SDH solar district heating

5th International
Solar District Heating
Conference

11-12 April 2018
Graz, Austria

www.solar-district-heating.eu

Proceedings

Supported by

This project has received funding from the European Union´s Horizon 2020 research and innovation programme under grant agreement No 691624

klima energie fonds

Das Land Steiermark
Wissenschaft und Forschung

Das Land Steiermark
Energie und Wohnbau

Gold sponsor

ENERGIE STEIERMARK

www.e-steiermark.com

Silver sponsors

AALBORG CSP - Changing Energy

www.aalborgcsp.com

ARCON SUNMARK

www.arcon-sunmark.com

Bronze sponsors

Savosolar

www.savosolar.com

Austroflex® Rohr-Isoliersysteme

www.austroflex.com

SOLID solarinstallation+design

www.solid.at

KBB SOLAR COLLECTORS

www.kbb-solar.com

GREENoneTEC 1 SOLAR COLLECTORS

www.greenonetec.com

austria solar WÄRME FÜR GENERATIONEN.

www.solarwaerme.at

wilo

www.wilo.at

SONNENKRAFT

www.sonnenkraft.com

www.isoplus.at

www.nmc.eu

www.absolicon.se

www.kyotherm.com

Media partner

www.solarthermalworld.org

www.solarthemen.de

www.ew-online.de

www.solarserver.com

The conference is organised by

Program committee

Scientific chairs

Christian Fink, AEE INTEC

Thomas Pauschinger, Steinbeis Research Institute Solites

Program committee members

Riccardo Battisti, Ambiente Italia

Jan-Olof Dalenbäck, Chalmers University

Christian Holter, SOLID

Heiko Huther, AGFW

Per Kristensen, Danish District Heating Association

Torsten Lütten, Savosolar

Gerald Moravi, Energie Steiermark

Cédric Paulus, CEA INES

Harald Poscharnig, GREENoneTEC

Alessandro Provaggi, Euroheat and Power

Matthias Sandrock, Hamburg Institute

Simone Skalicki, Region Styria

Per-Alex Sørensen, PlanEnergi

Table of Contents

2.1: Integration in urban district heating systems

2.2: Advanced system integration

4.2: Simulation tools and monitoring results

5.1: Land areas for SDH and roof integrated SDH concepts

5.2: Integration of thermal energy storage and heat pumps

6.2: Advanced system integration

THE ROLE OF THERMAL STORAGES AND SOLAR THERMAL IN TRANSITION TO CO_2 NEUTRAL HYBRID HEATING AND COOLING SYSTEMS IN CITIES.

Per Alex Sørensen
[1)] PlanEnergi, Jyllandsgade 1, 9520 Skørping, Denmark, +45 9682 0400, pas@planenergi.dk,

Matthias Sandrock
[2)] Hamburg Institut, Paul Nevermann Platz 5, 22765 Hamburg, Germany, +49 (0)40-39106989-0, sandrock@hamburg-institut.com

Abstract

When proposing solar thermal systems in connection to existing DH systems in cities, it is very often a problem, that the DH system is established for utilization of excess heat from power plants or from waste incineration. Therefore the base load in the district heating system is already "occupied" and solar thermal is not feasible because it will replace free heat.

The situation in many cities is even worse because there is much more heat in the summer period than needed. This is described a.o. in the Heat Roadmap Europe project (www.heatroadmap.eu) , where is is documented, that excess heat from power production, industrial production and waste incineration can cover more than the demand for heating all buildings in EU.

Several cities have as their ambition to within a period to complete a transition to CO_2 neutral heat supply or at least to reduce CO_2 emissions from heating of buildings remarkably. That will mean less heat from CHP plants using fossil fuels, less heat from boilers using fossil fuel and a need to fully utilize excess heat from other sources. This will demand thermal storages to store excess heat from summer to winter.

But in many cities this will still not be enough, so excess heat has to be supplemented from heat produced by solar thermal plants and heat pumps – and this can be feasible because a marginal extension of the storage capacity is relatively cheap. The result will be hybrid DH and cooling systems, where utilisation of fossil fuels is low or Zero and where extension of the systems to individual heated areas is possible.

1. INTRODUCTION

Excess heat from power production is enough to cover the total heat demand for buildings in EU (Persson, Möller and Werner 2014). In addition comes excess heat from waste incineration and industrial process. These resources can combined with long term storages and SDH be utilized in transition of cities towards 100% CO_2 neutral heating and cooling systems. The roles of the long term storages can be to

- Store heat from summer to winter.
- Energy management of multiple heat producers like e.g. CHP, solar thermal, heat pumps, industrial excess heat and geothermal heat.
- Store cold from winter to summer (if a heat pump is connected to the storage).

This document provides information about the possible potential for long term storages combining utilization of excess heat and SDH, status of demonstrated thermal storage technologies and a design study from Hamburg, where a hybrid system including thermal storage and a.o. SHD replaces a coal fired power plant.

2. POSSIBLE POTENTIAL FOR LONG TERM STORAGES AND SDH

In the Heat Roadmap Europe (HRE) project (www.heatroadmap.eu) the objective is to enable new policies and prepare the ground for new investments in district heating and cooling to decarbonize the energy system. The project is co-funded by the European Union and has developed into the current forth project "HRE4", where district heating and cooling possibilities are investigated in 14 EU member states (AT, BE, CZ, DE, ES, FI, FR, HU, IT, NL, PL, RO, SE, UK) covering 88% of the population, 92% of the heat demand in residential and service sector buildings and 89% of excess heat generating activities in whole EU28 (Persson, Möller and Weichers 2017). Mapping in the HRE4 project include mapping of heat demand and renewable heat sources divided in 1140 NUTS3 regions. The DH consumption is converted from point sources to areas. Tthe result for the Hamburg and Kiel areas in Northern Germany can be seen in Fig. 1.

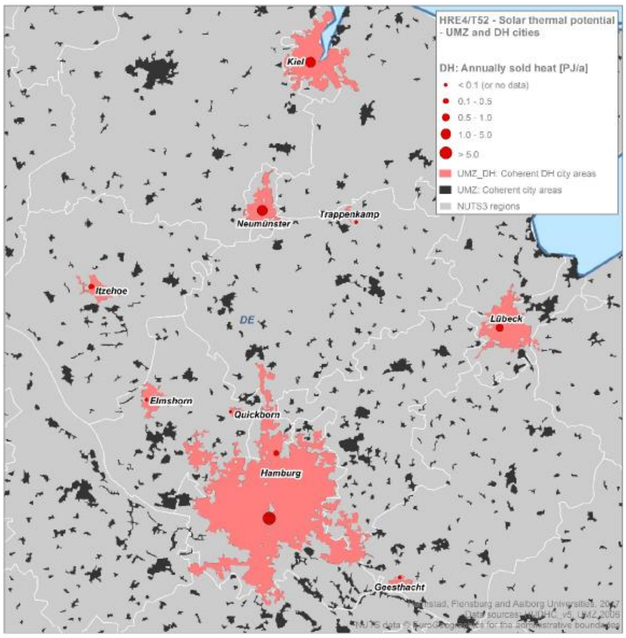

Fig1. City areas with DH in Hamburg-Kiel area (Persson, Möller and Weichers 2017)

To estimate the potential of long term heat storages at existing DH systems, the excess heat resource mapping has been combined with the DH mapping. And for the same Hamburg and Kiel areas, the result can be seen in Fig2.

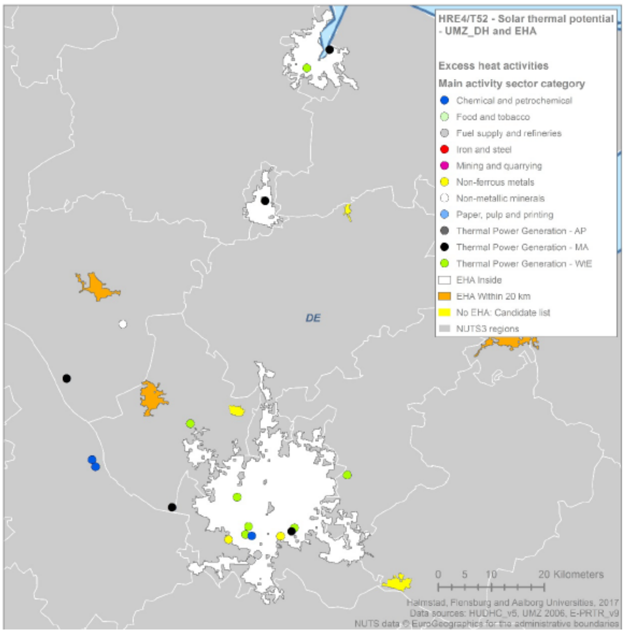

Fig.2. Excess heat activities combined with DH activities (Persson, Möller and Weichers 2017).

In Fig.2 the white areas indicate, that there are excess heat activities inside the DH area and the gold areas, that there are excess heat activities within 20 km from the DH borders.

Altogether 845 of 2.188 (39%) large-scale excess heat activities were found within coherent district heating city areas and 562 (26%) were found within 20 km of DH areas. In total there are 3.104 DH systems in the 14 member countries and 1.273 of these representing 150 mio. inhabitants have excess heat within 20 km. So the potential for further utilization of excess heat in DH systems and thus for implementation of long term storages is huge.

3. STATUS OF TECHNOLOGIES

Four storage concepts have until now been demonstrated as long term water storages in district heating and cooling systems. See Fig. 3.

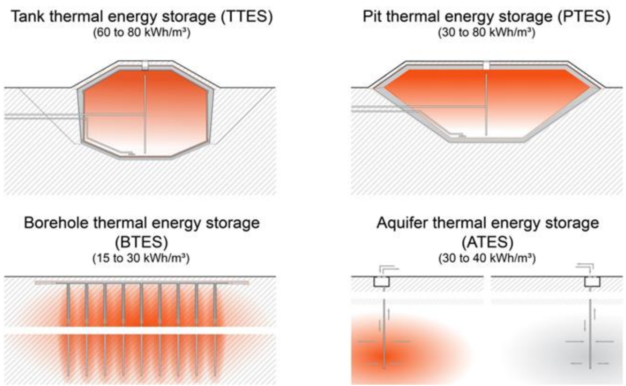

Fig. 3. Main concepts for long term storage (Solites).

Each storage concept has different capabilities. In Table 1 these capabilities are listed. The information are partly taken from SDH guidelines (Schmidt and Miedaner 2012) and updated with the latest results from Danish storages (Schmidt and Sørensen 2018).
Beside the four storage concepts also a hybrid storage (combination of TTES or PTES and BTES) has been demonstrated in pilot scale in Attenkirchen in Germany (Reuss e. al.)

Table 1. Comparison of storage concepts. Partly from SDH Guidelines www.solar_district_heating.eu.

TTES	PTES	BTES	ATES
Storage medium			
Water	Water	Soil/rock	Sand - water
Heatcapacity, kWh/m^3			
60 - 80	30 – 9,0	15 - 30	30 – 40
Storage volume for 1 m^3 water equivalent			
1 m^3	1 m^3	2 – 5 m^3	2 – 3 m^3
Geological requirements			
• Stable ground conditions • Preferably no groundwater • 5-15 m deep	• Stable ground conditions • Preferably no groundwater • 5–15 m deep	• Drillable ground • Groundwater favor-able • High heat capacity • High thermal con-ductivity • Low hydraulic con-ductivity ($k^f < 10^{-10}$ m/s) • Natural ground-water flow < 1 m/a • 30 – 100 m deep	• Natural aquifer layer with high hydraulic conductivity • Confining layers on top and below • No or low natural groundwater flow • Suitable water chemistry at high temperatures • Aquifer thickness of 20-50 m
Utilization			
• Short time storage up to 30,000 m^3 • Buffer tanks	• Long term storage for DH utilities pro-ducing more than 20,000 MWh/year • Long term/storage for industries (min. 30,000 m^3) • Short time storage from 30,000 m^3 for CHP-plants	• Long term storage for DH utilities pro-ducing more than 20,000 MWh/year • Long term storage for industries (min. 30,000 m^3) • Heat pump and buffer tank needed	• Cooling and heating of buildings • Long term storage in DH systems • Long term storage in industries • Heat pump needed for shallow applica-tions
Temperatures in hte storage			
5 – 95^o C	5 – 95^o C	-5 – 90^o C	2 - 20^o C for shallow systems 2-80^o C for deep-systems
Price/m^3 water equivalent			
100-200 € for tanks more than 2,000 m^3	20-40 € for storages more than 50,000 m^3	20-40 € for storages more than 10,000 m^3 water equivalent incl. buffer tank	4-35 €

The feasibility for a storage depends on price, operation costs, efficiency heat/capacity and lifetime. Normally the heat production price in a district heating system is 30 - 40€/MWh. If solar heat shall be stored the production price for the solar heat is maybe 20 €/MWh. If the storage efficiency is 80% the temperature difference is 50°C and the storage is only filled and emptied one time/year, this will mean that capital cost and operation cost of the storage may not exceed (40 or 30- 20/0,8) €/MWh or 5-15 €/MWh. If capital costs and operation cost are 7% of the investment, this means, that the investment in the storage has to be less than 12€/m^3 (5€/m^3 will result in a price for storing at 0.07 x 5€/m3/0.058 MWh/m^3 = 6€/MWh, 12€/m^3 will result in a price for storing at 0.07 x 12€/m^3/0.058 MWh/m^3 = 14.5€/MWh).

In the Danish 60,000 m^3 storage in Dronninglund storing solar thermal heat, the temperature difference is 80° C and the storage has two circles/year resulting in a better economy. The reason is, that the storage is used as heat source for a heat pump and also is used as buffer storage (Sørensen and Schmidt 2018).

So long term storing of solar produced heat needs cheap storages, cheap heat production prices, careful system integration and possible more functions to the storage (buffer tank, cold storage, storage for power-to-heat-to-power) to be economical feasible compared to the reference: fossil based production systems.

4. HAMBURG AS EXAMPLE

The City of Hamburg is a major city with 1.8 Mio. inhabitants in the North of Germany. Its district heating system is one of the oldest in Europe. Already in 1895 the heat supply of Hamburg's City Hall laid the foundation for the municipal district heating grid. Today, about 20% of Hamburg's heat demand – about 4.3 TWh/a – is covered by district heating.

During the 1990s the City of Hamburg sold the district heating system to the Swedish company Vattenfall. In the year 2013 the populace decided in a referendum to re-nationalise the district heating system. The City and Vattenfall agreed on a purchase option in 2019. The objective of the repurchase is the transition of the district heating system to renewable energies and waste heat use.

Hamburg Institut and PlanEnergi conducted a study for the City of Hamburg to establish how the share of renewable energies and waste heat can be increased considerably. In the first step options for the replacement of the co-generation coal power plant in Wedel which produces about 1/3 of Hamburg's district heat (1300 GWh/a) shall be developed.

The heat demand in Hamburg's district heating system is relatively low during the summer months. Then, only 150 MW are necessary. During the winter the heat demand increases to a maximum of 1500 MW. The summer load is mostly provided by the waste incineration plant Borsigstrasse (MVB).

For the study the district heating system was modelled in *EnergyPro* with the current generation portfolio. Furthermore, potentials for available renewable energies and necessary investments for their integration into the grid have been estimated.

In the modelling a cost-optimized operation of the heat sources in the course of the year is computed. The possible merit order of the production units has a large influence on the heat generation costs. Renewable heat plants have relatively high investment costs but relatively low operational costs (e.g. solarthermal). If those heat plants are only operated during the summer period for a few hours, heat prices increase due to fixed costs (capital costs).

For the replacement of the co-generation coal power plant Wedel the following heat sources are planned at the moment:

- 80 MW heat pump in a municipal wastewater treatment plant
- 18 MW industrial waste heat (steal / aluminium)
- 80 MW heat from a waste incineration plant
- 30 MW heat from biomass / RDF
- 12 MW solarthermal

The heat flows from industrial heat, waste incineration, solarthermal and heat pumps compete for the thermal load in spring, summer and autumn. Without seasonal storage their potentials cannot be used optimally and specific heat generation costs increase.

In Hamburg an aquifer heat storage is suitable for seasonal storage. The geological requirements are suitable and the underground conditions are well explored.

At a depth of about 270 m at the municipal wastewater treatment plant Dradenau a salinated aquifer exists in the "Braunkohlensande" layer. As the aquifer is not feasible for drinking water abstraction, it can be used to store heat. The aquifer is about 150 m thick and covered by an impervious "Glimmerton" layer.

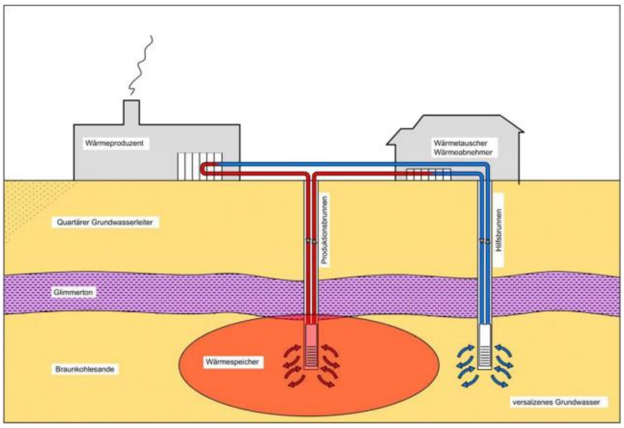

Fig 3. Concept of an aquifer heat storage system (Sandrock, Maaß Sørensen et.al. 2017)

For the utilisation a common water-water-system consisting of two extraction-/injection wells is proposed. It is planned to load the heat storage with a temperature of 80°C and unload with a temperature of about 65°C. Heat pumps and gas-fired boilers can increase the temperature of the stored water to the temperature level of the district heating grid. The flow temperature of Hamburg's district heating system lies between 90 and 133°C depending on the outside temperature.

A test drilling and heating of the aquifer has already taken place to enable a thermodynamic modelling of the heat storage. These measures were successful and make a successful realisation of the project seem probable. The thermal losses of the heat storage to their surroundings are estimated at about 15% based on the measurements.

During the first phase of the project a thermal power of the aquifer heat storage of about 30 MW is planned. Particularly the inexpensive heat flows from industrial waste heat and waste incineration (possibly also solarthermal) shall be stored for the heating period. The estimated investments costs for the heat storage itself (drilling costs and periphery) sum up to a moderate level of around 3 Mio. Euro. Larger investments are necessary for the large heat pumps and the gas-fired boiler.

By constructing additional wells, the storage capacity and the injection-/extraction capacity can be scaled up and be adapted to changing economic conditions. That way it is possible to integrate a large share of renewable energies and waste heat into the district heating system.

5. CONCLUSIONS

Altogether there are 3.104 DH systems in the 14 member countries and 1.273 of these representing 150 mio. inhabitants have excess heat within 20 km. So the potential for further utilization of excess heat in DH systems and thus for implementation of long term storages is huge. In many of these systems excess heat must be supplied by other sources, and that can open for solar thermal systems because the marginal cost of extending a long term storage can be low and solar thermal produced heat is fossil free and without air pollution.

Four concepts can be used as long term storages. They have all been demonstrated in full scale and valid test results exist. But to make long term storages and solar district heating feasible we need cheap storages, cheap solar heat production prices, careful system integration and possible more functions to the storage (buffer tank, cold storage, storage for power-to-heat-to-power).

An example of a long term storage combined with a.o. solar district heating has been calculated for Hamburg. Hamburg has favourable conditions for ATES (high temperature in the deep ATES and probably low investment costs for storing.

REFERENCES

Persson U, Möller B and Werner S (2014).
Heat Roadmap Europe: Identifying strategic heat synergy regions. Energy Policy. 74, 663-681.

Persson U, Möller B and Werner S (2017).
Heat Roadmap Europe. D2.3. A final report outlining the methodology and assumptions used in the mapping

Reuss M. et. al. (2005). Solar district heating with seasonal storage in Attenkirchen. ZAE-Bayern.

Sandrock M, Maaß C, Sørensen P A, et. al. (2017). Erneuerbare Energien im Fernwärmenetz Hamburg. Handlungsoptionen für einen kurzfristigen Ersatz des Kraftwerks Wedel.

Schmidt T and Miedaner O (2012). Solar District Heating Guidelines, Chapter 7.2 Construction concepts, cost and design guidelines for large scale or seasonal thermal energy storages.

Schmidt T and Sørensen P (2018). Monitoring results from Large Scale Heat Storages for District Heating in Denmark. 14th International Conference on Energy Storage, 25-28 April, Adana Turkey

Sørensen P and Schmidt T (2018). Design and Construction of Large Scale Heat Storages for District Heating in Denmark. 14th International Conference on Energy Storage, 25-28 April, Adana Turkey

MEASURES AND ENABLERS FOR INTEGRATING SIGNIFICANT SHARES OF SOLAR THERMAL ENERGY INTO URBAN DISTRICT HEATING NETWORKS – PRELIMINARY RESULTS FROM SHC TASK 55, SUBTASK A

Ralf-Roman Schmidt[1], Paolo Leoni[1], Markus Gölles[2], Sabine Putz[3], Anna Katharina Provasnek[3]

[1] AIT Austrian Institute of Technology GmbH, Vienna (Austria)

[2] BIOENERGY 2020+ GmbH, Graz (Austria)

[3] S.O.L.I.D. Gesellschaft für Solarinstallation und Design mbH, Graz (Austria)

Abstract

Introduction

The future of a lot of district heating (DH) networks is becoming more and more unsecure. Besides changing market conditions (especially energy prices), the need for decarbonisation imposes an increasing pressure to the operators of the networks for increasing the energy efficiency and share of renewables significantly. Solar thermal energy could be a suitable renewables energy source for substituting high shares of the existing fossil fuel based supply and therefore reduce the CO2 emissions of DH networks significantly. However, there are a couple of challenges (high network temperatures, high costs for collectors and long term storages, see also figure 1) that need to be overcome in order to enable a higher penetration of solar energy, especially in urban district heating networks.

Strengths • Small running costs and no risks • No CO2 emissions • Local technology suppliers	*Weaknesses* • High specific investment costs • Competition to base load supply • Long term storages not economically viable
Opportunities • By trend decreasing temperature levels in the network • Increasing need for reducing CO2 & subsidies for renewables	*Threats* • Collectors can be damaged (e.g. natural disasters) • Long payback times reduce flexibility

Figure 1: SWOT Analyses (Strengths, Weaknesses, Opportunities and Threats) of solar thermal integration into DH networks (simplified summary)

Method

This contribution describes preliminary results from subtask A of the IEA SHC Task 55. The focus of the IEA SHC program is to “develop research projects (Tasks) to study various aspects of solar heating and cooling.“[1] In this tasks, international experts cooperate and contribute their individual knowledge to a bigger picture. The IEA SHC Task 55 focuses on integrating large solar heating and cooling systems into district heating and cooling networks. Within Task 55, subtask A analyses different measures and enablers on the DH networks side to integrate significant shares of solar thermal energy into urban district heating networks. This is including:

- The assessment and comparison of different cases studies for DH networks with high shares of energy from solar thermal collectors
- The analyses of transition strategies of “traditional” DH networks with high fossil shares to networks with high solar shares, including the underlying heat demand and energy price scenarios
- The identification of beneficial integration options including hydraulics, supply technology combinations, storage integration and control strategies

[1] http://mojo.iea-shc.org/operating-agents

- The evaluation of different strategies to reduce the temperature levels (supply and return) on DH networks

Results

Following main enablers and measures can be differentiated:

Short term flexibility measures: In DH networks, normally two distinct customer side heating peak heating loads occur at the same time of the day (typically morning and evening peaks). Solar thermal energy has its supply peak usually directly in-between the morning and evening peak and therefore can only partly be used for covering the heating load. Short term flexibility measures for overcoming this mismatch are state-of-the art and include centralized and customer side storages, utilization of the network as storage and customer side load shifting. In (Schmidt and Basciotti 2014) those measures have been compered based on a literature review and dynamic network simulations of a typical rural heating network in Austria.

Long term flexibility measures: Beside the short term mismatch, a major barrier for integrating solar energy in DH networks is their seasonal mismatch to the demand profiles. Here, two cases have to be differentiated: First, DH networks where the heat demand in summer times is covered by heat pumps, geothermal energy or industrial waste heat. For economic reasons, those sources should not be turned off. As a consequence, solar energy in summer times needs to be stored for transition times or winter. Second, DH networks where the base load is covered by supply units that consume fuels, e.g. CHP or biomass plants. Here, the solar energy can actually safe costs and could be economically beneficial. However, large shares of solar energy needs to be stored in a seasonal storage anyways.

Measures for reducing the return temperatures: Currently, many "traditional" existing DH networks are not designed for a significant share of solar thermal energy due to the relatively high network temperatures, often between 60°C (return) and 120°C (supply). The technical measures for transforming traditional DH networks towards low temperature systems are well known, mature and in principle straightforward in their implementation. They can be distinguished in following areas:

- building side optimization such as hydraulic balancing and the correct use of thermostatic radiator valves
- Detecting and minimizing errors and faults in substations and domestic hot water preparation
- cascading (using the return flow of high temperature customers as a supply to low temperature customers)

However, for reducing the system temperatures, investments on the building side have to be done; the heating system is often not designed for low supply and return temperatures as well as domestic hot water preparation often need a certain temperature level.

References

Basciotti, D. and Schmidt, R.R.: "Peak reduction in district heating networks: A comparison study and practical considerations", The 14th International Symposium on District Heating and Cooling, Stockholm, Sweden, September 7th to September 9th, 2014

Winterscheid, Carlo; Dalenbäck, Jan-Olof; Holler, Stefan: Integration of solar thermal systems in existing district heating systems, In Energy, 2017, ISSN 0360-5442, https://doi.org/10.1016/j.energy.2017.04.159.

Keywords: solar district heating; case studies; integration aspects; transition strategies; network performance; hydraulics; control strategies; return temperature reduction.

The Role of Solar Thermal in Urban Heat Supply – Pilot Scheme Freiburg "Gutleutmatten" in Freiburg

Axel Oliva [1], Mehmet Elci [1], Alexander Ripka [2],
Wolfgang Kramer [1], Sebastian Herkel [1]

[1] Fraunhofer Institute for Solar Energy Systems ISE, Heidenhofstraße 2, D-79110 Freiburg i.Br., Tel.: +49 761 4588 – 5698, E-Mail: axel.oliva@ise.fraunhofer.de
[2] badenova Wärmeplus GmbH & Co. KG

1. Introduction

In the course of an inner-city development the housing estate Freiburg "Gutleutmatten" with 500 accommodation units, a heated floor area of 38.000 m² and a heat demand of 2.200 MWh/a is being realized.
Within the frame of this project decentralized solar thermal systems will be integrated in a heat supply concept based on a combined heat and power (CHP) district heating system. The operation of the CHP system will be optimized on one hand regarding to the interaction with the power network and on the other hand concerning the reduction of heat losses in the distribution network. The assumption is that this kind of design and operation management will be constructive to supply an urban area on a medium and long-term point of view. Central objectives of the project are to implement a concept for the operation management and to derive general rules for comparable urban areas. This will be carried out considering the ongoing massive transformation process of the overall energy system.

2. Objectives of the project

Primary the role of solar thermal technology in supply of urban areas will be evaluated. This will be done considering prospective conditions of the energy business. The focal point will thereby put on an integral consideration of power and heat consumption and the corresponding supply network systems.
Secondary it will be demonstrated an innovative and economically promising solution for investors, the operator and finally the clients in the integration of solar thermal technology to deactivate the district heating network during summer time. The approach is a decentralized implementation of solar thermal into the supply systems of each connection unit to deactivate the CHP operated district heating network for time periods with high irradiation and so a high fraction of photovoltaics in the electricity grid. During these periods the operation of the CHP is supposed to be not economically due to the low corresponding feed in tariff.
In the concept the total heat demand will be covered by 38 decentralized solar thermal units including its decentralized storages and the heat produced by the central CHP unit. The total area of collectors will be about 2.100 m² producing about 740 MWh/a. By that the specific storage volume will be at 100 Liter/$m^2_{Aperture}$. This will lead to a total heat coverage of about 33 % that will enable a self-sustaining supply by solar thermal for long periods during summer time. The remaining 1,460 MWh/a will be supplied by the central CHP. The heat loss of the network will be at about 300 MWh/a where the reduced operation time is already taken into account.

3. Results

In the first step, the **concept** of the **heat supply system** and it´s variants on the building side will be introduced in a generic technological point of view and transferred to the real demonstrating object. In the next step the executed **open competitive** bidding is illustrated and its results are **economically analyzed**. Furthermore an understanding of **cost** is shown introducing indicators like the specific cost of solar thermal systems and levelized cost of heat. In the next step the actual **state of construction** is shown reflecting some raised questions concerning **quality of workmanship and operational consequences** that occurred during that first operational periods of commissioning the heat supply system. At least **simulation based results**, representing the entire housing estate are shown, introducing the operational modes of “switching of the heat network” and harmonizing the heat demand of the housing estate regarding to the SDH by “injection of solar thermal heat to supply neighbored buildings”, putting together the effects of heat and electricity demands and the related costs.

A Case Study of Solar District Heating in the Context of Technical, Ecological and Economic Framework Conditions

Stehle, M.[#1], Blesl, M.[#2]
[#]Institute of Energy Economics and Rational Use of Energy (IER), University of Stuttgart
Hessbruehlstraße 49a, 70565 Stuttgart, Germany
[1]Markus.Stehle@ier.uni-stuttgart.de
[2]Markus.Blesl@ier.uni-stuttgart.de

Solar district heating (DH) systems represent an innovative approach to increase the share of renewable energy in the heat market. However, the realization of solar DH systems is capital-intensive and different barriers, such as land availability for collector fields, prevent this. Once these barriers are overcome, solar DH systems can contribute significantly to reduce carbon emissions. Aside carbon saving potentials, issues on the economic efficiency of solar DH supply, but also the impact of solar DH supply on other heat supply technologies need to be considered. The use of DH supply technologies, such as combined heat and power systems (CHP), is affected by solar integration into the DH grid. The profitability of CHP systems is not only influenced by intermittent solar energy, but also by economic conditions, such as the development of the electricity prices at the power exchange (e.g. EPEX SPOT[1]). Thus, the question arises to what extent solar integration leads to the displacement of cogeneration systems and what displacement effect is greater: solar integration or economic conditions. To investigate this issue, the Easy District Analysis (EDA) tool, developed within the framework of IEA[2] DHC[3] Annex TS 1 (Blesl, Stehle 2017 and Schmidt, Kallert 2017), was applied.
EDA is a DH planning tool for urban planners and utilities that is intended to be used in the pre-planning phase of a district energy system. The focus of the EDA tool lies on the evaluation of the impact of grid temperatures (e.g. standard DH[4] vs. low temperature DH[5]), operation modes (technical[6] vs. economic[7] operation) and DH supply technologies (e.g. CHP DH supply with and without solar integration) on the use of DH technologies, primary energy consumption, carbon emissions and heat production costs.
With the EDA tool a case study was applied to an urban district with more than 140 multi-family houses. As a result, the case study indicates that the economic displacement

1 European Power Exchange for power spot trading
2 International Energy Agency (IEA)
3 District Heating and Cooling (DHC)
4 Supply line / return line: 90°C/ 60°C
5 Supply line / return line: 50°C/ 35°C
6 Full use of CHP capacity
7 Cost-minimal operation of DH technologies considering economic framework conditions

effect on the use of cogeneration plants turns out to be higher (-20 % use of CHP) than the additional displacement effect caused by solar integration (-13 %).

Aside displacements effects of solar integration, different DH temperature levels can be applied to examine the impact on solar DH supply. A temperature reduction from standard DH to low temperature DH can boost solar DH in terms of yield and solar fraction significantly (e.g. + 45 % yield) and thus, increase the carbon mitigation potential of solar-powered DH. This is not only explained by lower collector heat losses, but also by an increasing period of solar thermal feed (+ 32 % hours of solar feed) as lower grid supply temperatures are easier achieved. Heat production costs of solar DH supply are reduced with low temperature DH supply and thus, making solar DH more competitive compared to alternative heat supply options. Furthermore, the influence of different instruments, such as CO_2 tax, can be analyzed on the use of technologies and heat production costs of different variants of DH systems[8].

References

(Blesl, Stehle 2017)

Blesl, M., Stehle, M. (Editors): ANNEX TS1: Low Temperature District Heating for Future Energy Systems – Subtask A: Methods and Planning Tools. Final subtask A report of the IEA DHC Annex TS1: Low Temperature District Heating for Future Energy Systems, Institute of Energy Economics and Rational Energy Use (IER), University of Stuttgart, 2017.

(Schmidt, Kallert 2017)

Schmidt, D., Kallert, A. (Editors): Future Low Temperature District Heating Design Guidebook, Final Report of the IEA DHC Annex TS1: Low Temperature District Heating for Future Energy Systems, AGFW-Project Company, Frankfurt, Germany, 2017.

(SolnetBW II)

Solites, AGFW, Hamburg Institut, IER, KEA: SolnetBW II – Solare Wärmenetze für Baden-Württemberg, Laufzeit 2017-2019. Baden-Württemberg Programm Lebensgrundlage Umwelt und Ihre Sicherheit (BWPLUS) 'Transformation des Energiesystems in Baden-Württemberg – Trafo BW'.

8 **Acknowledgement**
The paper was supported by the project 'Solnet BW II – Solare Wärmenetze für Baden-Württemberg' in the framework of the BWPLUS program (Baden-Wuerttemberg Research Program Securing a Sustainable Living Environment). The authors would like to thank for the given financial support from the German state of Baden-Wuerttemberg and project management of Karlsruhe (PTKA) and would like to acknowledge the contributions of their colleagues.

SDH IN ITALY: INCENTIVE SCHEME AND DEVELOPMENT OF NEW PLANTS

Riccardo Battisti
Ambiente Italia Srl, Via Carlo Poerio 39, Milan, 20129, Italy,
Phone: +39 02277441, E-mail address: riccardo.battisti@ambienteitalia.it

Abstract – Solar district heating in Italy has still a very limited diffusion with just one example of relatively large plant in Varese and some smaller examples in other cities of the northern regions. However, perspective for the development of new plants are quite positive, thanks to a growing interest from the utilities and a very good incentive scheme available for solar thermal plants, including their application to district heating networks. The support mechanism, whose revision has been recently released under the name of 'Conto Termico 2.0', foresees an incentive over 5 years which, depending on the system cost, the plant size and the expected yield of the solar collector, can cover between 40 % and 65 % of the initial investment cost, thus constituting a potential driver for increasing the SDH market in the country.

1. INTRODUCTION

Thanks to a series of EU-supported projects on the topic of solar and renewable district heating, SDH could take off in Italy, starting completely from scratch. The first project, 'SDHtake-off', was then followed by 'SDHplus', 'SmartReFlex' and, finally, the currently ongoing 'SDHp2m' initiative.

Within these projects, capacity building towards utilities and local authorities were implemented and feasibility studies for real plants were carried out. Thanks to such preparatory activities, for instance, the first Italian SDH plant was initiated, and then completed, more than two years ago in Varese (Battisti, 2015).

2. MAPPING THE MARKET

2.1 The first example in Varese

In all, three SDH plants are up and running in Northern Italy. The first one has a gross area of 990 m² and was set up in Varese, a city close to Milan, in 2015. It is run by Varese Risorse, a utility that is part of the large A2A group of companies. Solar output is primarily used to preheat the make-up water for the nearby district heating network.

The solar thermal system was developed and installed by newly established Italian company SDH Energy, which was founded by former Sonnenkraft Italy staff to become the distributor for Arcon-Sunmark in Italy. The solar field consists of 73 flat plate collectors, type HT-HEATBoost35/10, which were produced by Danish company Arcon-Sunmark and have a gross surface area of 13.6 m² each. The Varese city grid, which is heated by a 5 MW^{el} gas turbine and five backup natural gas boilers offering a total capacity of 35 MW_{th}, has a length of 16 km and supplies thermal energy for domestic hot water and space heating to 150 large consumers. The grid operates with a supply temperature of 90 °C and a return temperature of 65 °C.

The solar thermal plant provides heat to already existing water storage systems with volumes of 215 m^3. To try and obtain a lower average working temperature for the solar collectors, however, the solar circuit can also pre-heat the cold water which is needed to restore water losses in the grid and which is taken from public water supply at 10 °C.

The solar plant operates dangerously close to the stagnation point during high irradiation because of the grid's high supply temperature. The special circumstances required a system to control the pumps in the solar circuit based on irradiation and supply temperatures in order to avoid stagnation.

The SDH plant in Varese (photo: Battisti R.)

The total investment cost, excluding the storage which was already present in the heating plant, was about 420,000 EUR, showing a specific cost of slightly more than 400 EUR/m^2. The foreseen subsidy over a period of five years is 275,000 EUR and the expected Internal Rate of Return for the investment is over 8 %.

Although the solar fraction is lower than 1 %, this first solar district heating plant in Italy can serve as a milestone for spreading this technology in southern Europe.

The first on-field results reported a very good performance of the solar plant, in line and even above expectations and initial simulations (Battisti, 2016).

2.2 Solar feed-in

The second example is quite a peculiar one since it is based on a previously existing solar thermal plant installed on the roof of a swimming pool in Lodi near Milan. In 2017, it was then connected to the local district heating network of utility Linea Reti e Impianti. The 200 m² collector field is operated by the owner of the sports facility, Sporting Lodi, and preheats the return line of the grid.

This case, therefore, can be regarded as a third-party access to the district heating network by an external operator and can constitute an interesting milestone for other similar situations.

The connection between solar field and network return line (photo: Linea Reti e Impianti)

2.3 SDH in mountain areas

The third SDH system was installed in the village of Sansicario in the mountainous region of northern Italy (Degiorgis et al., 2016). In 2016, it started feeding solar heat into a district heating network which mainly runs on gas-powered CHP units. This solar field, designed by engineering services company Degmar, consists of two different sections, one with flat plate and one with evacuated tube collectors (ETCs). Its total gross area is 63 m².

The reason for installing a mixed-collector system was to analyse the performance of both types in an existing district heating system. The ETCs show better performance, with specific heat production up to 500 to 600 W/m² on an hourly basis and conversion efficiencies near the theoretical curve. Only the monitoring data made it possible to resolve the issues with the flat plate collectors, and production is now close to that of the ETC field.

SDH plant in Sansicario (photo: Degmar)

The district heating network generates 23,573 MWh of heat each year. Net production is at 21,120 MWh because of 10 % network losses. The 5-kilometer pipelines provide heat for around 350,000 m³ of building space in the residential and tourism sector. In winter, supply is at 95 °C and return at 65 °C. Three engines powered by natural gas provide about 86 % of total production at an overall power of 3.6 MW_{th}. The remaining demand is met by auxiliary boilers, which have a combined capacity of 10.3 MW_{th}.

Mountain areas are also very promising zones for the combination of solar and biomass for local district heating networks: Two examples of very small SDH plants, in combination with biomass, are in operation in the Veneto Region and are reported in the map below.

2.4 Plants under development

The SDH map for Italy shows the examples described above and also a new 600 m² plant foreseen within the renovation works of the 'Mirafiori Nord' heating plant of the district heating network in Turin, when also a 2,500 m³ water storage will be added, most probably by 2020.

Another 500 m² SDH plant has been planned, in combination with heat pumps, for supplying heat to an extension of the district heating in Alessandria, a city in the region of Piedmont.

Finally, for the large district heating network in Brescia, in the region of Lombardy, an ambitious decarbonisation plan has been set up by the local utility A2A, including industrial waste heat recovery, low temperature networks and the use of solar thermal systems.

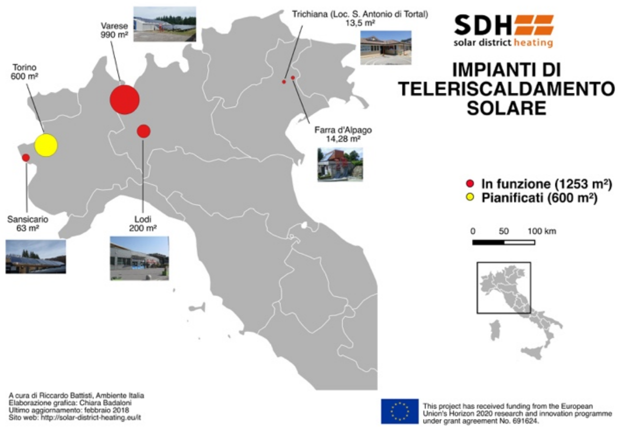

SDH plants in Italy: In operation and planned

3. ECONOMIC CALCULATIONS

3.1 The incentive scheme

In Italy an incentive scheme, 'Conto Termico', is operating at national level, supporting several renewable heat technologies as well as some energy efficiency measures for both private and public users.

Regarding solar thermal, the incentive mechanism, managed and operated by the state-owned company GSE, supports plants with a gross surface of up to 2,500 m². The subsidy is paid in two annual instalments for systems below 50 m² and in five for ones between 50 and 2,500 m². The amount of support depends on the system size, the application and the expected yield of the collectors. More specifically, the annual incentive is calculated as follows:

$$I_{a\,tot} = C_i \cdot Q_u \cdot S_l \quad (1)$$

where S_l refers to the system's gross area and C_i is a fixed parameter expressed in EUR/kWh, whose values span from 0.08 to 0.43 EUR/kWh depending on the application (domestic hot water, space heating, process heat, district heating and solar cooling) and on the system size. Finally, Q_u is the annual collector yield divided by the gross area of the collector type, as reported on the Solar Keymark certificate for the site of Würzburg at a temperature level depending on the final use of the solar heat; For SDH, for instance, the yield at 50 °C should be used for the calculation.

3.2 Solar heat cost

Assuming a 2,000 m² SDH plant with a specific cost of 400 EUR/m² (total investment of 800,000 EUR), the incentive could be calculated using a good quality collector with a Solar Keymark yield of 560 kWh/m² year at Würzburg and for a temperature of 50 °C.

The specific annual incentive is 50.4 EUR/m² and the total annual incentive for the plant is 100,800 EUR. The total incentive over the period of 5 years would then amount to 504,000 EUR, 63 % of the investment cost, very close to the maximum value of 65 % foreseen by the scheme.

Still large resources are available for 'Conto Termico', thus leaving a huge potential for small and medium-size SDH systems.

Beyond the incentive, the expected heat production cost can be calculated over, for instance, a period of 15 years, also assuming a 10-years bank loan with a 6 % interest rate and, therefore, a total cost of the investment of 1,280,000 EUR.

The real yield of the solar plant could be estimated to 500 kWh/m², thus bringing the total output in 15 years to 15,000 MWh.

Assuming a 1 EUR/MWh O&M cost, the total plant cost over the 15-years period is 1,295,000 EUR which is lowered to 791,000 EUR because of the incentive.

The solar heat would then have a cost of 53 EUR/MWh. This value is depending substantially on the financing cost: With a 4 % interest rate, it could go down to 42 EUR/MWh, even reaching 31 EUR/MWh in case of special 'green loans', for instance with a 2 % interest rate.

4. CONCLUSIONS

From a policy point of view, a relevant milestone was the inclusion of SDH in the Italian National Energy Strategy, released in November 2017. This inclusion was done thanks to a specific request sent by Ambiente Italia, partner of the SDHp2m project, during the open consultation phase of the strategy document.

A few SDH systems are in operation at the moment in Italy but both the positive attitude of several utilities and the good support scheme for solar thermal are really promising factors.

However, despite the favourable incentive environment for solar district heating in Italy, relevant barriers to faster deployment remain. First, the existing district heating capacity is restricted to the northern parts of Italy. A recently published study by GSE found that 78 % of district heating is concentrated in only three regions, namely Lombardy, Piedmont and Trentino-Alto Adige (GSE, 2015). An additional obstacle is the rather low gas price paid by utilities. Since they operate combined heat and power units, they are classified as electricity producers and are exempt from certain taxes. On top of this, there is a lack of awareness among utility operators and policymakers, and the number of specialised technology providers in the country is negligible. Other highly delicate issues are the visual impact of the collector field and competing land uses.

REFERENCES

Battisti R. (2015). Italy: First Solar District Heating System, 990 m² big. *Solarthermalworld.org.* http://www.solarthermalworld.org/content/italy-first-solar-district-heating-system-990-m2-big

Battisti R. (2016). Italy: First-Year District Heating Yield Better than Expected. *Solarthermalworld.org.* http://www.solarthermalworld.org/content/italy-first-year-district-heating-yield-better-expected

Degiorgis et al. (2016). Planning and operation of two small SDH plants as test site: Comparison between flat plate and vacuum collectors. *Proceedings of the 4th International Solar District Heating Conference*, 21-22 September, Billund, Denmark.

GSE (2015). Valutazione del potenziale nazionale di applicazione della cogenerazione ad alto rendimento e del teleriscaldamento efficiente. https://www.gse.it/documenti_site/Documenti%20GSE/Studi%20e%20scenari/Potenziale%20CAR-TLR%20nazionale%20e%20regionale.PDF

Towards Giga-Scale Thermal Energy Storage for Renewable Districts in Austria

Georg Engel[1], Ingo Leusbrock[1], Wim van Helden[1]

[1]AEE – Institute for Sustainable Technologies,
Feldgasse 19, 8200 Gleisdorf, Austria
Tel.: +4331125886262

E-Mail: g.engel@aee.at

Introduction and Motivation:
To reach the long-term goal of 100% renewable energy supply, district heating (DH) networks require large-scale thermal energy storage (TES) technologies such as pit and tank storage. As these systems need to be implemented in an urban environment, the required surface area should be minimised to compensate for the relatively high land price in an urban environment. These minimized costs can be achieved by moving the system below surface level and further decreased by allowing usage of the surface area for recreation or installation of solar collector fields. DH systems call for TES volumes up from 50,000 m^3 to as much as in the order of one billion litres, or 1 million m^3. Presently, large-scale thermal storages have been built and are in operation in Germany and mainly Denmark, with recent storages having volumes of nearly 200,000 m^3.
Experience with the existing plants is still limited due to the low number and short age of the storages. Improvements are needed on material performance and durability and on material and component development. Cost effectiveness and system integration call for higher storage density and thus higher temperatures, imposing even higher demands on the materials used. This and the requirements of vapour tightness, serviceability and durability of innovative solutions for lid, wall and liners call for novel materials and components as well as for improved durability testing methods. Additionally, the envisioned size of new giga-scale storage technologies and the construction in the subsurface require new construction methods.

Background:
The project giga_TES is an Austrian flagship- project targeting at the development of large-scale thermal storage concepts for renewable districts, with a focus on feasible Austrian implementations. The project consortium consists of key material and component industries, a major construction company, an engineering and two DH companies, backed by four Austrian and two foreign research institutes that have deep knowledge and experience in the field of materials, components and system technologies for very large thermal energy storages.

Goals:
The project pursues the following technical, economic and scientific goals:

(1) to develop a comprehensive overview with all requirements and relevant boundary conditions for the use and implementation of giga-scale storages and to implement a scientific decision-making tool for obtaining representative prospective application scenarios internationally and in Austria.
(2) to develop innovative and optimal construction methods for giga-scale TES with particular consideration of ground conditions. Based on five typical soil and rock profiles various ground engineering approaches for deep pit excavations will be assessed and their opportunities illustrated.
(3) to elaborate economic and practicable solutions for critical storage components which are the bottom slab, walls and the cover.
(4) to develop novel polymeric and inorganic materials for the construction of large-scale thermal energy storages along with testing and lifetime assessment methods for faster and more realistic screening and pre-qualification of such materials.
(5) to develop simulation models with different modelling depths, and to test and apply them to optimize the storage design for relevant boundary conditions. Furthermore, a methodology to predict the ground and ground water temperature increase depending on the specific geo-hydrological conditions and the storage design as well as a co-simulation platform for optimization of the system configuration and control strategies will be developed.
(6) to evaluate the added value and impact of large-scale storage in existing and future district heating systems and to analyse the sensitivities and mutual influence of system parameters on the overall performance, by that deriving operating windows and optimized system configurations for given boundary conditions, with separate attention to Austrian boundary conditions.

Discussion:
The project starts with the beginning of 2018. An overview of the goals and of the approaches how to achieve them will be presented at the conference.

Modular optimization-based energy management framework for cross-sectoral energy networks

Daniel Muschick[1], Andreas Moser[1,2], Markus Gölles[1]

[1]) BIOENERGY 2020+ GmbH, Graz (Austria)

[2]) Institute for Automation and Control, Graz University of Technology, Graz (Austria)

1. Introduction

To reap the highest benefit from the increased installation and integration of renewable energy sources, an effective, cross-sectoral energy management system (EMS) is needed. This EMS takes care of operating the individual components in such a way that the maximum amount of renewable energy from intermittent sources such as solar thermal or wind can be harnessed. Also, it tries to minimize operating and fuel costs as well as emissions by keeping the number of on/off cycles low and operating the heat and power producers in ideal conditions.

While proven to be attractive in numerous research projects, EMS capable of optimally operating cross-sectoral energy systems are not yet available on the market and three major challenges have to be faced:

1. Hybrid energy systems are still rather rare because of typically high investment costs and lack of experience with operating them. Without sufficient information on the long-term financial implications, tried-and-true but sub-optimal configurations as well as operating strategies are often implemented.
2. Once a hybrid energy system is installed and an EMS is available, the problem of actually implementing the directives given by the EMS on low-level controllers arises. A general guideline readily applicable to complicated configurations is still missing and a matter of current research.
3. Since the existing EMS mostly originate from (often academic) demonstration projects, they are tailor-cut to individual scenarios and do not easily scale to different configurations.

For these reasons, this talk will present a modular, optimization-based predictive energy management framework and showcase how it can help with each of these three challenges.

2. Modular optimization-based energy management framework

Structure of the developed modular cross-sectoral energy management framework

A modular EMS should consist of three parts (see Figure 1): a **load and yield forecasting algorithm** that provides information on the demand of the consumers (load) and intermittent production of renewable energy sources (yield); a **state estimator** that uses measurements to estimate energy levels in the storages and ultimately the overall state of the system; and an **optimization-based controller** which takes into account both the current state and the forecasts and determines a plan of operation (model predictive controller, MPC).

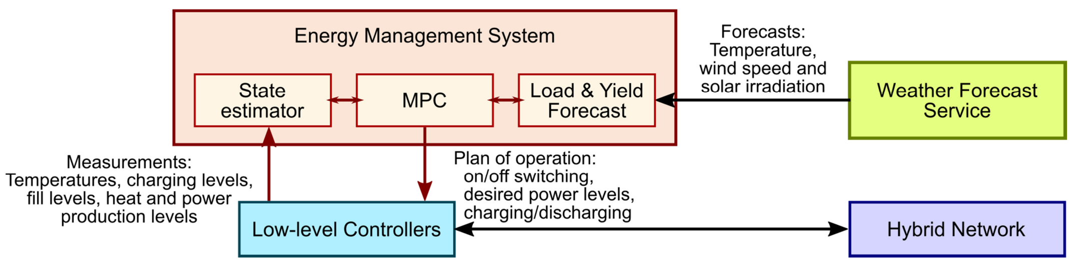

Figure 1: Structure of the developed modular cross-sectoral energy management framework

Modular framework for specifying energy configurations using standardized building-blocks

In order to address the challenges mentioned above, all three parts of the EMS need to be modular and able to adapt to different operating conditions and energy configurations. The energy configuration to be managed needs to be configurable from standard building blocks that represent the various technologies. These blocks represent sources (e.g. heating grid, solar thermal plants, biomass), sinks (e.g. feed-in into the grids), converters (e.g. heat pumps), distribution networks, and storages. The configuration is defined by specifying the connections between them and specifying e.g. the costs for buying from sources, rewards for selling to sinks, conversion efficiencies, storage capacities and minimum / maximum power levels; see Figure 2 for an example.

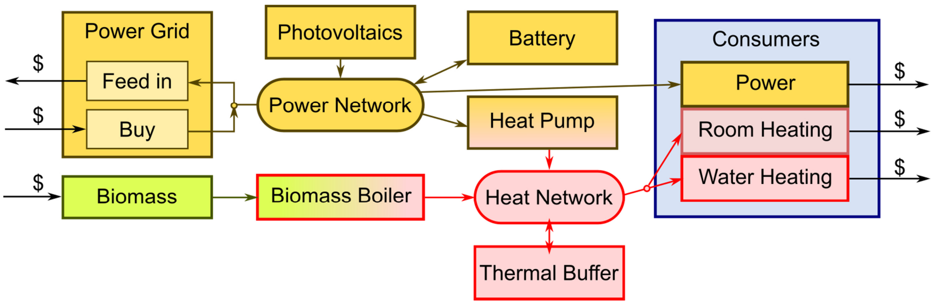

Figure 2: Energy configuration built from sources (biomass, power grid/buy, photovoltaics), sinks (power grid/feed in, consumers), converters (biomass boiler, heat pump), distribution networks and storages (battery, thermal buffer)

Automatic optimization problem generation

The predictive controller needs models of the individual components in order to predict the behavior of the system given a specific plan of operation. For scalability reasons, these should be as simple as possible, while retaining the ability to describe the essential characteristics of the components. Hybrid linear models stand out in that they can be expressed in a mathematical way easily accessible to optimizers (mixed logical dynamical models, MLD). They can be used to model on/off switching behavior, load-dependent conversion efficiencies and minimum output power requirements. Each block of the energy configuration is represented by a parametrized MLD model, and the interconnection configuration automatically determines an overall MLD model for the whole system. This, together with the predicted yield and load curves and cost definitions, defines a *mixed-integer* linear program (MILP) that can be solved even for medium-scale problems using state-of-the-art solvers such as GUROBI or CPLEX to give the optimal operating strategy.

Practical validation of the modular energy management framework

The practicability of the proposed method will be demonstrated on the basis of a local heating grid with three heat producers (biomass boiler, solar thermal in combination with a heat pump, oil boiler as backup) and 26 consumers where it has already been applied successfully. A screenshot of the control visualization, indicating the production power levels as well as the states of charge (SoC) of the storages, is displayed in Figure 3.

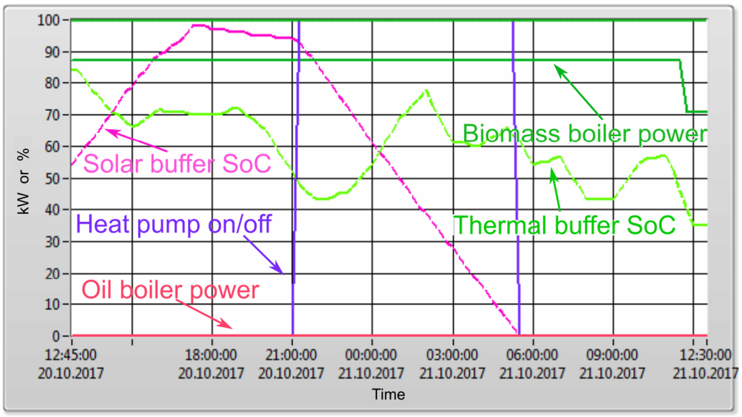

Figure 3: Example of a real-life operation of the energy management system of a local heating grid during autumn

3. Summary and Conclusion

The modular framework developed allows facility managers to quickly investigate different energy configurations in simulations and determine the most suitable configuration for their purposes. By relying on standardized building blocks, the EMS optimization problem can be automatically inferred and the interface to the low-level controllers can be automatically constructed, thus greatly simplifying the task of implementing the EMS in real world applications.

Within the talk the framework will be demonstrated and first practical results will be presented.

DATABASE FOR HEATING PLANTS BASED ON RENEWABLE ENERGIES IN STYRIA (AUSTRIA)

Julia Karimi-Auer and Simone Skalicki
Office of the Styrian Government – Department of Energy and Housing,
Landhausgasse 7, Graz, 8010, Austria,
Phone: +43 316 877 2729, email: julia.karimi-auer@stmk.gv.at, simone.skalicki@stmk.gv.at

Abstract – Austria's second largest federal province *Styria* is a European region with high potential for solar thermal energy and is participating in the current EC project SDHp2m (2016-2018) along with eight other European regions. The Styrian administrative body (Office of the Styrian Government) is a member of the SDHp2m project. Since 2016, Styria's administrative body maintains a publicly available database for heating plants in Styria that are based on renewable energies. As a part of the project SDHp2m the database was amended and furthermore used for investigating the operators' interest in the implementation of solar thermal support. This paper describes the background and the setting-up of the database and the information provided by it. In addition to that, the role of the database in the project SDHp2m is shown as well as its general benefits.

1. INTRODUCTION

Styria comprises 1.2 million inhabitants on 16 400 km² and is Austria's second largest federal province. Not including the city of Graz (280 000 inhabitants) there are more than 600 biomass based district heating plants all over Styria. The biomass plants' capacity ranges from about 40 kW to 20 000 kW (see Figure 1). The plants are usually based on solid biomass (wood) and are sometimes equipped with fossil boilers for peak demand coverage. Approximately 30 of those plants have solar thermal support.

Until 2016, there have been some non-coordinated databases for heating plants based on renewable energies with various data sources.

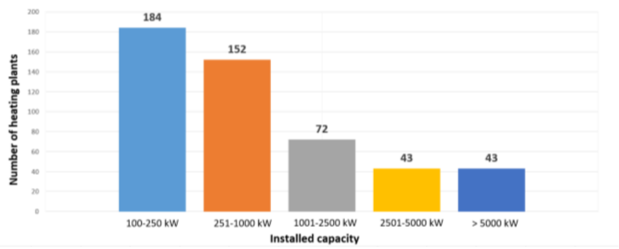

Figure 1: Biomass based district heating plants in Styria separated in groups based on the installed capacity

2. DEVELOPMENT OF THE DATABASE

In 2013, the Austrian statistical office (*Statistik Austria*) was asked to generate an EC-report about the use of biomass for heating purposes in Austria. Except for Austria's federal province of *Salzburg* there were no comprehensive databases concerning biomass plants available. Since there was now a specific need for such a database, the Office of the Styrian Government gathered the existing and partly private data and put it all together in one database with a new interface. By doing so, data protection issues also became important. For this reason all plant operators were informed in advance about the idea of an upcoming and publicly available database on biomass plants. The operators could choose about the grade of information that would be published (location as a minimum information). When the database was finished, also a GIS-based interface was added. Whereas the graphical interface is available to the public, the full database is only open to entitled persons of the Office of the Styrian Government and the Styrian Chamber of Agriculture.

3. CONTENT AND DESIGN OF THE DATABASE

The following table (Table 1) shows what kind of information is stored in the database. Of course, not all of the more detailed information parameters are available for every plant.

Master Data	Details	Heat Source
Address	First launch	Heat source
Plant operator	Number of clients	Manufacturer
Grid operator	Route length	Capacity
Contact person	Installed capacity	First launch
	Received subsidies	Comments
	Buffer storage	
	Biomass capacity	
	Overall capacity	

Table 1: Information stored in the database

The image below in Figure 2 shows the input mask of the database.

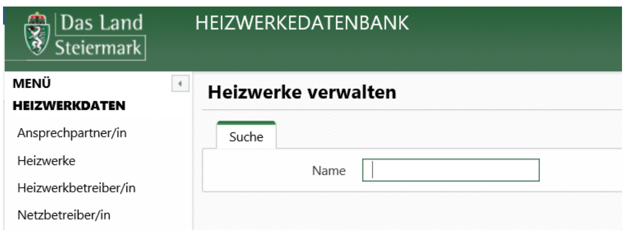

Figure 2: Input mask of the database

At the moment there are 620 biomass plants listed in the database.

Figure 3 shows the publicly available, GIS-based output of the database. As shown, the plants are graphically divided into the following subcategories: object supply with up to two heat consumers (53 heating plants), micro heating grids with up to 250 kW (138 heating plants), local or district heating grids with more than 250 kW (366 heating plants). For 45 heating plants there is no specific data available. 39 plants have solar thermal support.

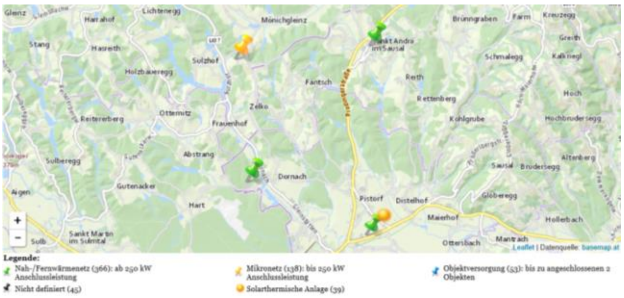

Figure 3: Publicly available GIS-based output of the database. Green pins indicate plants with an installed capacity of more than 250 kW, yellow pins indicate an installed capacity up to 250 kW, the sun symbol indicates solar thermal support.

4. BENEFITS OF THE DATABASE

The benefits of the database can be divided into in-house benefits (benefits of the administrative body) and external benefits (benefits for existing and future plant operators/customers):

The Office of the Styrian Government uses the database for strategic orientation when starting purposeful local incentive schemes or information campaigns. Furthermore, the database provides an overview about the status-quo, which is also used for EC reports.

For existing and future plant operators as well as customers the database offers an orientation about the existing heat supply facilities which helps when either planning a new heat plant or seeking for district heating connection.

5. CONTRIBUTION TO THE EC PROJECT

As a part of the EC project SDHp2m the existing database was amended (see chapter 5.1) and used for an investigation (see chapter 5.2).

5.1 Publicly available display of biomass plants with solar thermal support

Since the setup of the database in 2016, there has always been the possibility to feed the database with information about solar thermal support. As a part of the project SDHp2m a visualisation of plants with solar thermal support was added. So for the publicly available part of the database there is now a sun symbol for every biomass plant with solar thermal support (see Figure 3).

5.2 Investigation of the plant operators' interest in solar thermal support

The database was used for setting up a questionnaire which was sent to more than 213 plant operators in September 2017 (see Figure 4). Among other questions plant operators were asked whether they were interested in learning more about solar thermal integration for the biomass plants. There was quite a high response rate with 21 % (45 plant operators). 7 % (15 plant operators) holding 12 % of the heating plants (25 heating plants) showed interest in further consultation concerning solar thermal integration.

Those operators will be offered a two-day advisory service in spring 2018 including the following steps: a status analysis based on an on-site-analysis, a data collection focusing on summer loads and grid losses, a rough dimensioning of a solar thermal plant based on the heat demand and the available area, yield assessment and cost calculation, profitability calculation based on available subsidies and financing, final discussion with the plant/grid operator, written project report.

The advisory service is free for the plant operators and is paid by a grant amount of the SDHp2m-project and subsidies from the Styrian Government.

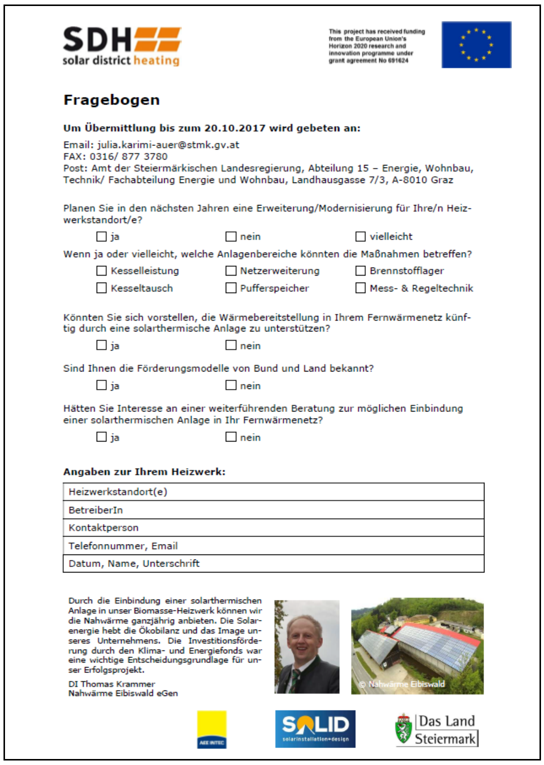

SDH solar district heating

This project has received funding from the European Union's Horizon 2020 research and innovation programme under grant agreement No 691624

Fragebogen

Um Übermittlung bis zum 20.10.2017 wird gebeten an:

Email: julia.karimi-auer@stmk.gv.at
FAX: 0316/ 877 3780
Post: Amt der Steiermärkischen Landesregierung, Abteilung 15 – Energie, Wohnbau, Technik/ Fachabteilung Energie und Wohnbau, Landhausgasse 7/3, A-8010 Graz

Planen Sie in den nächsten Jahren eine Erweiterung/Modernisierung für Ihre/n Heizwerkstandort/e?

☐ ja ☐ nein ☐ vielleicht

Wenn ja oder vielleicht, welche Anlagenbereiche könnten die Maßnahmen betreffen?

☐ Kesselleistung ☐ Netzerweiterung ☐ Brennstofflager
☐ Kesseltausch ☐ Pufferspeicher ☐ Mess- & Regeltechnik

Könnten Sie sich vorstellen, die Wärmebereitstellung in Ihrem Fernwärmenetz künftig durch eine solarthermische Anlage zu unterstützen?

☐ ja ☐ nein

Sind Ihnen die Förderungsmodelle von Bund und Land bekannt?

☐ ja ☐ nein

Hätten Sie Interesse an einer weiterführenden Beratung zur möglichen Einbindung einer solarthermischen Anlage in Ihr Fernwärmenetz?

☐ ja ☐ nein

Angaben zur Ihrem Heizwerk:

Heizwerkstandort(e)
BetreiberIn
Kontaktperson
Telefonnummer, Email
Datum, Name, Unterschrift

Durch die Einbindung einer solarthermischen Anlage in unser Biomasse-Heizwerk können wir die Nahwärme ganzjährig anbieten. Die Solarenergie hebt die Ökobilanz und das Image unseres Unternehmens. Die Investitionsförderung durch den Klima- und Energiefonds war eine wichtige Entscheidungsgrundlage für unser Erfolgsprojekt.

DI Thomas Krammer
Nahwärme Eibiswald eGen

© Nahwärme Eibiswald

AEE INTEC SOLID solarinstallation+design Das Land Steiermark

Figure 4: Questionnaire sent to the Styrian biomass plant operators in September 2017

5. CONCLUSIONS

As discussed in this article, the setup of a Styrian database for heating plants based on renewable energies offers various benefits for in-house usage as well as external use. Taking into consideration that the circle of users is quite limited, the yearly access with almost 800 visitors shows that the information offered, is used in practice.

REFERENCES

Website:
Styrian database of biomass based heating plants (*Steirische Heizwerksdatenbank*)
http://www.technik.steiermark.at/cms/ziel/116577771/DE/

PROPOSAL FOR NEW ISO STANDARD FOR GUARANTEED COLLECTOR FIELD PERFORMANCE

Jan Erik Nielsen
PlanEnergi
jen@planenergi.dk

Introduction

There is a significant and growing market of large-scale collector fields for district heating and various industrial applications in Northern Europe, China, South America, Middle East and others places.

There is a wish from the (potential) end users to have a check that the performance of their system meets the expectations given by the contractor.

In the European SDH projects as well as in the IEA SHC, procedures for Guaranteed Collector Field Performance has been developed and described in Fact Sheets. These procedures are mainly based on Danish experience and practice in the field.

Now, based on these procedures – and based on the new ISO Collector Test Standard EN/ISO 9806 – and based on inputs from interested ISO member countries - a new ISO standard for Guaranteed Collector Field Performance is proposed.

The Standard Proposal

The proposed standard specifies a procedure to give and check a guaranteed performance of large collector fields. The collectors in the field can be glazed flat plate collectors or evacuated tube collectors or concentrating tracking collectors. The standard will apply for all sizes of collector fields.

The performance guaranteed which is checked, is the thermal power output of the collector field – the document specifies how to compare a measured output with the guaranteed/calculated one.

The guarantied performance is given based on collector parameters from collector testing according to EN/ISO 9806 – taking into account uncertainties due to measurement uncertainty, pipe losses and others.

Only the hours with the collector field in more or less “full operation” are taken into account, so e.g. clear sunshine and no shadows are required for valid comparison between guaranteed and measured power.

The result of the procedure is a simple comparison of the average power measured versus guaranteed, for all valid periods – see fig. 1.

References

- EN/ISO 9806:2017*, Solar energy - Solar thermal collectors - Test methods*
- **SDH Fact Sheet 3.3** Performance guarantees (PDF) *,PlanEnergi, 2015*
- IEA SHC Fact Sheet 45.A.3.1 Performance guarantee - Collector field power output (R1), *PlanEnergi, 2015*

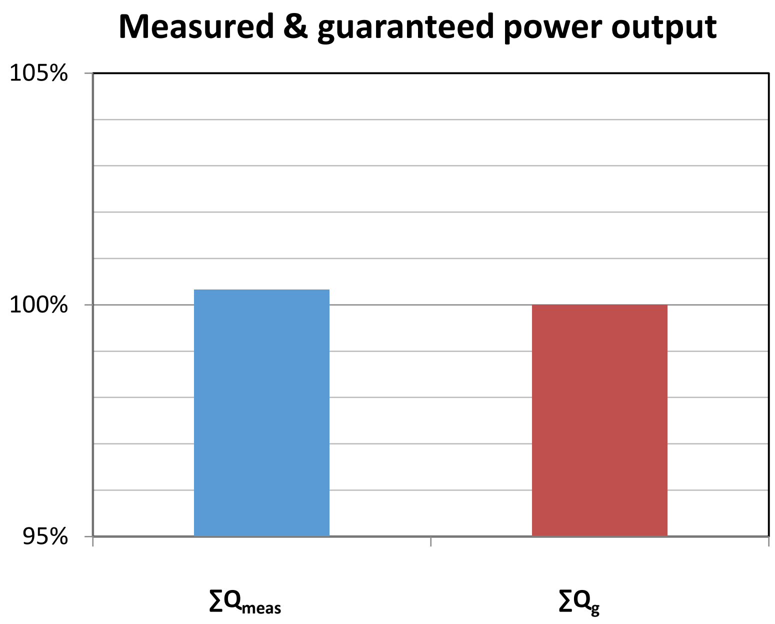

Figure 1. Example of a guarantee which is just fulfilled -
the average measured power (Q_{meas}) is a little more than the guaranteed power (Q_g)

Analyzation and Identification of Future Potentials of Solar District Heating Systems with Seasonal Thermal Energy Storage in Germany

Natalie Gohl*, Dominik Bestenlehner, Harald Drück

University of Stuttgart, Institute of Thermodynamics and Thermal Engineering (ITW)
Research and Testing Centre for Thermal Solar Systems (TZS)
Pfaffenwaldring 6, 70550 Stuttgart, Germany

Keywords: Solar district heating systems, seasonal thermal energy storage, integrated energy system

* Corresponding author. Tel.: +49 (0)711 685-63539; Fax: +49 (0)711 685-63503.
E-mail address: gohl@itw.uni-stuttgart.de

Introduction

Since the beginning of the 1990s, several large-scale solar thermal systems with collector areas of more than 1,000 m² combined with seasonal thermal energy storage were built in Germany. The solar fraction of these systems was planned to be in the range of 20 – 60 % of the total heat demand for space heating and domestic hot water preparation. The holistic review of nine solar district heating systems shown in Figure 1, which were realized as pilot systems in the research program Solarthermie2000 and Solarthermie2000plus is the basis for the work in the research project 'futureSuN – Analyzation, evaluation and development of future system concepts for solar district heating systems with seasonal thermal energy storage', which is funded by the German Federal Ministry for Economic Affairs and Energy (BMWi). The goals of this research project as well as first project results are introduced in the full paper of this contribution.

Figure 1: German solar district heating systems with seasonal thermal energy storage realized during the research projects Solarthermie2000 and Solarthermie2000plus. The systems reviewed in the project futureSuN are highlighted with a yellow frame.

The goals of the research project futureSuN are the extensive assessment of the solar district heating systems as well as the review and analysis of the experiences gained during their long-term operation. The holistic and comparative assessment of the reviewed systems creates the possibility to compare the systems in an objective way and to identify the strengths and weaknesses of the different concepts and technologies. A comparison to similar systems on international level will be carried out as well. Measures for optimization of the system efficiency will be identified from the review of the systems and communicated to the plant operators as a basis for system optimization.

A further aim of the project is the development of concepts for new sustainable solar district heating systems, which could lead to an extension of the range of functions of seasonal thermal energy storage. This includes for example the investigation if there are reasonable integrated energy usage concepts of solar thermal energy and excess electric energy for power-to-heat applications.

A general introduction of the research project as well as the current state of the project results will be presented in the full paper of this contribution. The focus will be on the presentation of the set of evaluation criteria for the energetic, ecologic and economic evaluation of the systems, which are defined in order to guarantee the comparability of the different systems as well as their holistic analyzation. Subsequently, the results of the analyzation of two of the solar district heating systems reviewed within the project on the basis of these criteria as well as possible optimization measures will be presented.

Acknowledgement
The activities described in this abstract are being supported by the German Federal Ministry for Economic Affairs and Energy (BMWi) based on a decision of the German Bundestag by Projektträger Jülich (PtJ) under grant numbers 0325897 A – C (Project futureSuN – Analyzation, evaluation and development of future system concepts for solar district heating systems with seasonal thermal energy storage). The authors gratefully acknowledge this support and carry the full responsibility for the content of this abstract.

EXPERIMENTAL SOLAR DISTRICT HEATING NETWORK OPERATION AT CEA-INES

Nicolas Lamaison[1, 2], Christian Tantolin[1, 2], Cédric Paulus[1, 2]

[1] CEA LITEN - 17 Rue des Martyrs, 38054 Grenoble (France)

[2] INES - 50 Avenue du Lac Léman, 73375 Le Bourget du Lac (France)

1. *Introduction*

In the frame of the 4GDH concept [1], the ability to integrate low temperature and renewable heat such as solar heat is a challenge that future District Heating System (DHN) will have to meet. In that context, the CEA-INES institute has decided to build an evolutionary solar DHN platform. Among the numerous purposes of that platform, the ones linked to the integration of solar energy into 4th generation DHN are i) the implementation and testing of various thermal solar panels technologies in a real DHN environment, ii) the comparison of centralized and decentralized reinjection of solar energy into a DHN and iii) the coupling with thermal storage.

Additionally, this DHN platform addresses other challenges of the 4GDH concept [1] since it is also designed i) to have low supply and return temperatures, ii) to be an integrated part of a smart energy system (connection with gas and electricity networks considered), and iii) to test innovative planning algorithm developed at CEA-INES [2]. The present work aims firstly at presenting in details this experimental solar DHN platform and secondly at showing preliminary results obtained during the first months of operation.

2. *Solar District Heating Platform presentation*

The solar DHN platform consists in a two-tube district heating network of about 200m long, supplying heat to one real building (tertiary) and to an emulated building (described later), as shown schematically in Figure 1. Supply temperature can be varied between 50 and 90°C. The main production unit of this DHN is a condensing gas boiler of 280kW. A solar field of 300m² (about 210kW) is also supplying heat to the network either in a centralized or in a decentralized fashion, as shown in Figure 1. Various solar panels technologies, i.e. single- and double-glazed serpentine copper flat plate, single- and double-glazed Multi-Port Extruded (MPE) aluminum flat plate and vacuum tubes are implemented (see Figure 2). The network is also equipped with a hot storage tank of 40m^3. The connection between the distribution network, the hot storage, the solar field and the condensing gas boiler is modular as highlighted in Figure 1. The latter allows testing different network architectures together with various control schemes.

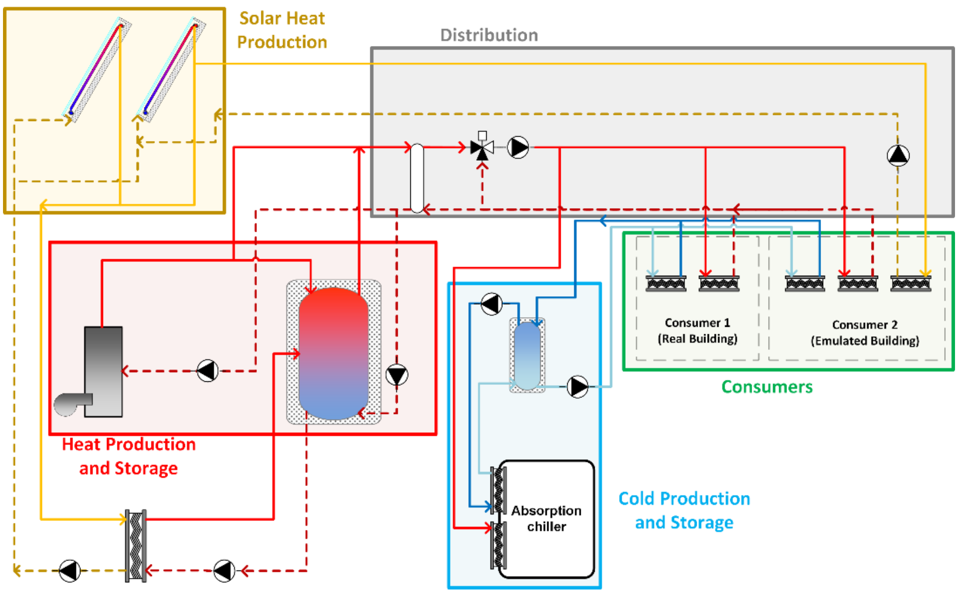

Figure 1: Schematic representation of the experimental solar district heating network at CEA-INES

As shown in Figure 1, a two-tube district cooling network alongside the heating network is also present with a 5m3 storage tank. It is planned to install in the coming months an absorption machine connecting the heating and cooling networks. The following additional extensions of the platform are also planned for the coming years:

*Corresponding author: e-mail : cedric.paulus@cea.fr / phone : +33 4 79 79 21 17

- A power-to-heat system (electrical boiler or heat pump) will connect the electrical network to the present DHN;
- A cogeneration unit will connect the gas network, the electrical network and the present heating network;
- A bidirectional substation will reinject solar heat in a decentralized manner at the emulated building location;
- Piping extensions will connect the present DHN to two extra building of CEA-INES.

Concerning the emulated building mentioned earlier, it consists in a TRNSYS building model simulation that calculates real time Domestic Hot Water (DHW) and space heating needs of the simulated building. These needs are then sent to a Labview program, which itself sends the required information to various thermo-hydraulic modules, composed of heat exchangers, valves, pumps and electrical resistances [3].

Figure 2: Thermal Solar Collector Field installed at CEA-INES micro-district heating network (left: flat plates aluminum MPE and copper serpentine, right: vacuum tubes)

3. *Preliminary Results*

Figure 3 presents the results of two consecutive days of operation of the present DHN in terms of powers, temperatures and mass flow rates variations. On the production side, only the solar panels were used while only on the consumption side, only the real building was supplied. It is seen that solar heat is stored during the days and used during the nights by the real building (clean rooms). The maximum power and the average energy production on the solar field reaches respectively 150kW and 2.7kWh/m²/day.

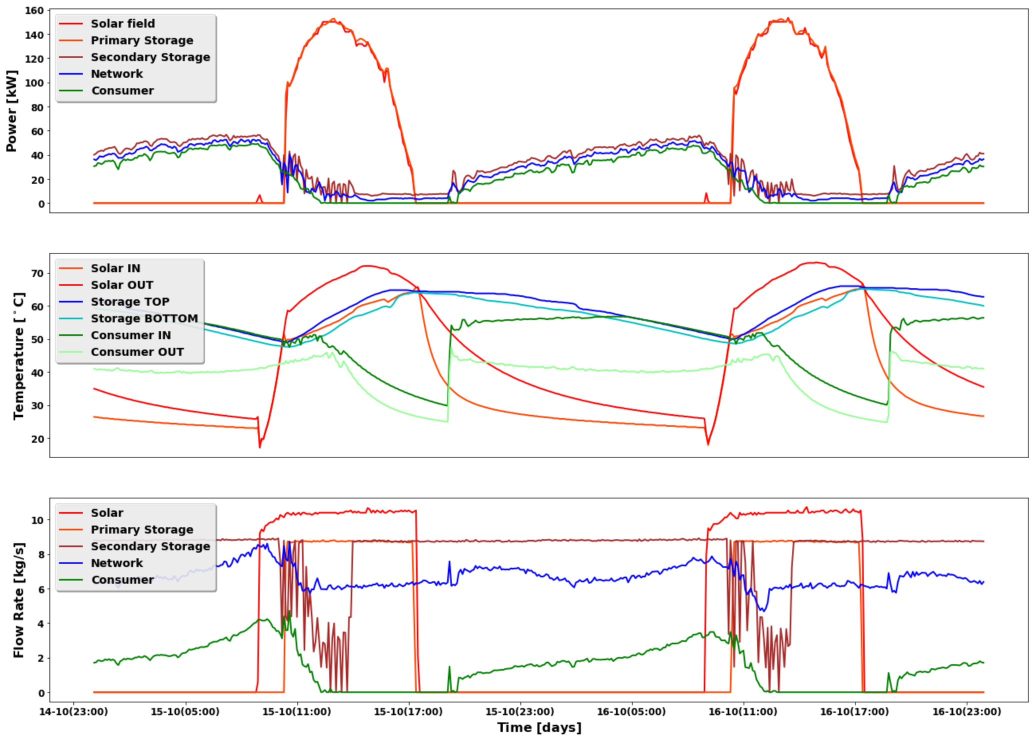

Figure 3: Operation for two consecutive sunny days of October 2017 (top: Powers variations, middle: Temperatures variations, bottom: Mass flow rates variations)

*Corresponding author: e-mail : cedric.paulus@cea.fr / phone : +33 4 79 79 21 17

[1] H. Lund *et al.*, “4th Generation District Heating (4GDH),” *Energy*, vol. 68, pp. 1–11, Apr. 2014.
[2] L. Giraud, R. Baviere, M. Vallée, and C. Paulus, “Presentation, Validation and Application of the DistrictHeating Modelica Library,” 2015, pp. 79–88.
[3] M. Albaric, J. Nowag, and P. Papillon, “Thermal performance evaluation of solar combisystems using a global approach,” presented at the Eurosun 2008, Lisbon, Portugal, 2008.

*Corresponding author: e-mail : cedric.paulus@cea.fr / phone : +33 4 79 79 21 17

THE ROLE OF SOLAR HEATING IN THE FUTURE HEAT SUPPLY PORTFOLIO: A TECHNO ECONOMIC ASSESSMENT FOR TWO DIFFERENT DISTRICT HEATING GRIDS

Richard Büchele, Marcus Hummel and Lukas Kranzl
Institute of Energy Systems & Electrical Drives, TU Wien, Gusshaussstr. 25-29/370-3, Vienna, 1040, Austria
+43-1-58801-370368, buechele@eeg.tuwien.ac.at

Ali Aydemir, Eftim Popovski and Tobias Fleiter
Fraunhofer ISI, Breslauer Straße 48, Karlsruhe, 76139, Germany

Abstract – In this paper the integration of solar thermal energy into two different district heating networks is assessed. In the first case the integration of larger scale solar thermal heat into an existing coal fired district heating network is assessed. In the second case the integration of small scale solar heat into a new settlement area with low energy buildings that will be entirely supplied by a new biomass based district heating system is assessed. For both analyses the levelized costs for different combinations of solar thermal collectors and thermal storages are calculated with the optimization tool energyPRO and the achievable solar fractions are compared. In general the analysis showed that levelized costs of solar thermal heat tend to be slightly higher than current supply portfolios but can compete with other renewable heating options and integrate a significant share of solar heat and thus reduce the use of valuable combustibles.

1. INTRODUCTION

The objective of this work is to identify possible design options of integrating solar energy in district heating systems and to assess their economic feasibility for the cities of Ansfelden in Austria and Herten in Germany. For these cases, a thorough analysis of the heating and cooling sector has been carried out (Büchele and Popovski, 2017a and 2017b) and heating and cooling strategies have been derived in close cooperation with the local authorities. The work has been carried out in the frame of the Horizon 2020 project progRESsHEAT (www.progresssheat.eu). The project included an intensive analysis of stakeholders, barriers and drivers, techno-economic modelling and the role of policies on the local, regional and national level. All these activities were embedded in an intensive stakeholder dialogue. The research question of the analysis presented in this paper is: What are the costs and opportunities for the integration of small and large scale solar heat in new and existing district heating systems in the two cities under investigation?

2. METHOD

2.1 Overall Method

To answer the research questions the following steps were carried out for each case study city: (1) Documentation and quantitative description of the current state of the district heating system in particular regarding heat supply, CO_2-emissions and costs of delivered heat. (2) Discussion of possible technological alternatives for the respective district heating system integrating solar heat. (3) Set up of a model of the current system and of the technological alternatives for the selected case studies in the modelling software energyPRO. (4) Performance of various calculations with the developed model for several settings of the supply portfolio, for solar thermal in particular regarding collector and storage size. (5) Analysis of the results in terms of resulting energy demand, share of renewable energy, CO_2-emissions and levelized costs of heat. (6) Derivation of conclusions regarding the overall feasibility of integrating solar energy in district heating based on a comparative discussion of the results.

Although this key approach was similar for both case studies, the specific questions and challenges were different due to the very different initial setting, which will be explained in the following:

2.2 The case study of Herten

For the case study of Herten the assessment focused on integrating large scale solar thermal fields with flat plate collectors from 1 000 to 50 000 m² in steps of 1 000 m² and two possible heat (pit) storages with 2 000 m³ and 10 000 m³ into the existing northern district heating subnetwork of the city, which is currently mainly supplied by coal. For this case no investments into network infrastructure or additional supply units would be needed, but the availability and costs of land and land-shaping for the solar thermal fields are important to be taken into account.

In the first step we calculated an hourly profile for the district heating network based on given annual data. The hourly demand profile was used to assess a realistic solar fraction as well as levelized costs of heat (LCOH) of solar thermal generation, which is only available at certain times of the year and particularly during summer. The hourly demand profile has been generated by fractioning the annual demand of the district heating network into hourly demand values. To do so 80% of the district heating demand has been modelled to be linear dependent on ambient temperatures accounting for space heating. A threshold value of 15°C ambient temperature was used. Above this threshold no space heat is demanded. The residual 20%-share of the district heating demand is modelled independent from ambient temperatures, assuming that it mainly results from residential hot water demand.

In order to find the solar thermal system with the lowest cost of heat the size of the solar field and the thermal storage were varied for all combinations as described above. Technical and economic assumptions such as efficiencies for the solar fields as well as capital costs for solar thermal plants including storage were taken from solar district heating guidelines (Sørensen, 2012) and are stated in Table 1. The lifetime has been assumed to be 30 years for the solar plants including storages.

With regard to land area necessary for the solar thermal fields nearby locations to the sub-systems connections have been assessed applying Geographic Information Systems. It has been assessed if the area for the fields chosen is available and if it is marked as agricultural area. This was based on the reason that agricultural land has served as area for solar thermal fields in several other projects. Thus, to allow the use of agricultural land for solar thermal fields is not uncommon. Furthermore, the price of agricultural land is by far lower than for areas dedicated for trade and industry. Costs of land are derived from a Geographical Information System from the state North Rhine- Westphalia (BORISplus, 2015), the values used are given in Table 1.

Table 1: Assumptions for the Herten case study

Parameter	Description
Solar thermal supply system	Solar thermal collectors: • Collector area 1 000 m² to 50 000 m² • Collector temperatures: 80°C/40°C • Start efficiency: 0,827 • Pipe losses: 4% • Investment costs including equipment: Cost function ranging from 200 €/m² to 400 €/m² • Fixed operation costs: 0.5 €/MWh
Thermal pit storage	• Storage Temperature top/bottom: 80°C/ 40°C • Storage volumes: 0 m³/ 2 000 m³/ 10 000 m³ • Storage capacities: 0 MWh/ 88 MWh / 440 MWh • Investment costs storage: 0 €/ 416 000 €/ 1 070 000 €
Cost of land	5.8 €/m²
Cost land shaping	6 €/m²
Economic Parameter	• Interest rate: 7% • Lifetime solar plants: 30 years • Lifetime heat storage: 30 years

2.3 The case study of Ansfelden

For the case study of Ansfelden possible supply options for a new settlement area without existing infrastructure were analysed. A 100% renewable district heating network supplying the entire settlement area by a biomass boiler with different combinations of solar thermal collectors and also solar PV in combination with a heat pump were considered. For this case study the levelized costs of heat (LCOH) included all costs arising from the installation and operation of all the components of the future district heating system.

The new settlement area under investigation includes an area of around 120 000 m² and according to current planning it will be covered by different types of mainly residential buildings and will have a plot ratio[1] of 0.45 to 0.55 per building lot. The expected buildings could consist of around 100 single-family houses, 200 row houses and 10 small multi-family houses. All of them are foreseen to be built as nearly zero energy buildings and therefore will have a very low heating demand. For each of the three building groups, the hourly demand and resulting heat load for space heating and domestic hot water is calculated.

All of the buildings in the new settlement area are assumed to be connected to a small low-temperature district heating network. The length of the network to connect all buildings is estimated to 1 500 m based on a rough calculation with a Geographic Information System. The expected supply and return temperatures are 65°C and 40°C, respectively. These low supply and return temperatures can be achieved because of the highly efficient buildings (low heating demand) and low-temperature radiators. Due to the low temperatures and pre-insulted pipes of the latest generation, the network losses are assumed to account for 10% of the annual transported heat.

According to the heat load of the buildings and the network losses a future demand profile for the district heating network was calculated smoothening the load over 4 hours. Still the high number of similar buildings with similar user profile lead to relatively high peaks of up to 2.9 MW and an annual total demand of 2.2 GWh.

Because no infrastructure exists yet, the network can be built from the scratch. Thus, synergies with other infrastructures like power lines and water channel can be used leading to lower installation costs of around 300 EUR/m of network.

The analysed district heating supply systems consists of a biomass-based boiler in combination with different sizes of solar thermal collectors and thermal storages as well as a heat pump and different sizes of photovoltaic collector fields.

The wood chip biomass boiler is the main supply device and with 2 MW of thermal output it is dimensioned to

1 Plot ratio is defined as the building floor area to the land area in a given territory

supply the demand in 98.3% of the hours (97.8% of energy). This means that in less than 7 days per year additional heating capacity is needed. An oil-fired boiler with 3 MW of thermal output works as back-up and peak load unit.

The area of solar thermal collectors is varied from 0 m² to 2 000 m² in steps of 200 m². They are combined with heat storages of 0 m³, 10 m³, 100 m³ and 500 m³. The solar thermal collectors are planned to be installed on the district heating station and the surrounding buildings in order to avoid spreading the solar collectors over all buildings of the settlement area.

The photovoltaic panels are varied from 0 kW_{peak} to 1 000 kW_{peak} in steps of 200 kW_{peak} and are used to drive a heat pump installed together with the PV panels. The heat pump is designed to support the system only in times when the PV system is generating electricity. Generated electricity, which cannot be used in the heat pump, is lost. The heat pump is designed to 500 kW of thermal output at an electrical input of 150 kW resulting in a COP of 3.3.

Therefore, 11 different sizes of solar thermal collectors and 4 different sizes of thermal storages together with 6 different sizes of photovoltaic panels make in total 264 combinations calculated for the case of Ansfelden. Table 2 summarizes all assumptions made for the calculation.

Table 2: Assumptions for the Ansfelden case study

Parameter	Description
Buildings	100 Single family houses, 200 Row houses and 10 Multi-family houses • Total built are: 56 300 m² • Specific space heating (SH)demand: 19 -24 kWh/m²y • Specific hot water (DHW)demand: 17 kWh/m²y • Total demand SH&DHW: 2 237 MWh • Maximum smoothened load: 2.9 MW
Network	• Length of DH network: 1 500 m • Losses: 10% of annual production • Capacity heat exchangers: 3.3 MW • Specific invest costs network: 300 €/m • Specific invest cost heat exchangers: 300€/kW
Supply Systems	Wood chip boiler • Thermal output power: 2 MW • Average annual efficiency: 85.3% • Specific investment cost: 250 €/kW • Fixed operation costs: 5 €/MWh • Cost wood chips: 66.8 €/t (25.6 €/MWh) Solar thermal collectors: • Collector area from 200 m² - 2000 m² • Collector temperatures: 70°C/40°C • Start efficiency: 0,80 • Pipe losses: 4% • Investment cost including equipment: Cost function ranging from 874 €/m² to 606 €/m² • Fixed operation costs: 0.5 €/MWh Ground source compression heat pump: • Rated electrical input power: 150 kW • Maximal thermal output power: 500 kW • Rated coefficient of performance: 3.3 • Investment costs: 1 000 €/kWth Photovoltaic cells • Installed areas 200 kWp – 1000 kWp • Aggregated losses module to grid: 5% • Investment costs including equipment: Cost function ranging from 1056 €/kW to 1041 €/kW Peak load and back up oil boiler • Thermal output power: 3 MW • Average annual efficiency: 85.3% • Investment cost: 100 €/kW • Fixed Operation Expenditures: 5 €/MWh • Cost of oil:0.7 €/l (71.4 €/MWh)
Thermal Storage	• Storage Temperature top/bottom: 65°C/ 40°C • Storage volumes: 0 m³/ 10 m³/ 100 m³/ 500 m³ • Storage capacities: 0 / 0.28 MWh / 2.75 MWh / 13.76 MWh • Investment costs storage: 0 € / 11 664 € / 39 000 € / 94 500 €
Economic Parameters	• Interest rate: 3% • Lifetime supply units & storage: 20 years • Lifetime network: 30 years

3. RESULTS

3.1 Results for Herten

The results for the district heating system in Herten show that the LCOH of the solar thermal collectors in combination with the pit storage can almost compete with the current heat supply from coal, but would slightly increase the cost of heat. In this case of course the solar heat would replace coal and therefore contribute to a significant CO_2 reduction. Furthermore in the case of Herten the integration of solar heat was the cheapest of the possible options to integrate renewable energy.

A visualisation of the evaluated cases is given in Figure 1 showing levelized cost of heat (LCOH), solar field size and storage size and the solar fraction representing the share of heat demand covered by the solar field during a year in the analysed district heating sub-system. It shows that the lowest LCOH for different field sizes can be achieved with corresponding storage sizes. Accordingly, systems without thermal storage have the lowest LCOH for small systems below 4 000 m² field area. However, with less than 5% the solar fraction is also very low for this system design. Between 5 000 and 22 000 m² of collector area systems with a relatively small storage of about 2 000 m³ have lowest LCOH achieving almost 20% solar fraction. Above 25 000 m² systems with 10 000 m³ storage become more cost-effective and can achieve a more than 5 percent higher solar fraction. The lowest LCOH of all calculated system configurations ranges between 40 and 50 EUR/MWh.

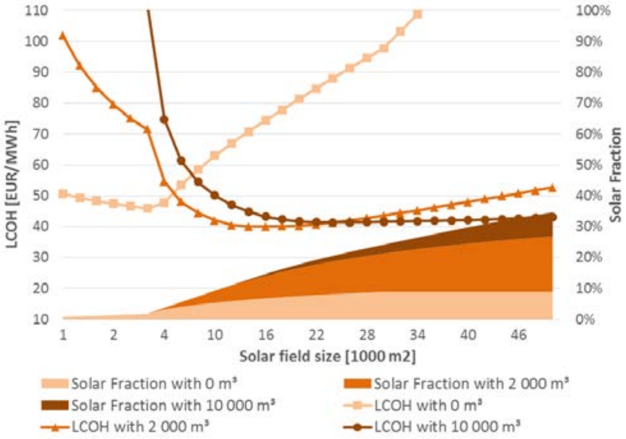

Figure 1: LCOH [EUR/MWh] of the large scale solar thermal system for the case of Herten

3.2 Results for the case of Ansfelden

Figure 2 shows the LCOH of the overall district heating network for the new settlement area in Ansfelden when integrating solar thermal collectors into a biomass based system. The results show that the cheapest heat supply for the new district heating grid would be achieved with the biomass boiler without additional solar thermal collectors but with a heat storage of 100 m³. This means that the resulting levelized costs of heat (LCOH) from the solar thermal system are higher than the heat generation costs of the assumed biomass boiler. However additional solar thermal collectors would only slightly increase the LCOH for the calculated system but could reduce the demand for biomass and therefore also reduce the risk for future price volatility of biomass. Futhermore costs and negative effects of transportation, which were not taken into account in the calculations could be reduced.

In our case for example the integration of 800 m² of solar collectors together with 100 m³ heat storage would increase the LCOH by around 10 EUR/MWh (+9.5%) and could reach a solar fraction of 15%.

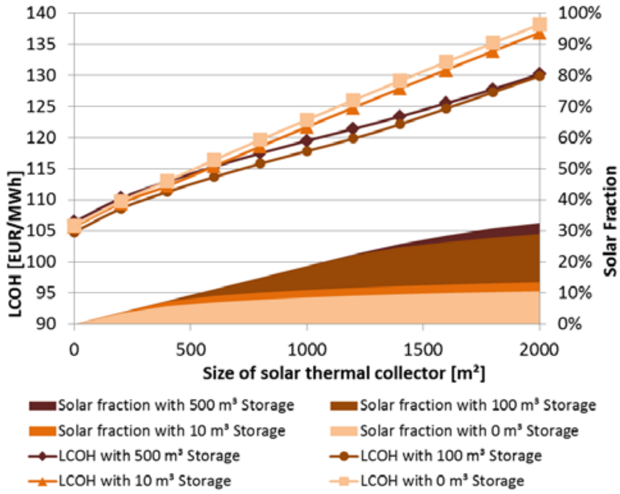

Figure 2: LCOH [EUR/MWh] of the overall district heating system for the new settlement area in Ansfelden when integrating solar thermal collectors into a biomass based system

Although the results seem to be different from the case of Herten, they show a very similar behaviour when only considering the costs for the solar thermal equipment and not for the overall district heating system: Figure 3 shows the results for the solar thermal system only, including solar thermal collector and heat storage but no investments into network nor other supply units. In this case the lowest LCOH for different collector field sizes can be achieved with different storage sizes. Up to around 200 m² of solar thermal collector the system without storage achieves the lowest LCOH resulting in solar fractions below 5%. For systems between 200 m² and 500 m² the combination with 10 m² of storage achieves the lowest LCOH resulting in solar fractions up to 10%. For systems between 500 m² and 1500 m² the combination with 100 m² of storage achieves the lowest LCOH resulting in solar fractions up to 25% and collector areas over 1500 m² achieve the lowest LCOH in combination with 500 m² of storage and can reach solar fractions above 30%. For small scale solar thermal systems the lowest LCOH of all system configurations are in the range of 80 EUR/MWh

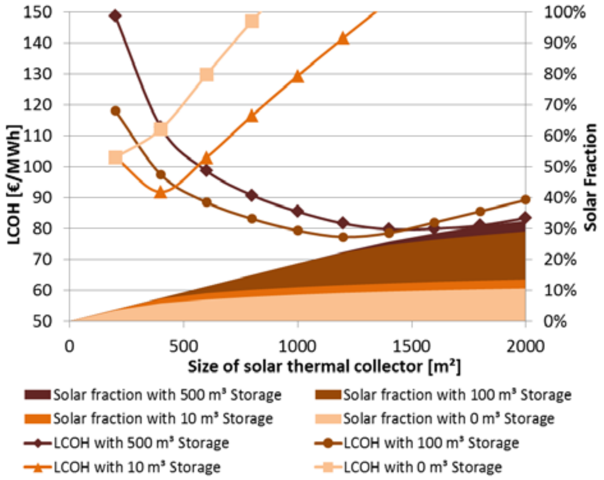

Figure 3: LCOH [EUR/MWh] of the solar thermal system only for the new settlement area in Ansfelden

Alternatively for the case of Ansfelden the integration of solar PV together with a heat pump was investigated. In this calculation the heat pump can only be driven by the local PV field and no connection to the grid is assumed. Hence the solar fraction in this case is defined as the share of total heat produced by the heat pump including the electricity from the solar PV and the ambient heat. Figure 4 shows the LCOH of the overall district heating network for the new settlement area in Ansfelden when integrating solar PV together with a heat pump into a biomass based system.

The results show that also in this case the cheapest heat supply for the new district heating grid would be achieved with the biomass boiler without additional solar PV but with heat storage of 100 m³. Compared to the integration of solar thermal collectors higher fractions of solar heat (including electricity from solar PV and ambient heat) can be reached at the same costs with the combination of solar PV and heat pumps. For example the integration of 400 kW_{peak} of solar PV together with a 150 kW_{el} heat pump and 100 m³ heat storage would also increase the LCOH by around 10 EUR/MWh (+9.5%) but could achieve a solar fraction of 42%.

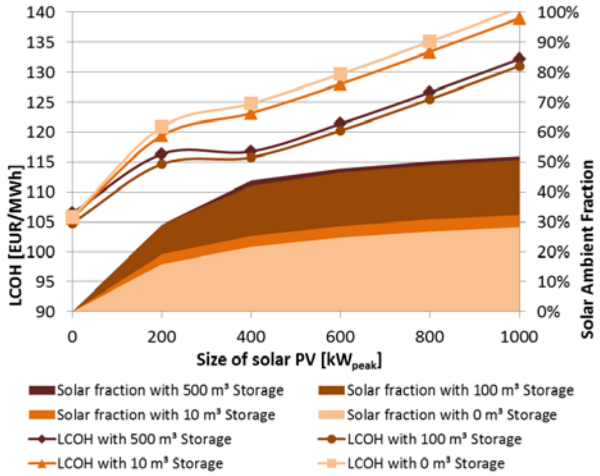

Figure 4: LCOH [EUR/MWh] of the overall district heating system for the new settlement area in Ansfelden when integrating solar PV and heat pump into a biomass based system

4. DISCUSSION AND CONCLUSIONS

For the case of Herten a big scale solar thermal system turned out to be an economically feasible solution for the integration of renewable heat into the existing coal based district heating grid. According to the calculation the integration of solar thermal heat would increase the current overall levelized cost of heat (LCOH) but reduce the CO_2 emissions significantly due to replacing coal by integrating a solar fraction up to 30%. However, the results also depend on several assumptions and input data, in particular the technical parameters and assumed investment costs. One of the biggest challenges for big scale solar systems near cities is the availability and price of land and land shaping. Moreover, for the decision also uncertainties regarding the future energy price development need to be considered

The case of Ansfelden shows similar findings in terms of effectiveness of integration of solar heat: Although the portfolio containing solar thermal collectors is not among the options with the lowest costs, a significant share of solar heat can be integrated at only moderately higher costs replacing combustibles that might be needed in other sectors like industry for higher temperature heat demands, and would also decrease the risk of price volatility of these energy carriers in the future. An integration of PV, heat pumps and a heat storage leads to higher shares of solar energy at similar costs than including solar thermal collectors. This result of course highly depends on the coefficient of performance of the heat pump and can be reached only with low flow temperatures and a well-designed heat pump. However, if this is the case, higher shares of solar energy can be integrated even if the heat pump only runs with local PV collectors not connected to the grid and economics would even improve, if excess electricity could be feed into the grid or purchased when electricity prices are low.

REFERENCES

BORISplus (2015), Aktuelle Informationen zum Immobilienmarkt in NRW: http://www.boris.nrw.de/ (last checked: 07.10.2015)

Büchele R. and Popovski E. (2017a) Assessment of local feasible renewable energy-based heating/cooling utilisation for Ansfelden and Herten. *Part of the reports D2.2 of the progRESsHEAT project*, Online available: http://www.progressheat.eu/Reports-publications-69.html.

Büchele R. and Popovski E. (2017b) Results of the quantitative assessment of selected policy packages for development area "Teilraum 31" (Ansfelden) and for Herten. *Part of the reports D4.1 of the progRESsHEAT project.* Online available: http://www.progressheat.eu/Reports-publications-69.html.

Sørensen P. A. (2012): Solar district heating guidelines. Introduction to SDH – from idea to operating system. Internet: www.solar-district-heating.eu (last checked: 17.08.2015).

INTEGRATION OF SOLAR THERMAL INSTALLATIONS INTO EXISTING DISTRICT HEATING SYSTEMS – AN OVERVIEW OF FEASIBILITY ANALYSIS TOOLS AND NECESSARY IMPROVEMENTS

Carles Ribas Tugores and Ingo Leusbrock
Thermal energy technologies and hybrid systems, AEE – Institute for Sustainable Technologies,
Feldgasse 19, Gleisdorf, 8200, Austria,
Tel.: +43 (0) 3112-5886-240, E-Mail: c.ribastugores@aee.at

Abstract – District heating in dense urban environments possesses significant CO2-reduction potential. It provides multiple possibilities for the hydraulic integration of renewable energies, storage technologies and waste heat utilization. Thus fossil fuels are being substituted and the flexibility of the energy system increases. Among the different possible energy concepts, the combination of large solar thermal plants with long term thermal storages and partly compression and thermal heat pumps is gaining interest in several countries such as Denmark (e.g. Silkeborg, Marstal) [11] and Austria (e.g. BigSolarGraz) [10]. A key step towards an optimum and feasible design for this type of systems is the robust and transparent assessment of the technical and economic aspects of the considered energy concepts during the feasibility analysis and the early stages of such a project. In this regard, the suitability of the four free available feasibility tools for the task are analysed and discussed with help of two scenarios. The review points out the suitability and limits of each feasibility tool. Furthermore, the approach followed in the Urban-DH-extended project to carry out feasibility analysis is presented. The approach mainly consists in the definition of different independent blocks (energy units; e.g. solar installation, thermal energy storage) which can be combined with each other to define any desired energy system in a simplified way.

1. INTRODUCTION

Within the Austrian research project Urban-DH-extended, which aim is to increate flexibility of existing district heating networks and share of renewables, three different district heating systems (Klagenfurt, Mürzzuschlag and Wien) are being analyzed. Different extensions for the current energy systems have been proposed. E.g. solar installation combined with long-term energy storage with/without heat pumps, increase operation hours of combined heat and power plant through addition of large thermal energy storage tank. The work carried out to assess until which extend the already available feasibility tools are suitable for the task is here presented. In this regard, the present work four available feasibility tools; Sunstore 4, SDH Online-Rechner, ScenoCalc Fernwärme (SCFW) and f-easy, are presented and reviewed with the help of two different scenarios for a small size district heating system. Furthermore, the modular approach for feasibility studies followed in the Urban-DH-extended project is briefly introduced and discussed.

2. FEASIBILITY TOOLS

2.1 Sunstore 4

As part of the European Project Sunstore 4, where several industrial companies such as Marstal Fjernvarme and SUNMARK as well as consulting companies such as PlanEnergie and Solites has been involved, an Excel-based feasibility tool has been made available on the project web page [5]. This tool allows carrying out feasibility studies for five different energy concepts, namely:

- Solar collector, seasonal water pit storage, heat pump and biomass CHP (ORC)
- Solar collector, seasonal water pit storage, heat pump and biomass boiler
- Solar collector, seasonal water pit storage and biomass boiler
- Solar collector, seasonal ground (borehole) storage, heat pump and biomass boiler
- Solar collector, short-term water tank storage and biomass boiler

The Sunstore 4 tool is based on the district heating grid in Marstal (Denmark) and includes data (default values) from that project. The tool can be used with other boundary conditions by selecting a different country/region, if location is changed, new price data and yearly solar radiation are used. The user can edit most of the suggested values. The feasibility tool is limited to these five energy concepts. In this regard, neither decentralized solar thermal plants nor different control strategies can be considered. Furthermore, district heating temperatures and thus temperatures at the solar installation are not part of the parameters. The obtained results are extensive; Results include a report per each energy concept, including investment costs, yearly costs and specific cost per MWh or m^2, as well as a short report comparing the different energy concepts.

2.2 SDH Online-Rechner

This feasibility tool is based on a simulation study done in TRNSYS [6]. Two main cases (decentralized solar thermal installation and centralized solar thermal installation with thermal energy storage) are considered [13]. For each case, parameter variations have been carried out. Location (weather data and reference load profile), collector type, collector orientation, tilt angle and area, district heating temperatures (supply and return), storage size (if applicable) are the main parameters. Missing simulation results due to lack of data, yields interpolation between available simulation results. The feasibility study is completed by considering some economic and ecological parameters, such as specific investment costs, funding rate, interest rate, electricity cost, reference energy source (e.g. gas) and its efficiency. The decentralized system does not consider any load in the district heating network and thus any restriction regarding the feed-in capacity. On the other hand, the centralized system does consider a reference load profile, which changes depending on the chosen location. Unfortunately, the list of available locations (weather and load data) cannot be extended.

2.3 ScenoCalc Fernwärme (SCFW)

SCFW is a calculation tool for the integration of solar installations in district heating systems [12]. It does use hourly weather data to calculate the solar gain. SCFW allows the user to define collector efficiency, consider heat losses in pipes of the solar installation and add efficiency losses due to the use of antifreeze fluid. Furthermore, one can choose between two control strategies, pre-heat or heat-to-supply. In the latter case, solar temperature needs to reach supply district heating system temperature. Solar heat is supplied directly to the district heating network when there is enough radiation and demand, otherwise heat is stored into the heat storage tank. It is possible to consider heat exchangers between the storage tank and solar installation as well as between the storage tank and district heating, and thus temperature difference between these subsystems. The district heating system is defined by a load profile with hourly values for load, supply and return temperatures. The SCFW tool does calculate in greater detail the solar gain and allows for some flexibility in the control strategy of the solar installation. Storage tank is but relatively simplified. The calculation tool lacks of an economic evaluation and therefore cannot be fully considered a feasibility tool.

2.4 f-easy

It is a tool for a first approach of sizing and economical balance of solar installation in district heating systems develop by PlanEnergi. The main inputs are; load on network, solar irradiation on horizontal, land area available, price per m^2 land, distance to network connection, average operating temperature and acceptable heat production price. Based on these main inputs a sizing for the solar installation with thermal energy storage is suggested. Notice the tool permits the user to overwrite some of the intermediate results such as collector area and storage volume. Further information can be found in [3].

2.5 Modelling tools

2.5.1 EnergyPro

EnergyPro is a commercial modeling software with more extensive capabilities than the previously mentioned feasibility tools [7]. It has flexibility on terms of system definition; the user can add different energy storages and sources, define efficiency curves and merit order for them. In this regard the software includes the possibility to optimize the merit of order of the considered energy sources including energy storages. The Modeled energy system, thermal and/or electrical, is then technically and economically evaluated based on the technical results and the introduced economic data. Furthermore, EnergyPro delivers an emission report to evaluate the environmental impact.

2.5.1 Dymola, OpenModelica

Dymola [2] and OpenModelica [9] are respectively a commercial and non-commercial software based on the Modelica non-proprietary object-oriented modeling language [4]. The field of application of Modelica is not energy specific. In this regard there are free and commercial libraries for a great variety of fields, namely combustion, noise, fuel cells, building performance simulations among others [8]. Thanks to the use of standardized interfaces within Modelica, the compatibility rate between different libraries is high. It allows the user to select the preferred model and if necessary write its own model and combine it with the already existing ones. So far there are no specific models for feasibility studies.

2.6 Urban-DH-extended Modelica based feasibility tool

Within the project Urban-DH-extended Modelica models for feasibility analysis purposes are being develop. They intend to cover the most important gaps identified during the review process of the existing feasibility tools, these are

- Limitation consideration of synergies. E.g. thermal energy storage could be used for several production units such as a solar installation and combined heat and power unit.
- Limited variety of energy concepts. One potentially interesting missing energy concept is the coupling of absorption heat pumps with solar installation and thermal energy storage.
- Flexibility in terms of control strategies. Heat is supplied and control options are limited to pre-heat or heat-to-supply temperature. Further interesting options are the use of stored heat to cover pick demands. Thus, having different control strategies for the solar installation and thermal storage which might be different over the year.
- Unknown effect on existing energy production units. The solar heat will substitute totally and/or partially some of the exiting production units. It yields change of the overall cost structure and therefore the system should be evaluated as a whole.

The followed approach to cover these gaps consist mainly in defining each production unit as an independent unit with a common main input and output signal. Namely the requested heat to be supplied (input) and the heat to be coped with the next unit (output). The basic model is extended accordingly to the production unit physics and needs. Some of the included models are below described.

Thermal heat storage is modelled with a cylindrical thermal energy storage as a core (slightly modification of the *FluidStorage* model from the BuildingSystems library [1]. Two different boundary conditions can be defined, one for the top and a second one for the bottom and side of the storage tank). During charge phase fluid is extracted from the bottom, heated up and stored into the top layer of the storage tank. In the discharge phase, mass flow direction is reverted and fluid is cooled down and stored into the bottom layer of the storage tank. Set point temperatures for the discharge and charge phase can be defined as a parameter (constant) or as input values (E.g. based on data from the district heating temperatures and/or solar installation unit). Furthermore, the models include an intern control to decide whether energy can be extracted or charged. Some of the parameters that can be edited are the heat loss coefficients for the bottom, side and top side of the storage tank, geometry parameters (height and diameter).

The solar installation model uses the *ThermalCollector* model from the BuildingSystems as a core [1]. Collector efficiency parameters, tilt angle, azimuth angle, and size are the main parameters to be defined. Just like the thermal storage tank, supply and return temperature can be here defined either as a parameter (constant) or as an input, e.g. data temperatures from thermal storage and/or district heating system. Furthermore, the model receives information through input connectors such as outdoor air temperature, direct and diffuse irradiation.

Some of the others simplified models being develop are boilers, combined heat and power plants and heat pumps (mechanical and absorption).

Besides the technical definition of the production units, all models include information to carry out an economic evaluation of the system such as heat production costs, electricity costs/revenue, expected life time, investment and maintenance costs, price change factor and interest rate.

Each system under study can be then analysed globally by adding and connecting the necessary production units and define more elaborated control strategies if needed. This approach allows for flexibility in terms of modeling detail as well as field of application (e.g. hybrid networks). A key issue here is to be overcome the main drawback, which is the time needed for modeling the different subsystems and subsequent combination of them to model the whole system.

3. CASE STUDY

3.1 District heating system

The case study deals with the integration of a solar installation into a small city district heating system located in Austria with a total yearly consumption of 35 GWh/a. It is assumed that supply temperature varies over the year between 70 and 90 °C and return temperature between 50 and 60 °C. A yearly average for the district heating network temperature yields around 70 °C.

For a quantitative comparison of the feasibility tools, two different cases are considered, namely the integration in the existing system of a,

- 5000 m^2 solar installation with a 600 m^3 water tank thermal energy storage tank (TTES)
- 34000 m^2 solar installation with a 68000 m^3 (water equivalent) pit thermal energy storage tank (PTES)

For both cases solar installation is south oriented with a tilt angle of 35 degrees. The distance to the district heating network is assumed to be 100 m.

3.2 Parametrization feasibility tools

In order to carry out a clear comparison it is beneficial to use the same parameter set. This is but not completely possible, mainly because the level of detail in which energy concepts are modelled are different per each tool and with it the necessary input data. The differences regarding the input data and limitations between feasibility tools are further discussed below.

Sunstore 4 does not consider any transmission losses (heat losses between solar installation and district heating network), merely storage heat losses. On the other hand, f-easy consider transmission losses but no losses of the heat storage. SDH Online and SCFW does consider both. Furthermore, SCFW allows to define heat exchangers between the district heating system and the storage as well as between the storage and solar installation and with them a temperature difference.

SDH Online and ScenoCalc (SCFW) use detailed weather data with hourly values. SCFW allows the user to import new weather data while SDH Online force the user to choose between six specific locations. On the other hand, the feasibility tools f-easy and Sunstore 4 simplify the weather conditions by using a yearly solar irradiation value. In this regard, SCFW, f-easy and Sunstore 4 are based on a Test Reference Year (TRY) for the case study location. Some key values are the yearly average outdoor air temperature (8,2 °C) and the yearly global solar radiation on horizontal (1100 kWh/a.m^2). For SDH Online there is no weather data available for the case study location. From the available data, Hamburg and Würzburg are the most suitable weather data because of similar average outdoor air temperature (8,8 °C / 9,4 °C) and yearly solar irradiation (952 kWh/m2/a / 1090 kWh/m2/a).

All feasibility tools have the possibility to specify the size of the solar installation and storage tank. SDH Online, SCFW and f-easy allow the user to directly specify it. In Sunstore 4 but, size is indirectly determined by defining an "expected net solar coverage" and the ratio "storage volume / collector area".

The efficiency of the solar installation and thus the net solar gain is calculated in different ways among the feasibility tools. Solar gain in f-easy is mainly affected by the chosen average operating temperature. In Sunstore 4 an annual efficiency value for the solar collector and thermal storage has to explicitly defined. SDH Online and SCFW have a more detailed approach. Efficiency is determined by choosing a solar collector. Likewise with the weather data, SDH Online restrict the user to choose between four specific solar collector technologies (specific efficiency values are unknown) while, SCFW allows the user to either select one of the available predefined collectors or deploy a new collector. Besides solar installation temperatures are indirectly set by defining the district heating temperatures. Other parameters to be defined are solar azimuth and tilt angle of the solar collectors.

4. TOOL COMPARISON – RESULTS

Since the Modelica models for feasibility study are still being develop and thus further adjustment and review of the models and parameter set is necessary, results are write down but left out of the comparison.
The results are obtained by using, when possible, the same input data.

4.1 Case 1: 5000 m² solar installation with a 600 m³ water tank thermal energy storage tank (TTES)

Main results of the feasibility analysis for the case 1 are summarized in Table 1.

Table 1: Main results for case 1

Feasibility tool	Net solar gain in MWh	Investment in million €
F-easy	1991	2,7
Sunstore 4	1750	1,6
SCFW (control to supply temperature)	1564	-
SDH Online (Centralized-Würzburg)	1569	1,8
SDH Online (Centralized-Hamburg)	1257	1,8
Modelica based	1317	-

The obtained net solar gains differ in a great extent from each other. The differences between results of SDH Online tool for different locations (Hamburg and Würzburg) highlight the importance of the weather data. Thus, the need of being caution with the direct use of the tool for other regions than the available locations.

Sunstore 4, f-easy and SCFW are parametrized based on the TRY weather data for the case study location. The solar installation is but simplified in different ways. Among these three feasibility tools, f-easy shows the most optimistic net solar gain. A closer look into f-easy shows how the size of the storage tank has no impact on the net solar gain. Notice that the size of the storage supposed to be one of the tool results. However, it is possible and foreseen that the user overwrites this value. It has but not the expect result, net solar gain remains constant and exclusively the economic results vary. Thus, analyse impact of storage size with this tool is not possible. Furthermore, the fact that there is a clear proportional relation between collector area and solar gains, even for big solar installations, shows that storage losses are not even indirectly considered, see Figure 1. Furthermore, the linearity of the net solar gain implies the non-consideration of relation between solar gain and heat load.

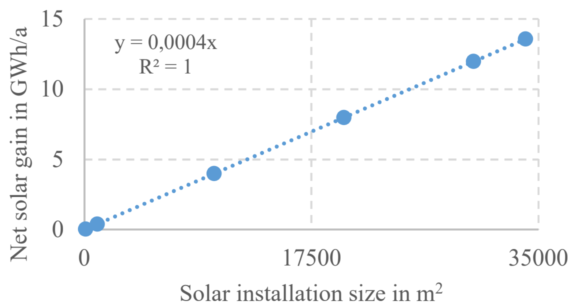

Figure 1. Relation between solar installation size and net solar gain of the f-easy tool with case 1-data set

A similar behaviour is observed in Sunstore 4 where the change of the storage size does not affect the value of the solar net gain. The thermal storage in Sunstore 4 is mainly defined by two parameters; the ratio storage volume-collector area and a percentage for the storage heat losses. A warning avoids the user to define unreasonable sizes for the thermal storage but are the parameters storage heat losses and annual solar collector efficiency which really affects the solar gain. In contrast, SDH Online and SCFW adapt the heat losses of the thermal storage to its size and thus changes on the storage size have a clear influence on the net solar gain.

The investment costs are similar for SDH Online and Sunstore 4. The higher investment cost of the f-easy tool is mainly explained by the 800.000 € corresponding to the land costs which are not considered by the other feasibility tools. Notice that SCFW does not calculate any cost.

4.2 Case 2: 34000 m² solar installation with a 68000 m³ pit thermal energy storage tank (PTES)

Main results of the feasibility analysis for the case 2 are summarized in Table 2.

In regard of the net solar gain, SDH Online shows again the dependency of the results to the chosen location. Results for f-easy are again the most optimistic followed by the Sunstore 4 and SCFW results. F-easy does not allow to choose a pit storage technology. Instead, a bond/borehole storage is chosen. The storage technology does not have any impact on the results of the net solar gain. It merely influences the investment costs.

Table 2: Main results for case 2

Feasibility tool	Net solar gain in MWh	Investment in million €
F-easy	13565	16
Sunstore 4	11800	8,8
SCFW (control to supply temperature)	11790	-
SDH Online (Centralized-Würzburg)	8592	13,7
SDH Online (Centralized-Hamburg)	7137	13,7
Modelica based	8713	-

In case 2 there is a great difference between the economic results of Sunstore 4, f-easy and SDH Online. Again, the land cost of f-easy, 5,1 million Euro, explain part of the difference. The specific investment costs for the solar installation are slightly different, see Figure 2. The investment cost of the solar installation for SDH Online, f-easy and Sunstore 4 are respectively 6.8, 6.8 and 7 million Euro.

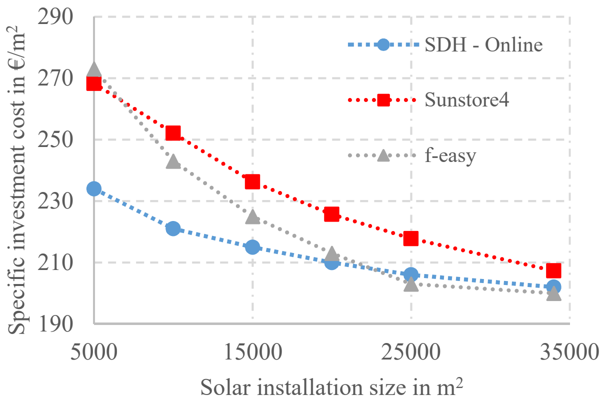

Figure 2. Specific investment costs used for the feasibility tools SDH Online (blue circle), f-easy (gray triangle) and Sunstore 4 (red square) as a function of the solar installation size.

Much greater difference is related to the pit storage tank costs, where specific costs from SDH Online are twice as higher as the ones from Sunstore 4, see Figure 3. The investment cost of the solar installation for SDH Online, f-easy and Sunstore 4 are respectively 3,7, 1,9 and 1,8 million Euro. The difference on the storage price explains part of the difference on the total costs, while a major part is explained by the fact that SDH Online applies surcharges for planning (10 %), equipment (7 %), building and site (5 %), measurement, control and regulation (3 %) as a percentage of the total investment costs.

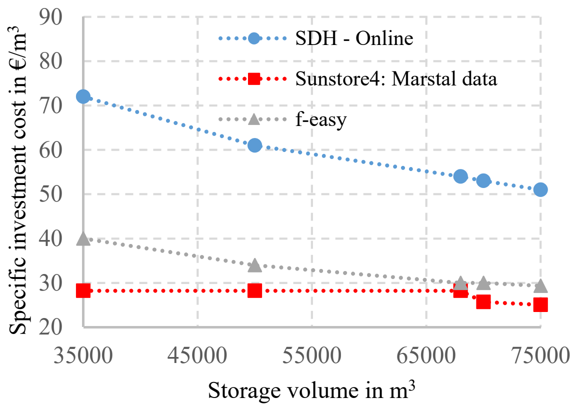

Figure 3. Specific investment costs used for the feasibility tools SDH Online (blue circle), f-easy (gray triangle) and Sunstore 4 (red square) as a function of the storage size.

5. DISCUSSION

The lack of reference values hampers the discussion regarding the quality and accuracy of the results. Considering the results from SCFW to be the most accurate (notice that SCFW presents the most detailed approach), it can be argued that the results from f-easy are over-optimistic and that Sunstore 4 are slightly more optimistic. Notice that f-easy does not take into account heat losses of the storage and therefore have more optimistic values for the net solar gain.

In regard of the applicability, with Sunstore 4 and f-easy is possible to get reasonable sizing for the solar installation and thermal energy storage. However, any of these two tools cannot be used to study the effect of the size of the storage on the system. Furthermore, in Sunstore 4 values for the yearly efficiency of the solar installation and storage have to be defined by the user. Here, even if reasonable values are suggested (default values), a previous work to estimate these values is necessary. Thus, making the consideration of e.g. operating temperatures and/or collector efficiencies a more complex task. On the contrary, SCFW and SDH Online present a more comprehensive approach, where physic parameters such as operating temperatures, solar collector and storage heat loss coefficients, among other parameters, have to defined. It is based on these parameters that the solar installation and heat storage efficiency are derived.

In regard of the transferability. All tools except SDH Online can be easily used for other locations. This is due to the importance of the weather data for such analysis and that SDH Online includes data for a limited number of locations (Barcelona, Frankfurt, Hamburg, Milan, Stockholm and Würzburg) which cannot be expanded.

In terms of flexibility, f-easy is the most rigid tool with a completely fixed energy concept (solar installation with thermal storage tank connected to a district heating system). SCFW is limited to the same system. However, small variations can achieve by activating/deactivating specific components: heat exchangers, storage tank, transmission pipes or even the district heating itself. Furthermore, it is possible to choose between two main control strategies, namely pre-heating (return mass flow rate from the solar installation is heated up 8 K and used to pre-heat the district heating network return flow. The missing necessary heat to rise the temperature up to the supply temperature is coped by a boiler) and control-to-supply temperature (solar heat is supplied when the supply temperature can be achieved). In addition, it can be assumed that the district heating is large enough so that solar heat gain can be delivered at any time. Under this assumption, heat storage and load data are not needed and therefore not used. With SDH Online mainly the same energy-system as SCFW can be considered: decentralized (solar heat is supplied at any time) and centralized (load data is considered. Solar heat is buffered and supplied when needed). The main differences are that the components considered are fix and depends on the chosen energy concept variation (centralized/decentralized). E.g. decentralized does not need a heat storage and that the pre-heat control strategy is not available (notice that this case could be eventually modelled by adapting/decreasing the heat load and the district heating supply temperature). Sunstore 4 presents the widest set of energy concepts, which were already listed in section

2.1 Sunstore 4. On the other hand, there is no flexibility on how the system is controlled, e.g. no control over operating temperatures, strategy: pre-heat/control-to-supply.

6. CONCLUSIONS

The reviewed feasibility tools are easy to use; It is possible in relatively few time to perform feasibility analysis for different energy concepts. The applicability of each tool is slightly different, Sunstore 4 and f-easy suggest reasonable sizing for each component of the system while SCFW and SDH Online allows the user to study the effect of different solar installation and thermal energy storage size. Excluding SDH Online all other tools can be directly used for a different location and boundary conditions. The accuracy of the results has not been assessed. In this regard, differences from up to 27 % and 16 % in the net solar gain are observed for the first and second case respectively (SDH Online and Modelica based feasibility tool results not considered).

The modelica based feasibility tool shows a great potential for carrying out feasibility analysis. The followed approach can deal with the observed limitations of the existing feasibility tools, listed in section 2.6 Urban-DH-extended Modelica based feasibility tool. In this regard the main two characteristics are,

- the flexibility of the modelling approach. Thus being able to adapt to the problem needs. New components can be implemented, existing ones adapted, and use them to model and analyse any energy concept.
- work in different level of detail. In this regard, it is possible to work on the component level; defining specific energy systems, or use system models; predefined models, e.g. solar installation with thermal storage, where the missing step is to parametrize the model and define proper boundary conditions.

The modelica based feasibility tools still needs some refining of the models and validation before a detailed comparison with existing tools can be carried out.

ACKNOWLEDGMENTS

The research leading to these results has received funding from the Austrian FFG Programme Stadt der Zukunft under FFG project no. 854666.

REFERENCES

[1] BuildingSystems library. https://github.com/UdK-VPT/BuildingSystems.
[2] Dymola. https://www.3ds.com/de/produkte-und-services/catia/produkte/dymola/.
[3] F-easy. http://solar-district-heating.eu/ServicesTools/SDHcalculationtools.aspx.
[4] Modelica. https://modelica.org/.
[5] Sunstore4 project. http://sunstore4.eu/.
[6] TRNSYS. http://www.trnsys.com/.
[7] EMD International A/S. EnergyPro. https://www.emd.dk/energypro/.
[8] Modelica Association. Modelica libraries. https://modelica.org/libraries.
[9] Open Source Modelica Consortium (OSMC). OpenModelica. https://www.openmodelica.org/.
[10] Patrick Reiter, Hannes Poier, and Christian Holter. BIG SOLAR GRAZ: Solar district heating in Graz - 500.000 m2 for 20 % solar fraction. In *4th International Solar District Heating Conference*, 2016.
[11] Solarthermalworld. Overview largest solar thermal installations worldwide. http://www.solarthermalworld.org/installations.
[12] Solites. ScenoCalc Fernwärme (SCFW). https://www.scfw.de/.
[13] Solites and AGFW. SDH Online-Rechner. http://www.sdh-online.solites.de/.

Towards intelligent and solar driven district heating: How simulation and energy master planning can contribute

H. Schrammel[a,*], F. Mauthner[a], I. Leusbrock[a]
a: AEE – Institute for Sustainable Technologies (AEE INTEC), Feldgasse 19, 8200 Gleisdorf, AUSTRIA; * = corresponding author, e-Mail: h.schrammel@aee.at

Background

Local energy utility companies are increasingly favoring local renewable and low-carbon energy sources (e.g., solar thermal, waste heat) for electricity and heat instead of using fossil fuels to actively contribute to achieving climate targets. This process requires long-term implementation strategies considering mutually social, technical and economic aspects.

As an example, the local multi-utility company Stadtwerke Gleisdorf GmbH has strong ambitions towards implementing a renewable district heating system as a substitute for local natural gas and other fossil based heating systems. Following this premises, the utility company started in 2009 with the construction of a biomass (two 850 kW_{th} biomass boilers) and solar thermal (300 m² gross collector area, 191 $kW_{p,th}$) based district heating system although a natural gas infrastructure was already established in large parts of the city. In the course of ongoing extensions, several larger consumers have been hydraulically connected, which were initially supplied by natural gas boilers via micro-grids. Moreover, further feed-in points for distributed solar thermal systems have been identified to increase the overall share of renewables. An overview of the current supply situation can be found in Table 1. Each station is equipped with feeding pumps as well as with thermal energy storages for load management.

Table 1: Overview current supply situation in Gleisdorf

	Station 1	Station 2	Station 3	Station 4
Biomass boiler	2 x 850 kW	-	-	-
Solar thermal	191 kW_{th}	182 kW_{th}	-	
Thermal storage	2 x 25 m³	2 x 13.7 m³	5 m³	6.2 + 7.1 m³
N-Gas boiler	-	-	1030 kW	2015 kW

In 2015, the total district heating system had a length of 5.1 km supplying 70 consumers with a load of 5.2 MW_{th} and a yearly consumption of 5,750 MWh (heat losses: 1,630 MWh, 22 %) were connected. Due to the hydraulic set-up and current operation strategy, natural gas boilers were used for base and peak load supply leading to around 30% of the final energy demand being supplied by natural while the remainder was supplied by biomass and solar thermal (68% biomass / 2% solar thermal).

Research questions (RQ)

The established district heating system with distributed conversion and storage units led to several challenges with regard to system hydraulics and operation control:

- Analysis and optimization of the thermal merit order of the conversion units including storage management
  - RQ1: Which boilers should be operated when in order to minimize heat generation costs, fossil fuel demand and energy efficiency?
- Assessment of current and future district heating operation characteristics
  - RQ2: What are the effects of further district heating extension as well as further integration of renewables and thermal storages on a) economics, b) emissions, c) physical parameters such as temperature and pressure levels and d) technical parameters such as electricity demand for pumping or full load hours of boilers?

- Optimization of overall district heating system performance by means of implementation of advanced control strategies and adapted system hydraulics
    - RQ3: What are the characteristic actuating variables in the control system today? What are the technical (control system, hydraulics) bottlenecks and how to overcome them?

Results

The status quo of the district heating system in 2015 as well as future scenarios were analyzed and optimized applying analysis of monitoring data, energy modeling (EnergyPLAN) and thermo-hydraulic simulations (simplex, STANET). Different measures to increase both energy efficiency and the share of renewables were identified, investigated and partially already implemented:

- Reduction of thermal losses in the distribution network by implementation of a weather-depended supply temperature control
- Adaptation / optimization of hydraulic set-up and control strategy of distributed boilers and pumps
    - to enable base load district heating supply via biomass boilers and solar thermal and
    - to reduce natural gas boiler operation to peak load hours by control of boiler merit-order / part load operation, improved control of the network heat pumps and storage management
- Installation of a roof-mounted solar thermal collector field with a gross collector area of 496 m² (316 $kW_{p,th}$) and impact-analysis for another 250 kW_{th} base load pellets boiler
- Assessment of customer substations and identification of critical operating conditions (above average supply and / or return temperatures)

We could show by simulation that the overall share of renewables in the system can be increased from 70% to 85% by optimized hydraulic integration of the wood-chip boilers (already implemented) and even increased up to 92% if additional renewables are integrated (solar thermal system already realized, pellets boiler pending). A total cost assessment based on real cost data from the utility company shows that levelized costs of heat may be decreased by 4-6% in a scenario with optimized integration of the wood-chip boilers combined with solar thermal and pellets boiler installed. In terms of emission, $CO_{2,eq}$ are reduced by 41-59% while NOx emissions rise by 17-22% and dust (PM10) by 32-36% respectively. Furthermore, new distributed consumers summing up to 4 MW_{th} of capacity can be integrated without critical effects on supply security, temperatures and pressures while boiler capacity only needs to be increased by 1.5 MW_{th}.

A major outcome and success story of the project is linked to improvements to the existing control system. A virtual controller based-on real-time district heating simulations was developed and programmatically linked to the existing control system via a standardized interface protocol. The virtual controller is already implemented and currently tested in actual operation.

Outlook

Further improvement potential has been identified for several customer substations (mainly high return temperatures) and is going to be further analyzed. Consequently, higher solar thermal yields are expected if network temperatures are being decreased and thermal storage management further improved.

Moreover, from a spatial energy planning perspective long-term strategies for renewable district heating extensions are developed in the framework of other ongoing research projects. Here, recommendations for local stakeholders (local government, city and landscape planning departments, energy utilities, etc.) are derived enabling long-term infrastructural changes in the community based on combined technical simulation and spatial planning knowhow. These recommendations are jointly developed with the local stakeholders in Gleisdorf and are part of the current efforts for a new spatial development and infrastructure plan for Gleisdorf.

CONTROLLING OF A DISTRIBUTED SOLAR DISTRICT HEATING PLANT: A DISTRICT HEATING CASE IN DENMARK

Andreas Zourellis[1] and Jes Donneborg[2]
[1] Aalborg CSP A/S, Address: Hjulmagervej 55, 9000-Aalborg (Denmark), phone: +45 50 30 00 25, email: azo@aalborgcsp.com
[2] Aalborg CSP A/S, Address: Hjulmagervej 55, 9000-Aalborg (Denmark), phone: +45 40 15 27 36, email: jdo@aalborgcsp.com

Abstract – The present document describes the performance and operation of a solar district heating plant in the southern suburbs of Copenhagen, in Solrød Kommune. The present decentralized plant is one of its kind since it is independently supplying with heat the district heating network by itself for consecutive weeks, even months fully automatically. This capability derives from the fact that a hot water accumulation tank of 1,250 m^3 is integrated in the system. This allows the solar field to charge the thermal storage tank with hot water with surplus heat during the day especially during the summer months. As a result the tank will be discharging that heat during night time and overcast days, allowing the operator to make major cost savings by not operating the natural gas fired engines. The plant has shown superiority in terms of temperature controlling in both the solar thermal field and the supply of the district heating network. The plant consists of 2,569 m^2 of flat plate collectors and has a peak capacity of 1.9 MWth. In its first year of operation it has managed to cover 28% of the annual heat demand with a production of approximately 1,300 MWh. During its guarantee period the plant has over performed 105% and it has covered almost the entire heat demand from May to September.

1. INTRODUCTION

By the end of September 2016 Denmark has reached a milestone regarding its solar thermal activity. More than one million square meters of solar collectors had been installed by that time [1]. Among those hundreds of thousands of flat plate collector square meters was the solar district heating plant of Solrød Kommune (Solrød Municipality) at the small town of Havdrup. Although the solar district heating plant is relatively small in size compared to the rest of Denmark, it has a unique characteristic. The plant in Havdrup is a distributed solar district heating system. This means that the solar plant is directly feeding the district heating grid with hot water. Normally “these plants use the grid as storage (as long as they provide a minor amount of heat in comparison to the total load of the district heating system” [2]. However, the solar plant in Havdrup due to the integration of a large hot water storage and its complex control philosophy can supply the heat to the grid 24/7 for several weeks especially during summer. That results in substantial savings for the district heating plant (Solrød Fjernvarme) as they are capable to completely shut down their gas boilers for a longer period.

2. DESCRIPTION OF THE SOLAR DISTRICT HEATING PLANT

2.1 Plant layout

The solar plant in Havdrup consists of 2,569 m^2 of GREENoneTEC flat plate collectors from the GK3003 product line, a technical house with all the technical equipment, instrumentation and heat exchanger and a hot water accumulation tank with a capacity of 1,250m^3. The GREENoneTEC panels have a 13.2m^2 gross collector area and a mix of single- and double glazed collectors are used in the solar field. These panels embed serpentine risers which helps the circulation as the water rises from the bottom footer to the top header as it gets warmer. The solar field includes 11 parallel rows of up to 20 solar panels connected in a series.

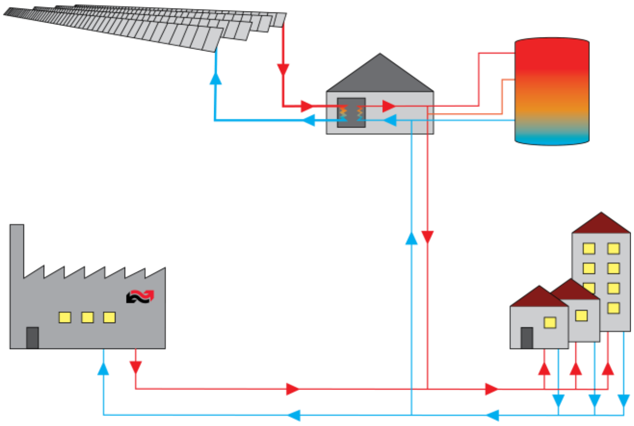

Figure 1: Havdrup distributed solar district heating plant

2.2 Mix of single- and double glazed collectors

As seen in Figure 2, due to space limitation the top two rows had to be bended in half. The first half of each row contains single glazed collectors while the second half consists of double glazed collectors in order to minimize the heat losses as the operating fluid (i.e. water/30% glycol) gets heated up by the sun.

At the north-west corner of the plant, the hot water accumulation tank and the technical building are located.

Figure 2: Solar district heating plant layout

2.3 Annual heat production targets

The plant is designed to supply heat to approximately 350 households (i.e. 1,200 inhabitants) covering as much as 28% of their annual heat demand during an average weather year. That way Solrød Fjernvarme is saving 233 tons of CO_2 yearly.

3. CONTROLLING A DISTRIBUTED DISTRICT HEATING PLANT

Figure 3 shows the SCADA system on site at technical control room. This also gives an overview of the different system components as well as various operational modes. The operational control philosophy of the plant in Havdrup has two main goals. It maintains a stable solar field outlet temperature not only in clear sunny days but in cloudy periods too.

Additionally, it supplies the district heating network with an accurate forward temperature, in the range of 65-75°C depending on the season. The control of the plant allows preheating early in the morning by recirculating the flow both in the primary and the secondary side, through the respective by-pass valves. Furthermore, it embeds two anti-freezing modes. The first one starts when the ambient temperature gets a few degrees lower than 0°C. For more aggressive cold weather with ambient temperatures around -10°C or below, the secondary anti-freezing mode kicks in, using heat either from the top of the tank or from the city grid.

During normal operation, the plant has the possibility to supply directly the heat to the grid through the assistance of a so called “city pump”. Since the plant is intentionally overdimensioned there are instances especially during summer, that there is surplus of heat produced. This heat excess is directed to the top of the accumulation tank.

As the top of the tank becomes hotter and hotter as the days pass by, it is important to maintain the stratification of the different temperature levels of the tank. Specifically, during morning hours when the plant has just completed preheating and the temperature of the hot water is still lower than both the top of the tank and the district heating, the flow is driven to the middle diffuser of the tank. These “middle” temperatures cannot be utilized and occupy significant space on the tank. For that reason, there is a shunting procedure. In cases, when the temperature coming from the secondary side of the heat exchanger is very high or at least higher than the desired temperature in the grid, the small shunt pump withdraws water from the middle of the tank to cool down the forward stream towards the city grid and get rid of these middle temperatures at the same time.

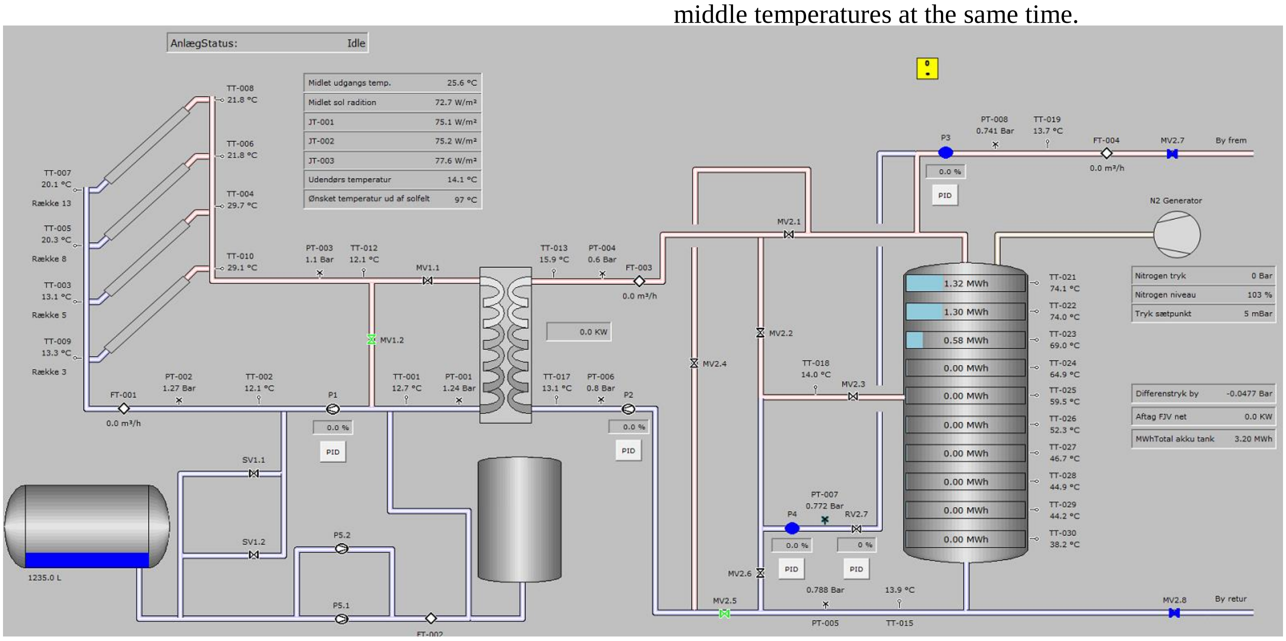

Figure 3: Screenshot of the SCADA system of the solar plant

For instances, when more than half of the tank is full with very high temperatures, the shunt pump withdraws cold water from the bottom of the tank and/or the return flow of the city.

Last but not least, when the tank gets more than ¾ full of hot water of around 90°C, then the operator gets a notification to manually operate the night cooling mode during the following night. In that way, significant part of the tank's hot content circulate at the solar field and eventually lose is energy to the surroundings. Before activating the night cooling mode, it is important to know what is the weather forecasted to be the following day. In case it is a cloudy day, then there is no reason for the operator to discharge the accumulated heat.

As a result there will be enough space to store the expected heat the coming day.

4. SOLAR DISTRICT HEATING PLANT MONITORING

The solar district heating plant in Solrød is already more than one year in operation and the results are more than satisfying. In Figure 4 the control of the outlet temperature of the solar field can be seen. This is a case of sunny and stable conditions. It becomes apparent that the outlet temperature is following with high precision the desired temperature setpoint which is adjustable by at any time.

In addition to that, Figure 5 shows how the outlet temperature of the solar field is maintained fairly constant in days with high radiation oscillations caused by passing clouds.

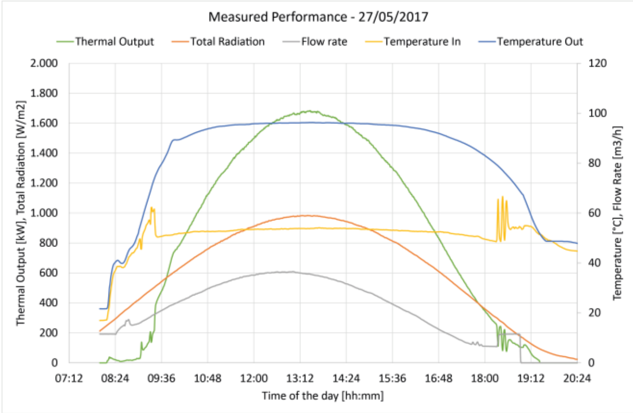

Figure 5: Field performance and collector outlet temperature control under clear sky conditions

It is worth noting at this point that the solar district heating plant in Solrød is expected to be doubled in the coming years resulting in an increased thermal energy yield. This implies that the system is already dimensioned to the full scale of the final solar field aperture area. All underground piping and hot water accumulation tank are over-dimensioned for the current size of the plant.

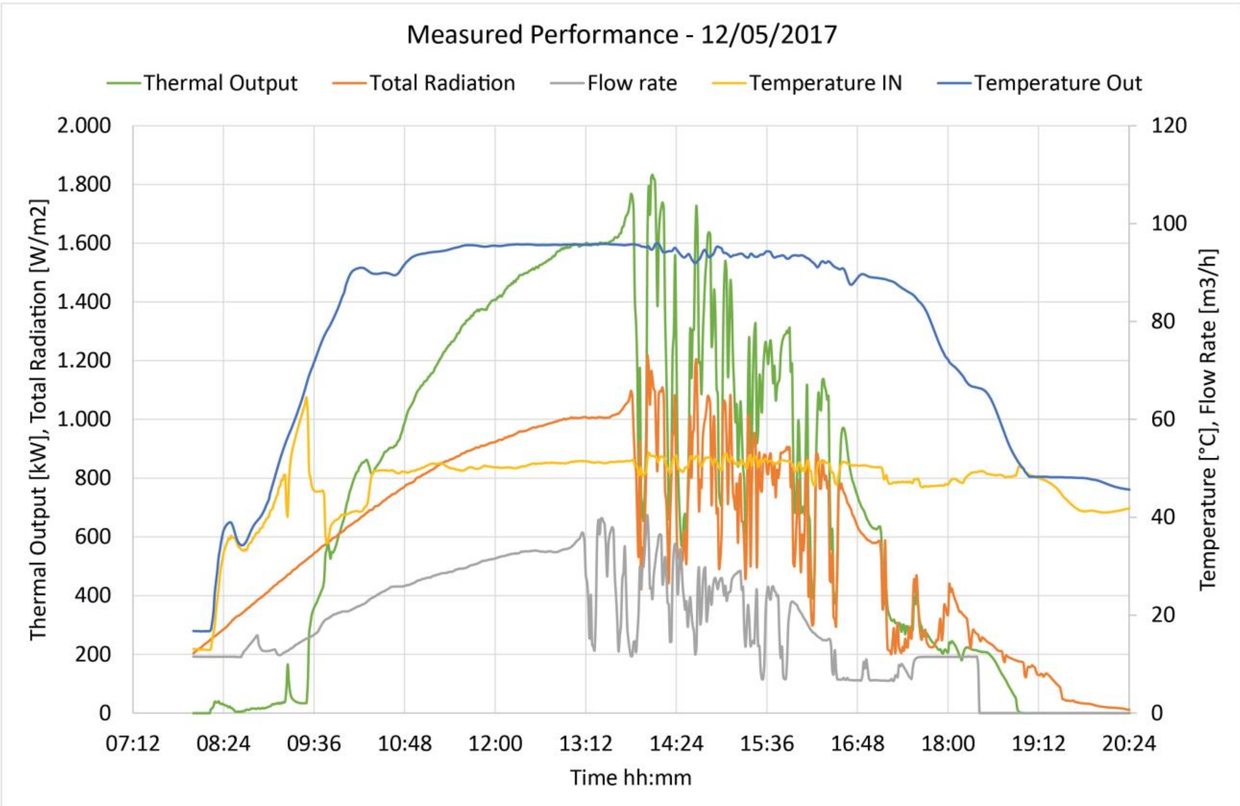

Figure 4: Field performance and collector outlet temperature control under unstable weather conditions

The immediate result, is that no night cooling was necessary to be activated during the whole summer of 2017, since the storage tank had enough "room" for the excess heat produced from the field. Thus, the plant was capable of supplying the district heating grid all the way from the beginning of May to late September. Figure 6[1] illustrates the energy level of the hot water accumulation tank in MWh during this period. As it can be seen, the energy inside the tank never dropped below 1.5 MWh meaning that there was always sufficient energy stored.

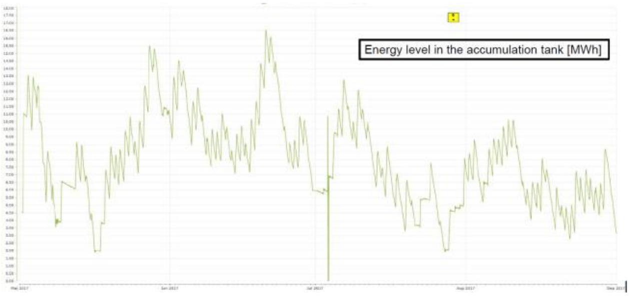

Figure 6: Hot water accumulation tank energy level from May 1st to September 30th 2017

Therefore, that resulted already in major cost savings for Solrød Fjernvarme, as the gas-fired engines were shut down throughout all that period and the city was using solar heat.

Figure 7 shows late days in May, where someone can see in greater details the temperature forward to the grid, the return temperature from the city to the plant as well as the heat content inside the storage tank.

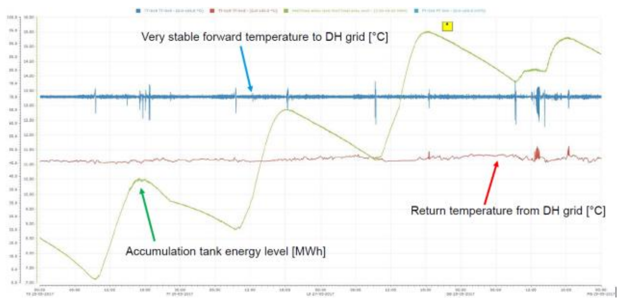

Figure 7: District heating supply and return temperatures and storage charge/discharge for the last week of May 2017

Even though instantaneous oscillations in the forward temperature of the solar plant to the city are not noticeable by the end-users, it is of great importance to deliver accurately the right temperature to the grid. Since, the solar plant is a decentralized entity, it is highly dependent on weather conditions and especially the solar radiation. However, the integration of the hot water accumulation tank balances the temperature that is supplied to the district heating grid, by shunting in colder water when the supply temperature starts to increase higher than the desired setpoint. In Figure 7 the precision and stability of supply temperature from the plant to the grid is shown (i.e. 70°C). The instant spikes take place during the transition from one operational mode to another which has as a result the opening and closing of the various valves. Therefore, there will be some "trapped" plugs of water with slightly lower or higher temperatures that will create this instant spikes which do not last more than a few seconds.

5. CONCLUSION

4.1 Thermal performance of the Solrød solar plant

The solar plant is regulated to maintain an outlet temperature of around 95-97°C and has proven to do so with excellent precision, even in unstable weather conditions.

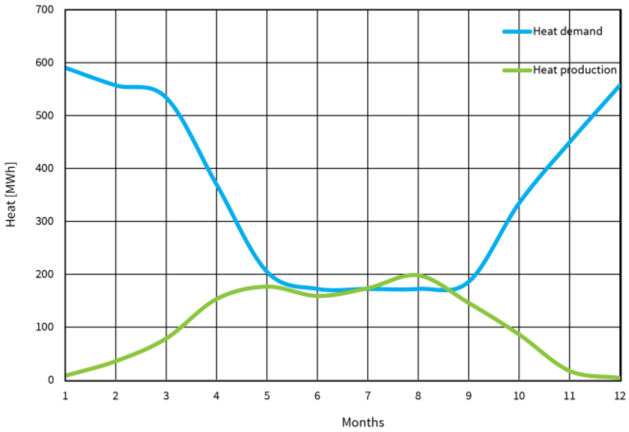

Figure 8: Annual thermal performance and demand curves

The plant has a peak thermal output of 1.8 MWth and an estimated yearly production of approximately 1,300 MWh. In a clear summer day the solar field can produce up to 12 MWh of heat. Figure 7 illustrates the annual thermal performance and demand in a monthly resolution.

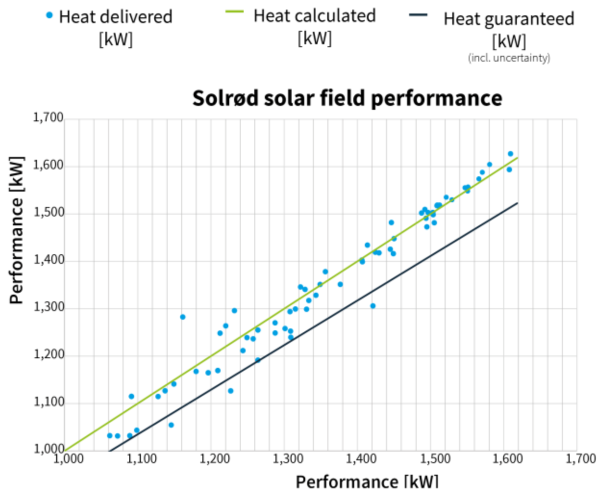

Figure 9: Measured vs. Calculated performance

[1] In Figure 6 there is one time that the energy content drops to zero due to a system restart

The plant has been delivered to the client at the end of spring 2017 and has been over-fulfilling its guaranteed performance since then, as it is shown in Figure 8. Until the end of June 2017 the plant was performing 5% better than the expected calculated performance

REFERENCES

[1] Million Square Meters Solar Thermal Collectors in Danish District Heating Plants. (2016, September 28). News and Articles. [URL: http://solar-district-heating.eu/NewsEvents/News/tabid/68/ArticleId/477/1-Million-Square-Meters-Solar-Thermal-Collectors-in-Danish-District-Heating-Plants.aspx]

[2] O. Miedaner, T. Pauschinger, J.O. Dalenbäck, “Categories of solar district heating systems” Solar District Heating guidelines, Solites, CIT Energy Management, Chalmers University, April 2012.

SOLAR CHP SYSTEM FOR LOW-TEMPERATURE DISTRICT HEATING NETWORKS

D'Antoni Matteo, Cozzini Marco, Fedrizzi Roberto
Institute for Renewable Energy, Eurac Research, Viale Druso 1, Bolzano, 39100, Italy,
Phone number: +39 0471 055614, email: matteo.dantoni@eurac.edu

Abstract – This paper considers a solar combined heat and power (CHP) system comprising parabolic trough collectors, a backup boiler, and an organic Rankine cycle engine. Its application is especially analysed in the context of a district heating and cooling network with a temperature of 20-30 °C, where distributed heat pumps are used as user substations. The case of a high temperature traditional network is however also considered. The analysis includes TRNSYS simulations for different geographical locations and different variants of the system configuration. Technical performances are presented in terms of energy outputs, which are then used for economic estimates. A similar analysis is carried out also for a flat plate collector field for heating only, in order to compare different possible ways of exploiting the solar resource. The solar-CHP configuration is found to yield acceptable economic performances, provided an extensive use of the backup boiler is considered. Environmental implications and alternative solutions are discussed.

1. INTRODUCTION

The current trend for district heating (DH) is to decrease the operating temperature, with the main goal of reducing thermal losses. The recently proposed 4th generation networks are expected to work at supply temperatures of the order of 50 °C, much lower than the 90 °C typically used in traditional 3rd generation networks (Werner et al., 2014; Lund et al., 2017). Within the H2020 FLEXYNETS project, even lower temperatures are considered, with the twofold purpose of opening the way to the exploitation of low-temperature waste heat (as the one available from cooling applications) on the one hand, and to introduce reversible heating and cooling networks on the other.

In this context, the traditional approach to DH should be entirely revised. Considering the importance of the coupling between thermal and electric sectors, as well as the importance of increasing the share of renewable energy sources (even more with heat pumps, introducing additional electric consumptions), an important chapter of this transformation should involve combined heat and power (CHP) systems. Traditional CHP is based on gas engines and it provides an efficient source for DH. A lower temperature network would have the benefit of decreasing the condensation temperature for these units, thereby increasing their efficiency. Thanks to this effect and having in mind the need to enhance clean energy sources, it is also interesting to consider a solar CHP system, composed of concentrating collectors coupled to an organic Rankine cycle (ORC) engine. Concentrating collectors, rather than the flat plate collectors usually mentioned in the solar district heating context, are crucial to reach the temperatures needed for ORC operation.

This system solution is the core of this paper, where different plant configurations (also including a boiler to extend the operation of the ORC and make the system more economically profitable) are considered. The yearly energy performance of the CHP system is evaluated by means of detailed TRNSYS simulations. A comparison with a flat plate collector field is also carried out.

2. BACKGROUND

The integration of heat pumps in district heating presents a series of interesting aspects. In the context of traditional DH networks, high-temperature heat pumps can be installed at facilities with cooling or refrigeration needs in order to reject heat directly to the network. While convenient in some cases, this way of recovering waste heat requires a relatively complex plant, which might reduce the willingness of some companies to start the connection. In the FLEXYNETS project, the opposite point of view is assumed: the network temperature is lowered at a nearly ambient temperature, so that direct integration of waste heat is always possible. Distributed heat pumps are instead considered as residential substations, making it possible to provide the desired temperature to the users.

This type of approach, while possibly more expensive in terms of installation costs, offers three important advantages: (i) a much easier integration of all waste heat sources located in the urban context, (ii) a strong coupling with the electric sector, with the possibility of applying demand side management to pools of small heat pumps coupled to local water storages (Pau et al. 2017; Monti et al., 2017), (iii) and a reversible system, able to simultaneously provide district heating and cooling (DHC) on the same pipes. The current electrification trend, also expected for the mobility sector, as well as the increasing decarbonisation of the electric grid, provide promising support to this option.

In this context, the role of CHP systems should be re-analysed. A lower temperature network can improve the electric efficiency of cogeneration systems, but the use of heat pumps to raise the temperature again, with corresponding electric consumptions, would largely reduce this benefit. Moreover, the overall environmental balance of this approach clearly depends on the nature of primary sources.

With these premises, it is interesting to consider the option of a CHP system with renewable sources. Here, we consider the solar source option, coupled to a boiler to extend its operation. In order to exploit a high level of flexibility, a gas boiler is considered for detailed modelling, though a biomass boiler could also serve to this purpose (biomass being considered renewable and carbon neutral under certain conditions).

In order to obtain temperatures high enough for cogeneration it is not possible to use flat plate collectors (FPC), but solar concentrating collectors are needed. In particular, this paper considers the case of parabolic trough collectors (PTC). Concentrating collectors can reach very high temperatures with special technologies (e.g., vacuum tubes and molten salts), but here less expensive and simpler collectors are considered, to operate in the range of 200-250 °C. They can then be coupled to ORC engines, which can easily be adapted to these source temperatures. This offers a compromise between efficiency and costs.

ORC engines are however rather expensive components. A common rule of thumb is that they are easily payed back when the yearly operation hours are of the order of 4000 or more. Since the solar availability is typically of the order of 2000 h per year, unless a rather large thermal storage is used, a backup boiler is needed.

Of course, since there are more efficient ways to generate electricity burning gas, some trade-off between the need of increasing the operation hours and the need to have a high renewable share. As already mentioned, biomass can also be considered to solve this conflict. The purpose of this work is however to offer a description of the gas-based system, as a starting point for future elaborations. A comparison with the alternative way of exploiting the solar resource via FPC is also presented.

3. METHODOLOGY

3.1 Energy concept

From a high-level point of view, the overall CHP energy system can be represented by a schematic single line connection diagram as shown in Figure 1 below. It is split into three parts, based on the used working fluid. Energy Generation Units (EGUs) use oil, Energy Distribution Units (EDUs) use water, and Energy Conversion Units (ECUs) interact with both oil and water. The main distinguishing point is their relative function in the energy system and in particular:

- EGUs generate thermal energy by utilizing solar or gas. Moreover, a small storage tank is included as an energy buffer.
- ECUs serve the primary purpose of conversion of thermal energy from the oil loop into either thermal energy in the water loop or electrical energy.
- EDUs are comprised of components responsible for meeting heating and cooling loads.

EGUs are responsible of delivering heat to the ORC. In this context, parabolic trough collectors are considered, which can be operated in series with or as an alternative to the gas boiler. The ORC can be designated as the central core of the CHP concept since it can produce simultaneously thermal and electrical energy, and the relative energetic output and system efficiency are dependent on its working conditions. The ORC is designed for a maximum inlet temperature at the evaporator of 245 °C and therefore thermal oil (Therminol SP) is selected as the heat transfer fluid to be used in solar collectors and other EGUs. The condensing heat of the ORC can be delivered to the network at a temperature range between 20 °C and 70 °C. As an alternative, the network temperature is raised directly by EGUs, solar collectors or gas boiler, which exchange heat with an intermediate oil-to-water heat exchanger. Although the presence of cooling schemes is not considered in this paper, EGUs can deliver heat for a sorption (ad- or absorption) chiller with a wide temperature range depending on the specific technology (250 °C - 65 °C). Minimum supply temperature is a function of the return temperature from the network and in any case cannot be lower than 7 °C. Condensing heat from the chiller could be rejected through a conventional wet cooling tower in order to guarantee a design return temperature to the chiller of 25 °C.

Besides the system represented in Figure 1, a FPC field will also be considered (scheme not reported in figure).

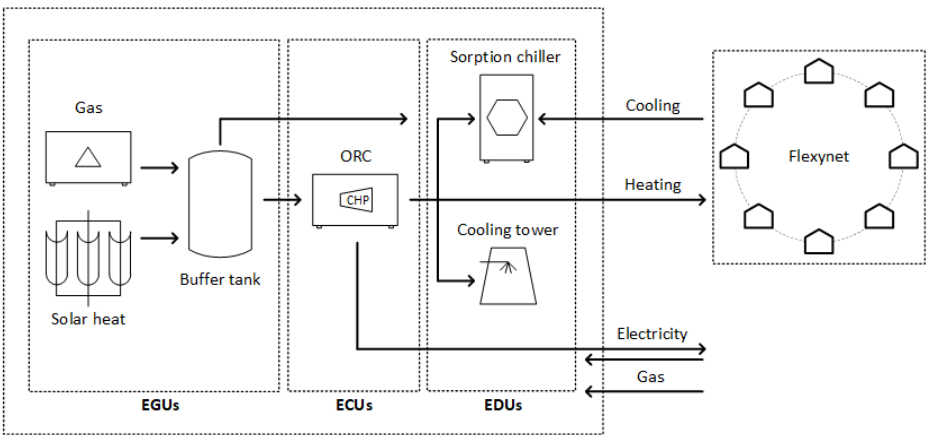

Figure 1. Single line diagram of the solar CHP system.

3.2 System layouts and working boundary conditions

The simulation platform for the assessment of different CHP layouts is carried out with the simulation software TRNSYS (Klein et al., 1979). The simulation approach adopted in the work is typical of energy potential studies where the network is assumed as an infinite load at constant return temperature and the CHP operates throughout the whole year (winter and summer) for delivering heating. This assumption mimics a condition where the solar CHP system covers a base load for the network, while variations with respect to this base load are covered by other units not considered here.

Solar PTC field, gas boiler and ORC unit are sized mutually in order to guarantee an optimal operation. EGUs as solar PTC field and gas boiler need to deliver heat to the ORC evaporator at a rather constant temperature, here fixed to 225 °C and therefore their capacity is sized accordingly. Performance characteristics of system components are derived from market available products (more information on the specific sizes of system components are listed in Table 1).

Table 1. Characteristics of CHP system components.

Parabolic trough collector (PTC) field		
Number of solar collector panels	12	-
Number of solar loops	3	-
Specific nominal power	537	W/m^2
Width of a single collector	2.37	m
Length of a single collector	26.16	m
Distance between rows	5.8	m
Flat plate collector (FPC) field		
Number of solar collector panels	72	-
Number of solar loops	12	-
Aperture area of a single module	10	m^2
Specific nominal power @ 70 °C	650	W/m^2
Gas boiler		
Nominal capacity	582	kW
Maximum outlet temperature	280	°C
Operation range	30…100	%
Avg. combustion efficiency	90	%
Organic Rankine cycle (ORC) unit		
Evaporator nominal capacity	530	kW
Electrical power output range	71-99	kW
Electrical power consumption	14	kW
Evaporator temperature range	185-245	°C
Condenser temperature range	20-70	°C

For PTC collectors, the efficiency curve of real collectors used in the BRICKER project is assumed. This is $\eta_{PTC} = 0.747\ \text{IAM} - 0.64(T_f - T_{amb})/\text{DNI}$, where IAM is the incident angle modifier, T_f is the average fluid temperature, T_{amb} is the ambient temperature, and DNI is the direct normal irradiance. Similarly, for FPC an efficiency curve valid for real collectors used in the InSUn project is assumed, namely $\eta_{FPC} = 0.811 - 2.71(T_f - T_{amb})/G_T - 0.01(T_f - T_{amb})^2/G_T$, where G_T is the global irradiance on the collector plane.

In the paper, four different variants of such generic solar CHP concept are compared. In the first layout, S01, a flat-plate solar collector (FPC) field transfers heat to the network through a heat exchanger (HEX). The working fluid in the solar loop is a glycol-water mixture operated at a constant mass flow rate of 40 kg/h/m^2. Configuration S02 is similar to S01 but FPCs are ideally replaced by high-temperature PTCs. In cases S01 and S02, almost the same collector aperture area (744 m^2 for PTCs and 720 m^2 for FPCs) is maintained. Clearly, cases S01 and S02 do not correspond to a CHP system, but just to a simple heat source. In configuration S03, PTCs deliver heat to an ORC that rejects its condensing heat into the network. Thanks to this configuration, the combined production of heating and generation of electricity is possible. The last concept, S04 integrates the presence of a gas boiler (BLR) that assists the PTC loop. This new component is sized in a way to deliver heat at 225 °C and it is always activated.

Note that the chosen sizing was tailored to the full configuration, i.e., PTC+BLR+ORC, so that the solar field peak power and the boiler minimum power (30 % of peak power) yield the ORC power (with a small difference to account for thermal losses in the circuits). In this way, the boiler is always on and ready to modulate to compensate the solar field fluctuations. For configuration S03, where only PTCs and ORC are included, it would be reasonable to reduce the ORC size to match (at most) the solar field peak power (of the order of 400 kW). For simplicity, however, the same sizes were kept for all configurations.

These four concepts are operated in two district heating conditions:

1. A traditional DH network characterized by a return network temperature $T_{netw,r} = 50$ °C, where the heat generation system has to guarantee a temperature rise (corresponding to the supply-return temperature difference) $\Delta T_{netw} = +30$ K.
2. A FLEXYNETS network characterized by a return temperature $T_{netw,r} = 20$ °C, where the heat generation system has to guarantee a temperature rise $\Delta T_{netw} = +10$ K.

For simplicity, the operating temperature of PTCs is fixed independently of the network temperature. Consequently, in configuration S02 the performance is not improved when lowering the network temperature. Conversely, for configuration S01 the collector temperature was properly adjusted: about 70 °C for the traditional case, about 45 °C for the FLEXYNETS case. Indeed, while configuration S02 in FLEXYNETS seems hardly interesting, it is useful to assess the efficiency improvement resulting for flat plate collectors in a low temperature context.

While the used numbers are realistic for the considered sizes, some overall improvement for a larger system could be expected. This point will be mentioned later in the context of economic estimates.

The dependency of thermal and electrical outputs from inlet temperatures into ORC's evaporator and condenser are taken into account by interpolating a performance matrix filled with manufacturer data. A similar approach is applied for combustion in the boiler.

Circulating pumps for oil and water loops are sized according to expected volumetric and mass flow rates and pressure drops. Power rated are derived from commercial available products. Pump consumptions are calculated both as electricity consumptions and as dissipated heat (additional thermal input to the system).

3.3 Control strategy

To integrate and run homogeneously all the components of the plant, an appropriate control strategy is developed. The architecture of the control rules consists of five elements listed in the following:

- Feedback signal is the information required from the sensors.
- Hysteresis is an elaboration of the acquisition signals in Boolean format. The hysteresis, in thermal systems, is useful to avoid continuous oscillation of the signal due to the nature of the system.
- Schemes represent the working modes used by the system. The schemes are defined as algebraic combination of hysteresis.
- Modulation refers to pumps and valves and it is used to scale the control signal of the component. The modulation can be either a fixed value or a function of another independent variable (temperature or mass flow rate).
- Control signal is the command given to the devices to be controlled; it is the combination of schemes and modulations.

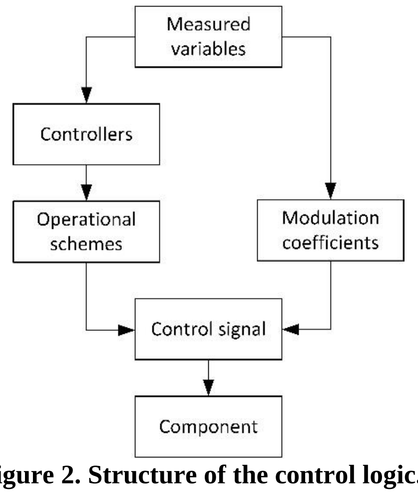

Figure 2. Structure of the control logic.

The activation of working schemes is based on real-time measured variables and in particular:

- T1: inlet oil temperature to the PTC solar field (used in configurations S02, S03 and S04).
- T2, T3: inlet and outlet oil temperatures to/from the gas boiler (used in configuration S04).
- T4: inlet oil temperature to the evaporator side of the ORC (used in configurations S03 and S04).
- T5: outlet temperature from secondary side of heat exchanger (used in configurations S01, S02 and S03);
- T6: inlet water temperature to the condenser side of the ORC (used in configurations S03 and S04);
- R1: DNI measured on collector absorber surface.

3.4 System analysis

The performance analysis of the CHP configuration is evaluated at the boundary comprising EGUs, ECUs and EDUs as shown in Figure 1. At this boundary, energy inputs, outputs and losses are quantified and in particular:

- System inputs: useful energy provided by the solar field (P1) and gas boiler (P2); electricity inputs for water and oil pumps, ORC power consumption.
- System outputs: heating production supplied to the network and electricity generated by the ORC.
- System losses: thermal losses from hydraulic components like pipes, buffers, storages and hydraulic junctions.

Inputs and outputs are used for calculating Final Energy (FE), Primary Energy (PE) and equivalent CO_2 production, according to the conversion factors reported below.

Besides energy efficiency indicators, economic performance figures are crucial for evaluating the profitability of different CHP configurations. Energy tariffs are referred for the network manager and typical of industrial customers. As well as environmental reference data, economic data are reported below.

Economic data. For each system block (FPC, PTC, ORC, BLR), investment costs as well as operation and maintenance costs where taken into account. The following values were collected from four different European projects (InSun, REEMAIN, BRICKER, FLEXYNETS) and from energy agency reports.

FPC:

- Investment cost per unit area: $c_{inv,FPC,A} = 400$ €/m^2 (InSun, deliverable 6.4). This is assumed to be the reference value for fields of a size of about 2000 m^2 (roughly 1 MW of thermal power). Costs typically decrease with the field size. A range of 300-600 €/m^2 seems in general a reasonable choice. These are considered overall costs, including balance of plant and installation.
- Operation and maintenance costs: these are assumed to be negligible. In practice, one expects electricity consumptions for pumping of the order of 1 % of the thermal power output. Pumping costs are here counted separately.

PTC:

- Investment cost per unit area: $c_{inv,PTC,A} = 400$ €/m^2 (data from InSun, FLEXYNETS). Again, this is assumed to be the reference value for fields of a size of about 2000 m^2 (roughly 1 MW of thermal power). Costs typically decrease with the field size. A range of 300-600 €/m^2 seems a reasonable choice in general. These are considered overall costs, including foundations, balance of plant, installation.

- Operation and maintenance costs: a yearly rate $r_{O\&M,PTC} = 0.5$ %, with respect to investment costs, is assumed (e.g., for buying spare parts). Similarly to FPC, pumping electric energy is of the order of 2 % of the thermal power output. Pumping costs are here counted separately.

BLR:

- Investment cost per unit power: $c_{inv,BLR,P} = 60$ €/kW (Danish Energy Agency, 2016).
- Operation and maintenance costs: a yearly rate $r_{O\&M,BLR} = 10$ %, with respect to investment costs, is assumed. The above reference (Danish Energy Agency, 2016) reports costs of about 1.1 €/MWh, which, assuming continuous operation throughout the year, would correspond to about 9 €/kW, i.e., 15 % of the investment. This value is here lowered to 10 % due to the modulating behaviour of the boiler.

ORC:

- Investment cost per unit thermal input power: $c_{inv,ORC,P} = 500$ €/kW (compatible with data from REEMAIN, BRICKER, FLEXYNETS). More generally, a range of 400-600 €/kW seems reasonable (overall costs).
- Operation and maintenance costs: a yearly rate $r_{O\&M,ORC} = 3$ %, with respect to investment costs, is assumed. Electricity self-consumption can be in the range 7-15 % of the electricity output and is counted separately.

For all components, a lifetime $L = 20$ years is assumed, though lifetimes of at least 25 years are realistic for most of these components.

As it can be seen, we assumed the same costs for FPC and PTC. Of course, depending on the company and the actual field conditions (e.g., type of ground), differences can arise. These effects are expected to lie within the given ranges.

Besides component costs, it is necessary to estimate energy costs. The following assumptions were done:

- Electricity costs. Electricity prices can vary significantly across Europe. Moreover, one has to take into account differences between residential and industrial costs, as well as taxes. Here we consider two options: (i) the cost for buying electricity, assumed to be equal to the 2015 EU average (as reported by Eurostat) for non-household costs including taxes, i.e., $c_{el,buy} = 147$ €/MWh; and (ii) the cost for selling electricity, assumed to be equal to the 2015 EU average for non-household costs excluding taxes, i.e., $c_{el,sell} = 87$ €/MWh. Ranges of +/- 50 % for these values can reasonably be considered (e.g., the average 2015 price for non-household electricity including taxes was 259 €/MWh in Denmark, against the 76 €/MWh of Sweden).
- Gas costs. Similarly to the case of electricity, the 2015 EU average for non-household users including taxes was assumed, i.e., $c_{gas} = 43$ €/MWh. Ranges of +/- 50 % hold also in this case.

Concerning the cost of the thermal energy sold to the network, we take as a reference the case of a gas boiler. In this case, the overall cost is higher than the pure gas cost. Assuming a boiler efficiency $\eta_{BLR} = 90$ %, one would get $c_{gas}/\eta_{BLR} = 48$ €/MWh. We therefore assume $c_{th} = 50$ €/MWh, rounding up to roughly take into account operation and maintenance costs. Again, a rather wide range of values could be considered in general.

With this information at hand, one can estimate the economic performance of the different considered configurations.

Economic performance is mainly compared through annualized costs. To this purpose, the interest rate $r_{int} = 3$ % is assumed. This corresponds to an annuity $a = r_{int}/[1-(1+r_{int})^{-L}] = 6.7$ %.

Environmental data. From this point of view, two types of information are considered: the primary energy factors for electricity and gas and their corresponding conversion factors in terms of CO_2 emissions. We assume the following, mainly taken from Ref. (IINAS, 2017).

Electricity

- Primary energy factor, $f_{ff,el} = 2.26$. This means that in order to produce 1 kWh of electricity, 2.26 kWh of fossil fuel energy are needed. With the increasing renewable share of the electricity mix, this value is expected to decrease. Values of 1.5-2 are already reasonable for some EU countries.
- Emissions, $f_{CO2,el} = 0.377$ t/MWh. As the primary energy factor, also this value depends on the actual electricity generation mix and is expected to decrease in the future.

Gas

- Primary energy factor, $f_{ff,gas} = 1.1$. This value includes the additional fossil fuel consumptions for, e.g., gas transport.
- Emissions, $f_{CO2,gas} = 0.25$ t/MWh.

With these values, it is possible to assess the environmental savings given by the different configurations with respect to the reference situation.

4. RESULTS

The developed model was used to estimate the system performances for the 4 different configurations mentioned above (S01-S04), 3 different geographic locations (Rome, Stuttgart, London), and 2 different network temperatures (see above). Hence, 24 simulations were run in total.

In the following, the main results are summarized, first recalling the main effects of changing geographical location and network temperature, then presenting actual results for the different configurations for the Rome climate and the lowest network temperature.

Effect of geographical location. The geographical location affects the performance of the solar field. The effect is different depending on the collector type: taking the Rome climate as a reference, the Stuttgart climate gives rise to a reduction in the output heat of the order of 40-50 % for flat plate collectors and of 50-60 % for parabolic trough collectors. The different effect on FPC and PTC can be explained by the different operation (FPC are fixed and exploit global irradiance; PTC include 1-axis tracking but exploit only direct irradiance). The given range takes into account the slightly different results depending on operation temperature and system configuration.

Effect of network temperature. The network temperature affects the performance of the ORC engine, correspondingly changing the condensation temperature. The lower the network temperature, the higher the ORC electric efficiency. Moreover, the network temperature affects the performance of FPC collectors, giving rise to different thermal losses (PTC are instead operated always at a high temperature, independent of the network temperature). In practice, one finds that reducing the condensation temperature from 50 °C to 20 °C, the ORC electric efficiency increases by 30-40 %, with negligible dependence on the location (the given range depends instead on the system configuration, the efficiency improvement being higher in the configuration without the boiler). The increase of the FPC efficiency when lowering the operation temperature from traditional to FLEXYNETS is instead of the order of 35-55 %, the improvement being higher for locations with lower solar irradiance (i.e., the benefit of adopting a lower network temperature is more evident for London, where the collector efficiency increases of about 55 %, than for Rome, where the efficiency increases of about 35 %).

Results of the different configurations. We compare the different configurations for the case of Rome and a FLEXYNETS network. Variations due to location or network temperature can be estimated according to the general comments made above. Fossil fuel savings are calculated with respect to a reference system where heat is generated by an industrial gas boiler and electricity is generated by the electric grid.

Configuration S01, FPC+HEX:

- Yearly final thermal energy output, $E_{th,out,fin} =$ 766 MWh.
- Yearly pumping consumptions, $E_{el,pump} =$ 7.7 MWh.
- Investment cost, $C_{inv} =$ 288 k€.
- Net present value $\mathrm{NPV}(r_{int}, L) =$ 265 k€.
- Internal return rate IRR = 11.4 %.
- Payback time PBT = 8 y (simple payback time 7 years).
- Levelized cost of energy, LCoE = 26.7 €/MWh.
- Yearly primary energy consumption of fossil fuel origin, $E_{ff} =$ 17.3 MWh, against reference consumptions of 936 MWh, with savings of 98 %.
- Yearly CO_2 emissions of about 2.9 t, against reference emissions of about 213 t, with savings of 99 %.

Configuration S02, PTC+HEX:

- Yearly final thermal energy output, $E_{th,out,fin} =$ 631 MWh.
- Yearly pumping consumptions, $E_{el,pump} =$ 14.4 MWh.
- Investment cost, $C_{inv} =$ 298 k€.
- Net present value $\mathrm{NPV}(r_{int}, L) =$ 118 k€.
- Internal return rate IRR = 6.9 %.
- Payback time PBT = 13 y (simple payback time 10 years).
- Levelized cost of energy, LCoE = 37.4 €/MWh.
- Yearly primary energy consumption of fossil fuel origin, $E_{ff} =$ 32.5 MWh, against reference consumptions of 771 MWh, with savings of 96 %.
- Yearly CO_2 emissions of about 5.4 t, against reference emissions of about 175 t, with savings of 97 %.

Configuration S03, PTC+ORC:

- Yearly final thermal energy output, $E_{th,out,fin} =$ 554 MWh.
- Yearly final electric energy output, $E_{el,out,fin} =$ 102 MWh.
- Yearly electric consumptions (pumping and ORC self-consumptions), $E_{el,in} =$ 41 MWh.
- Investment cost, $C_{inv} =$ 563 k€.
- The NPV at 20 years with an interest rate of 3 % is negative. This configuration is hence not economically viable with the considered parameters. Note that the sizing of the ORC is done for the configuration with the boiler and results unnecessary large for this configuration. Reducing the ORC size (e.g., to match the PTC field nominal power of 400 kW) would significantly reduce investment costs and yield a simple payback time of about 17 years.
- Yearly primary energy consumption of fossil fuel origin, $E_{ff} =$ 92.7 MWh, against reference consumptions of 908 MWh, with savings of 90 %.
- Yearly CO_2 emissions of about 15.4 t, against reference emissions of about 192 t, with savings of 92 %.

Configuration S04, PTC+BLR+ORC:

- Yearly final thermal energy output, $E_{th,out,fin} =$ 3910 MWh.
- Yearly final electric energy output, $E_{el,out,fin} =$ 742 MWh.
- Yearly electric consumptions (pumping and ORC self-consumptions), $E_{el,in} =$ 149 MWh.
- Yearly gas consumptions, $E_{gas} =$ 4313 MWh.

- Investment cost, C_{inv} = 598 k€.
- Net present value NPV(r_{int}, L) = 656 k€.
- Internal return rate IRR = 12.8 %.
- Payback time PBT = 8 y (simple payback time 7 years).
- Levelized cost of thermal energy assuming the buying price for electric energy, LCoE$_{th}$ = 38.7 €/MWh. Note that different possibilities for the allocation of costs in the case of cogeneration are possible (Frederiksen and Werner, 2014).
- Yearly primary energy consumption of fossil fuel origin, E_{ff} = 5082 MWh, against reference consumptions of 6456 MWh, with savings of 21 %.
- Yearly CO_2 emissions of about 1135 t, against reference emissions of about 1366 t, with savings of 17 %.

The levelized cost of energy is here calculated with the annuity method, i.e., LCoE $= \left(a\, C_{inv} + c_y\right)/E_{th,out,fin}$, where c_y are the yearly costs (operation and maintenance, electricity, and fuel; the yearly electricity production revenues, calculated using the market price for electricity, are subtracted from yearly costs when calculating the levelized cost of thermal energy in cogeneration mode).

It can be seen that configurations S01 (FPC+HEX) and S04 (PTC+BLR+ORC) are the most competitive ones, with very similar economic performances in terms of PBT and IRR. Note however that for the PTC+BLR+ORC configuration the assumption of continuous operation was made. This is convenient from the economic point of view (as it increases the number of operation hours of the ORC, allowing for a shorter payback), but it is questionable from the environmental point of view (due to the high gas consumption). Indeed, as a result of the extensive use of the boiler, the renewable share in the energy source mix is limited, giving rise to low-impacting savings (order of 20 %, for both fossil fuels and emissions).

This aspect could be changed with a reduced number of yearly operation hours for the boiler, though at the price of worse economic performances. As an alternative scenario, we therefore assume a system operating 50 % of the time (12 h/day, shutting down the boiler for the rest of the time). One can quickly make a rough estimate of the consequences in terms of PBT: since operation time is reduced by half, so are reduced revenues, so that one needs twice the time to pay back the investment. The PBT, which is $y_{PBT,full} = 8$ years at 100 % operation, then becomes of the order of 16 years (neglecting here details about interest rates). Conversely, one can approximately estimate the number of yearly operation hours h_y needed to get a given PBT of y_{PBT} years. Indeed, the product $h_y\, y_{PBT}$ yields the total number of operation hours to pay back the investment and is roughly constant (again neglecting interest rates). For example, if $y_{PBT} = 10$ (corresponding to a PBT equal to the 50 % of system lifetime) is considered acceptable, yearly operation hours can be reduced to $h_y/h_{y,full} = y_{PBT,full}/y_{PBT} = 80$ % (with obvious meaning of the subscripts).

It is also worth pointing out that, in the above estimates, the buying price for electricity was always assumed. In a FLEXYNETS network with significant electric consumptions due to heat pumps, it is indeed reasonable to assume the possibility to reuse internally all the electricity produced by the ORC. The use of the selling price for electricity would make the investment much less profitable. Indeed, assuming that the electricity produced in excess with respect to pumping energy and ORC self-consumptions is paid using the selling electricity price of 87 €/MWh, for configuration S04 (PTC+BLR+ORC) the NPV drops from 656 k€ to 127 k€, the IRR decreases from 12.8 % to 5.2 %, and the PBT increases from 8 to 15 years. The corresponding LCoE for thermal energy becomes 47.8 €/MWh, only slightly below the reference price.

Before closing this section, it is worth recalling the effects of network temperature and location. As mentioned above, the temperatures of a FLEXYNETS network improve the net ORC efficiency by 30-40 % with respect to a traditional DH network. The yearly electricity output, equal to 742 MWh with $T_{netw,r} = 20$ °C, is indeed only 573 MWh with $T_{netw,r} = 50$ °C (while electricity self-consumption is about 149 MWh in both cases). This would significantly reduce revenues. In practice, it turns out that with the conditions of a traditional network (and using the above economic reference value) the PBT of configuration S04 (PTC+BLR+ORC) increases from 8 to 12 years when using the buying price for all the sold electricity. Moreover, when using the selling price for the net electricity output, the PBT becomes longer than the assumed system lifetime (differently from the case with the FLEXYNETS temperature). Since in a traditional network it might be more difficult to self-consume all the produced electricity, this result shows the poor feasibility of a solar-CHP system in that context. Similarly, moving from Rome to norther climates reduces the convenience of the system due to the smaller solar fraction. For example, for the Stuttgart climate the PBT increases from 8 to 11 years.

5. CONCLUSIONS

The present work analysed a possible solar CHP system, comparing its performances with alternative configurations exploiting solar heat, for different locations and for different network temperatures.

The system was simulated in detail from a technical point of view, in order to calculate energy outputs including dynamic effects. These results were then coupled to economic estimates to assess the general feasibility of the system. Environmental figures were also provided.

It was found that, while clearly challenging, the considered system has some feasibility margin. In this respect, some comments are in order.

Due to the significant investment costs of current ORC systems, a large number of yearly operation hours is needed in order to make them economically convenient. This requires to extend operation beyond the period of solar availability. In this paper, the option of using a backup gas boiler was used. While technically and economically convenient, this is environmentally questionable. Alternative solutions can be provided by biomass boilers or thermal storages (with a proper relative sizing of solar field and ORC).

We have also shown that the FLEXYNETS context improves the feasibility of the considered solar-CHP system, taken as a single entity. Indeed, it lowers the condensation temperature of the ORC thereby increasing its efficiency. Moreover, it offers higher self-consumption opportunities (due to the presence of heat pumps), allowing to assume higher values for electricity. Looking to the entire picture, however, one should consider that if the generated electricity is mostly absorbed by heat pumps, the resulting solar-CHP + HPs system offers an energy output similar to a simple heating system. Other solar district heating options (e.g., with FPC) could then be more competitive, though the additional flexibility (including reversibility) provided by the thermal-electric hybrid system certainly brings some added value.

Finally, it is worth recalling the significant variability of many of the parameters used in these economic estimates. The reported ranges show that one can expect large differences from country to country, and possibly from now to a near future. Hence, in spite of the evident challenges posed by a solar CHP solution, it can be interesting to continue similar investigations, with the purpose of developing more diversified solutions for the next energy system.

ACKNOWLEDGMENTS

This work is part of the FLEXYNETS project, that has received funding from the European Union's Horizon 2020 Research and Innovation programme under grant agreement No. 649820.

REFERENCES

Danish Energy Agency, 2016. Technology Data for Energy Plants for Electricity and District Heating Generation, ch. 44.

Frederiksen, S., and Werner, S. (2014). *District Heating and Cooling*, 1st edn., ch. 11. Studentlitteratur.

IINAS (International Institute for Sustainability Analysis and Strategy), 2017. GEMIS – Global Emissions Model for Integrated Systems.

Klein, S.A., Beckman, W.A., Mitchell, J.W., Duffie, J.A., Duffie, N.A. et al. *TRNSYS 17, TRaNsient SYstem Simulation program*. University of Wisconsin, Madison, WI, USA (1979), www.trnsys.com.

Lund, H., Østergaard, P. A., Connolly, D., and Mathiesen, B. V. (2017). Smart energy and smart energy systems. *Energy* 137, 556–565.

Monti, A., Pesch, D., Ellis, K.A., Mancarella, P. (2017). *Energy Positive Neighborhoods and Smart Energy Districts*, 1st edn., ch. 2. Elsevier.

Pau, M., Cremer, J. L., Ponci, F., Monti, A. (2017). Impact of Customers Flexibility in Heat Pumps Scheduling for Demand Side Management. *Proceedings of the EEEIC / I&CPS Europe conference*, 6-9 June, Milan, Italy. DOI: 10.1109/EEEIC.2017.7977681. IEEE.

Werner, S., Wiltshire, R., Svendsen, S., Thorsen, J. E., Hvelplund, F., and Mathiesen, B. V. (2014). 4th Generation District Heating (4GDH). *Energy* 68, 1–11.

Performance of the 27000 m² parabolic trough collector field, combined with Biomass ORC Cogeneration of Electricity, in Brøndeslev Denmark

Bengt Perers[1], Simon Furbo[1], Zhiyong Tian[1],

Jan Holst Rothmann[2], Jacob Juul[2]

Thorkil Neergaard[3], Poul Vestergaard Jensen[3]

Jørgen Røhr Jensen[4],

Per Alex Sørensen[5], Niels From[5]

[1] Department of Civil Engineering, Technical University of Denmark, Nordvej Building 119, Kgs. Lyngby, 2800, Denmark, 0045-52781629, beper@byg.dtu.dk

[2] Aalborg CSP A/S, Aalborg (Denmark)

[3] Brønderslev Varme, Brønderslev (Denmark)

[4] NIRAS, Frederikshavn (Denmark)

[5] PlanEnergi, Skørping (Denmark)

SUMMARY

A new concentrating solar power (CSP) plant combined with biomass combined heating and power (CHP), using organic rankine cycle (ORC) technology has been taken into operation in Brønderslev, Denmark during spring 2018. The price for biomass is expected to increase with more and more use of this very limited energy source and then CSP will be cost effective in the long run, also in the Danish climate. Oil is used as heat transfer fluid in the high temperature PTC collectors in this application for district heating. Total efficiencies and costs, competitive to PV plants, are expected. The paper presents a performance analysis of the full scale CSP collector field of 27000 m^2 in the Danish climate during 2017.

key-words: concentrating solar power, combined heating and power, organic rankine cycle, TRNSYS

1. Introduction

The potential for installing ORC-units in Danish district heating plants with wood chip boilers is calculated to 30 utilities with more than 20,000 MWh in yearly heat production [1]. The first Danish plant (4 MW heat and 0.75 MW electricity) was implemented in 2011-12 in Marstal.

Aalborg CSP A/S has developed a concentrating solar collector array design. It has been demonstrated in several pilot plants. In the Brønderslev plant a further improved large collector array layout and control for operation temperatures up to 312°C is demonstrated.

The Brønderslev district heating company, expects lack of biomass in the future, resulting in higher prices. Therefore they implemented a CSP-plant, to supply the ORC with hot oil in periods with enough DNI (Direct Normal Irradiance). The collector array area is 27000 m^2 and the nominal peak power is 16 MW, see figure 1 and 2.

The collector array consists of very large 700 m^2 PTC (Parabolic Trough) collectors units with just one tracker each. Four such units are connected in series in each loop to reach a high flow velocity in the absorber tubes. The heat transfer media is a special thermal oil.

DTU has previously developed solar radiation models to determine the DNI availability in Denmark, see figure 3. They also investigated the potential performance for good PTC collectors utilizing direct solar radiation with promising results, see figure 8. Also a normal flat plate collector needs some direct radiation to reach operating temperatures and deliver heat.

Figure 1. The Brønderslev ORC-CSP biomass combined heat and power plant. The collector area is 27000 m^2 and nominal thermal power 16 MW.

The collector absorber tubes are of vacuum type giving extremely low heat losses even at high temperatures. This means that the collectors can start at extremely low beam radiation levels and that the tubes keep the temperature like a thermos flask between the sunshine periods.

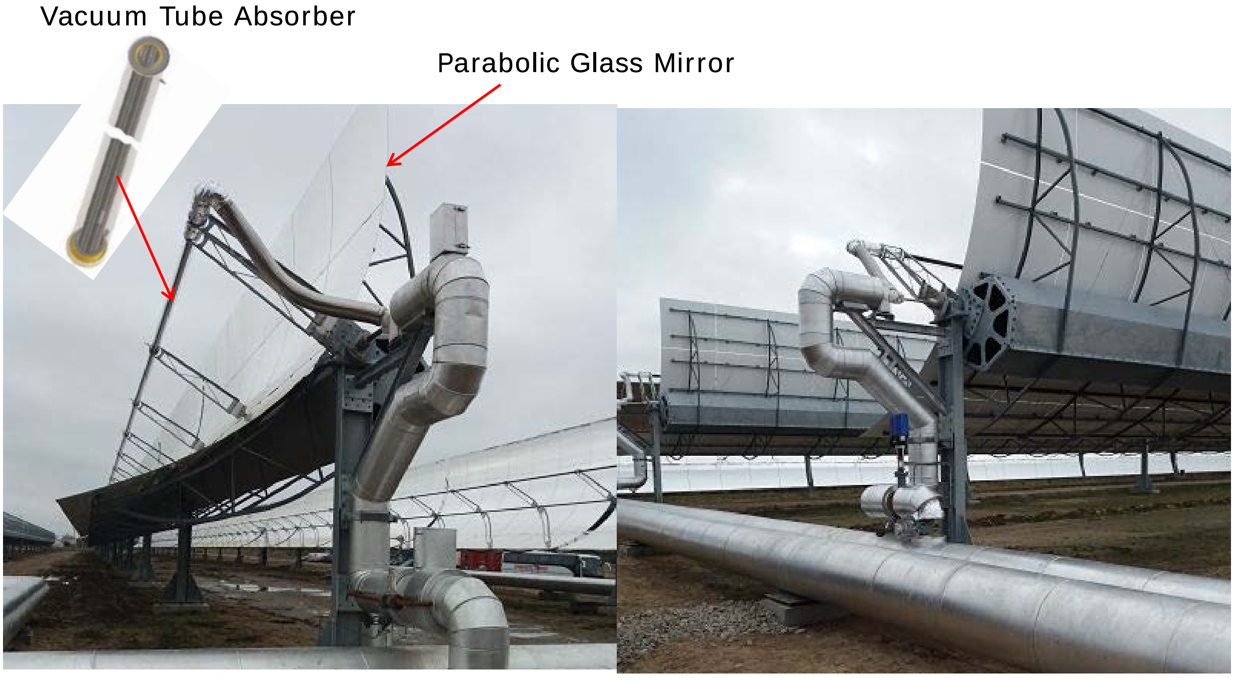

Figure 2. Closeup of the PTC collectors showing the vacuum tube absorbers, glass mirrors and the optimized mechanical trough metal structure. Only one tracker is needed for a 120 m long trough with almost 700 m^2 aperture area.

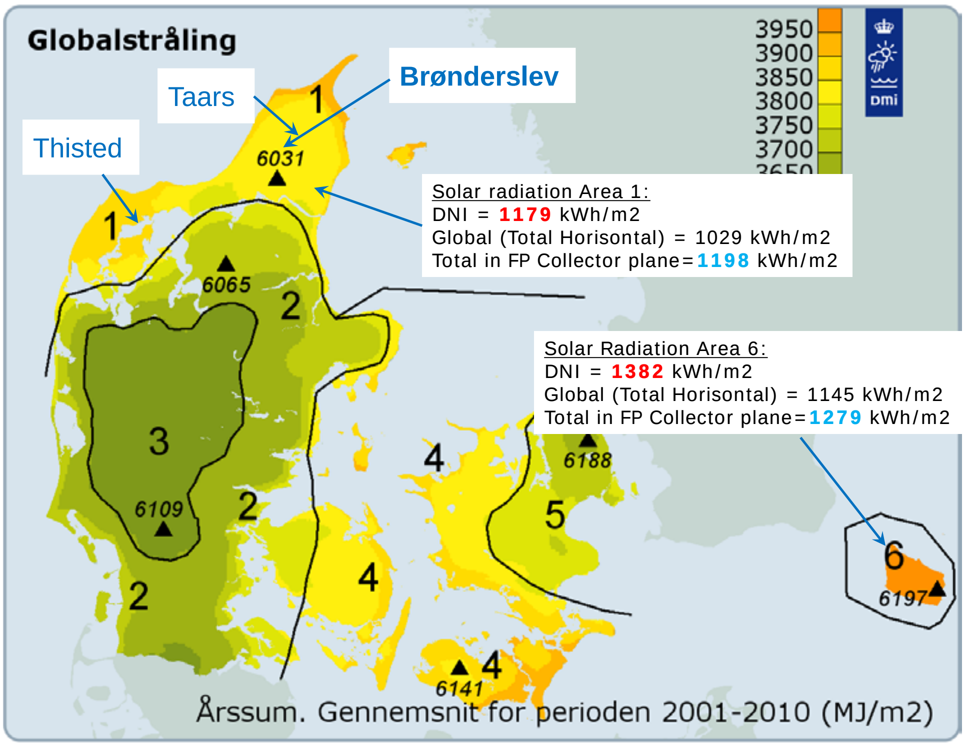

Figure 3. The Solar radiation distribution and availability in Denmark. Yearly Solar radiation for area 1:DNI=1179 kWh/m^2. Global (total Horisontal=1029 kWh/m^2. Total on Flat Plate Collectors=1198 kWh/m^2.Yearly Solar Radiation for area 6: DNI=1382 kWh/m^2. Global Radiaton=1145 kWh/m^2. Total on Flat Plate Collectors 1279 kWh/m^2.

2. The Plant Technology

The Italian Company Turboden has delivered the ORC unit. In the last 15 years Turboden has implemented ORC-units at about 300 places. Of these, approximately 250 plants are heated up with oil from biomass boilers and of these 250 plants, 170 are placed in Germany, Italy and Austria. One plant using CSP as heat source was implemented in Morocco in 2010 and three new plants are under implementation or planning in Italy. The technical efficiency when using solar as heat source is higher than 15%. CSP Solar power with ORC is thus as efficient as photovoltaic systems and on top of this the large fraction of ORC condenser heat, can be used for district heating in this plant design giving a favorable total efficiency. The ORC CSP principle is schematically shown in figure 4.

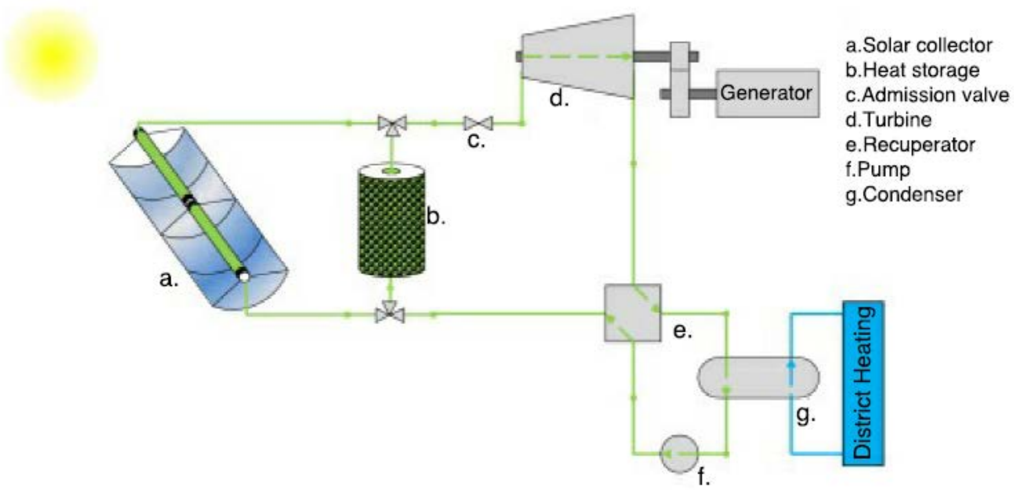

Figure 4. The ORC CSP principle. In this case the collector field is directly connected. In Brønderslev oil is used in the collector array.

The total Brønderslev system is shown in a simplified drawing in figure 5. The solar collector array can deliver heat both via the ORC machine or directly do district heating. The same for the biomass boiler, that also has a heat pump, to make use of waste heat from the biomass chimney and convert to district heating energy.

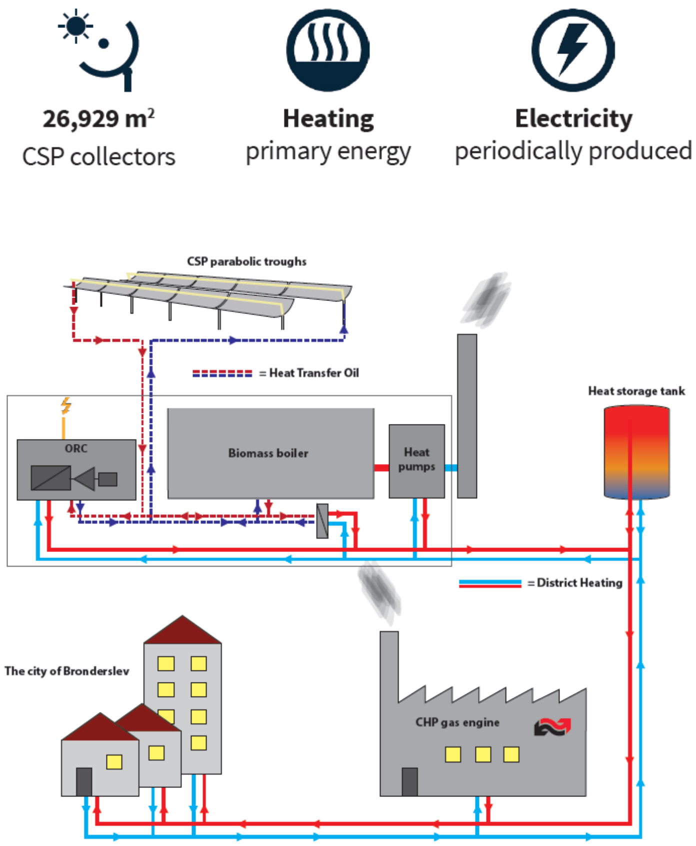

Fig.5. Flow sheet of biomass CHP-plant with ORC-power unit and feed-in of solar thermal energy both to the ORC and district heating network [3].

3. Measurements

To be able to analyze the collector field performance accurately the Brønderslev plant was instrumented carefully with advanced solar radiation equipment. Figure 6 shows the weather station and the DNI sensor measuring the direct or beam solar radiation coming from the sun disc. This sensor is very sensitive to dirt and is equipped with an air pressure cleaning device.

Figure 6. The weather station and DNI sensor for direct solar radiation measurements. Note the automatic air pressure cleaning system.

4. The 27000 m^2 CSP Collector field modelling

A detailed TRNSYS model has been developed for the full size collector field, so that control and performance can be investigated in detail.

Then effects of for example weather and operating conditions can be exactly taken into account and a true performance check can be made.

In figure 7 a comparison between modeled and measured power and temperatures is shown. The agreement is very good over the whole day. The thermal power delivered to the district heating network is also peaking close to the nominal 16 MW.

In figure 8 the solar radiation conditions with DNI (Direct Normal Incident radiation) and direct radiation in the tracking collector plane is shown for the same day. Also the incidence angle is given. This shows the effect of turning the tracking axis from exactly North South direction. The daily profile is then changed and may be adapted to the highest electricity price that at present often is in the mornings at around 8-10.

In figure 9 all relevant temperatures and the oil and water mass flow rates are shown. It can be seen that during this day the flow control is done only on the water side of the heat exchanger not on the oil side. The oil side shows very high temperatures compared to what is delivered to the district heating network. This control strategy can be optimized later when the plant is in full operation with ORC electricity production.

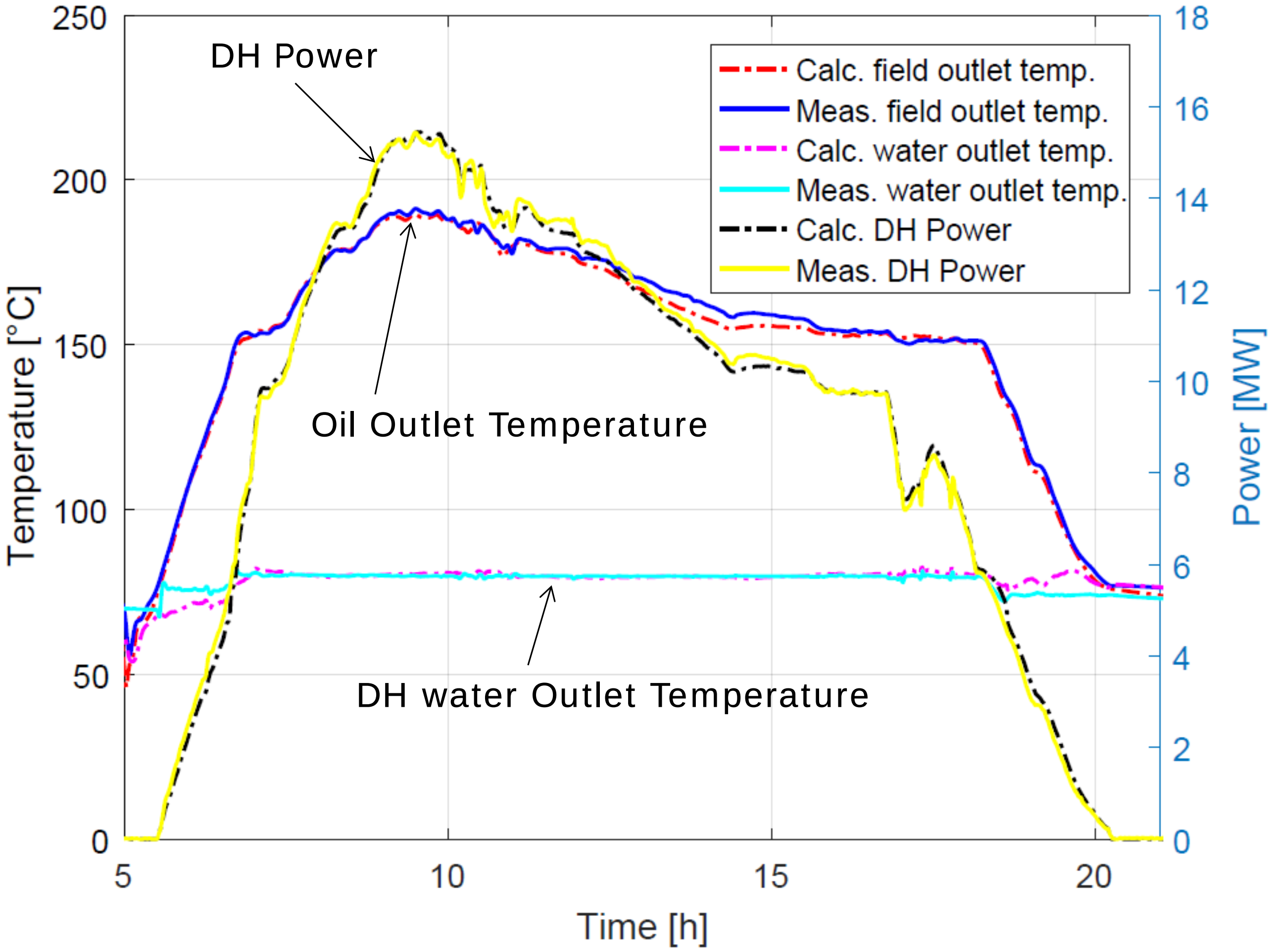

Figure 7. Detailed TRNSYS model validation for direct District heating operation. The match is very good concerning power but also temperature levels on water and oil side.

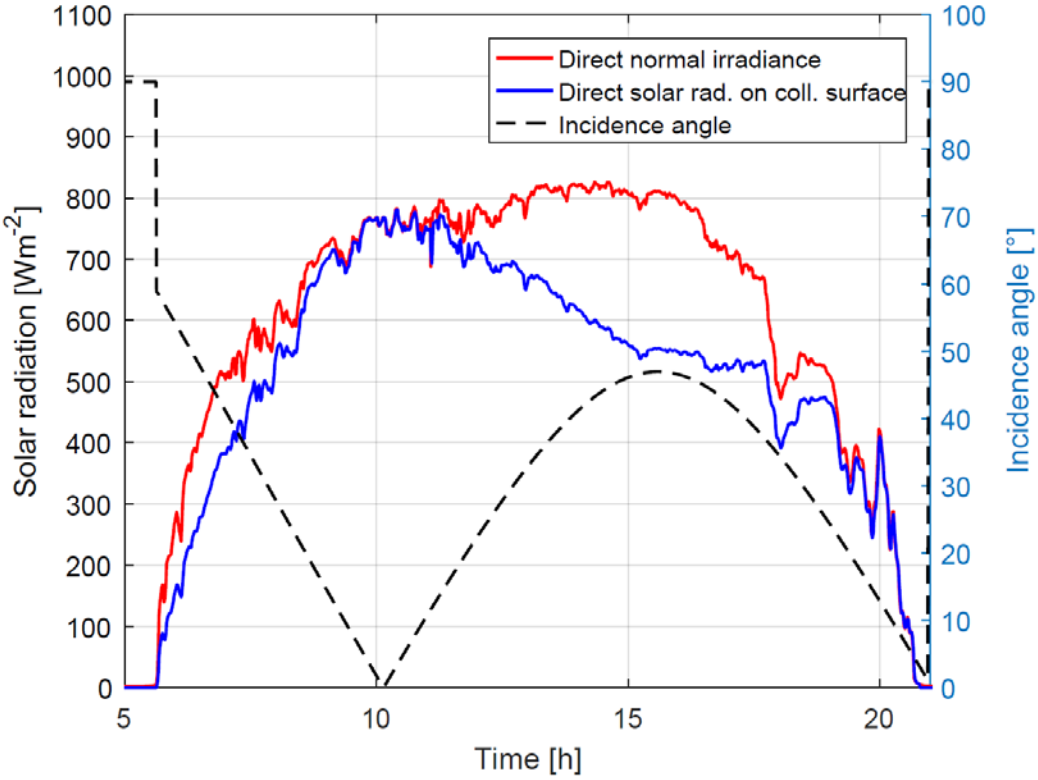

Figure 8. The solar radiation and incidence angles during the day shown for model validation in figure 7.

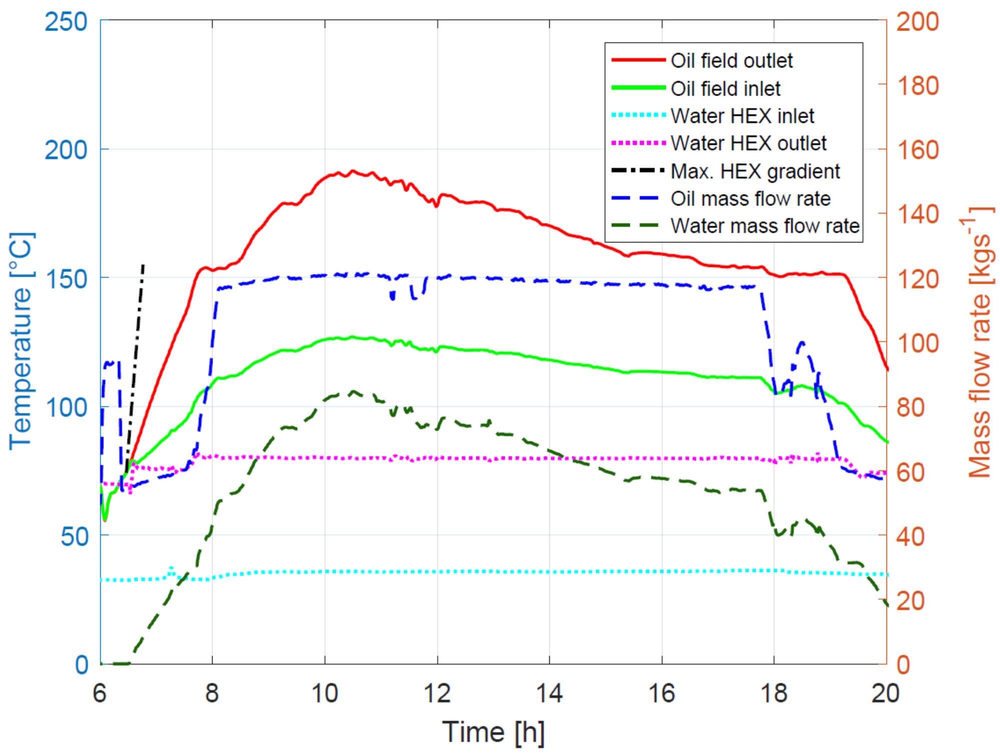

Figure 9. The most important temperatures and flows during the validation day in figure 7. The flow on the water side of the district heating heat exchanger is controlled to get a constant forward temperature to the district heating network.

Figure 10 shows the potential yearly thermal performance of a CSP solar collector field for different regions in Denmark determined with the validated model.

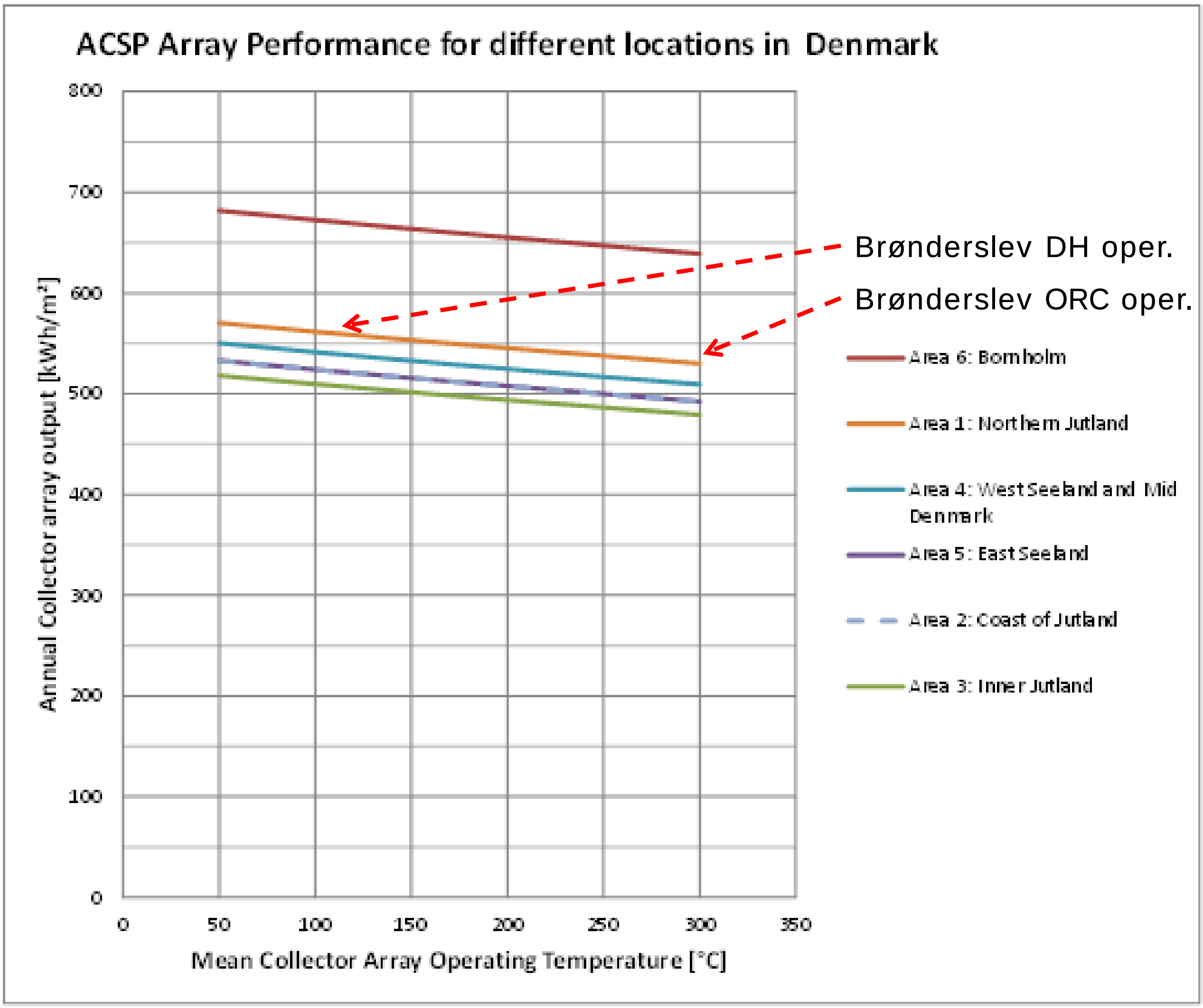

Figure 10. Potential CSP performance in different parts of Denmark at a wide temperature span. Bornholm has an extra favourable climate being and island. The difference between the other locations is surprisingly small. Danish reference year data and a validated collector model and parameters have been used.

5. Conclusions

The 27000 m^2 CSP array performance and control has been modelled in TRNSYS and a model validation is presented in this paper.

The first detailed results show a collector array performance close to the expectations.

References

[1] ORC og dampmotor til små flisfyrede varmeværker. Jan. 2011. Udført af Plan Energi for Dansk Fjernvarme 2011.

[2] Bengt Perers, Simon Furbo and Janne Dragsted. Thermal performance of concentrating tracking solar collectors. DTU Byg report R-292. August 2013.

[3] Aalborg CSP A/S. 2017.

[4] Bengt Perers, Simon Furbo and Janne Dragsted. Verification of high temperature performance for the 0.8 MW CSP test plant at Brønderslev. DTU Byg report SR-15.03. August 2015.

EFFICIENT HEAT DISTRIBUTION IN SOLAR DISTRICT HEATING SYSTEMS

Helge Averfalk and Sven Werner
School of Business, Engineering and Science, Halmstad University, P.O. Box 823, Halmstad, SE-301 18, Sweden

Abstract – This paper contains a short analysis showing the main benefit for solar district heating when a novel heat distribution concept with low temperatures is applied. The analysis is performed by comparing the annual solar heat output from a solar collector field for current heat distribution temperatures in Sweden with the corresponding output for the novel heat distribution concept. The results show that the new low temperature concept provides 66% more solar heat for a typical solar collector. Hereby, the solar collector field can be reduced with 40%, giving a corresponding cost reduction for solar heat generated. Another result is that the cost gradient for lower costs from lower return temperatures is five times higher for solar district heating compared to current heat supply in Swedish district heating systems. One major conclusion is that high heat distribution temperatures in current European district heating systems are a major barrier for the competitiveness of solar district heating.

1 INTRODUCTION

Most current solar district heating systems utilise conventional methods regarding district heating technology for heat distribution. The present heat distribution technology has been developed over the course of a couple of decades. During this period, end users heat demand has been high, compared to what might be expected from future new and renovated existing buildings. Furthermore, heat has conventionally originated from high temperature sources, commonly by fossil fuels that can generate high temperatures with ease. These two conditions have of course had an impact on technology development over the whole period.

In the future, however, these conditions are about to change. According to legislation from the European Union, such as the energy performance in buildings directive (European Union, 2010), heat demand from buildings will decrease, and according to the renewable energy directive (European Union, 2009), less availability of high temperatures from fossil fuels is expected. A somewhat common feature of renewable energy sources is that they will not be able to deliver high temperatures at the same extent as fossil fuels have done. This is especially valid for solar district heating, since higher temperatures are more difficult and expensive to achieve. Hence, low temperatures are essential to improve system efficiency of solar thermal systems. This conclusion can also be expressed as: high heat distribution temperatures in current district heating systems are a major barrier for solar district heating.

Thus, there is a challenge for current distribution technology to change in order to cope with surrounding factors that are in motion. As when, buildings have low heat demands, heat supply is derived from low temperature sources (renewable, recycled, and stored heat), and lower system temperature levels will be required. As it seems apparent that a change towards lower temperature levels is necessary, the important question arises: what should this change or enhancement of current distribution technology consist of?

This question is essential in the development of the fourth generation of district heating (4GDH) technology, defined in (Lund et al., 2014). This definition implies that the current technology generation is called the third generation of district heating (3GDH).

2 THE CONCEPT

In previous research we have worked with a principal concept for future innovative heat distribution technology in order to obtain lower annual average return temperatures (Averfalk & Werner, 2018). In said research, we have identified three important paths to achieve lower temperature levels in future district heating systems. These are:

- Three-pipe heat distribution networks
- Apartment substations in multi-family buildings
- Longer thermal lengths in heat exchangers

One of the major drawbacks of current heat distribution technology is the embedded temperature error that occurs when no heat demands exist. At such times, supply temperature water needs to be by-passed into the low-temperature return pipe, causing considerable higher return temperatures. This happens because of supply temperature drop at a no flow situation. We refer to this as temperature degradation. In current distribution technology, the operational strategy is to mix supply and return water, we refer to this as temperature contamination and we consider this a bad utilisation of exergy. And especially so, since the situation will occur more hours of a year when buildings thermal performance increase. Thus, the extent of this problem issue will grow by time.

We suggest three-pipe distribution networks as a strategy to avoid temperature contamination. By doing so we introduce a second return pipe in the distribution network, this additional return (recirculation) pipe should only be used to at times when it avoid temperature contamination, as seen in Figure 1.

We suggest apartment substations to eliminate domestic hot water circulation in multi-family buildings. This facilitates control of flow separation into ordinary (delivery) return and the new recirculation return, since domestic hot water circulation is a constant source of delivery flow. Furthermore, due to temperature requirements of domestic hot water circulation with regard to the Legionella issue, it also a source of high return temperatures (at least when compared to the ideal of the 4GDH systems).

In addition to this, we suggest heat exchangers with increased thermal lengths in order to decrease the logarithmic mean temperature difference between flows in a heat exchanger, with the purpose to decrease temperature levels further.

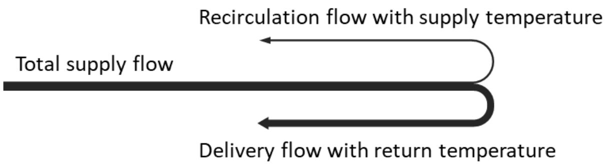

Figure 1. Denotes a conceptual depiction of the separation of total supply flow into a recirculation return flow and a delivery flow return.

In previous simulation work we have achieved results that indicate that these three changes achieve annual average return temperatures of around 20 °C for a small single-family house area, which is in line with ideal return temperatures of the 4GDH systems, as seen in Figure 2. Whereas, the ideal supply temperature is about 50 °C without requiring any auxiliary local heat supply. Various simulated annual average distribution temperatures from (Averfalk & Werner, 2018) are presented in Figure 3.

Simulation of heat losses, when comparing the situation in Figure 2, indicates that steady-state heat losses are equal. Currently, our research is still on a desk research level. However, we are interested to establish relationships with anyone that might be interested to take these ideas into a demonstration level project.

Figure 2. Presenting a standard configuration of twin-pipe (DN65 insulation series 3), to the left alongside with corresponding conceptualisation for a triple-pipe, to the right. The numbers are represented as annual averages temperatures for a single-family house area.

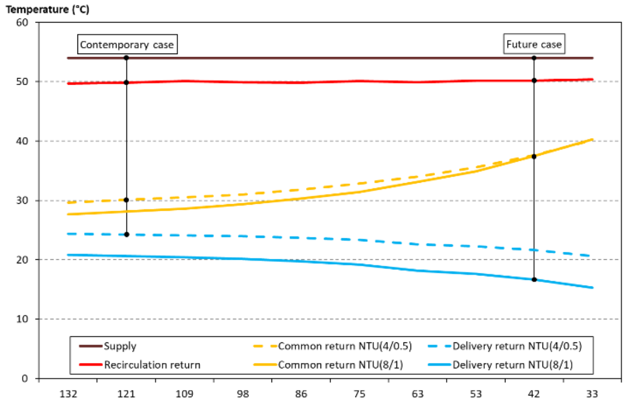

Figure 3. Annual simulation results regarding the case area temperature levels at the starting point to the distribution area. Horizontal axis displays the variation of heat power signatures, expressed as corresponding specific heat demands in kWh/m2, year. The two vertical lines point out two different simulation cases: one contemporary case with high heat demands to the left and one future case with low heat demands to the right. According to (Averfalk & Werner, 2018).

3 THE BENEFICIAL OUTCOME

The main economic value of lower annual average supply and return temperatures concerning solar district heating is higher conversion efficiencies in the solar collectors.

Other future economic benefits in 4GDH systems are:

- Lower heat distribution losses since lower temperatures than 3GDH systems
- Geothermal wells with higher capacities
- More easy access to low-temperature excess heat without heat pumps
- Higher COP in large heat pumps
- Higher recovery from flue gas condensation when using wet fuels, such as biomass and waste
- Higher power-to-heat ratios in steam CHP plants using biomass or waste
- Higher capacities in heat storages that also have access to high temperature heat sources

As an example, the economic difference for a solar collector field between different generations of heat distribution temperatures can be estimated in an analysis. The required input parameters for this analysis are the annual heat output with respect to mean fluid temperature, the installation cost for solar collectors, annual average network temperatures, the efficiency for the heat exchanger between the solar collector circuit, and the financial parameters of lifetime and hurdle rate.

The following input information has been used in the analysis:

- Annual heat output concerning Stockholm (Sweden) for Arcon-Sunmark HTHeatBOOST 35/10 solar collectors according to documentation in (Technical Research Institute of Sweden, 2016) and presented in Figure 4.

- Installation cost for solar collectors from Silkeborg, Denmark 2016 (225 euro/m^2 solar collector area).
- Annual average network temperatures of 86-47°C for a typical Swedish 3GDH system, according to (Frederiksen & Werner, 2013).
- Annual average network temperatures of 50-20°C for a new 4GDH system with novel heat distribution technology.
- Heat exchanger between the solar collectors and the district heating network with thermal length (NTU = number of thermal units) of 6.
- Annuities for lifetime of 20 years and 4% hurdle rate.

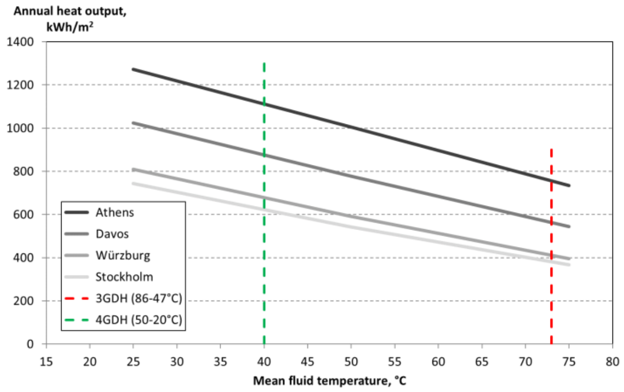

Figure 4. Annual heat output for four different locations from a typical solar collector with respect to mean fluid temperature, according to (Technical Research Institute of Sweden, 2016).

4 RESULTS

For the 3GDH system, the mean fluid temperature in the solar collector circuit becomes 73°C, since the temperature difference becomes 6.5°C from the thermal length of 6. The annual heat output from the solar collectors in Stockholm will be 379 kWh/m^2, according to Figure 4. The corresponding heat generation cost will be 43.7 euro/MWh from a collector investment of 594 euro per annual MWh.

For the 4GDH system, the mean fluid temperature in the solar collector circuit becomes 40°C, since the temperature difference becomes 5°C from the thermal length of 6. The annual heat output from the solar collectors in Stockholm will be 627 kWh/m^2, according to Figure 4. The corresponding heat generation cost will be 26.4 euro/MWh from a collector investment of 359 euro per annual MWh.

Hence, the considerable lower 4GDH temperatures increase the annual output from the solar collectors with 66 percent compared to current 3GDH temperatures. This gives a cost reduction of 17.3 euro/MWh or 40 percent. The cost gradient for a reduction of the return temperature with 27°C in a 4GDH system becomes then 0.64 euro/MWh,°C. The corresponding average cost gradient for Swedish 3GDH systems has been estimated to be about 0.13 euro/MWh,°C according to (Frederiksen & Werner, 2013). Hereby, solar collectors are five times more cost sensitive than traditional heat supply in district heating systems. This is an illustrative example of the main driving force for implementation of 4GDH systems in areas with new buildings.

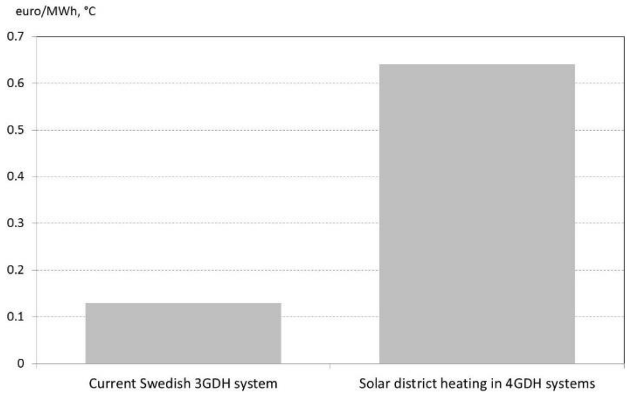

Figure 5. Examples of cost gradients for lower heat supply costs at lower return temperatures for 3GDH system based on conventional heat supply and 4GDH system based on solar district heating.

The total cost reduction of 17.3 euro/MWh obtained from the combination of solar district heating and lower heat distribution temperatures is considerable when comparing with the average price of district heating in Europe that is about 65-70 euro/MWh, according to (Werner, 2016).

The estimated cost reduction has also about the same magnitude as the total annual capital cost for distribution pipes in a district heating system. This cost can be estimated to be 14.7 euro/MWh for a distribution network with an average investment cost of 400 euro/m and linear heat density of 2 MWh/m.

5 DISCUSSION

This short analysis has been performed by comparing the novel heat distribution concept with current heat distribution temperatures in Swedish district heating systems. Many district heating systems in Europa apply higher temperatures (Averfalk et al., 2017). Hence, the identified benefit with the novel heat distribution technology will be higher when comparing with these higher network temperatures.

On the other hand, network temperatures are somewhat lower in Denmark than in Sweden (Gong & Werner, 2015). In these cases, the expected benefit with the novel heat distribution technology will be somewhat lower.

6 CONCLUSIONS

The following three main conclusions can be obtained from this short analysis:

- High heat distribution temperatures in current European district heating systems are a major barrier for the competitiveness of solar district heating.
- Considerable less solar collector area is required when the novel heat distribution technology with lower network temperatures are applied in new district heating systems.
- Solar district heating has a cost gradient for lower temperatures between 3GDH and 4GDH systems that is five times higher than the average cost gradient for current Swedish 3GDH systems.

7 REFERENCES

Averfalk, H., & Werner, S. (2018). Novel low temperature heat distribution technology. *Energy, 145*, 526-539. doi:https://doi.org/10.1016/j.energy.2017.12.157

Averfalk, H., Werner, S., Felsmann, C., Rühling, K., Wiltshire, R., Svendsen, S., . . . Quiquerez, L. (2017). *Transformation Roadmap from High to Low Temperature District Heating Systems. IEA-DHC TC annex 11*. Retrieved from http://www.iea-dhc.org/index.php?eID=tx_nawsecuredl&u=103&g=3&t=1509201202&hash=8e4700a1d635396eaf8e544945db6d89d735e567&file=fileadmin/documents/Annex_XI/IEA-DHC-Annex_XI_Transformation_Roadmap_Final_Report_April_30-2017.pdf

European Union. (2009). Directive 2009/28/EC of the European Parliament and of the Council of 23 April 2009 on the promotion of the use of energy from renewable sources and amending and subsequently repealing Directives 2001/77/EC and 2003/30/EC. *Official Journal of the European Union, 5*, 2009.

European Union. (2010). Directive 2010/31/EU of the European Parliament and of the Council of 19 May 2010 on the energy performance of buildings (recast). *Official Journal of the European Union, 18*(06), 2010.

Frederiksen, S., & Werner, S. (2013). *District Heating and Cooling*. Lund: Studentlitteratur AB.

Gong, M., & Werner, S. (2015). Exergy analysis of network temperature levels in Swedish and Danish district heating systems. *Renewable Energy, 84*, 106-113. doi:http://dx.doi.org/10.1016/j.renene.2015.06.001

Lund, H., Werner, S., Wiltshire, R., Svendsen, S., Thorsen, J. E., Hvelplund, F., & Mathiesen, B. V. (2014). 4th Generation District Heating (4GDH): Integrating smart thermal grids into future sustainable energy systems. *Energy, 68*, 1-11. doi:http://dx.doi.org/10.1016/j.energy.2014.02.089

Technical Research Institute of Sweden. (2016). *Solar Keymark Certificate: No. SP SC0841-14 for Arcon-Sunmark HTHEATboost 35/10*. Retrieved from http://www.estif.org/solarkeymark/Links/Internal_links/SP/SC0841-14.pdf

Werner, S. (2016). *European District Heating Price Series. Energiforsk-Fjärrsyn report no. 2016:316*. Retrieved from http://www.energiforsk.se/program/fjarrsyn/rapporter/european-district-heating-price-series/

CHALLENGES OF A CENTRAL OR DECENTRALIZED SOLAR SUPPLY OF SOLAR DISTRICT HEATING GRIDS

Markus Rabensteiner[a], Peter Schatte[b], Wolfgang Leitner[c] and Alois Kraußler[d]

[a] 4ward Energy Research GmbH, Headquarters, Reininghausstraße 13A, 8020 Graz, Austria, +43 (0)664 88 251 830, markus.rabensteiner@4wardenergy.at

[b] Hoval GmbH, Holzinnovationszentrum 1a, 8740 Zeltweg, Austria, +43 (0)664 600 555 311, peter.schatte@hoval.at

[c] Hoval GmbH, Holzinnovationszentrum 1a, 8740 Zeltweg, Austria, +43 (0)50 3655 341, wolfgang.leitner@hoval.at

[d] 4ward Energy Research GmbH, Site Vorau, Impulszentrum 1, 8250 Vorau, Austria, +43 (0)664 88 500 339, alois.kraussler@4wardenergy.at

Abstract – Energy management systems that guarantee a system-wide control of district heating systems are already state of the art. However, a bidirectional heat transfer station (for heat supply and uptake) in combination with an intelligent control strategy for the entire district heating system still has to be developed. While in a laboratory test, the properties of a prosumer are examined, a numerical model is used to investigate the effects of several prosumer on the entire district heating system. The simulation model, consisting of two parts, allows to investigate the bidirectional heat transfer station. The first model part depicts the primary side of the district heating system. Data from a real-life medium-sized district heating system is used as reference. The second part of the model forms the bidirectional heat transfer station and is individually set for each prosumer. A secondary storage exchanges energy with the decentralized heat source, the district heating system and the heating system of the consumer. The numerical model allows an energetic and economic investigation of district heating systems containing several prosumers. Hydraulic problems such as flow reversals can also be investigated. The simulation model has been validated on the basis of laboratory experiments.

1. INTRODUCTION

Local and district heating is an environmentally friendly heat supply by efficient energy generation plants, the use of combined heat and power and the use of residual and waste heat. About 24 % of all apartments in Austria are heated with local or district heating (FGW, 2016). However, operators (especially of smaller and medium-sized grids) are faced with economic challenges concerning decreasing heat demand due to better building standards (Averfalk and Werner, 2017; Lund et al., 2010). The exploitation of all optimization potentials by means of efficiency improvement measures (heating plant, grid and consumer), as well as the use of renewable heat is becoming increasingly important. The individual heat transfer stations, which form the link between district heat suppliers and end consumers, are of particular importance for an optimal district heating system. The following two points are essential for an efficient and economic supply:

- Control and operating strategies that exploit all optimization potentials, integrate favorable renewable heat sources and enable a high degree of utilization over year-round operating concepts.
- Development of a multifunctional heat transfer station which can be integrated into an optimized control strategy.

The development of bidirectional heat transfer stations in combination with intelligent control strategies for entire district heating systems is to be carried out in the course of the research project *MULTI-transfer* (Rabensteiner et al., 2017). The systems are studied both for new buildings as well as for the stock. A detailed consideration of two application cases on the secondary side is carried out:

- Solarthermics
- Waste heat integration by heat pumps (e.g. from refrigeration plants)

2. HYDRAULIC INTEGRATION

Measures on a single point in the grid (e.g. on the secondary side) can have effects on the entire grid. Therefore, the entire system has to be considered when a bidirectional heat transfer station is installed. The pressure in the district heating line is very important. Similar pressures on the primary and secondary side are advantageous. The integration of prosumers with certain infeed variants becomes more difficult at higher pressures in the primary circuit. The low flow in summer can lead to hydraulic problems when integrating prosumers. Today, there is almost no experience in the hydraulic design of such systems.

The integration of decentralized heat generators into the grid can be carried out directly, hydraulic separated by means of a heat exchanger or hydraulic decoupled via a hydraulic separator or with a decentralized energy storage. Prerequisites for a direct connection are that the decentralized heat source can withstand the high-pressure level and that only water is used. A hydraulic separation is always required for the integration of solarthermics and refrigeration systems.

The location of the prosumer in the district heating system is important. The stabilization of the system pressure is of utmost importance and allows easier feeding into the district heating system. Especially in the case of pipes made of steel, the temperature in the system must also be kept as constant as possible to avoid fatigue fractures due to thermal stresses (Kim et al., 2016). The location can limit the infeed of prosumers in already existing systems. In individual cases, the water column may even come to a standstill, particularly in cases of prosumer installations nearby to strand ends. According to Streicher (2005) there are basically three technical possibilities when feeding heat into existing district heating systems (compare Fig. 1):

- Flow from the return to the forerun
- Return rise
- Forerun rise

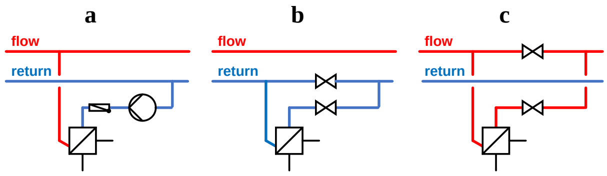

Fig. 1: *Hydraulic integration of decentralized heat suppliers: Flow from the return to the forerun (a), Return rise (b), Forerun rise (c)*

The abstraction of the heat transfer medium from the return line and the re-feed into the forerun line (Fig. 1a) requires a high pumping power because the differential pressure between forerun and return line has to be overcome. The small flow and the high differential pressure (up to 1 bar) could be problematic during infeed. There are only a limited number of pump manufacturers for such applications. The return temperature remains constant during infeed using this hydraulic integration variant.

The abstraction and re-feeding of the heat transfer medium takes place in the return line using the return rise (Fig. 1b). The pump energy is provided by the network pumps or by own heat exchanger pumps. A pressure-reducing valve must be provided in the return line in the first case in order to be able to control the flow through the heat exchanger. The heat exchanger pumps overcome the pressure losses of the heat exchanger, the control valve and the connecting lines. The efficiency of the centralized heat source is slightly reduced when a condensing boiler is used. Only additional energy can be introduced into the district heating system. The primary heat generator cannot be completely replaced. A return rise with the associated higher return temperatures is not advantageous in many smaller grids. However, a return rise can be quite useful in the case of relatively high temperature levels.

The heat transfer medium is abstracted from the forerun, passed through the bidirectional heat transfer station (heat exchanger) and fed back into the forerun, when using the forerun rise (Fig. 1c). As with the return rise, a pressure-reducing valve has to be installed into the district heating line – in this case, however, not in the return but in the forerun line. The pressure-reducing valve can be dispensed by installing a heat exchanger pump. The grid losses increase due to the higher grid temperature. The efficiency of the primary heat generator remains unchanged.

3. BIDIRECTIONAL HEAT TRANSFER STATION

Fig. 2 shows the hydraulic scheme of the bidirectional heat transfer station. This interconnection enables that heat can both be obtained from the grid and be fed into the grid by all three variants described above. 4 connection points are necessary at the district heating line. A speed-controlled pump is used on the primary side of the transfer station. Therefore, no pressure reducing valves are necessary in the corresponding district heating line. 4 and 2 three-way valves are installed on the primary and secondary side, respectively. By actuating these valves and switching on and off the corresponding pumps, various operating modes can be set. The associated interconnections can be seen in Fig. 3.

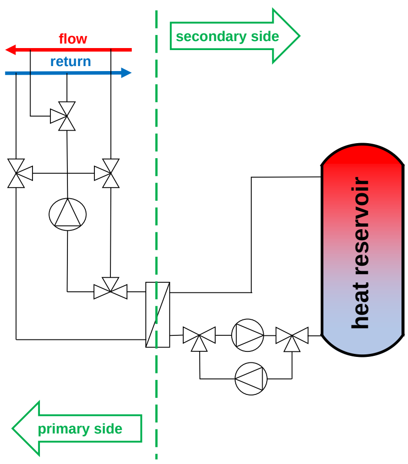

Fig. 2: *Hydraulic scheme of the bidirectional heat transfer station*

Initial cost calculations already show that this heat transfer station is a theoretical approach. The costs for the transfer station which allows all infeed variants are high. An installation is also complicated by the fact that 4 connection points on the district heating line are necessary. This means that additional lines are necessary at existing plants. The complexity is reduced for transfer stations that can only perform one infeed variant. Regardless of the chosen variant, however, at least 3 connection points are necessary, so that a new connection is inevitable for existing connections. The variant with the flow from the return to the forerun alone could preserve the two-line system.

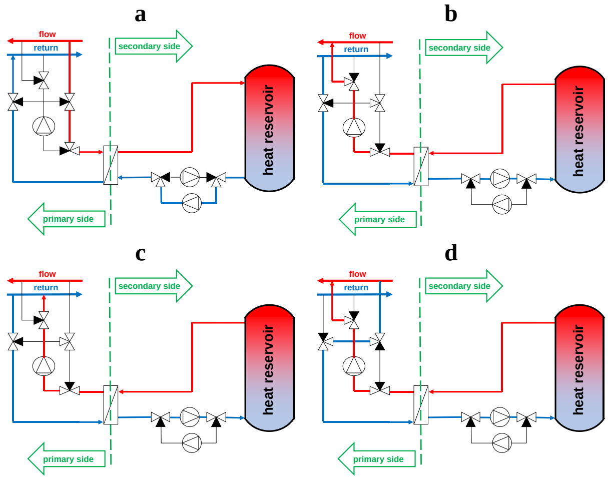

Fig. 3: *Switching of the bidirectional heat transfer station: Heat absorption from the grid (a), Flow from the return to the forerun (b), Return rise (c), Forerun rise (d)*

4. NUMERICAL MODEL

While in a laboratory test, the properties of a prosumer are examined, a numerical model is used to investigate the effects of several prosumer on the entire district heating system. The simulation model consists of two parts. The first model part depicts the primary side of the district heating system as detailed as possible, including the central heat source and the heat distribution system. Data from a real-life medium-sized district heating system is used as reference.

The second model (Fig. 4) forms the bidirectional heat transfer station and is individually set for each consumer/prosumer. The model considers stratified storages located at different consumers/prosumers. The model can be used to predict the time of heat input (into the district heating system) and the temperature level of this heat.

The illustrated simulation model in Fig. 4 calculates a prosumer with a solar thermal system. The model consists of different blocks. In the "Consumer" block, the data from the respective consumer of the reference district heating system are read in. Since a primary-side solar thermal system has already been installed at the heating plant on the reference district heating grid, real-time measured global radiation data can be acquired in the block "Solar data". The "Solarthermics" block calculates the available solar heat. The collector area was calculated according to the design diagram for solar collector surfaces for hot water preparation and heating support from Hoval GmbH. A solar coverage of about 25 % has been assumed. The size of the secondary storage was designed using the same diagram. The “Stratified storage” block calculates the

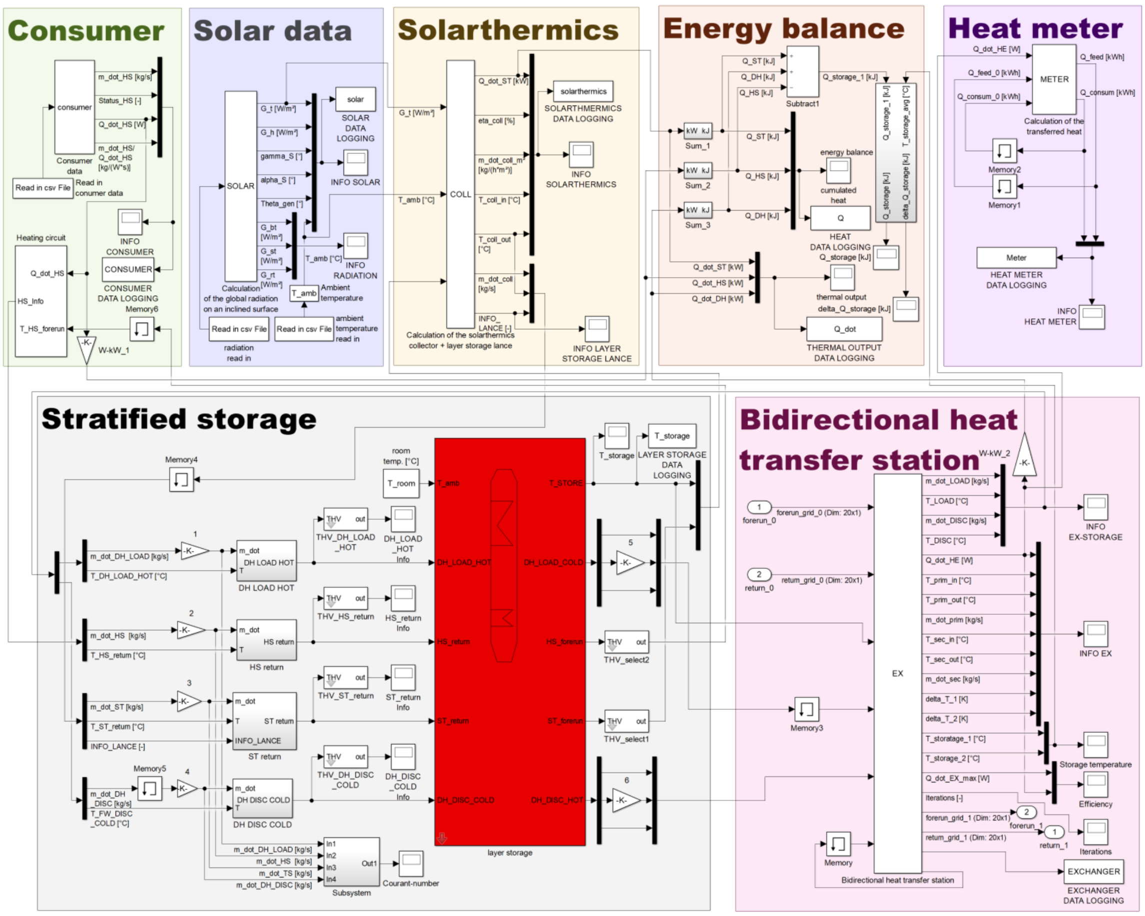

Fig. 4: *Simulation model of the bidirectional heat transfer station in Matlab/Simulink*

thermal stratification according to Eq. 1. The block called “Bidirectional heat transfer station” is the direct link between the grid and the prosumer and determines the operating mode based on the temperature in the storage and in the grid.

The two model parts allow an energetic and economical investigation of district heating systems with a large number of consumers/prosumers. This is enabled by combining the models. The primary side model receives data of the prosumers' strategy from the second model. Hydraulic problems such as flow reversals can also be investigated.

4.1 Control loops

The control loops of the simulation model are described with reference to Fig. 5. The heating circuit pump is controlled via the return temperature. A return temperature of 30 °C is assumed in the standard case. The heat output is taken from consumer data from the reference district heating system.

Three different operating options of the solar thermal system can be set. In the low-flow mode, the mass flow is 15 kg/(m²·h) in terms of the collector area. A mass flow of 40 kg/(m²·h) is set in the high-flow mode. In the matched-flow mode, the mass flow can vary between 1 and 50 kg/(m²·h). The mass flow is adjusted in 1 kg/(m²·h) steps in the just mentioned operation mode. The stratified storage is loaded via a stratified storage lance. Thereby, the return from the collector into the stratified storage can take place at different levels, but not at the same time. Normally, level 6 is fed. In the case of the matched-flow mode, the pump speed is controlled in such a way that the temperature of the feed medium corresponds to the storage temperature at level 6. If the mass flow rises above 50 kg/(m²·h), the inflow occurs one level higher (level 7). The higher temperature in the level above results in reducing pump speed and thus the volume flow is sinking. The infeed takes place up to level 11 with this control strategy. In the case of extreme solar irradiation, an injection at elevated temperatures can be carried out at the highest level. In the low- and high-flow mode, a stratified storage lance is also installed. The only difference between these variants is that the temperature cannot be adjusted to the respective level. This results in a slight disturbance in the thermal stratification.

The key factor as to whether the storage is charged or discharged is its temperature. The user can determine which temperature is to be used as the control variable for charging and discharging. The following selection options are available for the reference temperature:

- Average temperature in the storage
- Temperature of the lowest layer in the storage
- Temperature of the top layer in the storage

The corresponding three-way valves are activated, and the pump is switched on between heat exchanger and stratified storage if the reference temperature reaches a present value. During discharge, the corresponding reference temperature in the grid is used in addition to the reference temperature in the stratified storage. If the reference temperature in the stratified storage rises above a preset value, the storage temperature at level 11 is compared with the reference temperature in the grid. The reference temperature in the grid is the return temperature when using the return rise. Only when the highest storage

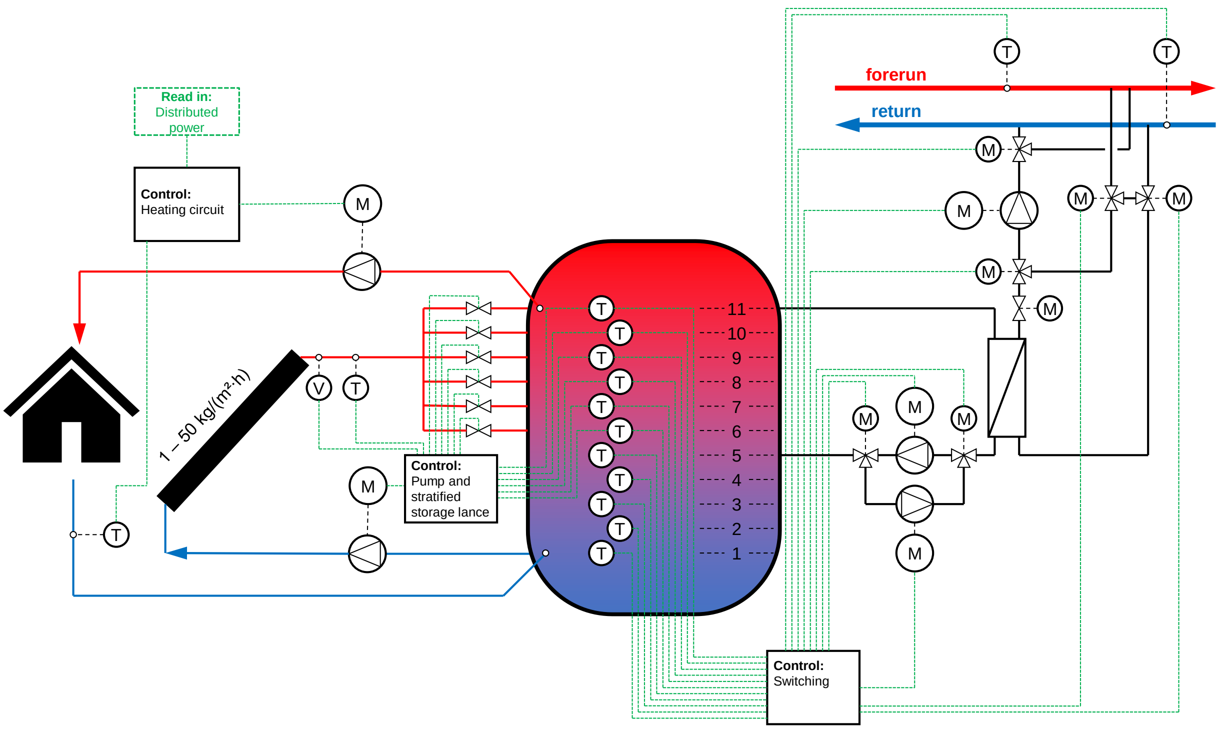

Fig. 5: *Control loops of the simulation model*

temperature (level 11) exceeds the return temperature in the grid, the heat flow from the prosumer towards the grid. For a possible infeed, the temperature in the uppermost layer of the storage must be significantly higher during the forerun rise. The forerun temperature of the grid is used as reference in this case. When using the infeed variant with the flow from the return to the forerun, the return temperature of the district heating line is also used as reference. In this case, indeed, it must be taken into account that, under certain circumstances, the resulting forerun temperature of the grid (after injection) decreases when the top storage temperature is lower than the forerun temperature of the grid (before feeding). However, there is nevertheless a heat flow from the prosumer to the grid, since this infeed variant increases the flow.

The loading of the storage occurs when the reference temperature in the storage falls below a pre-set value and the supply temperature in the grid is higher than the temperature in the uppermost layer of the stratified storage. For simulation purposes, a similar flow on the primary and secondary side is assumed. The maximum flow is determined either by the maximum flow rate of 2 m/s or by the maximum heat transfer capacity of the already installed heat transfer station of the individual consumers in the reference district heating system.

4.2 Influence of the reference temperature

For each of the following examples, a return rise as infeed variant is assumed. Charging and discharging takes place between 52 and 53 °C and 62 and 63 °C, respectively. The three examples differ only in the type of reference temperature. While in the first case, the average temperature in the storage is used, in the second and third case, the uppermost and the lowest temperature in the storage are used as reference.

Before describing the series of measurements, the mathematical model of thermal stratification will be explained briefly. The energy balance for each node of the stratified storage is calculated according to Eq. 1 (Solar-Institut Juelich, 1999).

$$\rho \cdot c_p \cdot \frac{dT_{node}}{dt} = \frac{(U \cdot A)_{loss}}{V_{node}} \cdot (T_{amb} - T_{node}) + \frac{\lambda_{eff}}{dh^2} \cdot \left(T_{node_{above}} + T_{node_{below}} - 2 \cdot T_{node}\right) + \frac{\dot{m}_{up} \cdot c_p}{V_{node}} \cdot \left(T_{node_{below}} - T_{node}\right) + \frac{\dot{m}_{down} \cdot c_p}{V_{node}} \cdot \left(T_{node_{above}} - T_{node}\right) + \frac{(U \cdot A)_{hx}}{V_{node}} \cdot (T_{hx} - T_{node}) \qquad \textbf{\textit{Eq. 1}}$$

The differences of the reference temperatures in the stratified storage and their effects on the operation of the bidirectional heat transfer station are listed below. Fig. 6 to Fig. 9 show the differences for a simulated day.

A thermal stratification is formed in the upper region of the storage when using the average storage temperature as reference (compare Fig. 6). There is no thermal stratification formation in the lower four levels. On the one hand, this is explained by the fact that charging and discharging via the grid takes only place between level 5 and 11.

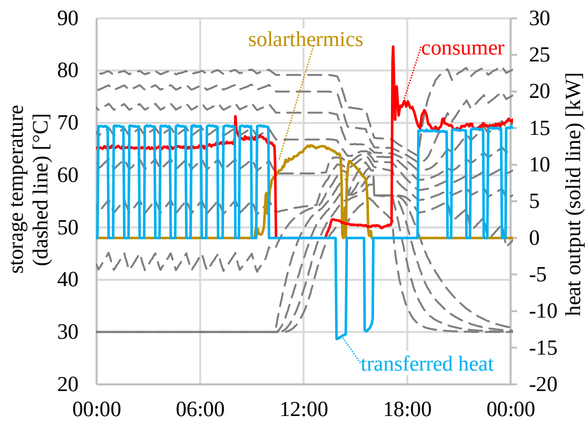

Fig. 6: *Storage temperature and heat output when using the average storage temperature as reference*

On the other hand, the mathematical model (Eq. 1) of the stratified storage simulation does not allow the consideration of temporal thermal stratification formation. During night and morning, the storage is periodically charged by the grid because of the constant heat transfer to the heating system (red line). A plus-sign in front of the transferred heat means that heat flows from the grid to the storage on the secondary side. Induced by solar yield, the average storage temperature rises, starting at about 10 am, so that no loading through the grid is required anymore. In addition, the heating system switches off immediately. The water is taken from the bottom layer during loading via the solar thermal system. A thermal stratification in the lower part of the storage is formed. The average storage temperature of 63 °C is exceeded at 2 pm. The transfer station switches to the infeed operation. When heat is feed into the district heating system, there is an increasing temperature drop with increasing storage height. The average storage temperature drops during discharging. After 35 minutes, the average storage temperature of 62 °C is already exceeded, resulting in termination of the discharge cycle. The short discharge cycle can be explained by the fact that discharging by heat transfer to the grid with 13.5 kW is considerably higher than the current solar yield (Shortly after 2 pm, there is a significant drop in the solar yield). A second discharge cycle starts at 3:30 pm. This leads to an increasing convergence of the lowest and highest storage temperature. In the evening, the solar yield drops back to zero and the heat absorption from the heating systems increases again. The average storage temperature decreases afterwards. A storage temperature of 52 °C is exceeded at about 6:30 pm and the storage has to be charged via the district heating grid. Due to the heating mode, return water with 30 °C reaches the lower part of the storage. Thus, the thermal stratification disappears again in this area.

Fig. 7 shows the system behavior when using the temperature of the uppermost layer as reference. The system is very sensitive. The charging cycles increase the temperature in the uppermost layer significantly, so that the reference value of 53 °C is reached quickly. Due to the short charging cycles, almost no thermal stratification occurs in the entire storage. The stratification arises only through the solar yield. In this variant, no discharge takes place via the grid for the day under investigation. After completion of the solar yield, the thermal stratification collapses again. The subsequent charging cycles are again very short. The storage capacity is only minimally used in this variant.

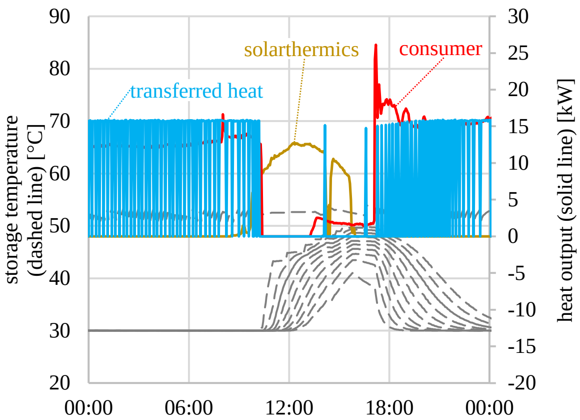

Fig. 7: *Storage temperature and transferred heat when using the temperature of the highest layer as reference*

Fig. 9 shows the system behavior when the temperature of the lowest layer in the stratified storage is used as reference. As it can be seen, the model can only adequately map this case. Since charging and discharging via the district heating system does not affect the lowest layer, the present reference temperature of the grid is the decisive factor for the operating state. The temperature in the uppermost layers corresponds approximately to the forerun temperature of the grid.

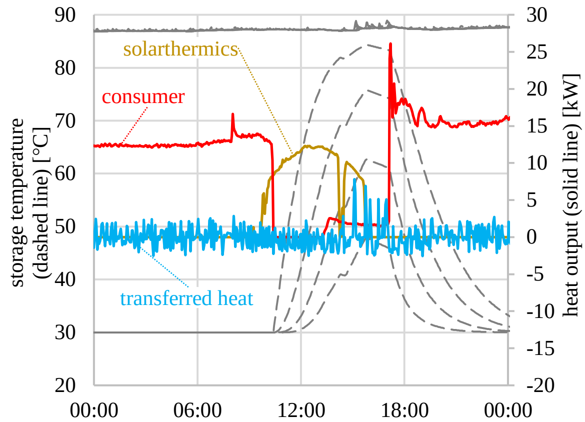

Fig. 9: *Storage temperature and heat output when using the temperature of the lowest layer as reference*

There is always a change from short charging and discharging cycles. Usually it should come to no discharge. Apparently, also short charging cycles occur when the flow temperature is below the temperature of the uppermost layer of the storage. Accordingly, it comes in a supposed charging cycle to a cursive discharge of the storage. Thus, in fact, a discharge of the storage occurs during a planned charging cycle.

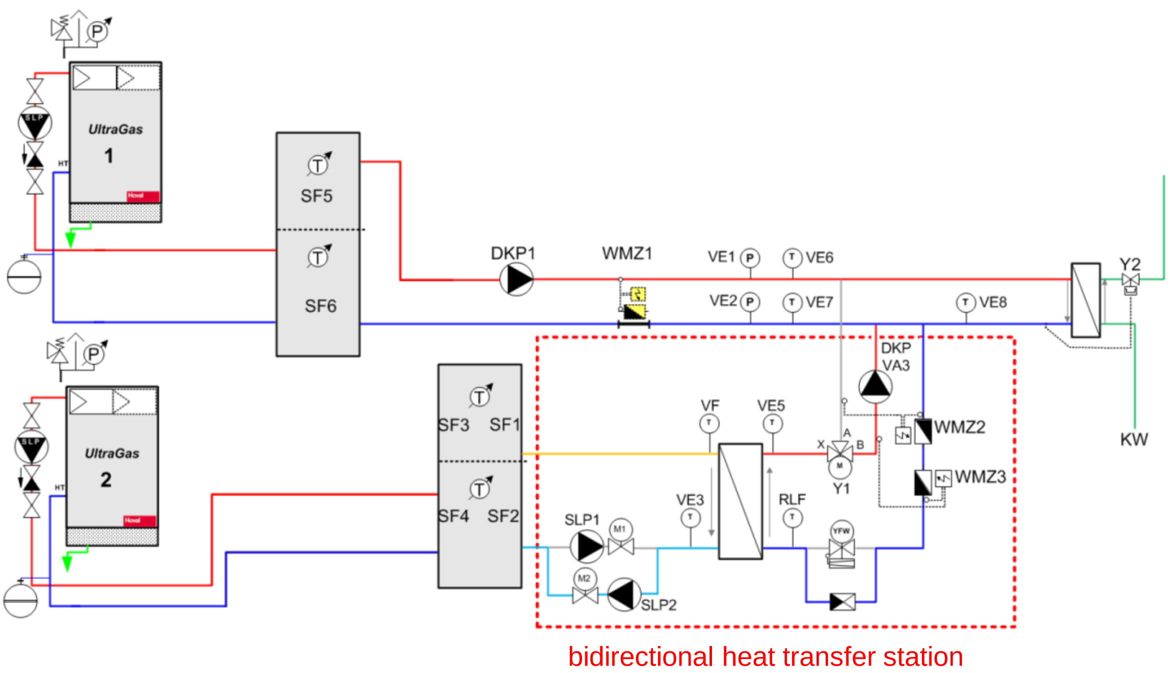

Fig. 8: *Laboratory test of the bidirectional heat transfer station*

4.3 Model validation by laboratory tests

The laboratory setup is shown schematically in Fig. 8. The central heat source of the district heating grid is simulated with a gas condensing boiler (UltraGas®, 50 kW). This boiler supplies a buffer tank. The pump DKP1 assumes the function of the network pump. Downstream consumers and prosumers are simulated by an adjustable heat exchanger. In addition to the heat absorption from the grid, the installed heat transfer station allows also an infeed by return rise. To overcome the pressure loss in the heat transfer station, the pump DKP VA3 is installed. Heat generation on the secondary side by the prosumer is also simulated by a gas condensing boiler (UltraGas®, 50 kW).

With regard to the simulation, the following changes occur for the laboratory operation:

- The loading of the stratified storage tank does not take place via a stratified storage lance.
- A discharge of the stratified storage tank can only take place via the grid. An extraction by the heating system was not included.

Fig. 10 shows the validation results for the plate heat exchanger. The dashed lines in this diagram and in the following indicate the measured values in the laboratory. The solid lines indicate simulation results.

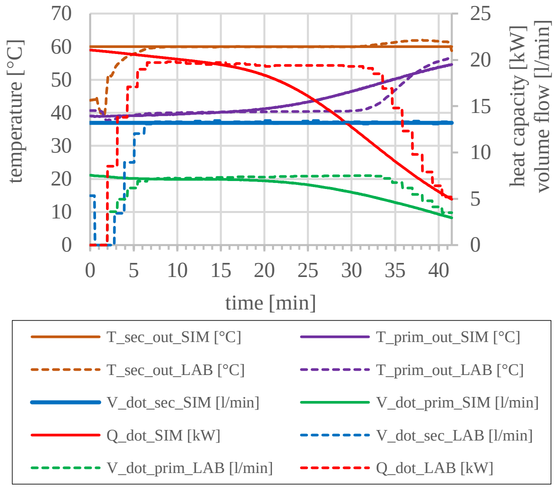

Fig. 10: *Validation of the heat transfer station (without consideration of inertia)*

The inertia of the system is not considered in Fig. 10. Effects of this neglection can be seen most clearly in the temperature difference of the secondary outlet temperature between simulation and laboratory in the first 5 minutes. While in the simulation over the entire loading cycle, the charge temperature is constantly 60 °C, the charge temperature in the laboratory test reaches this value only after 8 minutes. The reason for this behavior is the cooling of the line between heat transfer station and buffer storage. This neglection also leads to the fact that already at the beginning of the loading cycle, the transferred heat output has a maximum in the simulation. After that, the power drops. Unlike in the laboratory, the power decreases faster, so that in the study area, the amount of transferred heat is about the same size. Also in the simulation, there is a volume flow from the beginning on both the primary and secondary sides.

Taking into account the inertia of the heat transfer station, a line with a certain length was assumed between the transfer station and the secondary buffer. Thus, the cooling in the intermediate circuit could be well imitated (see Fig. 11 and Fig. 12).

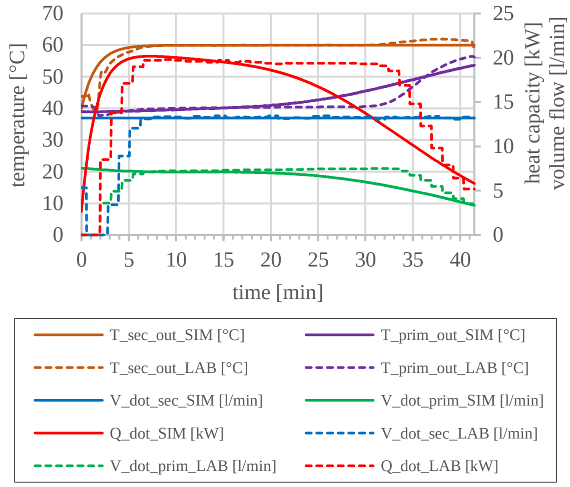

Fig. 11: *Validation of the heat transfer station (with consideration of inertia)*

For the comparison of the stratified storage temperatures in the buffer storage, the temperatures of the 11 nodes of the simulated stratified storage were used which are close to the installed temperature sensors. The uppermost storage temperature in the simulation fits very well with the measurement results, as shown in Fig. 12. With decreasing height, however, the deviation between simulation and measurement becomes larger. This can be explained by the fact that the transmitted heat output in the simulation is significantly higher in the first 5 minutes.

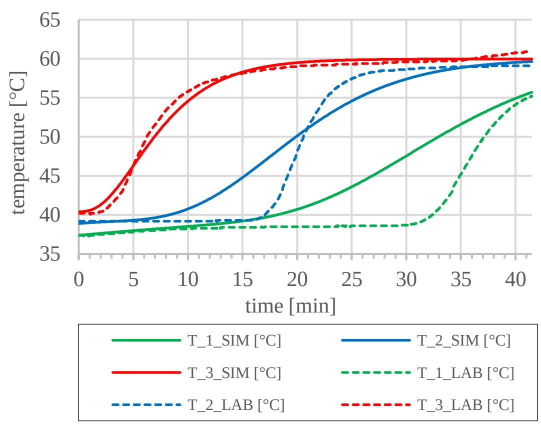

Fig. 12: *Validation of the buffer storage (with consideration of inertia)*

4.4 Simulation of strands

The installation of the model described above in certain areas of the district heating grid can endanger the security of supply of certain consumers and prosumers. Particularly in the area of strand ends, there is a potential danger for downstream consumers.

For example, when using the return rise, increased return temperatures may occur during infeed. This happens when the prosumer feeds and the downstream consumption is low at the same time. The risk of this scenario is particularly high, when solar thermal plants are installed on the prosumer sides. Due to the low demand of the downstream consumers/prosumers, the corresponding flow in the forerun and return line is low. A heat input by return rise has a huge impact on the return temperature. Prosumers which are located upstream on the same strand are confronted in this case with a very high return temperature, so that they can hardly feed-in at the same time with the same variant. In the case of forerun rise, however, the downstream prosumers are more affected through the high forerun temperature. An overall regulation of the consumers and prosumers in the line can solve this problem. In addition, a bypass at the heat transfer station of the last consumer in the strand can defuse this problem.

Problems may also arise during feed-in on strand ends by using the variant with the flow from the return to the forerun. This problem occurs when the prosumer is fed in and the temperature in the secondary storage is insufficient, thereby lowering the forerun temperature for the downstream consumers. Thus, under certain circumstances, the security of supply can no longer be guaranteed. Therefore, it is advisable to feed in only when the temperature of the uppermost layer in the stratified storage has exceeded the current flow temperature.

5. CONCLUSIONS

The numerical simulation of a bidirectional heat transfer station in Matlab/Simulink is explained in the present research work. The simulation model consists of two parts and takes into account both the primary side of the district heating grid and the secondary side with the decentralized heat source. The simulation model of the primary side was validated on the basis of measured data from the consumers, the boiler house and the grid points with the smallest differential pressure between forerun and return of a reference grid.

In a first sensitivity analysis, which is very important for the later validation by the laboratory measurements, the effects of different control parameters were described. It was shown that the average storage temperature is best used as a reference.

The validation of the simulation model of the bidirectional heat transfer station was carried out by means of laboratory tests. It turns out that the simulation model can reproduce the measurements relatively accurately. For faster load changes, however, the inertia of the system must be taken into account, which was carried out during the validation.

In the simulation of strands with several prosumers and consumers, problems have been raised that will be solvable by a cross-system control alone.

NOMENCLATURE

A_{loss}	Surface area for losses of one storage node	[m²]
λ_{eff}	Effective axial thermal conductivity	[W/(m·K)]
c_p	Heat capacity of fluid	[J/(kg·K)]
dh	Distance between two nodes	[m]
$\dot{m}_{down}$ $\dot{m}_{up}$	Vertical mass flow rate	[kg/s]
ρ	Density	[kg/m³]
T	Temperature	[K]
t	Time	[s]
U_{loss}	Heat loss coefficient	[W/(m²·K)]
V_{node}	Node volume	[m³]

REFERENCES

Averfalk, H., Werner, S., 2017. Essential improvements in future district heating grids. Energy Procedia 116, pp. 217-225

FGW, 2016. Zahlenspiegel – Erdgas und Fernwärme in Österreich. http://www.fernwaerme.at/media/uploads/misc/zahlenspiegel_2016.pdf

Kim, J., Kim, J., Cho, C., 2016. Experimental study for the reinforcement of district heating pipe. Transactions of the Korean Society of Mechanical Engineers A, Vol. 40, No. 3, pp. 245-252.

Lund, H., Möller, B., Mathiesen, B.V., Dyrelund, A., 2010. The role of district heating in future renewable energy systems, Energy 35, pp. 1381-1390.

Rabensteiner, M., Kraußler, A., Hummer, E., 2017. Simulation of bidirectional heat transfer stations in district heating grids. Book of abstracts: 3rd International Conference on Smart Energy Systems and 4th Generation District Heating.

Solar-Institut Juelich, 1999. CARNOT Blockset Version 1.0 – User´s Guide.

Streicher, W., 2005. Dezentrale Einspeisung von Erneuerbaren Energieträgern in Fernwärmenetze und Möglichkeiten der Biomasse KWK. Erneuerbare Energien für bestehende Fernwärmenetze, Graz, Austria, 20.04.2005.

EFFECTS ON DECENTRALIZED FEED-IN INTO DISTRICT HEATING NETWORKS – A SIMULATION STUDY

Sven Paulick and **Karin Rühling**
Institute of Power Engineering, Professorship of Building Energy Systems and Heat Supply,
Technische Universität Dresden, Dresden, 01062, Germany, +49-351 / 463-34440, sven.paulick@tu-dresden.de

Abstract – The effects of decentralized feed-in into district heating (DH) networks are investigated as part of the research project "Prognose der Auswirkungen dezentraler Einbindung von Wärme aus erneuerbaren Energien und anderen Wärmeerzeugern in Fernwärmenetze" (*DELFIN*). The study focuses on the thermo-hydraulic impact with the resulting requirements for components like pumps, pressure maintenance, pipes as well as on the net control strategy. The aim is to identify allowed locations, the scale and temperature level for feed-in stations in terms of solar thermal or combined heat and power (CHP) technology. Furthermore, the necessity of heat storages and their operation mode as part of the network regulation is considered. Finally, conclusions will be made about the overall efficiency of the district heating network according to feed-in and operating mode.

1. INTRODUCTION

This paper presents the latest results of the research project "Prognose der Auswirkungen dezentraler Einbindung von Wärme aus erneuerbaren Energien und anderen Wärmeerzeugern in Fernwärmenetze"[1] and is based on the previous research project *DEZENTRAL* (Heymann, Rühling, Felsmann, 2017). The project partners are *Solites*[2] and *AGFW*[3].

The results of the project *DEZENTRAL* have shown in detail, which effects can result with feed-in of decentralized heat into district heating networks. Flow reversal in part of the net branches, moving supply frontier or full supply of the decentralized producers can occur. The current project focusses on the impact in the network itself according to thermo-hydraulic effects and the consequent, alternating thermal stress of the pipes. Moreover, statements will be made about conditions when feed-in should be avoided according to network stability. Finally requirements for the feed-in pumps of the decentralized producers concerning to the location and local conditions in the network will be derived. A further aspect is the integration of a central thermal storage in the network. To prevent stagnation of installed solar thermal plants, the storage operation shall lead to a network load relief to decrease the stress in the network. Additionally, the following unloading can lead to a longer offline period of the central heat producer.

The simulation study focusses on two representative district heating networks with different structure and dimension to generalise the results for a wide field of application. The decentralized heat producers (DCP) are considered as solar thermal plants and combined heat and power units (CHP). A variation of decentralized heat producers according to size and position is part of the investigation as well as different operation modes of the central heat storage. Combined with two different weather locations the simulation study will have a large spread of results to derive.

This paper presents the status of the simulation study as well as the realization of consumer, decentralized producer and storage modeling. The first simulation results of both networks are presented including first insights in the flow conditions. Furthermore, the integration of the storage in several operation modes will be discussed.

2. SIMULATION

2.1 Simulation Tools

The simulation study is realized by a coupling of two different simulation tools. For the thermo-hydraulic simulation of the district heating network, TRNSYS-TUD is used, as an in-house development on base of the Transient System Simulation Tool (TRNSYS). The advantage of TRNSYS-TUD is the developed thermo-hydraulic solver, adopted for the usage of district heating networks. It leads, especially for larger mashed networks, to adequate time taken for the simulation. The modeling of the consumer, decentralized heat producer and the storage is realized in the modeling language Modelica. The reason to choose Modelica as a second simulation tool is on the one hand the possibility to read in large MATLAB-Files and on the other hand diverse functionalities for dynamic simulation. The coupling of both simulation tools is realized with the Functional Mock-up Interface (FMI), a tool independent standard for co-simulation (Blochwitz, Otter, et al., 2011). The coupling works on a so-called Master-Slave-Technology. The models of the simulation tools represent the slaves, whereas the master controls the

---

[1] DELFIN: Founded by Federal Ministry for Economic Affairs an Energy (FKZ: 03ET1358B)
[2] Steinbeis Research Institute for Solar and Sustainable Thermal Energy Systems
[3] AGFW - Der Energieeffizienzverband für Wärme, Kälte und KWK e.V.

data exchange between the slaves between simulations time steps. Figure 1 shows the principle for the here mentioned simulation study. The used FMI-Master is an in-house development that enables the communication to TRNSYS-TUD.

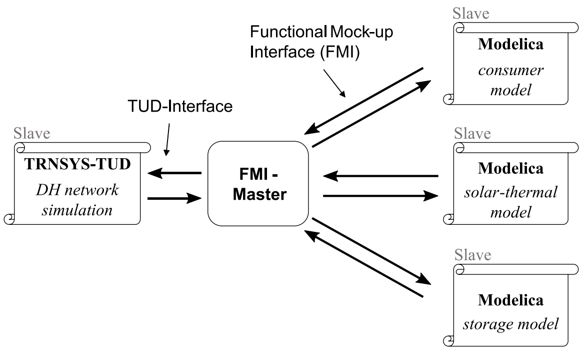

Figure 1: Schema of the coupling between TRNSYS-TUD and Modelica via FMI-Master

2.2 Considered District Heating Networks

Two different district heating networks are the research objects in the project. The first is a 3rd generation, radial DH network (following IEA-DHC Annex X classification), called Net G. The main characteristics are:

- installed load of 2.2 MW with a length of 2.65 km
- 51 consumers (in a range of 5.0 kw to 72.0 kW)

Up to five distributed decentralized heat producers (DCP) - in terms of solar thermal plants with each 100 m² gross area - are considered (compare Figure 2). A prospective integration of combined heat and power (CHP) units is planned.

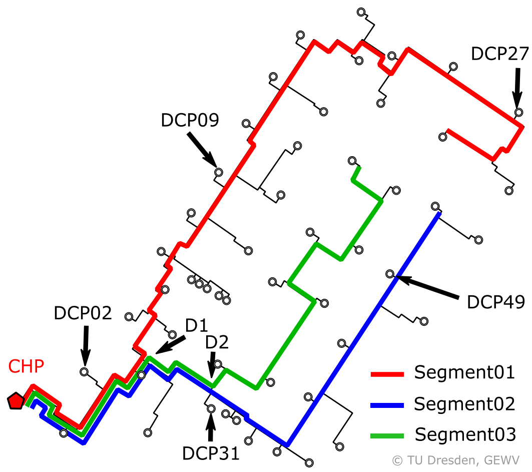

Figure 2: 3rd generation network - Net G - with central heat producer (CHP), segments and decentralized heat producer (DCP)

The second network is a 2nd generation, meshed DH network, called Net B, with the following main characteristics:

- installed load of 83 MW with a length of 41 km
- 485 consumers (in a range of 22 kW to 14.000 kW)
- four meshes
- further booster pump, installed in the return line

The simulation study focusses on the integration of up to 24 DCP in terms of solar thermal plants in this network. There are three different sizes of gross area installed with 500 m², 1000 m² and 5000 m², which are distributed in the network (compare Figure 3). The sizes correlate with the respective consumer at the location according to the installed load of $\dot{Q}_{Ci} > 500\,kW$, $> 1000\,kW$ and $> 5000\,kW$. Similar to Net G, decentralized CHP units will prospectively also considered.

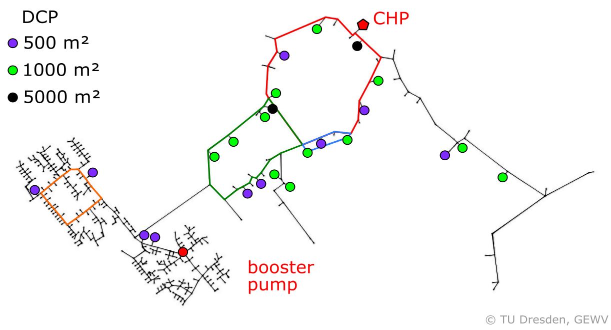

Figure 3: 2nd generation network - Net B - with central heat producer (CHP) and decentralized heat producer (DCP) according to size of collector gross area

The simulation study focusses on the two different weather data locations Würzburg and Potsdam (Germany), as regions with different radiation. The data source is *Deutscher Wetterdienst* (DWD), so original measured data is used for 2015. The reason is the possibly operation-mode for the CHP units according to EEX price-trend, which are combined with the respective weather data.

2.3 Principle of Consumer Modeling

Individual load profiles are crucial for a DH network simulation to prevent overestimated simultaneity in the network. The previous project *DEZENTRAL* used an adopted Typical-Day Method following VDI 4655 (2008). Measured data of consumer were adopted to specific weather data, and heat load profiles scaled to a given peak load. A detailed description can be found in (Heymann, Kretzschmar, Rosemann, Rühling, 2014).
However, this method was a pre-processing work and not suitable for larger DH networks, like Net B. Therefore, a new method was necessary that allows an online calculation of the heat load and return line temperature during the simulation. The developed procedure bases on linear regression models for 24 types of buildings (for

Net B) and two types of buildings for Net G. As data source, hourly measured data for heat load and return line temperature of one or two years as well as the respective weather data was considered. The data sources for the Net B are not from this original network, but from different unknown networks. This fact is a major advantage, because it allows using these regression models in several different DH network simulations.
As a first step, the identification of the major influencing parameters was done by regression analysis. The heat load of each building type $\dot{Q}_{Ti}$ mainly depends on the outlet temperature ϑ_o, the distinction of the working day W (equals one for working day, zero for a non-working day), the distinction of the heating period H (equals one for heating- and zero for non-heating period) and the hour of the day h, see equation (1).

$$\dot{Q}_{Ti} = f\ (\vartheta_o, {\vartheta_o}^2, W, H, h) \qquad (1)$$

The return line temperature ϑ_{RLi} of each building type additionally depends on the supply temperature at the consumer ϑ_{SLi} as well as on the current heat load of the respective consumer $\dot{Q}_{Ci}$, see equation (2).

$$\vartheta_{RLi} = f\ (\vartheta_o, {\vartheta_o}^2, W, H, h, \vartheta_{SLi}, \dot{Q}_{Ci}) \qquad (2)$$

As a result, a set of regression coefficients were derived for each building type dependent on the hour of the day h and the heating period H. During the simulation, in each time step the relevant regression coefficients are used together with the other influencing parameters to calculate the heat load and return line temperature of each building type. Finally, the heat load for each consumer $\dot{Q}_{Ci}$ is scaled to the installed heat load of the connection point of the consumer.
The distribution of the different regression models in the network was realised, for example in Net B, by information of the network operator about the type of consumer (e.g. residential building, industry).

The validation of the DH network simulation with measured data of the network operator (at the central heat producer) has shown an adequate result. The principle of using regression models from measured data of unknown networks was successfully tested. In that case, the problem of overestimated simultaneity was not present after the implementation due to an advantageous distribution of the consumer models. However, in case of a higher simultaneity the regression models can easily transformed regarding the heat load or time.

2.4 Decentralized Heat Producer

As mentioned before, two types of decentralized heat producers (DCP) are considered – solar thermal plants and combined heat and power units. The peak load of the DCP defer according to network G or B and the location within. The project partner *Solites* developed the model of the solar thermal plant. The model is implemented in an *EXCEL*-tool and contains the calculation of the insolation towards the inclined plane, the collector and the required components like heat exchanger and pipes. As an input, the supply and return line temperature at the feed-in point as well as the temperature setpoint is required. The possibly heat to the network is the result for each time step. For usage in a dynamic simulation, the model needed to be transferred into the modeling language Modelica for coupling with the network simulation of TRNSYS-TUD (see part 2.1).
All solar thermal plants in the simulation study has the following characteristics:

- 30° tilted collector
- southern orientation
- high-temperature flat plate collector
- water-glycol mixture
- target temperature equals setpoint reset curve of the network as $f(\vartheta_o)$ plus additional offset due to heat exchanger
- feed-in point to the DH network just right before a consumer

The installed peak load leads with the respective installed collector gross area to the following total peak load (see Table 1).

Table 1: Overview of collector size and peak load

	coll.-area [m²]	quantity	total coll.-area [m²]	total peak-load [kW]
Net G	100	5	500	350
Net B	500	10	5000	3500
	1000	12	12000	8400
	5000	2	10000	7000
	∑	24	27000	18900

The consequent ratio of the installed load of the network with the total peak-load of the installed solar thermal plants amounts to 15.9 % solar coverage for Net G, and 22.8 % solar coverage for Net B.

The integration of CHP units as the second category of decentralized heat producers is at the current state of the simulation study not yet implemented. It is planned to locate the CHP units just right before the consumers, similar to the solar thermal plants.

2.4 Storage Integration

The integration of a heat storage can be an element to reduce the impact of decentralized feed-in heat in the DH network. If solar thermal plants are installed in the network, the aim is to get as much as possible heat into the network. However, in times of highest solar heat gains, the heat demand in the network can be much lower. To prevent stagnation of the solar thermal plants in the network the integration of heat storages (central or decentral) can be one tool for net stabilisation and more effective operation. In this simulation study, one heat storage at the central heat producer is considered with different operation modes. The stagnation of all solar thermal plants installed is permitted, that means that an excess of heat in the network will directly load the storage. The heat storage is considered here only per energy balance sheet without thermal losses. As a first step, three storage operation modes (SO) were implemented, distinguished by the way of unloading:

- SO-P: permanent unloading allowed if necessary
- SO-D: daily unloading allowed between 8:00 PM and 8:00 AM if necessary
- SO-W: weekly unloading allowed between Friday 8:00 PM and Monday 8:00 AM

The loading of the storage is allowed at all times. For first investigations, the size is unlimited to get an overview of the required demand. Loading of the storage occurs when a flow reversal in the supply line at the central heat producer is present due to an excess of heat in the network. In that case, the heat into the storage $\dot{Q}_{ST,in}$ is calculated with the net mass flow $\dot{m}_{net}$ and the temperature difference of ϑ_{SL} and ϑ_{RL}, (compare Figure 4). The return line temperature ϑ_{RL} is equal to the lower storage temperature $\vartheta_{ST,l}$. As it is an energy balance sheet only consideration, the lower storage temperature needed to be defined for that case. Therefore, the lower storage temperature $\vartheta_{ST,l}$ was set to the mean temperature of the network return line between April and September, as the main operation time of the storage. This assumption leads to adequate results without considering complex storage modeling. For the heat into the storage $\dot{Q}_{ST,in}$, the following equation (3) applies:

$$\dot{Q}_{ST,in} = \dot{m}_{net} \cdot c_p \cdot (\vartheta_{SL} - \vartheta_{ST,l}) \qquad (3)$$

Similar, in case of unloading the storage the heat flow outside $\dot{Q}_{ST,out}$ is defined in equation (4):

$$\dot{Q}_{ST,out} = \dot{m}_{net} \cdot c_p \cdot (\vartheta_{ST,u} - \vartheta_{RL}) \qquad (4)$$

The upper storage temperature $\vartheta_{ST,u}$ has approximately the required temperature for the supply line ϑ_{SL}.
The simplified treatment of the heat storage is a sufficient method for investigations of required storage size and the effect of different storage operation modes. Prospective enhancements are conceivable regarding the consideration of heat losses and losses through convective mixing.

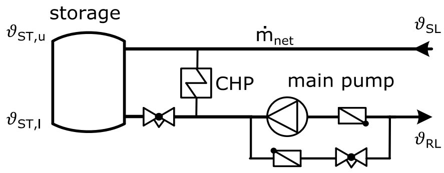

Figure 4: Heat storage integration at central heat producer (CHP)

3. RESULTS

The first representative results of the simulation are presented below. The analysis is done first via statistical evaluation of the annual simulation results by comparing the energy balances. Additionally the results of the storage operation modes will be treated. Finally the impact of decentralized feed-in to the network will be discussed on chosen examples.

3.1 Feed-In Results

For both considered networks, first results for energy balances can be made, however at the current status of the project they are named preliminary.
The solar net fraction SF is defined as the ratio of the solar heat input by DCP $\sum Q_{DCPi}$ to the sum of consumer demand $\sum Q_{Ci}$ plus heat losses Q_{loss} of the network, see equation (5).

$$SF = \frac{\sum Q_{DCPi}}{\sum Q_{Ci} + Q_{loss}} \qquad (5)$$

In Figure 5, the sum of DCP annual solar-thermal input $\sum Q_{DCP}$ and the solar fraction SF are shown for the considered plants in both networks according to the location.

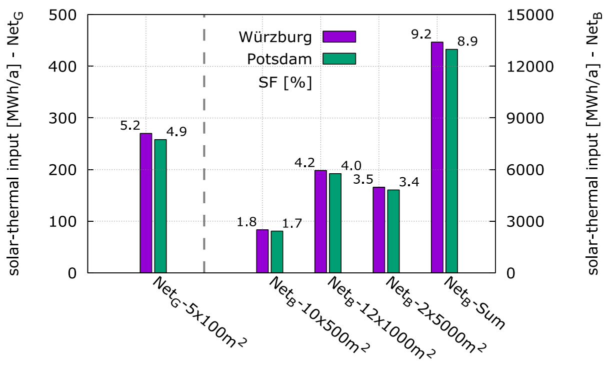

Figure 5: Solar-thermal input and solar fraction of all considered thermal plants acc. to location and network

In Net G, a solar fraction of around 5 % was reached at both location. The specific annual solar-thermal input leads to 515 kWh/(m²·a) for Potsdam and 540 kWh/(m²·a) for Würzburg. The sum of the consumer demand $\sum Q_{Ci}$ is 4893 MWh/a with losses of 304 MWh/a, for the example

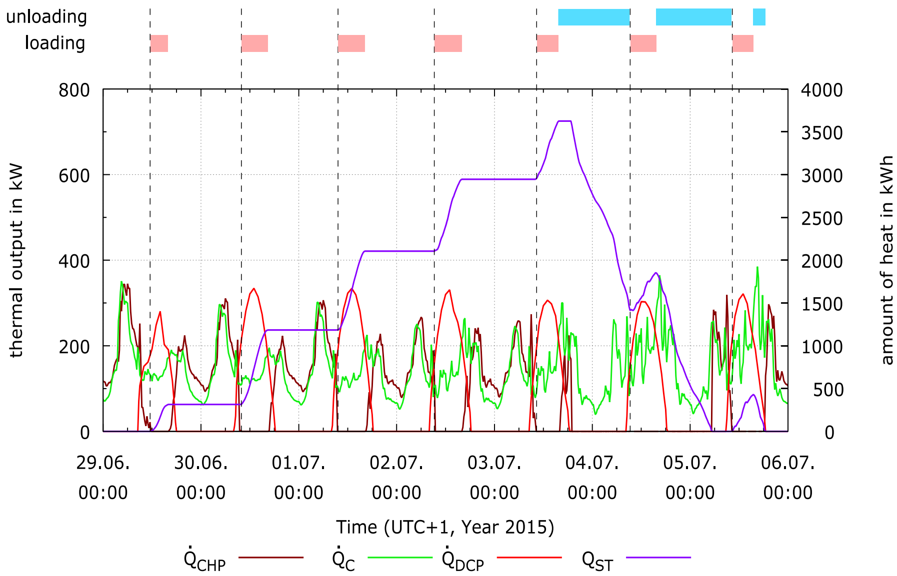

Figure 6: Example for weekly storage operation mode (SO-W) for Net G, Potsdam

of Würzburg. That means that the annual losses of the network are higher than the solar-thermal gains. For Net B, none of the variants with only one size of collector area reaches 5 %. However, the heat load in the network is much higher. If all solar thermal plants are installed, almost 9 % of solar fraction can be reached. The specific annual solar-thermal input leads to around 480 kWh/(m²·a) for Potsdam and around 497 kWh/(m²·a) for Würzburg. Here, the sum of the consumer demand $\sum Q_{Ci}$ is 134419 MWh/a with losses of around 9191 MWh/a, considered variant *NetB-10x500m²* for example. In that case, the losses of the network are more than three times higher than the solar-thermal gains.

The first simulation results have shown that the amount and size of installed solar-thermal plants leads to a realistic solar fraction for existing networks. Moreover, the specific annual solar-thermal input is around 500 kWh/(m²·a), which stands for a high gain and makes it suitable for the investigations in this project regarding the thermo-hydraulic impact of feed-in.

3.2 Storage operation

A further focus of the simulation study is the integration of the heat storage with the mentioned operation modes. Currently Net G was successfully tested with storage operation and Net B is in progress.

The main parameters of interest here are the maximum required volume of the storage $V_{ST,max}$ according to the operation mode as well as the sum of offline time of the central heat producer $\sum h_{CHP,off}$. In Table 2, the results are compared for Net G according to the operation mode for Würzburg. The results for Potsdam have slightly less sizes of $V_{ST,max}$, and are not mentioned here.

Table 2: Results of storage operation modes (Net G, Würzburg)

		SO-P	SO-D	SO-W
$V_{ST,max}$	[m³]	38	38	98
$\sum h_{CHP,off}$	[h]	596	523	556
$\sum h_{DCP,in}$	[h]	1636	1636	1636

The required size of storage strongly depends on the operation mode. For the weekly mode, the maximum volume $V_{ST,max}$ is around 2.5 times larger than for the other modes. As expected, the sizes for permanent and daily mode do not defer, because in both modes the unloading cannot reach the subsequent loading period to extend the necessary size. The comparison of the offline times of the central heat producer $\sum h_{CHP,off}$ reveals that the highest value is not the mode with the highest storage size. Here, the time of unloading seems more relevant. This effect can be explained by the heat demand while unloading. Operation mode SO-D and SO-W allow unloading starting from 8:00 PM where the heat demand is commonly higher than in the afternoon. It leads, compared to SO-P, to a faster unloading with shorter offline time of the central heat producer. However, the amount of hours is just the sum without recognizing minimum operation and offline times of CHP. The heat input of all decentralized heat producers $\sum h_{DCP,in}$ is at all storage operation modes equal, because of the same boundary conditions.

In Figure 6, the progress of weekly storage operation (SO-W) is presented with the amount of heat Q_{ST} in the storage, the overall consumer demand $\dot{Q}_C$ and the heat input of the central $\dot{Q}_{CHP}$ and decentral $\dot{Q}_{DCP}$ heat producer. There are five loading periods during working days with the following unloading, starting on Friday at

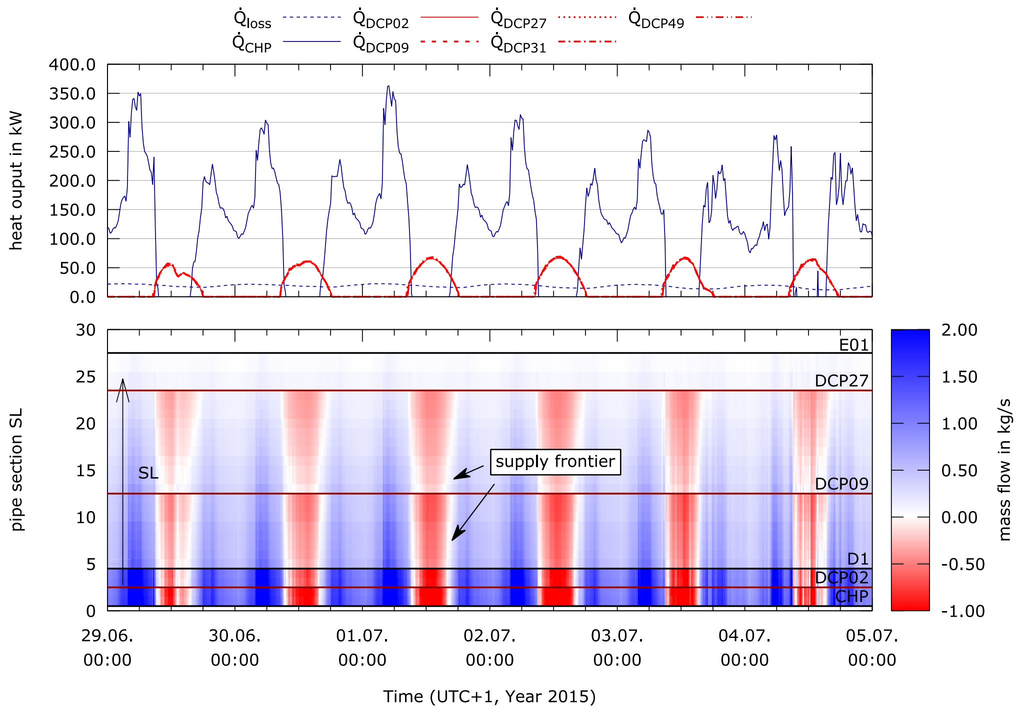

Figure 7: top: heat flow profiles, bottom: mass flow distribution; Net G, summer week, all DCP installed

8:00 PM. The loading of the storage is about a period of 103.25 h with a subsequent unloading about 34.75 h including a short reloading in between. That means that the central heat producer is offline for almost one and a half days, in case the maximum heat storage volume is installed.

3.3 Thermo-hydraulic Effects

The main aspect of the research project are the resulting effects of decentralized feed-in in the DH network. Therefore, the flow conditions needed to be investigated in detail. The following example presents the results of *Segment 01* of Net G (compare Figure 2). Similar analysis will be made for Net B, however simulations are currently ongoing.

Starting from the central heat producer, *Segment 01* has quite close the *DCP02*, followed by a network diversion *D1* and the further DCP´s (*DCP09* and *DCP27*) till the end *E01*. Figure 7 (top) shows the progression of the heat flows for representative summer week. The heat load of the five decentralized heat producers in the network $\dot{Q}_{DCP,i}$ proceed almost synchronous, because all of them have the same boundary conditions like collector type, tilt and installation. Smaller variations are caused by the slightly different temperatures at the feed-in point. The central heat producer is on every day for several hours offline, as seen in moments of $\dot{Q}_{CHP} = 0\ kW$. Here a full supply of the DCP´s occurs in the network. The resulting effect of the network can be seen in Figure 7 (below). This time equivalent diagram shows distribution of the mass flow (in supply line) over the length of *Segment 01*. The red colour indicates a flow reversal in the pipes due to an excess of heat in parts of the segment. The blue part with the different shades indicates fluctuations in the mass flow. The transition between both conditions is marked in white. The white zone indicates the supply frontier, where the flow velocity goes down to zero in this region (see the marked hint in Figure 7, below).

These alternating mass flow leads to alternating temperature profiles in the pipes. This is the main reason for thermal stress. Figure 8 shows the time equivalent temperature distribution of supply and return line. In the supply line, examples of supply frontier zones are marked. The temperature at these points is significant lower compare to the parts of feed-in, due to cool down of the stagnating flow. As the supply frontier is moving over time, an alternating thermal stress occurs at each pipe section. In the return line major fluctuations occur. During the night, the temperature is higher as a reaction of the consumer demand. The reaction of the moving supply frontier leads also to high fluctuation in the return line, to be seen as a shaded stream in the diagram along the line. Important to note is, that at the end of the return line (at the CHP) the temperature is almost homogenous. In the former project *DEZENTRAL*, high temperatures occur here in case of flow reversal. This was due to an installed bypass at the CHP instead of a storage, to use the network itself as short-term storage. The location had the highest thermal stress in the whole network. By installing the central heat storage at this point, the thermal stress might be reduced significantly. Further investigations to this topic will be part of the study in the near future.

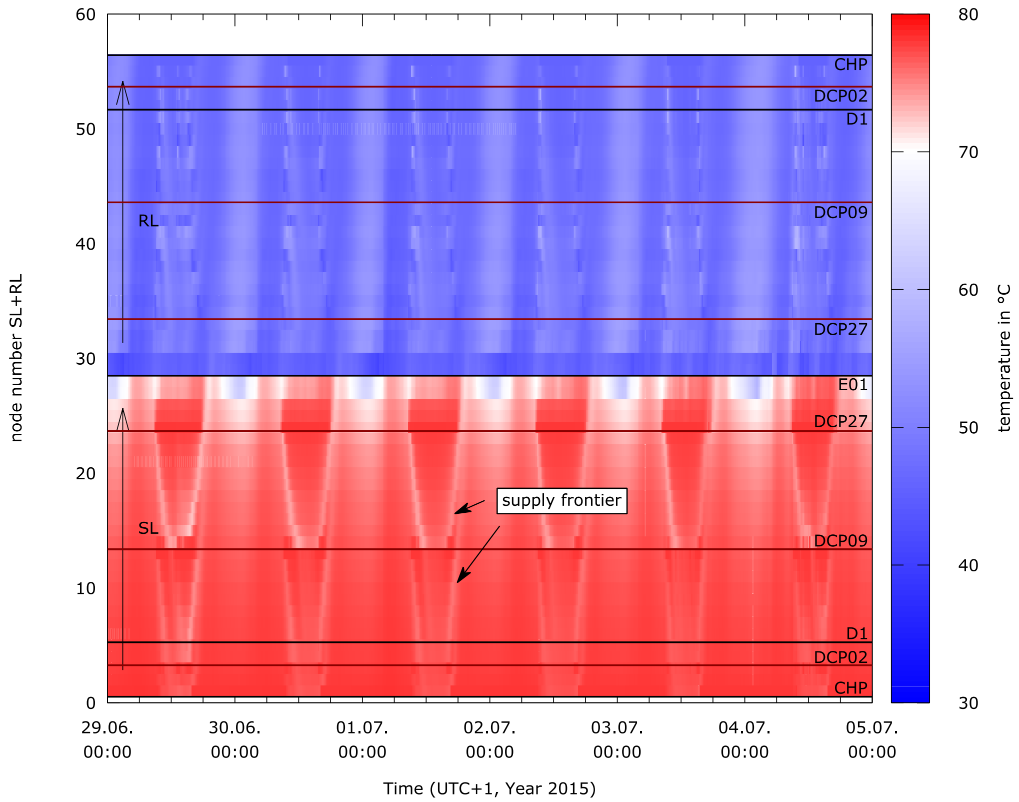

Figure 8: temperature distribution; Net G, summer week, all DCP installed

4. CONLUSION AND OUTLOOK

The realized *DELFIN* simulation studies shows further insights compared to the previous project *DEZENTRAL*. The developed principle of consumer modeling was tested successfully and validated with measurement data of the network operator. The selection and integration of the decentralized heat producers in terms of solar thermal plants has shown prospective relevant solar fraction rates for more renewable-based DH networks. Therefore, it can be the base for the following investigations. The study delivers first insights into the resulting operating conditions in the network and have shown a possibly reduction of thermal stress by integrating a central heat storage. However, this is a preliminary insight and further investigations are essential. The analysis of the heat storage integration has shown the necessity of distinction of various operation modes if energy efficiency is considered. However, finding an optimum between storage size, operation modes and possibly costs, will be interesting for the further investigations.

As a next step, the larger Net B with the four meshes and up to 9 % solar fraction will be considered in detail. Here the flow conditions in the mesh might change rapidly when large scale decentralized heat producer feeds in. Furthermore, the topic of thermal stress will be treated in detail. Finally, the project will be derive requirements for pumps, pressure maintenance, pipes and net control strategy as a result of the investigated thermo-hydraulic effects.

NOMENCLATURE

Symbols

h	hour	h
H	heating period	0 / 1
$\dot{m}$	mass flow	kg/s
Q	heat	kWh
$\dot{Q}$	heat flow	W
SF	solar fraction	%
V	volume	m^3
W	working day	0 / 1
ϑ	celsius temperature	°C

Abbreviations/Indices

C	consumer
CHP	central heat producer
DCP	decentralized heat producer
i, j	index
in	input / feed-in
l	lower
loss	losses
max	maximum
net	network
o	outlet
off	offline (out of operation)
out	output
RL	return line
SL	supply line
ST	heat storage
T	type
u	upper

REFERENCES

Blochwitz T., Otter M., Arnold M., Bausch C., Clauß C. Elmqvist H., Junghanns A., Mauss J., Monteiro M., Neidhold T., Neumerkel D., Olsson H., Peetz J.-V., Wolf S. (2011) *The Functional Mockup Interface for Tool independent Exchange of Simulation Models*, 8th International Modelica Conference 2011, Dresden

Heymann M., Rühling K., Felsmann C. (2017) *Integration of Solar Thermal Systems into District Heating – DH System Simulation*, Energy Procedia, 116, Seoul doi:https://doi.org/10.1016/j.egypro.2017.05.086

Heymann M., Kretzschmar T., Rosemann T., Rühling K. (2014) *Integration of Solar Thermal Systems into District Heating*, 2nd International Solar District Heating Conference, Hamburg

Experience from a new-built feed-in plant in Ystad

Gunnar Lennermo, Energianalys AB Sweden

On the roof of a handball arena in Ystad was a 534 m2 large solar-collector field installed in the spring 2017. The solar thermal plant is a feed-in plant with return/return (R/R) and return/supply (R/S) connections. Integrated in the control system there are a few different options to control the installation.
During the summer, the various operating cases have been used to determine whether the delivery of the feed-in substation is correct or not. Some changes from the tender documents was necessary to do and some errors in the original programming were found. All functions were not in place until mid-August. The owner was responsible to eliminate the air/gas in the system and this was not done properly until beginning of September. Due to this all test was not possible to do in the summer 2017.
The plant was handed over to the owner in beginning of October after the final inspection.
One of the conditions for the plant was that it should be built both as a R/R and R/S feed-in facility. The purpose of this was to be able to use low-radiation time for R/R-feed-in and time with high radiation for R/S-feed-in. Usually one kWh fed-in on the supply line is considered to have a higher value than one kWh fed-in on the return line. This position was also taken for the plant in Ystad even if no investigation has found that this is the case.
A R/R feed-in plant is very dependent on the flow in the return pipe and since the flow in the return line was not known, the possibility of building a R/R Solar Thermal plant was not considered.
The control system focused on switching to R/S as quickly as possible and then stay in R/S mode for as long as possible without any jumping between the two operating modes.
The agreement on which requirements are imposed on feed-in systems are only made between the two parties to which the installation relates. It this case is it a very big difference between Solar Thermal feed-in and Solar Electricity feed-in.

In the general discussion regarding R/S facilities the focus is on keeping a correct temperature of the feed-in flow while there is very little focus un fast changes in flow and on heat-power feed-in. The experience from other feed-in installations in Sweden is that, if there has been any complains or discussion from the district heating companies is it about fast changes in feed-in flow if the temperature is less than 10 K from the temperature set-point. Fast changes in feed-in flow and heat power immediately affect the central pumps in the DH-system and can in extreme cases causes water-hammers in the system.
If the control system is not designed to have at least as much focus on slow changes in feed-in flow as maintaining a correct feed-in temperature can the change in flow be very rapid. If it is an R/R+R/S-system, the risk is greater for large change in feed-in flow because it is very simple to change a valve position from R/S to R/R. The solar heat is still used, the system is not shut down as it will be if it is only a R/S-system.

It is possible to learn a lot from the Ystad ST plant as all data from many sensors is saved with a resolution on 5 seconds on a separate data-server. In an excel document is all parameters that is possible to chance collected together with a document where all changes are listed. Since not all function were in use during the summer of 2017, a better evaluation will be made after the summer of 2018.

Five of the most important questions will be presented

- Flow-balance and degassing or deaerator and GBT
- Switch from R/R to R/S

- Flow control in the solar thermal circuit
- Flow control in the R/S feed-in mood
- Switch from R/S to R/R

Flow balance. The plant consists of 36 large Savo-Solar solar collectors. The system is divided in 6 sub-circuits with 6 collectors in each row. The system sizing point is 0,25 l/min, m² active area which gives a temperature rise of 30 K, 48 to 78°C. If the flow in each sub-circuit has been the same has the pressure-drop variated between 68,8 kPa and 73,9 kPa. The difference is 5,1 kPa or 9,5 % of the pressure-drop in one sub-circuit. In reality will the pressure-drop be equal and the flow will differ which will give a temperature difference of 1,3 to 1,5 K at high radiation.
An under-pressure degassing unit was installed in early September to eliminate the gas in the system. The remaining gas volume in the system was measured with a GBT (M Heymann, TU Dresden).
Result; A degassing unit took in a few hours out the free gas in the system and the GBT was used to check the result and the temperature difference decreased to the appropriate and theoretical level.

Switch from R/R to R/S. The system always starts up as in R/R-mode. The chosen method to understand if the system can switch from R/R to R/S is to look at the temperature in the solar-circuit before the heat-exchanger. If this temperature is high enough can the system change to R/S but the system may not jump between R/R and R/S many times during a day. To avoid premature switching to R/S, a delay is entered in the control system and this delay, with a very low flow can cause a very high temperature in the solar collectors.
Result; A deferred switch to R/S with a very low flow can cause a too high temperature in the solar collectors.

Flow control in the solar circuit. When the system is in R/S mode, the ambition is to have a fixed temperature out from the collectors. This can be done in two different ways; the pump varies the flow to get a correct temperature at the sensor in the end of the sub-circuits and a flow is calculated based on the current solar radiation and this gives a set-point for the pump speed.
Result; A flow-controlled setpoint provides a more stable temperature, but since the efficiency decreases in the event of falling radiation, the calculation may need to be adjusted with a term due to radiation.

Flow control in the R/S feed-in mood. There are two alternative functions that control the feed-in flow. In one alternative is the pump speed controlled to feed-in a correct temperature and in the second alternative, the pump has a setpoint for the flow that is related to the flow in the solar thermal circuit.
Result; The option with a flow setpoint gives a more stable flow but the temperature varies more but still not very much. More test need to be done to investigate how high resolution is needed on flow sensor to get a sufficiently even flow.

Switch from R/S to R/R. The heat-power and flow feed-in should be as low as possible, when switching to R/R is made, because large flow and heat-power variations in the feed-in flow may interfere with other heat generations units in the district heating system.
Result; The discussion about which requirements are most important for an R/S feed-in plant must be taken. Is it more important to keep a correct feed-in temperature than that the change in feed-in flow and heat-power takes place slowly?

PRIMARY ENERGY BASED EVALUATION OF HEAT PUMPS IN DISTRICT HEATING SYSTEMS WITH MULTI-FUNCTIONAL THERMAL ENERGY STORES

Ochs Fabian
Unit for Energy Efficient Buildings, University of Innsbruck, Technikerstr. 13, 6020 Innsbruck, Austria, 0043 512 507 63603, Fabian.Ochs@uibk.ac.at

Abstract – District heating (DH) with multiple energy sources such as renewables and waste heat is considered as one key solution to successfully manage the transition to a more sustainable energy system. For a significant contribution of renewables (RE), large thermal energy stores (TES) are required. Heat pumps (HP) can be integrated in such systems with the aim of achieving higher share of REs and thus lower use of fossil fuels. Different concepts of integrating the HP in the DH system were proposed. One drawback of existing works was a simplified evaluation of the achieved primary energy (PE) savings. National conversion factors for PE are not purely based on facts, but are partly politically motivated. They differ significantly between the EU member states and are subject to change; seasonal variations of the electricity mix are not considered at all. A new method for a monthly PE evaluation is proposed considering the relevant parameters and allowing to include future development of the load (i.e. building stock) and electricity mix (share of REs) with seasonal variations. The impact on the use of HPs in DH systems with TES is discussed.

1. INTRODUCTION AND MOTIVATION

Large-scale thermal energy storage (TES) will be required regardless of the future composition of the energy system. In solar district heating systems, the solar contribution to the system can be increased with large-scale TES. Furthermore, with the storage of thermal energy the supply of electricity can be decoupled from the supply of heat, which is of importance in case CHP plants are integrated into district heating networks. There are three applications of TES:

- Buffer storage for short term energy storage (some 10 to maybe 50 000 m³)
- Large scale TES (some 1 000 to more than 100 000 m³) for long term / seasonal TES
- Large scale TES for multiple usages (e.g. solar heat and waste heat, heat pump)

Heat pumps (HP) can be integrated in such systems with the aim of achieving higher share of REs and thus lower use of fossil fuels. However, primary energy (PE) savings depend on the electricity consumption of the heat pump and the composition of the electricity mix.

2. UNDERGROUND THERMAL ENERGY STORE

Large freestanding tanks of up to about 100 000 m³ for short-term thermal energy storage (from some hours to a couple of days) in district heating systems can be considered as state of the art (see, e.g. Hedbäck 2012).

For very large-scale TES two types of hot water stores can be distinguished: tank and pit thermal energy storage (TTES and PTES), see Fig. 1.

With respect of building physics (moisture protection of the insulation), construction cost and maintenance/repair free-standing tanks will be the always first choice. However, in case of residential districts visibility is normally not desirable and at least in metropolitan areas the area should be usable (trafficable by foot or car).

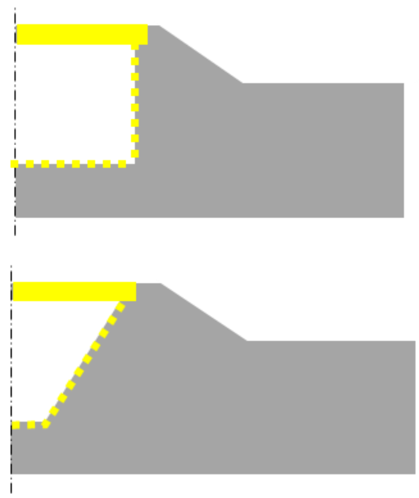

Figure 1: Buried tank (cylinder) vs. pit with or without insulation

Both types can be covered by a floating cover. In case of floating covers the area is not (fully) useful. A cylinder, which features a smaller cover area compared to a pit with the same volume, might be built with a self-carrying cover.

Dimensions of pilot and research tank thermal energy storages and pit thermal energy storages that have been realized over the last 25 years for solar assisted district heating systems, range from several 100 m³ up to 75 000 m³ (see e.g. Ochs 2010, SDH 2015). Even larger TES of up to 2 000 000 m³ are being developed in the Austrian FFG project Giga_TES.

The wall and the ground can optionally be insulated as indicated by the yellow dashed line, pits were in the majority of cases build without further insulation.

3. LARGE-SCALE TES AND HP FOR SDH

3.1 System integration and energy balance

A heat pump (HP) can be inegrated into the Solar assisted district heating (SDH) system to reduce or even replace the fossil backup (BU), see Fig. 2. Storage losses decrease when the temperature level is further decreased by the heat pump. The performance of the solar collectors might be improved. However, the driving energy i.e. the electricity has to be considered in the energy balance and thus the composition of the electricity mix. The integration of the HP has to be planned carefully.

Generally, a compression heat pump can be integrated in different ways:

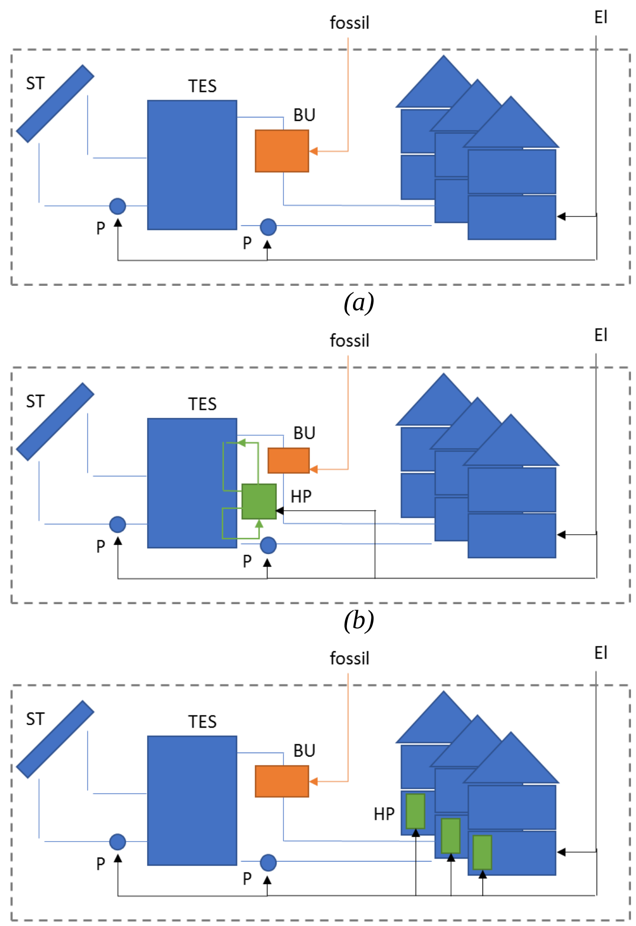

Figure 2: Integration of HP into SDH systems with TES and components of the Energy Balance (a) without HP, (b) with central HP, (c) with decentral HP

As low temperature heat source, environmental energy (either ground water, ground or air) can be exploited. Alternatively, the (lower part) of the TES can be used as source and finally, the return of the district heating could be used (central at the TES or decentral in the buildings).

The sink (at high temperature level) can be either the flow of the DH, the (upper part) of the TES or directly the buildings in case of decentral HPs.

The condenser can be connected to the upper part of the TES, directly to the flow branch of the district heating system (which requires a heat pump with high power (or low contribution of the heat pump with regard to the load). Alternatively, an additional buffer tank, which is connected to the flow branch of the district heating system can be heated with the condenser of the heat pump (see Fig. 3, bottom). With an additional buffer tank back-mixing can be avoided which occurs in particular in case of TES with low h/d-ratio such as pit TES. However, further investment costs and additional thermal losses of the buffer tank have then to be considered.

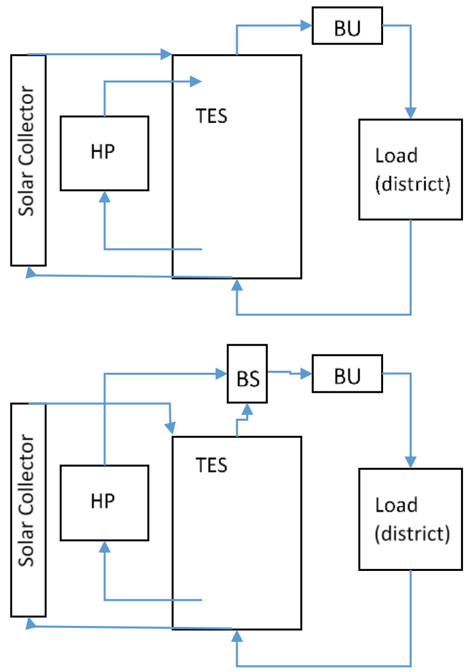

Figure 3: Solar assisted district heating system with large-scale TES and heat pump, (top) without additional buffer store, (bottom) with additional buffer store; HP: Heat Pump, TES Thermal Energy Store, BS: Buffer Store, BU: Backup Heater (Ochs F., 2015)

In this paper, the environmental benefit (in terms of primary energy savings) of integrating a heat pump in such a system by improving the stratification of the store or enable further discharge of the store (below the level of return flow temperature) and thus increase the solar yield is investigated. A primary energy and economic analysis is required.

Absorption heat pumps can be integrated, too, if high temperature excess heat is available, but this is not the focus of this paper.

3.2 Review of HP in SDH

SDH systems with heat pump was already investigated in theory and in practice by several authors. The plants in

Rostock (ATES, D), Attenkrichen (Tank-BTES hybrid, D), Neckarsulm (BTES, D), Crailsheim (BTES, D), Eggenstein (Gravel-water pit, D), Munich (tank, D) and Marstal (hot water pit, DK) are operated with a heat pump (see e.g. saisonalspeicher.de, or IEA SHC Task 45).
Marx (2015) investigates the integration of heat pumps into solar assisted district heating systems. Heat pumps coupled with TES systems in combination with the smart grid concept are seen by some authors (e.g. Arteconi et al. 2013, Sørensen et al 2013, Dröscher et al. 2013) as a promising technology for load management.

4. MONTHLY PRIMARY ENERGY CONVERSION FACTORS

It is well known that electricty and heat heat have different (technical) value. In order to compare the electric and fossil energy consumption, the related primary energy consumption (or CO_2 emissions) can be used. The primary energy (PE) is caluclated with the primary energy conversion factors for electrictiy and fossil energy (here gas), respectively $f_{PE,el}$ and $f_{PE,fossil}$

$$PE = f_{PE,el} \cdot E_{el} + f_{PE,fossil} \cdot E_{fossil} \qquad \text{eq. 1}$$

National conversion factors for PE/CO_2 are not purely based on facts, but are partly politically motivated. They differ significantly between the EU member states and are subject to change, e.g. Germany (ENeV) 1.8 since 2016 (2.4 before), Austria 1.91 since 2015, 2.62 before (OIB-6, 2015, (OIB-6, 2011). Seasonal variations are not considered at all.

Due to the volatile share of renewable energy in the grid (see e.g. the energy balance for Germany in 2015 (e.g. data from ENTSO-E), a net energy balance to evaluate different efficiency and energy concepts can be misleading.

Heating and DHW preparation do not yet contribute significantly to the electric grid load in central European countries such as Germany and Austria (electric heating and heat pumps have a share in the range of 5 %, BEDW 2013, Statistik Austria, 2016)

Furthermore, for the electricity mix, the share of renewables within the time frame of consideration (e.g. 20 years) should be included and not - as usually done - the current (or even past status). A significantly increased share of renewable electricity can be expected in the near future in particular in summer (PV), while in winter it is likely that there will be only a moderate increase (further extension of wind power). In Fig. 4 a simplified model to qualitatively represent the availability of the different RE sources over the course of the year is shown.

Availability of hydro energy is relative homogeneous (however lower in winter and higher in summer), but further development/extension is hardly possible Solar energy is significantly lower in winter than in summer. It has a large potential. Wind energy availability is again relative homogeneous with higher share in winter and thus has the potential to compensate to some extend the winter lack of Solar energy. Biomass is not considered here. Biomass can be stored, but it can be expected to have a very limited potential for the building sector as it will be required for industry and mobility, see e.g. Feist 2018.

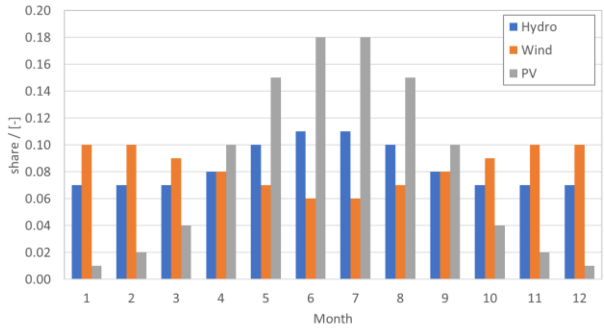

Figure 4: Simplified model of the seasonal avialability of different REs (Hydro, Wind, PV), based on ENTSO-E

For the above mentioned reasons, a monthly evaluation based on monthly primary energy factors is proposed, which can be used to calculate a more representative environmental impact considering the point of time of the consumption.
With different shares of hydro, wind, PV and fossil energy in the electricity mix, based on the distribution in Fig. 4, the primary energy conversion factor can be calculated on monthly basis.

$$f_{PE} = f_{PE,hyd.} \cdot w_{el,hyd.}/w_{el} + f_{PE,wind} \cdot w_{el,wind}/w_{el} + f_{PE,PV} \cdot w_{el,PV}/w_{el} + f_{PE,fos.} \cdot w_{el,fos.}/w_{el} \qquad \text{eq. 2}$$

The PE conversion factors in kWhPE/kWhel used for the following calculation are shown in the Tab. 1.

Table 1: PE conversion factors kWh_{PE}/kWh_{el}

RE	**f_{PE} / [kWhPE/kWhel]**
Hydro	0.01
Wind	0.05
PV (off-site)	0.1
Fossil	2.4

In addition to the availability of RE, the load curve influences the electricity consumption. In Fig. 5 (a) an example of the monthly contribution of RE and fossil energy to cover the load of a Passive House (PH) is show for the case 10 % hydro, 10 % wind and 10 % PV are assumed. The same is shown in Fig. 5 (b) for a low energy house (LEH) with higher energy demand and longer heating period.

The resulting monthly primary energy conversion factors for the case of a PH load with 10 % hydro, 10 % wind and 10 % PV) is shown in table 2. Furthermore, the cases of a low energy house load curve (LEH) with also 10 % hydro, 10 % wind and 10 % PV (10-10-10) and with 10 % hydro, 30 % wind and 50 % PV (10-30-50) are compared.

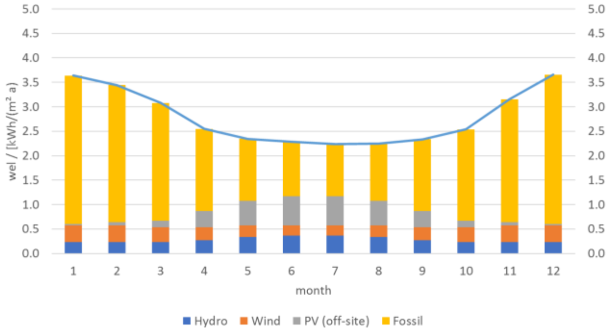

(a)

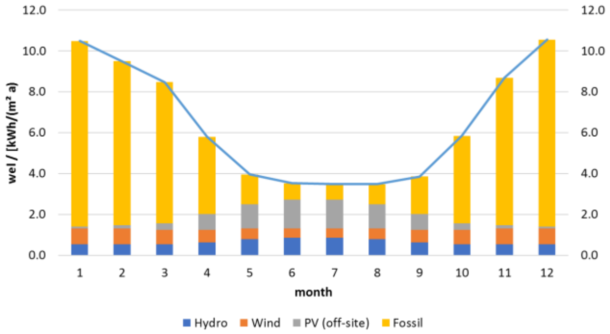

(b)

Figure 5: monthly contribution of RE and fossil energy to cover the load of (a) a Passive House (PH) and (b) a low energy house with each 10 % hydro, 10 % wind and 10 % PV

Table 2: Monthly primary energy factors for three different scenarios PH 10-10-10 (Passive house load curve, 10 % hydro, 10 % wind, 10 % PV); LEH 10-10-10 (Low energy house load curve, 10 % hydro, 10 % wind, 10 % PV) ; LEH 10-30-50 (Low energy house load curve, 10 % hydro, 30 % wind, 50 % PV)

Month	PH 10-10-10	LEH 10-10-10	LEH 10-30-50
1	2.01	2.1	1.7
2	1.96	2.0	1.5
3	1.89	2.0	1.2
4	1.60	1.6	0.1
5	1.33	0.9	0.1
6	1.20	0.6	0.1
7	1.18	0.6	0.1
8	1.28	0.7	0.1
9	1.53	1.2	0.1
10	1.78	1.8	0.7
11	1.92	2.0	1.4
12	2.01	2.1	1.7

5. CASE STUDY

5.1 Boundary conditions and assumptions

A virtual case study was selected with the following boundary conditions and assumptions:

- » Climate of Vienna
- » Low energy buildings with 60 kWh/m²/year
- » Heating season from October to May
- » DHW demand of 20 KWh/m²/year
- » DH with 15 % losses
- » DH Temperatur 60 °C
- » Max. storage temperature < 100 °C
- » Min HP discharge temperature 30 °C
- » Solar collector field efficiency 32 %
- » TES Losses ca. 10 % (medium term storage, 20 % long term storage)

5.2 Methods

All calculations are performed in Microsoft Excel® with a simplified monthly energy balance. The results have been cross-checked with the SDH Tool (lookup table generated with TRNSYS simulations).

It is assumed that the required flow temperature of the DH system is low enough and TES temperature is high enough such that post-heating is not required.

Furthermore, the heat pump can provide sufficiently high temperatures in case the storage is discharged to temperatures below DH temperature.

The seasonal performance factor of the heat pump is calculated based on the simple approach with the Carnot performance factor:

$$COP = \eta_{Carnot} \cdot Thot/(T_{hot}-T_{cold}) \qquad \text{eq. 3}$$

5.3 Variants

The variants considered in this study are summarised in Tab. 3. Four solar collector field sizes are considered see Fig. 6, resulting in “no”, “small”, “medium” and “high” excess heat.

Table 3: Variants of the district heating (DH) with small, medium and large Solar thermal plant (ST) and without or with thermal energy storage (TES) as well as with or without heat pump (HP)

Nr		A_{ST} / [m²]		V_{TES} / [m³]
1	DH with small ST	4 500	no TES	-
2	DH with medium ST	18 000	no TES	-
3	DH with medium ST	18 000	TES	78 000
4	DH with large ST	22 000	TES	73 000
5	DH with large ST	22 000	TES, HP	62 000
6	DH with xlarge ST	25 000	no TES	-
7	DH with xlarge ST	25 000	TES, HP	73 000
8	DH with xlarge ST	25 000	large TES	115 000
9	DH with xlarge ST	25 000	smaller TES	72 000
10	No DH, no ST	-	HP	

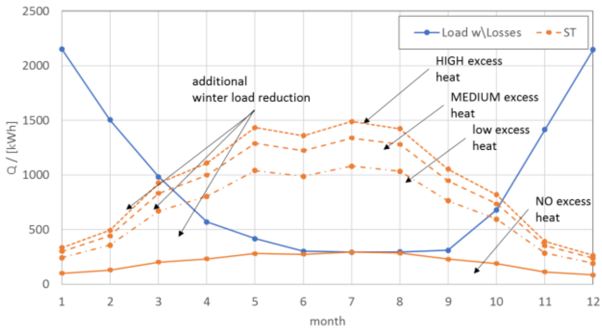

Figure 6: Example of a load curve (monthly values) and three different cases of excess heat (i.e. heat produced by the ST plant)

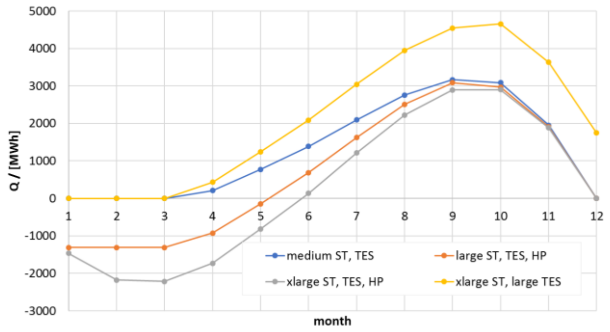

Figure 8: Monthly charging status of the four variants with large TES. medium ST, TES (3); large ST TES, HP (5); xlarge ST TES, HP (7); xlarge ST large TES (8);

6. RESULTS

The additional winter load reduction that can be achieved by increasing the ST field is limited. A significant reduction of fossil energy in winter can only be achieved by using large-scale TES (Fig. 6). Depending on the amount of excess heat, the TES can be dimensioned such that is fully charged when the available ST energy is just enough to cover the load, which is between end of September and beginning of October in the example in this work, see also Fig. 7. Then, the TES is imediatelly used to cover the difference between load and available ST energy, as shown schematically in Fig. 7.

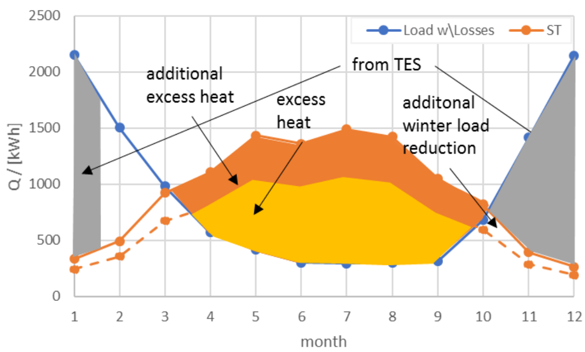

Figure 7: Example of variant 8 DH with xlarge ST (25 000 m³), large TES (115 000 m³); Load curve and contribution of direct solar (compared to medium ST).

Depending on the size of the ST field and correspondingly the size of the TES, it is discharged until December or January. For the rest of the heating season, the gap between the load and the available ST energy has to be covered by fossil energy.

Alternatively, a HP can be used to further discharge the TES (below return flow temperature) and thus extending the discharge period and in the same time reducing fossil energy use. The monthly charging status of the TES is shown for four different examples in Fig. 8.

Table 4 summarizes the results of the contributions of solar thermal, TES usage and fossil energy usage for the 9 SDH variants and the reference variant with decentral HPs (variant 10). The monthly results can be found in the appendix.

Table 4: Summary of the contributions of ST (direct and excess), TES, HP and fossil (gas) energy in MWh for the 9 variants of DH and a decentral HP system (variant 10) in comparison

Nr	Load	ST dir	ST exc.	TES	HP	HP el.	Gas
1	11065	2413	-	-	-	-	8652
2	11065	4532	3521	-	-	-	6533
3	11065	4532	3521	3169	-	-	3365
4	11065	5034	4942	2970	-	-	3061
5	11065	5034	4942	4281	1851	539	1210
6	11065	5277	4942	-	-	-	5788
7	11065	5277	5816	5119	2885	670	0
8	11065	5277	5816	4653	-	-	1136
9	11065	5277	5816	2904	-	-	2885
10	9600	-	-	-	9600	3957	-

The directly used ST and the ST Excess heat are shown in Fig. 9. The contribution to cover the load by directly used ST, by the TES (direct) and by the TES with the use of a HP as well as by fossil energy is shown in Fig. 10.

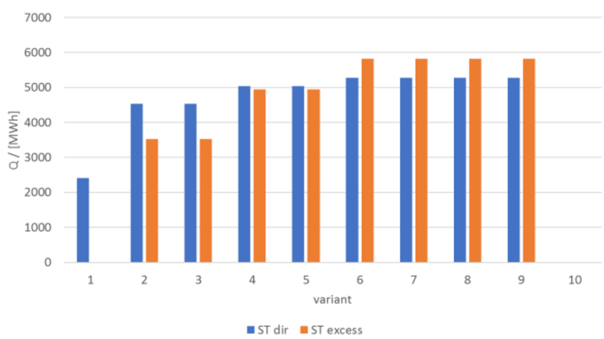

Figure 9: Directly used ST and ST Excess heat for the 9 SDH variants with ST (and TES)

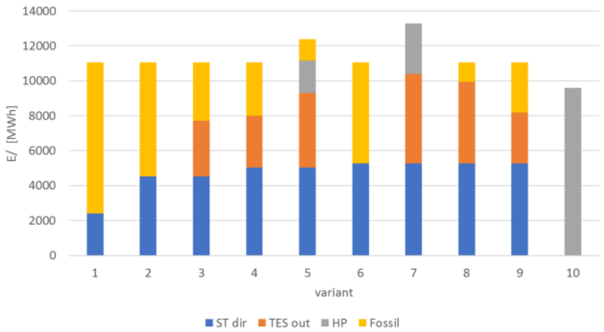

Fig. 10: Contribution to cover the load of directly used ST, of TES (direct) and of TES with HP as well as fossil for the 9 variants as well as the heat delivered with HP in case of decentral HPs (variant 10)

The ST energy and the energy used from the TES can be considered for free (disregarding energy reqired for the pumps and control), while the fossil energy (here gas) and the electricity to drive the HP have to be purchased. The purchased energy is shown in Fig. 11 for the 10 cases.

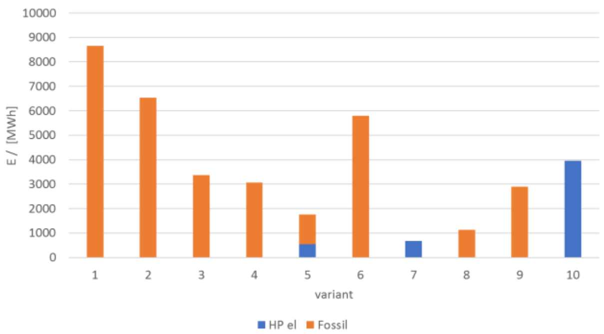

Figure 11: Purchased energy, i.e. electricity to drive the heat pump and fossil energy (gas) for the 9 SDH variants and the reference with decentral HPs

In order to compare the purchased gas and electricity from the point of view of environmental impact, the related CO_2 emissions or primary energy demand have to be calculated. As discussed in section 4, in order to consider appropriately the time of the electricity consumption monthly primary energy conversion factors are used. The results are summarized in Fig. 12 and compared with the case of constant (i.e. average) primary energy conversion factor. Furthermore, for variant 10, a the case with high share of RE in the electricity mix (10-30-50, see Tab. 2) is compared.

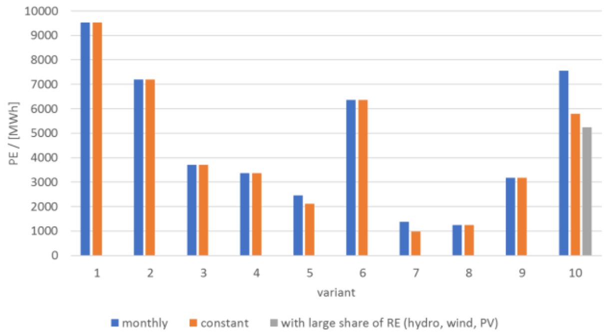

Figure 12: Primary energy, i.e. electricity to drive the heat pump and fossil energy (gas) for the 9 variants and the reference with decentral HPs

7. DISCUSSION

Clearly, the variants with the large ST plants and thus with the highest share of excess heat have the overall lowest primary energy demands. Contrariwise, the district heating system with small ST (without excess heat) has the highest PE demand. And even variant 2 with medium ST has a PE demand, which is even higher than the variant 10 with decentral heat pumps, if a constant PE conversion factor is used. However, if the point time of electricity consumption is considered and monthly PE conversion factors are used, the variant with decentral HPs features the highest PE demand (with exception of variant 1 with the small ST). On the other hand, if a high share of RE (hydro, wind, PV) is assumed as can be expected to be the case in the near future the decentral HP performs better then variant 2 and 6 with larger ST without TES.

In case a TES is used in a DH with high excess heat, the primary energy consumption can be significantly reduced. It depends again on the share of RE (hydro, wind, PV) in the electricity mix, whether it is better to discharge a smaller TES with a heat pump or whether to invest in a larger TES (compare variant 7 with 8). With constant primary energy conversion factor, the benefit of the heat pump use is overestimated (variant 5 and 7).

8. CONCLUSIONS AND OUTLOOK

Sustainable and responsible use of resources is required in order to mitigate climate change. Micro-economic goals usually consider only the capitalized investment costs and/or the purchased energy. On macro-economic scale, the (non-RE) primary energy (PE) use and CO_2-emissions have to be reduced (while nuclear energy has to be avoided.)

The mismatch between (electricity) demand and RE availability should be considered, e.g. by means of time dependent (e.g. seasonal or monthly) primary energy conversion factors, a method was suggested in this paper.

It is obviously not trivial to predict the future composition of the electricity mix. However, some general trends are predictable. By applying (simple) models for the future composition of the electricity mix, at least the environmental impact of different technologies (such as ST, HP etc.) can be better understood and technology ranking for future energy scenarios can be performed in a more robust way.

It is of major relevance in which time of year the HP is operated (i.e. when electricity is consumed) and thus whether fossil fuels are replaced or not. Energy savings in winter have higher value, which is reflected by the new evaluation method. The proposed monthly PE evaluation considers the relevant parameters and allows to include future development of the load (i.e. building stock) and electricity mix (share of REs) with seasonal variations. The impact on the use of HPs in DH systems can be better understood by evaluating the primary energy savings based on monthly primary energy conversion factors.

It could be shown that integration of a HP in a SDH can have environmental benefits, but careful planning is required. However, first of all, a significant reduction of the energy demand of the building stock is a prerequisite for a sustainable energy system.

Future work should concentrate on approving the assumptions made by comparing with a more detailed simulation model. Furthermore, large TES have to be developed and optimized in terms of costs and design for ideal integration into SDH systems. Finally, different scenarios for the future development of the electricity mix should be investigated and their impact on the optimal system design and control strategy of SDH systems.

ACKNOWLEDGEMENT

This work is part of the Austrian flagship project „Giga_TES“, Klima- und Energiefond, FFG, Project number: 860949, January 2018 – December 2020.

REFERENCES

BEDW, Wie heizt Deutschland, BEDW-Studie zum Heizungsmarkt, Juli, 2016.

BEDW, Energie-Info, Stromverbrauch im Haushalt, Berlin, 2013.

Hans-Martin Henning, Andreas Palzer, A comprehensive model for the German electricity and heat sector in a future energy system with a dominant contribution from renewable energy technologies. Pt.I: Methodology, Renewable & sustainable energy reviews 30 (2014), pp.1003-1018 ISSN: 1364-0321 2014

ENTSO-E European Network of Transmission System Operators for Electricity https://www.entsoe.eu

Wolfgang Feist, Passivhaus – das nächste Jahrzehnt. In: Tagungsband zur 18. Internationalen Passivhaustagung, Aachen, April 2014.Hedbäck, 2012: Dr. sc. techn. Anders Hedbäck, Danderyd, Schweden, 2012

Fabian Ochs, Simulation Based Optimization of Pit and Tank Thermal Energy Storage for Solar District Heating Systems, SDH Conference 2015, Toulouse, France, 2015.

Fabian Ochs, Andreas Zottl, Herman Schranzhofer, Richard Heimrath, Christian Halmdienst und Daniel Reiterer, „Store4Grid - Optimierte Erdbeckenwärmespeicher für Nahwärmenetze,“ Wien, 2015.

Fabian Ochs, Evaluation of Efficiency and RE Measures considering the future Energy Mix, 7th IBPC, Syracus, USA, 2018, abstract submitted.

OIB-6 Richtlinie 6, Energieeinsparung und Wärmeschutz, Österreichisches Institut für Bautechnik, 2011

OIB-6 Richtlinie 6, Energieeinsparung und Wärmeschutz, Österreichisches Institut für Bautechnik, 2015

Helmut Strasser, Norbert Dorfinger, Boris Mahler, Stadtwerk: Lehen _ Solar energy in urban community in City of Salzburg, Austria SHC 2012, Energy Procedia 30 (2012) 866 – 874

Roman Marx, Integration von Wärmepumpen in solare Nahwärmeanlagen mit saisonaler Wärmespeicherung, 978-3-8440-3476-9, Shaker Verlag, 2015

SDH Online , http://www.sdh-online.solites.de/Tool/2#

Statistik Austria, Bundesanstalt Statistik Österreich, 2016 https://www.statistik.at/web_de/statistiken/energie_umwelt_innovation_mobilitaet/energie_und_umwelt/energie/energieeinsatz_der_haushalte/index.html, 2017

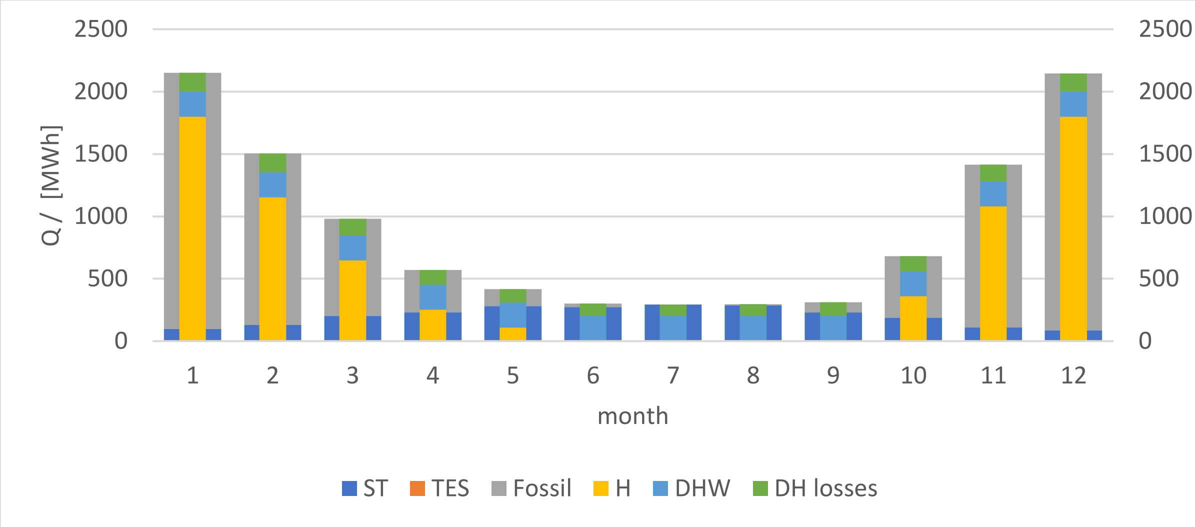

1: DH with small ST, no TES

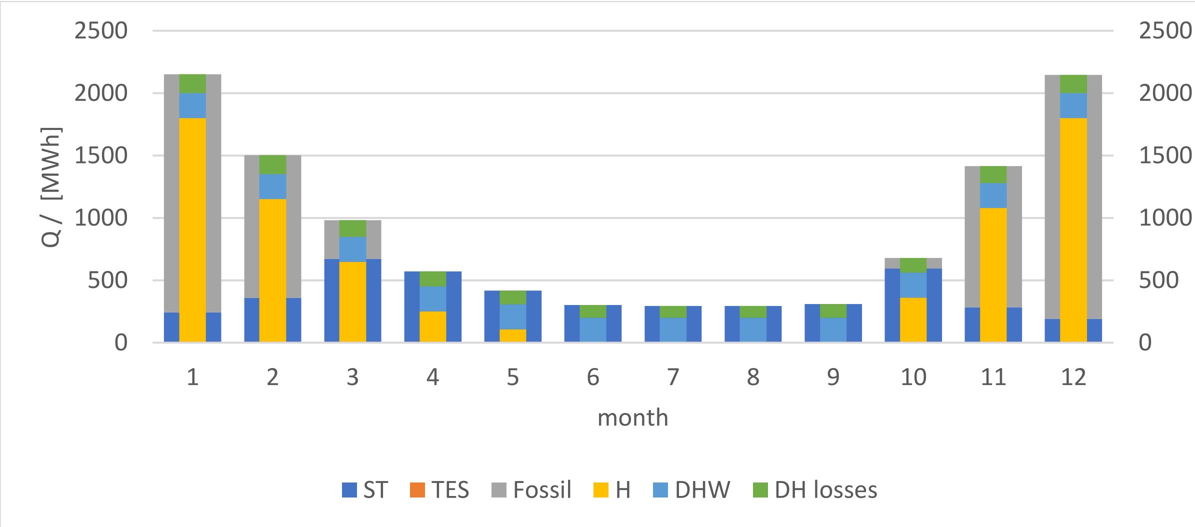

2: DH with medium ST, no TES

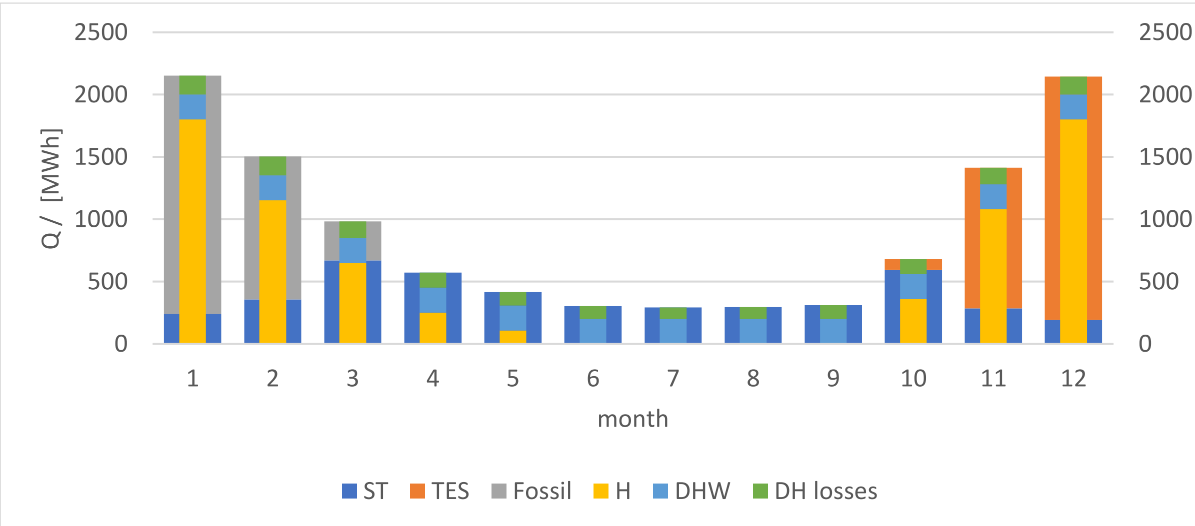

3: DH with medium ST, TES

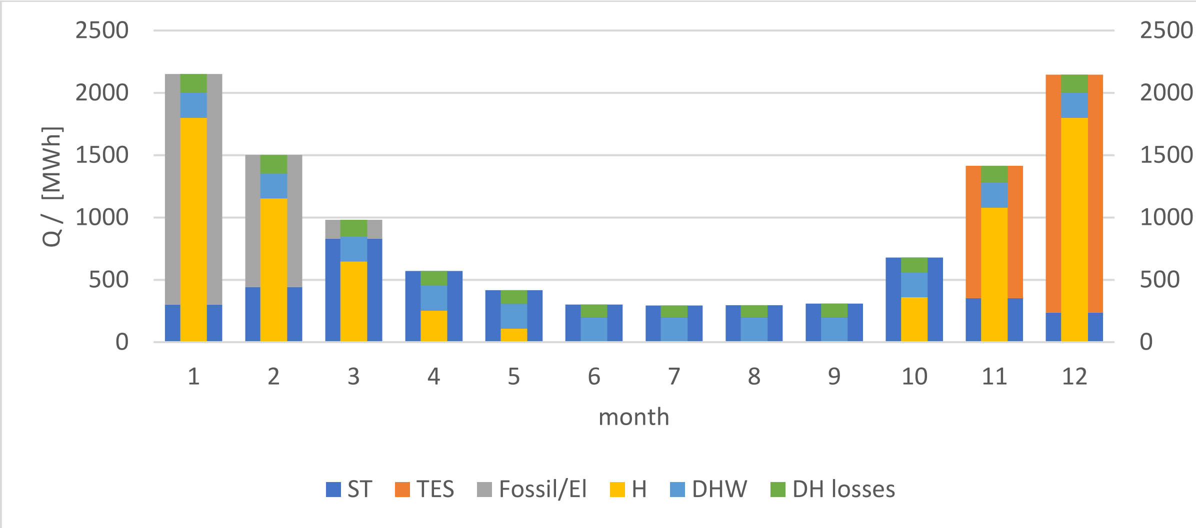

4: DH with large ST, TES

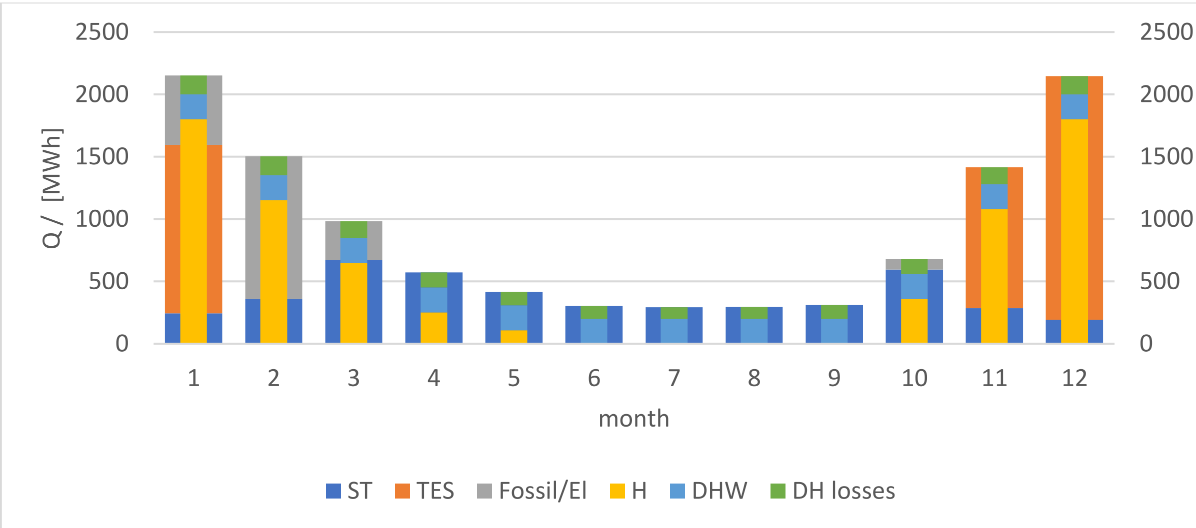

5: DH with large ST, TES, HP

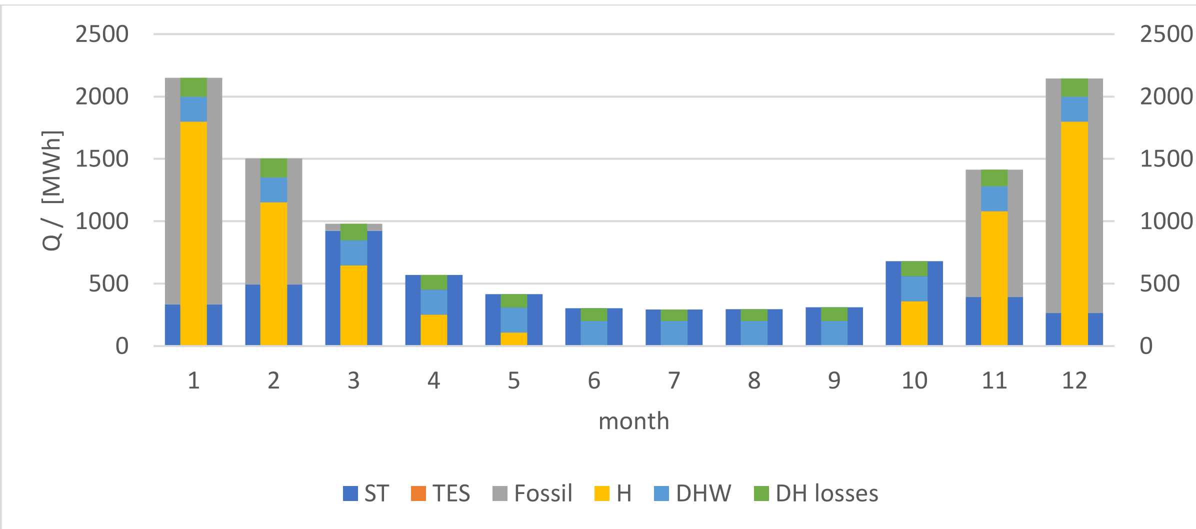

6: DH with xlarge ST, no TES

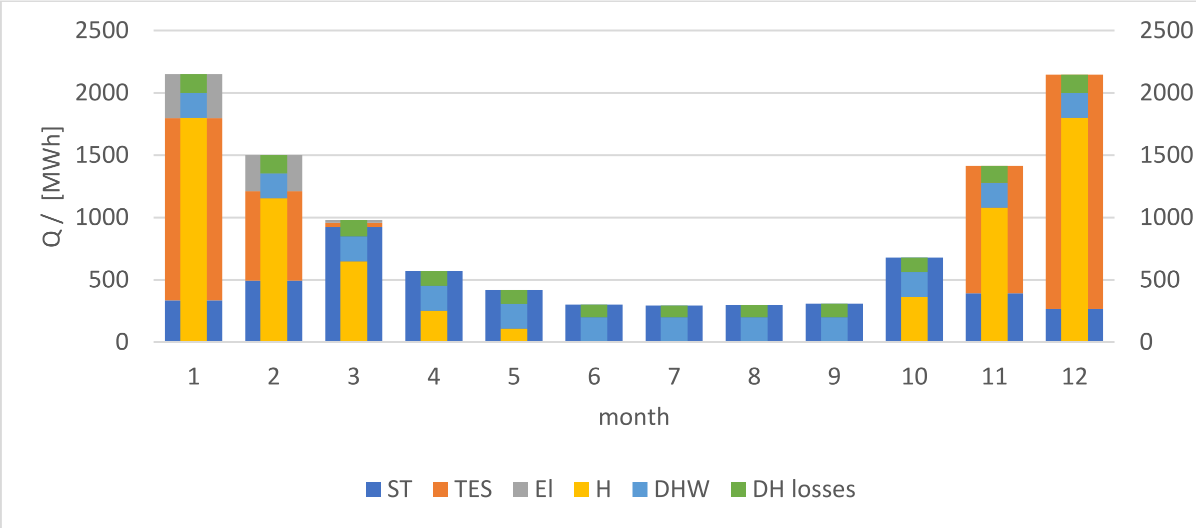

7: DH with xlarge ST, TES, HP

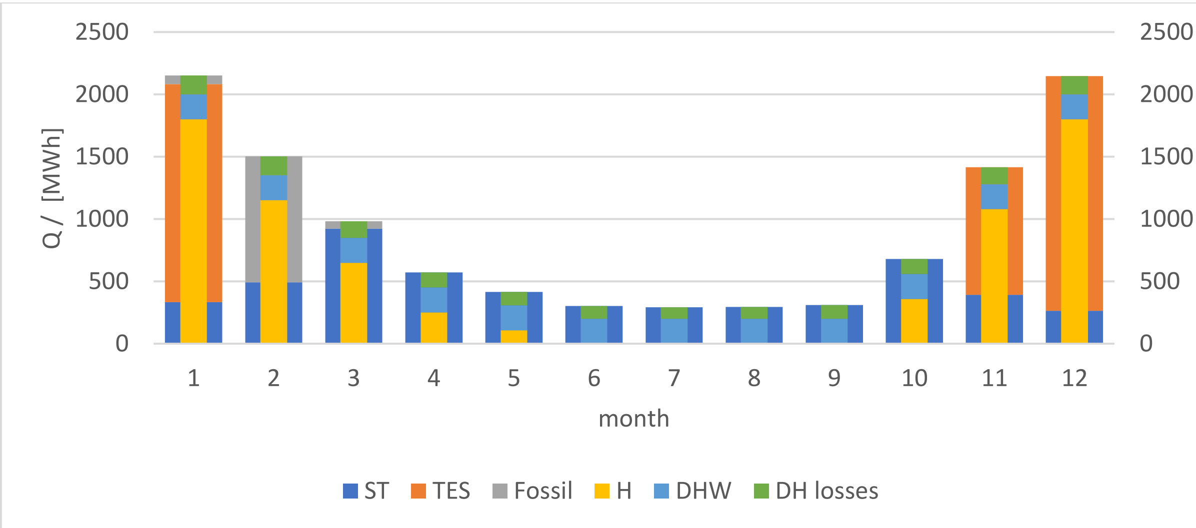

8: DH with large ST, large TES

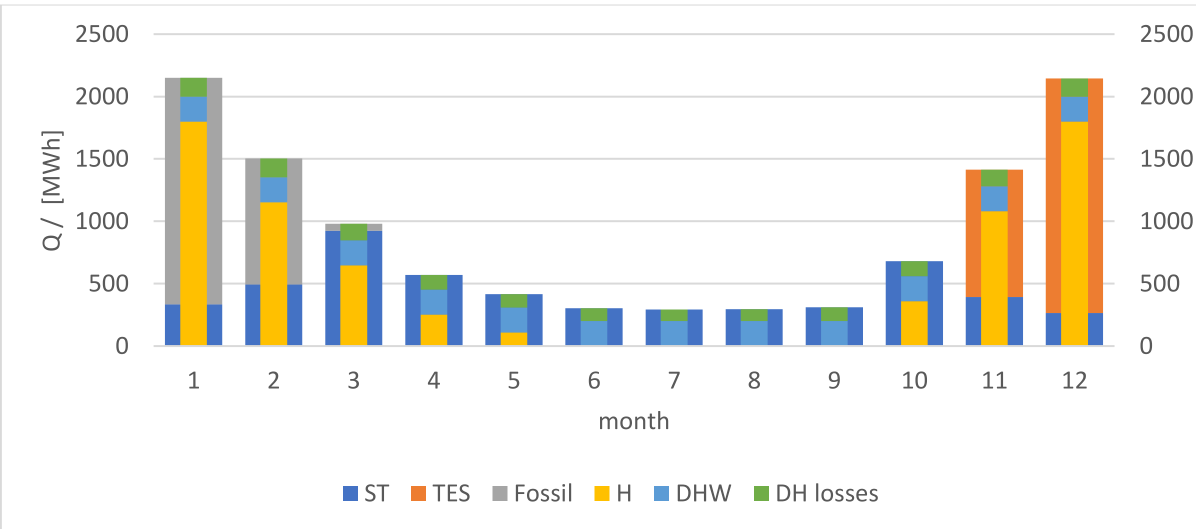

9: DH with xlarge ST, smaller TES

OPTIMIZING EFFICIENCY OF BIOMASS-FIRED ORGANIC RANKINE CYCLE WITH CONCENTRATED SOLAR POWER:
A **C**ombined **H**eat- and **P**ower case in Denmark

Jes Donneborg[1] and Jelica Matoricz[2]

[1] Aalborg CSP A/S: Jes Donneborg, MSc Economics and Business Administration, Executive Vice President, Aalborg CSP A/S, Address: Hjulmagervej 55, 9000-Aalborg (Denmark), phone: +45 40 15 27 36, email: jdo@aalborgcsp.com

[2] Aalborg CSP A/S Jelica Matoricz, MSc International Marketing, International Marketing Manager, phone: +45 52 73 37 96

1. Concentrated Solar Power in Denmark

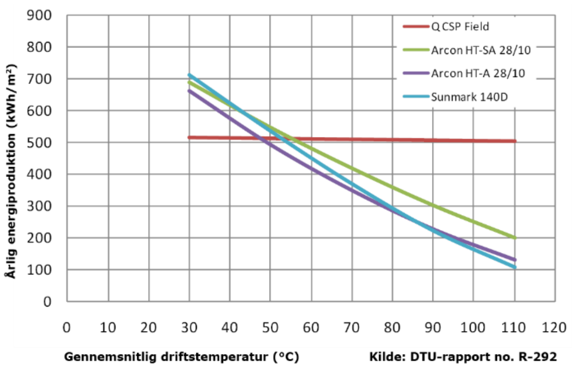

Figure 1: CSP surpasses performance of flat panels in Danish climate

Concentrated solar power (CSP) plants have so far mainly been built to produce electricity for export to the grid, however, numerous advantages have been identified in industrial setting as well. Due to the technology's flexibility to produce high and mid temperature heat, it provides an ideal solar-thermal solution for industrial purposes. Parabolic trough CSP plants are typically found in countries around the solar belt, but economic viability has also been proven in a place with limited solar resources, in Denmark, where efficiency of the system was monitored and compared with flat solar-thermal panels. The report concluded that CSP produces more energy above 50 °C, provides a better economy over the system's 25-years lifetime and ensures a year-round energy production even in Nordic climate conditions compared to flat panel systems [1].

2. CSP as a flexible add-on to a biomass-fired ORC

In December 2016, a world first CSP plant went into operation in the northern part of Denmark (town of Brønderslev). The plant's uniqueness lies in the facts that it was designed to be integrated with a biomass-fired Organic Rankine Cycle (ORC) which is currently still under construction and is expected to go online in Spring 2018. This combined solution will be the first large-scale system in the world to demonstrate how CSP, with an integrated energy system design can optimize efficiency of ORC even in areas with less sunshine, in this case Denmark.

Figure 2: Image of the concentrated solar power plant in Brønderslev, Denmark

Figure 3: Engineering drawing of the solar field

The solar energy plant was delivered by Danish renewable energy specialist Aalborg CSP, and it is based on the company's own CSP parabolic trough technology. The plant consists of 40 rows of 125m U-shaped mirrors with an aperture area of 26,929m^2.These mirrors collect the sunrays throughout the day and reflect them onto a receiver pipe, which sums up to 5 kilometre receiver tubes. This receiver pipe is surrounded by a special glass vacuum tube and inside this runs - only heated by the sun - thermal oil with temperatures up to 330 °C. This high temperature is able to drive an electric turbine to produce **electricity**, but the flexibility of the system also allows production of lower temperatures for **district heating** purposes. The solar heating system can thus alternate between providing heat and power or deliver heat exclusively. To maximize yield of energy, the waste heat is utilized and sent to the district heating circuit whereas electrical power is generated at peak price periods.

The achievement of the world's first CSP system combined with a biomass-ORC plant is supported by the Danish Government's Energy Technology Development and Demonstration Programme (EUDP).

Figure 4: Aalborg CSP's parabolic trough

3. Monitoring performance during the first solar season

The peak performance of the plant is set to reach 16.6 MWth and the annual yield is expected to be 16,000 MWh of thermal energy. Since the CSP-plant went into operation in the end of 2016, it has been meeting the expected operational goals.

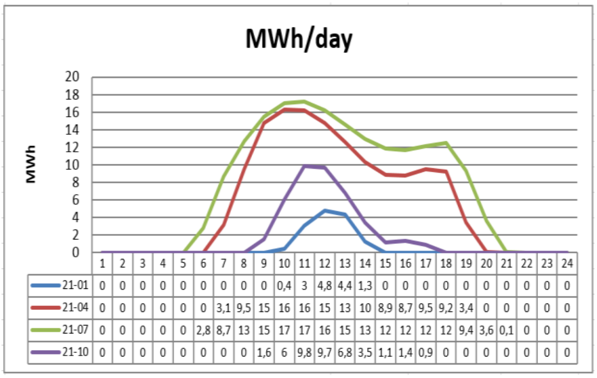

	1	2	3	4	5	6	7	8	9	10	11	12	13	14	15	16	17	18	19	20	21	22	23	24
21-01	0	0	0	0	0	0	0	0	0	0,4	3	4,8	4,4	1,3	0	0	0	0	0	0	0	0	0	0
21-04	0	0	0	0	0	0	3,1	9,5	15	16	16	15	13	10	8,9	8,7	9,5	9,2	3,4	0	0	0	0	0
21-07	0	0	0	0	0	2,8	8,7	13	15	17	17	16	15	13	12	12	12	12	9,4	3,6	0,1	0	0	0
21-10	0	0	0	0	0	0	0	0	1,6	6	9,8	9,7	6,8	3,5	1,1	1,4	0,9	0	0	0	0	0	0	0

21 January: 14 MWh **21 April:** 138 MWh
21 July: 180 MWh **21 October:** 41 MWh

Figure 3: Daily production data from each season of 2017

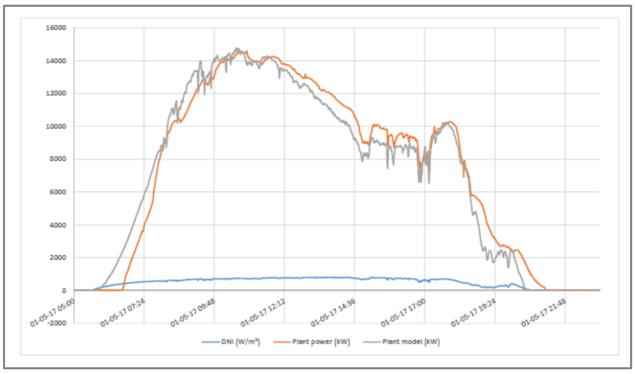

Heat calculated: 132,6 MWh **Heat delivered:** 130,1 MWh

Figure 6: Daily production data from 1 May, 2017

References

[1] B. Perers, S. Furbo and D. Janne , "Thermal performance of concentrating tracking solar collectors," Technical Univeristy of Denmark (DTU) Civil Engineering Report R-292 (UK) Department of Civil Engineering, Denmark, 2013.

Model-based control strategies for the integration of large-scale solar plants into district heating grids: evaluation of the required technical adjustments and the potential for performance improvement

Peter Innerhofer[*1],Viktor Unterberger[2,3], Bernhard Gerardts[1], Klaus Lichtenegger[2],Markus Gölles[2]

*) Corresponding author: tel: +43 316 292846, fax: +43 316 29284028; email: p.innerhofer@solid.at
1) S.O.L.I.D. Gesellschaft für Solarinstallation und Design mbH, Puchstraße 85, 8020 Graz, Austria
2) BIOENERGY 2020+ GmbH, Inffeldgasse 21b, 8010 Graz, Austria
3) Institute for Automation and Control, Graz University of Technology, Kopernikusgasse 24, 8010 Graz, Austria

Introduction

The control of large-scale solar thermal plants constitutes a major challenge, mainly for the following reasons. First, these plants exhibit highly dynamic behavior due to external disturbances by varying weather conditions, in particular the effective solar radiance and the ambient temperature. Second, the throughput time of the piping and collectors are high and varying with the pump speed. When the solar thermal plant additionally should be integrated in a district heating grid the control problems get even more complex.

In order to deal with these challenges the control strategies applied are often hierarchically structured. On a high-level basis, typically a set of rules defines the general mode of operation (e.g. feeding the heat into a district heating grid vs. storing it in a local buffer storage in case of presence of on-site consumers). On the low-level basis, control tasks such as controlling mass flows and temperatures are mainly handled separately for each subfield of the solar plant respectively part of the heat distribution system using simple linear PID controllers. On both levels of control typically neither the non-linear and coupled characteristics of the different components are considered, nor is information on future conditions and requirements taken into account. Therefore these default strategies applied on both levels usually do not yet utilize the full potential of the integration of modern solar thermal plants into district heating grids, mainly resulting in efficiency losses, even unused solar energy and increased re-parameterization efforts.

Model based control strategies would be a promising solution to better cope with these challenges, by taking into account the physical characteristics of the plant and incorporate weather forecasts. However, there exists nearly no experience regarding the practical steps necessary to apply such model-based control strategies in large scale solar thermal plants.

For this reason this contribution aims for presenting insights and experiences from a real implementation of model-based control strategies for a large-scale solar thermal plant integrated into a district heating grid. Next to all aspects which have to be considered within the implementation also a data-driven evaluation of the potential for efficiency increase by the application of model-based control strategies in large-scale solar thermal plants integrated into district heating grids should be presented.

Part I – Implementation details

The experiences evaluated come from the implementation of a model-based control strategy currently performed at a plant with 3.855m² of collectors, a feed-in point to the district heating grid and a local consumer with 500kW peak demand supplied through a heat store with 64m³. A peculiarity to this plant are the 3 different orientations of its collectors, south-west, south and south-east and its varying collector string size, see Figure 1. Solar plants are often optimized and constraint on the useable space. Due to these facts, the feed temperatures of the collector strings systematically vary within a single day since the zenith angle of the sun changes respectively. This behavior is even increased when the solar radiance is at partial load i.e in transition periods or winter.

Figure 1: Setup of the collectors at the solar thermal plant considered (Wasserwerk Andritz)

At the start of the project, additional sensors and actuators where added. First, to get more precise measurement data and consequently to create more reliable models serving as basis for the subsequent control development. Second, to be able to control the flow of each collector string and therefore regulate the feed temperatures separately.
The most important sensors and actuators which were installed are a reliable non-shaded pyranometer in horizontal mount, flow sensors and control valves for each collector string and pressure and temperature sensor in the return and flow of each collector row (Figure 2). Additionally a heat meter was installed in the main collecting pipe.
Important to the installations are the position of the sensors for example the pressure sensors. They are used to measure the pressure difference over each collector string. In order to do so, they need to be placed before the control valves. Also important are the flow coefficients of the control valves. They need to fit the overall pressure loss of a collector row to regulate the flow effectively.
With all the sensors installed, it was possible to conduct experiments, collect measurement data and create the respective models. In a first step cold experiments were executed during the night with simple flow regulations to evaluate the pressure-flow relationship of the solar pump in combination with the control valves.
In a next step warm experiments were conducted during the day to incorporate the temperature pressure correlation.

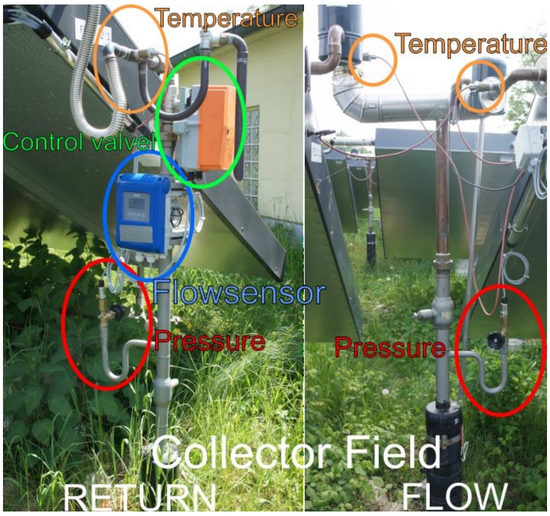

Figure 2: Additional Sensors and Actuators

Next step in the project is to implement the control strategies currently under development and show first results on the real-scale solar thermal plant.

Part II - potential for efficiency increase
In general, the method used for the evaluation is based on a comprehensive analysis and categorization of representative measurement data combined with simulation studies. Additionally, the method distinguishes between the potential within the high-level control and the low level control. The improvement in the high level control mainly results from the explicit consideration of forecast data as well as predicting the optimal behavior for all components. The improvement in the low-level control results for instance from avoiding the typical oscillating behavior. For the plant considered an increase of the annual efficiency of 3% by a model-based high-level control and 5-8% by a model-based low-level control could be shown. Finally, these two results lead to a potential of 8-10% for the overall efficiency increase achievable by the employment of model-based control strategies.

Thermal performance analysis and comparison between measured performance and modelled performance of a parabolic trough solar collector array

Janne Dragsted, Bengt Perers, Simon Furbo, Weiqiang Kong
Department of Civil Engineering, Technical University of Denmark, Kgs. Lyngby 2800, Denmark
+45 45251862, jaa@byg.dtu.dk

Keywords: Parabolic trough solar collector, thermal performance analysis, solar collector field.

SUMMARY

A new Parabolic Trough solar collector is investigated and tested at the test facilities at the Technical University of Denmark. The performance is measured at different inlet temperatures in order to evaluate the efficiency. The measured thermal performance is compared with modelled thermal performance of the same Parabolic Trough solar collector.

1. Introduction

In the summer of 2017, a parabolic trough solar collector, see figure 1, was installed at the test facilities at the Technical University of Denmark. The aim of the tests is to investigate the thermal performance of the solar collector and compare measured data with modelled values describing the solar collector. The solar collector is made up of four troughs installed in series and intended for operating temperatures of 80-90 °C

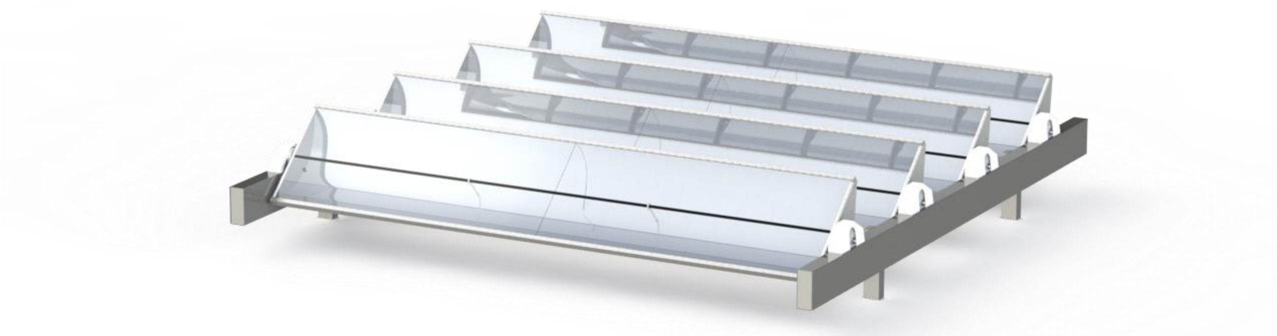

Fig 1. Sketch of the parabolic trough solar collector.

2. Measuring and monitoring system

The test facilities for testing solar collectors at the Technical University of Denmark have been in operation over two decades. The measurement consists of in- and outlet temperature, ambient temperature, flowrate, total- and diffuse solar radiation on the plan of the trough. The inlet temperature is varied from 20 °C to 80 °C and the efficiency is analysed.

Fig 2. Picture of the parabolic trough solar collector.

3. Results

The thermal performance of the solar collector, see figure 2, is evaluated under Danish weather conditions at a high inlet temperature of 80 °C. A comparison is carried out of measured and modelled performance.
The efficiency of the collar collector is evaluated.

Reference

[1] S. Furbo, B. Perers, W. Kong, Z. Tian, H.-E. Kiil, A. W. Larsen, R. Bang Madsen, New CPC based hybrid collector for solar heating plants, SDH Conference 2016 final Aug 15 2016

[2] Z. Tian, B. Perers, S. Furbo, J. Fan, Annual measured and simulated thermal performance analysis of a hybrid solar district heating plant with flate plate collectors and parabolic trough collectors in series, Applied Energy, Volume 205, November 2017, Pages 417-427.

MEASUREMENT-BASED DESCRIPTION OF THE TEMPERATURE DISTRIBUTION IN LARGE ATMOSPHERIC HEAT STORAGE TANKS

Luise Umbreit, Andreas Herwig and Karin Rühling
Institute of Power Engineering, Professorship of Building Energy Systems and Heat Supply,
Technische Universität Dresden, Dresden, 01062, Germany, +49-351 / 463-32971,
Luise.Umbreit@tu-dresden.de

Abstract – The presented research project uses an innovative measurement technology to investigate large atmospheric heat storage tanks which are operated with water as storage medium. There is already sound knowledge about heat storage systems at small scales as used in single buildings in literature and software engineering as well. On the other hand, for large atmospheric heat storage tanks there are only a few scientific descriptions in literature and simulation models available. The measurement data combined with simulation results are used to gain further insight into load management in district heating especially with respect to increasing levels of renewable based feed-in. In this publication, the focus is set on particular aspects concerning the physics of one-zone and two-zone atmospheric heat storage tanks.

1. MEASUREMENT TECHNOLOGY

In order to investigate their physical behaviour under real operation conditions four one-zone and two two-zone heat storage tanks at scales between 2,000 m^3 and 43,000 m^3 had been equipped with a distributed temperature sensing (DTS) measurement system. The DTS-measurement principle (Figure 1) is based on the RAMAN-effect to gain precise information about the temperature distribution both in space and in time along one single glass fibre cable (Smolen and van der Spek, 2003). The measurement data had been used to create animated visualizations that depict the operation mode of the heat storage tanks in general (Rühling et. al., 2016). Due to realizing an adapted measurement concept for each monitoring and developing appropriate analysis algorithms more detailed information can be revealed. Hence, different physical effects on thermal stratification within heat storage tanks can be proven. This paper presents some subset results for both researched types of heat storage tanks.

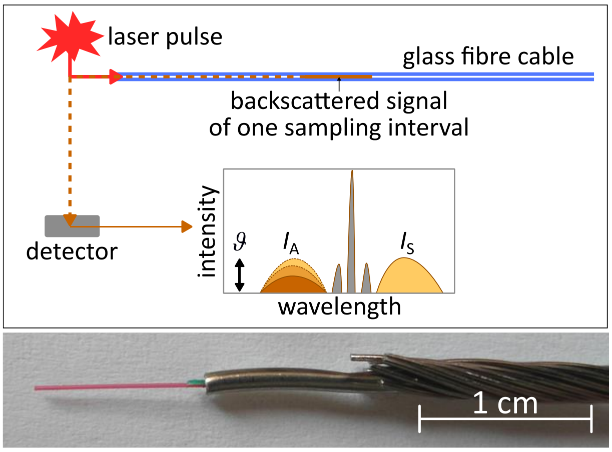

Figure 1: Top: Scheme of the DTS-measurement system. Corresponding to the RAMAN-effect, the frequency-shifted backscattering signal of a laser pulse running through a glass fibre cable features two components: The Stokes signal I_S and the Anti-Stokes signal I_A The space- and time-resolved temperature ϑ of the fibre can be determined from the detected intensity ratio of both components.
Bottom: Structure of the stainless steel sheathed glass fibre cable installed in the heat storage tanks.

2. ATMOSPHERIC ONE-ZONE HEAT STORAGE TANKS

2.1 General physics and operating mode

A common and widely realized type of large atmospheric heat storage tanks is based on the design of HEDBÄCK. They are built as pressure-less standing cylinders with one radial diffuser at the bottom and one at the top of the storage volume. During the charge process, warm water is entering the tank through the top radial diffuser and cold water is leaving through the bottom radial diffuser. While discharging the heat storage tank the flow is directed reversely. As both radial diffusers are concentric with the cylindrical storage tank they induce a radial free jet (Figure 2). In most cases the charging and discharging temperatures are well defined, hence a thermal stratification with a layer of high temperature above one layer of lower temperature is formed, with a thermocline in between. This heat storage tank design is optimized for capacities of up to several 10,000 m^3 of water. More than 100 of these heat storage tanks had been built during the past decades.

The grade of stratification inside the heat storage tank limits the amount of heat which can be discharged at the required supply temperature level. Therefore a good understanding of the main factors that have an impact on the stratification is important for both: to give advice to the operation management and to generate valid models of this type of heat storage tank.

Main influences on the thermal stratification within the heat storage tank had been mentioned in (Herwig and Rühling, 2014).

2.2 Measurement concept

The measurement concept includes the DTS-measurement system and additional operating data of the heat storage tank as well. As shown in Figure 2 the DTS system captures the temperature field vertically at four radial and two additional circumferential positions: R1, R2, R3=U3, R4 and U1 and U2. Supplementary operating data is available for 19 vertically aligned PT100 temperature sensors, supply and return temperatures, volume flow and pressure at the bottom of the heat storage tank.

The temperature resolution is limited by random noise that can be reduced by averaging consecutive measurements. However, time resolution must be considered carefully. The presented work uses an average time of one minute. For this mean type the conditions inside the heat storage tank are assumed as sufficiently constant. As the focus is set on radial homogeneity of the temperature field in this study, temperature differences are formed at the same height between the six vertical positions. By the use of one-minute averages the DTS-system achieves a resolution, defined by the 1-σ standard deviation, of about 0.1 K for the radial temperature differences. The spatial resolution along the cable is 0.35 m.

By a step of calibration, the mean temperature of vertical measuring points is optimised to eleiminate small perturbations of the DTS system. Consequently, the measured temperature profiles can be compared only in terms of their shape, but not in terms of their absolute position. Since the corrections are only in the range of a few hundredths of a K, this aspect should not be discussed further in the following.

2.3 Radial homogeneity of the temperature field

The radial homogeneity of the temperature field is investigated based at the four positions R1 to R4. The position R3 represents the reference section which is used to compare the temperatures obtained at the other positions.

In Figure 3 solid lines on the right side represent the temperatures at the four radial positions during a standstill phase of the highly charged heat storage tank. Dashed lines on the left side related to the scale at the x2 axis indicate the temperature differences to R3 in each case. The gray lines marked with D indicate the position of the two diffusers. The temperature differences to R3 occurring in Figure 3 remain at very small scales over the entire height of the heat storage tank and are caused by the random noise

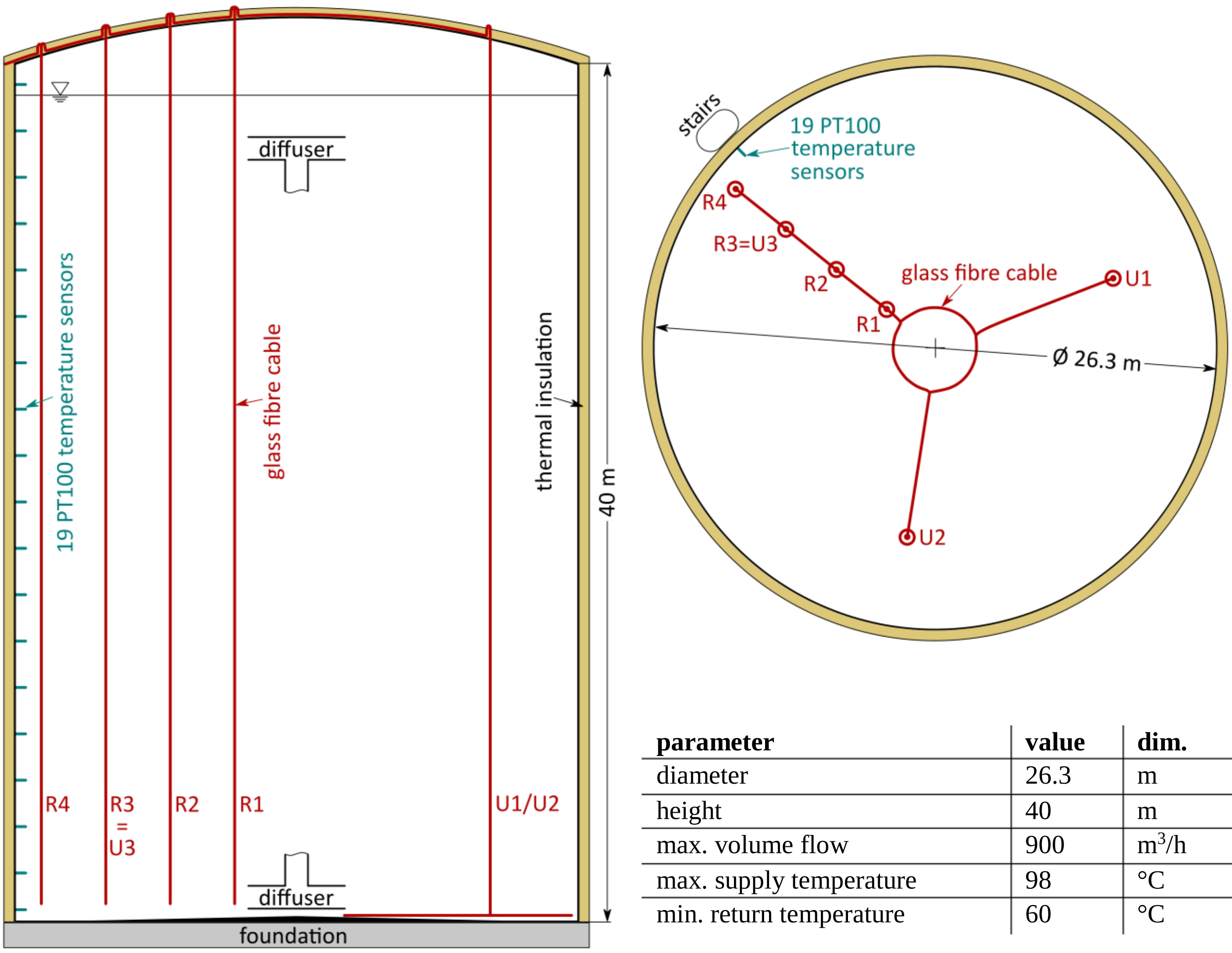

parameter	value	dim.
diameter	26.3	m
height	40	m
max. volume flow	900	m^3/h
max. supply temperature	98	°C
min. return temperature	60	°C

Figure 2: Measurement concept of the atmospheric one-zone heat storage tank and main design parameters

of the DTS system. Thus, for cases with no charging or discharging radial homogeneity of the temperature field can be assumed. Therefore, this case is considered as reference case for further investigation.

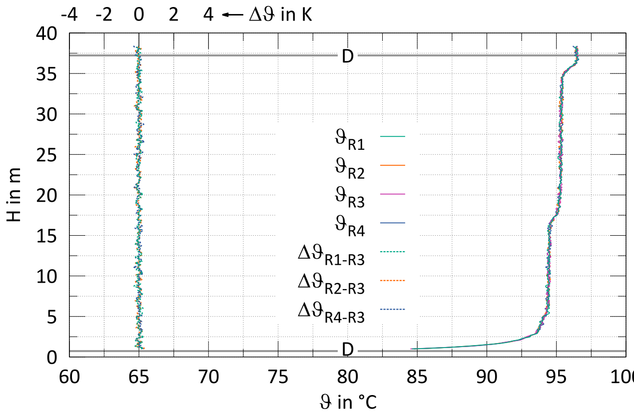

Figure 3: Temperature profile at the four radial positions and Temperature difference to R3 with scale on x2-axis. Reference case, 15 June 2016, 12.00 am

In the measurement period from 04 May to 30 June 2016 the largest radial deviation of 3.8 K occurs at 00.28 am on 31 May between R1 and R3 (dashed lines on the left side of Figure 4). It is located in the lower half of the thermocline at about 31.5 m. The maximum radial deviation is caused by an inversion lasting 1.45 h while a discharging process where water enters the heat storage tank at almost 77 °C with a volume flow of 500 m^3/h through the lower diffuser. The surrounding fluid has a temperature of 67.5 °C leading to a buoyancy of the incoming fluid, which is associated with strong convective mixing. Nevertheless, all observed radial temperature differences are smaller than 0.4 K in the cold layer, which extends to a height of 30 m (Figure 4). Thus, the inversion does not affect the radial homogeneity in the cold layer significantly compared to the reference case with radial differences up to 0.3 K (Figure 3).

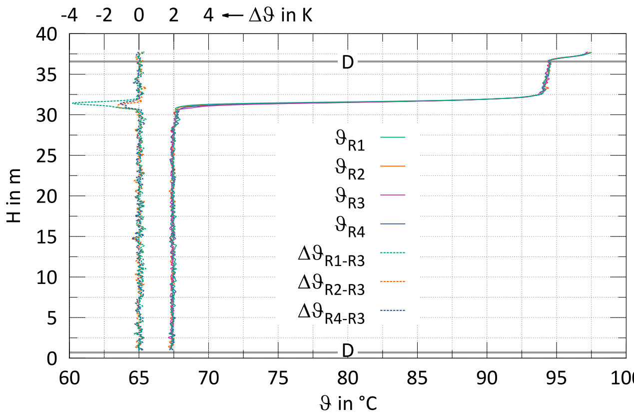

Figure 4: Temperature profile at the four radial positions and Temperature difference to R3 with scale on x2-axis. Reference case, 31 May 2016, 00.28 am

A detailed animated analysis over successive time steps suggests the following thesis for the radial deviations of up to 3.8 K located in the thermocline: Due to its high vertical density gradient the thermocline represents a barrier to the upward convection movement which was caused by the inversion at the lower diffuser. The upward momentum of the convection flow is dissipated by the natural density stratification in the thermocline, bringing it into a slight oscillation. Thus, the temperature profiles in the area of the thermocline seem to be vertically shifted by 0.1 to 0.2 m during this phase. Meanwhile cold water mixes into the thermocline and chills it. The warm storage layer above the thermocline, however, remains unaffected. By the end of the inversion the temperature profiles regain congruence within a few minutes. However, inversions up to this magnitude represent a rare operating case and the described case occurred during commissioning phase of the heat storage tank.

Finally, the radial homogeneity of the temperature field for a typical charging phase of 12 h without pronounced inversions shall be discussed. The maximum volume flow is 850 m^3/h. Again, the temperature difference between R1 and R3 is evaluated. Evaluating all temperature differences between R1 and R3 over the total height of the measuring section 466,727 individual temperature differences can be determined from 660 1-minute averages. The obtained dataset is characterized by a very good radial homogeneity of the temperature field. Only 1 % of the temperature differences are outside the range of ±0.3 K with a maximum deviation of 0.8 K.

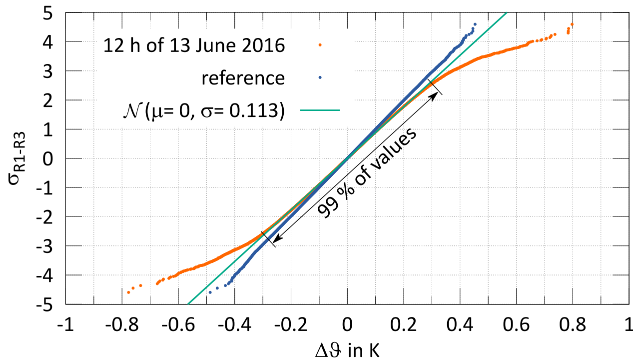

Figure 5: Normal probability plot of temperature differences R1 to R3 while a period of maximum charge flow, 13 June 2016 from 12.00 am to 12.00 pm; reference case, 13 h of 15 June 2016 while a period of no volume flow

A more detailed analysis of this distribution is possible by a comparative analysis with the reference case presented in the normal probability plot (Figure 5). Here, normally distributed data is arranged along a line of constant slope. For the reference case the dataset of 466,621 points approximates the normal distribution very good (blue in Figure 5). This means that in the reference case the temperature differences in radial direction consist in fact only of random noise of the DTS-measurement. The measured 466,727 temperature differences during the charging phase are depicted in orange in Figure 5. Their standard deviation had been calculated to 0.113 K. The straight green line in Figure 5 would result from a perfect normal distribution with just this standard deviation of 0.113 K. In the top and bottom regions, the orange data deviates from the linear curve.

Therefore, the temperature differences greater than ±0.3 K cannot be explained by the random noise of the DTS-system, which is approximately normally distributed. They must be caused by the temperature field of the heat storage tank. By analyzing the supplementary operating data it was found that the largest radial deviations (>0.6 K) in Figure 5, as already described with reference to Figure 4, are correlated to short term temperature inversions at the upper diffuser. In the period shown for Figure 5, however, the inversions are less pronounced than the inversion of over 9 K, which caused a radial temperature difference of 3.8 K in Figure 4. The inversions during the period shown in Figure 5 reach 2 to 3 K for the temperature difference between the water entering the heat storage tank through the upper diffuser and the surrounding water of the warm layer. Short-term perturbations of the density stratification associated with this 2 to 3 K temperature deviations at the diffuser are thus sufficient to cause very small deviations in the otherwise radially homogeneous heat storage tank.

3. ATMOSPHERIC TWO-ZONE HEAT STORAGE TANKS

3.1 General physics and operating mode

The atmospheric two-zone heat storage tank is also based on HEDBÄCK and is shown as an example in Figure 6 (not to scale). It has the same design features as the one-zone atmospheric heat storage tank, but is divided into two zones by an insulated, dome-shaped intermediate floor. The intermediate floor can be considered dimensionally stable.

The two storage zones each have two radial diffusers for charging and discharging. Moreover the two-zone heat storage tank features a vertical compensation pipe. This is an open ended pipe which serves as a hydraulic connection between the upper and lower storage zone. The length of the pipe and the amount of additional openings depend on constructive and functional requirements. The permanent exchange of fluid between the two storage zones is important for two reasons:

The density changes occurring in the upper storage zone through charging and discharging have a direct effect on the filling level due to approximately constant fluid mass

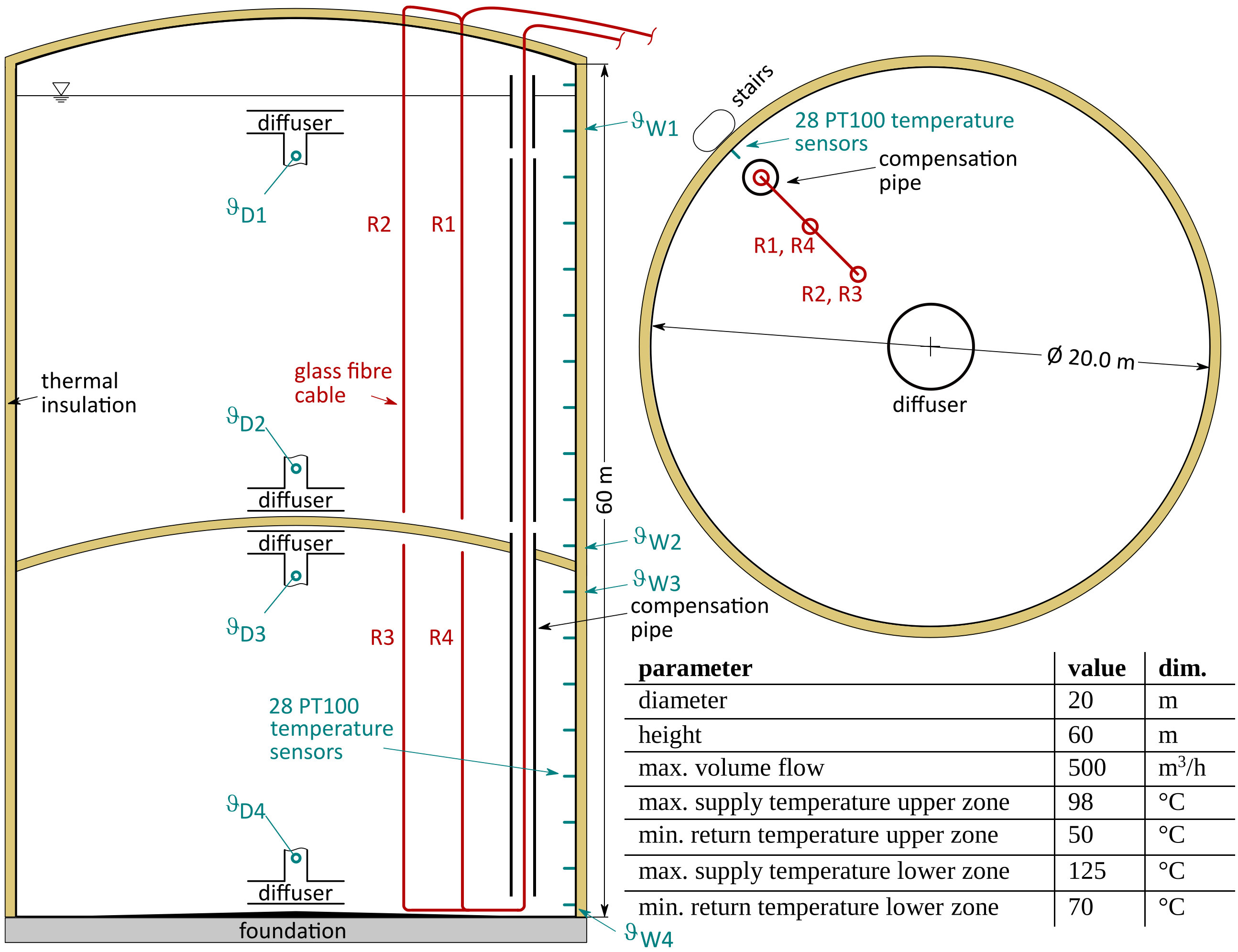

parameter	value	dim.
diameter	20	m
height	60	m
max. volume flow	500	m^3/h
max. supply temperature upper zone	98	°C
min. return temperature upper zone	50	°C
max. supply temperature lower zone	125	°C
min. return temperature lower zone	70	°C

Figure 6: Atmospheric two-zone heat storage tank. Sketch, measurement concept and main design parameters

in the storage tank. In the lower storage zone, however, the volume is constant due to the fixed position of the intermediate floor. Since there is no further expansion tank available for the heat storage tank, the density changes occurring during charging and discharging of the lower storage zone must be compensated for by a mass flow via the compensation pipe.

Moreover, it acts as a safeguard against underpressure or overpressure in the lower zone (e. g. as a result of operating errors).

On the other hand, the exchange of fluid between the two storage zones may encourage undesirable effects:

The compensating pipe primarily conveys fluid from one storage zone to the other, or as a side effect within a storage zone itself in case of additional openings in the compensating pipe. Thus a flow in the immediate vicinity of the respective opening is induced as fluid leaves the compensation pipe. Furthermore, this fluid usually has not the same temperature as the surrounding fluid when entering the respective layer within a storage zone. Due to the necessarily occurring convective mixing, the thermal stratification existing within a storage zone can be influenced negatively.

Nevertheless, the hydraulic coupling of both storage zones has an important effect, which is an essential feature of the two-zone heat storage tank:

The pressure level in the upper region of the lower storage zone below the intermediate floor is sufficiently high to store water at temperatures above 100 °C. Currently, temperature levels of up to 130 °C are in use. These temperature levels do not mark the physical limits but meet the local applicable safety measures.

Thereby, the volume-specific heat capacity of the two-zone heat storage tank is higher compared to a single-zone heat storage tank of the same size. Thus, the higher total investment costs can be super-compensated with respect to the amount of stored energy.

The constructive design of the two-zone atmospheric heat storage tank is not akin to that of the pressurized heat storage tank, since

- the maximum pressure level reached is not higher than with a single-zone atmospheric heat storage tank of the same height
- the heat storage tank is operated as a displacement heat storage tank at atmospheric conditions, and
- the intermediate floor experiences only a small pressure difference.

For atmospheric two-zone heat storage tanks there are two application possibilities: If heat is to be provided at two different temperature levels, both the lower and the upper storage zone can be used actively for heat storage. Alternatively, the sole active operation of the lower storage zone is possible. In this case the upper storage zone serves as pressure load and may be used as water reservoir, for example.

3.2 Measurement concept

The measurement setup features vertical temperature profiles at two radial positions both in the upper and lower zone of the heat storage tank as well as in the compensation pipe (Figure 6). The vertical temperature profiles at positions R1 in the upper zone and R4 in the lower zone had been captured at the same radial distance from the diffusers. The same applies to the vertical profiles at R2 and R3. DTS-measurements had been carried out alternating for the upper and lower zone with an average time of 10 s each. Subsequently, time averaging had been applied to groups of three datasets so that a measuring time of 30 s for one cable represents an average value for one minute of physical time.

Supplementary operating data is available in 1-minute resolution for volume flow of the upper and lower zone, pressure at the bottom, supply and return temperatures for both the upper and lower zone and 28 vertically aligned PT100 sensors.

3.3 Nominal operation, interaction between the upper and lower zone

To show the nominal operation of the two-zone heat storage tank the data record of one measurement day, 26 March 2015, had been chosen according to the following requirements:

- pronounced thermal stratification both in the upper and lower zone as well
- charging or discharging at moderate volume flows both in the upper and lower zone with visible changing of the state of charge
- visible influence of the thermal stratification by the interaction of the two zones through the compensation pipe.

Figure 7 depicts subset operating data including the supply and return temperatures ϑ_D1-ϑ_D4 which had been captured in the corresponding supply and return line. Furthermore, the PT100 temperatures ϑ_W1-ϑ_W4 at the highest and at the lowest position within the two zones of the heat storage tank are shown. The corresponding volume flow is only measured for the return line connecting pipe for each zone. At the other diffuser almost the same inverse mass flow is assumed. Here, positive volume flows indicate charging and negative volume flows indicate discharging.

The lower zone experiences discharging from 00.00 am to 08.00 am with a volume flow of less than 50 m^3/h (or 10 % of nominal volume flow), supply and return temperatures are 118 °C and 73 °C.

Subsequently, there is a phase with zero volume flow followed by discharging in two phases beginning at 00.30 pm, supply (ϑ_D3) and return (ϑ_D4) temperatures are 125 °C and 73 °C.

The upper zone is charged with a volume flow of 50 m^3/h (or 10 % of nominal volume flow) throughout the day. Supply (ϑ_D1) and return (ϑ_D2) temperatures remain constant at 95 °C and 52 °C.

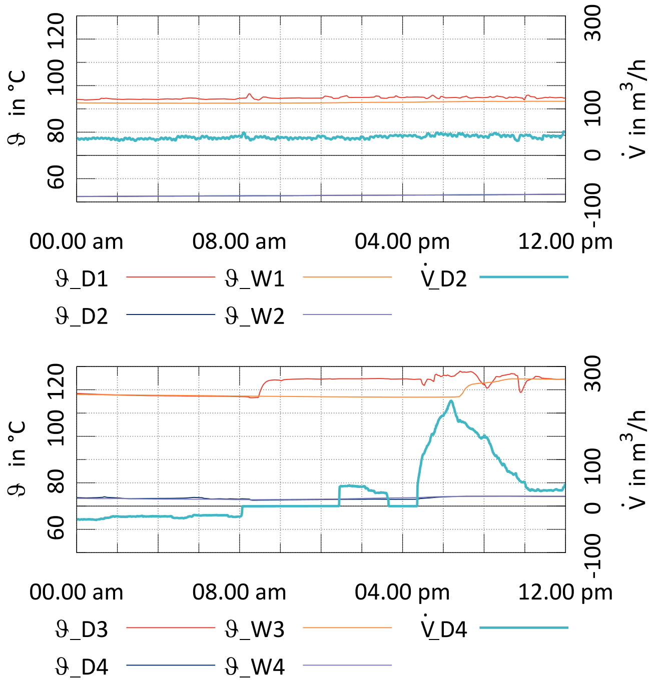

Figure 7: Operating data for upper (top) and lower zone (bottom), 26 March 2015

The evolution of the vertical temperature profile in time generated by post-processing the DTS-measurements is depicted in Figure 8 by height-to-temperature plots. There is one graph for each the upper and lower zone including the temperature profiles every four hours at the radial positions R1 and R4 respectively. The inner temperature profiles R2 and R3 had not been taken into account as they serve to investigate radial homogeneity of the temperature field. However, radial effects are supposed to be small and not to determine main characteristics of the temperature field.

Additional marks in the graphs indicate the positions of the radial diffusers ("D"). In case of the upper diffuser of the upper zone the range where the diffuser can move is marked. The letter "B" marks the position of the intermediate floor within the graph of the upper zone.

General description of the temperature field:

Good thermal stratification can be observed both in the upper and lower zone. Since the pressure level in the lower zone is higher than in the upper zone the temperature level of the lower zone can exceed that of the upper zone. This results in a remarkable aspect of the two-zone heat storage tank: The highest temperature can be found under the intermediate floor at the top of the lower zone and the lowest temperature can be found directly above the intermediate floor at the bottom of the upper zone.

Furthermore, there is obviously more than one thermocline in the lower zone which is the regular case and occurs due to fluctuating supply and return temperatures. However, in the presented case no further fluctuations occur which facilitates the discussion of the evolution of the temperature profiles in time for the two zones.

The same applies to the upper zone. Here, only one thermocline is pronounced whereas the other ones are only implied. In addition for the upper zone several influences on the shape of the temperature profile have to be discussed.

Moreover, the vertical temperature gradient within a pronounced thermocline is higher for the lower zone than for the upper zone.

Evolution of the temperature field in the lower zone:

The temperature profile is shifted vertically while charging and discharging. Between 00.00 am and 08.00 am it moves slightly upwards due to discharging. At 12.00 am the state of charge of the lower zone is identical to 04.00 am as the temperature profile has reached the same position. From this point on the two cycles of charging cause the temperature profile to move downwards. The covered distance between 04.00 pm and 08.00 pm is especially high due to the high volume flow. In addition a third thermocline from 117 °C to 127 °C is formed by the increased level of supply temperature.

During the whole process the shape of the temperature profile remains nearly the same for the thermoclines and the temperature levels at H = 2…4 m and H = 11…17 m. In the upper region above the upper thermocline a slight lowering of the temperature level of approximately 1.5 K can be observed.

Convective mixing is not considered to be the reason for this effect because there is no source of cold fluid entering the lower zone in this region. Heat losses through the surface are not dominating here because they would influence the entire temperature profile. Hence, the lowering of the temperature level in the upper region must be caused by thermal conduction through the intermediate floor. Underneath the intermediate floor the water is cooling down and mixes with fluid of the upper layer, as described in (Huhn, 2007). Subsequently, the upper layer is chilled evenly.

The minimum temperature level is reached at 12.00 am. Afterwards the charging processes combined with an increased supply temperature form a layer with fluid at a higher temperature and a third thermocline which is already implied by the temperature profile at 04.00 pm. The influence of thermal conduction on the temperature level cannot be discussed for the time after 12.00 am as the thermocline at 04.00 pm is not fully developed and the supply temperature is not stable. But the temperature profile at 12.00 pm implies that again the warm layer is cooling down.

The temperature profiles show that the influence of thermal conduction can be proven by the DTS-measurements. This effect could not be detected by the conventional operating data since the shape of the temperature profile is not resolved sufficiently. The modelling of thermal conduction through the intermediate floor is not presented in this paper and is considered as future work.

Evolution of the temperature field in the upper zone:

Figure 8 shows that constant charging of the upper zone is shifting the temperature profile downwards. As the volume flow remains nearly constant the displacement speed is also nearly constant which can be estimated regarding the distance covered by the thermocline at 49 m starting at 00.00 am. The vertical temperature gradient within the thermocline is not influenced. Obviously, the thermocline at about 58 m does not get affected by the charging process. That is because this region marks the transition from the fluid to the vapour space. This is a region above the water level where steam gets induced to keep an approximately constant temperature.

Contrarily to the lower zone the shape of the temperature profile changes more considerably. The following aspects can be observed as marked in Figure 8:

a) The thermal stratification in the region from 52 m to 57 m gets more pronounced during the entire day.

b) At its lower end the thermocline gets blurred meaning that the transition to the temperature level of 54 °C smoothens.

c) The temperature level from 27.5 m to 36 m increases. As a result, the thermocline at 35 m disappears.

Knowing that the compensation pipe features two additional openings, one in proximity of the lowest vertical position of the upper diffuser and one at the bottom of the upper zone, there are two possible influences on the temperature profile in region a):

- Flow leaving the upper diffuser at supply temperature
- Flow leaving the compensating pipe through the upper opening

The first point is likely to influence the temperature profile in the upper layer within region a) since the flow leaving the upper diffuser should form a layer of approximately the same temperature level as the supply temperature.

The lower layer within region a) is outside the sphere of influence of the upper diffuser and must be caused therefore by the flow leaving the compensation pipe. The measurement data shows that the temperature level slightly decreases while the layer gets more pronounced.

Regarding the discharging process in the lower zone from 04.00 pm the fluid originating from the bottom of the lower zone enters the compensation pipe at a temperature of about 74 °C. Since the compensation pipe features a second opening at the bottom of the upper zone permanent exchange between fluid in the compensation pipe and the heat storage tank is possible. For this reason, the temperature level within the compensation pipe is shifted to about 62 °C as fluid is transferred to the upper opening. This chilled fluid enters the upper zone and mixes with the surrounding fluid. Subsequently, a layer of about 87 °C is formed.

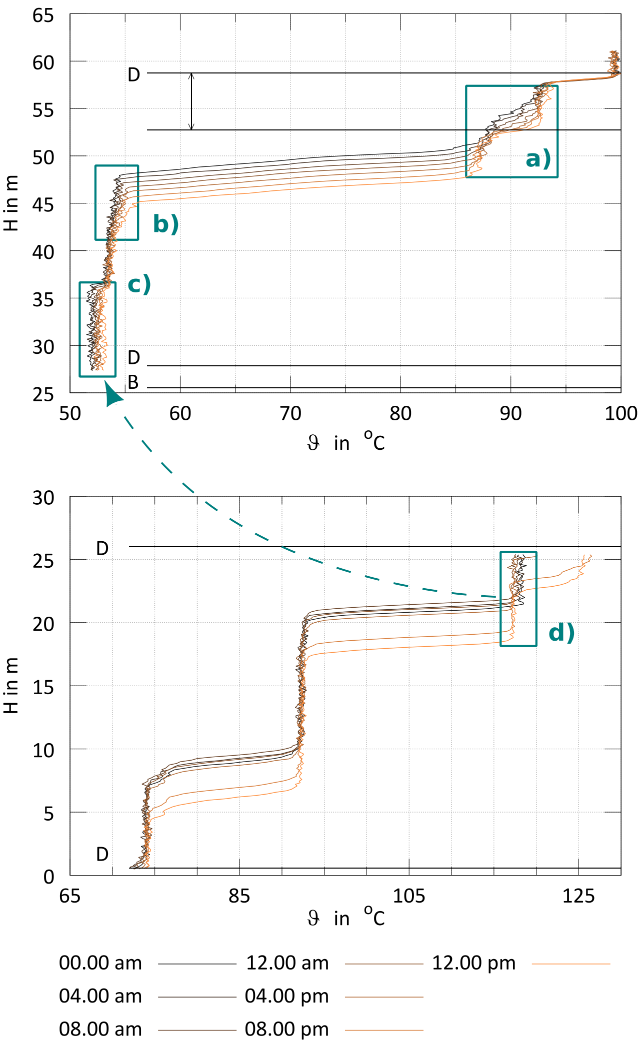

Figure 8: Evolution of temperature profile for the upper (top) and lower (bottom) zone, 26 March 2015

Besides, a small amount of fluid leaving the compensation pipe may also fall through the thermocline and influence the temperature profile in region b). This process could be observed by animated visualization of the DTS-measurements including the temperature profile within the compensation pipe, which is not presented in this paper. The volume of fluid transferred through the compensation pipe for the discharging process of the lower zone from 04.00 pm to 12.00 pm could be estimated to 32 m^3 which is about 0.4 % of the total volume of the lower zone. Nevertheless, this small amount of fluid is able to cause the changes in the temperature profile in the lower layer of region a) which could be confirmed by an energy balance.

For region c) there are four possible influences:

- Flow leaving the lower diffuser at return temperature
- Thermal conduction within the upper zone
- Thermal conduction through the intermediate floor
- Flow leaving the compensation pipe

As there is no fluid leaving the lower diffuser, the first point is deniable. Thermal conduction within the upper zone requires a sufficiently high temperature gradient but is unlikely to act over distances of several metres. However, thermal conduction through the intermediate floor must be taken into account since heat losses in the upper layer of the lower zone had been observed. The heat transfer through the intermediate floor is therefore indicated by a green arrow. Finally, a possible influence might be fluid originating from the bottom of the lower zone and leaving the compensation pipe through the lower opening at the bottom of the upper zone. It may rise up and mix with fluid of the cold layer of the upper zone.

4. FUTURE WORK

One-Zone heat storage tanks

- Evaluate further measuring periods
- Proof of circumferential symmetry
- Creating a simple 1 D model that comprises the main effects on the vertical temperature profile

Two-Zone heat storage tanks

- Proof of radial (and circumferential) homogeneity
- Design of a universal assessment criteria for thermal stratification
- Quantifying thermal losses towards the boundaries and within the heat storage tank, i.e. thermal conduction through the intermediate floor
- Characterizing the flow within the compensation pipe

4. CONCLUSIONS

Large atmospheric heat storage tanks offer a technically approved and cost efficient way to store energy at the temperature level of district heating systems. The DTS-measurement system was found to be an appropriate mean to investigate this type of heat storage tanks in detail.

One-Zone heat storage tanks

In the measuring period of two months, the heat storage tank shows a pronounced radial homogeneity. Only temperature inversions due to warmer fluid leaving the lower or colder fluid leaving the upper diffuser cause radial temperature deviations up to a few Kelvin. These deviations quickly fade away with the end of inversion. The actual thermal stratification of the heat storage tank is hardly affected.

Two-Zone heat storage tanks

The measurement data shows a prove-of-concept for the two-zone heat storage tank design. In this case both the upper and lower zone are used actively to store heat at different temperature levels each. Despite detected inner thermal losses good thermal stratification in both zones can be observed. Besides thermal conduction within the storage medium of a single zone thermal conduction through the intermediate floor and the flow through the compensation pipe are assumed as main influences on inner thermal losses. The latter is a direct consequence of the upper zone serving as pressure maintenance of the lower zone. Hence, to a certain degree an influence on the thermal stratification is expected and unavoidable.

ACKNOWLEDGEMENT

This research project was founded by German Bundesministerium für Wirtschaft und Energie (FKZ 03ET1322A).

REFERENCES

Smolen J. J. and van der Spek A. (2003) *Distributed Temperature Sensing – A DTS Primer for Oil & Gas Production*, Shell International Exploration and Production B. V., The Hague, The Netherlands.

Rühling K. et. al. (2016) *Erhaltung der Marktfähigkeit von KWK Anlagen mittels Einbindung von Umweltenergie*, Abschlussbericht Forschungsvorhaben – FKZ 0327831 (BMWi). AGFW-Projektgesellschaft für Rationalisierung, Information und Standardisierung mbH, ISBN: 3-89999-057-9

Herwig A. and Rühling K. (2014) Fibre-Optic distributed temperature sensing of large hot water storage tanks. *14th International Symposium on District Heating and Cooling*, 7-9 September, Stockholm, Sweden.

Huhn R. (2007) *Beitrag zur thermodynamischen Analyse und Bewertung von Wasserwärmespeichern in Energieumwandlungsketten*, PhD Thesis, Technische Universität Dresden.

Metrological and computational analysis of solar integration in a district heating system with variable temperatures

Tobias Ramm, Michael Klärner and Tobias Schrag

Summary

This paper introduces Dollnstein's district heating system with variable supply temperatures and the implemented measurement concept. The system uses solar thermal collectors as well as photovoltaics together with heat pumps. The metrological analysis shows very good results regarding the efficiency of the integrated solar thermal system. A first computational analysis verifies the benefit of the solar thermal feeding at lower temperature levels. In addition, a first analysis of the electrical power production by photovoltaics and the heating demand is performed. This analysis may show additional potential to provide thermal energy by the combination of photovoltaics and heat pumps and improve the solar share.

Keywords: district heating systems, variable temperatures, solar thermal, photovoltaics, metrological analysis, low-exergy, heat pumps, coupled energy systems, system modelling

1. Introduction

Currently district heating systems are following different approaches to reduce the greenhouse gas emissions and therefore the environmental impact of heating systems. On the one hand, the efficiency of the system and the integration of renewables or waste heat is tackled. On the other hand, the integration of the heat supply in the overall energy system is focused. This work addresses both issues with the focus on the use of solar energy.

2. Case study Dollnstein

The village of Dollnstein has implemented one of the first local district heating systems with variable temperatures. The hydraulic diagram of the system is shown in Fig. 1. During the heating period, the grid supplies the consumers with a temperature level of approx. 70 °C. To improve the

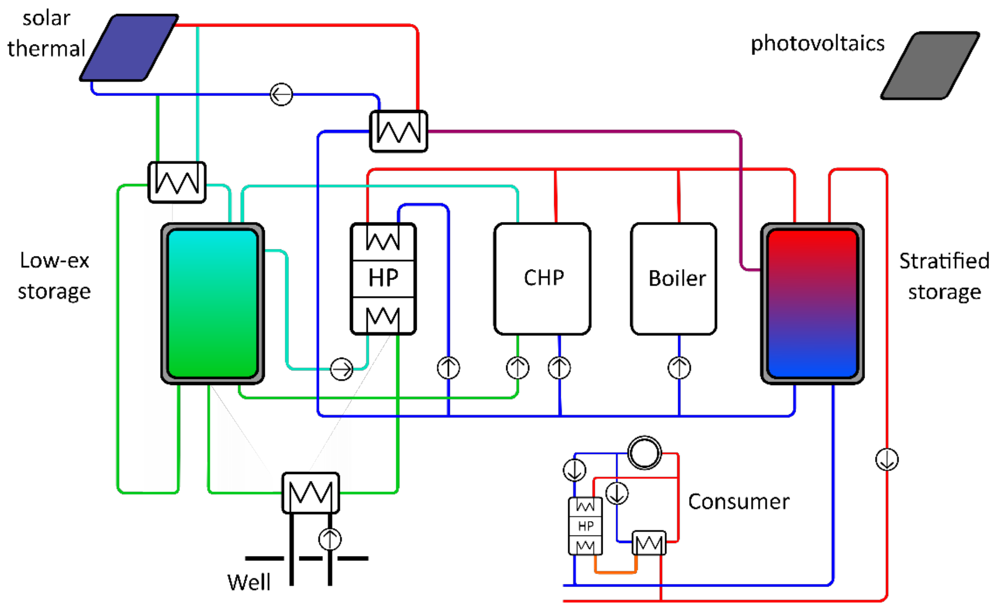

Fig. 1 Hydraulic diagram of the heating system

technical efficiency and economic viability, the supply temperature is lowered to approx. 30 °C during the summer period. Decentralized heat pumps provide the necessary temperature for hot water preparation using the heat grid as heat source. The solar thermal system with a size of 100 m² feeds, depending on the temperature levels of the storages and the fluid flow temperature, into the low-exergy storage or the stratified storage. A Photovoltaic system, which is also part of the system, is one option to supply the heat pumps with electrical power.

3. Measurement concept and data evaluation

The measurement concept allows a detailed analysis of every single component of heat and power generation as well as every electrical und thermal consumer and the overall system. The measurement concept was not fully implemented for the whole investigated period. The measurement results indicate a very good thermal efficiency of the integrated solar thermal system. The monthly production per square meter installed collector area is shown in Fig. 2. The results lead to the estimation, that the yield for the year 2017 is between 560 and 620 kWh/m²a, whereby the yield within the measured seven months is 504.5 kWh/m². The ratio of the solar thermal energy of the centralized heat production is 63 % in July and 70 % in August.

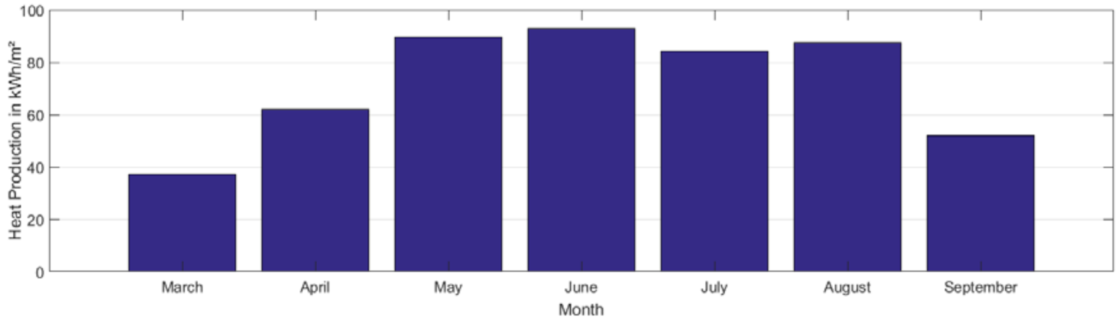

Fig. 2 Specific solar thermal production from March to September of the year 2017

In addition, a first analysis of the electricity produced by photovoltaics and the heat demand of the consumers is performed. Due to this analysis, a theoretical possible solar fraction can be calculated. This overall solar fraction contains the directly produced heat by the solar thermal collectors and the indirect produced heat by photovoltaics combined with central and decentralized heat pumps.

4. Computational analysis of the heating system focused on solar integration

A model of the heating system using the software MATLAB/Simulink with the Carnot-Toolbox is developed. First computational analysis show the benefit of low temperatures for the solar thermal system and will be presented at the conference.

5. Results

The solar thermal collectors show very good thermal yields. During summer, there is a very high ratio of solar production. The actual computational model was validated. The developing of an enhanced computation model is necessary to investigate the behaviour of the system together with the grid and find favourable control strategies to extend the usage of the electrical power by the photovoltaics for heat production by heat pumps. In future, there will be also measuring data of the electricity demand for the heat pumps available. This allows doing more accurate and detailed analysis of the electricity demand of the heat pumps and makes it possible to compare the electricity demand and production in a high resolution of time.

Use of drones to evaluate the thermal performance of solar collector fields

Janne Dragsted, Simon Furbo
Department of Civil Engineering, Technical University of Denmark, Kgs. Lyngby 2800, Denmark
+45 45251862, jaa@byg.dtu.dk

Keywords: Drone, flow distribution, solar collector field, thermal performance.

SUMMARY

Solar collector fields are increasing in size, therefore new methods are developed for evaluating the thermal performance. Here the use of drones with infra-red camera are investigated as an easy way of insuring an good flow distribution and avoid boiling in large solar collector fields.

1. Introduction

Solar collector fields consist of a high number of parallel connected solar collector rows with different numbers of serial connected solar collectors, see figure 1. In order to achieve a high thermal performance of the solar collector fields and by that reach the high energy saving potential of the fields, it is important that the flow distribution for the solar collector fluid in the fields is reasonable even. That is: The flow rate through each collector row must be proportional to the collector area of the row, so that the return fluid temperature from each row is almost the same.

As the solar collector fields are getting larger and larger it is difficult, expensive and time consuming to determine the flow distribution during different weather and operation conditions by use of conventional flow meters.

Fig 1. Solar collector field in Denmark.

2. Results

Measurements of surface temperatures of solar collectors will be carried out with a drone with an infra-red camera, see figure 2. The measurements will be analysed in such a way that it will be elucidated how accurate the solar collector fluid temperature can be determined by means of the measurements. Measurements with a drone of surface temperatures of solar collectors in the end of different parallel connected rows in a solar collector field will also be carried out. Based on these measurements and on temperature measurements of solar collector fluid temperatures it will be evaluated if drones with infra red cameras are suitable for an easy and fast check of the flow distribution in solar collector fields.

Fig 2. Drone with infra-red camera

Reference

[1] F. Bava, S. Furbo, Development and validation of a detailed TRNSYS-Mathlab model for large solar collector fields for district heating applications, Energy, Volume 135, 2017.

[2] S. Furbo, B. Perers, F. Bava, Thermal performance of solar district heating plants in Denmark, Proceedings of Eurosun 2014.

MODELLING FAULTY BEHAVIOURS OF LARGE SOLAR THERMAL SYSTEMS

Gaëlle Faure[1,2], Mathieu Vallée[1,2], Cédric Paulus[1,2] and Tuan Quoc Tran[1,2]

1 Univ. Grenoble Alpes, INES, F-73375 Le Bourget du Lac, France

2 CEA, LITEN, 17 rue des Martyrs, F-38054 Grenoble, France

Summary

This paper presents the modelling and simulation of several faults that can affect a large solar thermal system. We give an overview of our methodology, based on component modelling. In particular we describe the solar collector model. We then show the results of the simulation of the behaviour of the complete system subject to faults.

Keywords: fault modelling; fault analysis; large solar thermal system

1. Introduction

Large solar thermal systems (LSTS) can provide renewable and cheap energy to district heating networks and industrial processes. The total area of such installations in operation in Europe reached 1 million m^2 at the end of 2015 (Mauthner, Weiss, and Spörk-Dür 2016). Since these installations require long-term investment, fault detection and diagnosis methods (FDD) can ensure a better return on investment. However, few work exists in this direction (Ohnewein et al. 2006; Shahbazfar et al. 2012).

In order to develop a FDD method, main prerequisites are a good overview of which kind of dysfunctions can affect the plant as well as the observation of the behaviour of the system subjects to the different dysfunctions. The first step was addressed in a previous paper (Faure et al. 2016). Data to achieve the second step can be produced either by experimental or simulation means. However obtaining experimental data of a faulty system is in general not possible or limited to one specific fault and one specific system. On the other hand, a model is flexible and allows a better understanding of how react a system to a fault. In this paper, we present the application of this option: the modelling of the behaviour of a LSTS under some faults:

- faults that can affect solar thermal collectors,
- a bad hydraulic balancing,
- excessive thermal losses of the pipes.

2. Description of the study

We performed a state of the art survey which showed that there are very few attempts to accurately model the faulty behaviour of a LSTS. In particular, the modelling of faults that can affect a solar thermal collectors has been made using a simple regression solar collector model which use performance parameters of the NF EN ISO 9806 or ASHRAE norm (Kalogirou et al. 2008; de Keizer 2012). The drawback of this kind of model is the difficulty of choosing and tuning the parameters to properly represent a fault inside the solar collector.

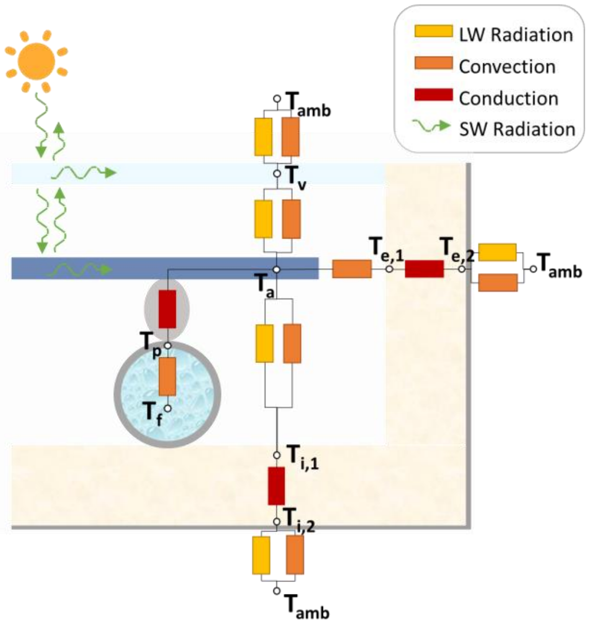

Fig. 1: Simplified representation of the developed solar collector model.

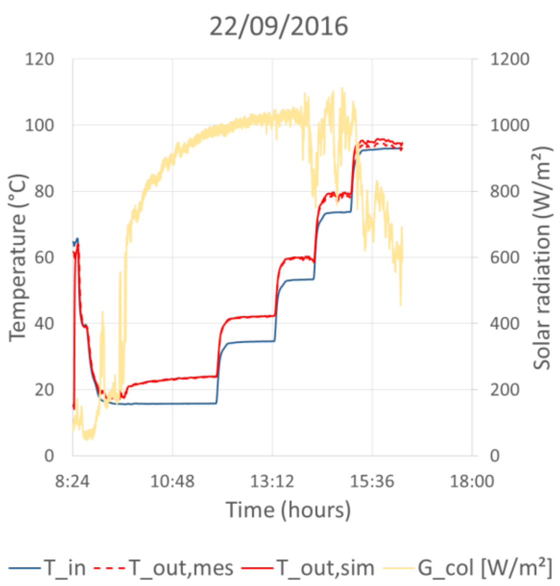

Fig. 2: Validation of the solar collector model with experimental data.

We developed a physical detailed model of solar collector which represents each parts of the collector and the physical interactions between these parts. In this way, it becomes easy to model one fault that affect a solar thermal collector. The model was validated with a simple model and experimental data.

This solar collector model was then integrated in a model representing the whole primary loop of a LSTS. Primary loop comprises the solar thermal collectors, the solar pump, the heat exchanger between primary and secondary loop, the pipes between solar collectors and the heat exchanger and the pump controller. This model was developed in the Modelica language, which enables a modular modelling and thus make modifications of the plant easier. It was parametrized with typical parameters of such installations.

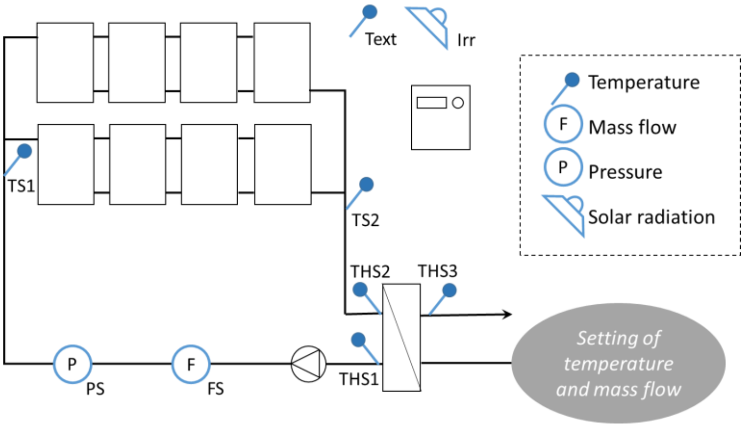

Fig. 3: Schematic representation of the simulated system and observed variables, which corresponds to a typical monitoring.

Finally, faults are implemented in the primary loop model by modifying appropriate parameters. Several simulations were performed for each fault by varying the severity of the fault, the number of impacted solar thermal collectors (in the case of faults affecting them) and the type of hydraulic configurations.

3. Conclusion

The simulations highlighted the faults that impact the most the behaviour of the system and thus have to be detected in priority. Moreover, the analysis of the results can help to choose and design the most appropriate method to detect and diagnose these critical dysfunctions, diagnosis meaning identifying the type of the fault as well as its location and severity.

4. Acknowledgement

This project has received support from the French State Program Investment for the Future bearing the reference (ANR-10-ITE-0003).

5. References

Faure, Gaëlle, Mathieu Vallée, Cédric Paulus, and Quoc Tran Tran. 2016. “Reviewing the Dysfunctions of Large Solar Thermal System: A Classification of Sub-Systems Reliability.” In *ISES Conference Proceedings (2016)*. Palma de Mallorca (Spain).

Kalogirou, Soteris, Sylvain Lalot, Georgios Florides, and Bernard Desmet. 2008. “Development of a Neural Network-Based Fault Diagnostic System for Solar Thermal Applications.” *Solar Energy* 82 (2): 164–72. doi:10.1016/j.solener.2007.06.010.

Keizer, Corry de. 2012. “Simulation-Based Long-Term Fault Detection of Solar Thermal Systems.” Kassel University.

Mauthner, Franz, Werner Weiss, and Monika Spörk-Dür. 2016. “Solar Heat Worldwide - Markets and Contribution to the Energy Supply 2014.” 2016 edition. Solar Heating and Cooling Programme. International Energy Agency.

Ohnewein, Philip, Angela Dröscher, Klaus Schgaguler, Franz Feichtner, Ernst Meißner, Peter Luidolt, Alice Köstinger, Richard Heimrath, Michael Jaindl, and Wolfgang Streicher. 2006. “IP-Solar: Development of a Web-Based Monitoring and Diagnostics Tool for Solar Thermal Systems.” In *Eurosun 2006*.

Shahbazfar, R., A.C. de Keizer, S. Kuethe, U. Jordan, and K. Vajen. 2012. “Fault Detection and Fault Diagnosis for Large Scale Solar Thermal Systems.” In *Proc. of Eurosun 2012, Croatian Solar Energy Association*. Rijeka, Croatie: International Solar Energy Society (ISES).

Thermal performance analysis and comparison between measured performance and modelled performance of a parabolic trough solar collector array

Janne Dragsted, Bengt Perers, Simon Furbo, Weiqiang Kong
Department of Civil Engineering, Technical University of Denmark, Kgs. Lyngby 2800, Denmark
+45 45251862, jaa@byg.dtu.dk

Keywords: Parabolic trough solar collector, thermal performance analysis, solar collector field.

SUMMARY
A new Parabolic Trough solar collector is investigated and tested at the test facilities at the Technical University of Denmark. The performance is measured at different inlet temperatures in order to evaluate the efficiency. The measured thermal performance is compared with modelled thermal performance of the same Parabolic Trough solar collector.

1. Introduction

In the summer of 2017, a parabolic trough solar collector, see figure 1, was installed at the test facilities at the Technical University of Denmark. The aim of the tests is to investigate the thermal performance of the solar collector and compare measured data with modelled values describing the solar collector. The solar collector is made up of four troughs installed in series and intended for operating temperatures of 80-90 °C

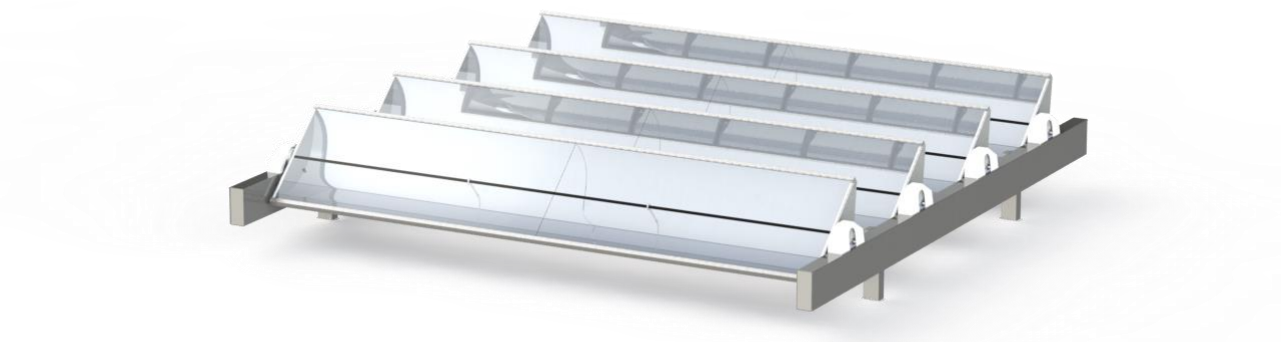

Fig 1. Sketch of the parabolic trough solar collector.

2. Measuring and monitoring system

The test facilities for testing solar collectors at the Technical University of Denmark have been in operation over two decades. The measurement consists of in- and outlet temperature, ambient temperature, flowrate, total- and diffuse solar radiation on the plan of the trough. The inlet temperature is varied from 20 °C to 80 °C and the efficiency is analysed.

Fig 2. Picture of the parabolic trough solar collector.

3. Results

The thermal performance of the solar collector, see figure 2, is evaluated under Danish weather conditions at a high inlet temperature of 80 °C. A comparison is carried out of measured and modelled performance.
The efficiency of the collar collector is evaluated.

Reference

[1] S. Furbo, B. Perers, W. Kong, Z. Tian, H.-E. Kiil, A. W. Larsen, R. Bang Madsen, New CPC based hybrid collector for solar heating plants, SDH Conference 2016 final Aug 15 2016

[2] Z. Tian, B. Perers, S. Furbo, J. Fan, Annual measured and simulated thermal performance analysis of a hybrid solar district heating plant with flate plate collectors and parabolic trough collectors in series, Applied Energy, Volume 205, November 2017, Pages 417-427.

Adaptive forecasting methods for the prediction of future solar yield of solar thermal plants and heat demand of consumers

Viktor Unterberger[1,2], Thomas Nigitz[1,2], Mauro Luzzu[1], Peter Innerhofer[3], Daniel Muschick[1], Markus Gölles[1]

[1]) BIOENERGY 2020+ GmbH, Graz (Austria)

[2]) Institute for Automation and Control, Graz University of Technology, Graz (Austria)

[3]) S.O.L.I.D. Gesellschaft für Solarinstallation und Design mbH, Graz (Austria)

1. Introduction

Solar thermal energy as an volatile energy source is highly depending on time of the day and weather conditions. Therefore solar thermal systems are set up with buffer storages in order to decouple the occurrence of heat production from heat consumption at least at a certain degree. Furthermore solar thermal plants must always be combined with one or more controllable energy systems in order to supply the connected consumers with heat in case there is lack of solar energy and there is no heat stored in the buffer storage. In such configuration an efficient energy management system which maximizes the generation of solar thermal energy is of high importance.

For such energy management systems the most promising approach to optimally plan generation, storage and consumption of heat would be predictive control strategies which can explicitely consider the available information on the future conditions. To utilize their full potential forecasts for both the future solar yield as well as the future heat demand of the consumers have to be taken into account.

Unfortunately, most of the available forecasting methods for solar yield as well as for heat demand are tailored for a specific application, not adaptive and mathematically complicated. Because of their complex mathematical structure (e.g. artificial neural networks), it is not possible to easily implement them on off-the-shelf PLCs used in solar thermal plants respectively district heating grids. Thus, they cannot serve as a general basis for predictive control strategies, which is why the development of general, simple and adaptive forecasting methods for the solar yield as well as for the heat demand is a prerequisite for the application of efficient predictive control strategies.

This contribution presents **forecasting methods** for both the solar yield (section 2) as well as the heta demand (section 3) which are **adaptive**, **easy to implement** and **suitable for use in predictive controllers** in solar thermal plants or district heating grids. All methods shown in this contribution are **using real weather forecast data** from a weather service provider and are verified with **real measurement** data from representative plants.

2. Forecasting method - solar yield

In principal the solar yield of solar collectors can be described by a static collector model according to the European Standard EN12975 which is based on a simplified energy balance. However, the analysis of measurement data from large-scale solar thermal plants shows that applying this model, with its parameters taken from the datasheet of the collectors, does not directly lead to satisfying results when it is used to forecast the solar yield of a plant. This is because the model parameters are only valid for stationary conditions in the laboratory and not for the conditions occurring in the daily operation. Furthermore, these model parameters would have to change over time to account for polluted collector surfaces decreasing the optical efficiency, or for the decay of materials leading to higher convective heat losses of the collector.

The method developed generally also bases on this static collector model and is therefore valid for a lange range of collectors. However, within the new method the collector parameters are continuously adapted using measurement data. For this purpose it uses the past values of the measured solar yield, the measured ambient temperature as well as the measured global solar irradiation. The depency on the time of the day is considered by using different parameter sets for different times of the day. By this procedure the influence of pollution of the collector fields, of the decay of the materials as well as of local shading is automatically considered.

Furthermore, no manual parameterization is necessary.

Fig. 1 shows an exemplary forecast of the solar yield (red) for a sunny summer day of a subfield with a size of 152 m² built in 2009 in comparrision to the actual measured solar yield (blue).

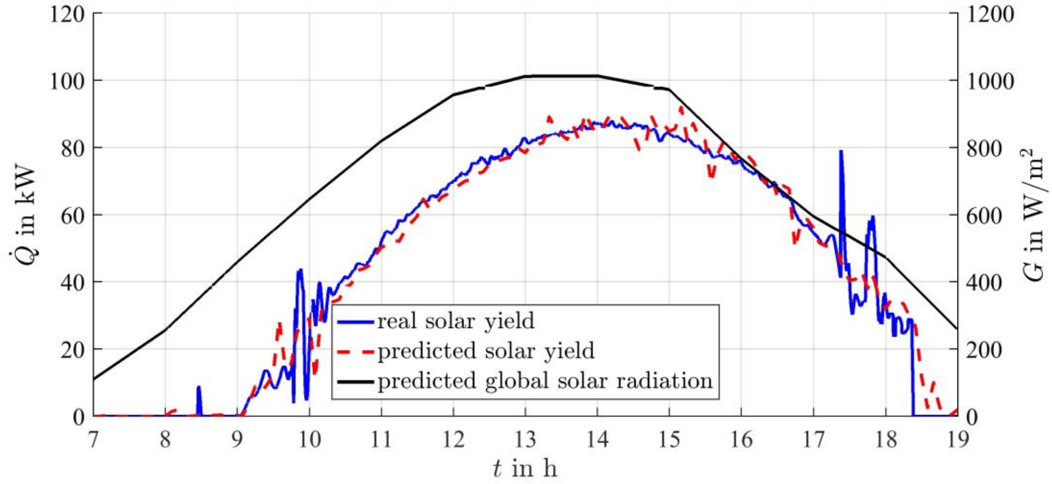

Fig. 1: Comparison of measured (blue) and predicted (red) solar yield together with the forecast for the global solar radiation (from conventional wheater forcast data, black) for a collector field with a size of 152 m².

3. Forecasting method - heat demand

The method developed for forecasting the heat demand of different types of consumers (from buildings to heating grids) is based on the empirical analysis of the correlation between weather data and heat load data of different types of consumers ranging from private households to industrial buildings. The analysis revealed that, for a given time of the day, an approximately linear correlation exists between load demand and ambient temperature . Also, there is a characteristic dependency of the heat load on the time of the day. It was found that the individual days of the week do not have to be considered explicitly, but a distinction between working days and weekends/holidays turned out to be necessary. The method thus predicts the heat demand of the consumers based on distinct linear models for every hour of the day, and corrects it by using the current prediction error as well as basic expert knowledge. The parameters of the method are updated at every iteration, taking into account the measured heat flow and ambient temperature of the previous days. By keeping the data window length short, the method easily adapts to changing seasons and consumer behaviors. Fig. 2 shows an exemplary forecast for the heat demand (red) of an office building in comparison to the heat actually needed (blue).

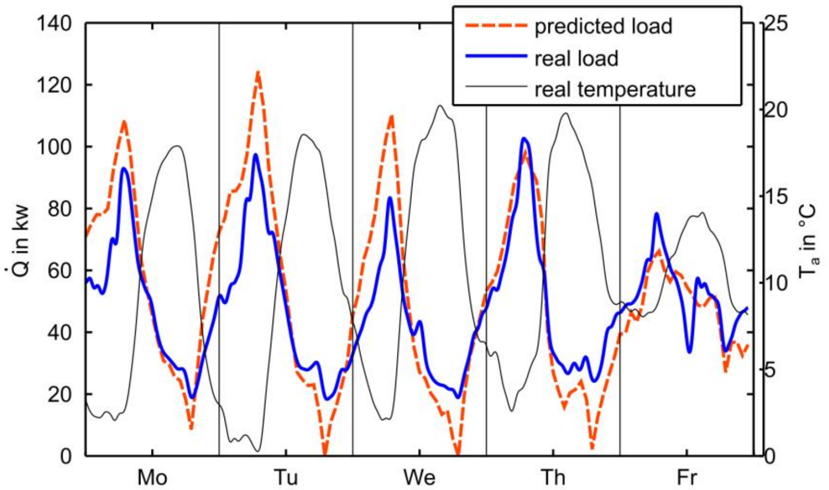

Fig. 2: Exemplary prediction of the heat demand (red) of an office building (connected load: 35 kW) compared to the actual (measured) heat demand (blue) together with the (measured) ambient temperature (black) for a typical work week.

PERFORMANCE OF OVERGROUND HOT WATER STORES IN SEGMENTAL CONSTRUCTION FOR SOLAR AND CHP DISTRICT HEATING SYSTEMS

Thorsten Urbaneck, Fabian Findeisen, Jan Markus Mücke, Bernd Platzer
Chemnitz University of Technology, Department of Mechanical Engineering, Institute of Mechanics and Thermodynamics, Professorship Technical Thermodynamics, 09107 Chemnitz, Germany, thorsten.urbaneck@mb.tu-chemnitz.de

Markus Gensbaur, Stephan Lang, Dominik Bestenlehner, Harald Drück
University of Stuttgart, Institute of Thermodynamics and Thermal Engineering (ITW), Research and Testing Centre for Thermal Solar Systems (TZS), 70550 Stuttgart, Germany

Timo Herrmann, Robert Beyer
farmatic tank systems GmbH, Kolberger Str. 13, 24589 Nortorf, Germany

Abstract – Hot water stores represents an integral part of heating systems. A new store design offers numerous benefits compared to currently at the market available storage technologies, in particular pressure vessels and conventional flat-bottom tanks. This paper delivers first results regarding the performance of a demonstrator with the new design, which is basically a small-scale tank with a volume of approx. 100 m³. The test store is equipped with a radial diffuser for constant charging temperatures and high volume flow rates as well as a stratification device for variable temperatures. Experiments underline the advantageous behaviour regarding stratification and heat losses. In addition, long-term tests with high temperatures were carried out. Further investigations are in progress to identify optimization potentials e. g. regarding the reduction of thermal bridges, which is a topic in a later phase of the project.

1. INTRODUCTION

Thermal energy stores can significantly improve the efficiency and environment-friendliness of the heat supply by storing heat surpluses and supplying heat to the consumer on demand. This requires technologies for cost-effective storage systems with low energy losses.

In a store using the displacement principle, a water exchange takes place by direct charging and discharging. A thermal stratification inside the store is achieved by separating water with different temperatures through buoyancy. There are significant optimization potentials regarding currently at the market available storage technologies, in particular pressurized stores and flat-bottom tanks (Urbaneck et al., 2016a). Pressurized stores allow higher storage densities as well as higher temperature differences but often have low storage volumes, higher heat losses and higher investment costs. However, flat-bottomed tanks combine large volumes with relatively low costs. A drawback of two-zone storages is that a second zone resp. a higher fill level is required to apply a hydrostatic load. Furthermore, for safe operation of conventional one-zone stores low-pressure steam or a protective gas in the attic is mandatory. This leads to higher heat losses, unfavourable thermal stratification and operation conditions plus unused storage volume.

A new storage design eliminates these disadvantages and offers numerous benefits (Urbaneck et al., 2016b, 2017). A demonstrator was already built in cooperation with industrial and scientific partners as part of the OBSERW project (Urbaneck, 2018). This work gives a short description for the store design and presents first operation results.

2. DESCRIPTION OF THE NEW STORE DESIGN

The construction is shown in Fig. 1. The main novelty is an indoor, protected floating ceiling, with a directly attached upper charging device (e. g. a radial diffuser). A flexible connection allows the free movement of the floating ceiling between a top and bottom dead centre. During charging of the tank a gravity current can occur directly at the ceiling, which is an essential prerequisite for a good thermal stratification. When discharging, hot water is sucked straight along the ceiling, which allows the full use of the hot zone. The aim is to operate the store with a maximum temperature of 98 °C. But the elimination of a hydrostatic pressure relief means that there is a risk of falling below the steam pressure limit. This has to be avoided, as it could lead to cavitation or other transient effects during discharging. A free-form radial diffuser lowers the local pressure drop due to his flow-optimized shape and thus improves operation safety (Findeisen et al., 2017). A flexible sealing and the pressure compensation pipe ensure volume and pressure compensation in both store and attic. This allows the store in combination with a pressure-increase or pressure-reduction installation, to provide functions such as pressure maintenance as integration into heat supply networks. The pressure compensation pipe is also used for independent ventilation (e. g. during commissioning) and secures the store against overpressure and negative pressure. This may also occur,

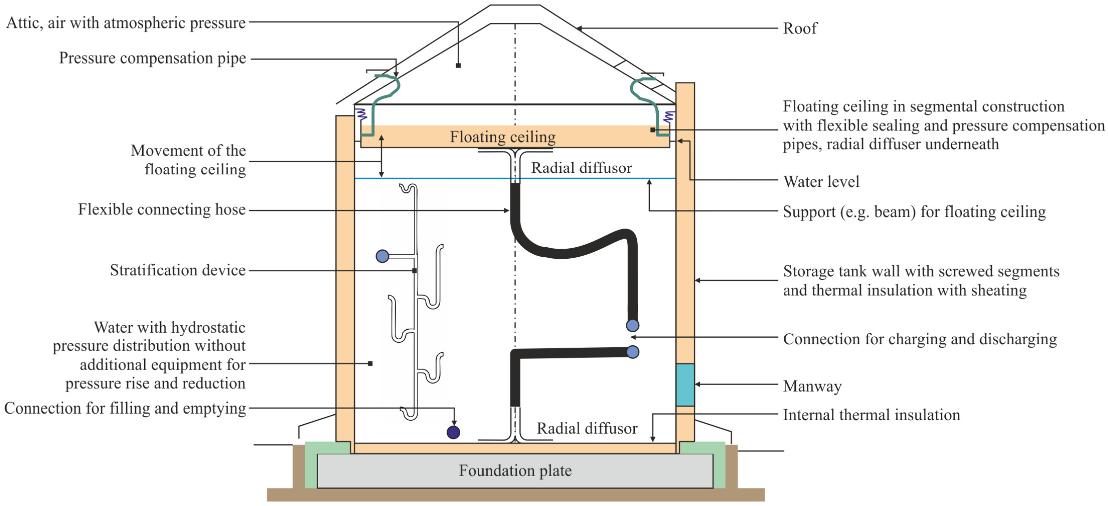

Figure 1: Overground thermal energy store in segmental construction with floating ceiling and directly mounted radial diffuser, stratification device not displayed here

for instance, when the appliance is not in use and water level falls while the floating ceiling rests on the support (bottom dead center). The floating ceiling and the flexible sealing avoid a gas input into the water and thus avoid corrosion in the system. Furthermore, flexible sealing lips are located at the edge of the ceiling to suppress free convection between the ceiling and the storage wall. As a result, heat losses are reduced and the flexible sealing is less thermally stressed. For the construction of the ceiling, bolted and sealed segments are provided which can be easily filled with a blow-in thermal insulation material. The use of plates is also conceivable. Compared to other constructions, the thermal insulation is located directly on the hot zone, which is topologically the best solution. The roof protects the thermal insulation from weather influences. Since the attic can be equipped with ventilation, drying is possible if humidification occurs.

Figure 2: Demonstrator in Nortorf, Germany, approx. 100 m³, single-zone store

3. FIRST OPERATION RESULTS

3.1 Introdution of the Demonstrator

The demonstrator of the new store design is basically a compact small-scale tank with a height of 5.12 m and a volume of approx. 100 m³ (Fig. 2). The store is equipped with its own heating and cooling circuit in the nearby factory hall of farmatic tank systems GmbH (left in Fig. 2). This allows numerous tests under specified boundary conditions with relatively low energy and time effort. Fig. 3 shows the radial diffuser mounted to the floating ceiling as well as the stratification device mounted to the segmented and sealed tank wall. A detailed presentation of the demonstrator was already published by Urbaneck et al., 2017.

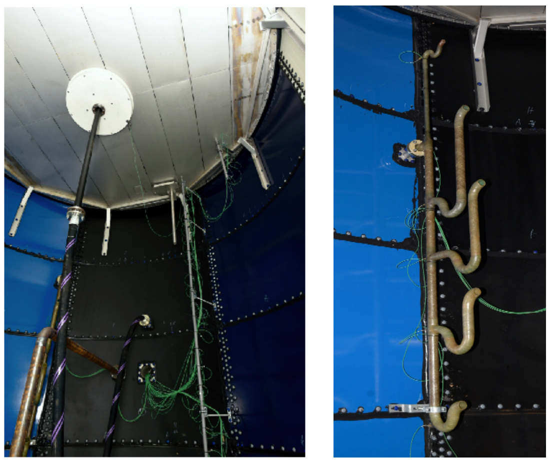

Figure 3: Radial diffuser and temperature measurement (left), stratification device (right)

3.2 Charging with Radial Diffusers

Radial diffusors usually serve as charging device for applications with constant charging temperatures. They can handle high volume flow rates and are mainly used for short term thermal energy storage.

Tab. 1 gives an overview about the naming of the experiments regarding volume flow rates $\dot{V}$ and temperature differences ΔT that were performed with the demonstrator. The experimental program is limited by the thermal performance of the boiler system (approx. 230 kW) in the heating circuit.

Table 1: Experimental program for charging with a radial diffuser

$\dot{V}$ [m³/h]		4.86	9.72	14.58	19.44
$\dot{V}/\dot{V}_{max}$ [%]		25	50	75	100
ΔT [K]	5	V25_T5	V50_T5	V75_T5	V100_T5
	10	V25_T10	V50_T10	V75_T10	V100_T5
	15	V25_T15	V50_T15		
	20	V25_T20	V50_T20		
	30	V25_T30			

Fig. 4 shows the vertical temperature distribution inside the store when it is 42 % loaded (dimensionless time $t^* = t / t_{100\%} = 0.42$). For the temperature differences and volumetric flows examined, it can be seen, that a relatively sharp defined warm zone is formed. It is remarkable that the temperature in the warm zone hardly deviates from the charging temperature at slight temperature differences. As the charging temperature rises, a so-called long tail effect occurs in the warm zone (Urbaneck, 2012). The long tail effect describes the asymptotic approximation of the temperature profile to an ideal temperature profile. The ideal temperature distribution corresponds to a rectangular profile with minimum and maximum storage temperatures and is identical to the profile of a plug flow (ideal displacement).

For a complete charging of the tank the development of the temperature profile is shown in Fig. 5 for V25_T20 (Tab. 1). Within the stratification layer, the vertical temperature rise remains almost constant, while the transition to the cold or warm zone is flattened over time and less steep. The mean temperature in the warm zone is approx. 49.2 °C at the end of the test and deviates less than 1.0 K from the charging temperature. The height of the stratification layer starts at about 0.16 m and triples up to the end of the charging process. This is mainly because of external heat losses during the charging time of almost 24 h.

The results show that the radial diffuser fulfills its function and is suitable for use in large hot water tanks. The charging device offers a narrow thermal stratification layer and thus a high usable volume for applications that require a high stratification quality.

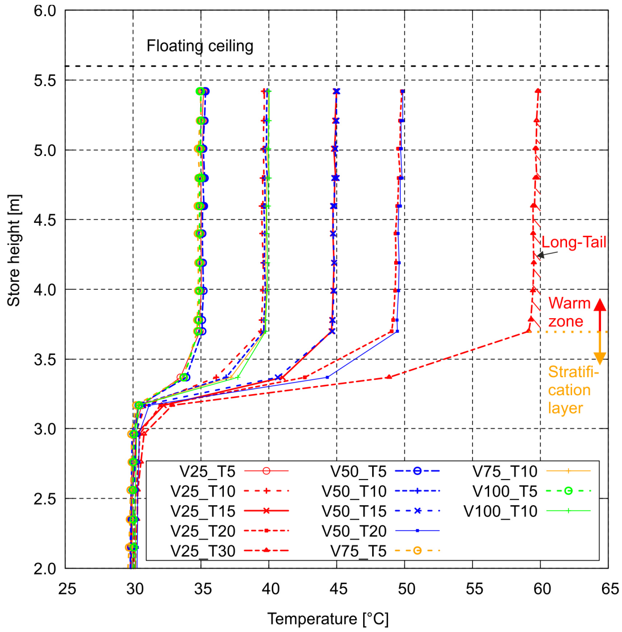

Figure 4: Vertical temperature distribution inside the demonstrator at the end of the test and marking of the long tail in V25_T30; $t^* = 0.42$

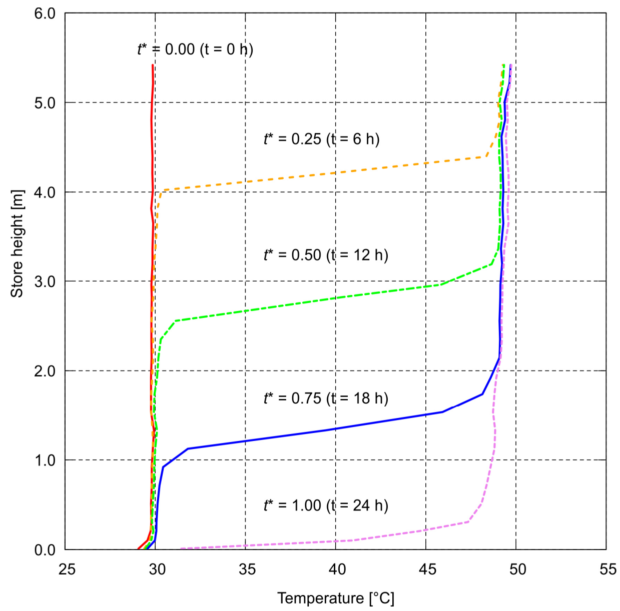

Figure 5: Development of the temperature distribution inside the store until fully charged (V25_T20)

3.3 Charging with Stratification Device

The aim of a stratification device is to create a thermal stratification or to maintain the thermal stratification in case of an existing stratification. The inflow of the charging fluid into the store takes place in the stratification device via five openings without additional control and regulation mechanisms. A detailed description of the operating principle of the stratification device can be found in Lohse (2010). Figure 6 shows a sketch of the stratification device as well as the installation situation in the demonstrator and names the individual outlets.

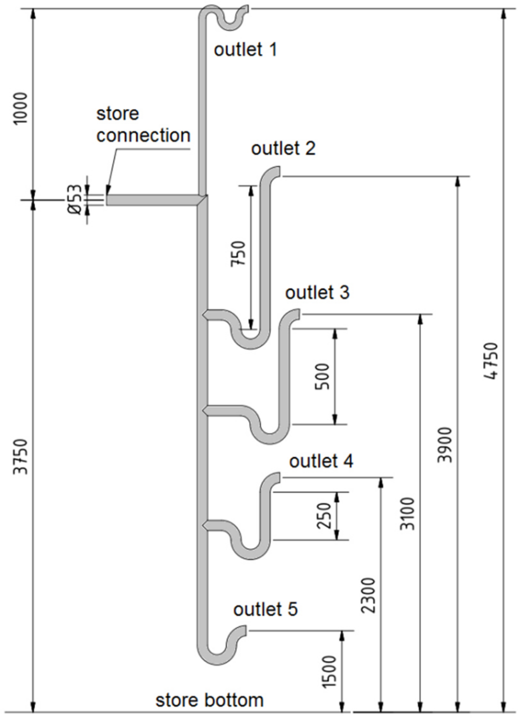

Figure 6: Drawing of the stratification device

The results presented here shows the so called test sequence 'jump profile'. In the jump profile, the demonstrator with an initial store temperature of 30 °C is first charged with a constant volume flow rate of 1.0 m³/h and a temperature of 50 °C. As soon as the stratification layer has approximately reached outlet 4 (see Fig. 6), the inflow temperature is reduced to 35 °C. This results in the formation of a new temperature layer. The temperature difference between the hot water store and the charging fluid in case of the jump profile is selected in such a way that they provides a representative operating state of the store.

Fig. 7 shows the temperature distribution over the store height at different times during the charging of the demonstrator with the test sequence under the above mentioned conditions. Furthermore, the outlet heights 1 to 5 of the stratification device and the time course of the inflow temperature are shown. As expected, charging takes place first in the upper store area and the store fluid temperature increases above outlet 1 and outlet 2. The temperature of the warm zone asymptotically approaches the charging flow temperature. With increasing test duration, the nearly linear temperature distribution shifts to lower layers. After a test duration of approximately 50 hours, the charging flow temperature is reduced to 35 °C with a constant volume flow rate. Due to the temperature distribution in the store at this time, an inflow of charging fluid at outlet 4 can be expected. Accordingly, a second stratification layer is built up in the store at 35 °C below outlet 4.

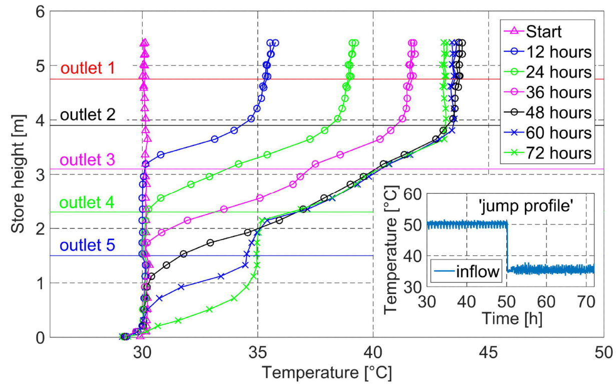

Figure 7: Temperature distribution over the store height during charging with the stratification device and a test sequence called ’jump profile’

The test sequence shows the expected operation behavior of the stratification device and that the design process was successful. There is potential for optimization when setting up the warm zone at the beginning of the charging process.

3.4 External Heat Losses

With the measured temperature- and heat-flux-density-values in the wall structure and the floating ceiling of the demonstrator, it is possible to calculate the effective thermal conductivity. The values are plotted in Fig. 8 above the corresponding mean temperature and temperature difference between storage fluid and environment for a 101-day measurement period. In addition, the measurement results for the thermal insulation material Rathipur (Co. Rathi, 2018) from a two-plate apparatus (TPA) laboratory measurement of the ITW (Lang, 2017) are shown. The mean value of the TPA measurement was determined from eight individual measurements, including a sample of the demonstrator batch. The error bar represents the largest identified deviation of an individual measurement from the mean value. Different samples can cause these deviations. Reasons for the scattering can be, for instance, different bulk densities and particle size distributions of the samples (Mücke et al., 2017).

The upper diagram in Fig. 8 shows that a large part of the measuring points are located within the error bar of the laboratory measurement and that the identified increase in heat conductivity with the mean sample temperature also occurs at the demonstrator. The lower diagram shows a slight increase in thermal conductivity with increasing temperature difference between storage medium and environment. A possible explanation for this is the generally higher mean temperature with increasing temperature difference.

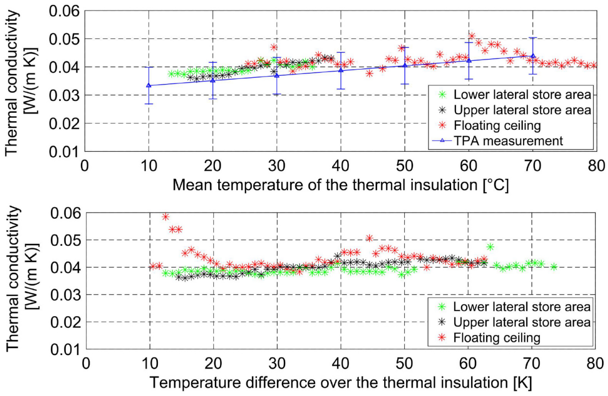

Figure 8: Mean values of effective thermal conductivity for the measurement period of 101 days applied over the associated mean temperature of the thermal insulation and the temperature difference between storage fluid and ambient air

Contrary to the findings from Mücke et al. (2017), there is currently no evidence of natural convection in the wall structure, based on the available data. There are ongoing investigations regarding natural convection, especially tests with higher temperatures in the wall structure. Furthermore, it must be noted that a comparison between Mücke et al. (2017) and the demonstrator is not necessarily correct due to the different dimensions of the wall structures. Therefore natural convection might still occur in wall structures with different dimensions.

The thermal conductivity determined in Fig. 8 is not influenced by thermal bridges due to the mounting position of the heat flow measuring plates. This confirms the good agreement of these values with the material values from the analyses with the TPA. It is also evident that the design value of the thermal conductivity of the used insulation material Rathipur ($\lambda_{\mathrm{Rathipur}}$ = 0.036 W/(m K), Co. Rathi, 2018) is also approximately achieved in an practical installation situation (in a wall area not influenced by thermal bridges).

The theoretical total heat loss rate of the demonstrator is 17.7 W/K, assuming the material values of Rathipur (Co. Rathi, 2018) and one-dimensional heat conduction. Taking the temperature-dependency of the thermal conductivity into account leads to an increase in the theoretical total heat loss rate to 19.2 W/K at a mean temperature of the insulating material of 50 °C. A first comparison of these theoretical results with the total heat loss rates determined from the field test shows that the actual total heat loss rate is significantly higher. Since the effective thermal conductivity in a wall area which is not influenced by thermal bridges matches the values from laboratory analyses, this can be attributed to thermal bridges in the wall, ceiling and floor areas. Further investigations on the thermal bridges and the total heat loss of the demonstrator are currently carried out.

3.5 Hot Test and Temperature Durability of the Store

The resistance of the sealants in the segmented wall structure to thermal stress due to temperatures up to 98 °C is analyzed by a so-called hot test with maximum charging temperature. After charging is complete, a 12-hour standstill phase follows, until the maximum store temperature falls below 90 °C. An analysis of the temperature and humidity sensors in the wall and ceiling construction during the hot test does not indicate the presence of leaks. Thermal stresses and resulting expansions between the bolted wall segments also do not lead to obvious leakages. Furthermore, the results show that the change in the height of the floating ceiling allows compensation of the volume expansion of the storage water. Therefore, the hot test can be considered successful.

4. OUTLOOK

The experiments have shown further possibilities for optimizing the design. With respect to the thermal stratification, improvements can be achieved by mounting the stratification device right under the ceiling or even directly to it. This would lead to a much favourable development of the warm zone with less mixing and temperature reduction.

Optimization regarding the external heat losses is primarily possibly by reducing the thermal bridges in the construction. There are two main areas where this can be achieved. The first area is the wall structure. The brackets that hold the outer panel in place should be manufactured out of alternative materials such as glass-fibre reinforced plastics. Currently there are stainless steel brackets with a thermal separation in use.

The second area is the edge of the floating ceiling and the flexible sealing (see also Fig. 1). This is mainly due to the uninsulated sealing. Additional thermal insulation of the sealing therefore promises a considerable optimization potential.

5. CONCLUSION

The investigations on the charging behaviour show that the radial diffuser and the stratification device fulfil their function very well and are suitable for use in large hot water stores. The radial diffuser offers a narrow stratification layer and thus a high usable volume for applications that require a high stratification quality.

The stratification device provides the desired layering behaviour for applications with varying operating conditions. In the tests carried out here, a functional proof for store heights up to 5 m was provided. The construction of the warm zone offers optimization potential. E. g. installing the stratification device directly below the floating ceiling can be advantageous.

An initial evaluation of the external losses at the demonstrator shows increased heat losses compared to the expected losses according to the material values of

Rathipur. However, the unimpaired wall and ceiling constructions (not affected by thermal bridges) have the expected thermal insulation properties when compared to laboratory analyses. The increased heat losses are thus due to thermal bridges.

The new construction is leakproof and can absorb thermal and mechanical tensions. Special material investigations are still pending. The test results show that the new design is suitable for larger stores (500 ... 6000 m³) and that the desired advantages compared to other designs are actually achieved.

With the construction and operation of the demonstrator, important findings were gained and the design of thermal storage tanks was improved. However, further work is still needed to investigate the remaining optimization potentials.

ACKNOWLEDGEMENT

The realization of the project and the scientific work is supported by the German Federal Ministry for Economic Affairs and Energy (BMWi) on the basis of a decision by the German Bundestag (funding reference: 03ET1230A/B/C). The authors gratefully acknowledge this support and carry the full responsibility for the content of this paper.

REFERENCES

Co. Rathi, 2018. www.rathi.de/produkte/rathipur-daemm granulat-kd/

Findeisen, F., Urbaneck, T., Platzer, B., 2017. Radial Diffusers in Stratified Hot Water Stores: Geometry Optimization with CFD. Proceedings of the 6th International Conference on Solar Heating and Cooling for Buildings and Industry (SHC 2017), Abu Dhabi (UAE)

Lang, S., 2017: Internal work. University of Stuttgart, Institute for Thermodynamics and Heating Technology (ITW)

Lohse, R., 2010; Einfluss von Beladeeinrichtungen auf die thermische Schichtung in Warmwasserspeichern. TU Chemnitz, Dissertation

Urbaneck, T., 2012: Kältespeicher: Grundlagen, Technik, Anwendung. Oldenbourg Verlag, 2012. ISBN 3486719882

Mücke, J.; Urbaneck, T.; Platzer, B., 2017: Versuchsstand zum praxisnahen Test von Wandaufbauten für thermische Energiespeicher – Materialuntersuchung des Einblasdämmstoffs aus Polyurethan-Hartschaum-Partikeln. 24. Energie-Symposium Nutzung regenerativer Energiequellen und Wasserstofftechnik, Stralsund, 09.11. bis 11.11.2017, Hochschule Stralsund – ISBN 978-3-9817740-3-0, p. 73-81.

Urbaneck, T.; Platzer, B. and Findeisen, F., 2016a: Warmwasserspeicher – Stand der Technik und Entwicklungen. HLH., 67, Nr. 07-08, p. 16-21. ISSN 1436–5103

Urbaneck, T.; Findeisen, F. and Platzer, B., 2016b: Thermischer Energiespeicher in Form eines Flachbodentanks. german patent, DE102016100649A1

Urbaneck, T.; Findeisen, F.; Mücke, J.; Platzer, B.; Gerschitzka, M.; Lang, S.; Bestenlehner, D.; Drück, H.; Herrmann, T.; Beyer, R., 2017: Development of Overground Hot Water Stores in Segmental Construction for Solar and District Heating Systems Within the Project OBSERW. Proceedings of the 6th International Conference on Solar Heating and Cooling for Buildings and Industry (SHC 2017), Abu Dhabi (UAE)

Urbaneck, T., 2018: project description OBSERW. www.obserw.de. version: 29.01.2018

EXPERIMENTAL IDENTIFICATION OF EFFECTIVE THERMAL CONDUCTIVIETIES IN WALL CONSTRUCTIONS WITH BLOW-IN INSULATION FOR THERMAL ENERGY STORAGE TANKS IN SEGMENTAL CONSTRUCTION

Jan M. Mücke, Thorsten Urbaneck, Bernd Platzer
Chemnitz University of Technology, Department of Mechanical Engineering, Institute of Mechanics and Thermodynamics, Professorship Technical Thermodynamics, 09107 Chemnitz, Germany,
Phone: +49 371 531-34877, Fax: +49 371 531-834877, jan-markus.muecke@mb.tu-chemnitz.de

Abstract – This paper describes a new test rig to investigate real wall structures e. g. for thermal energy storage tanks and effective thermal conductivities of the used insulation material. The fundamental approach of the test rig is the possibility to investigate sealant, insulation material and wall segment in one unit as well as the large scale of the samples (approx. 1.90 m * 1.90 m * 0.50 m). Within the OBSERW project (Overground Stores in Segmental Construction for Heat Supply Systems), the Chemnitz University of Technology, Professorship Technical Thermodynamics built such a test rig and investigated a bulk material out of polyurethane foam called Rathipur. In this paper the results for the effective thermal conductivity of the material are being presented. The values imply the occurrence of natural convection inside the tested wall structure. This is the case despite relatively low Rayleigh-Numbers, where according to literature no natural convection should occur. The results show that in reality, without the installation of convection brakes, not only insulations with larger particles but also bulk materials with relatively small particles (such as Rathipur) may be significantly impaired by convective effects. In the examined temperature range the total thermal losses increase by a maximum of approximately 16 % of the expected value if there was only heat transfer by conduction.

1. INTRODUCTION

Thermal energy storage can contribute a large part to the increase of the use of renewable energy. A core issue is the reduction of heat losses through the outer surface while maintaining, resp. decreasing costs for thermal insulation materials. Within the OBSERW project (Overground Stores in Segmental Construction for Heat Supply Systems [1]), the Chemnitz University of Technology, Professorship Technical Thermodynamics has developed a test rig for the practical study of multi-layered wall structures (TR-WS). The project is part of the energy storage initiative of the Federal Government of Germany [2].

2. TEST RIG FOR PRACTICAL TESTING OF MULTI-LAYERED WALL STRUCTURES

The TR-WS (Figure 1 and Figure 2) allows practical investigations of various insulating and sealing materials as well as wall segment materials in one unit. The strategy is to test new wall structures on a small-scale prior to actual use. This approach offers some significant advantages compared to large-scale testing in the field. There are defined and realistic conditions in the laboratory with high reproducibility. The construction and operation costs are relatively low in comparison to a full-scale store. There is a low risk of malfunctions and it is possible to run a high number of test cycles. The essential difference to conventional test rigs for determining thermal conductivity (e. g. two-plate apparatus) or other tests (e. g. for sealants) is the possibility to examine a representative surface element (RSE). The element represents a typical wall-segment including insulation material, wall segment, joints and seals. The test rig is used to set the typical boundary conditions on the inside and outside. Thus the heat and mass transfer in the RSE is reproduced accurately. The dimensions of the insulation samples examined are also significantly larger than in other experimental studies. Furthermore, it is possible to inspect vertical and horizontal wall structures, since the test rig is mounted in pivoting bearings. Currently it is being used to investigate the effective heat transfer in the wall structure and for long-term tests of the materials (temperature resistance, tightness). The test of sealing materials and wall segment materials is conducted automatically while operating the test rig. The results of these investigations however are not part of this article.

The test rig consists of a hydraulic circuit (not shown here) with which water is pumped through a tub (Figure 2). The temperature is precisely adjustable and simulates the conditions on the inside of a storage tank. Figure 1b shows the structure including the installed measurement technology. The front view shows the wall segment (measuring 1.00 m * 1.00 m) out of an enamelled steel sheet with a thickness of 3 mm, as it is also used for real tanks in segmented construction. This wall segment was glued to the tub (Figure 2) in accordance with the intended construction technology (sealing and adhesive: Sikasil AS-70). The examined heat insulation material made of polyurethane foam particles (PUR granulate) is located on the front side. The front is enclosed with a smooth metal sheet. An approx. 0.50 m thick insulation layer is installed

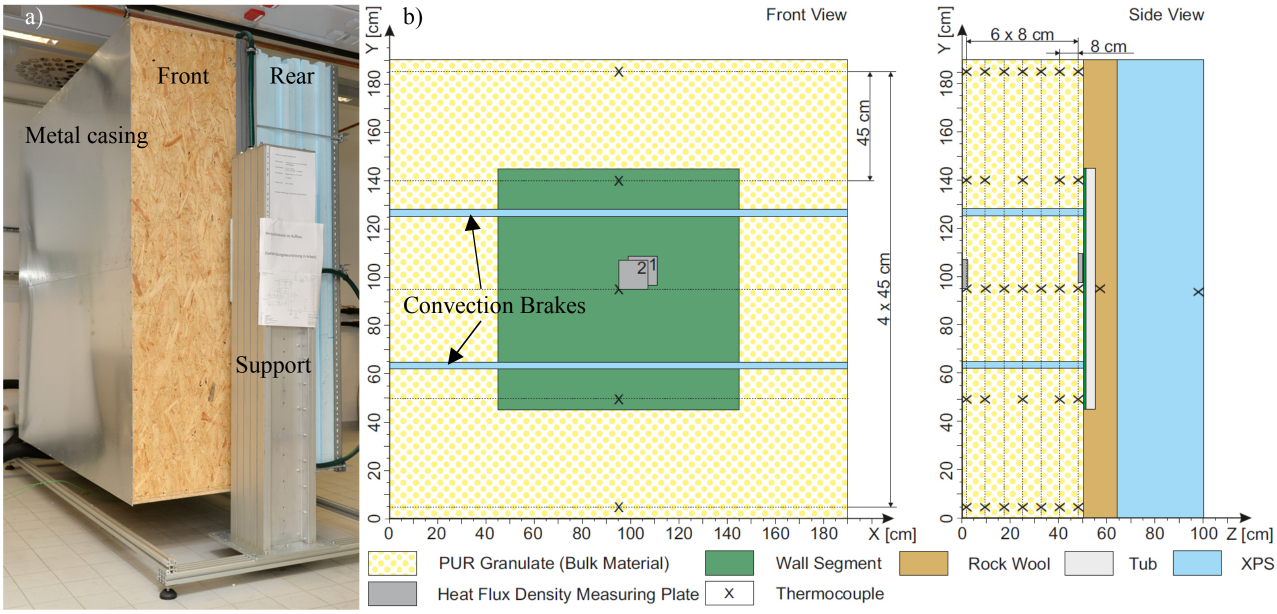

Figure 1: a) Test rig for practical testing for multi-layered wall structures; b) schematic structure of the test rig, cross section of the front- and side-view with measurement instrumentation

in each direction to suppress the geometrical heat losses. Rock wool and extruded polystyrene foam (XPS) are used on the rear side.

To determine the effective thermal conductivity, which is used as a measure of effective heat transfer in the RSE, heat flux measuring plates and thermocouples are used. The heat flux measuring plates are located centrally on the surface of the wall segment and on the inside of the cover plate. In addition there are overall 31 thermocouples in the examined bulk material. They are installed at five different heights (Figure 1b, front view, distance 45 cm) and in seven different layers (Figure 1b, side view, distance 8 cm). This configuration enables recording of vertical and horizontal temperature profiles in the wall structure.

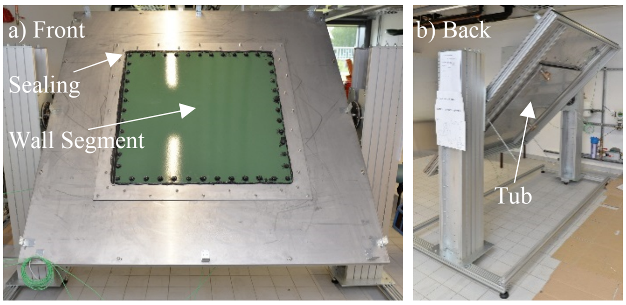

Figure 2: Front (a) and back view (b) of the TR-WS under construction without insulation material and measurement equipment

3. MATERIAL INVESTIGATION

In the first phase of the OBSERW project [3] a bulk material made of PUR foam particles (Rathipur, Figure 3 [4]) is used to insulate the wall and ceiling.

Figure 3: Polyurethane foam granulate Rathipur

The results of first material investigations on Rathipur (RP) can be found in Lang [5] and Gerschitzka [6]. This article presents, amongst others, the results of further studies. As can be seen in Figure 3, Rathipur consists of particles of different sizes, which also differ in shape (polydisperse bulk material). Rathipur is also subject to significant material fluctuations. The test rig described above is not suitable for all material analyses. In order to be able to characterize the bulk material more precisely, additional substance analyses were carried out. Among other things, the mean particle diameter, the settled apparent density (after shaking the material on a vibrating plate) and the external porosity were determined. Table 1 summarizes the results.

Table 1: Particle diameter, mean value of the density and the outer porosity for Rathipur [9]

d [mm]	d_m [mm]	$\rho_{settled}$ [kg/m³]	$\psi_{e,RP}$ [%]
ca. 1-16	5.3	29.0	53

The particle size varies from very small particles of about 1 mm to larger particles of about 16 mm. The average density was 29 kg/m³. This is well below the manufacturer's stated material parameter of 40-50 kg/m³. These are two examples for the significant fluctuations of the material.

4. EFFECTIVE THERMAL CONDUCTIVITY

Since the test rig is located in a laboratory with relatively constant temperatures (approx. 23 °C), the graphs for the effective heat conductivity over the mean temperature inside the insulating material and over the temperature difference between tub and surroundings are qualitatively equivalent. Figure 4 shows the calculated heat conductivity over the mean temperature of the insulation material. Results from the TR-WS in vertical orientation indicate a significantly higher effective thermal conductivity than expected (e.g. compared to the thermal conductivity measurements at the University of Stuttgart, Institute of Thermodynamics and Thermal Engineering (ITW) with a guarded hot plate apparatus with the same Rathipur samples [5] or the manufacturer's data [4]). The reason for the increased effective thermal conductivity seems to be free convection in the wall structure. If one compares the values for horizontal (TR-WS horizontal) and vertical orientation of the test rig (TR-WS vertical) in Figure 4, the latter variant shows a strong increase at higher temperatures (respectively larger temperature differences).

In previous works the ITW was able to identify free convection in bulk materials with larger particles (e.g. foam glass gravel) [7]. Other resources however suggest that in bulk materials with comparable outer porosity and representative particle size as in Rathipur no convection occurs [8].

The possibility to detect free convection at the TR-WS is due to the described different experimental setup than at a conventional guarded hot plate apparatus. As mentioned above, the wall structure can not only be observed horizontally but also vertically with a horizontal heat flux (real wall structure). Furthermore the investigated sample size is significantly larger than in conventional test rigs, therefore additional effects can be observed.

To confirm the occurrence of free convection in the wall structure convection brakes (CB, plates made of XPS with almost identical thermal conductivity as Rathipur) are placed in the bulk material. The convection brakes divide the bed into three horizontal segments, each with a height of approximately 0.60 m. This change in the set up reduces the effective thermal conductivity significantly. With this configuration (TR-WS horizontal CB and vertical CB in Figure 4) free convection is suppressed so well that values of the effective thermal conductivity approximate the horizontal data (TR-WS horizontal).

Figure 5 shows the recorded temperature curves parallel to the wall segment. The different colors correspond to different distances to the surface of the wall segment. In this case, the mean temperature in the tub is 60 °C. The wall segment is located on the right and the outer plate on the left. The curves have a similar shape for horizontal orientation and vertical orientation with convection brakes. The central area (at a height of 0 cm) has the highest temperatures. Due to the outer surfaces without heating and the larger transmission surface to the surroundings, the temperatures for the outer measuring points decreases.

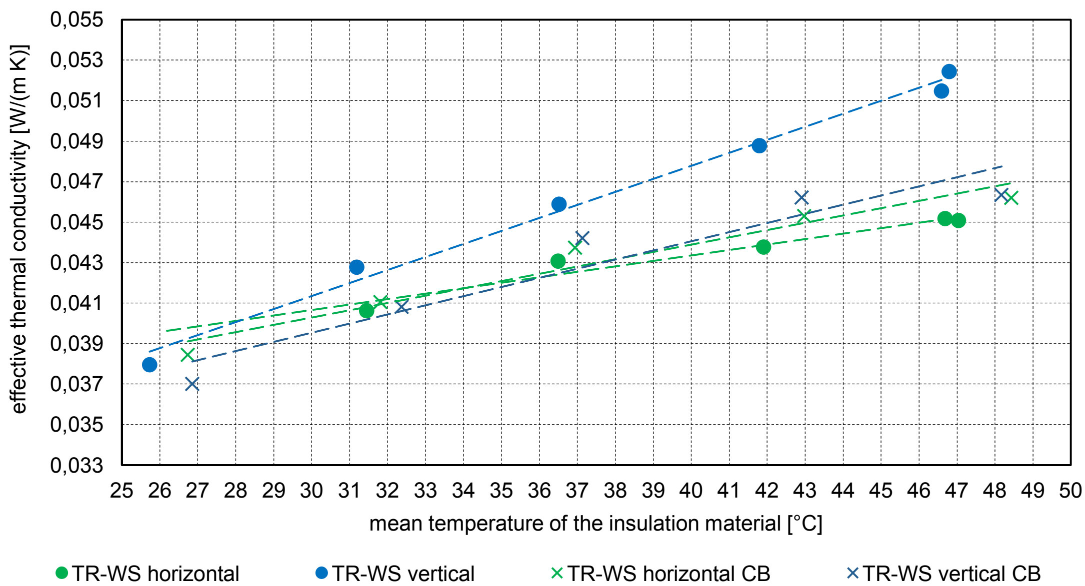

Figure 4: Thermal conductivity of Rathipur as a function of the mean temperature of the insulation material (at a room temperature of approx. 23 °C the mean temperature differences between tub and laboratory was 7 K, 17 K, 27 K, 36 K and 46 K. See also Table 2.)

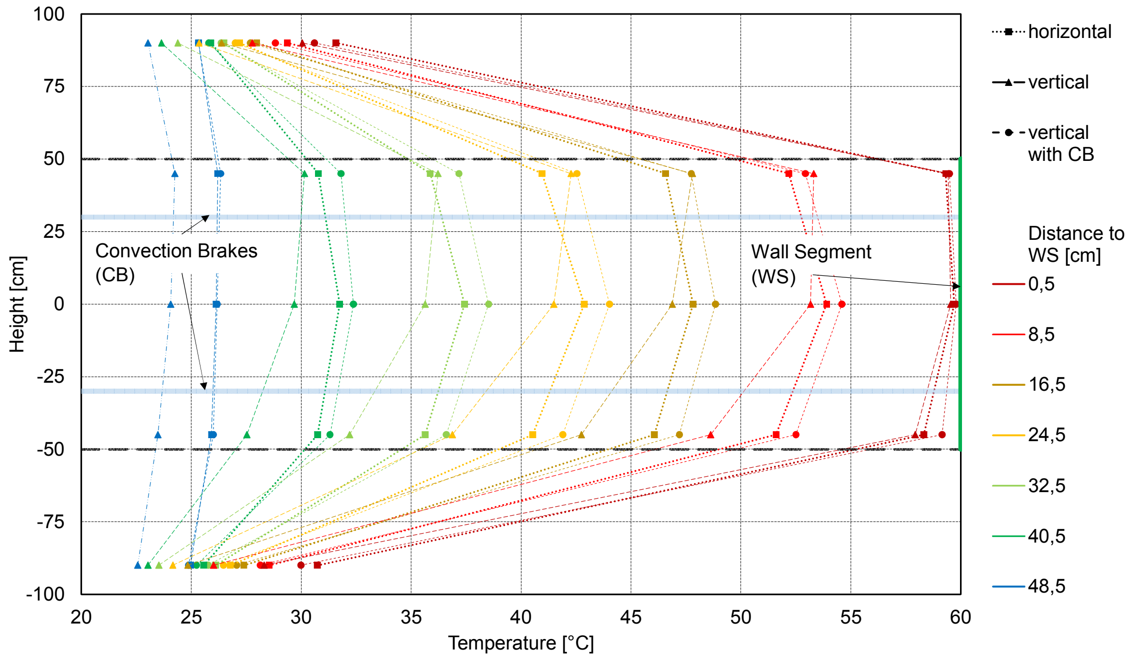

Figure 5: Temperature profiles over the height (vertical position) or width (horizontal position) of the test rig with and without convection brakes (CB); 60 °C water temperature in the tub

The temperature profile for the vertical position without convection brakes however differs significantly from the two other profiles. The heating of the air near the wall segment results in higher temperatures at the measuring points at a height of 45 cm than in the centre. In addition, the temperatures at the lower measuring points are significantly lower (height: -45 cm). The results therefore show that an air flow heats up over the entire segment height. In addition the temperature distribution near the outside cover of the test stand (distance to the wall segment: 48.5 cm) speaks in favour of a downward directed air flow that cools down. The temperature profiles over the test rig height in vertical position without convection brakes therefore confirm the occurrence of free convection in the bulk material.

Table 2 shows a comparison of the effective thermal conductivity of Rathipur as measured at the TR-WS with and without CB.

Table 2: Effective thermal conductivity for Rathipur in the TR-WS in vertical position with and without convection brakes (CB) in relation to the mean temperature of the insulating material and the temperature difference between tub and laboratory.

Without CB			CB		
T_m [°C]	ΔT [K]	λ_{eff} [W/(m K)]	T_m [°C]	ΔT [K]	$\lambda_{eff,KB}$ [W/(m K)]
25.7	8.6	0.038	26.9	6.5	0.037
31.2	17.8	0.043	32.3	15.5	0.041
36.5	26.9	0.046	37.1	25.8	0.044
41.8	36.6	0.049	42.9	34.3	0.046
46.6	47.0	0.053	48.2	43.8	0.047

In order to better assess the influence of convection, the convection factor ε_k, introduced by Michejew [10]:

$$\varepsilon_k = \frac{\lambda_{eff}}{\lambda}, \tag{1}$$

is being used. Here λ is the material parameter for Rathipur.

If the convection factors are based on the effective thermal conductivity for the horizontal orientation and assuming that no convective effects occur there, the losses for the vertical position are a maximum of about 16 % at a mean temperature inside the insulating material of about 48 °C (ΔT = 46 K, Table 3). The additional losses are most probably higher with further increasing mean temperatures in the insulating material and therefore also increasing temperature differences between the tub and the surroundings.

Table 3: Comparison of the convection factor ε_K for values in horizontal and vertical position with and without CB at the TR-WS

T_m [°C]	ΔT [K]	ε_K Without CB	ε_K CB
26	7	1.00	0.99
32	17	1.05	0.99
37	27	1.07	1.01
43	36	1.11	1.02
48	46	1.16	1.00

When using convection brakes, only a very small increase of approx. 2 % can be observed. This difference lies within the range of the measurement uncertainty of the used heat

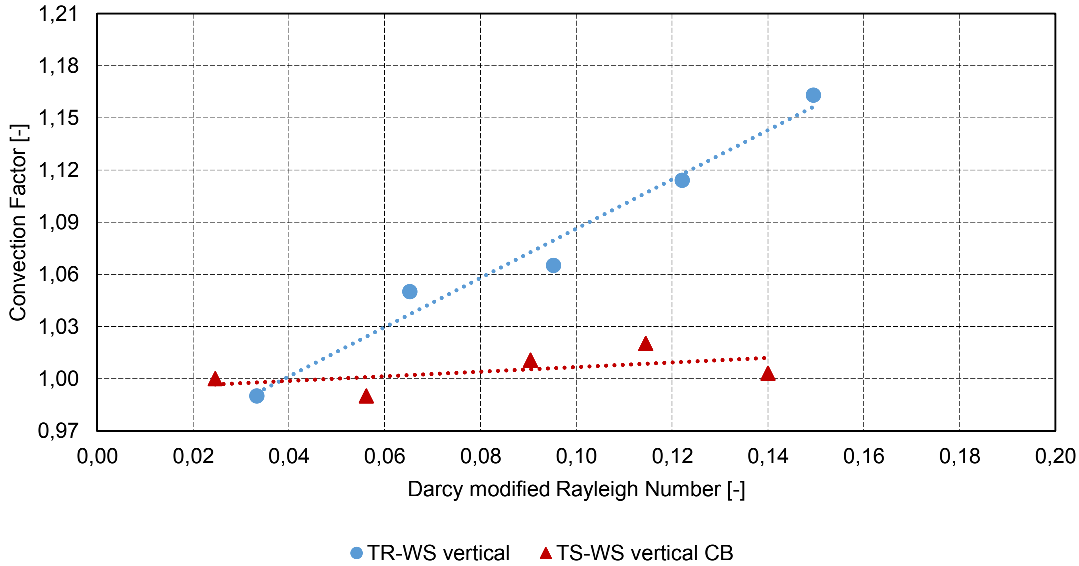

Figure 6: Convection factor ε_K as a function of the Darcy modified Rayleigh number *Ra at the TR-WS**

flux measuring plates. Thus the free convection could most likely be effectively eliminated with the usage of CB.

Figure 6 shows the Rayleigh numbers modified according to Darcy (*Ra**) as a function of the convection factor for the values from Table 3. *Ra** is calculated as follows [11]:

$$Ra^* = Ra * Da = K \frac{g * \beta_f * l * \Delta T}{\nu_F * a_{\text{bulk}}}, \tag{2}$$

with the Darcy number *Da*, the thermal diffusivity of the bulk material a_{bulk}:

$$a_{\text{bulk}} = \frac{\lambda_{\text{bulk}}}{(\rho * c_p)_f}, \tag{3}$$

the permeability *K* after Rumpf, Gupte:

$$K = \left(\frac{d^2}{5.6}\right) * \Phi^{5.5} \tag{4}$$

and the characteristic length *l* being the thickness of the investigated insulation layer (0.50 m, Figure 1b). Temperature-dependent material values for air and Rathipur are being used. The ITW's measurements [12] serve as material parameters for Rathipur. According to this data no free convection occurs in the TR-WS at $Ra^* < 0.04$.

A comparison between temperature profiles with a low and a high temperature inside the tub exemplifies this (Figure 7 and 8). The difference between the gradients without

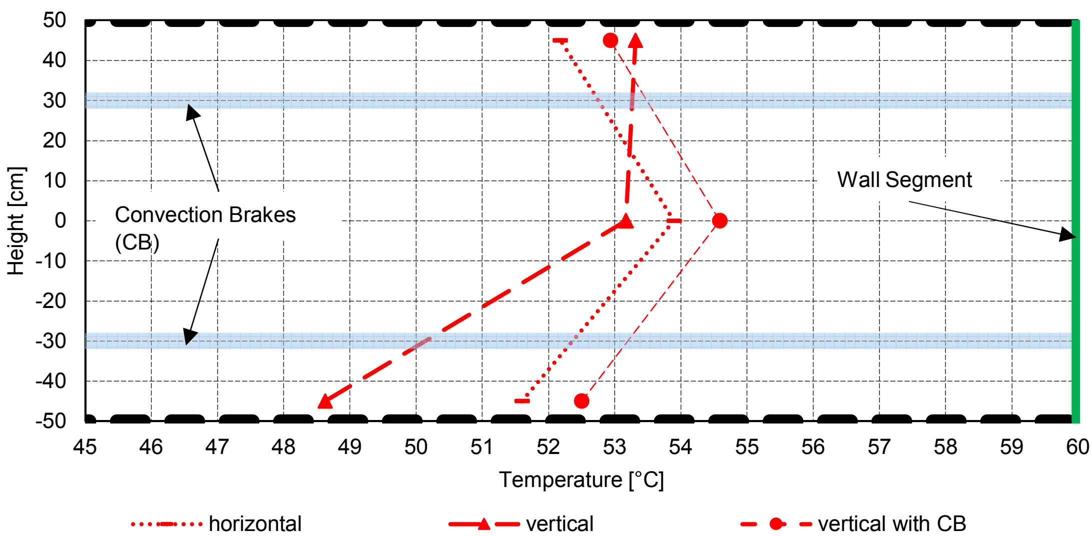

Figure 7: Parallel temperature gradients in Rathipur (front side of the TR-WS) for vertical and horizontal position, 60 °C mean temperature in the tank, 8.5 cm distance to the wall segment, with and without convection brakes

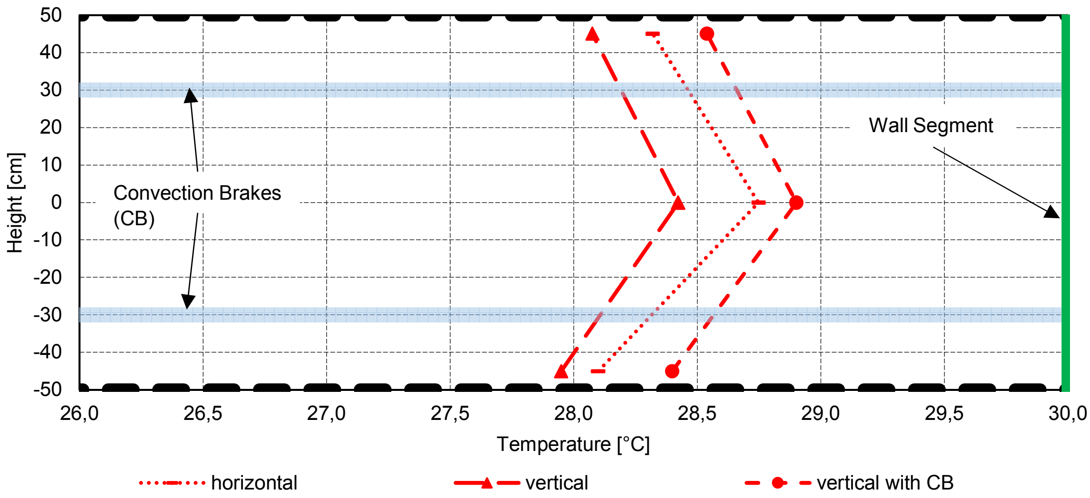

Figure 8: Parallel temperature gradients in Rathipur (front side of the TR-WS) for vertical and horizontal position, 30 °C mean temperature in the tank, 8.5 cm distance to the wall segment, with and without convection brakes

any CB at 60 °C and 30 °C is clearly visible. At 30 °C (*Ra** approx. 0.03) all three curves are similar. In contrast to the higher temperatures, there is obviously no or almost no free convection in the TR-WS.

Comparison with references shows that free convection in the TR-WS occurs despite very low Rayleigh numbers. In the VDI heat atlas or in DIN EN ISO 10456, critical Rayleigh numbers of 2.5 respectively 15 and 30 are given [11], [13]. However, it should be noted that, according to ITW investigations, a comparison of Rayleigh numbers is only permissible with a similar characteristic length (similar geometry) of the investigated construction and permeability of the bulk material [7].

5. CONCLUSIONS

The results show that the material is very well suited for thermal insulation of wall and ceiling constructions. The generally good thermal conductivity values in the range of 0.04 W/(m K) demonstrate this. However, it should be noted that convective effects may occur. In reality, without the installation of convection brakes, not only insulations with larger particles but also bulk materials with smaller particles (d_m approx. 5 mm, comparable to Rathipur) can significantly be impaired by convective effects. Due to these additional losses, the total thermal losses increase by approx. 16 % of the expected value if there was only heat transfer by conduction. At higher mean temperatures of the insulating material respectively higher temperature gradients between the wall segment and the outer surface of the test rig these values will most likely increase further. These findings have also confirmed the experimental approach (construction of the TR-WS). Investigations at a 100 m³ storage tank (demonstrator) are currently in progress.

ACKNOWLEDGEMENT

The realization of the project and the scientific work is supported by the German Federal Ministry for Economic Affairs and Energy (BMWi) on the basis of a decision by the German Bundestag (funding reference: 03ET1230B). The authors gratefully acknowledge this support and carry the full responsibility for the content of this paper.

SYMBOLS AND ABBREVIATIONS

Latin Letters

Symbol	Name of Symbol	Dimension
a	thermal diffusivity	m²/s
c_p	specific heat capacity	J/(kg K)
Da	Darcy number	-
d	particle size	m
g	apparent gravity	m/s²
K	permeability	m²
l	characteristic length	m
Ra	Rayleigh number	-
Ra^*	Darcy modified Rayleigh number	-
T	temperature	K, °C

Greek Letters

Symbol	Name of Symbol	Dimension
α	heat transfer coefficient	W/(m² K)
β	thermal expansion factor	1/K
ε	convection factor	-
λ	thermal conductivity	W/(m K)
Φ	porosity	-
ν	kinematic viscosity	m²/s
ρ	density	kg/m3

Abbreviations

bulk	bulk material
CB	convection brake
eff	effective

f	fluid
ITW	University of Stuttgart - Institute of Thermodynamics and Thermal Engineering
PUR	polyurethane foam particles
RP	Rathipur
RSE	representative surface element
TR	test rig
TR-WS	test rig for the practical study of multi-layered wall structures
XPS	extruded polystyrene foam

REFERENCES

[1] Urbaneck, T. et al.: www.obserw.de. Website for the project (in German): Overground Stores in Segmental Construction for Heat Supply Systems (OBSERW), energy storage initiative of the federal government (BMWi), funding reference 03ET1230 A/B/C, 2018.

[2] German Federal Ministry for Economic Affairs and Energy: www.forschung-energiespeicher.info, 2018.

[3] Findeisen, F. et al.: Development of Overground Hot Water Stores in Segmental Construction for Solar and District Heating Systems within the Project OBSERW. International Conference on Solar Heating and Cooling for Buildings and Industry, Abu Dhabi, 2017.

[4] Co. Rathi: http://www.rathi.de/produkte/rathipur-daemmgranulat-kd/, 2018.

[5] Lang, S.; Bauer, D.; Drück, H.: Neue Untersuchungen zu Wärmedämmstoffen für thermische Energiespeicher. 5. OTTI Fachforum Thermische Energiespeicher, Neumarkt i.d.Opf., Germany, 30.06. – 01.07. 2016.

[6] Gerschitzka, M.; Marx, R.; Lang, S.; Bauer, D.; Drück, H.: New Developments related to Thermal Insulation Materials and Installation Techniques for Overground Seasonal Thermal Energy Stores. GREENSTOCK 2015, 13th International Conference on Energy Storage, Beijing, China, 2015.

[7] Bauer, D.; Drück, H.; Lang, S.; Marx, R; Plaz, T.: Weiterentwicklung innovativer Technologien zur solaren Nahwärme und saisonalen Wärmespeicherung. Universität Stuttgart, Institut für Thermodynamik und Wärmetechnik, Forschungs- und Testzentrum für Solaranlagen (TZS), Stuttgart, 2016.

[8] Holzbecher, E.: Modeling Density-Driven Flow in Porous Media. 1. Auflage Berlin: Springer-Verlag, 1998.

[9] Roscher, W.: Internal Works. Technische Universität Chemnitz Institut für Mechanik und Thermodynamik, 2017.

[10] Michejew, M. A.: Grundlagen der Wärmeübertragung. 3. Auflage Berlin. VEB Verlag Technik 1964.

[11] VDI e.V.; VDI-GVC: VDI-Wärmeatlas. 11. Auflage Berlin Heidelberg. Springer-Verlag 2013.

[12] Lang, S.: Internal Works. Universität Stuttgart Institut für Thermodynamik und Wärmetechnik (ITW), 2017.

[13] Yagi; Kunii: Studies on Effective Thermal Conductivities in Packed Beds, Tokyo, Japan, 1957.

RADIAL DIFFUSERS IN STRATIFIED HOT WATER STORES: SIMULATION OF THREE-DIMENSIONAL FLOW BEHAVIOR WITH CFD

Fabian Findeisen, Ullrich Kroll, Thorsten Urbaneck, Bernd Platzer
Chemnitz University of Technology, Department of Mechanical Engineering, Institute of Mechanics and Thermodynamics, Professorship Technical Thermodynamics, 09107 Chemnitz, Germany, fabian.findeisen@mb.tu-chemnitz.de

Abstract – Radial diffusers are used in thermal energy stores as charging- and discharging devices in combination e. g. with solar thermal (matched flow operation mode) or CHP plants. They are essential for a good thermal stratification inside the storage tank. This paper describes the three-dimensional flow behaviour during charging of the tank for an isothermal and a non-isothermal test case. Numerical results show, that in the non-isothermal case (charging of a cold store with hot water) a highly asymmetric and unidirectional flow can occur. Besides of the thermal conditions inside the radial diffuser the effect mainly depends on the geometry of the transition area from the connection hose to the radial diffuser. As a result, strong mixing effects reduce the stratification quality significantly. The simulations are validated by experiments. Countermeasures to retrieve a symmetrical outflow will be presented.

1. INTRODUCTION

Thermal energy stores can make heat surpluses available to the consumer if necessary. A thermal stratification inside the storage tank is achieved by separating water with different temperatures through buoyancy. In a store operating according to the displacement principle, a water exchange takes place by direct charging and discharging. Hereby, radial diffusers can serve as charging and discharging devices (CDS) in order to realize high volume flow rates in combination with constant charging temperatures. This is the case, e. g. for solar thermal plants in matched flow operation mode, district heating networks or combined heat and power (CHP) plants. They consist of radial plates guiding the flow through a narrow gap horizontally into the storage tank.

In this contribution the three-dimensional flow within the radial diffuser will be discussed using Computational Fluid Dynamics (CFD). The investigations are part of the OBSERW project [Urbaneck, 2018]. Former studies already described the performance of radial diffusers with different shapes in different hot water store sizes by using a two-dimensional simulation model [Findeisen et al. 2016, 2017a, 2017b]. By mounting the diffuser to the ceiling of the tank the thermal stratification could be significantly improved. The results underlined the benefits of a new storage type with a floating ceiling developed in the OBSERW project [Urbaneck et al. 2017]. Moreover, a new free-form radial diffuser with a flow optimized shape was presented, which enables charging and discharging with temperatures up to 98 °C by reducing the risk of falling below the steam pressure limit (see also Findeisen et al., 2017c).

2. CFD METHODOLOGY

To discuss the three-dimensional flow behaviour an isothermal and a non-isothermal case will be investigated in this paper. The isothermal case represents the state when the stratification inside the store is fully development. The non-isothermal case also considers the development of the stratification at the beginning of the charging process when the fluid inside the tank has a lower temperature.

A three-dimensional model was used to perform the simulations with ANSYS CFX [ANSYS, 2015]. The CFD model for the non-isothermal case takes buoyancy into account. The k-ω-SST model serves as a turbulence model (Reynolds-averaged Navier-Stokes approach, RANS). Additional production and dissipation terms capture the effects of density gradients on the turbulent flow. Also a Large Eddy Simulation (LES) will be applied for the isothermal case. Although LES is a highly demanding simulation method in terms of computational demands it also yields as very accurate compared to simpler approaches like RANS. The utilized LES turbulence model is called WALE. Findeisen et al. (2016) describes the modelling in detail. The boundary conditions at the inlet as well as the initial condition in the tank are determined by the operating conditions in Tab. 1 (assumption: constant volume flow and constant charging temperature). The investigation considers two different shapes of CDS as shown in Fig. 1:

- CDS_0: Reference geometry with sharp-edged transition from the connecting hose to the radial diffuser and
- CDS_1: Radial diffuser with a round edge in the transition area (constant radius, r = 75 mm).

The new free form diffuser from Findeisen et al. (2017c) with a round transition but a varying radius will not be part of this paper. Since the overall flow effects are qualitatively similar to CDS_1, however, the results can be transferred.

To ensure that the flow topology in the pipe is similar to the conditions in reality, the connection hose of the radial diffuser has a 90°-manifold. The investigation therefore not only describes the flow in the radial diffuser, but also in the connection hose through which a non-ideal inflow into the radial diffuser will be present.

Tab. 1: Operation conditions and geometrical parameters of the simulation model

$h_{diffuser}$ [mm]	40	d_{store} [m]	5.12
d_{hose} [mm]	68.8	$d_{diffuser}$ [m]	0.96
$\dot{V}_{in}$ [m³/h]	19.44	T_{in} [°C]	70
V_{store} [m³]	116.76	T_{store} [°C]	40

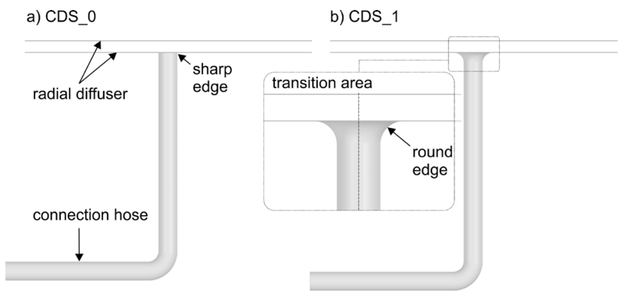

Figure 1: Schematic view of CDS_0 with sharp and CDS_1 with a round edge in the transition area

3. CFD RESULTS

3.1 Isothermal Simulation with LES

This section focuses on the isothermal three-dimensional turbulent flow behaviour within the charging system. Initially, the calculations were carried out without a storage tank. A more detailed explanation of the LES model can be found in [Findeisen et al., 2018].

Fig. 2 shows the flow distribution in the radial diffuser as well as the vortice structures. The flow in the radial diffuser is almost equally distributed, whereby fluctuations and turbulences of varying intensity can be observed in the circumferential and radial direction. Such spatial structures are typical for vortex-resolved simulations because they correspond to the chaotic, three-dimensional and unsteady behaviour of turbulent flows.

The comparison of LES with the results of an isothermal RANS model in accompanying investigations further shows that in the simpler k-ω-SST model there is too much expansion of the separation area after the 90°-manifold and the flow separation occurs too early in the transition area of the radial diffuser. But all in all, the RANS approach delivers a good result that is essentially consistent with the LES result and requires significantly less computing effort. However, it is important to ensure the correct resolution of the flow boundary layer (see also Deschamps, 1988).

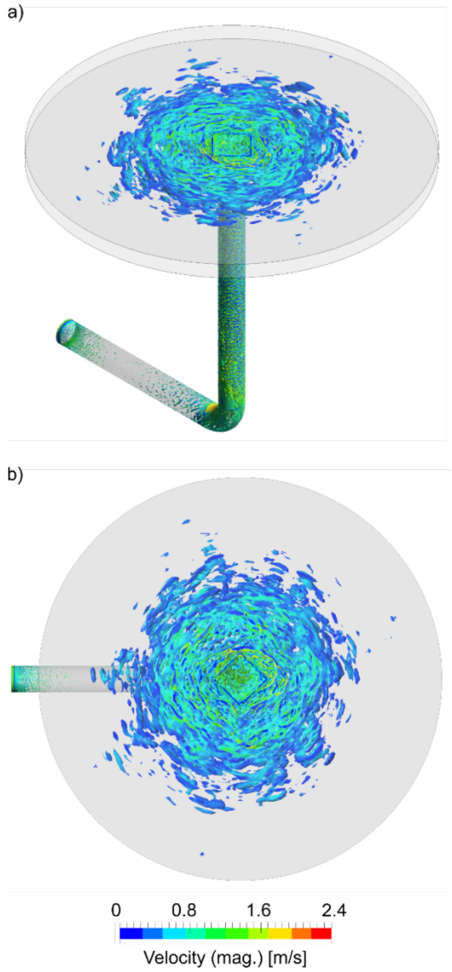

Figure 2: Vortice structures colored according to magnitude of velocity, CDS_1, LES, t = 6 s

3.2 Non-isothermal Simulation with RANS

A special phenomenon can now be observed in the non-isothermal 3D-CFD simulations including the storage tank. Fig. 3 illustrates the temperature field in the vertical section as well as the warm zone[1] (red volume).

In Fig. 3a (CDS_0) there is still a practically symmetrical outflow, as it would be expected on the basis of the isothermal investigation from sec. 3.1. However, in the case of a rounded transition between the connecting hose and the diffuser (CDS_1), a strongly asymmetrical and one-sided outflow occurs (Fig. 3b). The main flow emerges at higher speed and, thus, is stronger reflected by the side wall of the tank. All in all, it takes significantly longer to build up a warm zone because of strong mixing effects during beginning of the charging process.

[1] The isovolume of the warm zone includes fluid with a temperature above 67 °C according to the 10 / 90 %-Method [Findeisen et al. 2016].

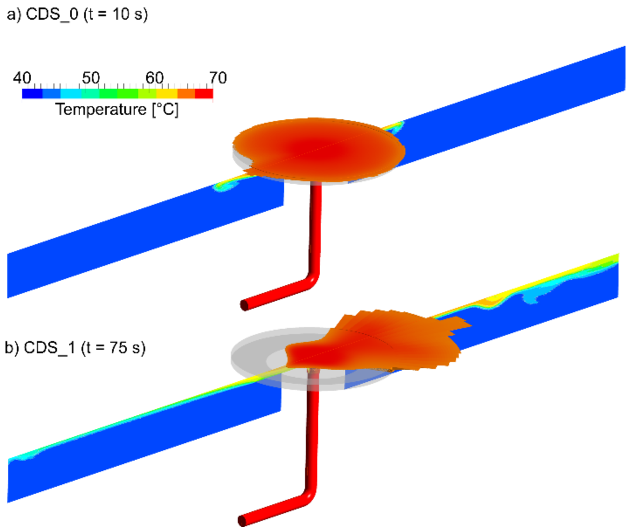

Figure 3: Symmetrical (a) or strongly asymmetrical flow (b) with different CDS, red: Volume of the warm zone ($T > 67$ °C) and temperature field in the vertical section

Fig. 4 illustrates the start of the charging process within the vertical section of CDS_1. When the warm fluid hits the upper diffuser wall, it is distributed analogous to an impact jet on a flat plate. Thus, it is almost evenly distributed. After 5 s, however, the jet moves more and more towards the right wall of the transition area. After 10 s, finally, a main flow in one direction has developed. The jet is now slanting towards the upper diffuser wall and is no longer distributed symmetrically. Instead, a secondary flow is formed that points in the direction from which the jet has initially come.

That a non-symmetrical outflow exists at all was only an assumption based on individual experiments. E. g., by performing a three-dimensional measurement of the flow field in a hot water storage tank Herwig and Rühlig (2015) showed a strongly asymmetrical outflow. From technical literature, however, it is known that a fluid jet can be deflected towards and, under certain conditions (distance, angle, flow velocity), attaches to an adjacent wall. This effect is also called Coandă-effect (Coandă, 1911). Once the jet has formed, it usually remains stable and does not change its direction any more, as viscous forces in the boundary layer have a stabilizing effect.

From the isothermal simulations it is known that the flow profile at the end of the inlet section does not actually show axial symmetry, but is slightly elevated along one pipe side. Nevertheless, in the calculations with a homogeneous temperature field, an almost uniform outflow can be observed. Therefore, the directed outflow in the non-isothermal case cannot be attributed solely to the velocity profile.

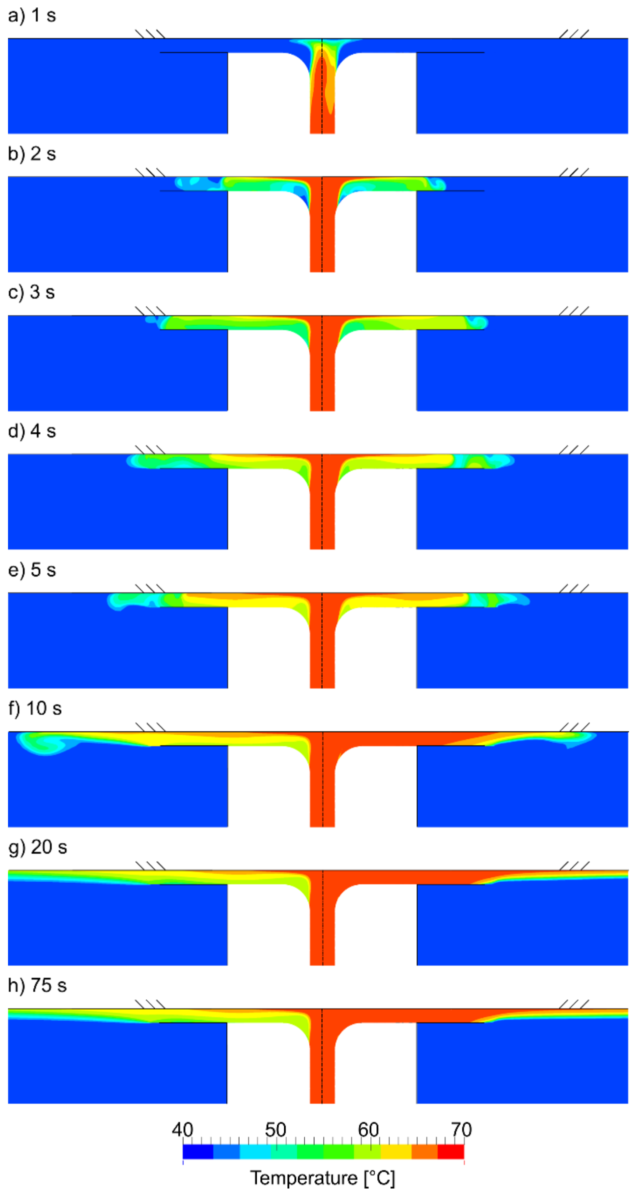

Figure 4: Beginning of charging process in CDS_1, evolution of temperature field in cross section of the 3D-CFD model

According to Coandă (1911), a jet can only be diverted if the system of jet and environment is not in equilibrium. Since in the isothermal case the outflow characteristic did not change, a stable system can be assumed. In the non-isothermal case, the flow is unstable in regions where there is a difference in temperature or density. It is remarkable that an unstable flow condition does not only exist in the radial diffuser, but already in the connection hose. This can be observed in Fig. 5.

Contrary to the idea of a plug flow, the fluid does not move through the hose as a stable flow. Instead, there is already mixing, especially after the 90°-manifold. This leads to the development of single jets as it can be observed in Fig. 5b.

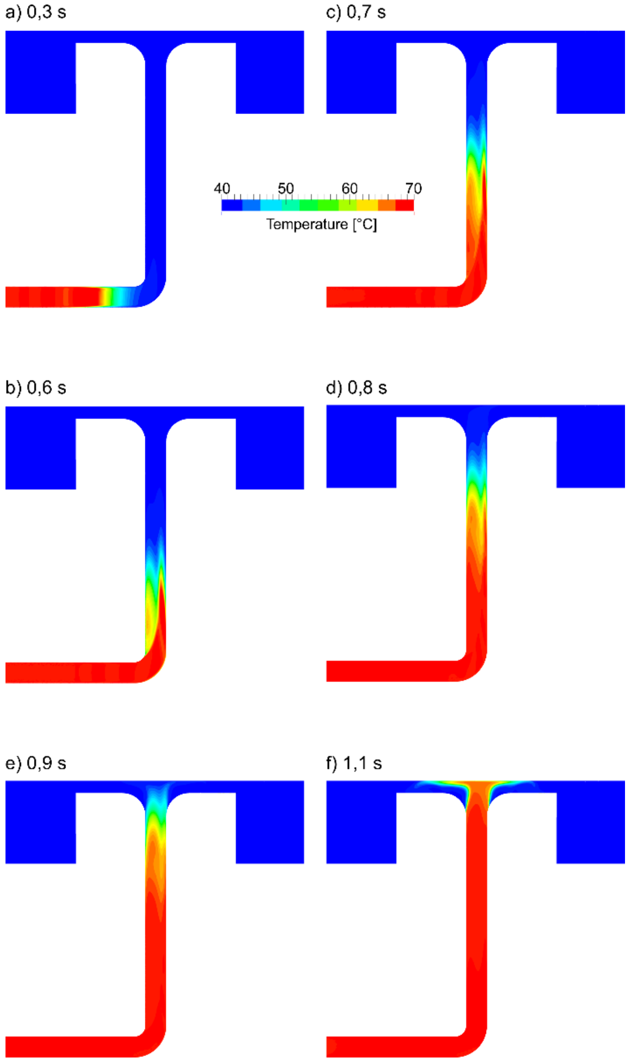

Figure 5: Evolution of the temperature field in the cross section of the connecting hose of CDS_1

In order to avoid the one-sided outflow, the installation of guide plates (Urbaneck et al., 2007) can force a guidance of the flow in different circumferential directions. Therefore, in the transition area eight vertical baffles staggered around 45° were placed, so that in principle eight single channels or segments are created. As shown in Fig. 6, this measure leads to the formation of multiple single jets over the radial diffuser. The flow follows the guide plates instead of attaching to the wall of the transition area. However, there is not yet an even flow over the entire diffuser circumference. How to achieve this, will be one topic of the next section.

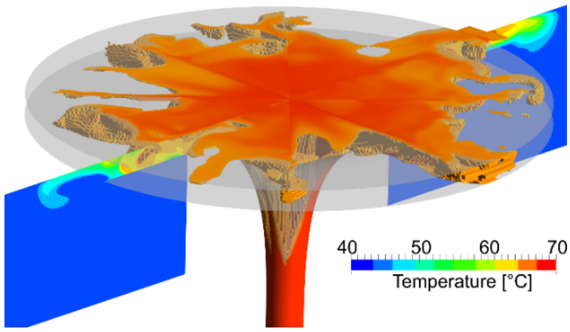

Figure 6: CDS_1 with guide plates, red: Volume of the warm zone (T > 67 °C) and temperature field in the vertical section

4. Experimental Validation

The aim of this section is to validate the simulation results and to show measures how to restore a symmetric flow. Therefor experiments in the laboratory of the Technical University of Chemnitz, Professorship Technical Thermodynamics, were performed. The test rig is shown in Fig. 7. It is basically a rectangular tank that has a dividing wall in order to get a square ground area in the right part of it (Fig. 7c). The CDS is placed in this part of the tank. Dividing the tank was necessary in order to minimize the different distances between the CDS outlet and the side walls of the tank. An optimum solution would be a cylindrical tank but the test rig was initially built for experiments on linear diffusers, where a rectangular shape is more appropriate. Table 2 gives the main parameters of the tank and the radial diffuser. Since the investigation of three-dimensional flow effects is the main topic, dimensionless quantities for buoyancy and flow behaviour like Froude and Reynolds number between the CFD simulation and the experiments were not respected.

Tab. 2: Operation conditions and geometrical parameters of the test rig

$h_{diffuser}$ [mm]	5	l_{tank} [mm]	600
d_{hose} [mm]	22	$d_{diffuser}$ [mm]	325
$\dot{V}_{in}$ [m³/h]	2	T_{in} [°C]	40
V_{store} [m³]	0.5	T_{store} [°C]	20

The investigations were carried out with a downscaled 360°-model of CDS_0 and CDS_1 (r = 75 mm, radius not downscaled) from the 3D-CFD simulations. To visualize the flow, black ink was added into the hose. The test rig has two supply lines (upper/bottom) in order to study the influence of the length of the inlet pipe.

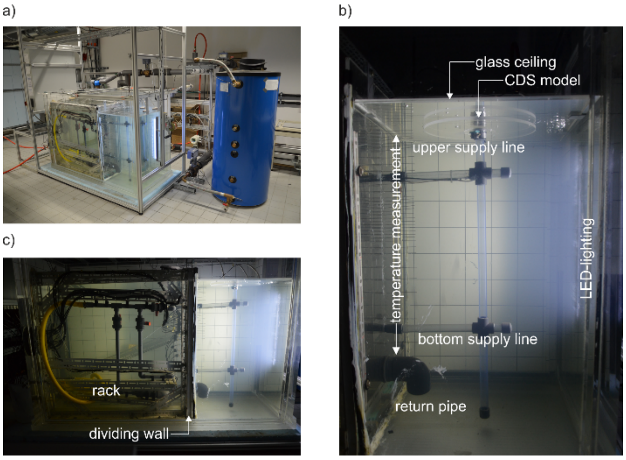

Figure 7: Test rig (a) with separated tank (b, c) in the darkened laboratory

Fig. 8 compares the outflow of both CDS. In the case of the sharp-edged transition (CDS_0, Fig. 8a), the outflow is distributed over the entire diffuser circumference. However, the flow is not rotationally symmetric, as single jets were generated. The flow pattern can be qualitatively compared with the result of the LES calculation in Fig. 2.

In the case of a round transition area (CDS_1, Fig. 8b), the flow get deflected in one direction, while fluid is sucked into the diffuser on the opposite side. This is accompanied by a considerable decrease of stratification quality. These results are similar to the 3D-CFD simulations.

Nevertheless, there are differences between simulation and experiment. While the 3D-LES calculation showed, that there is an almost uniform outflow in CDS_1 for isothermal conditions, this can not be observed in the downscaled model. In the experiment the effect persists also if there is practical no difference between the temperatures of the charging fluid and the fluid in the tank. This suggests that the flow velocity as well as the CDS dimensions have a significant influence on the occurrence of the effect. To clarify the relationship between flow, resp. thermal conditions and geometry further studies are necessary.

However, the results show clearly that for the investigated store, resp. tank yields, that high local flow velocities and the formation of jets is disadvantageous for the stratification quality. A high velocity jet is always accompanied by increased mixing effects in the CDS, a stronger reflection at the side walls of the tank and highly turbulent as well as complex flow patterns. In order to achieve less mixing and a better stratification quality a homogeneous outflow with minor velocities is useful. The CDS works best when the flow momentum is reduced by spreading and distributing the charging fluid over the largest possible area. Anyway, a prerequisite is the mounting of the CDS at the ceiling of the storage tank in order to secure the formation of a density current as described by Findeisen et al. 2016.

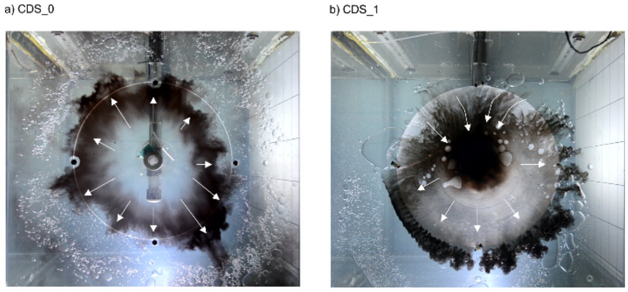

Figure 8: Addition of ink to the flow in a 360°-model of CDS_0 and CDS_1, view from above, $\dot{V}_{\mathrm{in}}$ =2 m³/h, ΔT =20 K

Besides of validating the simulation results, it's also possible to investigate measures to regain a symmetrical outflow. E. g., in the 3D-CFD simulations from the last section the installation of guide plates led to a star-shaped outflow. In order to reproduce this behavior in the experiments, such an installation part was installed in the transition area of CDS_1. As in the simulation from Fig. 6, now, the disappearance of the main jet and the formation of several single jets can be observed (Fig. 9). However, the jets still have a relatively high exit velocity and in between there are mixing areas. Nevertheless, the results show that the installation of guide plates as proposed by Urbaneck et al. (2007) has a very positive effect on the flow distribution in radial diffusers.

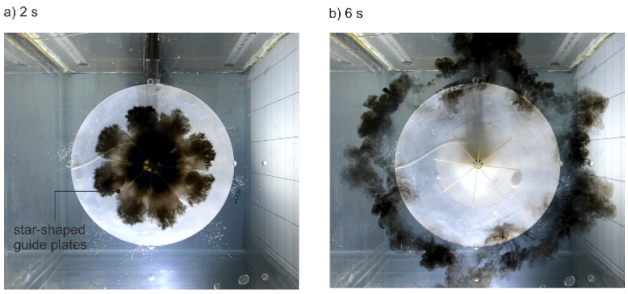

Figure 9: Flow in CDS_1 with star-shaped guide plates, view from above, $\dot{V}_{\mathrm{in}}$ =2 m³/h, ΔT =20 K

In order to improve the flow pattern and to increase the momentum loss, CDS_1 is extended in a second step by a built-in part to generate an additional pressure drop. This part can be designed as a perforated plate as it is already in operation for radial diffusers in cold water stores (Urbaneck et al., 2007). Due to the narrow diffuser gap in the downscaled model this was not practicable for the test rig, thus, a metal foam was used in the experiments.

It should be noted that such a part can in principle also lead to a high pressure reduction, which is considered unfavorable especially for operating the diffuser in suction mode with temperatures up to 98 °C. However, calculations have shown that the pressure reduction is uncritical when the mounting part is placed not too close to the transition area. In the radial diffuser mainly comparatively low velocities are still present, thus, the pressure reduction is uncritical.

That the built-in part leads to a very good uniformity of the flow is shown in Fig. 10. Before the black-colored flow reaches the metal foam it is still relatively chaotic (as in Fig. 8a). Shortly thereafter (Fig 10a) it passes through the metal foam ring and emerges almost symmetrically out of it. Contrary to the large turbulences in the other examples, very fine strands can be observed, which is due to the fine structure of the foam. Finally, a relatively even flow emerges over the entire diffuser circumference and in the further course (Fig. 10b) larger turbulence bundles also arise again. All in all, the outflow is more uniform than with CDS_0 in Fig. 8a.

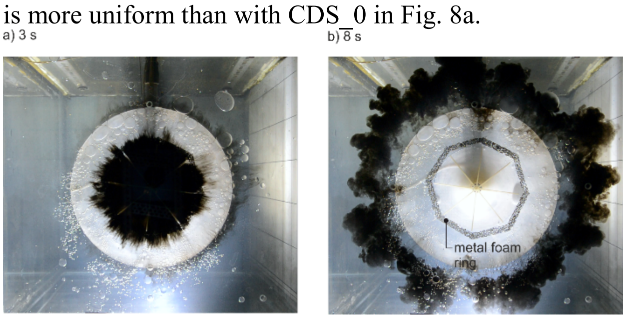

Figure 10: Flow in CDS_1 with star-shaped guide plates and a metal foam ring, view from above, $\dot{V}_{in}$ =2 m³/h, ΔT =20 K

Fig. 11 shows the temperature distribution in the tank for both CDS and two different temperature differences without additional built-in parts. The reflection of the accelerated main jet of CDS_1 on the tank side wall clearly leads to strong mixing and a worse stratification quality.

Fig. 12 illustrates the influence of the built-in parts on the temperature profiles. As expected, by using guide plates the temperature distribution the stratification quality is significant higher than in CDS_1 without any additional parts. In addition to that, the temperature in the warm zone is even higher than in CDS_0. The result with metal foam is slightly better than only with guide plates. In the end, the qualitative improvement of the flow pattern is accompanied by a quantitative improvement.

To investigate the influence of the inlet pipe length the experments were also performed with a short, resp. long pipe (upper/bottom supply pipe in Fig. 7). While for CDS_0 there was no remarkable difference in the temperature profiles, CDS_1 showed a slight improvement. Espeacially for small temperature differences the temperatures in the warm zone were up to 1 K higher.

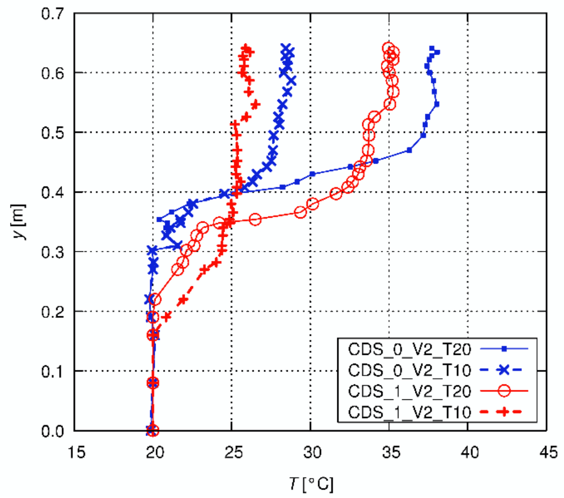

Figure 11: Vertical temperature profile for CDS_0 and CDS_1, $\dot{V}_{in}$ =2 m³/h, ΔT =10, resp. 20 K, t^* = 0.25

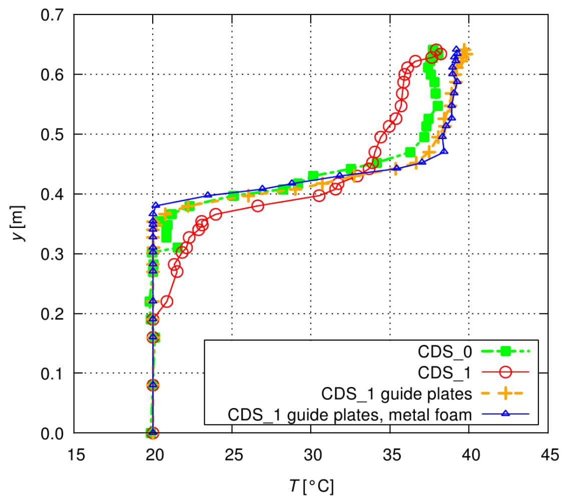

Figure 12: Vertical temperature profile for CDS_0, CDS_1 and CDS_1 with built-in parts, $\dot{V}_{in}$ =2 m³/h, ΔT =20 K, t^* = 0.25

5. CONCLUSIONS

This paper investigated the three-dimensional flow behavior in radial diffusers for thermal energy stores. Numerical investigations using CFD with RANS and LES, as well as experiments in the laboratory were carried out.

The investigations highlighted a special phenomenon: Due to a transition area with a relatively large radius between the connecting hose and the radial diffuser, a strongly asymmetrical and unidirectional flow can occur. Distinct mixing effects along the resulting main jet reduce the stratification quality. The numerical results were validated by experiments in the laboratory.

However, as previous studies already showed (Findeisen et al. 2017c), a round transition area (ideally with a varying radius; a so called free form diffuser) is necessary for operation with charging and discharging temperatures up to 98 °C. In order to handle the effect, guide plates in the transition area prevent the unidirectional outflow and improve stratification quality. In combination with built-in parts to generate an additional pressure drop, resp. a higher momentum loss (perforated plates or metal foam) the best results regarding flow pattern and stratification quality can be achieved.

ACKNOWLEDGEMENT

The realization of the project and the scientific work is supported by the German Federal Ministry for Economic Affairs and Energy (BMWi) on the basis of a decision by the German Bundestag (funding reference: 03ET1230A/B/C). The authors gratefully acknowledge this support and carry the full responsibility for the content of this paper.

REFERENCES

ANSYS Inc., 2005-2015. ANSYS CFX. Canonsburg (USA)

Coanda, H., 1911. Lifting apparatus. USA Patent US3261162A

Deschamps, C. J., Prata, A. T. and Ferreira, R. T. S., 1988. Application of the k-e Model to Turbulent Flow in Compressor Valves. Proc. 2 Brazilian Congress of Mechanical Engineering, Rio de Janeiro. p. 259–262

Findeisen, F., Urbaneck, T., Platzer, B., 2016. Radiale Diffusoren in Warmwasserspeichern – Funktionale Optimierung mittels CFD, Teil 1: Grundlagen und Modellierung. HLH, 10, p. 20-28. ISSN 1436-5103.

Findeisen, F., Urbaneck, T., Platzer, B., 2017a. Radiale Diffusoren in Warmwasserspeichern – Funktionale Optimierung mittels CFD, Teil 2: Optimierung des Be- und Entladeverhaltens. HLH, 2, p. 25-33. ISSN 1436-5103.

Findeisen, F., Urbaneck, T., Platzer, B., 2017b. Radiale Diffusoren in Warmwasserspeichern – Funktionale Optimierung mittels CFD, Teil 3: Detaillierte Untersuchung des Beladeverhaltens. HLH, 6, p. 19-27. ISSN 1436-5103.

Findeisen, F., Urbaneck, T., Platzer, B., 2017c. Radial Diffusers in Stratified Hot Water Stores: Geometry Optimization with CFD. Proceedings of the 6th International Conference on Solar Heating and Cooling for Buildings and Industry (SHC 2017), Abu Dhabi (UAE)

Findeisen, F., Urbaneck, T., Platzer, B., 2018. Radiale Diffusoren – Untersuchung des dreidimensionalen Strömungsverhaltens mittels CFD (Teil 1). Chemie Ingenieur Technik. accepted paper. ISSN 1436–5103

Herwig, A. and Rührling, K., 2015. Kriterien zur Bewertung der Energieeffizienz von Wärmespeichern: Teil 2 – Chancen einer neuen Messmethodik. Euro Heat & Power. 44, Nr. 4, p. 28–35. ISSN 1613–0200

Urbaneck, T.; Uhlig, U. and Barthel, U., 2007. Charging and/or discharging system and method for charging and/or discharging a thermal energy storage with an insert provided between the diffuser plates. EP 2003414A2.

Urbaneck, T., Findeisen, F., Mücke, J., Platzer, B., Gerschitzka, M., Lang, S., Bestenlehner, D., Drück, H., Herrmann, T., Beyer, R., 2017. Development of Overground Hot Water Stores in Segmental Construction for Solar and District Heating Systems Within the Project OBSERW. Proceedings of the 6th International Conference on Solar Heating and Cooling for Buildings and Industry (SHC 2017), Abu Dhabi (UAE)

Urbaneck, T., 2018. project description OBSERW. www.obserw.de. version: 29.01.2018

INVESTIGATION OF THE INTEGRATION OF A NEWLY DEVELOPED OVERGROUND HOT WATER STORE IN A SOLAR DISTRICT HEATING SYSTEM

Markus Gensbaur, Natalie Gohl, Dominik Bestenlehner, Harald Drück
Research and Testing Centre for Thermal Solar Systems (TZS)
Institute of Thermodynamics and Thermal Engineering (ITW)
University of Stuttgart, Pfaffenwaldring 6, 70550 Stuttgart, Germany,
Phone: ++49 (0)711 685-63628, email: gensbaur@itw.uni-stuttgart.de

Abstract – This contribution describes a newly developed overground hot water store based on a segmental construction principle and investigations related to the integration of this store in an existing solar district heating system in Crailsheim, Germany. The integration is investigated by means of annual system simulations. The transient simulation software TRNSYS 17 is used to perform the simulations of the entire solar district heating system. A validated model of the existing solar district heating system is used as reference system. The reference system is extended by the newly developed overground hot water store, using different integration variants of the store. Furthermore, an extension of the solar collector area and an increase of the capacity of the installed heat pumps are investigated. The objective of these studies is to demonstrate the benefit of an extension of the storage capacity by integrating an additional hot water store in a large solar district heating system.

1. INTRODUCTION

Solar district heating systems with and without seasonal thermal energy stores (STES) are investigated in various publications, for example in (Bauer et al., 2010), (Fisch et al., 1998) and (Xu et al., 2014). An evaluation of the system operation can be carried out by analysing monitoring data. A comparison of different existing system configurations is possible by using typical performance parameters, like solar fraction or store efficiency. If no monitoring data are available, for example in case of theoretical system modifications, system simulations studies can be used. In the field of solar thermal applications, the system simulation software TRNSYS is often applied (Gerschitzka, et al., 2015a), (Pahud, 2000), (Sibbitt et al., 2012). This contribution describes TRNSYS system simulation studies related to the integration of an overground hot water store in an existing solar district heating system and the evaluation of different integration configurations of the store.

The presented results are part of the research project CROW (Extension and optimization of the solar district heating system Hirtenwiesen II in Crailsheim and accompanying research on solar district heating and seasonal thermal energy storage) and the research project OBSERW (Overground storages in segmental construction for district heating systems). The German Federal Ministry for Economic Affairs and Energy (BMWi) partly finances both projects.

One aim of the project CROW is to promote and demonstrate the technology of central solar heating plants with seasonal thermal energy storage (CSHPSS) especially with high solar fractions. For this purpose, modifications and extensions of the existing CSHPSS in Crailsheim, Germany are investigated in this project. Figure 1 presents typical monitoring results of the heat demand of the district heating net Hirtenwiesen II and the solar thermal energy delivered by the solar collectors in Crailsheim. It can be seen, that there is a heat demand in winter, which cannot be covered by solar thermal energy, and in summer there is more solar thermal energy available than heat demand in the district net Hirtenwiesen II. This illustrates the purpose of the seasonal thermal energy store in the existing CSHPSS. An increase of the collected solar thermal energy caused by an increase of the solar collector area would also require additional STES capacity. The strong decrease of the solar thermal energy in September is caused by the control strategy of the CSHPSS.

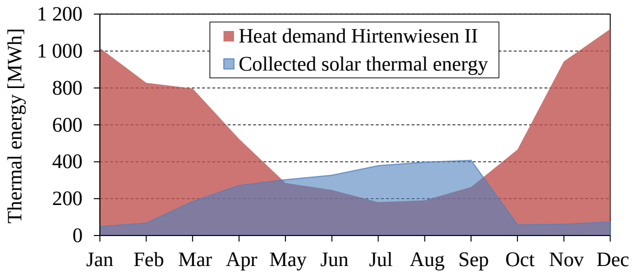

Figure 1. Heat demand of the district heating net Hirtenwiesen II and collected solar thermal energy for the CSHPSS in Crailsheim; monitoring results of the year 2016

The aim of the project OBSERW is the development of an unpressurized and water-based thermal energy store in segmental construction for district heating systems with water volumes between 500 m^3 and 8000 m^3. The segmental construction of the store and the pourable thermal insulation of polyurethane granule lead to low production costs compared to conventional welded STES with comparable volumes. A first application of the polyurethane granule in a STES is documented in (Chmielewski et al., 2014) and the segmental construction principle is often used for cold water stores (Urbaneck et al., 2015). A so-called OBSERW store with a volume of

100 m^3 was built for demonstration proposes and is currently operated in Nortorf, Germany. Furthermore within the project OBSERW, several test facilities and CFD models for the investigation of newly developed stratification devices, the heat transfer within the granule thermal insulation and the accelerated aging of the sealing material (Gerschitzka, et al., 2015b) are have been built up. A detailed description of the project, of the OBSERW store construction and of the project progress can be found in (Urbaneck et al., 2015). In figure 2 an OBSERW store with a volume of 100 m^3, its segmental construction of the tank and the granule recycling material polyurethane are shown. The thermal insulation material is blown-in the annulus between the tank and the grey-coated cover sheet in the mantel area and in the space at the top of the store.

Figure 2. Picture of the 100 m^3 OBSERW store in Nortorf, Germany (left), of the segmental construction of the tank (right) and of the granule recycling material polyurethane (top right)

2. METHODS

The transient simulation software TRNSYS 17 is applied to perform simulation studies of the solar district heating system in Crailsheim. A validated model of the existing solar district heating system is used for the simulation of the reference system, see section 2.1. A hot water store extends this reference system as described in section 2.3.

2.1 Reference system

The current solar district heating system in Crailsheim, Germany consists of three solar collector fields connected to two separate heating centers, a borehole thermal energy store for seasonal thermal energy storage and two buffer stores for short-term thermal energy storage. Additionally a compression heat pump is integrated in the system in order to discharge the borehole thermal energy store to lower temperatures. The district heating net named Hirtenwiesen II supplies approximately 300 apartments, a school and a sports hall with heat. Furthermore, solar excess heat can be transferred to the district heating net Hirtenwiesen I, which is supplied by a thermal power station consisting of two gas boilers and a combined heat and power plant. If there is not enough solar thermal energy available to cover the heat demand in the district net Hirtenwiesen II, the thermal power station also supplies thermal energy to this net. Figure 3 shows a scheme of the current system or reference system respectively.

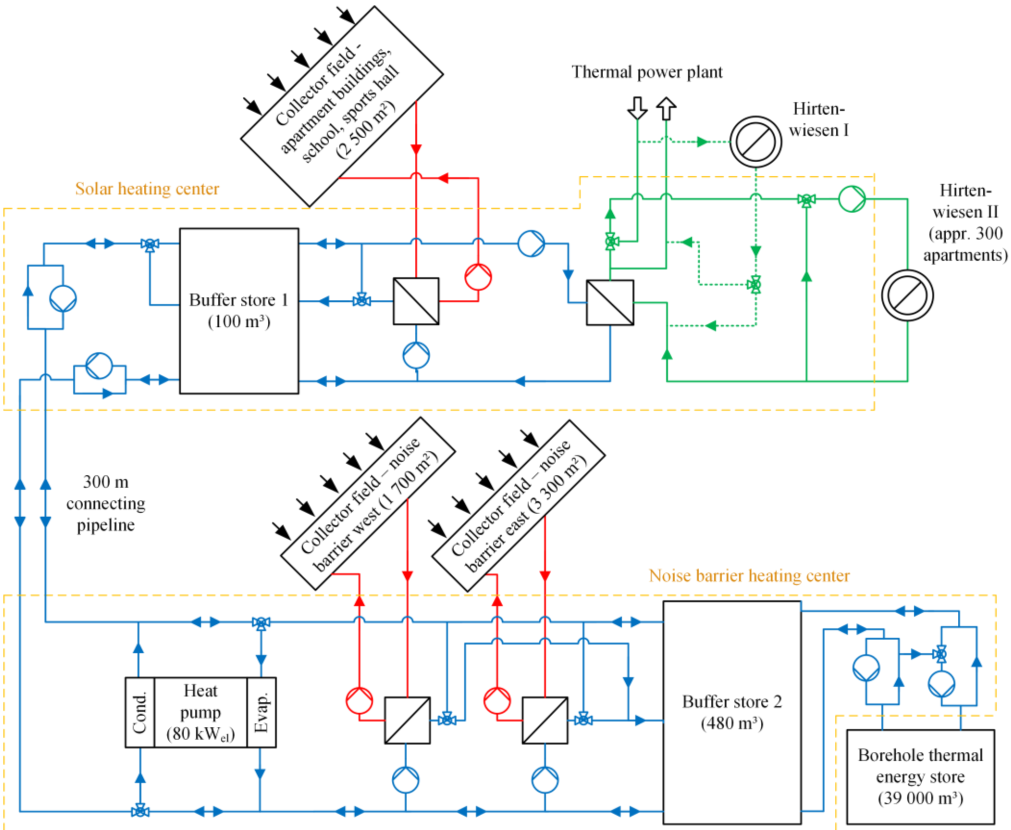

Figure 3. Scheme of the existing CSHPSS in Crailsheim, Germany (reference system)

Figure A1 in the appendix shows a picture of a small-scaled model of the CSHPSS in Crailsheim and figure A2 shows a photo of the CSHPSS in Crailsheim. Furthermore, the main components of the reference system are explained in table A1 of the appendix.

2.2 Model validation and sensitivity analysis

This section explains the validation of the reference model using measurement data of the year 2016. Table 1 shows the comparison of different annual energy amounts. These are calculated from the monitoring results of the CSHPSS in Crailsheim and the TRNSYS simulation results. The table presents the annual amount of thermal energy charged into and discharged from the BTES (Borehole Thermal Energy Store) $Q_{BTES,char}$ and $Q_{BTES,dischar}$, the annual heat demand of the district net Hirtenwiesen II Q_{HWII} and the annual amount of thermal energy transferred to the district heating net Hirtenwiesen I Q_{HWI}.

$Q_{Loss,HC}$ represents the heat losses of both buffer stores, the heat losses of the connection pipelines and the heat losses of the hydraulic components of both heating centers and Q_{STE} represents the annual amount of thermal energy transferred from all solar collector fields into the heating centers.

Table 1. Comparison of measured and simulated annual thermal energy amounts of the CSHPSS of Crailsheim for the year 2016

Annual energy amount	$Q_{BTES,char}$ [MWh]	$Q_{BTES,dischar}$ [MWh]	Q_{HWII} [MWh]	Q_{HWI} [MWh]	Q_{STE} [MWh]	$Q_{Loss,HC}$ [MWh]
Simulation	647	412	6 861	158	2 581	245
Measurement	731	419	6 862	175	2 577	204
Relative difference [%]	11	2	0.1	10	0.2	17

Overall, there is a good agreement between the simulated and measured annual thermal energy amounts. The slight differences between the measured and calculated values for $Q_{BTES,char}$ as well as $Q_{Loss,HC}$ can be explained by differences of the initial BTES and buffer store temperatures at the beginning of the calculation as a certain temperature has to be assumed for the start of the simulation. Furthermore model uncertainties of the BTES can have an influence on the results. The validation with monitoring data of the year 2015 shows similar results.

Figure 4 shows a sensitivity analysis of the solar fraction of the reference system, based on simulation results. It can be seen, that especially a decrease of the heat demand of the district net Hirtenwiesen II Q_{HWII} and an increase of the collected solar thermal energy Q_{STE} leads to an increase of the solar fraction. Based on this finding, the reference system is extended by an additional solar collector field and an OBSERW hot water store, see section 2.3.

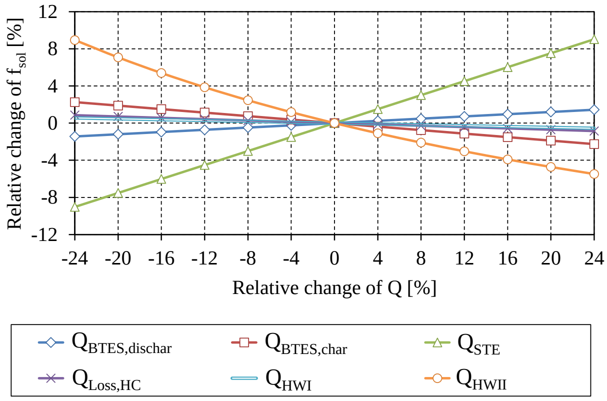

Figure 4. Sensitivity analysis of the solar fraction (2016)

2.3 Extensions of the reference system

Five extension variants are investigated for the integration of the hot water store into the heating center located close to the noise barrier (so-called noise barrier heating center). The figures A3 to A6 in the appendix show the different integration schemes. In variant 1 the additional hot water store can be discharged by buffer stores 1 and 2 and be charged only by buffer store 2. Variant 2 is similar to variant 1, but the additional hot water store can be discharged only by buffer store 2. In variant 3 the hot water store is charged only if the buffer store 2 is at least charged 80 volume-percent. The variant 4 is created to investigate the influence of the extension of long-term thermal energy storage capacity by a parallel charging of the BTES and the additional hot water store. The integration of the store in variant 5 is identical to variant 1, beside the application of a more complex control strategy.

Table 2. Parameters of the hot water store used in the variants investigated for the extension of the existing reference system

Component	Description
OBSERW store (TRNSYS type 340, modified)	Ideal thermal stratified operation, volume $V = 500 - 16\,000\ m^3$, heat loss rate[a] (UA) = $135.4 \cdot (V / 800)^{(1/2)}$ W/K, height $h = (V \cdot 4 / \pi)^{(1/3)}$ m, number of nodes for the vertical discretization of the store volume: 145

[a] The dependency of the heat loss rate from the store volume is calculated based on the European standard EN 12977-3:2012. The so calculated heat loss rate of a store with a water volume of 4 000 m^3 is for example similar to the theoretical calculated heat loss rate of a store with thermal insulation material of a thickness of d = 20 cm and a thermal conductivity of $\lambda = 0.043$ W/(m·K). This thermal conductivity is similar to the one of the measured polyurethane granule at a mean temperature of 62 °C used as thermal insulation in the OBSERW store (Gerschitzka, et al., 2015b).

The store's parameters for the TRNSYS simulations are summarized in table 2. Furthermore, some modifications in the reference system model were performed. The heat demand is slightly increased from 6 862 MWh to 7 000 MWh and the parameters of the collector field "noise barrier east" are modified to model vacuum flat plate collectors.

This modified reference system is denoted as extended reference system in the following. All simulation studies have a simulation duration of three years to obtain for the third year results being independent form the initial temperatures of the stores. Hence, for the determination of the results used for the evaluation only the third year is considered. Further investigations concerning the model parameters of the hot water store show, that the effective vertical thermal conductivity, the increase of the number of nodes for the store volume discretization and the assumption of ideal stratified charging have a negligible influence on the annual solar fraction of the CSHPSS and the efficiency of the hot water store.

Beside the investigation of the integration of an additional hot water store, the influence of an additional heat pump and of an additional solar collector field are investigated. Table A2 in the appendix shows model parameters of the additional heat pump and the additional solar collector field. These additional modifications are applied only on one of the investigated integration variants.

3. RESULTS

The following section presents the results of the simulation study. For each integration variant of the extended reference system, several hot water store volumes in the range from 500 m^3 to 16 000 m^3 are investigated. Figure 5 and figure 6 show the solar fraction and the store efficiency of the hot water store for the integration variants as described in section 2.3. Variant 2 and 4 reach a maximum related to the solar fraction between a volume of 4 500 m^3 and 5 000 m^3. Variant 1, 3 and 5 reach a maximum solar fraction between a volume of 8 000 m^3 and 9 000 m^3. Variant 5 shows the highest results concerning the solar fraction. The fluctuation in the solar fraction are due to effects caused by the individual control strategies. In an ideal case a continuous trend without any fluctuations could be expected. Figure 5 also shows that even a hot water store with a volume of 500 m^3 increases the solar fraction for all variants compared to the extended reference system. The solar fraction decreases for high store volumes because of the increased thermal energy losses of the store.

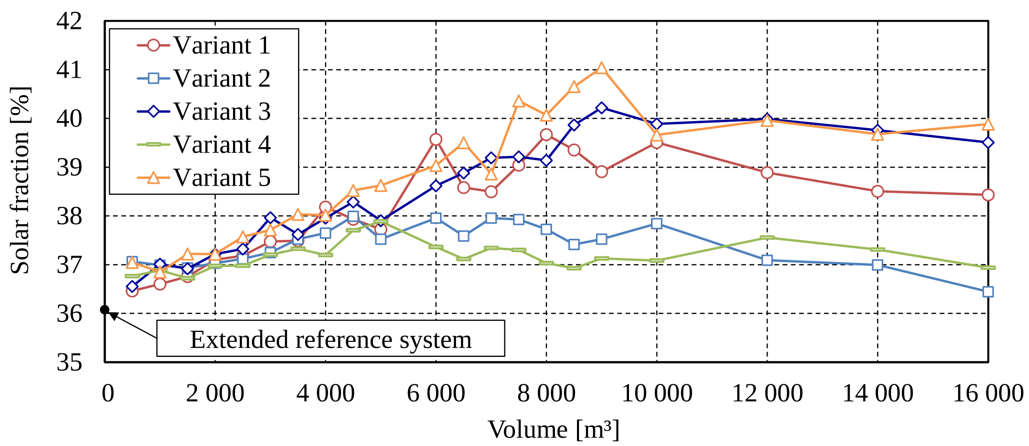

Figure 5. Solar fraction as function of hot water store volume for all integration variants of the extended reference system

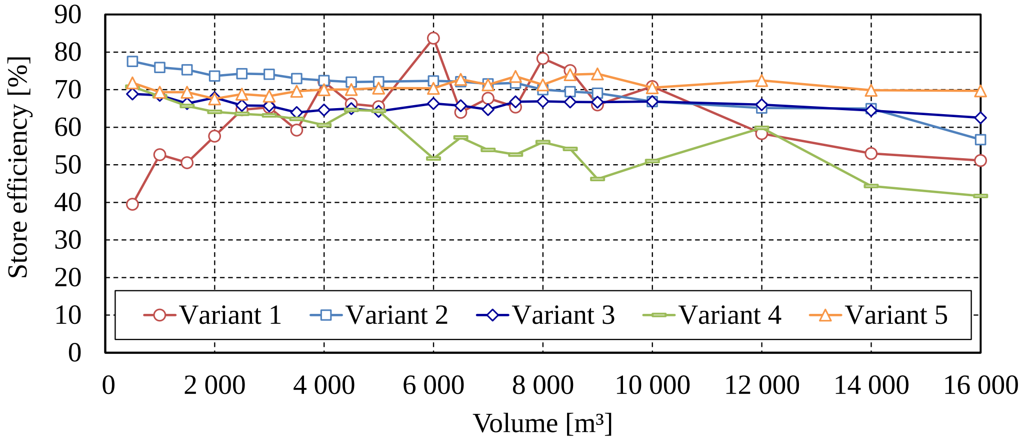

Figure 6. Store efficiency as function of hot water store volume for all integration variants of the extended reference system

Figure 6 shows for the variants 2, 3, 4 and 5 only a slight dependency between the hot water store volume and the store efficiency (see nomenclature) in the considered volume range. The store efficiency decreases with increasing store volumes. Variant 1 shows a maximum in store efficiency, probably because of control strategy problems of the CSHPSS at lower store volumes.

Figure 7 and figure 8 present the solar fraction for all variants as a function of the additional solar collector area for a hot water store volume of 8 000 m^3 and as a function of the hot water store volume for an additional collector area of 2 000 m^2. Furthermore, in figure 8 the influence of an additional heat pump is presented exemplary for variant 5 in comparison to all other variants.

All variants show a strong dependency of the solar fraction on the additional collector area. In the range from 0 m^2 to 3 000 m^2 an almost linear increase occurs. Assuming an additional collector area of 2 000 m^2, figure 8 demonstrates, that an increase of thermal capacity results in an increase of the solar fraction for the complete considered volume range, except for variant 4. Finally, figure 8 presents that concerning the solar fraction an additional heat pump with a maximum electrical power consumption of 80 kW along with the best variant 5 leads to a further strong increase of the solar fraction.

4. CONCLUSION

The assessment of the extension of the extended reference system with an additional hot water store is done by means of the parameters solar fraction and store efficiency. A variation of the store volume and five integration variants is considered. Furthermore two additional modifications of the extended reference system are investigated. These modifications are the extension of the collector area and the integration of an additional heat pump.

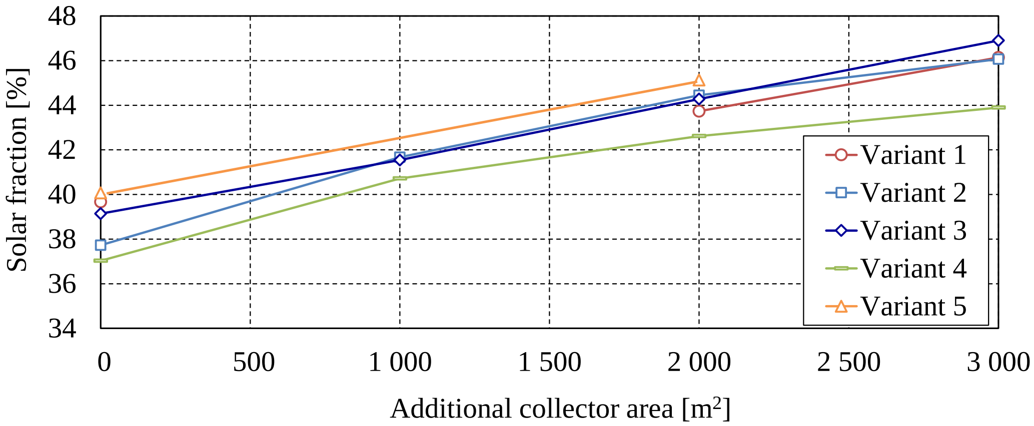

Figure 7. Solar fraction as function of the additional collector area for all extension variants of the extended reference system (additional hot water store volume 8 000 m^3)

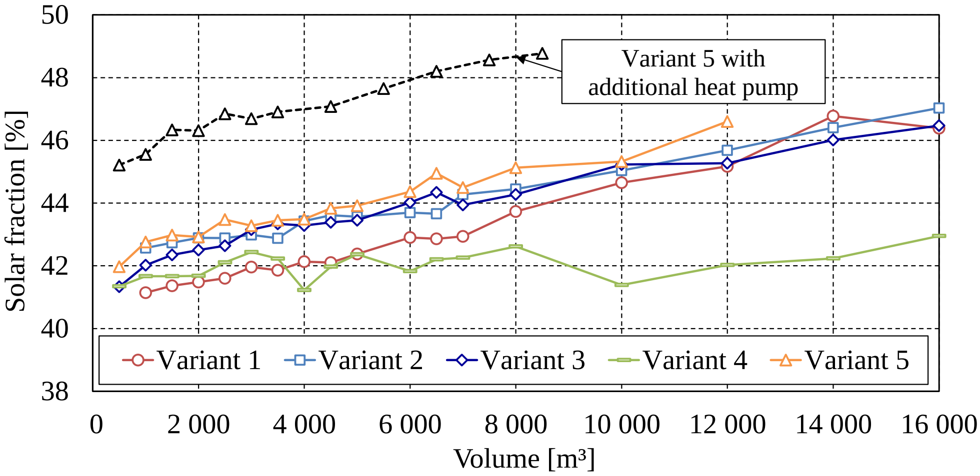

Figure 8. Solar fraction as a function of the hot water store volume for all extension variants of the extended reference system with 2 000 m^2 additional solar collector area and an additional heat pump (variant 5)

It can be stated that the volume of the integrated hot water store has a strong impact on the solar fraction of the CSHPSS. Furthermore, high store efficiencies can be reached, premised a suitable integration variant is chosen. For example the extension of the CSHPSS in Crailsheim with a 8 000 m^3 hot water store in variant 4 leads to an increase of the solar fraction of approximately Δf_{sol} = 4 %-points. For this extension of the extended reference system, an increase of the solar collector area leads to a solar fraction increase for all variants of approximately Δf_{sol} / A= 2.4 %-points / 1 000 m^2 solar collector area. An integration of a second heat pump in variant 5 also shows a solar fraction increase compared to variant 5 without second heat pump of approximately Δf_{sol} = 3.4 %-points for a hot water store volume in the range between 500 m^3 and 8 500 m^3.

REFERENCES

Bauer D., Marx R., Nußbicker-Lux J., Ochs F., Heidemann W., Müller-Steinhagen H. (2010). German central solar heating plants with seasonal heat storage, *Solar Energy*, 84, 612-623.

Chmielewski M., Starosielec B., Żach J., Aguirre P., Esteban J. C. M. (2014). D7.1 Report on design and installation of demonstration plants, *Document of the research project EINSTEIN (Effective integration of seasonal thermal energy storage systems in existing buildings)*, [online: www.einstein-project.eu/moduluak /estatikoak/dokumentuak/einstein-el-71-v1.pdf]

Fisch M. N., Guigas M., Dalenbäck J. O. (1998). A review of large-scale solar heating systems in europe, *Solar Energy*, 63, 355-366.

Gerschitzka M., Lang S., Bauer D., Drück H. (2015a). Potentials of high-efficient thermal energy stores for solar district heating applications. *Proceedings of 3rd Solar District Heating Conference (SDH 2015)*, Toulouse, France.

Gerschitzka M., Marx R., Lang S., Bauer D., Drück H. (2015b). New developments related to thermal insulation materials and installation techniques for over ground seasonal thermal energy stores. *Proceedings of 13th International Conference on Thermal Energy Storage (Greenstock 2015)*, Peking, China.

Pahud D. (2000). Central solar heating plants with seasonal duct storage and short-term water storage: design guidelines obtained by dynamic system simulations. *Solar Energy*, Vol 69, No 6, 495-509.

Sibbitt B., McClenahan D., Djebbar R., Thornton J., Wong B., Carriere J., Kokko J. (2012). The performance of a high solar fraction seasonal storage district heating system - five years of operation. *Energy Proceedia*, 30, 856-865.

Urbaneck T., Platzer B. (2015). Overground storages in segmental construction for district heating systems (OBSERW) - Project overview. *Proceedings of 13th International Conference on Thermal Energy Storage (Greenstock 2015)*, Peking, China.

Xu J., Wang R. Z., Li Y. (2014). A review of available technologies for seasonal thermal energy storage. *Solar Energy*, 103, 610-638.

ACKNOWLEDGEMENT

The activities described in this publication are being supported by the German Federal Ministry for Economic Affairs and Energy (BMWi) based on a decision of the German Bundestag by Projektträger Jülich (PtJ) under grant numbers 0325869B (research project CROW: Extension and optimization of the solar district heating plant Hirtenwiesen II in Crailsheim and accompanying research on solar district heating and seasonal thermal energy storage) and 03ET1230C (research project OBSERW: Overground storages in segmental construction for district heating systems). The authors gratefully acknowledge this support and carry the full responsibility for the content of this publication.

ABBREVIATIONS

BTES	Borehole thermal energy store
CFD	Computational Fluid Dynamics
CROW	Research project: Extension and optimization of the solar district heating plant Hirtenwiesen II in Crailsheim and accompanying research on solar district heating and seasonal thermal energy storage
CSHPSS	Central solar heating plants with seasonal thermal energy storage
Cond	Condenser
Evap	Evaporator
HWS	Hot water store
OBSERW	Research project: Overground storages in segmental construction for district heating systems
STES	Seasonal thermal energy store

NOMENCLATURE

A_{coll}	Area of a collector field [m^2]
a_1	Collector heat loss coefficient [$W/(m^2 \cdot K)$]
a_2	Collector temperature depended heat loss coefficient [$W/(m^2 \cdot K^2)$]
h	Height [m]
f_{sol}	Solar fraction ($f_{sol} = Q_{Sol,net} / Q_{Net}$) [%]

(UA)	Heat loss rate of the store [W/K]
d	Thickness of the thermal insulation [cm]
Q	Thermal energy [MWh]
$Q_{BTES,char}$	Annual amount of charged thermal energy into a BTES [MWh]
$Q_{BTES,dischar}$	Annual amount of discharged thermal energy from a BTES [MWh]
$Q_{HWS,char}$	Annual amount of charged thermal energy into a hot water store [MWh]
$Q_{HWS,dischar}$	Annual amount of discharged thermal energy from a hot water store [MWh]
Q_{STE}	Annual amount of transferred solar thermal energy from the solar collector fields into the heating centers [MWh]
$Q_{Sol,net}$	Annual amount of supplied solar thermal energy to the district net Hirtenwiesen II [MWh]
Q_{Net}	Annual amount of consumed thermal energy by the district net Hirtenwiesen II [MWh]
Q_{HWI}	Annual amount of transferred thermal energy to district heating net Hirtenwiesen I [MWh]
Q_{HWII}	Annual amount of heat demand of the district net Hirtenwiesen II [MWh]
$Q_{Loss,HC}$	Annual amount of overall heat losses of both heating centers and connecting pipelines [MWh]
P_{el}	Electrical power consumption of the heat pump [kW]
V	Thermal energy store volume [m^3]
λ	Thermal conductivity [W/(m·K)]
η_s	Thermal energy store efficiency ($\eta_s = Q_{HWS,dischar} / Q_{HWS,char}$) [%]
η_0	Optical collector efficiency [-]

Appendix

Table A1. Main components of the reference system

Component	TRNSYS Type	Description
Borehole thermal energy store	346 (modified)	80 double-U-shaped borehole heat exchangers with a depth of 55 m, BTES volume V = 39 000 m^3
Buffer stores	340	Hot water stores in ideally stratified operation, buffer store 1: volume V = 100 m^3, heat loss rate (UA) = 101 W/K, height h = 12.5 m, buffer store 2: volume V = 480 m^3, heat loss rate (UA) = 123 W/K, height h = 14.5 m, number of nodes for the vertical discretization of the store volume for: 145 (buffer tore 1) and 175 (buffer store 2)
Flat plate solar collector	301	Summarized collector field area A_{coll} = 7 500 m^2, heat loss coefficient a_1 = 4.60 W/(m^2·K), temperature dependend heat loss coefficient a_2 = 0.012 W/(m^2·K^2), optical collector efficiency η_0 = 0.80
Heat pump	850 (modified)	Maximum electrical power consumption P_{el} = 80 kW

Table A2. Additional modifications of the noise barrier heating center

Component	Description
Additional heat pump (TRNSYS type 850, modified)	Combined maximum electrical power consumption of both heat pumps P_{el} = 2 x 80 kW = 160 kW
Separate solar collector field (TRNSYS type 301)	Collector field area A_{coll} = 0 m^2 to 3 000 m^2, heat loss coefficient a_1 = 0.41 W/(m^2·K), temperature dependend heat loss coefficient a_2 = 0.007 W/(m^2·K^2), optical collector efficiency η_0 = 0.82

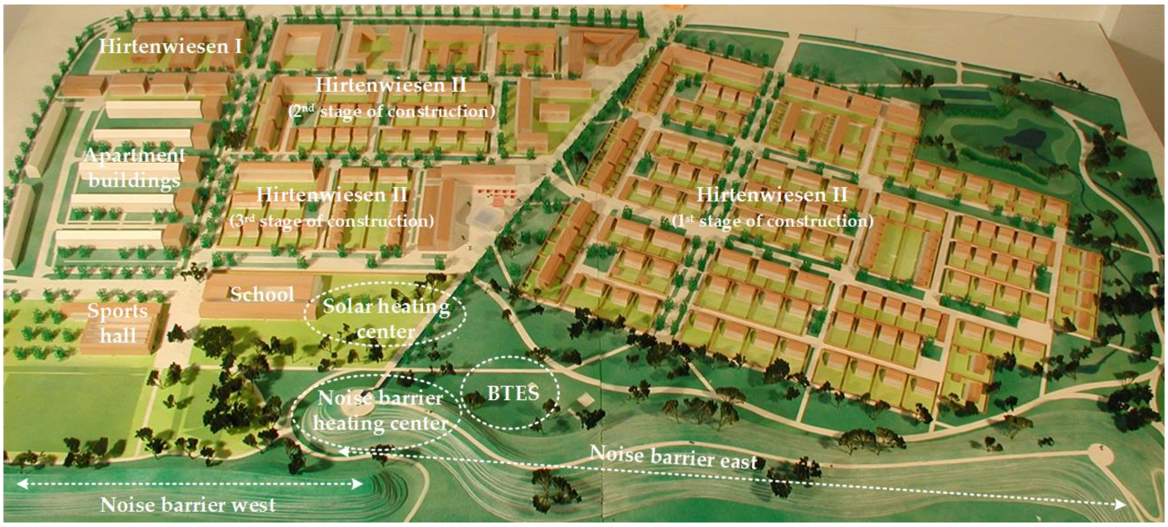

Figure A1. Picture of a small-scaled model of the CSHPSS in Crailsheim (reference system)

Figure A2. Photo of the CSHPSS in Crailsheim

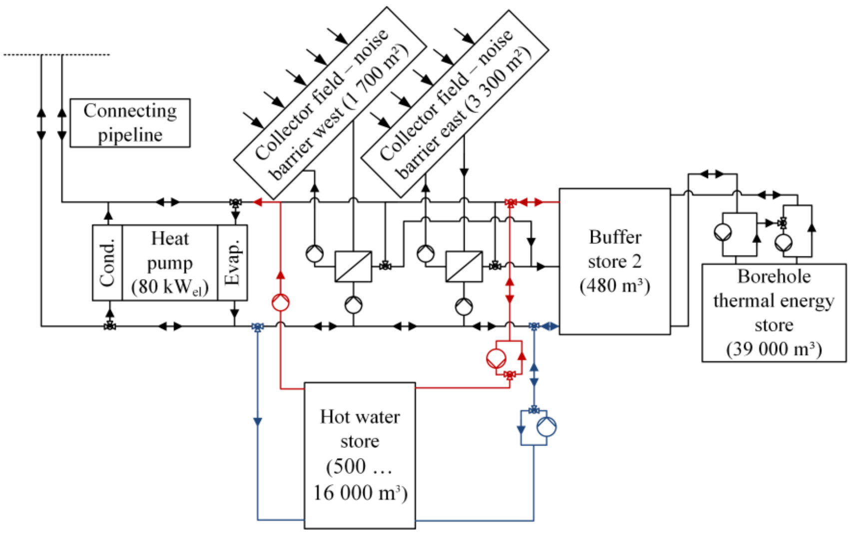

Figure A3. Scheme of the modified noise barrier heating center of the CSHPSS Crailsheim (variant 1)

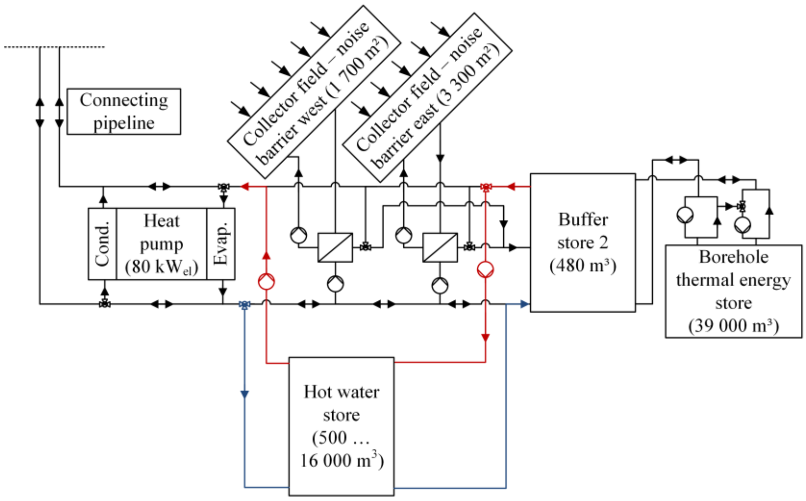

Figure A4. Scheme of the modified noise barrier heating center of the CSHPSS Crailsheim (variant 2)

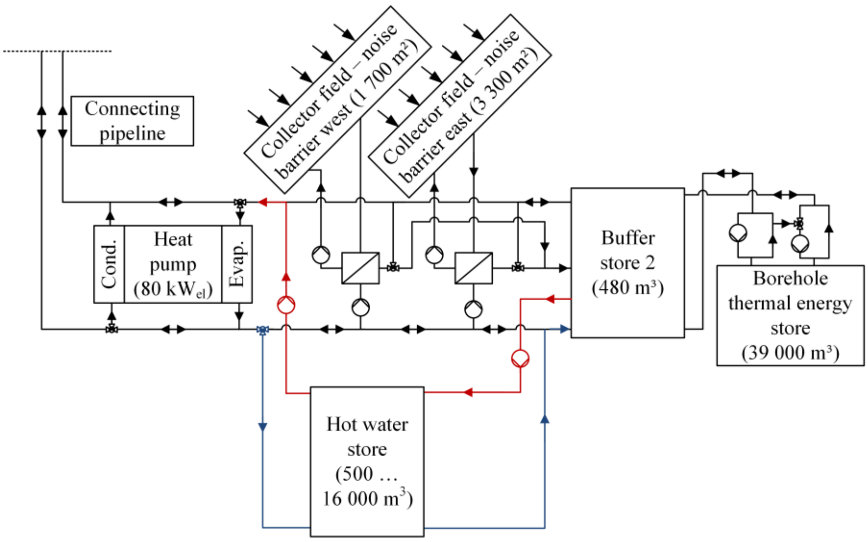

Figure A5. Scheme of the modified noise barrier heating center of the CSHPSS Crailsheim (variant 3)

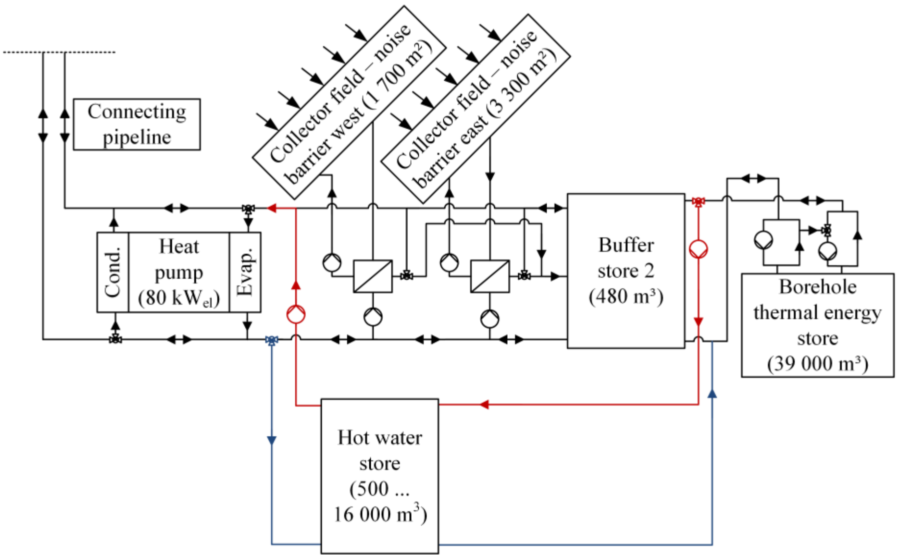

Figure A6. Scheme of the modified noise barrier heating center of the CSHPSS Crailsheim (variant 4)

Floating thermal collectors on top of seasonal water pit storages

Arch. Dimitar Paskalev, Eng. Valentin Vasilev, Eng. arch. Milan Rashevski

2018

Institute for Zero Energy Buildings, 183 Rakovski str., Sofia, Bulgaria
paskalev@izeb.eu
+359888531538

The solar irradiation hitting the top of the water pit storages is sufficient to heat up the water volume if it is harvested. The concept develop integration between solar thermal collectors with the floating heat insulation in a system, that will allow to harvest the solar irradiation and at the same time to keep it for seasonal usage. As result of the proposed system the usage of land for solar fields aside of the seasonal storages will be avoided and the total cost of the SDH will be diminished. The system is solving problems like wind, evacuationg of rain water, melting the snow, and other maintanance issues. In addition the system can be applied in existing water volumes, near by urban areas, where water volume is used without need of any building process and laining. It is evaluated optimal depth of the seasonal water pit as function of the harvested energy and the expected losses. It is evaluated expected minimization of the total installation cost, comparing with installation where solar field is placed in a land aside of the seasonal storage.

1. INTRODUCTION

Ground mounted collector areas for district heating are seen in e.g. Sweden, Denmark, Austria and Holland. They are oriented towards south and the distance between the solar collector rows and the angle from horizontal is optimised for each place and collector type. Normally for 1 m2 solar collector 3-4 m2 land is needed. The distance between the solar collector rows is normally at least 4.5 m (depending on the collector height) – measuring from the front of a collector row to the front of the next row – allowing people to move around between the rows. Larger distances give higher production because of less shadowing but also higher costs for ground and piping. [1].

The seasonal storages are crutial solutions for achieving bigger solar energy fraction in the DH mix. In order to use the full capacity of the solar field, assuming very little consumtion of DHW in the summer months, approx 65% of the harvested energy needs to be stored for seasonal use. Converted in water storage volume it is evaluated, that each 1m2 collector aperture needs 11m3 water volume (Table 1).

Pit thermal energy storages (PTES) are constructed without static constructions, by means of mounting insulation and a liner in a pit. The design of the lid depends on the storage medium and geometry, whereas in the case of gravel- or soil / sand-water thermal energy storages the lid may be constructed identical to the walls. The construction of a lid of a water PTES requires major effort and is the most expensive part of the thermal energy storage. Typically it is not supported by a construction underneath but floats on top of the water. By definition, pit thermal energy storages are entirely buried. In large PTES the soil dug from the ground is used to create banks which make the storage somewhat higher than the ground level. The lid can be only equipped with a membrane for rain and UV protection. [2]. Typical section is shown in Fig. 1.

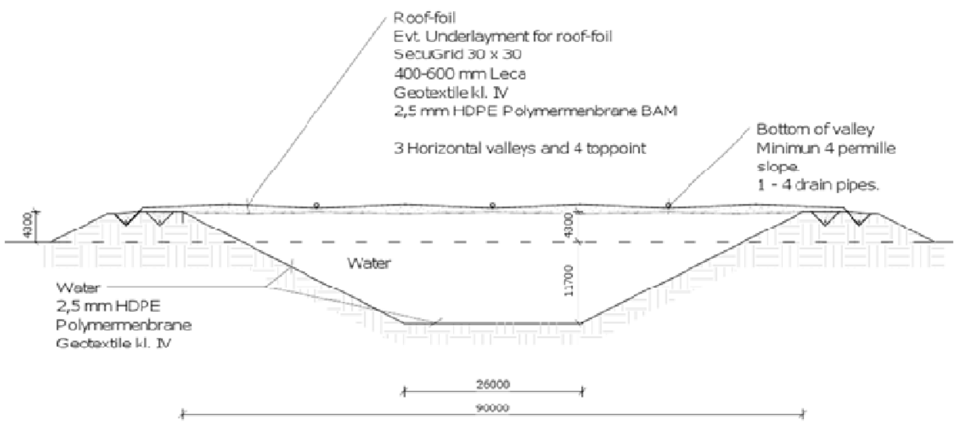

Fig. 1: Construction cross section of the 75,000 m³ PTES in Marstal. (Source: PlanEnergi)

solar radiation at 1m2 aperture area in Varna, Bulgaria						
	0 degree			35 degree		
Month	Hm	COP	harvested	Hm	COP	
1	44	53%	23	71	53%	37
2	61	67%	41	88	67%	59
3	108	78%	84	133	78%	104
4	144	81%	117	157	81%	128
5	191	83%	159	188	83%	157
6	206	85%	175	191	85%	163
7	214	86%	184	204	86%	176
8	193	86%	166	205	86%	176
9	132	83%	110	161	83%	134
10	87	79%	69	122	79%	96
11	52	67%	35	82	67%	55
12	38	50%	19	62	50%	31
Yearly	1470		1182	1664		1314
summer	to be stored		795			805
winter	direct use		387			509
% storage of total			67%			61%
storage volume m2			11			11
after 20% losses and heat capacity 60kWh/m3						

Table 1. Solar radiation at 1m2 aperture area of collectors at 0 and 35 degree inclination and needed storage volume for 100% heating use in Kinder garden (excl. DHW consumption), Varna, Bulgaria

2. PROBLEM DEFINITION

The successful integration of SDH in the urban areas is facing the problem of the land use and related costs and general lack of free space. Land areas are needed for both – collector fields and storage. PTES has proven to be one of the most feasable storage sollutions, however, not including investment for land use, which can be significant in urbanised areas. Furthermore, pit storages include sophisticated and expensive cover lid with low static bearing capabilities. The area of this cover lid is significant compared to other storage types and implies high land costs. In addition, long distances from the solar field to the DH network are causing additional losses and infracstructure investments. In this sense, it is very logical to look for technical opportunities to use this area for solar collector field.

The main technical challenges to locate solar collectors on the top of the floating lid are:

- Low bearing capacity of the lid cover
- Evacuation of rainwater
- Mechanical wind resistance of the collectors
- Penetration and lid tightness issues
- Difficult maintanance of the floating lid cover

Those problems are the reason why up to date no SDH with floating sollar fields has been built. It is necessary not just to adopt and adjust existing storage and collector sollutions, but create an entirely new system, as a result of integrated design, able to overcome the challenges listed above.

3. CONCEPT

The proposed system solves integration between solar thermal collectors with the floating heat insulation on top of the seasonal water storages. It will allow to harvest solar irradiation and at the same time to keep it for furher use. It is fully prefabricated, modular and easy to install on top of the water volume (Fig3.)

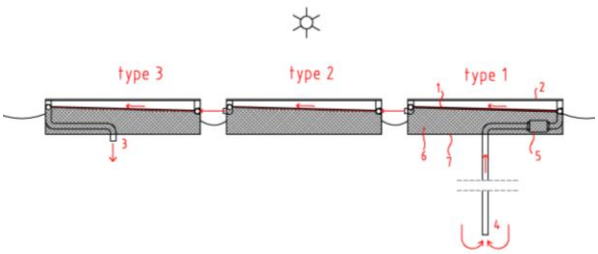

Fig. 3 Floating collectors principle:
The absorption surface (1) is mounted below horizontal glass top (2), covering the floating heat insulation plate (6). There are 3 types of collectors: Type 1 – including input hose (4) sucking cold water from the bottom of the storage volume through the pump (5), Type 2 – transfering collector, Type 3 – including output hose, that injects hot water on the top layer of the storage volume. There are strings formed after connection of the three collector types (with multiple type 2 collectors on each string, depending on design requirements). The collectors are connected with fast plug in connections (both - pipes and bodies), forming solid floating platform. The bottom of the insulation plate is covered with high temperature water resistent linen (7), preventing the insulation from getting soaked with water.

4. DETAILED SOLUTION

The proposed modular collector field is floating over the PTES, integral part of its design and is assuring for both: harvesting and storing the solar energy. It injects the thermal energy directly into the top level of the storage with no additional thermal losses.
As being modular and rigid – the system is assembling very fast, by clicking together plug in connections. In addition a silicone strip is closing the gaps between the panels. Vacuum drainage system is integrated. Such system does not need any slopes of the roof surface in order to evacuate the rain water out of the storage surface. Details are shown on Fig. 4.

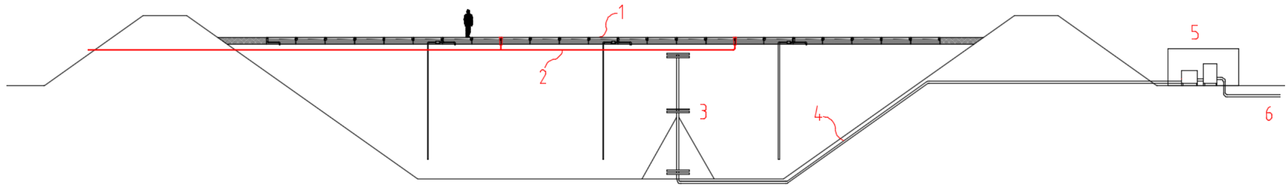

Fig. 4 Principle of floating collectors on top of the hot water pit storage
The floating collectors (1) are forming solid floating platform on top of the hot water pit storage. The vacuum drainage system is evacuating the rain water outside of the storage volume (2). The collectors are sucking cold water from the bottom of the volume, transferring it from the collector's aperture surface, and when heated – injecting it on the top of the volume. All the pumps of the Type 1 collectors are working with variable flow and managed from automation system. The thermal energy is distributed from the distribution column (3) through the pipelines (4) to the power station (5), where the heat exchangers, circulation pumps and water treatment system are installed. If needed – the output energy can be preheated. From the power station the energy is transferred to the DH network (6).

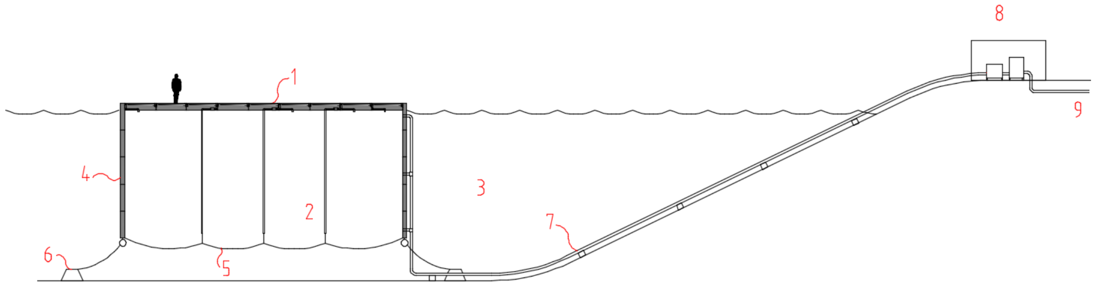

Fig. 5 Principle of the Floating cell
The floating collectors (1) are forming solid floating platform on top of the existing water basin (3). Surrounding heat insulation panels (4) are separating the hot and treated water (2) from the water of the basin. The bottom membrane (5) is closing the volume of the treated water. There is no need for heat insulation at the bottom: the heat is stratified in a normal way in the upper part of the volume, reaching the bottom temperature similar to the exterior basin temperature. Distribution tubes (7) laid on the basin bed are transporting the thermal energy from the floating cell to the power station (8), where the heat exchangers, circulation pumps and water treatment system are installed. If needed – the output energy can be preheated. From the power station the energy is transferred to the DH network (9).

Moreover, the proposed system can work as independent solar heat collector and storage cell, mounted inside an existing water volumes (lakes or seashore bays). The proposed system may achieve radically low investment cost compared to existing PTES. Principle scheme is shown on Fig. 5

5. BUSINESS OPPORTUNITIES

The total cost of SDH is a function of installed collector field, price of the land and cost of the seasonal storage:

T (total cost euro/m2 apreture area) = C (cost of installed collectors) + L (price of the land) + St (storage cost)

According to IZEB studies on the SDH market [3] the cost of the collectors depends on the origin, qaulity and warranty given. The cost of the land is significant factor, that may impact on the SDH commercial viability when applied in urban areas. The construction cost of PTES is already confirmed by many successful projects to be the most cost efficient solution at the moment. [4]

With the proposed system there are savings in the following aspects:

- Land for the collectors field
- Heat insulation on the back of the collectors
- Auxiliary mechanical support for the collectors
- Storage basin excavation (in case of floating cells in existing basins)

In addition some negative sides of the state of the art PTES are overcome:

- The sophisticated cover installation, and the filling up process is becoming easier: just filling up the volume and installing the moduls with fast plug in connection.

- Rain water evacuation with pupming from the center is replaced with standard vacuum drainage system, where no slopes are needed, and where evacuation tubes are mounded below the floating collectors.
- The system consists of small size panels, easy for production and instalation with low installation costs

6. CONCLUSIONS

The floating collectors on the top of PTES represent an integral solution overcoming most of the technical and financial challenges for locating collector fields over storage facilities. Early calculations estimate a price reduction (incl. Price for land use) between 15 and 20% compared to conventional SDH technologies. This solution allows achievement of SDH facilities with close to 100% solar fraction and reduces significantly energy transport losses. It will introduce SDH concept to urbanized areas, increase general social awareness and contribute for better air quality. This promising technology gives new perspectives and opportunities for the SDH sector. Modular, scalable and prefabricated design approach will both reduce prise and increase productivity.

7. CALL TO ACTION

This new integral solutions requires significant R&D effort in order to find industrial implementation. There are still some technical challenges which need to be solved and industrial production requires close cooperation of research and business partners. Institute for Zero Energy Buildings is looking for organizations sharing a vision for low-carbon EU perspectives.

8. REFERENCES

Literature:

1. Per Alex Sørensen (2012), PlanEnergi, *Where to place the solar collectors, p3*., SDH guidelines, http://solar-district-heating.eu
2. Per Alex Sørensen (2012), *Storage, p5*., PlanEnergi, SDH guidelines, http://solar-district-heating.eu
3. Paskalev, Rashevski, Kamburov, (2016), *„Анализ на технико-икономическите възможности за реализация на слънчева топлофикация в България“p65.*, sdh.bg
4. Per Alex Sørensen (2012), *Storage, p11*., PlanEnergi, SDH guidelines, http://solar-district-heating.eu

SEASONAL THERMAL ENERGY STORAGE OF SOLAR ENERGY IN ABANDONED COAL MINES

Dieter Patteeuw and Lieve Helsen
Department of Mechanical Engineering, KU Leuven, Celestijnenlaan 300A, box 2421, 3001 Leuven (Heverlee), Belgium, lieve.helsen@kuleuven.be
EnergyVille, Thor Park, 8310, 3600 Genk, Belgium

Virginie Harcouët-Menou, Rutger Baeten, Koen Allaerts and Ben Laenen
VITO, Boeretang 200, 2400 Mol, Belgium
EnergyVille, Thor Park, 8310, 3600 Genk, Belgium

Abstract – The use of abandoned coal mines as seasonal thermal energy storage for solar energy is investigated from a technical and economical point of view. This usage is contrasted with using abandoned coal mines as a low temperature heat source for a heat pump, which is the common use in the literature. These two choices are compared for a case study: the city of Genk in Belgium. Genk has 3 mines with a historical combined total production of 175 million ton of coal that were operated until 1988. The underground has been entirely flooded, resulting in an artificial underground water reservoir of 16,7 million m^3. Furthermore, the city of Genk has a population of 65,000 inhabitants and hence, there is a significant heat demand in the proximity of the abandoned coal mines. This study features the comparison of two configurations for exploiting the mines as heat storage or heat source for a swimming pool in Genk, with a yearly heat demand of 2700 MWh. The best configuration depends on the activated underground volume. For this particular case, when activating a stone drift with a diameter of 4.22 m, a stone drift of up to 2 km in length is more suited for thermal energy storage, regenerated by solar energy. If a stone drift of more than 5 km can be activated, the abandoned coal mine is more suitable as a low temperature heat source for a heat pump.

1. INTRODUCTION

Seasonal thermal energy storage (STES) is a crucial technology to increase the share of solar energy within the heating sector. Sensible thermal energy storage is the main mechanism for attaining STES, as opposed to latent and chemical STES which are rarely demonstrated on a large scale (Xu, Wang and Li, 2014). In Belgium, STES is typically attained in an indirect way by using a heat pump, which extracts heat from or injects heat in an aquifer (Vanhoudt et al., 2011) or a borehole heat exchanger (Antonov, 2016) (Žáčeková, Váňa and Cigler, 2014). In Belgium, these systems are typically installed for buildings with a significant cooling demand, for which the ground can deliver the cooling directly during summer and in this way regenerates the ground during summer, such that the heat stored can be used as an interesting source for a geothermal heat pump. This application for shallow geothermal heat and cold benefits from the average temperature of 10°C of the shallow underground in Belgium. The aquifer or borehole heat exchangers act subsequently as a “cold storage”.

This paper looks at another alternative in the underground for STES, namely abandoned mines. Worldwide, there have been a few applications of using water from abandoned mines, as summarized in Table 1. From this table, it is clear that the mines are mostly used directly for

Table 1: Overview of minewater projects based on (Ramos, Breede and Falcone, 2015) (Watzlaf and Ackman, 2006) (Verhoeven et al., 2014)

Country	Town	Extract depth (m)	Extract temp. (°C)	Inject depth (m)	Mass flow rate (m³/h)	Supply temp. heating/cooling (°C)	Thermal power (kW)	End-use (size in m²)
Canada	Springhill	140	13-25	30 m	14.4		11 heat pumps	Industry (14000)
Germany	Ehrenfriedersdorf	110		110			138	Mining
Germany	Freiburg (castle)	60	10.2		10.8	42 / 19	130	Castle
Germany	Freiburg (university	216	18	216		55 / -	260	University
Germany	Marienberg	105	12.4	105	124–2000		310	Recreation
Germany	Wettelrode	283	12–13	163	90–150	50 / -	47	Mining (400)
Netherlands	Heerlen	700 (heat)	27–32	350	0-230	45 / -		Multiple
		250 (cool)	16	350	0-230	- / 16		(500000)
Russia	Novoshakhtinsk	50-150	12–13			95 / -	40000	Multiple
Spain	Asturias		17–23			50 / 7	4600	Multiple (85000)
UK	Shettleston	100	12	Below water table		55 / -	2 heat pumps	Residential
UK	Lumphinnans	170	14.5	Strata layer		45-53 / -	Heat pump	Residential
USA	Kingston		16		20.5	50 / -		Recreation (1580)
USA	Park Hills, MO	120	14	122	17	22 / 24	113	Municipality (753)
USA	Scranton, PA	122	14			- / 13		University

cooling or as a source for a heat pump, i.e. similar to the use of the aquifer or borehole heat exchanger in Belgium. In Table 1, the highest temperatures are extracted from a mine in Heerlen, The Netherlands (Verhoeven et al., 2014) (Ferket, Laenen and Van Tongeren, 2011), which is only 40 km away from Genk, Belgium. Genk has 3 mines with a historical combined total production of 175 million ton of coal that were operated until 1988. Modelling of water ingress after closure of the mines indicates that the underground has been entirely flooded by now, resulting in an artificial underground water reservoir of 16.7 million m^3. The deepest mine corridors, at a depth of 1000 meter, each have a volume between 100 to 500 thousand m^3, surrounded by rock at a temperature of about 40 to 45°C. Furthermore, the city of Genk has a population of 65,000 inhabitants and hence, there is a significant heat demand in the proximity of the abandoned coal mines.

The water temperature in the deepest mine corridors makes these corridors an interesting option for “hot storage”. This matches the low-temperature heat demand in Genk well. Given the low potential of waste heat from industry nearby, there is little competition nearby from other heat sources when looking at district heating. As can be seen in Table 1, the mine water is usually used as a low temperature heat source, but not as a thermal energy storage. The exception to this is Heerlen, where one part of the mine is used as a cold storage and another part as a heat storage.

In this paper, we investigate the use of the abandoned coal mine as a heat storage or heat source. Two system configurations are considered in this study. In the first, the mine is merely a heat source and there is no active recharging of the mine. In the second configuration, solar thermal panels are added to recharge the mine. This paper presents the comparison of these two system configurations in a case study for Genk, with a variable size of the mine corridors that is activated.

2. METHODOLOGY

This Methodology section is organised as follows. In order to compare the two system configurations, a case study in Genk, Belgium, is chosen and described. Next, a model for a horizontal mine corridor, called a stone drift, is presented and verified with respect to a finite element model. Finally, the two system configurations are discussed.

2.1 Case study description

From an overview of large buildings in Genk, the public swimming pool ‘SportinGenk’ was selected as an interesting case study to start exploring the thermal potential of the abandoned coal mines. As shown in Figure 1, the swimming pool (S in Figure 1) is only about 1.2 km away from the central mine shaft of the abandoned coal mine of Winterslag (M in Figure 1). The mine of Winterslag has an open space of about 4.8 million m^3, part of which is located closely to the swimming pool. Large parts of the mine are more than 700 m deep, at a temperature of more than 30°C. This makes it a very interesting heat source for a swimming pool.

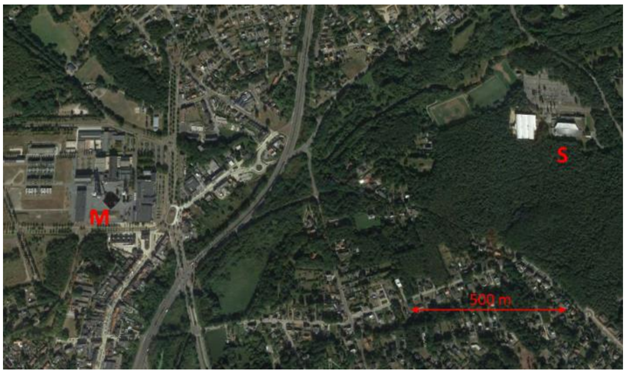

Figure 1: Top view of swimming pool (S) and abandoned mine shaft (M). Image from Google Earth.

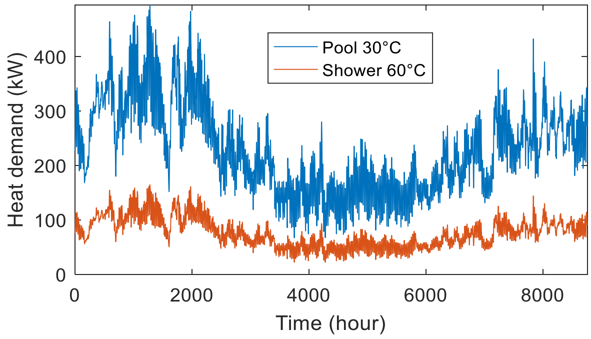

Figure 2: Assumed heat demand profile for the swimming pool, split up in the low temperature heat demand for the pool and high temperature heat demand for the showers.

The swimming pool of Genk is is equipped with a combined heat and power (CHP) plant of 300 kW_{el} and 450 kW_{th}. On top of this there are two backup condensing gas boilers of 450 kW_{th} each. The swimming pool and changing rooms are equipped with floor heating. Given this floor heating and the large heat demand for refreshing the swimming pool water at around 30°C, a large part of the heat demand is at a low temperature. Higher supply temperatures are needed for the showers, as well as for the ventilation of the other rooms, specifically the cafeteria, judo room, fitness room and other areas. We estimate the yearly heat demand of the swimming pool to be 2700 MWh. Based on (Schrier, 2001), we determine that 25% of the heat demand is at a high supply temperature of 60°C and 75% of the heat demand is at a low supply temperature of 35°C. Starting from normalized heat demand measurements for another pool, the heat demand profiles for the swimming pool of Genk are determined in Figure 2.

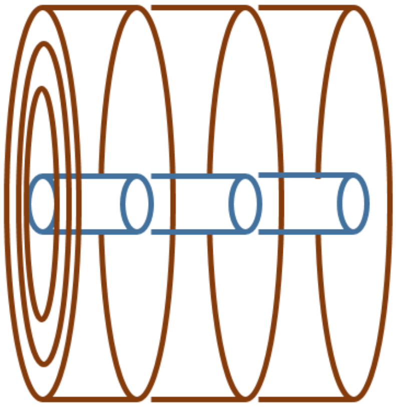

Figure 3: Discretization of a stone drift and the soil around the stone drift

2.2 Stone drift model

The horizontal corridors of the mine (called stone drift throughout this paper) are modelled in Modelica to allow for efficient system simulations. Figure 3 shows conceptually how the stone drift and the soil around it is modelled in Modelica. The water in the stone drift and the soil around it are discretized in the longitudinal direction. On top of that, the soil around the stone drift is discretized in the radial direction, with the discretization scheme of Eskilson (Eskilson, 1987). The water in the stone drift is modelled as mixing volumes and hence, plug flow is not taken into account. Finally, the geothermal heat flux is not modelled since it has a low thermal power and is hard to represent in the cylindrical model.

The Modelica model is verified with respect to a finite element model implemented in TOUGH2 (Pruess, Oldenburg and Moridis, 1999). Figure 4 describes the set-up of the verification study. A stone drift initially at 25°C receives from one side colder water at 10°C at a mass flow rate of 5.6 kg/s. Figure 4 summarizes all parameters of the case study, except the convective heat transfer coefficient, which has a constant value of 2 W/m²K.

Both the TOUGH2 model and the Modelica model are

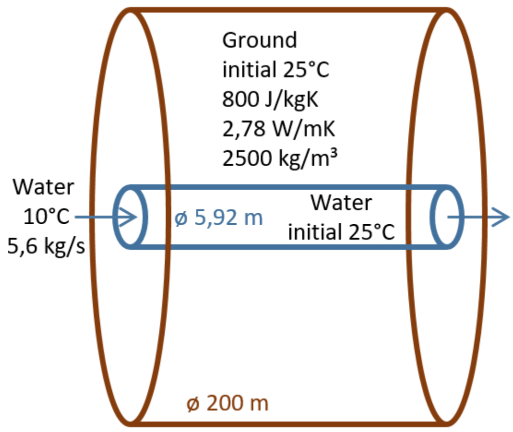

Figure 4: Verifcation case study of the stone drift model

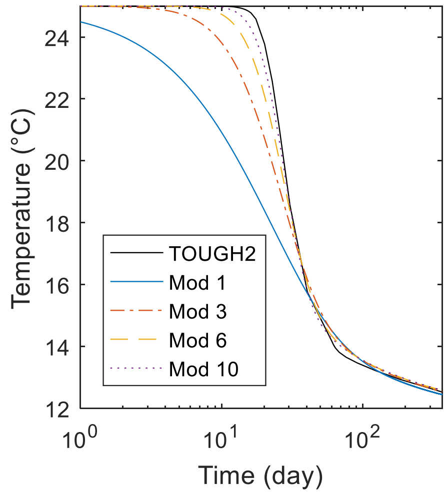

Figure 5: Verification of the stone drift Modelica model (using 1, 3, 6 or 10 longitudinal discretizations) with respect to the TOUGH2 model: temperature of the water exiting the stone drift after injecting water at 10°C

simulated for 1 year. The temperature of the water exiting the stone drift is plotted as a function of time in Figure 5. Four variations of the Modelica model are tested, using different longitudinal discretizations, respectively 1, 3, 6 and 10 discretizations. All four variations appear well equipped to estimate the long term (>100 days) thermal behaviour of the stone drift. Over a full year, the mean absolute error (MAE) is 0.43°C, 0.22°C, 0.15°C and 0.10°C for 1, 3, 6 and 10 discretizations respectively. However on the short term, the Modelica model without longitudinal discretization (Mod 1) is totally unsuitable for representing the stone drift. Over the first month, the MAE is namely 3.74°C, 1.61°C, 0.74°C and 0.29°C for 1, 3, 6 and 10 discretizations respectively. Hence, with 10 longitudinal discretizations (Mod 10), the Modelica model differs less than 0.5°C from the TOUGH2 model output. For the sake of completeness, also 3 (Mod 3) and 6 (Mod 6) longitudinal discretizations are shown in Figure 5. Throughout the rest of this work, the Mod 10 model is used in order to attain sufficient accuracy.

2.3 Heating system lay-out

As mentioned in the introduction, two system configurations are studied in this paper. Figure 6 schematically illustrates these configurations. For the sake of simplicity we assume that one long stone drift is activated, so we don't consider multiple pathways of the water as is usually the case in abandoned coal mines, see (Ferket, Laenen and Van Tongeren, 2011). This stone drift is assumed to be at a depth of 735 meter and at a starting temperature of 32.5°C. The stone drift has a diameter of 4.22 meter. The soil around the stone drift has a thermal conductivity of 2.3 W/mK, a density of 1280 kg/m³ and a specific heat capacity of 800 J/kgK. The pump extracts the water from the stone drift at a mass flow rate of 108 m³/h and provides this mass flow

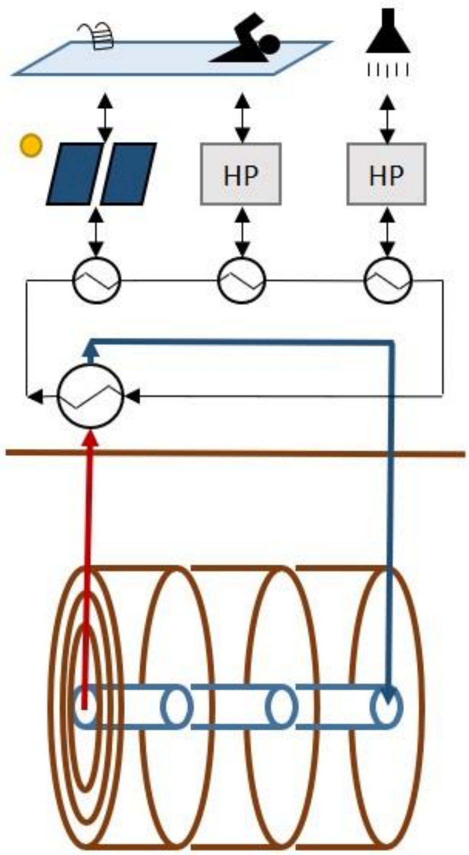

Figure 6: Schematic overview of the possible system configurations. The heat pump (HP) always secures sufficient heat supply. A solar collector field can be added for preheating the water from the mine and regeneration in summer.

rate throughout the whole year. Since the pressure drop calculations can be quite challenging for this system, we neglect the expenses for pumping in this study. Both configurations studied use this pump continuously throughout the year, so it will not make a difference when comparing the two configurations. The length of the stone drift which is hydraulically activated, is varied in this study between 1 and 10 km.

The first configuration is called 'Heat Pump', abbreviated to 'HP'. In this configuration, the stone drift is solely used as a source for the heat pumps (HP in Figure 6). Two drillings are made in a stone drift (blue and red arrows). The water within the stone drift is circulated towards a heat exchanger. If the temperature is sufficient to supply the heat demand of the pool directly, this option is used first. After this, two heat pumps are active. One for supplying the pool with heat at a supply temperature of 35°C and one for supplying the showers with a supply temperature of 60°C.

The heat pump is modelled using the 'Carnot_TCon' model of the 'Buildings library' (Wetter et al., 2014) in Modelica. This model supplies a constant supply water temperature. The coefficient of performance (COP) is determined based on Carnot and normalized to a nominal COP value at design temperature levels. The nominal value of the COP is based on (Bettgenhäuser et al., 2013):

$$COP = a \cdot \frac{T_{supply}}{T_{supply} - T_{source} + b}$$

with T_{supply} the nominal supply water temperature and T_{source} the nominal source temperature, which is assumed 25°C in this study. The parameters a and b are taken for a ground coupled heat pump of (Bettgenhäuser et al., 2013), namely a is 0.5 and b is 10. The heat pumps are sized in order to deliver the peak heat demand based on Figure 2.

The second configuration is called 'Solar', abbreviated to 'Sol'. In this configuration, a solar thermal collector field is installed. For modelling this thermal collector, the ASHRAE93 model is used from the 'Buildings library' (Wetter et al., 2014) with the parameters of the FP - Therma-Lite, HS-20, a glazed flat plate collector. We assume 10,000 m² of these flat plate collectors in this study, with a southward orientation and a tilt of 30°C. These solar collectors preheat the water that is directed towards the heat pumps. If the solar collectors are warmer than the water coming out of the mine, a secondary circuit pump is activated and the water that exchanged already heat with the mine water is further heated by solar energy. The heat pumps can then deliver the last temperature lift in order to supply the heat demand at the desired supply water temperature. If the water is still at a higher temperature than the mine water after heat supply to the heat pump, the solar collectors are heating up the mine water too.

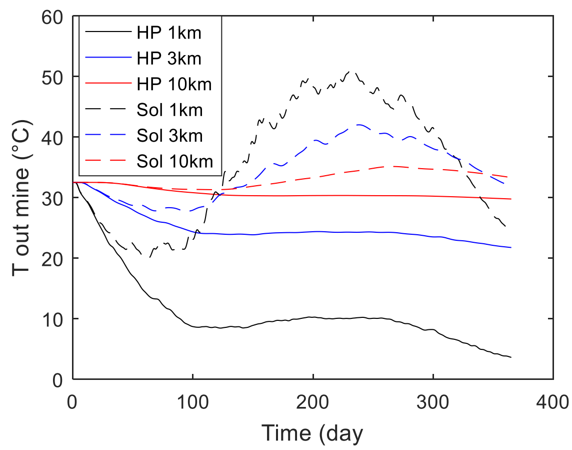

Figure 7: Temperature of the water coming out of the mine, throughout the year for a stone drift length of 1, 3 or 10 km. In the heat pump (HP) configuration, this temperature substantially drops. In the solar (Sol) configuration, the temperature rises throughout the summer and hence, heat is stored in the mine.

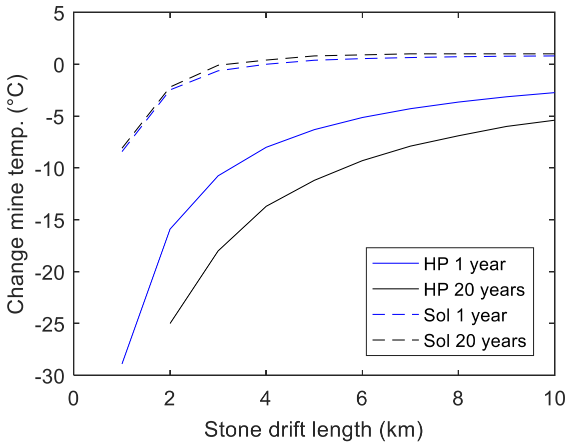

Figure 8: Change in temperature of the water exiting the mine after 1 and 20 years.

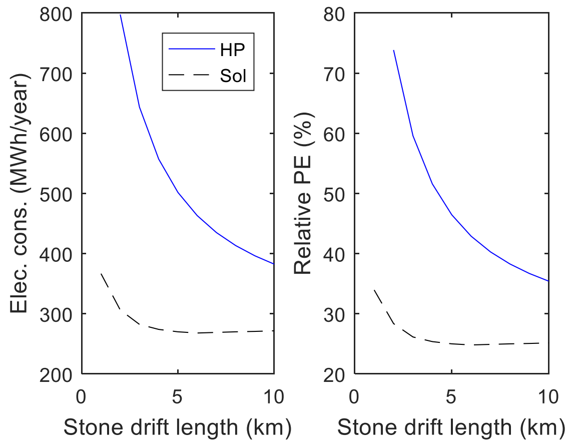

Figure 9: Yearly electricity consumption of the heat pumps (left), also expressed in relative primary energy (PE) use (right) compared to 2700 MWh supplied with a gas boiler.

To wrap up, the HP configuration can be seen as the heat extraction scenario. In this case, we solely extract heat from the mine. In the Sol configuration, flat plate collectors are installed to supply part of the heating in summer but also regenerate (heat) the mine for later use. In this case, the stone drift acts as a storage. For both configurations, the activated stone drift length will be varied in order to compare both configurations.

3. RESULTS

Both HP and Sol configurations are simulated for one year. Figure 7 shows the temperature exiting the mine throughout a year for multiple stone drift lengths. In case of a 1 km stone drift, solely extracting heat (‘HP 1km’ in Figure 7) is clearly not sustainable. The temperature of the water in the stone drift drops to 5°C after 1 year, which means a temperature decrease of 28°C in one year (the first year). When the stone drift is longer, this configuration gets more sustainable, with for a 10 km stone drift a temperature decrease of only 2.5°C in one year (the first year). In the case of a long stone drift length, a large horizontal surface area is activated. In this case, the geothermal heat flux can become influential. However, this is hard to represent in this cylindrical model and will be considered in future work.

When the solar collectors are added, the temperature throughout the year follows a significantly different path. The heat pumps still lower the stone drift temperature in the beginning of the year (in winter), but the stone drift is substantially heated throughout summer. The stone drift acts as a thermal energy storage: the temperature of the stone drift clearly rises and this is not directly lost due to heat losses. The amplitude of the temperature variation is larger the shorter the stone drift is.

Figure 8 shows the difference in stone drift water temperature after 1 year and 20 years of operation. For the HP configuration, the temperature quickly drops after 1 year of operation. Comparing this temperature drop to the one after 20 years, we observe that almost half of the temperature drop happens within the first year. After this first year, the decline per year is more steadily. The HP configuration with 1 km of stone drift reached 0°C after 1 year and 1 month, after which the simulation was terminated. With a 2 km stone drift, the heat pump was able to run for 20 years while the water in the stone drift reached a temperature of 7.5°C. For longer stone drifts, the temperature drop decreases, resulting in higher mine temperatures and hence higher heat pump efficiency.

For the Sol configuration, the system is in equilibrium: after 1 year, the same temperature difference is reached as after 20 years (Figure 8). The same stone drift temperature profile is repeated each year. The temperature drop for the Sol case remains limited for all stone drift lengths and reaches zero at a stone drift length of 3 km, after which a slight temperature increase occurs.

The difference in stone drift water temperature between the HP and Sol configuration gets smaller as the stone drift length increases (Figure 8). This has an effect on the yearly electricity consumption of the heat pumps, which converges for longer stone drift lengths, as Figure 9 (left) shows. The yearly consumption is also expressed in terms of relative primary energy use, compared to the use of a gas boiler (Figure 9 (right)). To this aim, the electricity consumption is translated to primary energy by using a factor of 2.5. This primary energy consumption is compared to the case where the full 2700 MWh of heat demand would be supplied by a gas boiler. This metric is easier to interpret. For short stone drift lengths and a HP configuration, the primary energy savings are rather limited: about 25%. The heat pump configuration clearly needs a significant stone drift length in order to deliver large primary energy savings. The Sol configuration on the other hand, delivers substantial primary energy savings (up to 75%), even for shorter stone drift lengths. Notice in the Sol configuration how the electricity

Table 2: Optimistic and pessimistic price assumptions for the investment, running costs and interest rate. Collector price based on (Nielsen and Battisti, 2012) Connecting pipe price based on (Frederiksen and Werner, 2013). Other data from personal communication with practitioners.

	Price per unit (EUR)		Units
	Optimistic	Pessimistic	needed
Drillings towards the mine	400k/drilling	600k/drilling	2 drillings
Connecting pipe	300/m	600/m	1500 m
Heat pump	200/kW	200/kW	650 kW
Flat plate solar collectors	150/m²	225/m²	10000 m²
Electricity	150/MWh	180/MWh	-
Interest rate	3%	7%	-

demand (Figure 9) stabilizes at a stone drift length of 3 km. From this point onwards, it's clearly not needed anymore to activate a longer stone drift. The electricity use even slightly goes up for longer stone drift lengths (Figure 9), which indicates a higher heat loss to the surrounding rock. For this case, the optimal stone drift length is 5 km. But as one can notice, this is a weak optimum, as a stone drift length between 3 and 7 km almost performs equally.

Finally, the choice between the heat pump and Sol configuration will be based mainly on cost. Table 2 shows the considered ranges for major cost components. We assume that the system runs for 20 years except for the connecting pipe and drillings, for which we take an economic lifetime of 40 years. The length of the connecting pipe is 1500 m, based on Figure 1. Hence, we assume that the multiple stone drift lengths can be activated with a same distance covered above ground. In other words, for the longer stone drift lengths, we assume that parallel paths can be activated.

Based on Table 2 and the electricity consumption data in Figure 9 (left), the cost for supplying 2700 MWh per year is shown in Figure 10. From this figure, it appears that the Sol configuration shows a very large spread in cost. This is mainly attributed to the cost of the flat plate solar collectors. When these show a low cost and the interest rate is favourable, then the Sol configuration can economically compete with the HP configuration for a stone drift length of up to 5 km. For larger stone drift lengths, the HP configuration clearly outperforms the Sol configuration, for the whole range of cost assumptions.

One can interpret Figure 10 also in a more abstract way. For this particular case, up to 2 km stone drift length, the stone drift is more favourable as an energy storage. Starting from 4 km stone drift length, the stone drift is more favourable as a heat source. Off course, these values are highly case dependent, as they depend on technical and economical parameters.

Finally, Figure 10 compares both configurations to the typical range of the natural gas price for Belgian

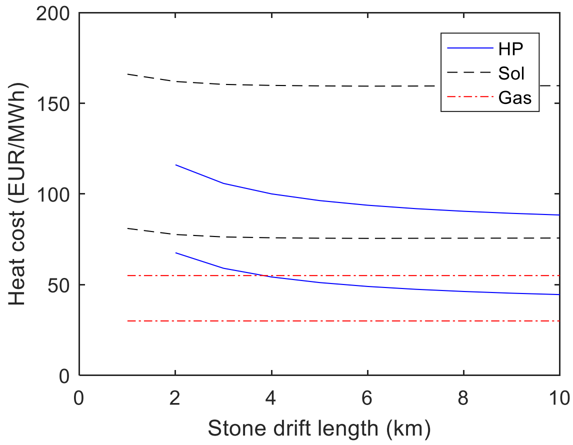

Figure 10: Cost ranges for supplying 1 MWh of heat for the heat pump and solar configuration. This is compared to a typical price for natural gas (Gas). The top and bottom lines are the pessimistic and optimistic cost estimates, respectively;

consumers with a yearly demand in the range of 2700 MWh. These days, the natural gas price is more towards the lower end of the range, but this price is known to fluctuate strongly over the years. When comparing both the HP and Sol configuration to the natural gas price, it is clear that both configurations are not very competitive with natural gas in an economic sense. Only the HP configuration in favourable conditions and long activated stone drift lengths, can compete directly to a natural gas boiler. Hence, the choice for these configurations will be driven more by environmental reasons, namely the reduction in primary energy use as shown in Figure 9.

4. CONCLUSIONS

This paper compares the use of abandoned coal mines as a thermal energy storage for solar energy ('solar') and as a low temperature heat source for a heat pump ('heat pump'). To this aim, a thermal model of a mine corridor (or stone drift) was developed in Modelica. The aforementioned comparison was performed for a swimming pool in Genk. In the solar configuration, the temperature of the stone drift is stable already from year one onwards. Substantial primary energy savings of up to 75% can be achieved with this configuration. Furthermore, it is economically competitive with respect to the heat pump configuration for shorter stone drift lengths (up to 2 km) in this case study. The heat pump configuration could be attained for 20 years as soon as the stone drift length was longer than 2 km. However significant temperature drops (up to 25°C after 20 years) are observed in the stone drift for small lengths. For a 2 km stone drift length, the primary energy savings are rather limited (around 25%). The heat pump configuration needs a longer stone drift length to show interesting primary energy savings and to compete with the solar configuration. For a stone drift length larger than 5 km in this case study, the heat pump configuration is on average cheaper than the best case solar configuration. Hence the choice between both configurations depends on the ratio between heat demand and available stone drift volume.

ACKNOWLEDGEMENTS

This study is part of the research project `Towards a sustainable energy supply in cities'. This project receives the support of the European Union, the European Regional Development Fund ERDF, Flanders Innovation & Entrepreneurship and the Province of Limburg.

REFERENCES

Antonov, S. (2016). *Short and Long Term Optimal Operation and Robustness Analysis of a Hybrid Ground Coupled Heat Pump System with Model Predictive Control.* Department of Mechanical Engineering. Leuven, KU Leuven (Doctoral dissertation, PhD dissertation: 156 pp).

Bettgenhäuser, K., Offermann, M., Boermans, T., Bosquet, M., Grözinger, J., von Manteuffel, B., and Surmeli, N. (2013). *Heat pump implementation scenarios until 2030, appendix*. Tech. rep., Ecofys.

Duffie J.A., and Beckman W.A. (1991) *Solar Engineering of Thermal Processes*, 2nd edn. pp. 54-59. Wiley Interscience, New York.

Eskilson, P. (1987). *Thermal analysis of heat extraction boreholes.* Department of Mathematical Physics. Lund, Sweden, University of Lund (Doctoral dissertation, PhD dissertation: 264 pp).

Ferket, H. L., Laenen, B. J., and Van Tongeren, P. C. (2011). Transforming flooded coal mines to large-scale geothermal and heat storage reservoirs: what can we expect. *Mine Water—Managing the Challenges*, 171-176.

Frederiksen, S., and Werner, S. (2013). *District heating and cooling*. Studentlitteratur.

Nielsen, J. E., and Battisti, R. (2012). *Solar district heating guidelines, feasibility study fact sheet 2.3.* Solar-district-heating.eu

Pruess, K., Oldenburg, C. M., and Moridis, G. J. (1999). *TOUGH2 user's guide version 2* (No. LBNL--43134). Ernest Orlando Lawrence Berkeley National Laboratory, Berkeley, CA (US).

Ramos, E. P., Breede, K., and Falcone, G. (2015). Geothermal heat recovery from abandoned mines: a systematic review of projects implemented worldwide and a methodology for screening new projects. *Environmental Earth Sciences*, 73(11), 6783-6795.

Schrier, P.J. (2001). *ISSO-publicatie 59: grote zonneboilers: initiatief, ontwerp, uitvoering en beheer*, pp. 43. Stichting ISSO, Rotterdam. (in Dutch)

Vanhoudt, D., Desmedt, J., Van Bael, J., Robeyn, N., and Hoes, H. (2011). An aquifer thermal storage system in a Belgian hospital: Long-term experimental evaluation of energy and cost savings. *Energy and Buildings*, *43*(12), 3657-3665.

Verhoeven, R., Willems, E., Harcouët-Menou, V., De Boever, E., Hiddes, L., Op't Veld, P., and Demollin, E. (2014). Minewater 2.0 project in Heerlen the Netherlands: transformation of a geothermal mine water pilot project into a full scale hybrid sustainable energy infrastructure for heating and cooling. *Energy Procedia, 46*, 58-67.

Vlaams tijdschrift voor Sportbeheer. (2008). Gerenoveerd Genks zwembad opent. *Vlaams tijdschrift voor Sportbeheer*, 191, 5-9. (in Dutch)

Watzlaf, G. R., and Ackman, T. E. (2006). Underground mine water for heating and cooling using geothermal heat pump systems. *Mine Water and the Environment*, 25(1), 1-14.

Wetter, M., Zuo, W., Nouidui, T. S., and Pang, X. (2014). Modelica buildings library. *Journal of Building Performance Simulation*, *7*(4), 253-270.

Xu, J., Wang, R. Z., and Li, Y. (2014). A review of available technologies for seasonal thermal energy storage. *Solar Energy*, *103*, 610-638.

Žáčeková, E., Váňa, Z., and Cigler, J. (2014). Towards the real-life implementation of MPC for an office building: Identification issues. *Applied Energy*, *135*, 53-6.

MODESTO – A MULTI-OBJECTIVE DISTRICT ENERGY SYSTEMS TOOLBOX FOR OPTIMIZATION

Annelies Vandermeulen[a,b,c,1], Bram van der Heijde[a,b,c], Dirk Vanhoudt[b,c], Robbe Salenbien[b,c] and Lieve Helsen[a,b]
[a] Department of Mechanical Engineering, KU Leuven, Celestijnenlaan 300 bus 2421, 3001 Leuven, Belgium
[b]EnergyVille, Thor Park, Waterschei, 3600 Genk, Belgium
[c]VITO, Boeretang 200, 2400 Mol, Belgium

Abstract – Optimization of district energy systems (heat, electricity and gas) is an important part of the evolution towards a more sustainable energy system. It can be used to support short- and long-term decisions and it leads to further insights regarding the behaviour of the energy system as a whole, resulting in better integration of intermittent renewable energy sources (RES). However, optimization of these energy systems is not trivial, due to large-scale systems, a broad range of time constants, nonlinearities, etc. Additionally, the requirements of the optimization model are very case and goal specific. To facilitate these optimizations, *modesto* – a Multi-Objective District Energy Systems Toolbox for Optimization – is being designed, a Python package that allows easy setting up of energy system optimization models, while offering flexibility to customize to specific cases. This paper presents the current state of *modesto*, a case study illustrating the toolbox's principle and the future expansions that are planned.

1. INTRODUCTION

Climate change and environmental pollution call for a transition to a more sustainable energy system. This energy system will most likely be a multi-carrier energy system, where electricity, gas and thermal networks work in unison. However, the separate development and operation of these energy subsystems is already challenging, let alone the joint development and operation. In this context, this paper presents modesto – a Multi-Objective District Energy Systems Toolbox for Optimization, see Figure 1. As the name indicates, it is a toolbox that provides optimization tools for district energy systems, although in its current state it focuses on thermal systems.

Figure 1: The logo of modesto

When developing such a toolbox it is imperative to be aware of existing energy modelling and optimization tools. Overviews of existing tools have been made by Connolly *et al.* (2010) and van Beuzekom, Gibescu, and Slootweg (2015). The reviews show that many tools are already in existence. However, each of these tools considers different parts of the energy system (electrical, thermal, multi-carrier etc.), and uses different techniques (including simulation or operational optimization) on different time and geographic scales. However, concerning tools that resemble *modesto* (optimization of district energy systems, with a focus on thermal systems), few equivalents can be found: according to Connolly's overview, only the following optimization tools have a similar goal:

- *COMPOSE* (Aalborg University n.d.) is a free modelling tool for multi-carrier energy systems to assess whether energy projects can support RES intermittency. One of its strengths is its ability to take into account uncertainty, and is hence, suited for risk and uncertainty analyses.
- *energyPRO* (EMD international A/S n.d.) is a commercial modelling tool for techno-economic design of multi-carrier energy projects. It focuses on cogeneration or trigeneration, which can be used in combination with district heating.
- *HOMER* (HOMER Energy LLC. n.d.) is a commercial tool that focuses on optimization of micro hybrid electricity systems. Although capable of modelling district heating (in a limited way), its focus is mostly on the electricity system.

Beyond Connolly *et al.*'s overview, the following energy modelling tools seem relevant as well:

- *OSeMOSYS* (Howells et al. 2011) is a systems optimization model for long-run energy planning. The focus seems to be on the electricity system, although heating is included in the output streams. Welsch *et al.* (2012) expanded the OSeMOSYS environment to be compatible with smart grid optimization.
- *JModelica* is a Modelica-based open source platform for optimization, simulation and analysis of dynamic systems (Modelon AB 2017) and has been used on at least one occasion for operational optimization of district heating and cooling systems (Schweiger et al. 2017).
- *DER-CAM* or Distributed Energy Resources Customer Adoption (Stadler et al. 2014; Steen et al. 2015) is a MILP-based optimization tool to support investment decisions in energy systems including distributed energy resources. The objective is to minimize carbon emissions and annual costs for customer site systems or micro grids.
- *oemof* (oemof Developing Group 2017) is an open source optimization platform for multiple energy

[1] annelies.vandermeulen@energyville.be

carriers. It is able to connect multiple regional energy systems and has flexible time steps.

- *MODEST*[2] (Model Optimization of Dynamic Energy Systems with Time dependent components and boundary conditions) was developed as a linear optimization tool to find the optimal operation of energy systems from a cost perspective (Åberg and Henning 2011; Åberg, Widén, and Henning 2012). MODEST is aimed at local, regional and national spatial scales and can handle time divisions flexibly.
- *Urbs* (Dorfner 2016, 2017) has the intention to optimize the installed capacity of different types of energy technologies (including storage) in a given energy system, while supplying a specified demand profile. It uses a time step of 1 h, but appears to be intended for a larger geographic scale than *modesto*, although it is flexible to be changed to the needs of the user.

Table 1: The list of symbols

Symbol	Description	Unit
c_p	Specific heat capacity of water	$J\ kg^{-1}\ K^{-1}$
E	Energy use	J
h	Optimization horizon	s
$\dot{m}$	Mass flow rate	$kg\ s^{-1}$
$\mathcal{J}$	Objective function	J or €
$\dot{Q}$	Heat flow rate	W
S	Slack value	J or €
T_{mix}	Mixed temperature	K
T_{ret}	Return temperature	K
T_{sup}	Supply temperature	K
α	Objective weighting function	/ or € J^{-1}
β	Slack penalization weight	/
$\mathcal{C}$	Set of components	
$\mathcal{C}_{out,n}$	Set of components extracting water from node n	
$\mathcal{C}_{in,n}$	Set of components injecting water into node n	
$\mathcal{S}$	Set of slacks	
c	Component index	
n	Node index	
s	Slack index	
t	Time index	

Clearly, the motivation to develop *modesto* does not stem from a lack of energy system optimization tools However, all available tools in their many shapes and flavours do not natively provide the ability to optimize district energy systems with a focus on dynamic behaviour of thermal system components, except for Schweiger at al's work (2017) with *JModelica*, although it should be noted that *JModelica* is unable to solve mixed integer linear problems, which is where *modesto* comes into play.

modesto is a package that, given a network topology, allows easy setting up of optimization problems for district energy systems, although it is limited to district heating at the moment. *modesto* contains models for different typical components found in district energy systems (such as energy storage, energy conversion and energy transportation systems). Often, goals and cases require different models putting emphasis on different dynamics. For this purpose, *modesto* provides different models for the same type of component.

The toolbox is still under development, with the current focus going to district heating systems, but the eventual goal being multi-carrier energy systems. Thus, this paper mostly discusses the tool in the context of district heating.

This paper presents the current status of *modesto*. More specifically, Section 2 discusses the structure of the toolbox, presenting the different component models and the way they are interconnected. Section 3 presents possible applications for *modesto*, while Section 4 shows an example case study. Section 5 discusses possible further developments and, finally, Section 6 concludes this paper. All symbols used in this paper are listed in Table 1.

2. STRUCTURE

This section gives an overview of the *modesto* structure. Firstly, the toolbox is considered as a black box, with the discussion only focusing on the in- and outputs of the toolbox. Secondly, the internal structure of the toolbox is presented in more detail, with first a general overview, followed by a more detailed look at the separate district heating network components and optimization objectives.

2.1 In- and outputs

An overview of all in- and outputs of *modesto* is shown in Figure 2.

A first input is a NetworkX object (Hagberg, Schult, and Swart 2008), describing the configuration of the energy network by using a graph consisting of nodes and edges. Applied to a district heating network, the nodes represent points in the network where a customer, heat source and/or thermal energy storage (TES) system is/are connected to the network or where two or more pipes intersect. The edges connect the nodes and represent the district heating pipes. This input gives *modesto* all required information about the topology of the network and enables the toolbox to set up the network's model.

A second input allows changing the optimization settings. At the moment this includes:

[2] Any similarity between the names of MODEST and *modesto* is purely coincidental; the authors only found out about this existing tool later. Although both are energy optimization tools, *modesto* is aimed at being more flexible towards multiple energy optimization problems, while confining itself to district scale.

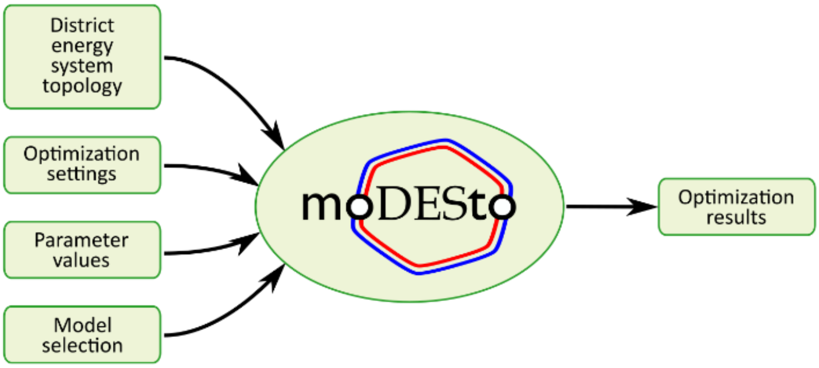

Figure 2: A black-box overview of modesto

Box 1: List of the main assumptions and limitations of the current status of *modesto*.

1. The network is assumed balanced, i.e. the mass flow in a component's supply and return line are always the same.
2. No pressure drops are considered. Hence, only tree shaped networks without loops can be optimized.
3. All component models and the resulting network model are linear, resulting in either a linear program (LP) or a mixed integer linear program (MILP).
4. Building substation models are modelled in a very simplified way, with the temperature differences across the heat exchanger assumed to be known and constant.

- *The selection of the solver*: All solvers that are compatible with Pyomo (Hart et al. 2017) are possible. Currently, the standard solver is set to Gurobi (Gurobi Optimization Inc. 2016), which is used with an academic license. However, tests with CPLEX (IBM Corp. 2016) are being carried out with similar results.
- *The optimization horizon*: This time horizon determines the time period for which the optimization is carried out. It can range from a short-term optimization, generally used for optimal control to long-term optimization, generally used for optimal design.
- *The time step*: *modesto* generates discrete models of district energy systems. The time step setting determines the discretization of the problem.
- *The objective*: Several standard objectives are already available, including minimization of energy and cost, CO_2 and return temperature. It can be extended to primary energy use, share of RES…

A third input sets the parameters values of the optimization problem. Using this input enables the user to easily change e.g. the dimensions of a component, which is useful in optimal design. Another possibility is to change the disturbances to the energy system, such as weather predictions, or boundary conditions such as electricity prices, which is mostly relevant if the optimization is used in a control context with a moving horizon (see Section 3).

A final input allows changing the model selection. As discussed in Section 2.3, some component models differ in the assumptions that are made, leading to a model library.

modesto's goal is to optimize an energy system. Hence, the main output of the toolbox is the optimization's result. *modesto* incorporates a function that provides easy access to all results. In the future, extra plotting functions will be added to visualize results facilitating easy analysis. However, when analysing the results, it is important to realize the assumptions made within *modesto*. Therefore, a short overview of the main assumptions is given in Box 1.

2.2 Internal structure

Using the inputs as they are shown in Figure 2, *modesto* sets up the optimization problem of the given network automatically. The Python package Pyomo (Hart et al. 2017) is used as compiler and the Python package pandas (McKinney 2010) handles data (such as weather and prices).

Given the network topology (the NetworkX object), *modesto* composes the whole optimization problem. Firstly, all component and edge models (heat users, sources, storage and pipes) are built, depending on which model types were selected by the user. These models have a structure as shown in Figure 3. Each component has a return and supply temperature and mass flow rate, with the relationship between them determined by the component model.

Subsequently, *modesto* creates all node models, which describe the interconnections between the components. An example is shown in Figure 4, where a node with four components is shown. Figure 4 also shows the conservation equations contained in a node model. *modesto* does not consider pressure drops (yet), hence the only relevant conservation equations are mass - Eq. (2), and energy - Eq. (3) till (6).

These node models create interconnections between all components, leading to a single model for the entire district heating network.

2.3 Component models

The main components in a district heating network can be split in four groups: 1) those that create a heat demand, 2) heat sources, 3) thermal energy storage systems, and 4) network pipes. A short overview of the models available in *modesto* is given below. The main assumptions that are made in these component models are listed in Box 1.

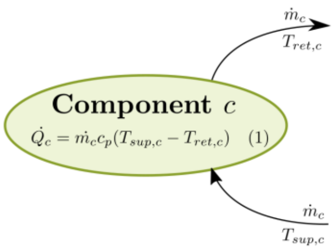

Figure 3: An example illustrating the component model structure.

Regarding components that represent a heat demand, two models have been implemented. A first model, is a simple fixed profile that describes the deterministic heat extracted from the point in the network to which it is connected. This model is presented in Figure 3 (using assumption 4 in Box 1). A second model is an equivalent resistance-capacitance (RC) model describing the building's dynamics. This model creates the possibility to use the building's thermal inertia as a thermal energy storage system which can be used to create extra flexibility. These models are based on the work of Reynders, Diriken and Saelens (2014) and Protopapadaki, Reynders and Saelens (2014).

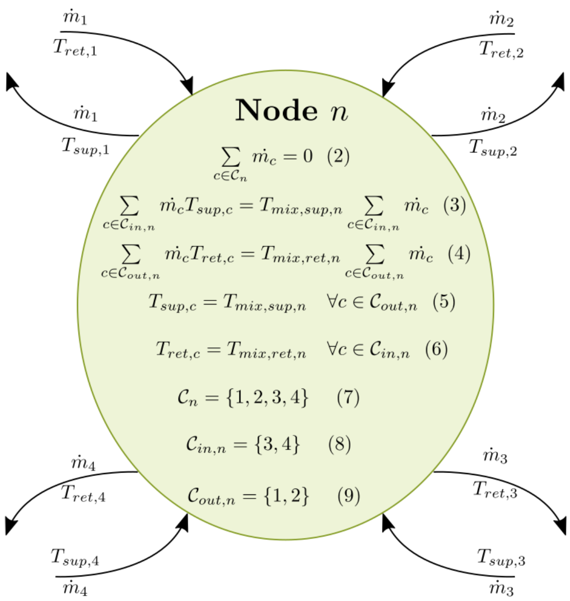

Figure 4: The structure of the model describing a network node.

Two heat source models are available at present. The first model can have limitations on maximum power, ramp rate and efficiency (or COP). If none of these limitations are activated, it is an ideal heat source. The second model is, similar to the heat demand models, a fixed profile, i.e. the heat injection at this point in the network is known in advance. It can be used to model e.g. solar thermal collectors assuming weather predictions are perfect and there is no curtailment. Heat profiles for solar thermal collectors (van der Heijde et al. 2018) are available in *modesto*.

Regarding thermal energy storage systems, a stratified storage tank model (Steen et al. 2015; Vandewalle and D'haeseleer 2014) has been implemented. The model assumes perfect stratification at a fixed high and low temperature. Mass flow rates in and out of the tank can be constrained.

Three pipe models have been implemented in *modesto*, each differing in the assumptions that are made, making them suitable for different applications. A first, very simple model is a perfect pipe, with no heat losses, mass flow limits nor time delays. A second model has limits on mass flow rates and heat losses, but is based on steady-state assumptions and hence requires constant temperatures (van der Heijde, Aertgeerts, and Helsen 2017). A third pipe model, based on Benonysson's node method (Benonysson 1991) no longer requires steady-state assumptions and constant temperatures and is hence suited to analyse time delays in the network. However, to ensure the linearity of the problem in this case, the mass flows in the network need to be known perfectly in advance. This can be ensured by using fixed heat demand models only.

2.4 Objectives

Different objectives have been implemented in *modesto*, including energy use, operational energy cost, CO_2 emission and return temperature minimization. These objectives are set up in the following way.

Firstly, the objective in each component is defined. Taking for example energy and cost optimizations: a heat source has in both cases the following objective:

$$\mathcal{J}_c = \sum_{t=1}^{h} \alpha_{c,t} E_{c,t} \tag{10}$$

With $\mathcal{J}_c$, the component's contribution to the overall objective, $\alpha_{c,t}$ equals 1 in case of an energy optimization or equals the heat source's energy price [€/kWh$_{\mathrm{primary}}$] in case of a cost optimization. $E_{c,t}$ is the heat source's primary energy use during time step t.

Other possible contributions to the objective include the slacks, which are optimization variables that are added to inequality constraints for robustness. The value of all slack variables is integrated in the objective function using a penalization weight β in order to discourage the use of these slacks, leading to the following expression for the problem's objective:

$$\mathcal{J} = \sum_{c \in C} \mathcal{J}_c + \beta \sum_{s \in \Omega} S_s \tag{11}$$

3. POSSIBLE APPLICATIONS

modesto is designed in such a way that it can be used for different goals and can be easily implemented within other tools. Two possible applications are shortly presented here, with a description on how *modesto*, designed to solve an optimal control problem, could be used.

3.1 Model predictive control

Optimal control has already been used often in the literature to reduce the district heating network's operational costs (Benonysson, Bøhm, and Ravn 1995; Korpela et al. 2017) or to provide demand side management to integrate RES (Salpakari, Mikkola, and Lund 2016). However, optimal control only correctly tracks the optimal case if there are no mismatches between reality and model and if there are no prediction errors.

To account for these unavoidable errors, model predictive control (MPC) can be used instead. It combines optimal control (*modesto*) with feedback control, applying the optimal control signals to the actual network, as can be seen in Figure 5, regularly recalculating a new optimal control strategy making use of new predictions and measurements. Verrilli et al.'s work is a recent example of an MPC for district heating (Verrilli et al. 2016).

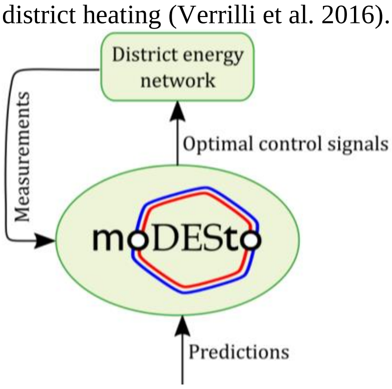

Figure 5: The flow chart of an MPC using *modesto* to control a district energy network

3.2 Integrated optimal control and design

modesto can be used for integrated optimal control and design as well; design parameters are varied throughout multiple runs of the optimal control problem. The variation with the best objective function value is chosen as the best design. The integrated optimal control problem helps to provide a fair basis of comparison for various designs, whereas a control based on simpler rules might fail to do so. A flow chart describing the integrated optimal control and design process is shown in Figure 6.

4. A CASE STUDY

This section shortly presents a case study to illustrate the possibilities of *modesto*.

4.1 Case description

The case considers an imaginary district energy system consisting of three residential areas, connected by a thermal network and heated by a central heat production plant (e.g. ORC plant fed by geothermal energy). This configuration is considered as the base scenario. As a future scenario, a large solar thermal collector array is added. To get the solar fraction as high as possible, large TES tanks are added at the solar array network node. Furthermore, to make the (backup) central heat supply as constant as possible (which is beneficial to e.g. a geothermal ORC plant which requires a stable output power), a short-term storage tank is added near the backup plant.

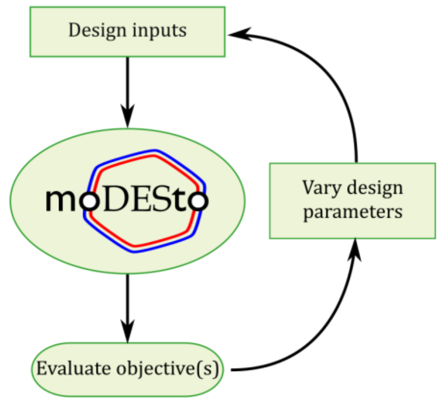

Figure 6: Flow chart describing the integrated optimal design and control process using *modesto*.

The lay-out of the network is shown in Figure 7, with the extension for the future scenario in dashed lines. All optimization runs consider a horizon of a full typical meteorological year with a time step of 6 h. For actual modelling purposes, this is a large time step, but this choice was made for the sake of a quick showcase and comparison. The modeller can freely choose the time step.

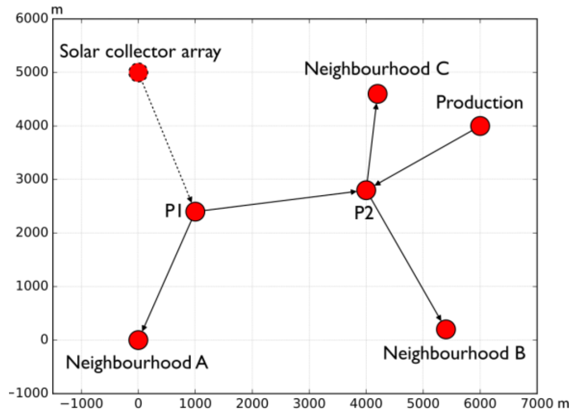

Figure 7: Lay-out of the case study. Base scenario in full lines and circles, future scenario extension dashed.

For both scenarios, the same weather input profiles are used, as well as the same heat demand for the neighbourhoods. These profiles are shown in Figure 8. The design parameters considered for both cases are summarized in Table 2. The total annual space heating and domestic hot water energy demand of the neighbourhoods is 185 GWh/a. The thermal network is operated at a supply and return temperature of 70°C and 30°C, respectively.

4.2 Base scenario

The base scenario considers the existing neighbourhoods with a single heat generation plant at node "Production" and limited short-term TES tank at the same location. The storage buffer near the heat generation plant is effectively used as a short-term storage. The evolution of its state of charge (SoC) varies rapidly, and is hence not shown on a separate graph. The heat input profile from the central heat generation plant (at node "Production") is shown in Figure 9. In this case, the central heating plant is sized according to the minimum nominal power needed for the year optimization, by iteration. Apart from the slight attenuation by the short-term storage tank, the heating profile follows the load variations (Figure 8 – bottom). In total, 199.5 GWh/a of heat has to be injected into the network.

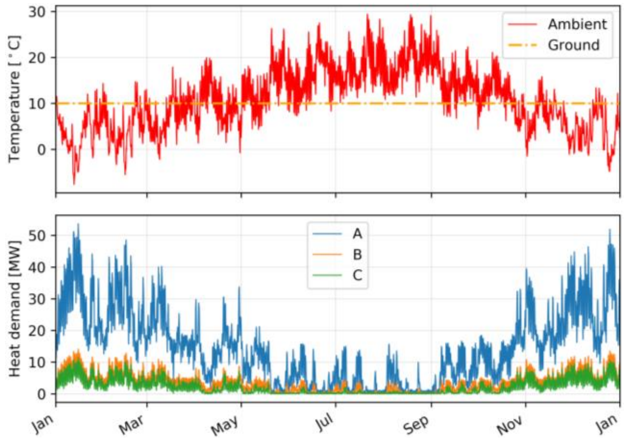

Figure 8: Ambient ground input temperature profiles (top) and heat demand per neighbourhood (bottom).

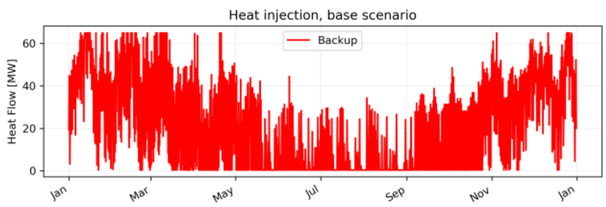

Figure 9: Heat injection from central generation plant in the base scenario.

4.3 Future scenario

In the future scenario, a large solar thermal collector array of 300 000 m^2 is added at the node "Solar Collector Array". A large seasonal TES pit is built at the same location. Additional long-term storage tanks are installed at neighborhoods A and C. The heat injections from the solar thermal collector (STC) array and the backup heating plant are shown in Figure 10. In this system, 93.2 GWh/a of backup heat (from the central production plant) is still needed.

Figure 11 shows the evolution of the energy stored in all of the TES systems. For the seasonal storage systems, the seasonality is clear. These tanks are discharged during winter, and recharged during summer. The short-term storage tank shows a lot more charge/discharge cycles in the SoC diagram, but due to the limited capacity of the tank this is barely distinguishable on the energy diagram (Figure 11 – top).

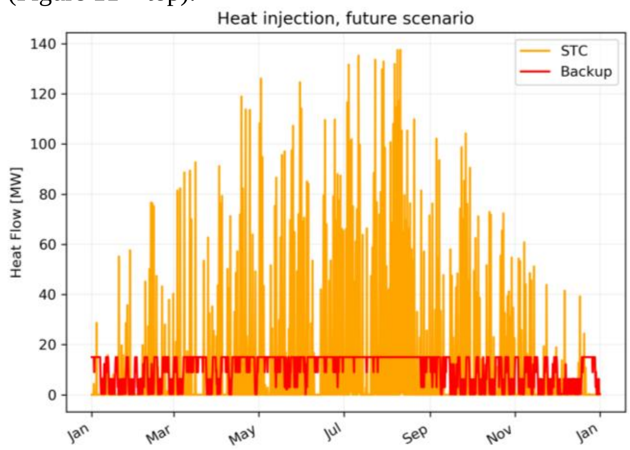

Figure 10: Injection of heat by the solar thermal collector (STC) array and the backup heating plant in the future scenario.

4.4 Comparison

Two scenarios were chosen, using very similar network lay-outs, to illustrate that modesto is a very flexible tool that allows calculating various cases with only limited code changes. The addition of the new network node with

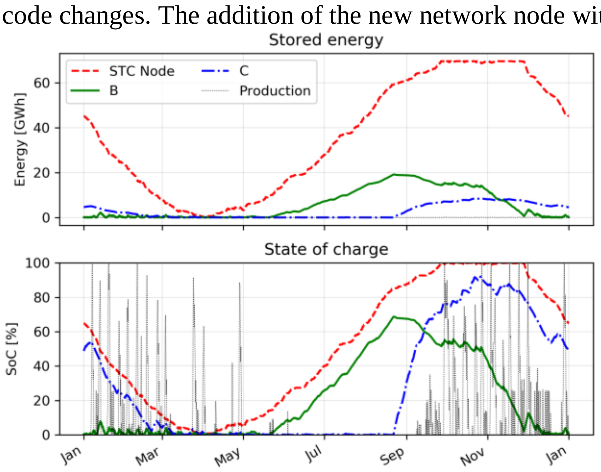

Figure 11: Evolution of stored energy (top) and state of charge (bottom) of the various storage systems in the future scenario.

the solar thermal collectors is accomplished with two extra lines in the network configuration code; another 5 lines are added to configure the parameters of the two added systems. Adding storage in an existing node only requires changing the dictionary of components in those nodes in the NetworkX input, and adding few lines for the parameters again.

The chosen scenarios led to a MILP problem. To solve the future scenario for a full year until a MIP optimality gap of around 1.8 % (best feasible solution found) takes not more than 60 seconds on a Dell Latitude E7470 device

Table 2: Design parameters of system components for the base and future scenarios.

Node	Component	Base scenario	Future scenario
Solar collector array	STES	/	1 500 000 m^3
	STC array	/	300 000 m^2
Production	Heat generation plant	65 MW	15 MW
	Short-term storage tank	3000 m^3	3000 m^3
Neighborhood A	STES	/	600 000 m^3
Neighborhood B	STES	/	200 000 m^3

with an Intel® Core™ i7-6600U 2.60 GHz with 2 cores (4 logical processors); the device has 16 GB RAM and runs Windows 10 as operating system. The base scenario can be reduced to a linear problem (all binary variables presolved) with negligible solution time.

5. FUTURE WORK

modesto is still a work in progress, with many plans for possible expansions. What follows is an overview of the most important planned expansions.

As already mentioned, *modesto* is meant for district energy systems in general, though currently it only focuses on district heating. Hence, in the future, multi-carrier energy systems will become possible as well. Additionally, extra objectives will be added, with the possibility to combine multiple objectives with weights.

The assumptions in Box 1 give an indication of other planned expansions, including non-linear optimization, pressure drops in the network and unbalanced networks.

Furthermore, extra components will be added, being mainly extra heat source models for e.g. CHP's and heat pumps, and extra thermal energy storage systems, such as borefields, aquifers, phase change materials (PCM), etc.

Finally, to simplify the use of *modesto*, methods to plot the optimization's results will be developed and an extensive documentation will be made.

6. CONCLUSION

This paper gives an overview of *modesto*, a toolbox for the optimization of district energy systems, designed in such a way that it can easily be used for different goals and cases. Both the interface and internal structure are presented in detail. Additionally, a short overview of implemented component models and objectives is given.

To illustrate possible uses of *modesto*, a case study is presented and analysed which confirms *modesto's* flexibility in handling changes in design and inputs. A conventional district heating scenario is compared to a future case with a large ratio of solar thermal input and large seasonal energy storage systems.

Finally, the future plans are elaborated on, the main ones being an expansion from district heating systems to multi-carrier energy systems (including the electricity system), and introducing more component models, both for new components that are not included yet, and new models for components already included but modelling different/ more/less dynamics.

ACKNOWLEDGEMENTS

This study is part of the research project "Towards a sustainable energy supply in cities". This project receives the support of the European Union, the European Regional Development Fund ERDF, Flanders Innovation & Entrepreneurship and the Province of Limburg. The authors also would like to acknowledge the financial support of VITO for the PhD Fellowships of Bram van der Heijde and Annelies Vandermeulen.

REFERENCES

Aalborg University. "COMPOSE - ENergyInteractive.net." http://energyinteractive.net/COMPOSE.ashx (February 7, 2018).

Åberg, M., and D. Henning. 2011. "Optimisation of a Swedish District Heating System with Reduced Heat Demand due to Energy Efficiency Measures in Residential Buildings." *Energy Policy* 39(12): 7839–52. http://linkinghub.elsevier.com/retrieve/pii/S0301421511007208 (November 4, 2014).

Åberg, M., J. Widén, and D. Henning. 2012. "Sensitivity of District Heating System Operation to Heat Demand Reductions and Electricity Price Variations: A Swedish Example." *Energy* 41(1): 525–40. http://linkinghub.elsevier.com/retrieve/pii/S0360544212001296 (May 19, 2014).

Benonysson, Atli. 1991. "Dynamic Modelling and Operation Optimization of District Heating Systems." PhD thesis, Technical University of Denmark (DTU).

Benonysson, Atli, Benny Bøhm, and Hans F. Ravn. 1995. "Operational Optimization in a District Heating System." *Energy Conversion and Management* 36(5): 297–314.

van Beuzekom, I., M. Gibescu, and J.G. Slootweg. 2015. "A Review of Multi-Energy System Planning and Optimization Tools for Sustainable Urban Development." *2015 IEEE Eindhoven PowerTech*: 1–7. http://ieeexplore.ieee.org/lpdocs/epic03/wrapper.htm?arnumber=7232360.

Connolly, D., H. Lund, B. V. Mathiesen, and M. Leahy. 2010. "A Review of Computer Tools for Analysing the Integration of Renewable Energy into Various Energy Systems." *Applied Energy* 87(4): 1059–82. http://dx.doi.org/10.1016/j.apenergy.2009.09.026.

Dorfner, Johannes. 2016. "Open Source Modelling and Optimisation of Energy Infrastructure at Urban Scale." Technischen Universität München.

———. 2017. "Urbs: A Linear Optimisation Model for Distributed Energy Systems — Urbs 0.7.1 Documentation." http://urbs.readthedocs.io/en/latest/index.html (February 9, 2018).

EMD international A/S. "energyPRO." https://www.emd.dk/energypro/ (February 7, 2018).

Garegnani, Giulia et al. 2016. "EPLANopt: EnergyPLAN Optimization Library." https://gitlab.inf.unibz.it/URS/EPLANopt (February 20, 2018).

Gurobi Optimization Inc. 2016. "Gurobi Optimizer Reference Manual." https://www.gurobi.com/ (February 7, 2018).

Hagberg, Aric A., Daniel A. Schult, and Pieter J. Swart. 2008. "Exploring Network Structure, Dynamics, and Function Using NetworkX." *Proceedings of the 7th Python in Science Conference (SciPy 2008)* (SciPy): 11–15.

Hart, William E. et al. 2017. *Pyomo - Optimization Modeling in Python. Second Edition.* Springer.

van der Heijde, Bram et al. 2018. "Using Representative Time Slices for Optimization of Thermal Energy Storage Systems in Low-Temperature District Heating Systems." In *Submitted to the 31st International Conference on Efficiency, Cost, Optimization, Simulation and Environmental Impact of Energy Systems*, Guimarães, Portugal, 1–13.

van der Heijde, Bram, Arnout Aertgeerts, and Lieve Helsen. 2017. "Modelling Steady-State Thermal Behaviour of Double Thermal Network Pipes." *International Journal of Thermal Sciences* 117: 316–27.

HOMER Energy LLC. "HOMER Energy." https://www.homerenergy.com/ (February 7, 2018).

Howells, Mark et al. 2011. "OSeMOSYS: The Open Source Energy Modeling System: An Introduction to Its Ethos, Structure and Development." *Energy Policy* 39(10): 5850–70. https://www.sciencedirect.com/science/article/pii/S0301421511004897 (February 7, 2018).

IBM Corp. 2016. *IBM ILOG CPLEX Optimization Studio*. https://www.ibm.com/support/knowledgecenter/SSSA5P_12.7.0/ilog.odms.studio.help/pdf/usrcplex.pdf (February 23, 2018).

Korpela, Timo et al. 2017. "Utilization of District Heating Networks to Provide Flexibility in CHP Production." *Energy Procedia* 116: 310–19. http://dx.doi.org/10.1016/j.egypro.2017.05.077.

Kummert, Michaël. 2007. "Using Genopt With Trnsys 16 and Type 56." *Program* 5: 1–11.

McKinney, Wes. 2010. "Data Structures for Statistical Computing in Python." In *Proceedings of the 9th Python in Science Conference*, Austin, Texas, USA, 51–66.

Modelon AB. 2017. "JModelica.org." http://www.jmodelica.org/ (February 9, 2018).

oemof Developing Group. 2017. "Open Energy Modelling Framework - A Modular Open Source Framework to Model Energy Supply Systems." https://doi.org/10.5281/zenodo.438676#.Wn3CDc35H20.mendeley (February 9, 2018).

Prina, Matteo Giacomo et al. 2016. "Smart Energy Systems Applied at Urban Level : The Case of the Municipality of Bressanone-Brixen Introduction." *International Journal of Sustainable Energy Planning and Management* 10: 25–26.

Protopapadaki, Christina, Glenn Reynders, and Dirk Saelens. 2014. "Bottom-up Modelling of the Belgian Residential Building Stock: Impact of Building Stock Descriptions." In *9th International Conference on System Simulation in Buildings*, Liege, Belgium, 1–21.

Reynders, Glenn, Jan Diriken, and Dirk Saelens. 2014. "Bottom-up Modeling of the Belgian Residential Building Stock : Influence of Model Complexity." In *9th International Conference on System Simulation in Buildings*, Liege, Belgium, 1–19.

Salpakari, Jyri, Jani Mikkola, and Peter D Lund. 2016. "Improved Flexibility with Large-Scale Variable Renewable Power in Cities through Optimal Demand Side Management and Power-to-Heat Conversion." *Energy Conversion and Management* 126: 649–61. http://dx.doi.org/10.1016/j.enconman.2016.08.041.

Schweiger, Gerald et al. 2017. "District Heating and Cooling Systems – Framework for Modelica-Based Simulation and Dynamic Optimization." *Energy* 137: 566–78. http://linkinghub.elsevier.com/retrieve/pii/S0360544217308691.

Stadler, M., M. Groissböck, G. Cardoso, and C. Marnay. 2014. "Optimizing Distributed Energy Resources and Building Retrofits with the Strategic DER-CAModel." *Applied Energy* 132: 557–67. http://dx.doi.org/10.1016/j.apenergy.2014.07.041.

Steen, David et al. 2015. "Modeling of Thermal Storage Systems in MILP Distributed Energy Resource Models." *Applied Energy* 137: 782–92.

University of Wisconsin. 2017. "TRNSYS - A Transient Systems Simulation Program." https://sel.me.wisc.edu/trnsys/ (February 9, 2018).

Vandewalle, J., and W. D'haeseleer. 2014. "The Impact of Small Scale Cogeneration on the Gas Demand at Distribution Level." *Energy Conversion and Management* 78: 137–50. http://dx.doi.org/10.1016/j.enconman.2013.10.005.

Verrilli, Francesca et al. 2016. "Model Predictive Control-Based Optimal Operations of District Heating System With Thermal Energy Storage and Flexible Loads." IEEE Transactions on Automation Science and Engineering 14:2: 1–11.

Welsch, M. et al. 2012. "Modelling Elements of Smart Grids - Enhancing the OSeMOSYS (Open Source Energy Modelling System) Code." *Energy* 46(1): 337–50. http://dx.doi.org/10.1016/j.energy.2012.08.017.

Multi-Objective Optimization of a District Heating Networks Energy Supply Systems Structure and Dimension

***Prof. Dr.-Ing.* M. Adam and *M.Sc.* J. Gottschald**
Centre of Innovative Energy Systems, University of Applied Sciences Duesseldorf,
Muensterstrasse 156, Duesseldorf, 40476, Germany,
+49211 4351 3575, +49211 4351 19502, jonas.gottschald@hs-duesseldorf.de

Abstract – The authors present a new method for a time-efficient optimization of a district heating networks energy supply systems structure and its dimension, using both, an ecological and economical target. The method is applied to a planned innovative district heating network in Germany with multiple heating suppliers. The method is based on a combination of sampling, modelling and optimization algorithms and allows for fast calculation of the Pareto Front, which includes all potentially optimal solutions. Furthermore, the method offers remarkable potential for visualizing the results.

1. INTRODUCTION

Energy supply companies are striving to design future-proof supply concepts that are as sustainable and thus attractive as possible for the reflected customer, affordable and guarantee a secure supply. The planner has a range of commercial (software) tools for dimensioning and sizing: From annual time series by means of spreadsheets to detailed simulation tools. In most cases, these tools are sufficient for the simple systems for local and district heating, which are still common today, often consisting of a CHP module, and heat backup (e.g. gas boiler). In the sense of energy turnaround, increasingly complex heating networks are now being created that are fed from conventional and renewable heat sources (Federal Ministry of Economic Affairs and Energy, 2017). The number of different producers also increases the planning effort. With solar heating as an example, in addition to a large number of hydraulic circuits or switch-on sequences, etc., it is also necessary to dimension the collector type, the solar field size and the storage tank volume to such an extent that the economic and ecological criteria as well as the security of supply are met.

2. BASELINE AND SIMULATION MODEL

In this article, the authors deal with the optimised design of a planned local heating network with a renewable energy share for a new housing estate in North Rhine-Westphalia, Germany. With 120 residential units and a total living space of approximately 15.600 m², the annual heat demand for heating, domestic hot water and grid losses is estimated at 950 MWh. For this purpose, a heating requirement of 40 kWh/(m²·a) and a domestic hot water requirement of 15 kWh/(m²·a) were assumed. An important feature of the grid is the planned low grid temperature of 50°C in the inlet flow and 30°C in the return flow. These are advantageous for the integration of renewable energies, especially for solar thermal energy and heat pumps.

In a first design step, an analysis of the possible plant technology takes place. You can choose between two fossil heat generators in the form of a gas-powered CHP module and a gas boiler, an electric heat pump with air or soil as a heat source and a central solar thermal system with short-term or long-term heat storage. The generator configurations examined in this preliminary analysis differ in the composition of the generation park, with all configurations including a cogeneration module for base-load coverage. The planning of the weather-independent generators is carried out on the basis of annual production lines (Figure 1), while a supplementary solar thermal system is also taken into account in Figure 2. As a result, a combination of CHP module, gas boiler, solar thermal energy and geothermal heat pump is prioritised.

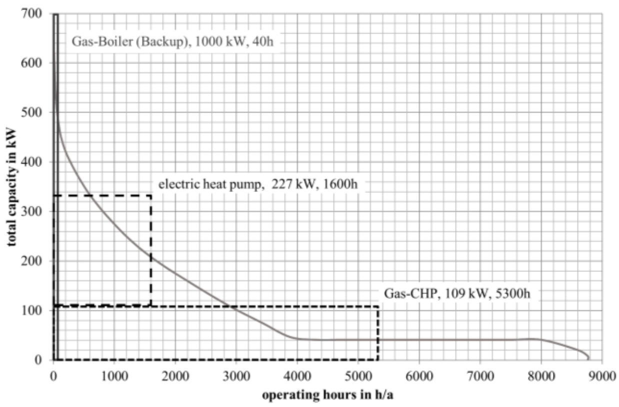

Figure 1: Exemplary design of generators according to the annual production line

The generators examined in the preliminary analysis show constant power, collector field size and storage volume based on the annual duration line or empirical values. However, this design does not have to be the optimum for the planned energy supply system. A different composition (smaller/larger heat pump, solar field size etc.) of the generators can lead to better ratios between heat costs and primary energy factor. In general, it is interesting to see which primary energy factors are attainable at which heat costs in the best case and what the corresponding system configurations look like. Determining this via "manual" parameter variations would be very time-consuming given the large number of possible configurations.

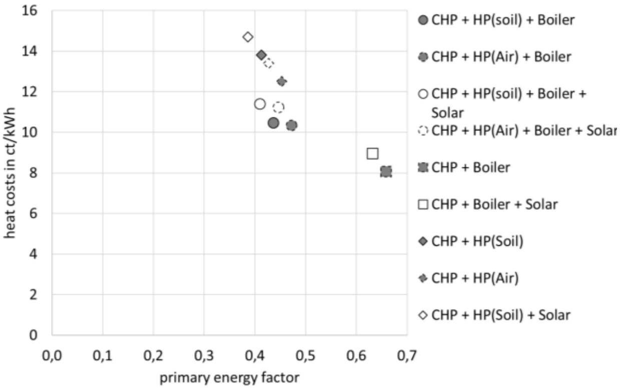

Figure 2: Results of the design according to annual production line for the examined systems

In addition, the design of such complex energy supply systems involving fossil and renewable generators, some of these depend on the weather, requires detailed annual simulations. The heat load profile required for this is generated in the following with regard to the heating load over utilization hours, heating limit, standard design temperature and the yearly course of the outdoor temperature. The domestic hot water load is determined with the DHWcalc (Jordan and Vajen 2003) software, which displays the hourly domestic hot water (DHW) consumption on a statistical basis. Grid losses are taken into account with a surcharge of 15% of the total useful heat requirement.

3. SIMULATION MODEL

In the second design step, a simulation model for the energy supply system is created according to the energy balance method in the form of a spreadsheet calculation, i.e. the heat requirement is covered by the generation park at all times in the simulation year. A model is created for each generator, i.e. CHP module, electric heat pump, solar collectors, solar storage tank and gas boiler. For this purpose, the spreadsheet uses a large number of device-specific characteristics (including investment cost functions and efficiency curves) as well as annual curves (e.g. outdoor temperature, global radiation and heat demand) in hourly resolution for the location of Duesseldorf, Germany. A fixed power-on sequence is used to control the individual heat generators to cover the heat demand: If solar heat is present in the storage tank or the collector field can provide power, it is used to cover the heat demand. If the heat requirement exceeds the available solar heat, the CHP module goes into operation first. If its output is not sufficient, the electric heat pump follows and at peak load times the gas boiler starts.

The model allows variable generator configuration by setting the device heat output of CHP module, electric heat pump and gas boiler as well as collector field size and storage volume. With the setting of 0 kW, for example, individual devices can be removed from the generator configuration. The primary energy factor and the heat costs of the energy supply system are defined as target values. The primary energy factor for electricity from the public grid in Germany is currently 1.8 and for natural gas 1.1. The calculation of the primary energy factor for the CHP module is carried out according to the current credit method (DIN V 4701-10 2003). The calculation of the heat costs includes capital costs (e.g. investment costs), maintenance and operating costs (e.g. energy costs, CHP subsidies, taxes, etc.).

4. DESIGN OF EXPERIMENTS AND MODELLING

The simulation model is the basis for the optimization of a "super-structure". A "super-structure" consists of all heat generators (cogeneration module, gas boiler, solar thermal energy with heat storage tank, heat pump, etc.) which are to be considered for the real operation and from which the optimum structure is to be selected. In order to ensure that the heat demand can always be covered, a gas boiler is integrated into the system structure as standard in this investigation, which supplements the total output of the heat generators to the required nominal value. The optimization should answer the question of the optimal structure (which components are to be used?) and the optimum dimensioning of the components (e.g. nominal thermal output of the CHP module, solar field area, heat storage capacity etc.) with regard to the heat costs as an economic and primary energy factor as an ecological target. A common approach to do this is the formulation of an optimization model by mixed-integer linear programming (MILP, see (P. Voll, 2013)). The disadvantage of MILP is that the computing time increases exponentially with the number of time steps in the time series, the target values can only be optimized individually or sequentially, and the graphical visualization of the general system behaviour is insufficient.

In contrast, the approach of the authors consists of an iterative process, which allows a sufficiently precise approximation of the non-linear system behaviour depending on exemplary selected parameters (only three parameters for reasons of clarity and representability are used in this example; a larger number allows the methodology with no problems) with as little effort as possible. The generated approximation model not only allows a fast visualization of the general system behaviour, but also the multi-criteria unweighted system optimization associated with many system evaluations.

The three selected parameters and the associated limits of the experimental space shows Table 1.

Table 1: Parameters and their respective lower and upper limits in the experimental space

Parameter	Lower limit	Upper limit
solar field size	0 m²	4000 m²
heat storage volume	0 m³	600 m³
heat pump capacity	0 kW	1000 kW

The non-parametric approximation model is trained and validated on the basis of simulation data. The model has the simplest possible structure to prevent an over-adaptation to the training data and the associated poor prognosis or approximation of unknown data. The training is initially provided on the basis of a factorial two-stage test design with one test point in each corner of the experimental space. In order to validate the prediction quality of the network, the authors use a uniformly distributed experimental design whose test points are optimized with regard to a distance measure and a correlation criterion. As long as the forecast quality of the model is insufficient on the validation data, additional test points are randomly selected, simulated and added to the training data set. The model is retrained and tested on the validation data.

Ultimately, 51 simulations and 131 simulations are required for a sufficiently accurate approximation of the heat costs and the primary energy factor. Figure 3 gives an overview of the distribution of the test points of the training data set in the experimental space for the primary energy factor (left) and the heat cost (right):

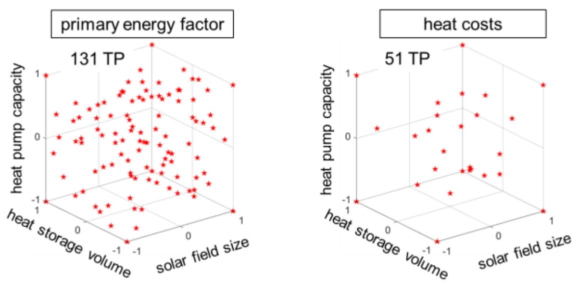

Figure 3: Test points in the experimental space for a sufficiently precise approximation of the validation data set, primary energy factor (left) and heat costs (right)

In order to evaluate the approximations, an independent test data set is generated in addition to the training and validation data set, which does not correlate in any way with the previously used data. The trained models approximate the test data set, which allows an independent qualitative and quantitative assessment of the prediction quality. The qualitative prognosis quality as a comparison between the new test data values and the prognosis values of the approximation model is shown in the so-called prognosis/observation plots in Figure 4. For comparison, Figure 4 also shows the prognosis/observation data pairs for the case of a quadratic effective area regression as an approximation, which were formed on the identical training data set (which shows only minor amalgamations of the main effects):

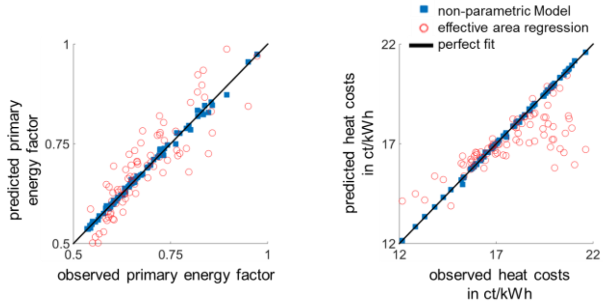

Figure 4: Prediction/observation plot of primary energy factor (left) and heat costs (right). Approximated using an artificial neural network (blue squares) and a regression of the effective area (red circles)

It can be seen that the non-parametric approximation model is more capable of representing the nonlinear system behaviour than a quadratic effective area regression. The approximation of the test data set shows that the models produced are very good generalizers and therefore ideal for a general analysis of the system.

5. MULTI-CRITERIA OPTIMIZATION

Often, two target values of interest have divergent curves in the experimental space and therefore different optimal positions. If you are interested in both target values and want to find particular efficient settings and visualize them with the help of a Pareto-front panel, unweighted multi-criteria optimizations (Konak, Coit and Smith, 2006) can be used best. The algorithm used starts with a random selection of parameter sets or configurations (heat pump capacity, solar field size, storage volume). The individual combinations of factor levels (configurations) and result values are evaluated on the basis of their relation to the optimum and their distribution. The best ones are combined according to their binary coding. In addition, the binary values of individual factor levels can vary randomly. The newly created combinations of factor levels are simulated again and form the next generation of system configurations. The process of coding and random variation of binary values starts again. If the combinations of factor levels and result values do not improve significantly or if a maximum number of generations has been created, the algorithm terminates. This stochastic optimization method is also capable of overcoming local optima, but also uses a large number of (>>1000) system evaluations. A (re-)simulation of the optimal configurations determined by the optimizer secures the results in retrospect.

6. CONCLUSION

It was shown that iterative modelling combined with experimental design methods allows a very precise and time-efficient approximation of system behaviour. The approximation model, which requires only one thousandth of the simulation time for calculating the target variables compared to the original simulation model, enables complex, varying analysis methods, in particular the multi-criteria, unweighted optimization of the system configurations. The result is a pareto-front of configurations that represent a not improvable compromise with respect to the evaluation criteria chosen, i.e. primary energy factor and heat costs, see Figure 5. The results shown below apply to the boundary conditions selected here for the local heating network to be supplied, costs, weather conditions, etc.

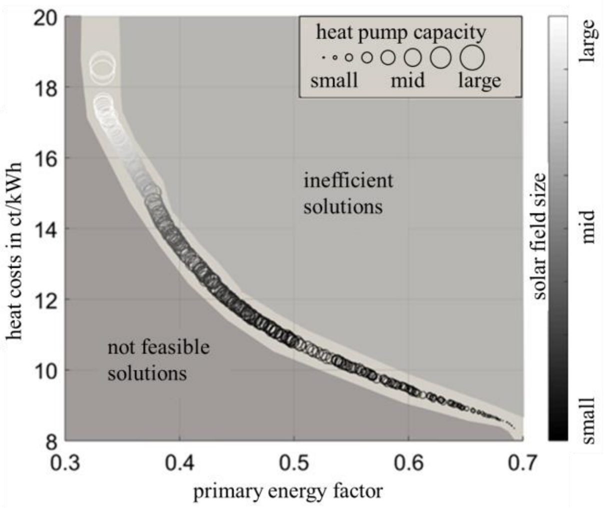

Figure 5: The pareto-front of the system configurations for supplying the local heating network

Each circle in Figure 5 represents a system configuration. The circle diameter stands for the heat pump capacity and its colour for the size of the solar field size. The solar storage volume also varies, but is not shown here because of the analogy to the solar field size. The configurations with the highest primary energy factor but lowest heat costs (lower right-hand corner in the figure) form systems containing only the CHP module and the gas boiler. Starting from this point and along the front, the heat pump capacity (large circles) increases, while the solar field is initially small or not (black circles) present. In this section of the pareto-front, the use of a heat pump is more effective than a solar thermal system, which can also be seen in the flat gradient (moderate increase in the heat costs with strong improvement of the primary energy factor) of the front. This occurs up to a primary energy factor of approx. 0.45 and a heat costs of approx. 12 ct/kWh. Above this point, the heat pump capacity remains approximately constant (same circle diameter) while the solar field size grows steadily (circle colour increasingly brighter). A larger solar thermal system is more efficient in this area than a larger heat pump.

Using the pareto-front, the appropriate configuration for the energy supply system can now be determined by selecting the desired primary energy factor/heat costs combination. One methodical advantage is the considerable visualization potential. Thanks to the design as a pareto-front, polyoptima can be clearly displayed and correlations can be read off easily.

7. OUTLOOK

The next steps of the authors concern the further development of the methodology towards a better applicability in simulations with long simulation times (>1h), a robust optimization and an even simpler applicability. Due to the robust optimization, it will be possible to deliver also robust best-configurations independent of fluctuating boundary conditions (e.g. weather, energy costs). A further planned step is the generalization of the method to a possible use with any simulation software as well as the improvement of the experimental design methods.

REFERENCES

Federal Ministry for Economic Affairs and Energy Germany (2017) Förderbekanntmachung zu den Modellvorhaben Wärmenetzsysteme 4.0 („Wärmenetze 4.0“), Berlin

U. Jordan*, K. Vajen** (2003) DHWcalc: Software zur Generierung von Trinkwasser-Zapfprofilen auf statistischer Basis, *Technical University of Denmark DTU, **University of Kassel, https://www.uni-kassel.de/maschinenbau/en/institute/ite/fachgebieteleitung/about-us/downloads.html

DIN V 4701-10 (2003) Energy efficiency of heating and ventilation systems in buildings - Part 10: Heating, domestic hot water supply, ventilation, Beuth Verlag GmbH, Berlin

P. Voll (2013) sOptimo: Strukturoptimierung von Energieversorgungssystemen - am Beispiel von Industrieparks

A. Konak, D. W. Coit, A. E. Smith (2006) Multi-objective optimization using genetic algorithms: A tutorial, *In Reliability Engineering & System Safety, Volume 91, Issue 9, 2006, Seite 992-1007, ISSN 0951-8320, https://doi.org/10.1016/j.ress.2005.11.018*

A novel simulation model, for the annual yield of parabolic trough collectors, including shading in the field. Simulation and validation

Bengt Perers[1], Janne Dragsted[1], Simon Furbo[1], Zhiyong Tian[1]

Jonatan Mossegård[2], Joakim Byström[2] , Olle Olsson[2]

Benjamin Ahlgren[3], Emma Johansson[3], Kajsa Lundberg[3] ,

[1] Department of Civil Engineering, Technical University of Denmark, Nordvej Building 119, Kgs. Lyngby, 2800, Denmark, 0045-52781629, beper@byg.dtu.dk

[2] Absolicon Solar Collector AB (Sweden)

[3] Umeå University (Sweden)

SUMMARY

A new concentrating parabolic trough collector (PTC) design is under market introduction by Absolicon Solar Collector AB. To support the sales and marketing and increasing the general scientific knowledge about these collectors, this work is done to create a tool for quick performance estimates, at any place on earth where solar radiation data is available. A special simulation tool for this collector and array design, is under development to manage different axis directions and also tilt of the tracking axis. Also shading between the collector rows is carefully corrected for. This was found to be an important factor for collector fields of this design and necessary to optimize the field design. The model is also validated against long term measurements at DTU on a small demonstration PTC collector array and also checked against other simulation tools using the same parameters and weather data.

key-words: concentrating solar collector, global performance, parabolic trough, array shading.

1. Introduction

A new concentrating parabolic trough collector (PTC) design is under market introduction by Absolicon Solar Collector AB, see an illustration in figure 1. To support the sales and marketing and increase the scientific understanding of this collector type this work is done to create quick performance estimates at any place on earth where solar radiation data is available. Both a small demo array tested at DTU (Technical University of Denmark) and simulations have shown that accurate treatment of both direct and diffuse shading in an array is important to get accurate annual performance results. The diffuse shading will not be fully solved in this paper but the main effects are corrected for. This is often neglected for PTC collectors. This also has influences on PTC collector testing that is not yet fully taken into account, as it involves the anisotropy of the diffuse radiation, that is not yet fully characterized for this collector type. But validation, figure 2, shows that there already is a good agreement between measured and calculated thermal performances.

Figure 1. A photo impression of a collector array with Absolicon PTC collectors.

2. The Simulation Tool

The simulation program, in this project, is developed in TRNSYS and then transferred to a simple to use TRNSED version, to make it easier for non TRNSYS experts, to use the tool.

The type of weather data .TM2, has been chosen to have a large global coverage for average year climate data, and still keep a good accuracy.

The TRNSYS work is focused on an accurate but simplified modelling that is directly connected to standardized collector test results and the model used there. Compared to simplified tools like ScenoCalc also shading between collector rows is modelled carefully. Also ease in changing between many climate files has priority.

A main goal is also to get a fast tool, to allow many simulations in a short time. This is needed for optimization runs and also investigations of the variability of performance globally from country to country and for different locations within a country. The correlation to DNI, sunshine duration and latitude is of special interest.

A validation of the simulation tool is shown in figure 2. It is in the form of an Input/Output diagram [2] that allows measured and simulation results to be compared, even if the weather data is not exactly the same.The test is done at DTU in the northern part of Copenhagen and The TRNSYS weater data is for Taastrup just west of Copenhagen.

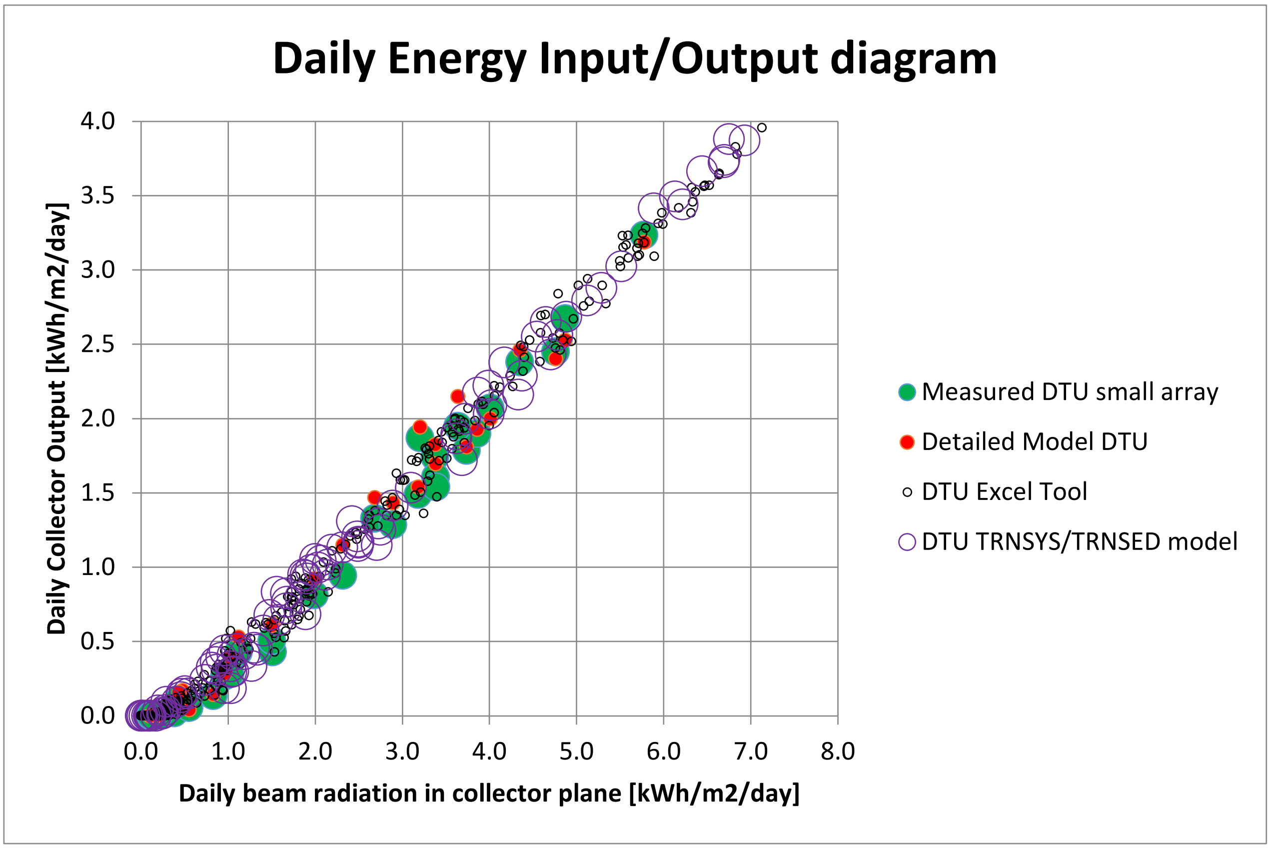

Figure 2. Validation of the simulation tool (large rings) versus small array measurements at DTU (green dots), An excel DTU tool (small rings) and DTU detailed modelling (red dots). The Input/Output diagram [2] allows measured and simulation results to be compared, even if the weather data is not exactly the same.

3. Results

Preliminary studies have shown that in the climates where most people live, the difference between North-South (NS) and East-West (EW) tracking axis-direction is not so large for a collector field, as one could expect. But this is first when taking array shading between rows into account. Though for a single trough without near and far shading, most often NS axis, gives the highest annual performance, as is commonly assumed. The annual distribution of the thermal performance is most even for East West axis directions so a larger solar fraction is possible then.

The daily distribution of energy output varies with axis direction and of course latitude. This can be used to adapt solar energy production to the load from case to case. The annual energy production for an array is not affected so much by the axis orientation as one could expect se figure 3.

Therefore axis directions in between classical NS and EW, like SE or SW can be utilized to match the load better and maybe give easier installation on site, if the ground area or roof borders are not perfectly NS and EW [1]. Figure 3 shows the annual thermal performance variation with tracking axis direction. 0= North South, -90 and 90 is East West direction. Note that there is a tendency to better performance in between the classical tracking axis directions N-S and E-W. This is an example for a standard array with closely packed troughs with row distance 1.4 m, trough width 1.06 m and 20 rows.

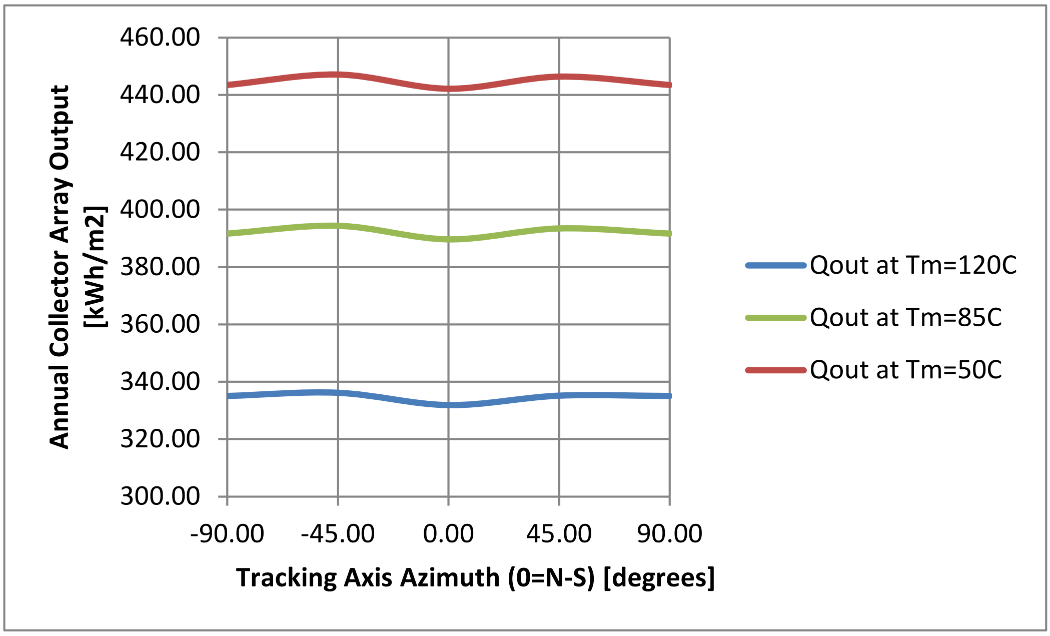

Figure 3. Annual thermal performance variation with tracking axis direction. 0= North South -90 and 90 is East West direction. Note that there is a tendency to better performance in between the classical axis directions. Weather data is from North Jutland.

Further it is found that even small tracking axis tilt angles towards the equator, can improve the performance quite significantly especially at high latitudes. Preliminary studies have shown that small axis tilts increases the performance by 1% per degree tilt at high latitudes like in Denmark. We think this extra enhancement above the effect of more beam radiation in the PTC collector plane, by tracking axis tilt, is partly due to less inter-array shading.

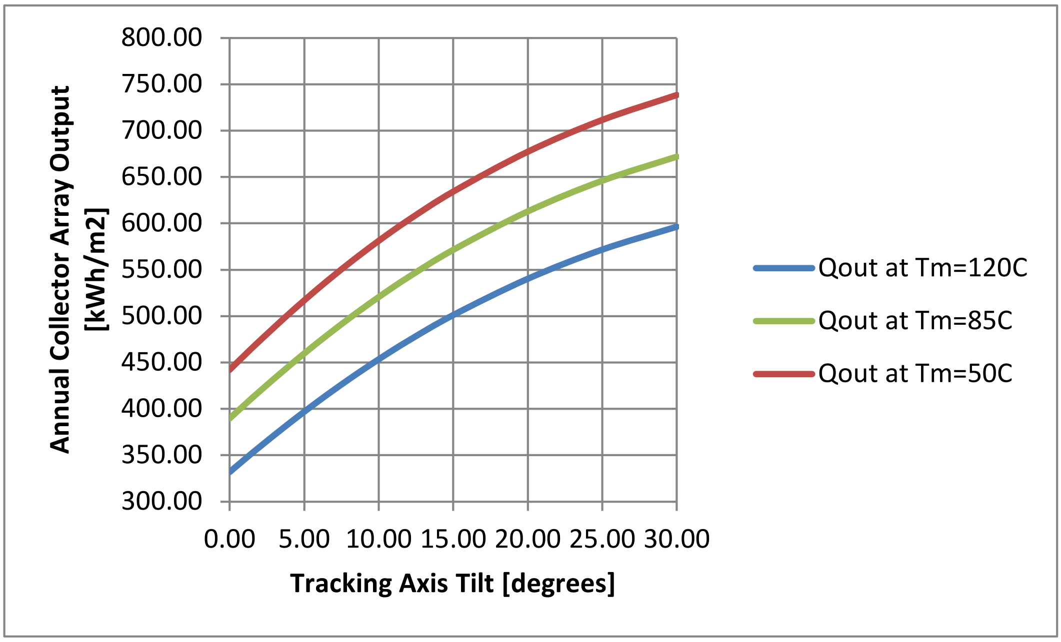

Figure 4. Performance enhancement by tracking axis tilt, for a PTC operating in the North Jutland climate.

4. Conclusions

- A simulation tool is under development to investigate performance of PTC collector arrays worldwide.
- The tool has been validated against measurements on a small array at DTU in Denmark.
- The calculations so far indicate that the exact tracking axis direction is not so critical in a wide range of latitudes. This gives a freedom in installation of an array depending on local conditions for load profile and available area for the collector field.
- A load adaptation can be achieved by optimizing the axis direction for each case.
- Even small tilts of the tracking axis towards the equator can give significant annual performance improvements at high latitudes.

References

[1] Bengt Perers, Simon Furbo and Janne Dragsted. Thermal performance of concentrating tracking solar collectors. DTU Byg report R-292. August 2013.

[2] Bengt Perers, Heimo Zinko, Per Holst. Analytical model for the daily energy input/ output relationship for solar collector systems. Document D11:1985. ISBN 91-540-4359-X. Swedish Council for Building Research.

RELATED, A FLEXIBLE APPROACH TO THE DEPLOYMENT AND CONVERSION OF DH NETWORKS TO LOW TEMPERATURE, WITH INCREASED USE OF LOCAL SOLAR SYSTEMS

Roberto Garay Martinez, Victor Sanchez Zabala
Sustainable Construction Division, Tecnalia, c/ Geldo, Edificio 700, 48160, Derio, Spain, +34 667 178 958, Roberto.garay@tecnalia.com

Abstract – District heating (DH) systems are key systems for the de-carbonization of heating energy in European Cities. In order to allow for this transition, while guaranteeing competitive energy costs, conversion of DHs is required. DH operation temperature needs to be reduced in order to increase the performance of renewable systems and operation criteria needs to be adopted for the introduction of weather-dependent, distributed heat sources such as solar systems.
This paper presents the RELaTED decentralized Ultra-Low Temperature DH network scheme, and its adaptation to several operational schemes such as new and existing DH networks, with different levels of complexity. Transitory phases in the conversion process are discussed.

1. INTRODUCTION

District heating (DH) systems are one of the most energy efficient heating systems in urban environments, with proven reliability within many decades already. DHs have traditionally been designed to be operated in a hierarchized way, with central energy production facilities delivering heat to a variety of distributed consumption locations.

DHs are identified as key systems to achieve the de-carbonization of heating energy in European Cities. (European Commission, 2016) Renewable and waste heat sources are foreseen at the same time as de-carbonized heat sources and the way to guarantee competitive energy costs with limited influence of fossil fuel supply price volatility. To achieve this, a transition is needed in DHs, comprising not only measures to improve overall performance (temperature level reductions, improvement of substations, etc.), but to guarantee system viability as a whole in a context (Harrestrup & Svendsen, 2015) of reduced heat loads with the transition to NZEB (Near Zero Energy Buildings).

RELaTED deploys a decentralized, Ultra-Low Temperature (ULT) DH network concept, which allows for the incorporation of low-grade heat sources with minimal constraints, larger shares of renewable energy sources (RES) and distributed heat sources. ULT DH reduces operational costs due to fewer heat losses, better energy performance of heat generation plants and extensive use of de-carbonized energy sources at low marginal costs.

In the transition towards NZEB and PEH (plus energy houses), RELaTED allows for a prosumer scheme, where positive buildings deliver energy to the grid.

2. DE-CARBONISED HEAT SOURCES

Modern DH networks are one of the most resource efficient heat production systems. In some countries, DHs are linked to intense use of Combined Heat and Power (CHP) and Heat pump technologies, linked to renewable energy sources such as geothermal fields, biomass and waste incineration.

Along the last decade, already in several EU locations, large ST systems have been successfully connected to DH networks under commercial operation. (SDHplus, 2015)

Linked to variations of solar resources and electricity costs-for heat pump heating-, over the year, several DH networks have incorporated large scale thermal storage systems. (Gadd and Werner, 2015),)

In fact, for some concept districts such as the (Drake Landing Solar Community) full solar cover of heating loads has been achieved with a mixture of ST and seasonal storage even in cold climates in continental Canada at 50ºN.

Although very dependent on local availability, waste heat streams from industrial and commercial (e.g. supermarkets) sources, are relatively stable sources of heat. Large scale industrial processes are active all year-round, resulting in minimally carbon intensive processes.

(Vesterlund et Al., 2017) studied the configuration of the DH network in Kiruna, SE, where a large iron mining setting provided a de-carbonised heat recovery source. In all calculations where industrial waste heat was introduced, the optimal situation made use of the maximum capacity of the industrial waste heat (15MW), it provided. The relative relevance of this heat source was 30% of the winter peak load (49MW) and 38% of the winter average load (39MW).

With unprecedented performance levels in fuel-based heat production processes, improvements in performance levels will only have minimal impact in the route to DH de-carbonisation. The transition will require the large scale integration of ST systems, and waste heat resources. Linked to load reduction in the progressive transition to NZEB performance levels, with progressive connection of BIST into the DH, a de-carbonised DH environment can be achieved.

3. LIMITATIONS OF CURRENT DH NETWORKS

DH systems date back more than 100 years. Originally with steam as as heat carrier, DH has evolved through the 20th century into systems at lower temperature. With most of the systems in Europe developed over the decades of 1970 & 80, typical DH systems deliver presurized water at about to about 80°C to consumers. In Nordic countries, district heating developed rapidly in the nineties into areas with lower heat density, requiring more efficient distribution networks. Supply temperatures were reduced even further. In these systems, heat is supplied at 60-70ºC, supported by modern building codes in those regions, where new radiator systems are sized for operation at 60°C/30°C.

DHs deliver heat for space heating (SH) and domestic hot water (DHW) preparation. With the trend towards more insulated buildings-NZEB, heat loads for SH are steadily decreasing, which, in combination with improved substation design, allow for even further temperature reductions of the supply temperature. However, the preparation of DHW imposes limits to this temperature fall, due to the need to avoid legionella-related issues. Depending on specific national regulations, storage temperatures in the range of 55-75ºC are prescribed, depending on storage size and SHW preparation method.

(Olsen et Al.,2008) and (Christiansen et Al. 2012), among others, have investigated in alternative DHW preparation methods with DH service temperature as low as 50ºC. In many alternatives, traditional DHW preparation methods are substituted by "innovative methods". In these concepts, mains water is primarily heated by the DH, and then complemented by electric heaters/boosters up to the required temperature levels. In more advanced alternatives, heat pumps are used for such purposes.

4. CONCEPTUAL DEVELOPMENT OF THE RELATED ULT DH SYSTEM

RELaTED builds over existing evidence (Brand et al.,2016 and Gudmundsson, et al., 2014) that DH supply temperatures as low as 45ºC, are suitable for heat supply to define its ULT DH concept.

In RELaTED every single building is converted into an energy node, where so-called triple function substations (3FS) allow for bi-directional heat exchange between the building and the network, with the additional functionality of grid injection of excess local solar heat. In fact, adaptations are made to Building Integrated Solar Thermal (BIST) systems in order to adapt them to Low Temperature (BILTST), with reduced local storage, as the connection to the DH makes it redundant.

Additionally District-heating connected Reversible Heat Pump systems (DHRHP) allow for recovery of exhaust heat from cooling applications (e.g. air conditioning, ventilation, etc.).

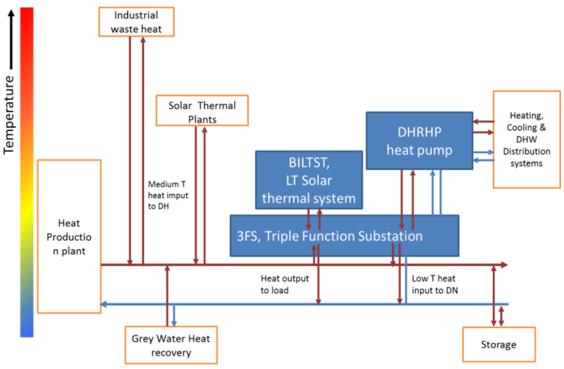

Overall RELaTED Concept

Even before the consideration of further technological improvements, ULT temperature levels substantially improve the performance of heat production systems. It is estimated that CHP performance can be improved by a factor 2 to 5, considering (Lowe, 2011). Furthermore, ULT allows for the integration of virtually any waste heat source from industry, sewage, etc.

RELaTED builds atop of the existing trend for integration of large solar thermal plants systems in DH networks, some of them comprising large seasonal storage systems. RELaTED incorporates large ST plants, but also provides the famework for the integration of BIST into the main ULT DH concept. With lower fluid temperature when compared regular BIST integration levels, performance levels are expected to rise by 20%, due to lower heat loses. An additional 20% rise is calculated when avoiding local storage due to direct DH connection. The RELaTED ULT network acting as a perfect heat sink avoids storage stagnation situations, thus allowing for larger ST performance levels.

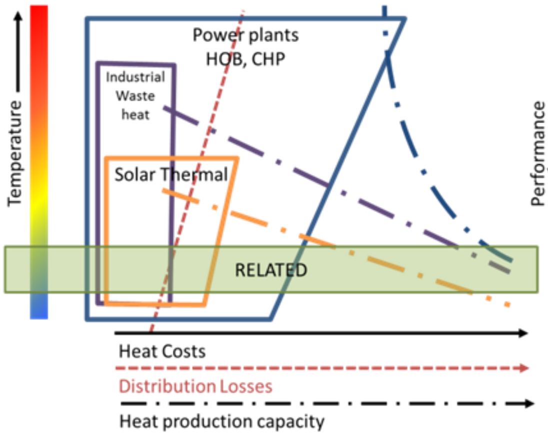

Temperature & performance levels, cost of heat, & other critical parameters in heat production for DH networks.

DHRHP systems allow for the de-coupling of temperature levels in DH network and Building level HVAC systems. With the DH as heat source, stable tempertures at 35-40ºC ensure stable COP levels of 6-7 for the DHRHP all-year-round. These units provide an economic way for the preparation of DHW, while at the same time allowing for the connection of buildings with higher temperatures in their HVAC design (i.e. older buildings).

The RELaTED concept, when implemented with a substantial share of RES provides a robust framework to ensure the economic viability of DH networks, in the context of the transition of the building stock to NZEB along the following decades.

5. RELATED IN NEW DH NETWORKS

The RELaTED ULT DH concept is directly applicable to DHs in the context of new urban developments. In these cases, previous experiences are directly applicable, allowing for SH at 45ºC. Sizing of heating networks in buildings and the overall DH infrastructure would be made according to the expected heating temperature, with standard calculation procedures.

As defined before, DHW loads are key issues, where, electric heating would be applied, either by means of electric boosters or heat pumps (depending on the rated power). (Brand et Al., 2016) tested an electric booster system connected to a DH network at 40ºC. In this experimental work, the use of electricity accounted to 30% of the DHW perparation energy, or 3% of the overall energy consumption.

RELaTED proposes an advanced 3FS substation concept, where local ST systsms can be connected into the DH network, and substations allow for LT distribution systems, with the potential use of electric boosters. In some cases, where cooling loads are present or high temperature heating systems are used, DHRHP systems provide an alternative to electric boosters.

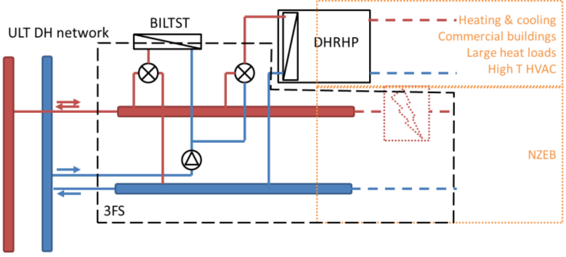

3FS concept & connection with ULT network, BILTST, DHRHP & Electric booster systems

In this scheme, RES systems are integrated since the beginning of the system, according to the possibilities, requirements, and interest in each particular building. 3FS allow for the integration of sparse BILTST systems into the network, without the need of specific investment at DH level.

6. RELATED IN EXISTING DH NETWORKS

Intetgration of ULT in existing networks is a complex mission. Existing networks are commonly composed by many subnetworks, each serving buildings constructed over decades according to different energy codes.

The 3FS scheme, with particular adaptations can be optimized to operate in three different environments:

- ULT DH networks
- Higher temperature DH network: 3FS can be integrated at higher tempeatures, while the (sub)network where it is integrated is not fully capable of operating at LT
- Temperature cascading concept: 3FS, when incorporated only in part of the DH subnetwork can be used to extract heat from the return pipe of the DH system. Thus allowing for the densification of a DH network without further changes to the pipes. For this purpose, an additional pump would be required This configuration could later be transformed into a general purpose 3FS when lowering the supply temperature in the DH.

7. TRANSITORY PHASES

The conversion of a DH network is a complex process, which needs to be performed stepwise in order to guarantee continous SH and DHW services. Although relatively long SH service interuption in summertime is possible, DHW is required all-year-round. Thus network conversions need to be carefully scheduled. Successful transitions require that all buildings within a network are equipped with an updated substation (ULT or 3FS), prior to temperature reductions in each subnetwork. As a further step, temperature in transmission pipes can be reduced, with inproved performance in heat production plants.

Along the process, waste heat streams an ST plants can be incorporated at any phase, as long as their compatibility with current temperature levels is ensured.

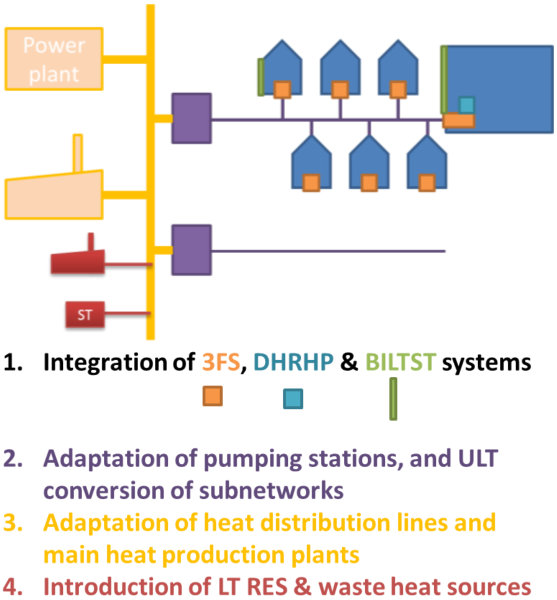

Stepwise conversion process of a DH into ULT

8. EXPECTED DEVELOPMENT

RELaTED is an ongoing research & development, with expected demonstration activities along the 2018-2021 period. The overall ULT concept, integration of 3FS, BILTST & DHRHP subsystems, industrial waste heat, large ST & waste incineration plants will be demonstrated in 4 selected locations:

- Green field development in VINGE, DK
- DH network with large share of biomass in TARTU, EE
- Large DH network with incorporation of large RES resources in BELGRADE, SR
- Corporate DH network in IURRETA, ES

Successful demonstration of RELaTED in this context will show the potentialities of the system under various climatic conditions, heat production mix & DH design/operation cultures.

9. CONCLUSIONS

RELaTED presents a promising ULT DH concept, backed-up by existing evidence that large ST fractions, Industrial waste heat and ULT DH allow for substantial de-carbonisation of heat delivery in the context of DH networks.

RELaTED will implement this concept over a set of diverse DH networks, allowing for the validation of the concept prior to full scale implementation.

ACKNOWLEDGEMENTS

Research output presented in this paper has performed under project RELaTED (RELaTED, 2017). RELaTED project partners are: TECNALIA, Danish Technical Institute, Fortum Tartu, Beogradske Elektrane, Basque Government, Metro Therm, Nibe, Aventa, Industrias IMAR, Basque Energy Agency, Mazovia Energy Agency, Institute of Baltic Studies, FEDARENE, El Taller De Comunicación y CIA.

This project has received funding from the European Union's Horizon 2020 research and innovation programme under grant agreement No 768567.

REFERENCES

Brand M. et al. (2016),District heating substation with electrical heater supplied by 40°C district heating water. SDDE16 International Conference on District Energy

Christiansen C. H., Dalla Rosa A., Brand M., Olsen P. K., Thorsen J. E. (2012), Results and experiences from a 2-year study with measurements on a new low-temperature district heating system for low- energy buildings

Drake Landing Solar Community (2017/12/19), http://www.dlsc.ca/

European Commission, An EU Strategy on Heating and Cooling (2016)

Gadd H. and Werner S. (2015), Thermal energy storage systems for district heating and cooling, In Advances in Thermal Energy Storage Systems ,Woodhead Publishing Series in Energy, edited by Luisa F. Cabeza, Woodhead Publishing, Pages 467-478, ISBN 9781782420880

Gudmundsson, et Al. (2014), Ultra-Low Temperature District Heating And Micro Heat Pump Application – Economic Analysis. 14th International Symposium On District Heating And Cooling

Harrestrup M. Svendsen S.(2015), Changes in heat load profile of typical Danish multi-storey buildings when energy-renovated and supplied with low-temperature district heating, l Journal of Sustainable Energy, 34:3-4, 232-247, DOI: 10.1080/14786451.2013.848863

Lowe R. (2011), Combined heat and power considered as a virtual steam cycle heat pump, Energy Policy, Volume 39, Issue 9

Olsen P.K., Lambertsen H.,Hummelshøj R., Bøhm B., Christiansen C.H., Svendsen S., Larsen C.T., Worm J. (2008), A new low-temperature district heating system for low-energy buildings, 11th International Symposium on District Heating and Cooling, Reykjavik, Iceland

RELaTED, REnewable Low TEmperature District, EU h2020 GA nº 768567 (2017-2021), www.relatedproject.eu

SDHplus- New Business Opportunities for Solar District Heating and Cooling, EC-IEE, 2012-2015, http://solar-district-heating.eu/SDHrelatedprojects/AboutSDHplus.aspx

Vesterlund M., Toffolo A., Dahl J. (2017), Optimization of multi-source complex district heating network, a case study, Energy, vol 126, doi: 10.1016/j.energy.2017.03.018

DESIGN OF CONSUMMER THERMAL SUBSTATIONS FOR THE INTEGRATION OF DISTRIBUTED SOLAR TECHNOLOGIES IN DISTRICT HEATING SYSTEMS

Victor Sanchez Zabala, Roberto Garay Martinez,
Sustainable Construction Division, Tecnalia, c/ Geldo, Edificio 700, 48160, Derio, Spain, +34 661 174 917,
vfrancisco.sanchez@tecnalia.com

Abstract – In most cases, building service designers choose between Solar thermal (ST) and District Heating (DH) technologies for their integration in buildings. By doing so, only a fraction of the buildings within a particular district is used for ST, while at the same time energy intensity in DH networks can be reduced. In some cases, building-integrated solar thermal systems are connected to DH networks by means of dedicated pipes. In all these cases, sub-optimal situations are reached with lower fraction of renewable heat, reduced network strength and/or additional heat losses.
In this paper, a consummer substation concept is proposed with reversible heat flow and net metering, which avoids local thermal storage in the solar loop. Adaptations required for multi-dwelling buildings are presented.

1. INTRODUCTION

With limited energy resources to meet the requirements of a steadlily increasing population, there is a clear trend towards the implementation of energy efficiency (EE) measures and de-carbonisation of the energy supply for heating applications.

In the EU context, EPBD policies and national regulations require of increasing levels of building energy performance levels and incorporation of Renewable Energy Sources (RES) such as solar thermal (ST) technologies.

In the context of individual buildings, ST systems are composed by a solar collector field, a thermal storage system, and an alternative heat source such as a boiler, which delivers complementary heat during peak consumption periods without solar radiation in winter. Due to techno-economical optimisation, in most common cases, ST technologies are only sized to cope part of the heat load of buildings.

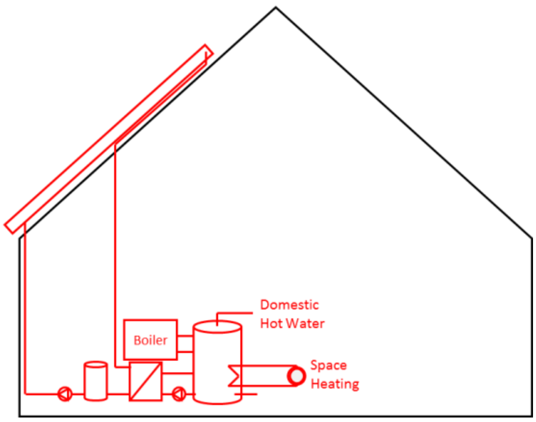

Schematic of Drainback ST system. Auxiliary elements are not represented.

District heating (DH) systems are highly efficient heating systems which have been developed & operated over decades in urban environments. To-date, DH has been supplied mainly by large fossil-fuel fired boilers, or Combined Heat and Power (CHP) systems, although other implementations incorporate waste heat from large industrial settlements, or substitute fossil fuels with biomass.

In the last years, a number of satisfactory experiences have proven the commercial application of large ST plants and Thermal Storage (Werner, 2017). Thses plants act as a substitute for polluting energy production systems. Following these experiences and its potentiality to integrate waste heat streams, DHs are identified as key systems to achieve the de-carbonization of heating energy in European Cities. (European Commission, 2016). RES integration achieves the dual objective of de-carbonization of heat sources and the limitation of heating cost exposure to the volatility of fossil fuel price.
In many areas, the feasibility of installation of centralized ST plants is limited by geographical constraints and scarcity of land in larger cities.

DH configuration has evolved over time in order to adapt to increasing EE needs and variation in heat loads with the modernisation of buildings and their heating systems. Temperature levels have been substantially reduced and substation configuration improved, among other measures.

With an expected switch towards Nearly Zero Energy buildings (NZEB) over the next decades, heat loads to be supplied are expected to reduce substantially, and measures will need to be taken to ensure the economic viability of DH systems.

With an increased share of NZEBs in districts, it is to be expected that heat production in these buildings may frequently exceed local needs in these buildings. DHs should take profit of these heat which would otherwise be wasted. With steady reductions in operational Temperatures in DH, oportunities to do so are increased.

To do so, it is required that subsations at building level are adapted and suitable heat purchase tariffs and net metering are applied.

2. CURRENT DH SUBSTATION CONFIGURATIONS

District heating substations are devices whose main function is the connection of loads to DH networks in a standardized manner. Each DH operator specifies particular considerations regarding design & construction of substations in order to achieve homogeneous service levels within the network.

Considering that medium-large DH networks commonly comprise thousands of consumers connected into the DH network (DH network in Belgrade serves CA 1 million inhabitants), industrialized substations have been developed to guarantee common connection criteria with simplified engineering, installation and commissioning works.

In most common applications, substations comprise: several heat exchangers, which serve as a physical barrier to avoid local leakage to cause mayor failure of subnetworks serving; regulation valves & controllers, which serve to ensure standardized return temperature levels in the DH; heat meters, for billing purposes; and auxiliary devices.

2 common configurations are possible:

- Substation with heat exchanger for space heating and thermal store for DHW preparation. In this configuration, the thermal store is heated by means of an inmersion heat exchanger which de-couples DHW from the DH circuit. This configuration is valid both for individual dwellings but also for centralised heat deliveries within multi-rise buildings.
- Substation with 2 heat exchangers. DHW production requires of substantially larger sizing of the pipework, high quality/capacity heat exchangers and precise instrumentation. Limitations are imposed to the laying of DHW pipework within the building. This configuration commonly applies only to individual housing/apartments.

In multi-rise buildings, the use of centralised DH substations imposes a relatively high service temperature for DHW preparation due to the need to keep DHW storage tanks and pipes at legionella-safe temperature levels.

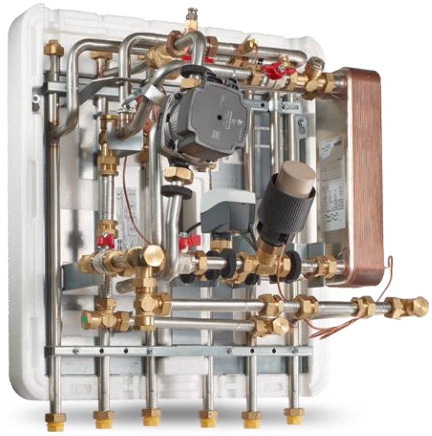

Appartment Substation for direct space heating and DHW preparation (Source: METRO THERM)

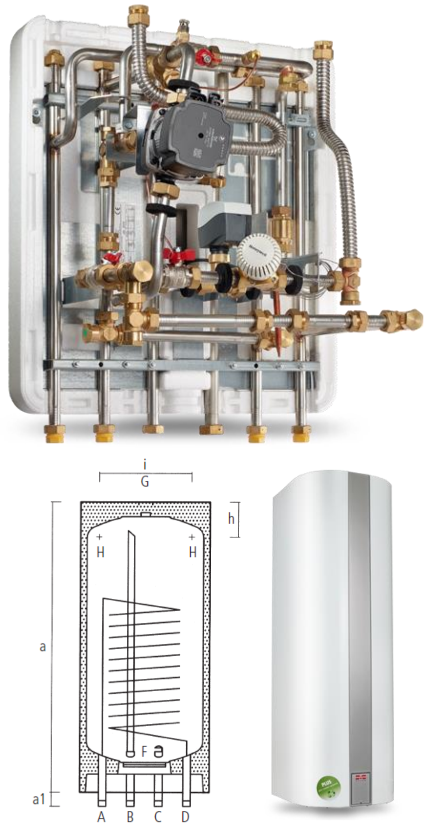

Substation with indirect preparation of DHW, and compatible DHW storage tank (Source: METRO THERM)

When low-temperature DH networks are implemented, substations at dwelling level are commonly selected. In these, lower temperature lossess occur as centralised HVAC plants are avoided, and lower temperature levels are possible due to smaller DHW loads, and the possibility to satisfy these by means of instantaneous heating with heat exchangers.

Modern substations are sized to perform correctly at temperature levels in the viccinity of 55ºC, but lower temperatures are also possible under request, as long as the DHW preparation process is complemented by other means (e.g. electric boilers, heat pumps,…).

In Industrial settings, different types of substations may be possible. These are not analized in this work.

3. DH-CONNECTED ST SYSTEMS

In the last decade, there has been a large boost in the construction and operation of large ST plants, connected to DH networks.

Depending on the size of the system, available ST capacity, etc, large seasonal thermal storage systems have been installed along with these systems.

These systems are not connected to buildings directly, and they are operated by DH operators directly or as independent heat producers. As such, their interconnection schemes are not relevant in terms of substation definition for de-centralised ST systems. Nevertheless, these setups demonstrate that ST is a viable source of heat in the context of DH networks, and that there should be room for de-centralised ST in systems with limited access to land for large ST installation.

Sources such as (Solar District Heating) show the actual status of the technology.

The recurrent use of thermal storage along with ST technologies in DH clarifies that such storage is critical to get the most of ST systems at DH level, by capturing solar energy during summer months and making it available during winter period. However, for relatively small ST systems, with heat production not exceding heat loads in summer, this storage could be limited to inter-daily needs.

4. DISTRIBUTED, DH-INTEGRATED ST SYSTEMS

Solutions for the integration of ST systems in buildings have been extensively investigated and demonstrated over decades already. Requirements on minimal solar fractions are imposed in building codes acros Europe, which can even be satisfied by means of off-the-shelf systems. Most common ST solutions incorporate ST collectors, in a presurized circuit, which delivers heat to a stratified storage tank. Auxiliary heating devices-most commonly, natural gas boilers- are incorporated in parallel to meet heating needs in buildings when the solar resource is insufficient. Many reviews on ST systems and case studies can be found in literature such as (Hadorn, 2015)

DH connection of these systems can be performed under various approaches. Following the general interaction scheme expressed above, DH can be used as an alternative heat source for those moments where the ST system is not able to cope with the heat load in the building. In this case, Buildings behave as regular DH connected buildings, but with a reduced heat load during periods with ST heat production. There is no possibility to inject any ST excess heat into the DH network.

However, this approach limits the potentialities for the use of excess ST energy outside the building itself. (Gavalda, and others) studied the potentialities of reconficuration of individual ST installations to deliver excess heat to the DH network in Barcelona, where the surplus energy delivered to the DH reached 50% of the total heat produced. With ST sized for winter use, almost no surplus energy is delivered in winter period, but surplus energy accounting to 1.5-2 times the heat production in january is delivered monthly during the spring, summer and autum periods.

These figures are valid for the case of ST installations operating at its regular temperature (e.g. 60-70ºC of heat delviery temperature.

A further improvement in the interconnection would be such that the ST system is connected to operate at lower temperature -thus higher performance levels. In this context, excess heat is delivered into the return pipe of the DH.

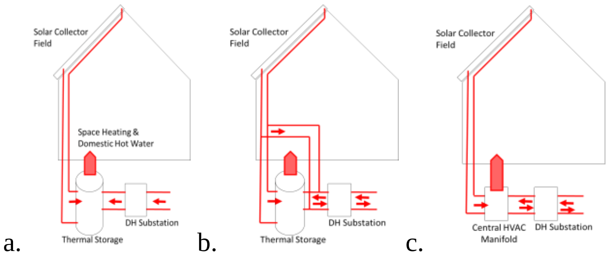

Connectio Schemes of ST systems to DH. a. ST & DH in parallel. b. Delivery of excess heat to DH. c. Hibrid system without ST storage

DH systems are large hydronic sytems. Due to its large capacity, and considering the relatively small share of ST systems connected to the network, DH systems can be considered as an ideal heat sink. Under these circumstances, all heat produced by the ST system, is consummed by final users consummed to the network. Shall ST integration in DH be massive, DH operators should steadily incorporate thermal storage to the network. Anyhow, the cost of large scale thermal storage is substantially smaller to incorporating storage to each ST unit.

Extensive cost reviews of thermal storage for ST systems state that cost can be reduced by a factor 4-6 when large storage sizes & technologies are applied (Mauthner and Herkel). Considering present cost of thermal storage techonlogies for ST systems, DH connected systems could easily reduce their present cost by 50-100€/m². As stated before, these cost would only be partially transferred to the DH operator for situations with large fractions of ST integrated in the district.

5. POTENTIALITIES OF DH-INTEGRATED ST SYSTEMS

DH connection of distributed ST systems provides several advantages over insulated ST systems.

From the Energy point of view, the yearly solar energy yield is substantially increased. (Gavalda and others) states that with DH-connected ST, yearly heat production in the range of 654 kWh/m2 are possible. This figure almost doubles the performance of insulated ST systems.

With these figures, payback period of ST systems can be substantially reduced.

Additionally, in common DH systems, there is only a small share of buildings with ST systems connected to the DH network. In this context with marginal contributions of ST systems to the DH network, there is no need to configure ST systems to raise fluid temperature to the overall flow temperature in the DH network. ST systems may be confirgured to deliver the maximum possible heat to the return pipe of the DH system.

Considering performance levels declared in a Solar Keymark certified flat plate ST collector, performance of the collector itself is improved by an average 0.58% for every ºC of reduction in the operation temperature of the ST field. This reduction is greater for ST systems operating at 70-90ºC (0.7%). Considering DH operational conditions with ATs in the range of 30ºC, the performance level of ST ststems can be improved by ~20%.

Also, by selecting the connection scheme withoun local storage (c), local heat losses in the storage tank are avoided.

All this can be converted in a 80-140% of increase in the heat output of the ST systems along the year. Even when considering that the cost of heat during summer times might be reduced by 30%, there is a substantial increase in the economic output, in the range of 60-100%.

Additional improvements can be achieved due to the professional operation of the DH connected ST system. Under this scheme, maintenance costs can be substantially reduced while at the same time better service level can be achieved.

Furthermore, with DH connected ST systems as those defined in this work, DH operators could potentially deliver Energy Services uner ESCO approaches. “Rent-Your-Roof” approaches, which are developped as investment-free alternative for the installation of PV in buildings, can then be applied to the installation of ST systems.

6. PROPOSED OPERATIONAL SCHEME

ST heat production and heat load curves are not coincident. During winter time, it can be expected that all ST will be used within the building. During summer time, heat production can be expected to be larger than heat needs within the building. For this reason, in order to utilize correctly the heat captured by the ST installation, this heat should be made available both at local level, and delivered to the DH network.

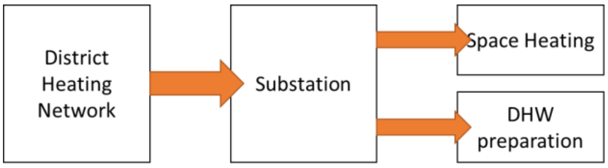

Heat delivery scheme in state of the art DH substations

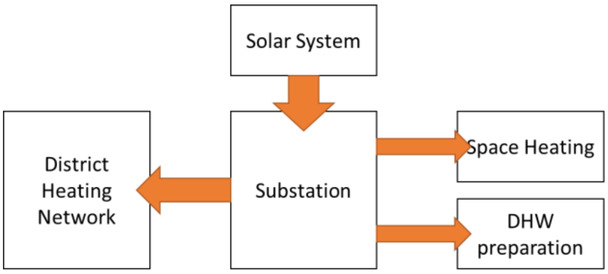

Proposed heat delivery scheme for ST energy

Considering this operational scheme, the integration of ST systems in DH, as proposed in this work, requires a heat purchase policy to be implemented by Dh operators. Bi-directional and/or net-heat metering devices should be installed in the substation.

7. LIMITATIONS OF CURRENT SUBSTATIONS

Currend DH substations are conceived for heat delivery from the DH into the building. Both for space heating and DHW. There are different configurations, depending on the use of direct/indirect methods for space-heating and DHW, but in terms of flexibility, all substations are operated in the same manner. Under these configurations, no bi-directional heat transfer is possible.

In order to propose suitable substations for the new operational scheme, the following items need to be considered:

- 3-service substations are required: Solar, Space heat, DHW
- Bi-directional and/or net heat meters are needed
- Reverse pumping needs to be incorporated in order to pump water from the return pipe back into the flow pipe
- Control needs to be coordinated with ST loop

8. ALTERNATIVE SUBSTATION DESIGNS FOR DH-CONNECTION OF ST

The proposed substation configurations are based on a 3-heat exchanger concept. Each of theser heat exchangers independizes on of the circuits within the building: Space Heating, DHW and ST system.

Depending on the configuration of each particular ST system, the solar part of the circuit can be configurated as required. Variations such as presurized/drainback systems, with water and/or thermal fluids, and pontential local storage are possible.

For Space heating and DHW, regular DH substation configurations are proposed. Again, depending on network and building particularities, DHW storage can be added.

2 configurations are presented which differ in the connection of the ST loop with the DH grid:

- 2-pipe configuration: ST is connected at high temperature
- 3-pipe configuration: ST heat can be delivered either at high or low temperature levels.

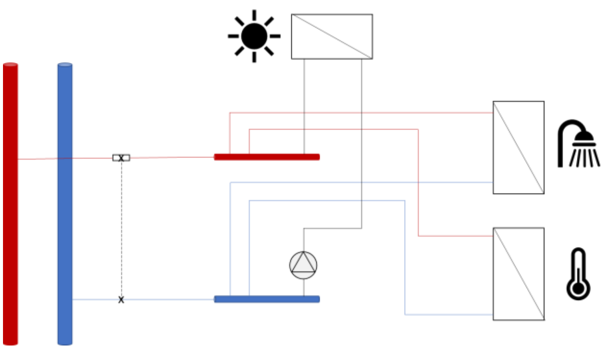

Proposed substation concept with a 2-pipe arrangement

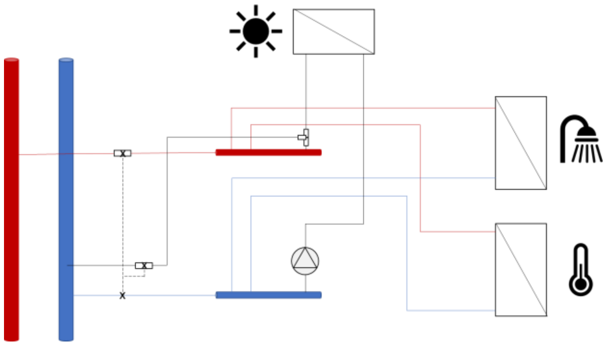

Proposed substation concept with a 3-pipe arrangement

The 2-pipe substation can in principle be used to connect ST systems into buildings with already-existing DH connections (2 pipe). Of course, an agreement would be required for energy billing with a net-metering approach.
3-pipe substations imply changes in the connection of the building to the distribution network. As such, it is only recommended for large buildings, or for situations where changes are expected in the network anyhow. In this case, a net-matering approach is followed for heat consummed/injected at high temperature, while a secondary meter is used to account for heat injected at lower temperature, potentially at a lower price.

9. CONCLUSIONS

The incorporation of distributed ST in DH networks presents a clear opportunity to de-carbonize heat production in such environments. At the same time, this kind of installations presents substantial benefits over issolated ST systems:

- Heat production is much larger
- Cheaper system, as thermal storage is no longer needed
- Provide better economic metrics due to the possiblity to sell excess heat
- ST systems are better commissioned

At the same time, these installations need to be promoted by DH operators, with the implementation of heat purchase strategies.

Substations need to be adapted to the new configuration, with additional heat exchangers for the ST system, net meters, and reverse pumping capacity.

10. FUTURE WORK

Substations for the connection of ST into DH networks will be developed within (RELaTED, 2017). Within this project, several substation concepts will be engineered, prototyped, tested and deployed over 4 pilot DH setups across Europe. Deployment of such devices is expected in 2019.

ACKNOWLEDGEMENTS

Research output presented in this paper has performed under project RELaTED (RELaTED, 2017). RELaTED project partners are: TECNALIA, Danish Technical Institute, Fortum Tartu, Beogradske Elektrane, Basque Government, Metro Therm, Nibe, Aventa, Industrias IMAR, Basque Energy Agency, Mazovia Energy Agency, Institute of Baltic Studies, FEDARENE, El Taller De Comunicación y CIA.

This project has received funding from the European Union's Horizon 2020 research and innovation programme under grant agreement No 768567.

REFERENCES

European Commission (2016), An EU Strategy on Heating and Cooling

Hadorn J. C. (2015), Solar and Heat Pump Systems for Residential Buildings, Wiley, Berlin.

Gavalda O., Gonzalez D., Carrera A., Garcia R. (2015), Análisis De Potencial Y Oportunidades De Integración De Energía Solar Térmica En Redes De Calor. Las Grandes Redes De Barcelona, IDEA, Madrid

Mauthner F., Herkel S. (2016), Classification and benchmarking of solar thermal systems in urban environments, IEA SHC Task 52.

Solar District Heating, Advanced policies and market support measures for mobilizing solar district heating investments in European target regions and countries, EU, GA nº691624, http://solar-district-heating.eu/

Werner S. (2017), International review of district heating and cooling, Energy 137, 617-631

Energy integration and performance evaluation of a new concept of advanced solar district heating/cooling networks for energy supply in buildings

Kane M., Grosjean S., Kaempf J.

Laboratory for Thermal Energy (LTE), Mechnical Engineering Department at the University of Applied Sciences and Arts of Western Switzerland, HES-SO, Pérolles 80 ▪ PO BOX 32 ▪ CH-1705 Fribourg, Switzerland, tel +41 (0)26 429 68 42 (direct)**, malick.kane@hefr.ch**

District heating (DH) networks are becoming an energy-saving and cost-effective alternative to conventional conversion systems (boilers, killers, combined heating and power systems) and appear as a vector of the energy transition because of the diversity of the energy sources that can be used for their operation. They are increasingly used in cogeneration and more efficiently when operating with lower temperature levels. Indeed, many previous works, carried out in several European countries, notably in Switzerland, Great Britain but also in countries such as Denmark and Sweden were able to demonstrate the application of renewable energy sources such as biomass, solar thermal and geothermal energy and / or waste heat recovery for DH energy supply. These works were carried out on traditional networks (eg steam, superheated water and/or hot water with temperature levels in general above 60°C), hence relatively high temperature levels compared to ones required for heating new and high-performance buildings (below 30°C). In addition to the linear thermal losses related to the high differential temperature between the networks and the environment, the heat transfer processes that occurred on the substations (decentralized heat exchangers connected to the network system to supply heat to buildings) are clearly inefficient with significant exergy losses.

Recent developments have led to so-called “anergic” networks operating at low temperature levels (~ 8/12 °C), which use decentralized heat pump (HP) substation units for heating and domestic hot water production. These HPs make it possible to raise the temperature to approximately 30°C for space heating and 55°C for the preparation of hot water. Such advanced networks have the advantage of being able to serve both for heating (in winter) and cooling (in summer). The performance of these heat pumps depends strongly on the temperature of the network.
The high differential temperature between the DH network and the level of energy supply for heating and hot water process in the building corresponds to an important consumption of electricity in the decentralized HP units.
The proposed study concern a new concept of advanced heating/cooling networks that operates with optimal temperature levels, using an intelligent centralized energy conversion unit able to integrate and manage different renewable and residual energy sources (solar thermal, geothermal and waste heat). In winter, the temperature of the DH network could be chosen higher than 30°C, thus enabling simple heat exchangers to be used for heating purposes. Compared to an “anergic” low-temperature network, only hot water production requires the use of decentralized heat pump units. The latter operate even more efficiently to raise the temperature up to more than 55°C (low temperature differential between sources of the heat pump). In summer, the temperature of the DH network could be reduced to a lower value (around 15°C), allowing to use the same heat exchangers for free-cooling the buildings.

A typical application for a set of high performance buildings in the BlueFactory district (Fribourg, Switzerland) has been considered. The demands for heating, cooling and electricity as well as the temperature of the required

hot water are first estimated for each building. It allows to determine the key parameters for the design and operation of the advanced heating/cooling network such as the pinch temperatures of heating and cooling, the nominal capacity of the network and the range of the working conditions (flowrates, minimum heating/cooling capacity). Hydraulic and thermodynamic models have been developed for all components in order to simulate different structures of advanced thermal networks where the performances in term of pressure drop and thermal losses on the pipes and exergy losses on the substations (heat exchangers and heat pumps for space heating and domestic hot water preparation) are determined in function of the temperature of the network. A general energy/exergy modelling have also been performed in function of the temperature to evaluate the various options of the substations in term of exergy efficiency. These different model results have then been applied: first to simulate the performance of a reference system based on an "anergic" low-temperature (8/12°C) advanced heating/cooling network; then to evaluate the influence of different local heat sources on the temperature of the network (solar thermal and geothermal contributions, waste heat recovery from the residual hot water); and finally to evaluate the required heat from the centralized EC unit to control the temperature of the network. Results show that an exergy efficiency of the substations units of more than 55% can be achieved for the proposed concept, reducing electricity consumption of about 20% compared to the "anergic" DH network.

IMPACT OF SOLAR SHARE ON OPTIMAL SUPPLY TECHNOLOGIES AND SEASONAL THERMAL STORAGE SIZE IN SOLAR DISTRICT HEATING SYSTEMS

Hrvoje Dorotić, Tomislav Pukšec, Neven Duić

University of Zagreb, Faculty of Mechanical Engineering and Naval Architecture

e-mail: hrvoje.dorotic@fsb.hr

ABSTRACT

District heating systems are on a way to the fourth generation of the district heating (4DH) systems which can merge different sectors such as: heating, cooling, power and transport. In addition to this, they can integrate various low-temperature renewable energy sources such as geothermal and solar. Due to the high interconnectivity of energy streams and various possible technologies, optimization of such systems presents a challenge which needs to be tackled. Solar district heating systems are well-known and proven technology in EU with solar shares reaching more than 50%, despite high related investment costs. In order to integrate solar energy and district heating systems, detailed analysis should be carried out in order to select the most suited combination of classical district heating supply technologies, thermal storage size and solar share. In addition to this, power-to-heat technologies are also present in these systems, therefore electricity market should also be taken into account. In this paper, relation of solar share on optimal supply capacities and seasonal thermal storage size in the solar district heating systems has been studied. Optimization was carried by using mixed integer linear programing, with the code written in MATLAB and solved by using SCIP solver which is part of Opti Toolbox, MATLAB add-in. The hourly based model is capable of optimizing capacities and one-year operation of supply technologies such as: electrical heater, heat pump, heat-only boiler, cogeneration and seasonal thermal storage, for specific solar share, i.e. solar thermal collectors' capacities. Objective function is defined as minimization of total cost of the system, which includes discounted investment and the overall running costs. This paper shows which technologies and capacities should be utilized in order to minimize investment and running costs for predefined heating demand and solar fraction of the solar district heating system. The impact of increased solar share on the total greenhouse gas emissions, levelised cost of heat, seasonal thermal storage and utilized technologies size has been presented. Furthermore, sensitivity analysis on solar collector type has also been carried out: the optimization procedure was performed for flat plate and evacuated tube collectors. In order to choose the most suited solution, decision making criteria has been modelled which takes into account economic feasibility and total environmental impact of the system.

Key words: solar district heating, optimization, mixed-integer linear programming, seasonal thermal storage

COMPARATIVE ANALYSIS OF BIOMASS/SOLAR DISTRICT HEATING SYSTEM IMPLEMENTATION IN DENMARK AND CROATIA

Borna Doračić[1], Jakob Worm[2], Tomislav Pukšec[1], Neven Duić[1]

[1] *Faculty of Mechanical Engineering and Naval Architecture, Department of Energy, Power Engineering and Environment, University of Zagreb, Ivana Lučića 5, 10 000 Zagreb, +385 1 6168242* [2] *PlanEnergi, Vestergade 48H, DK - 8000 Aarhus*

e–*mail:* borna.doracic@fsb.hr

ABSTRACT

District heating systems present a significant factor in reducing the primary energy consumption and the environmental impact of the European heating sector. The combination of biomass and solar district heating can be particularly interesting for existing district heating or new district heating for smaller rural cities, which mostly use individual heating solutions based on fossil fuels or biomass. Despite using biomass, most of the individual heating systems are old and do not use filtration, resulting in high emission of particles and significant health problems for the population in the area. Therefore, modern hybrid district heating solutions provide a clean, efficient and comfortable way of supplying renewable heat to the final consumer and contribute to the security of supply, price stability, local economic development, local employment, etc. These two energy sources complement each other in a way that solar heating requires no fuel, while biomass heating can store the chemical energy of fuel and release it during winter when solar irradiation is significantly lower. Moreover, it is beneficial and often crucial to integrate heat storage when designing such systems. For short term storage, buffer tanks can be used, but solar energy can also be directly stored during summer in seasonal pit/basins for long-term storage. Finally, the main benefits of this hybrid concept are that the biomass demand, as well as the maintenance needs of the biomass boilers are reduced.

Despite its substantial potential, there is a significant mismatch when it comes to the share of district heating in heat supply of European countries. While some countries, e.g. Denmark have already highly developed renewable heating solutions and a high share of district heating in the heat supply, others have a low share and mostly use fossil fuels. Croatia is one of these examples where only around 14% of heat is supplied by district heating and most of these systems are old and inefficient. Therefore, the main goal of this work was to demonstrate the feasibility of biomass/solar district heating implementation in a small rural town in Croatia, which currently only uses individual heating solutions. The heating system has been modeled in energyPRO tool and the output provided the optimal operation of the system on the hourly level. In addition, the comparison has been made with one Danish city in order to assess the importance of different framework conditions for successful implementation of such systems.

Key words: renewable district heating; biomass; solar; energyPRO; comparative analysis

THE MANY FACES OF SOLAR DISTRICT HEATING IN GERMANY

Laure Deschaintre, Oliver Miedaner, Thomas Pauschinger and Carlo Winterscheid
Steinbeis Research Institute for Solar and Sustainable Thermal Energy Systems Solites, Meitnerstr. 8, Stuttgart, 70563, Germany,
+49 (0)711 673 2000 - 0, info@solites.de

Abstract – This publication aims at giving an overview of the recent developments within the solar district heating (SDH) market in Germany. It focuses on the diversity of the technologies and business models implemented in the last years and offers an analysis based on concrete examples.

1. INTRODUCTION

Solar district heating can support the heat transition in Germany as well as at European level. For this reason, its development is supported by public funded projects:

- at national level with Solnet4.0 [1]
- at regional level with SolnetBW II in Baden-Württemberg [2], as well as in Thuringia and Hamburg within the European Horizon 2020 project SDHp2m [3]

Thanks to these projects, the developing market is closely monitored and analysed. The paper aims at presenting the specificities of the German market as well as perspectives of its development.

Solar district heating plants find application in a wide range of concepts and within very different boundary conditions. The main differences are:

- The type of connection to the district heating plant (centralized vs. decentralized feed-in) (see figure 1)
- The kind and the size of the district heating networks in which they are integrated. They range from districts or villages to large cities as supply areas.
- The type of operator of the plant

At European level, the largest market, by far, is Denmark. One of the main differences of the German market compared to the Danish one is the multitude of existing legal status of heat suppliers. Whereas Denmark has almost exclusively cooperative-owned district heating, in Germany operators are sometimes citizen cooperatives, but more often municipalities themselves, municipal utilities or private companies.

This variety, combined with technological specificities of the solar district heating plants, implies a large panel of possible business models. This paper will describe these different organizational and financial models based on concrete examples realized within the last years.

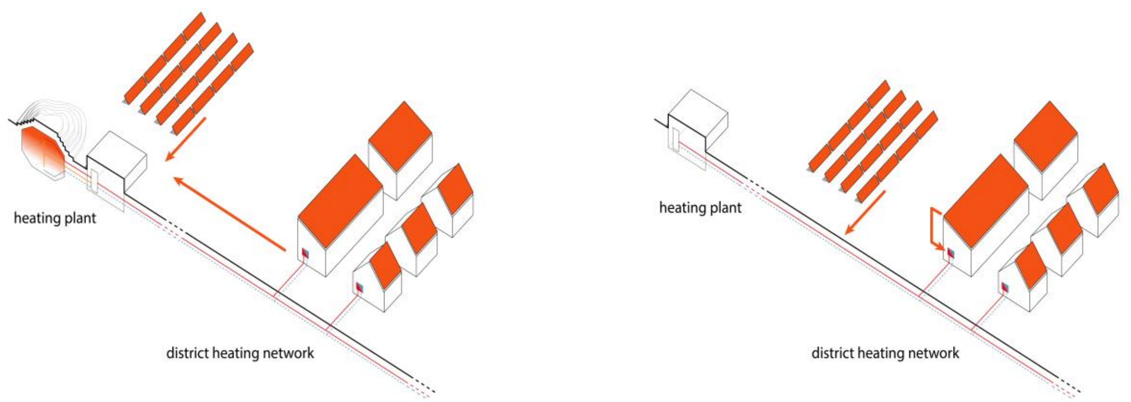

Figure 1: On the left, central solar district heating plants: the solar collectors deliver heat to a main heating central. On the right, decentralized solar district heating plant: the solar collectors are placed at suitable locations and connected directly to the district heating network on site.

2. THE GERMAN MARKET

Currently in Germany, 25 solar thermal plants with a nominal power of 35 MWth in total are connected to a district heating system. 8,8 MWth are in concrete planning or construction. Based on the good incentive situation, a doubling of the installed power can be foreseen in the next years. Between 1995 and 2012 eleven large-scale solar thermal plants were installed as pilot projects within the Solarthermie2000 and Solarthermie2000+ programs. These plants still represent a significant part of the plants currently installed in Germany. Since 2013 however, several new plants were built. A significant part is installed in rural areas, so-called "Energiedörfer", in which in general a solar thermal plant between 1000 and 3000 m² collector area is installed on the ground and combined with a biomass heating plant. The solar thermal plant covers herby the total summer load. Moreover, the plant erected in Senftenberg, Brandenburg in August 2016 represents an important milestone since the municipal utility of Senftenberg decided to build the 8 300 m² plant based solely on economic criteria. As of now, it is the largest solar thermal plant in Germany and feeds around 4 GWh annually into the city's district heating network with a total supply of 100 GWh. The plants that are currently in preparation aim for the integration of large collector areas over 10 000 m² in urban district heating networks. The map presented in Figure 2 allows locating the planned and existing plants and Figure 3 presents the market development from a time perspective.

2.1 SDH for villages and rural areas

District heating systems supplying heat to small cities and communities in rural areas allow a fast and comprehensive transition of the heat supply to local, renewable resources. For example, the combination of a large-scale solar thermal plant to cover the summer load and a biomass heating plant is an economically interesting concept to supply local networks with renewable heat.

In Büsingen, the 1 090 m² collector plant provides all the heat supplied by the district heating network in summer, avoiding an uneconomical part-time operation of the biomass boiler. The district heating net, in operation since 2013, provides 100 buildings with 100% renewable heat.

The district heating plant of Büsingen was built by the local energy supplier Solarcomplex, who also operates the plant. After this first experience, Solarcomplex decided to implement this successful model in further projects of "energy villages" in the region. They are realizing a second solar district heating plant in Randegg with 2 400 m² complementing an existing biomass plant. A plant with an expected area of 6 000 m² is also in planning in Schluchsee.

Figure 4: Solar district heating plant in Büsingen, source Solarcomplex

The model was also replicated further away from the Lake Constance region with the projects in Hallensdorf. In Hallensdorf, the operator is the green-electricity supplier Naturenergie AG. Operators can also be local utilities like the Stadtwerke Radolfzell who is building a plant in Liggeringen with 1 200 m², or the municipality itself like in Neuerkirch-Külz und Ellern.

In such projects, the involvement and participation of citizens are essential success factors. The economical feasibility of the project depends on the connection rate to the new district heating network. Sometimes, they are even themselves the motor of the change, as in Breklum and Mengsberg. Here the first citizen cooperative owned solar district heating plants are being built.

These projects have a positive impact on the economical development in the region. Furthermore, they are very efficient since they allow to completely turn the heat supply of the whole villages from a usually very low renewable energy part to 100% in a few years.

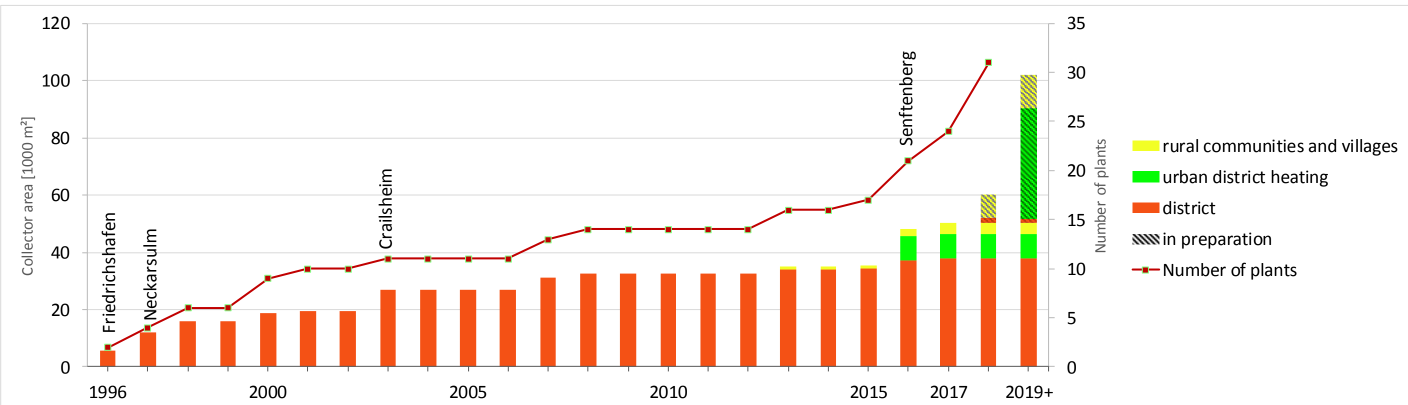

Figure 2: Development of solar district hating plants in Germany (accumulated) – Status September 2017 – Source: Solites

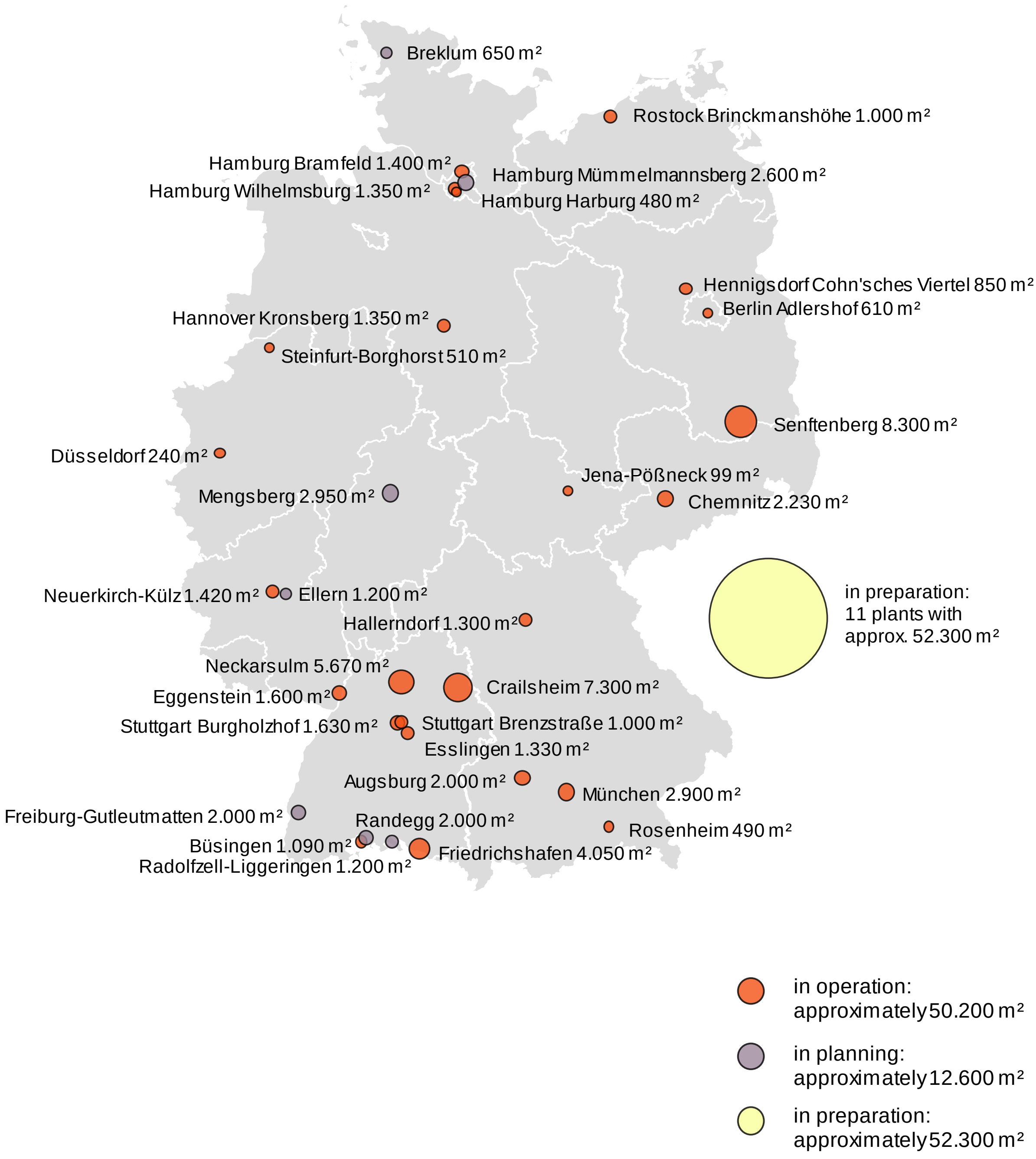

Figure 3: German solar district heating plants – September 2017 – Source: Solites

2.2 SDH in districts

In cases of renovation or new construction of urban quarters, local heating networks are a valid option for heat supply. Depending on the building type and equipment, such networks can be operated at low temperatures, which are favourable for integrating solar thermal plants. Such systems usually reach up to 20% solar contribution to the total heat supply but the integration of a seasonal heat storage can increase the solar fraction up to 50%.

In Crailsheim, the starting point was the refurbishment of a former military area. A high school and a sport facility were built, and the military buildings transformed in apartments. All the buildings are connected to a sub-district heating network, operated by the local utility. All in all, 7 300 m² solar thermal collectors are feeding into the district heating network. One part is integrated in the roofs of the refurbished buildings, and another part is mounted on the nearby noise protection wall (figure 5). They are combined with a buffer tank storage of 400 m³ and a borehole thermal energy storage of 37 500 m². The solar fraction over the year is 50%.

Figure 5: Solar district heating plant in Crailsheim

2.3 SDH in cities and urban areas

Large urban district heating systems are usually operated with heat from combined heat and power plants, heating plants or industrial waste heat. Sometimes, decentral integration of large-scale solar thermal plants can be a suitable choice to increase the share of renewable energy sources if areas are not available close to the heat central.

In Senftenberg, Brandenburg, the largest solar thermal plant of Germany with 8 300 m² solar thermal collectors area was inaugurated. It should deliver 4 GWh to the district heating network every year. The area of 2.2 hectares where the plant is built is located on a previous waste disposal site of the City of Senftenberg, where the recultivation process ended last year.

In Berlin Adlershof, a plant is in operation since 2017 on the roofs of two out of five newly built buildings with a very interesting business model. Every kWh of solar heat which is not needed in the buildings is fed into the district heating network and accounts for one kWh that will be delivered by the district heating network in the winter. The 613 m² evacuated-tube collectors produce more heat over the year than the heat consumption of the five buildings, even if only two of the roofs are covered. The surplus heat is free for the district heating operator. On the other hand, the housing company has a guarantee that it does not need to buy heat and can define a relatively cheap fixed rent including heat costs. Thanks to the fact that the network is used as storage, only 10 m³ of storage volume is needed for the five buildings. As soon as these are loaded, the additional heat is fed into the district heating network.

2. GERMAN FRAMEWORK

Some German regions have recognized the potential of solar district heating and actively promote its development, via favourable policies and financing possibilities.

Baden-Württemberg has its own incentive programme and strategy name [4,5] and supports its own market development projects with SolnetBW II. The objective of the project is to increase the application of solar district heating networks in Baden-Württemberg. Therefore, the project partners want to work together with local stakeholders within ‘real labs’, e.g. on removing barriers regarding the availability of land areas, on energy and economic system analysis issues, on knowledge transfer to planners and project developers, etc.

The region Thuringia is involved as partner in the SDHp2m from policy to market project and is implementing supporting measures at policy level as well as developing favourable incentive frameworks. Also

Hamburg is one of the target region of the project and addressing the issue via market development activities.

Several further regions have shown interest to become active in this field.

At national level, the incentives available for the construction of SDH plants are very interesting.

The MAP (Marktanreizprogramm) of the Federal Ministry of Economic Affairs and Energy aims at promoting measures for the use of renewable energies in the heat sector. It includes the following incentives:

- Solar thermal plants larger than 40 m² feeding their heat into district heating networks receive up to 40% of the investment costs. Alternatively the performance related incentive for solar thermal plants can be chosen: The yearly collector yield (according to the Solar Keymark certificate) is subsidized as one single investment support with 0,45 €/kWh. The subsidy is limited to 45 to 65% of the investment by the "Allgemeine Gruppenfreistellungsverordnung (AGVO)".
- Existing district heating networks using mainly heat from renewable energies receive 60 €/m and 1800 € per substations
- Thermal heat storages larger than 10 m³ mainly used by renewable energies receive 250 €/m³

Since the 1st of July 2017, the German Ministry for Economic Affairs and Energy has established a new subsidy scheme for 'District Heating Pilot Projects 4.0' ("Wärmenetze 4.0"). In order to get funding, district heating networks have to cover at least 50 % of the annual heat consumption from renewable energy sources or waste heat.

A district heating network 4.0 has a maximum supply temperature of 95°C. Innovations like long-term thermal energy storages or coupling of the electricity and heat sector via large heat pumps or electric boilers are promoted. Via a fundamental orientation towards low-temperature district heating networks, the German Federal Ministry for Economic Affairs and Energy aims at enabling a large range of technologies. Support is foreseen for so-called cold district heating networks with 20°C supply temperature as well as for classic district heating systems as long as the supply temperature does not exceed 95°C. However, no more than half of the renewable heat supply should be generated from biomass. Therefore, most of the projects realized so far with 20% of solar heat and 80% of biomass wouldn't be eligible as pilot project in the framework of this new funding guideline.

The objective at political level is to prove the economical and technical feasibility in at least twelve cases thanks to feasibility studies. Moreover, at least six district heating networks should be built or fundamentally transformed by 2020. The district heating networks should have at least 100 connections or a minimum heat supply of 3 GWh per year.

Cost efficiency has high priority: The heat supply from supported networks should be as competitive as heat supply from fossil fuels. Support is foreseen for new construction or transformation of existing networks but low-temperature sub-networks are also eligible. Two stages are planned. In a first step, feasibility studies are supported up to 60% (max. 600 000 €). In a second step, the realization of the networks can be financed up to 50 % (max. 15 millions). In addition, an allowance up to 80% for information activities (max. 200 000 €) to potential users is foreseen, in order to reach a high connection rate. Moreover, the participation of local research organizations is sponsored up to 100 %.

The gradation of the subsidy is new. The district heating grid gets a subsidy of 20 % (or 30 % if the applicant is a Small or Medium Enterprise). In addition, there is a 'sustainability bonus' of up to 10 percent: One can receive 0,2 % for every full percentage point of renewable energies or waste heat fraction exceeding the minimum requirement of 50 %.

Another innovation is the 'cost efficiency bonus' for especially low heat prices. If the heat price falls below 10 cents per kilowatt hour, this bonus increases step by step. For a heating price of only 5 cent the maximum subsidy of 10 % of eligible costs would be reached. Long-term thermal energy storages are considered standard for district heating networks 4.0 unless it can be demonstrated that their implementation in the system is not economically feasible.

3. PERSPECTIVES

The Federal Ministry for Economic Affairs and Energy, published the EGS „Energieeffizienzstrategie Gebäude" in November 2015. The scenario implies a constant contribution from district heating networks until 2050 of 80 TWh/a for the heat production in Germany. Meanwhile, the contribution from solar thermal energy, including individual systems, industrial applications and district heating application, should increase from 3 TWh/a in 2008 to 80 TWh/a.

Considering a fraction of solar thermal in district heating networks from 15%, the contribution of solar thermal in this application would be 12 TWh/a. In order to reach this, a total collector area of 30 millions m² installed on a land area of round about 7500 acres would be necessary, corresponding to a total capacity installed of 21 GW until

2050. Yearly, the construction of around 1 million m² per year is therefore necessary.

This paper shows that solar district heating is developing in many different sectors and showing an encouraging trend in the last years and in the previsions. Still many efforts are necessary to reach the ambitious and challenging aims outline above.

REFERENCES

[1] Solnet4.0- Innovative Lösungs- und Entwicklungskonzepte zur Marktbereitung für solare Wärmenetze, FKZ 03EGB0002A

[2] SolnetBW II – Solare Wärmenetze für Baden-Württemberg, Baden-Württemberg Programm Lebensgrundlage Umwelt und ihre Sicherung (BWPLUS) ‘Transformation des Energiesystems in Baden-Württemberg – Trafo BW‘, BWT17005, www.solnetbw.de

[3] SDHp2m – Solar District Heating, from policy to market – Horizon 2020 under grant agreement number 691624

[4] Förderprogramm Energieeffiziente Wärmenetze des Landes Baden-Württemberg, Feb. 2016, www.um.baden-wuerttemberg.de

[5] Solar district heating in Baden-Württemberg – Overcoming barriers and market introduction within the project SolnetBW, O. Miedaner, Solites and H. Böhnisch, KEA, Conference proceedings, 4th International solar district heating conference in Billund, 21-22 September 2016

SUPPORTING POLICY FOR SOLAR DISTRICT HEATING AS A COMPONENT OF THE THERMAL ENERGY TRANSITION IN THURINIGA

Dr. habil. Martin Gude and Aline Isabel Kornmann
Thuringian Ministry for Environment, Energy and Nature Conservation, Beethovenstraße 3, Erfurt, 99096, Germany,
Phone Number: +49 (361) 57-3911336, Fax Number : +49 (361) 57-3911302, e-mail address:
Aline.Kornmann@tmuen.thueringen.de

Abstract – This paper describes the supporting policy for solar district heating as a component of the thermal energy transition in Thuringia, Germany. To contribute to the internationally stated climate protection targets at local level, Thuringia is pursuing a double strategy and focussing the reduction of heat demand and the increase of heat production from renewable energies. An examination of the heat supply system, which is dominated amongst others by district heating systems, showed that the potentials of geothermal and solar thermal energies are not tapped yet. Currently, in Thuringia one pilot solar district heating plant is in operation while other projects are under examination or conception. Supporting policy for solar district heating in Thuringia has different levels: Currently the State Government is discussion and voting over a Draft Law of the Thuringian Climate Law, which could set concrete climate protection targets with respect to greenhouse gas emission reduction potentials within the heating sector. Furthermore the State Government is discussing a Draft of an Integrated Energy and Climate Strategy that contains concrete measures to tap the greenhouse gas emission reduction potentials of the heating sector in Thuringia. Additionally, several supporting services for stakeholders are or will soon be available in Thuringia, such as a Solar Calculation Tool, information handouts and a supporting service at the Thuringian Energy- and GreenTech-Agency (ThEGA).

1. INTRODUCTION

Thuringia may contribute to the internationally stated climate protection targets at local level. Therefore it is necessary to promote the “Thermal Energy Transition” as an essential part of the “Energy Transition” at political level. To take advantage of the greenhouse gas emission reduction potentials the heating sectors bears for a “Thermal Energy Transition” Thuringia is pursuing a double-strategy: not only the overall heat demand should be reduced, but the share of renewable energies and efficient technologies on the heat supply should be increased as well.

2. SOLAR DISTRICT HEATING IN THURINGIA

An examination showed that the regional heat supply system in Thuringia is dominated amongst by natural gas and oil boilers also by district heating systems and is rather heterogeneous. Moreover, the examination showed that in 2010 the share of renewable energies on the heat supply in Thuringia already has been significantly higher than in Germany.

An essential part of this heat from renewable energies has been supplied by biomass (about 85%), which potentials in Thuringia are nearly exploited. However, the potentials of other renewable energies, such as geothermal and solar thermal energy are not tapped yet. Due to this, and Thuringia’s settlement structure with lots of rural areas, combining biomass and solar thermal in district heating systems could be one promising approach to increase the share of renewable energies within the heating sector. Furthermore, Thuringia’s cities have a high share of multiple dwelling units, which often are either already connected to the cities district heating grid, or could possibly get connected to a local grid, integrating solar thermal collectors on their roof areas. Beside these two promising approaches, the Thuringian Ministry of Environment, Energy and Nature Conservation (TMUEN) is pursuing several activities to support the market roll-out of renewable energy sources and solar district heating by addressing different target groups and following different approaches. The participation as a Level A-partner within the EU Horizon 2020-project “SDHp2m” is underlining these activities.

Currently, in Thuringia one pilot solar district heating plant in Jena-Pößneck is in operation, while other solar district heating-projects are under conception and several feasibility studies concerning the integration of renewable energies within the heating system at regional level are in progress.

3. POLITICAL FRAMEWORK

Already in 2014 the Thuringian Solar Thermal Initiative was founded and a funding of decentral photovoltaic and solar thermal plans as well as energy storage systems was established.

Since 2014 the Thuringian energy and climate politics concerning solar district heating has been developed further and the following key points of the regional policy are supporting renewable energy sources and solar district heating:

3.1 Climate Law

In 2017 the Thuringian Ministry of Environment, Energy and Nature Conservation (TMUEN) has developed a Draft Law of the Thuringian Climate Law, which was accepted by the State Government after two interdepartmental coordination processes and finally handed over to the State Parliament for further discussion and voting over it in January 2018.

The Draft Law of the Thuringian Climate Law, which is under discussion within the State Parliament since February 2018, could build, when getting accepted by the State Parliament, an essential part of the present energy politics of Thuringia concerning renewable energy sources and solar district heating amongst others. The Draft Law of the Thuringian Climate Law is containing for example the following cornerstones:

- Reduction corridors for greenhouse gas emissions of 80 to 95% until 2050 with respect to the greenhouse gas emissions in 1990
- Reorganization of the regional energy supply system to 100% renewable energies on a yearly balance until 2040
- Role model function of public administration, especially climate neutrality for state department by 2030
- Development of regional climate concepts, heat analysis or heat concepts by municipalities
- Development of supply concepts by municipal utilities
- Transition to a climate-neutral building stock until 2050
- Climate adaption measures

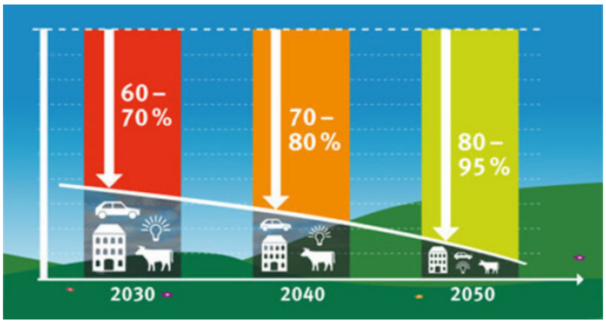

Figure 1: Greenhouse gas emission reduction target corridors within the draft of the ”Thuringian Climate Law” (base year 1990)

The Climate Law is focusing amongst others the greenhouse gas emission reduction potentials of the heating sector. These potentials of the heating sector should be tapped through cooperation with regional stakeholders:

Following the Draft Law of the “Thuringian Climate Law”, municipalities could develop heat analysis and heat consumption concepts. Administrative districts and municipalities could develop or update existing climate protection concepts, which would contain aspects of heat analysis and heat consumption concepts as well. These climate protection concepts should describe, how greenhouse gas emissions could be reduced and the usage of renewable energies be extended. Furthermore, heat analysis for municipalities should contain an analysis of heat consumption and available heat sources. Heat concepts should contain measures for reducing heat demand and the expanding of renewable energies. In this manner, options for actions or concrete projects at local level might arise.

Furthermore, operators of district heating networks would have to develop concepts for their local heat supply system, to meet the targets of the transformation of the Thuringian energy supply system up to a mix of 100% renewable energies on a yearly balance until 2040. Implementation steps have to be part of these concepts, which need to be updated at the latest every ten years. District heating network operators have to publish product information for consumers (share of renewable energies) as well as information about the environmental impact (carbon dioxide emissions and primary energy factor) of their heat supply system.

Building owners, with regard to their economic conditions, would have to ensure that the particular heat demand of a building will be covered from renewable energy sources by 25% by 2030 to reach the persuaded climate neutrality of the consumption sector of existing buildings. This target might be reached through a connection to a district heating network providing more than 25% heat from renewable energy sources.

These actions should lead not only to energy savings and increasing energy efficiency within the heat supply system but to an increasing share of renewable energy sources within the heat supply system.

While the Draft Law of the Thuringian Climate Law specifies climate protection targets, it does not describe a step-to-step proceeding to meet these targets set. Therefore, the development of an Integrated Energy and Climate Strategy that will collect concrete measures is foreseen within the Draft Law of the Thuringian Climate Law.

A draft of the Integrated Energy and Climate Strategy was under development in 2017 within cooperation with regional stakeholders and experts in a broad public discussion.

3.2 Integrated Energy and Climate Strategy

Involving regional stakeholders and the general public, a draft of the Integrated Energy and Climate Strategy (IEKS) that will collect concrete measures to foster the realization of the targets set within the Draft Law of the Thuringian Climate Law was under development in 2017. Within two workshop-series with experts and taking into account the general public as well as representatives of institutes and associations personally and online the draft of the Integrated Energy and Climate Strategy has been developed step-by-step.
The final draft has been handed over to the State Government for further discussion in January 2018.

Content-related, renewable energy sources district heating is taken into account here as well. The field of action „energy supply system" contains the following measures that could help to reach the climate protection target set within the Draft Law of the Thuringian Climate Law:

- Development of concepts for a CO2-neutral heat supply system for public district heating systems and transparent product information
- Support for the expansion of local heating grids with renewable energies
- Development of a Coordination Unit and Forum for Dialog concerning the Energy Transition in Thuringia
- Pilot projects for the transition of a district heating system from high temperatures to low temperatures
- Development of a strategy concerning the energy supply system stability and the integration of options for flexibility including integrated energy
- Improvement of financing conditions for the development of renewable-energy-projects, energy-efficiency-projects, combined heat and power-projects and excess heat-projects
- Pilot project for the integration of geothermal energy in hybrid systems
- Continuation and further development of the incentive Instrument SolarInvest
- Provisioning of state-owned areas for the exploitation of renewable energies

3.3 Financing and Funding

In Thuringia three funding programs, that complement with national funding programs concerning solar district heating directly and indirectly are already existing or under development. The funding programs GreenInvest, KlimaInvest and SolarInvest, that are addressed to different target groups due to different focusses, presently are available in Thuringia:

- Within the GreenInvest program, companies can receive funding for advice services, feasibility studies and exemplary investments in projects with renewable energies and energy efficient technologies targeting at a greenhouse gas emission reduction with up to 80%. Obligatory condition is a pilot character of the measures.

- Within the KlimaInvest program, municipalities can receive funding for the development of greenhouse gas emission reduction or heat concepts with up to 40%. Advice services and professional trainings can be promoted with up to 80%. Furthermore, municipalities can receive a 100% funding for a 7500 € climate protection-starter package, such as initial advice services.

- Within the SolarInvest program for example municipalites, companies, housing cooperatives and citizen cooperatives can receive funding for investments in heat storage systems and correlating advice service and feasibility studies, amongst others. Citizen cooperatives can receive funding for investments in heat storage systems with up to 40%, all other target groups can receive funding with up to 20%. Advice services are supported with up to 80% funding.

Furthermore a funding program of the Thuringian Ministry of Infrastructure and Agriculture (TMIL) concerning investments in district heating systems with renewable energies in rural areas is under coordination.

4. TOOLS, MANUAL AND CONSULTING

Several tools, that can support stakeholders with developing and implementing renewable energy sources and solar district heating projects, are under construction:

4.1 Tools

In 2017 a webbased software application called Thuringian Solar Calculator has been developed and will be launched in 2018. This tool aims at an increasing generation of heat and power from solar energy in Thuringia in general. It should support different user groups, such as house owners, planners, municipalities or companies to exploit the potentials of solar energy by identifying potential areas for installing solar thermal collectors or photovoltaic modules on any roof or open area in Thuringia. Identification of potential areas for the exploitation of the potentials of solar energy contains calculations of the yield and the economics of possible solar energy plants in Thuringia.

Concerning solar district heating, beside roof areas also any open area in Thuringia can be chosen for calculations by marking a certain polygon-shaped area manually. The allocation of this area with solar thermal collectors runs automatically but adjustments such as adding, removing or shifting collector modules can be taken into account.

Also the type of solar thermal collectors (flat plate or vacuum tube collector) can be chosen for calculations. Solar yield and costs for investing are calculated and results can be printed and saved as PDF-document.

A detailed concept for public relation activities in May and June 2018 has been developed in cooperation with the Thuringian Energy- and GreenTech Agency (ThEGA) to inform potential users as well as multipliers about the implementation of the "Thuringian Solar Calculator". This concept includes for example the offer of information events and workshops, the printing of leaflets and brochures and the presentation of the "Thuringian Solar Calculator" online and at fairs.

Furthermore it is important to support stakeholders with the usage of the "Thuringian Solar Calculator". On this account, the "Thuringian Solar Calculator" will be linked to the "Servicestelle Solar" (Solar Service Center) at the Thuringian Energy- and GreenTech Agency (ThEGA), which offers practically oriented consulting e.g. for municipalities, citizen and companies concerning the identification of potential areas for implementing solar thermal and photovoltaic plants, correlating business models and subsidy possibilities.

Furthermore, a webbased waste heat cadaster for Thuringia has been launched in May 2017, where possible sources of excess heat are listed and located. This tool should foster the integration of excess heat in the heat supply system and could build a further starting point for renewable energy district heating.

Finally, a webbased system for heat energy analysis of quarters is currently under development and will be a helpful tool for municipalities, planners or municipal utilities to analyse the local heat demand and identify local renewable energy sources for heating by comparing economic aspects of different technical solutions.

4.2 Manual "Future Sun!"

The brochure "Future Sun!" was developed with regional stakeholders and experts and is available online and printed. It contains a question-answer-catalogue as well as three case studies concerning solar district heating and can give interested stakeholders an overview on technical, organizational and juridical aspects of solar district heating.

4.3 Consulting

Beside information material such as the manual "Future Sun!", also consulting service dealing with renewable energies is available in Thuringia:

The Thuringian Energy- and GreenTech-Agency (ThEGA) builds the point-of-contact for technical questions related to energy and climate topics in Thuringia. Stakeholders can receive consulting and further information in topic-related workshops and events. So, the Thuringian Energy- and GreenTech-Agency (ThEGA) is supporting and connecting stakeholders.

For example, the Thuringian Energy- and GreenTech-Agency (ThEGA) is offering an advice service for representatives of municipalities concerning energy management and renewable energies in their municipal buildings.

Moreover, currently the "Solar Service Center" with respect to the well settled and successful "Wind Service Center" is under development at the Thuringian Energy- and GreenTech-Agency (ThEGA). The "Solar Service Center" offers consulting and support in connection with the topics of solar thermal and photovoltaic and its establishment is linked to the development of the "Thuringian Solar Calculator", which will be maintained and announced by the Thuringian Energy- and GreenTech-Agency (ThEGA).

5. CONCLUSIONS

The Thuringian Ministry of Environment, Energy and Nature Conservation (TMUEN) is pursuing several activities to support the market roll-out of renewable energy sources and solar district heating by addressing different target groups and following different approaches.

So, the stakeholders in Thuringia currently receive support at several levels: political, financial and content-related support for developing solar district heating projects is available. Still, it is foreseen to intensify activities concerning information and advice services to stimulate further demonstration projects.

Especially low prices for gas and oil are high barriers for an implementation of solar district heating. And beside this, concerning the market roll-out long and intensive planning processes are necessary and include several barriers for stakeholders. To overcome these barriers, stakeholders need to get supported in different fields, as described.

REFERENCES

IFOK GmbH und Leipziger Inistut für Energie GmbH (2017) *Zwischenbericht zur Erarbeitung der IEKS.*

Thüringer Landesregierung (2017). *Thüringer Gesetz zum Klimaschutz und zur Anpassung an die Folgen des Klimawandels (Thüringer Klimagesetz – ThürKlimaG). Gesetzentwurf der Landesregierung.*

Wesselak, V. et. al. (2013) *Energiemonitoring für Thüringen. Abschlussbericht 2013.*

SDH MARKET SUPPORT IN THE FRENCH REGION AUVERGNE-RHONE-ALPES

Mathieu Eberhardt, Auvergne Rhone-Alpes, 18 rue Gabriel Peri, 69100 Villeurbanne, France

F: +33(0)4 72 56 33 57, e-mail: mathieu.eberhardt@auvergnoerhonealpes-ee.fr

Most European regions have defined ambitious objectives for the reduction of greenhouse gas emissions and the transition of their energy systems.

The regional council of Auvergne-Rhône-Alpes has adopted in 2014 a Regional Scheme on Climate, Air and Energy, which sets up targets regarding the development of renewable energy sources. For instance, the main objective is to achieve 29.6% of RES in final energy consumption by 2020. Heat consumption represents more than the half of the total energy consumption so developing RES DHC is a relevant action to achieve this goal.

The regional council and its Regional Energy Agency are involved in the European H2020 project named SDH p2m. This project, started in 2016, gives the opportunity to implement advanced policies and market support measures for mobilizing solar district heating in Auvergne-Rhône-Alpes.

The objective of the presentation will be to show how to develop solar district heating in region through the SDH p2m project.

Many actions have been implemented like the mobilization of relevant stakeholders through a regional committee, the implementation of framework improvements and the mobilization of projects and investments.

The flagship actions and the first results of the project will be presented during the conference. It includes:

- Better access to financing
- Study case on 3 existing DHC
- Tool box for professionals
- Local authorities network animation (TEPOS)

PREFERENCES FOR DISTRICT HEATING IN EUROPE RESULTS FROM AN EUROPEAN CROSS-COUNTRY STUDY

Adriano Profeta and Thomas Krikser
PROKRIBUS GmbH, Kniegasse 23,
37213 Witzenhausen, Germany, Phone: +49 5531/8140643, Mail: profeta@prokribus.de

Sebastian Grimm and Heiko Huther
AGFW Projekt GmbH, Stresemannallee 30,
60596 Frankfurt/Main, Germany, Phone: +49 69/6304-200, Mail: s.grimm@agfw.de

Abstract – Space heating demand accounts for a large fraction of the overall residential energy demand. For example, private households in Germany consumed about 1570 PJ for heating in 2015. Recent policy goals for energy efficiency and GHG emission reductions require specific (policy) measures in building new houses and renovating existing houses. To develop efficient and tailored policy measures, it is crucial to understand the key determinants and heterogeneity of these choices. In this context the expansion of district heating is often mentioned as one option for becoming more independent from fossil fuels. In this paper we focus on private consumers and municipalities preferences for district heating from renewables. The results show that district heating was favoured over the other studied main heating alternatives. Our results indicate that in Germany, France and Austria the private consumers prefer district heating in comparison to other heating options. Furthermore, if the district heating stems from renewables the private consumers are willing-to-pay a tremendous additional price premium 2.90 to 3.60 € variable costs (per m^2 and year). Likewise, the municipalities have the WTP for district heating from renewables in all analysed countries.

1. INTRODUCTION

The heating system is an essential component of the maintenance and improvement of comfort in the home, as heat energy is required for heating rooms, incoming air and household water. Space heating demand accounts for a large fraction of the overall residential energy demand. For example, private households in Germany consumed about 1570 PJ for heating in 2015. This amounts to more than 69% of the total final energy demand for residential purposes (AGEB, 2016). In Germany, residential heat supply is mainly based on the two fossil fuels, heating oil and natural gas. According to German federal ministry for economic affairs and energy (2018), in 2016 about 46.7% of the existing homes were using gas for heating, while about 24%, had an oil-based residential heating system (RHS). Moreover, 44.4% of the newly built homes were equipped with a gas-fired RHS (BDEW, 2017). Due to this important role of oil and gas, residential heating is strongly linked to policy considerations related to global warming, the security of energy supply, and increasing energy prices.

At the societal level, studies have emphasized the potential for renovations to reduce greenhouse gas emissions (GHG). Recent policy goals for energy efficiency and GHG emission reductions require specific (policy) measures in building new houses and renovating existing houses. To develop efficient and tailored policy measures, it is crucial to understand the key determinants and heterogeneity of these choices. In particular, old houses with oil boilers represent a significant potential for the replacement of non-renewable fuel with some alternative heating system or fuel with lower GHG emissions. In 2017, 0.49 million Germans indicated to renovate their private heating systems within the next two years. Another 1.26 million are thinking of renovating but the final decision has not already been made (VuMA 2018). Therefore, existing houses represent a significant potential source of emission reductions compared to new house construction. In this context the expansion of district heating is often mentioned as one option for becoming more independent from fossil fuels. In general district heating is becoming more important in Germany. Whereas in the year 2000 only 7% of all new constructed private building were supplied by district heating this value increased to 24% in 2016 (BDEW, 2017). From many experts district heating from renewables is seen as one important path for decarbonising the EU energy system (Connolly et al., 2014).

In this paper we focus on private consumers and municipalities preferences for district heating from renewables. The term private consumers comprise homeowners as renters as well. We applied a so-called Discrete-Choice-Experiment (DCE) for comparing different heating alternatives (district heating from fossil fuels, district heating from renewables, heat pump and gas condensing boiler). The DCE-method allows a detailed analysis of consumer and municipalities preferences for the different heating alternatives. From the result the additional willingness-to-pay a price premium for district heating from renewables can be calculated.

In previous studies employing choice modelling, customer, home and spatial characteristics have been emphasized, while the heating system attributes have mostly been excluded due to issues with data availability. Furthermore, these studies mostly rely on ownership data; in such cases, choice is understood as ownership or availability rather than the actual purchase of a heating system. For example, Vaage (2000) and Braun (2010) analyzed the determinants of (actually) owning the heating system, using Norwegian and German cross-sectional household data, respectively. However, there is a growing body of literature including system attributes in the choice models (e.g. Willis et al. 2011). Jaccard & Dennis (2006) incorporated the estimated key parameters (discount rate, intangible costs and degree of heterogeneity) from the choice model into an energy-economy policy model.

Our study extends previous works employing choice modelling by explicitly presenting environmental impacts for each labelled heating system as absolute emission levels and customizing the choice sets according to the availability of district heat. Utilizing our choice modelling results, we then aim to simulate the willingness-to-pay for different heating systems.

2. Material and Methods

2.1 Questionnaire and sampling

The amount of examined alternatives and attributes is rather limited in CE studies as individuals cannot consider too many of them at the same time. Hence, we began discussions with experts to determine the most relevant main and supplementary heating technologies available today and the most important attributes with what we could describe these technologies in a realistic way.

In this study, the objective is to examine preferences of individuals and municipalities who are or will potentially making heating system decisions. Correspondingly, the relevant population for this kind of investigation includes all individuals who are building or planning to build a new detached house as well as homeowners who are replacing or planning to replace their existing heating system as well as renters who consider the heating system and the associated costs when they are looking for a new flat (i.e. all adult Germans potentially belong to this group). Furthermore we analyse the preferences of the municipalities too due to the fact that they have a decisive impact on the urban planning.

The consumer sample of the survey was drawn from an online-panel from the company respondi. For Germany 490, for France 490 and for Austria 520 respondents completed the survey. The municipality data used were acquired from a questionnaire mailed to all German municipalities. Approximately 3 weeks after the questionnaire had been sent, a follow-up reminder (including a copy of the questionnaire) was sent to non-respondents. A total of 274 replies for Germany. In Austria and France the questionnaire was sampled by partners of the Horizon 2020 project SDHp2m. In this way 23 questionnaires for Austria and 39 questionnaires for France were received. Tables 1 to 3 presents descriptive statistics for our sample.

Table 1. Demographics of end-users, municipalities in Germany

Consumers (490)		Municipalities (n=274)	
Gender			
Male	49.2%		
Female	50.8%		
Income		Party affiliation of mayor	
< 1,300€	21,2%	Independent	38.3%
1,300-2,600€	36.9%	CDU/CSU	32.6%
2,600-3,600€	23.5%	SPD	18.9%
3,600-5000€	12.4%	Others	10.2%
>5,000€	5.9%		
Age		Position	
18-30	22.5%	Mayor	22.6%
31- 45	26.4%	Administration	19.2%
46-65	43.1%	Administration	43.7%
> 65	8%	Others	14.5%
Place of residence		Place	
Small town	16.4%	Small town	36.4%
Small city	19.8%	Small City	37.5%
Medium city	22.9%	Medium City	18.9%
Big City (<100k)	18.8%	Big City (> 100k)	7.2%
Big City (> 100k)	22.1%		

Table 2. Demographics of end-users, municipalities in Austria

Consumers (n=520)		Municipality (n=23)	
Gender			
Male	49.2%		
Female	50.8%		
Income		Party affiliation of mayor	
< 1,300€	20,8%	ÖVP	65.2%
1,300-2,600€	37.1%	SPÖ	30.4%
2,600-3,600€	22.5%	Not indicated	4.3%
3,600-5000€	13.8%		
>5,000€	6.3%		
Age		Position	
18-30	27.5%	Mayor	9.1%
31- 45	36.7%	Administration	45.4%
46-65	32.0%	Administration	36.4%
> 65	3,8%	Others	9,1%
Place of residence		Demographics	
Small town	34.0%	Small town (pop.	27.3%
Small city	17.9%	Small City	27.3%
Medium city	9.2%	Medium City	0%
Big city	15.0%	Big City	45,5%
Big city	23.8%		

In addition to questions on socio-demographic characteristics and agreements with statements on energy and heating systems, a discrete choice experiment (DCE) for heating systems was included in the questionnaire. After the DCE, respondents were asked about their current heating system, whether they had replaced the original heating system in the last years and whether they had any plans to replace or renovate the current primary heating system in the future.

Table 3. Demographics of consumers and municipalities in France

Consumers (n=490)		Municipalities (n=39)	
Gender			
Male	52.2%		
Female	47.8%		
Income		Party affiliation of mayor	
< 1,300€	14,7%	Independent	33.3%
1,300-2,600€	38.0%	LR	20.5%
2,600-3,600€	24.9%	PS	5.1%
3,600-5000€	15.9%	Others	15.4%
>5,000€	6.5%	Don't know	25.6%
Age		Position	
18-30	10.6%	Mayor	35.9%
31- 45	32.7%	Administration	10.3%
46-65	46.7%	Administration	25.6%
> 65	10%	Others	28,2%
Place of residence		Demographics	
Small town	35.7%	Small town	64.1%
Small City	22.4%	Small City	25.7%
Medium City	23.5%	Medium City	7.7%
Big City	7.8%	Big City	2.6%
Big City	10.6%		

The DCE of heating systems was conducted using 12 hypothetical choice sets offering 3 heating system alternatives with varying, alternative-specific levels of pre-determined attributes: 1) annual operating cost, 2) , investment cost 3), primary energy factor, 4) CO_2 emissions and 5) price risk (Table 4). The heating systems in the choice sets were 1) district heating from fossil fuels, 2) district heating from renewables, 3) district heating from fossil fuels, 3) ground heat/heat pump and 4) gas condensing boiler. The investment costs had the levels 4,000 €, 6,000 €, 8,000 € and 10,000 € for the private consumers and 40,000 €, 45,000 €, 50,000 € and 55,000 € for the municipalities.

Table 4: Attribute and characteristics in the DCE

annual operation costs/m^2	6 €	8 €	10 €	12 €
investment costs* in €	4 k 40k	6 k 45 k	8 k 50 k	10 k 55 k
primary energy factor	0.0	0.7	0.8	1.1
CO_2-emission in kg CO_2/ m^2/a	0.4	13	14	20
price risk	low	middle	high	

*(without 3,000 € for ventilation system)

The respondents were asked to choose for each choice set the heating option that they would choose if they buy/construct a new house or renovate their actual systems and if there were no other options available. In addition, they got the information that they should assume that their house respectively flat was currently located near a heating network respectively connected to such a network. The investments costs were related to a house/flat with 120 m^2. For the municipalities the investments costs were related to a housing complex with six flats. Furthermore, the choice task was slightly adapted. The participants from the municipalities should imagine, that in their municipality a new housing estate will be constructed. The task then was to choose the heating alternative that has the highest utility for the municipality and their inhabitants.

Although choice sets are hypothetical and the only choices are those stated, choice experiments appear to be the most appropriate method. A researcher using choice experiments has full information about non-chosen alternatives, can vary attribute levels independently, is able to elicit willingness-to-pay measures for nonfinancial system attributes and, therefore, overcomes possible drawbacks of revealed preference data.

The choice of attributes and their levels (Table 4) was based on earlier studies, on feedback from experts and on a pre-test of the questionnaire. We decided to use the same levels of investment cost and required own work for both house size classes, as we did not find these attributes to vary significantly. The annual operating cost and CO_2 and fine particle emissions were calculated based on the energy consumption of an average detached house, the efficiency of a heating system and unit price/emission of a fuel and expressed as annual totals in the choice experiments.

In total, 12 different (unlabelled) choice sets were generated using the Software NGene (Choicemetrics, 2012), allowing for the main effects to be identified and estimated without confounding. The choice sets had different orderings of the heating systems to eliminate possible ordering effects in choices. See Table 5 for a choice set example.

Table 5: Choice-Set example private households

	alternative 1	alternative 2	alternative 3
	District heating renewables	District heating fossil fuels	Heat pump
annual operation costs/m^2	12 €	12 €	6 €
investment costs*	6,000 €**	6,000 €	8,000 €
primary energy factor	0,0	0,7	0,8
CO_2-emissions in kg CO_2/ m^2/year	0,4	14	13
price risk	low	low	high

*(without 3,000 € for ventilation system)

In addition to the choice tasks, the questionnaire included questions on the respondents' attitudes and socio-demographic characteristics were recorded.

2.3 Statistical modelling

The discrete choice experiment method is specifically based upon 1) the characteristics theory of value, which assumes that the utility to homeowners is derived from the characteristics of the heating systems, and random utility theory (RUT). The choice experiments were analysed with logit models using the software NLogit 4.0. Multinomial Logit (MNL) models were estimated to gain insight into the data. In choice analysis, it is assumed that the utility U_i of choosing alternative *i* out of a choice set of J alternatives is composed of the observed utility V_i capturing the effect of the variables tested in the experiments, and the random error term ε_i capturing the unobserved utility (Hensher et al., 2015). The observable component V_i is assumed to be a linear relationship of observed attribute levels *x* of each alternative *j* and their corresponding weights (ß). In this study, all cost attributes represented metric variables. The heating options 'gas', 'district heating fossil fuels', 'district heating renewables' and 'heat pump' entered the model as dummy-variables with the option 'gas' set to zero as reference. The costs were included as metric variables and assumed to have a squared effect on the observable component of the utility as follows:

$$U_i = \beta_{ac}\text{annual costs}^2 + \beta_{ic}\text{investment costs}^2 + \beta_{dc-renew}\textit{district heating renewabels} \\ + \beta_{dc-fossil}\textit{district heating fossil fuels} + \beta_{heat\ pump}\textit{heat pump} + \varepsilon_i$$

The probability (Prob) that alternative *i* is chosen out of a choice set of J alternatives is given by (Hensher et al., 2015):

$$\text{Prob}_i = \frac{\exp V_i}{\sum_j^J \exp V_j}$$

3. Results

3.1 Germany
Consumers

The estimation results for Germany demonstrate that 'district heating from renewable energies' is the most preferred heating alternative whereas the reference base alternative 'gas' is least preferred (see Table 6). The second place takes 'district heating from fossil fuels' followed by the option 'heat pump'. The described effects are all highly significant in comparison to the reference base 'gas' and differ significantly from each other.

As expected the cost parameters ('variable costs' & 'investments cost') are negative and significant. In the model for these both variables their squared terms resulted in a better model fit and were therefore used for the final estimation. For an economic evaluation of the described positive effect sizes market simulations were calculated with the help of the estimated cost parameters.

Table 6. Estimation results Germany (N=490)

Coefficients		
	Estimate	Std. Error
district heating renewable+	2.02***	0.06
district heating fossil	1.03***	0.08
heat pump	0.26***	0.04
variable costs^2	-0.02***	0.01
investment costs^2 * 1000	-0.05***	0.01
Log-Likelihood	-5200.6	

Significance codes: 0=***, 0.001=**, 0.01*
+The heating alternative 'gas' is the basis with an estimate value of zero to which the competing heating alternatives are compared

Furthermore, for this purpose, investment costs for all heating alternatives were set equal to 6,000 €. The variable costs for the base option 'gas' were set to 6 €/m^2/a whereas the variable costs for the other alternatives were successively increased (starting point 6 €) up to the point where they attained the same market share as the base alternative. For this simulation, a situation with only two alternatives were hypothesized.

Figure 1 illustrates the calculated willingness-to-pay in comparison to the reference basis. The participants are willing to pay 7.1 € higher variable costs per m^2/year for 'district heating from renewable energies' than for 'gas'. The WTP for 'district heating from fossil fuels' is about 40 % lower with 4.2 €. The WTP for the alternative 'heat pump' is 1.3 €.

The results clearly show that 'district heating from renewable energies' is the most favourite heating option for the consumers. The ranking of the other alternatives is 'district heating from fossil fuels', 'heat pump' and 'gas'. It is to highlight that the participants revealed a significant additional WTP for 'district heating' just for the fact that is from renewable energies. The WTP is 2.9 € higher for this option than for 'district heating from fossil fuels'.

Figure 1. WTP for the different heating systems

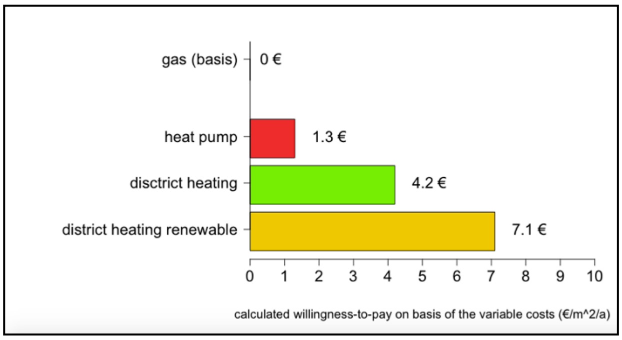

Source: own calculation.

Municipalities

The estimation results for Germany demonstrate that ‘district heating from renewable energies’ is likewise the most preferred heating alternative for the municipalities whereas the reference base alternative ‘gas’ is least preferred (see Table 7). The second place takes ‘heat pump followed by the option ‘district heating from fossil fuels’. The described effects are all highly significant in comparison to the reference base ‘gas’ and differ significantly from each other. As expected the cost parameters (‘variable costs’ & ‘investments cost’) are negative and significant. In the model for these both variables their squared terms resulted in a better model fit and were therefore used for the final estimation.

Table 7. Estimation results Germany (N=274)

Coefficients		
	Estimate	Std. Error
district heating renewable+	2.14***	0.08
district heating fossil	0.39***	0.10
heat pump	0.46***	0.06
variable costs^2	-0.01***	0.01
investment costs^2*10000	-0.01***	0.01
Log-Likelihood	-2768.5	

Significance codes: 0=***, 0.001=**, 0.01*
+The heating alternative ‘gas’ is the basis with an estimate value of zero to which the competing heating alternatives are compared

For an economic evaluation of the described positive effect sizes market simulations were calculated with the help of the estimated cost parameters. Furthermore, for this purpose, investment costs for all heating alternatives were set equal to 30,000 €. The variable costs for the base option ‘gas’ were set to 6 €/m^2/a whereas the variable costs for the other alternatives were successively increased (starting point 6 €) up to the point where they attained the same market share as the base alternative. For this simulation, a situation with only two alternatives were hypothesized.

Figure 2 illustrates the calculated willingness-to-pay in comparison to the reference basis. The participants are willing to pay 9.7 € higher variable costs per m^2/year for ‘district heating from renewable energies’ than for ‘gas’. The WTP for ‘heat pump is much lower with 3.0 €. The WTP for the alternative ‘district heating from fossil fuels’ is 2.7 €. The results clearly show that ‘district heating from renewable energies’ is the most favorite heating option for the municipalities. The ranking of the other alternatives is ‘heat pump’, ‘district heating from fossil fuels’ and ‘gas’.

Figure 2: WTP for the analyzed heating alternatives

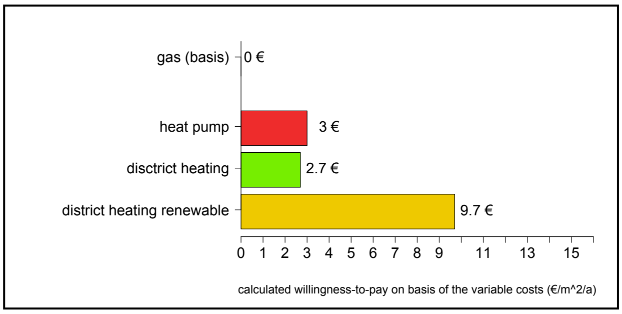

Source: own calculation.

It is to highlight that the participants revealed a significant additional WTP for ‘district heating’ just for the fact that is from renewable energies. The WTP is 7 € higher for this option than for ‘district heating from fossil fuels’.

3.6 Austria

Consumer

The estimation results for Austria reveal that ‘district heating from renewable energies’ is the most preferred heating alternative whereas the reference base alternative ‘gas’ is least preferred (see Table 8). The second place takes ‘district heating from fossil fuels’ followed by the option ‘heat pump’. The described effects are all highly significant in comparison to the reference base ‘gas’ and differ significantly from each other. As expected the cost parameters (‘variable costs’ & ‘investments cost’) are negative and significant. In the model for these both variables their squared terms resulted in a better model fit and were therefore used for final estimation.

Table 8: Estimation results Austria (N=520)

Coefficients		
	Estimate	Std. Error
district heating renewable+	2.24***	0.06
district heating fossil	1.06***	0.08
heat pump	0.67***	0.04
variable costs^2	-0.01***	0.01
investment costs^2*1000	-0.01***	0.01
Log-Likelihood	-5802.6	

Significance codes: 0=***, 0.001=**, 0.01*
+The heating alternative ‘gas’ is the basis with an estimate value of zero to which the competing heating alternatives are compared

For an economic evaluation of the described positive effect sizes market simulations were calculated with the help of the estimated cost parameters. Furthermore, for this purpose, investment costs for all heating alternatives were set equal to 6,000 €. The variable costs for the base option ‘gas’ were set to 6 €/m²/a whereas the variable costs for the other alternatives were successively increased (starting point 6 €) up to the point where they attained the same market share as the base alternative. For this simulation, a situation with only two heating alternatives were hypothesized.

Figure 3 illustrates the calculated willingness-to-pay in comparison to the reference basis. The participants are willing to pay 8.4 € higher variable costs per m²/year for ‘district heating from renewable energies’ than for ‘gas’. The WTP for ‘district heating from fossil fuels’ is circa 50 % lower with 4.8 €. The WTP for the alternative ‘heat pump’ is 3.3 €.

Figure 3: WTP for the analysed heating alternatives

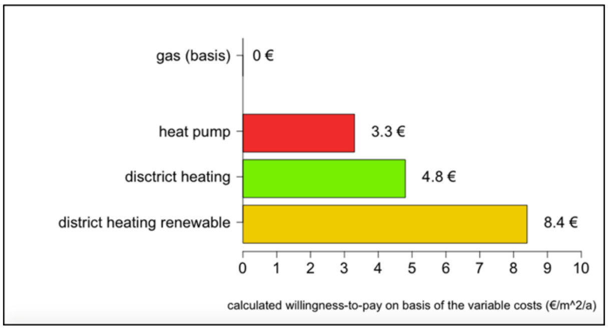

Source: own calculation.

Municipalities

The estimation results for Austria demonstrate that ‘district heating from renewable energies’ is the most preferred heating alternative whereas the reference base alternative ‘gas’ is least preferred (see Table 9). The second place takes ‘district heating from fossil fuels’ closely followed by the option ‘heat pump’. The described effects for the heating systems are all highly significant in comparison to the reference base ‘gas’ and differ significantly from each other.

As expected the cost parameters (‘variable costs’ & ‘investments cost’) are negative. Nonetheless, the effect of the investments costs was not significant what may be is due to the low sample size and the applied selection process for the sample. In the model for these both variables their squared terms resulted in a better model fit and were therefore used for final estimation.

Table 9: Estimation results Austria (N=23)

Coefficients		
	Estimate	Std. Error
district heating renewable+	4.48***	0.52
district heating fossil	2.12***	0.55
heat pump	2.02***	0.36
variable costs^2	-0.10*	0.01
investment costs^2*10000	-0.01	0.01
Log-Likelihood	-160.31	

Significance codes: 0=***, 0.001=**, 0.01*
+The heating alternative ‘gas’ is the basis with an estimate value of zero to which the competing heating alternatives are compared

For an economic evaluation of the described positive effect sizes market simulations were calculated with the help of the estimated cost parameters and according to the approach applied for the German case. Figure 4 illustrates the calculated willingness-to-pay in comparison to the reference basis. The participants are willing to pay 16 € higher variable costs per m^2/year for ‘district heating from renewable energies’ than for ‘gas’. The WTP for ‘district heating from fossil fuels’ is circa 50 % lower with 9.8 €. The WTP for the alternative ‘heat pump’ is 9.5 €.

The results clearly show that ‘district heating from renewable energies’ is the most favorite heating option for the municipalities. The ranking of the other alternatives is ‘district heating from fossil fuels’, ‘heat pump’ and ‘gas’. It is to highlight that the participants revealed a significant additional WTP for ‘district heating’ just for the fact that is from renewable energies. The WTP is 6.2 € higher for this option than for ‘district heating from fossil fuels’.

Figure 4: WTP for the analysed heating alternatives

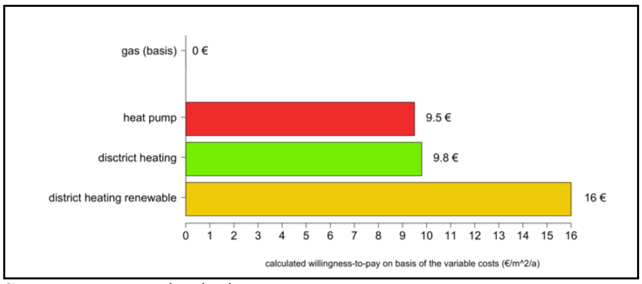

Source: own calculation.

3.7 France

Consumer

The estimation results for France demonstrate that ‘district heating from renewable energies’ is the most preferred heating alternative whereas the reference base alternative ‘gas’ is least preferred (see Table 10). The second place takes ‘district heating from fossil fuels’ followed by the option ‘heat pump’. The described effects are all highly significant in comparison to the reference base ‘gas’ and differ significantly from each other. As expected the cost parameters (‘variable costs’ & ‘investments cost’) are negative and significant. In the model for these both variables their squared terms resulted in a better model fit and were therefore used for the final estimation.

Table 10: Estimation results France (N=490)

Coefficients		
	Estimate	Std. Error
district heating renewable+	2.25***	0.06
district heating	1.16***	0.08
heat pump	0.52***	0.05
variable costs^2	-0.01***	0.01
investment costs^2*1000	-0.01***	0.01
Log-Likelihood	-5200.6	

Significance codes: 0=***, 0.001=**, 0.01*
+The heating alternative ‘gas’ is the basis with an estimate value of zero to which the competing heating alternatives are compared

Figure 5 illustrates the calculated willingness-to-pay in comparison to the reference basis. The participants are willing to pay 8.4 € higher variable costs per m^2/year for ‘district heating from renewable energies’ than for ‘gas’. The WTP for ‘district heating from fossil fuels’ is circa 40 % lower with 5.1 €. The WTP for the alternative ‘heat pump’ is 2.7 €.

Figure 5. WTP for the analyzed heating alternatives

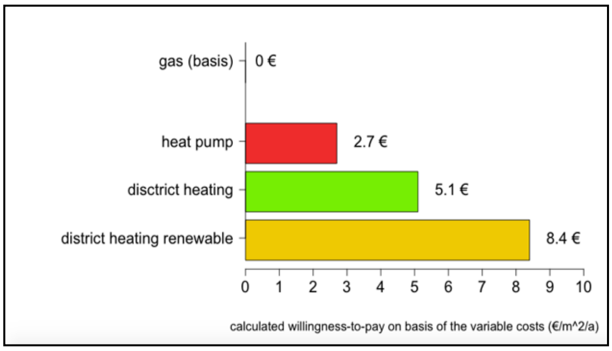

Source: own calculation.

Municipalities

The estimation results for France demonstrate that ‘district heating from renewable energies’ is the most preferred heating alternative for the municipalities whereas ‘heat pump’ and ‘district heating’ are not significantly different from the base alternative ‘gas’ (see Table 11). As expected the cost parameters (‘variable costs’ & ‘investments cost’) are negative. In the model for these both variables their squared terms resulted in a better model fit and were therefore used for the final estimation.

Table 11: Estimation results France (N=39)

Coefficients		
	Estimate	Std. Error
district heating renewable+	2.95***	0.01
district heating	0.38	0.26
heat pump	0.30	0.10
variable costs^2	-0.01*	0.01
investment costs^2*10000	-0.01	0.84
Log-Likelihood	-311.39	

Significance codes: 0=***, 0.001=**, 0.01*
+The heating alternative ‘gas’ is the basis with an estimate value of zero to which the competing heating alternatives are compared

Figure 6 illustrates the calculated willingness-to-pay in comparison to the reference basis. The participants are willing to pay 10.3 € higher variable costs per m^2/year for ‘district heating from renewable energies’ than for ‘gas’. The WTP for ‘heat pump is circa much lower with 1.1 €. The WTP for the alternative ‘district heating from fossil fuels’ is 1.9 €.

Figure 6. WTP for the analyzed heating alternatives

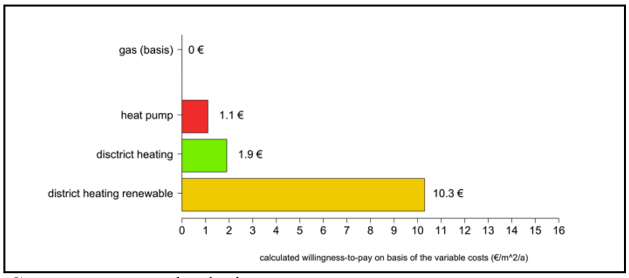

Source: own calculation.

5. DISCUSSION

The results revealed that district heating was favored over the other studied main heating alternatives. This finding is in line with the results of earlier studies (Mahapatra and Gustavsson, 2008, 2010; Rouvinen and Matero, 2013). District heat serves as a common source of space heating especially for new detached houses in Germany. However, the most popular heating technology sources are the gas and oil based system. Other heat pump technologies (e.g., exhaust air heat pumps) have also become prominent in the residential heating market (Motiva, 2012).

Our results indicate that that in Germany, France and Austria the private households prefer district heating in comparison to heat pump. Furthermore, if the district heating stems from renewables the private consumers are willing-to-pay a tremendous additional price premium 2.90 to 3.60 € variable costs (per m^2 and year).

For the municipalities the heating options district heating from fossil fuels and heat pump were of similar importance. Comparable to the results for the private households the municipalities are willing-to-pay a significant price premium if the district heating stems from renewables.xp

Acknowledgements

The project **S**olar **D**istrict **H**eating and actions from **P**olicy **to** **M**arket (SDHp2m) has received funding from the European Union's Horizon 2020 research and innovation programme under grant agreement No 691624

This project has received funding from the European Union's Horizon 2020 research and innovation programme under grant agreement No 691624

REFERENCES

AGEB (2016), Anwendungsbilanzen, Stand 10/2016 www.ag-energiebilanzen.de, retrieved on 05.03.218

BDEW (2017), Beheizungsstruktur im Wohnungsneubau in Deutschland 2016.

Braun, F. (2010), Determinants of households' space heating type: a discrete choice analysis for German households, Energy Policy, 38 (10), 5493–5503.

ChoiceMetrics (2012), Ngene 1.1.1. User Manual & Reference Guide (Sydney, Australia: *Choice Metrics,* 2012).

Connolly, D., Lund H., Mathiesen, B.V., Werner, S., Möller, B., Persson, U., Boermans, T., Trier, D., Østergaard, P.A., and S. Nielsen (2014), Heat Roadmap Europe: Combining district heating with heat savings to decarbonise the EU energy system, Energy Policy, 65, 475-489.

German federal ministry for economic affairs and energy (2018), Energiedaten 2018.

Hensher, D., Rose, J. and Greene, W. Applied Choice Analysis: A Primer (Cambridge, England: Cambridge University Press, 2015).

Jaccard, M., and M.Dennis (2006), Estimating home energy decision parameters for a hybrid energy and economy policy model, *Environmental Modeling and Assessment*, 11, 91–100.

Mahapatra, K. and L. Gustavsson (2008), An adopter-centric approach to analyze the diffusion patterns of innovative residential heating systems in Sweden, *Energy Policy*, 36 (2), 577–590.

Mahapatra,K. and L. Gustavsson (2010), Adoption of innovative heatings systems – needs and attitudes of Swedish homeowners, *Energy Efficiency*, 3,1–18.

Motiva (2012), Heating System Alternatives for Detached Houses. Available from: http://www.motiva.fi/files/7201/Pientalon_lammitysjarjestelmat_2012.pdf)

Rouvinen, S. and J. Matero (2013). Stated preferences of Finnish private homeowners for residential heating systems: a discrete choice experiment, Biomass and Bioenergy, 57, 22-32.

Vaage, K. (2000), Heating technology and energy use: a discrete continuous choice approach to Norwegian household energy demand, Energy Economy, 22 (6), 649–666.

VuMa (2018). Umfrage zu geplanter Modernisierung der Heizungsanlage. In: Statista, retrieved on 08.03.18 from https://de.statista.com/statistik/daten/studie/181347/umfrage/geplante-modernisierung-der-heizungsanlage-in-den-naechsten-2-jahren/.

Willis, K., Scarpa, R., Gilroy, R., and N. Hamza (2011), Renewable energy adoption in an ageing population: heterogeneity in preferences for micro-generation technology adoption, EnergyPolicy (39), 6021–6029.

IEA SHC TASK 55: „TOWARDS THE INTEGRATION OF LARGE SHC SYSTEMS INTO DHC NETWORKS“ - CONTRIBUTING PROJECTS AND RESULTS

Putz, Sabine, Ing. ; *Provasnek, Anna Katharina, Dr.**

Mrs. Sabine Putz, OPERATING AGENT IEA SHC Task 55
SOLID, Puchstrasse 85, A-8020 Graz
s.putz@solid.at
+43 316 292840-45

Key words: Solar District Heating (SDH), Solar District Cooling (SDC), Solar thermal systems, Solar thermal large-scale installations, modular construction, networks, solar fraction

Looking closely at the contributing projects and listening to outside market information is vital to the success of SHC Task 55. Without the right team in place, any Task and its objectives can be challenged. Because of this, the OA of Task 55 has connected its core expert participants, their projects and stakeholders in 4 dynamic Subtask teams.

Examples of current projects, contributing to SHC Task 55, are heat_portfolio, BiNe2, UrbanDHExtended, optENgrid, giga-TES, BIG SOLAR, NEWsdhSOL, ISORC, or a solar heating project from Tibet. Many more projects have registered their contributions in Task 55 and will be presented at the 3rd Expert Meeting in Abu Dhabi. Participants can already look forward to discuss case studies such as "Solar District Heating Inspiration and Experiences from Denmark" in greater technical and economic details. The interest into solar thermal energy installations increases, but still strong measures are necessary to promote the technology across countries and energy policy frameworks. So how can the share of solar thermal energy be increased in district heating and cooling networks globally? Today, technical, economic, and policy measures still restrict a profound market development and limit the integration of large scale solar systems into different types of energy networks (Solar Heat Worldwide 2014)1, despite the huge potential of the technology to provide heat based on renewable sources. Several technical design characteristics determine the specific energy output of the systems, such as collector field losses, low temperature operations, or low return temperatures into solar collectors critical to storage losses. One major specific problem of regions with strong seasons are system and operational losses during winter times. The integration of solar thermal large scale applications into district heating networks is problematic: Solar radiation is low while temperatures of the district heating network are high (90°C – 140°C flow temperature). Additionally, the performance of collectors and their performance in field constructions does not correspond to their designated lab test results. Storages, hybrid technologies (industrial waste heat, heat pumps, or storage types) and optimized system components have to be aligned with all-year system requirements of district heating and cooling networks to guarantee a high solar fraction.

IEA SHC Task 55 integrates past findings and extends research towards district heating and cooling networks, main system components and hybrid technologies. Additionally, the Task aims to provide options on how to best integrate solar thermal large scale installations in combination with hybrid technologies (such as seasonal heat storages or adsorption heat pumps) into district heating and cooling networks. The main contributions of SHC Task 55 projects provide information on:

- Low cost and high performance large-sized SDH/SDC systems, their main components and guidelines for their construction
- Simulation of the integration of large seasonal storages, hybrid technologies and large collector arrays into different district heating networks
- A description of crucial components of modular conception and construction of SDH/SDC systems
- An elaboration of business and financing calculation models
- The validation of measurement methods of tests on field collector performances and singular collector tests in the laboratory
- Country reports, license requirements, feasibility studies and a database on large SDH/SDC systems in established and new markets

Increasing the solar fraction within a large-scale district heating system requires a holistic investigation of the total heating installation. These focal points are the core of the list of international projects and their results which will be presented.

HOW TO MODEL FUTURE DISTRICT HEATING SYSTEM WITH SMALL AND LARGE SCALE SOLAR SYSTEMS?

Keith O'Donovan, Gerald Schweiger, Basak Falay and Ingo Leusbrock
Department of Thermal Energy Technologies and Hybrid Systems, AEE Intec, A-8200, Feldgasse 19, Gleisdorf, Austria, Ph.: +43 (0)3112-5886, Fax.: +43 (0)3112-5886-18, office@aee.at

Abstract – Simulation and later optimization and operation of DH systems - particularly those with inputs from fluctuating renewable energy sources – faces several overriding challenges, especially when the complexity of the DH system increases. The benefits in using Modelica modelling language to model and simulate such systems are outlined and investigated and how it can be integrated in an overall workflow from network plan to later post processing. Firstly a methodology is presented to illustrate how one can extract data from a given CAD drawing of a network and implement it into a dynamic thermo-hydraulic model. The advantage of using the Python package NetworkX as a post processing tool to help visualise network dynamics is demonstrated. To showcase the overall workflow, a chosen network was implemented both with and without the addition of thermal storage and solar thermal technologies. The results outline the relative contribution of each technology to the overall network performance, with the storage tank successfully aiding in increasing the share of renewable energy contribution to the network and subsequent CO_2 emission reduction.

1. INTRODUCTION

Increased integration of renewables such as solar thermal and flexibility measures such as storage and heat pumps represent a major challenge for future district heating systems, both for planners and operators. To design such systems that integrate large shares of fluctuating renewable energy sources while improving the overall efficiency and flexibility of district heating systems requires sophisticated simulation, optimization and control methods and tools.

Previous research has shown that district heating and cooling infrastructure has the potential to play a key role in sustainable energy systems (Lund, H. et al. 2014, Schweiger G. et al, 2017). Multiple options exist for increasing energy system flexibility, including combining different energy domains, increasing supply and demand flexibility, integrating energy storage technologies and increasing the transmission capacity of the national grid as well as interconnections to other countries. In order to investigate these challenges and opportunities for future systems, many of the standard simulation tools and methods are unsuitable, because they often rely on simplified models, static relationships and single-domain approaches (J. Allegrini, et al. 2015). One consequence of this among others, is that they are frequently unable to capture the dynamic behavior of such complex systems and interaction between included components.

Recent advances in object-oriented, physical modeling of energy systems has led to potential for developing novel tools for system planning and operation control that focus specifically on these new challenges. The modeling language Modelica is a promising candidate to become standard for industry and academia in the field of dynamic modelling, and in particular, modelling of multi-domain systems (Fritzson, P. 2015). Modelica is a well-established modelling language in industry (7% of German power production is based on Modelica models (Wetter M. and van Treeck C., 2016) and academia. A general distinction can be drawn between block diagram modelling (also known as causal modelling) using imperative programming languages and equation-based modelling (also known as acausal modelling). Equation-based languages are most advantageous for:

- representing the physical structure of systems as it enables the modeler to model the system directly by means of physical equations. The causality of how to solve the equations is not decided during the modelling stage, which means that the usual need for manual conversion of equations to a block diagram is removed.
- reusability, extensibility, adaptability of models and
- being simple to code and read.
- Are preferable for optimization tasks (Schweiger, G. et al. 2017)

A disadvantage of these methods is that it is more difficult to go from a mathematical model to the numerical solution algorithm. Highly elaborated tools are required to handle them efficiently.

In the following, we describe a framework for modelling and simulating such networks using Dymola as a simluation environment with an example focusing on converting an existing network to an ugraded version representive of the 4th generation of distrct heating. The impacts of large-scale solar units, prosumers, decentralized renewables etc. are investigated. We will thus highlight the differences between standard tools for planning and design of the systems with our approach and show the added value in terms of accuracy and representation of dynamics, which will become a vital feature of future DH systems.

2. OVERRIDING CHALLENGES IN SIMULATION

2.1 Complex System Dynamics

Future district heating systems are pushing towards higher flexibility through integration of fluctuating renewable heat sources (solar, geothermal), large thermal energy storage and Power-to-Heat technology to shave load peaks. Each of these components require sophisticated control strategies in order to operate in such a way that the overall flexibility and renewable energy fraction is increased. Model Predictive Control (MPC) uses for instance real time weather data to constantly readjust the network supply temperate in order to minimise heat losses over a short term horizon. These varying temperatures at the producer lead to temperature wave propagations along the network with delay times up to a couple of hours for customers located many kilometres from the production site. This aspect cannot be captured by static simulation tools.

In order to accurately capture such dynamic phenomena, the tool needs to solve the heat equation in space and time. Modelica is a powerful language for solving such partial differential equations which is equipped with a number of implicit and explicit solvers to do so. In order to easily interpret results, post processing and visualisation methods are favourable. A study has been carried out to visualise simulation results from Modelica models using graph drawing in Python which allows the user to easy debug any physically unrealistic dynamics in the system (Fuchs, Streblew and Müller, 2015). The work in this paper has been adapted to help visualise the simulation results.

2.2 Optimisation Tasks and Aggregation

A key progression from simulation is the ability to perform dynamic optimisation on a network in order minimise key performance indicators such as end energy use, supply temperatures, costs, CO_2 emissions at every time step in the simulation. This is achieved by defining an objective function which expresses the intended minimising variable as a function of other related variables. A number of constraints are then applied to represent the boundary conditions of the network such as min and max allowable heat flows, temperatures, pressure drops etc.

Dynamic optimisation for a network of any considerable size requires huge computational effort and in most cases is only achievable by firstly aggregating the network down to a small fraction of its original size. There are two largely recognized aggregation methods known as the German and Danish methods. Both methods merge pipes and consumers in series and parallel while conserving properties of the original network. Aggregation methods are based on steady state assumptions and thus are most appropriate when applied to quasi-stationary networks, but dynamic aggregation has been applied with varying levels of success (Larson, 2015).

3. MODELLING APROACH

3.1 Converting a Network representation to executable Modelica code.

To manually build a district heating network simulation model of any significant level of detail would be an arduous and time consuming task, not to mention highly prone to human error. A more effective approach is to implement an automated work flow to go from a CAD drawing of the network plan all the way to executable Modelica code. This is done in a number of steps:

1. Assuming the network representation has embedded GIS data, one can export main pipeline, producer and consumer coordinates from the CAD (see Fig 1. (a)) using Python script.
2. Using the Python Package, NetworkX, pipes and consumers can be represented as a collection of connected "edges" and nodes" respectively. Both have a dictionary format which stores data and parameters such as coordinates, loads, temperatures, pipe diameters, and insulation thickness' etc.
3. Another Python script translates this plan to executable Modelica code which can be run in Dymola for simulation (see Fig 1. (b)).

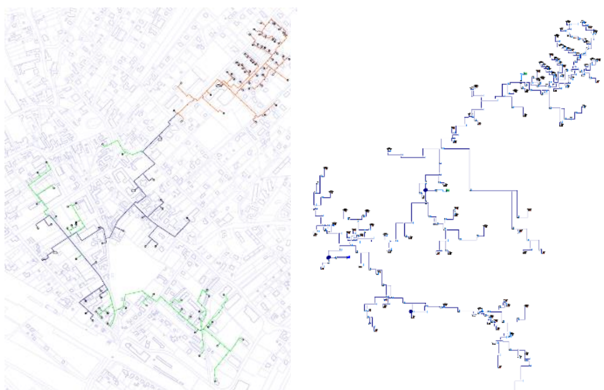

Figure 1: (a) Actual Network Plan (b) Modelica respresntation of network after Python manipualtion

4. 4th GENERATION DISTRICT HEATING SCENARIO COMPARISON

4.1 Use case definition

The following example demonstrates the capabilities of Modelica in modelling and simulating a DHN by taking an existing network and upgrading it to a typical 3-4th generation network with the addition of small and large scale solar collectors. The results aim to demonstrate the capability of Dymola in capturing a number of complex dynamic effects.

4.2 Base Case

The base case represents the network which supplies the town of Gleisdorf located in the south east of Austria with planned network extensions already in place. The specifications for this base case do not reflect exactly those of the network, but serve rather as a potential future situation. The simulated network consists of:

- 116 consumers
- Mean supply return temperatures 88/55^{o}C
- Three production sites:
    - Base load supplied by Biomass plant – capacity 3.5MW
    - Peak load supplied by a gas boiler of capacity 2MW
    - Constant 300kW$_{th}$ from CHP
- Approx. 7km of pipeline.

Consumer load profiles were used from existing load data from the year 2015. The main pressure control is implemented at the Biomass plant in the south east which provides a pressure drop such that the minimum pressure drop in the network at some critical consumer (usually the furthest away) is at least 0.5bar. The required mass flow is then computed indirectly as a function of the pressure drop.

4.3 Upgraded Case

The upgraded case was kept like above with the addition of:

- Four flat plate solar collector sites with a total collector surface area of 1,500m^2 (2x600m^2 + 250m^2 + 50m^2)
- The 50m^2 collector supplies a building directly with excess solar being fed back into the net. The building thus acts as a prosumer.
- 750 m^3 thermal storage tank next to the Biomass plant.

The purpose of the storage tank is to allow for increased hours of the biomass plant, thus increasing its operating efficiency. Excess heat from the Biomass plant is stored in the tank during periods of low demand and discharged during times of high demand. Aside from increasing the output of the biomass, the additional heat from the tank will help reduce the dependency of the gas boiler during periods of high demand, thus reducing the overall CO_2 emission levels.

A stratified tank model developed by Modelica Buildings Library (Berkley), is used for the simulation. A control strategy is implemented to assess when to charge and discharge the tank based on current network demand levels and minimum and maximum permissible tank temperatures. The biomass plant was configured to run at a constant output of 3MW with any surplus heat used to charge the tank during times of low demand. At times of higher demand, the tank is then discharged into the network cover the remaining load. Only when the tank is fully discharged and total net load is above 3MW is the gas boiler switched on. The idea is reduce the dependency on the gas boiler while also operating the biomass boiler at a more efficient output level. The tank is considered to be fully charged when the temperature of the storage medium reaches that of the network supply right through. The tank is considered to be fully discharged when the temperature of the storage medium reaches that of the network return temperature right through.

For the solar facilities, a weather data file for the local conditions is read at every simulation time step with the global irradiance, G, angle of incidence, θ and ambient air temperature T_{amb} serving as inputs to the collector model.

The collector model itself assumes a flat plat collector with a collector area, A, in a horizontal configuration. An average collector temperature of 70 degrees is specified and the collected heat can therefore be calculated from Eq. (1).

$$\dot{Q}_{solar} = \eta A G \qquad \text{Eq. (1)}$$

Where η is the collector efficiency calculated from Eq. (2)

$$\eta = F\left(a_0 - \frac{a_1(T_{colector,avg} - T_{amb})}{\max(G,0.0001)} - \frac{a_2(T_{colector,avg} - T_{amb})^2}{\max(G,0.0001)}\right) \qquad \text{Eq. (2)}$$

Where F is a function of the angle of incidence θ, a_0 , a_1 and a_2 are constants and properties of the collector itself. These are typically found in an accompanying technical data sheet provided by the manufacture.

The mass flow is achieved via a circulation pump which only switches on once the irradiance exceeds a specified minimum value $G_{min.}$ See Figure 2.

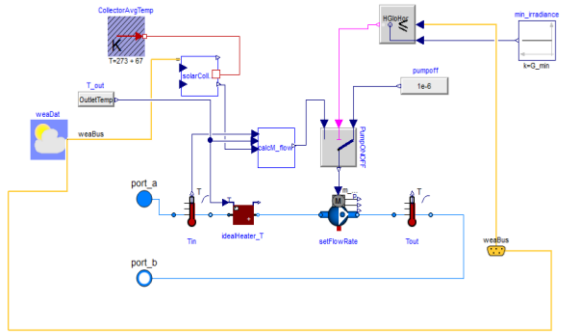

Figure 2: Solar collector model with pump control - G, θ and T_{amb} are read from the weather data.

5. RESULTS AND DISCUSSION

5.1 Visualisation

Both networks were simulated over a four month long time from spanning from Jan 1st to April 30th. A dynamic simulation produces vast amounts of data with pressure and mass flows and temperature being calculated at each pipe component at every time For a relatively large network such as the one simulated here, visualisation of the network results is necessary in order to assess the dynamics of the system. By reading the result file in Python and assigning result variables to each pipe and consumer node in the network representation created using NetworkX, a visualisation of any variable of interest can be obtained whether it be the pressure, mass flow or temperature distribution, either as a figure at a certain point in time or as a video to represent the dynamics. Figure 3. gives a representation of the network supply pressure distribution at a high and low demand period.

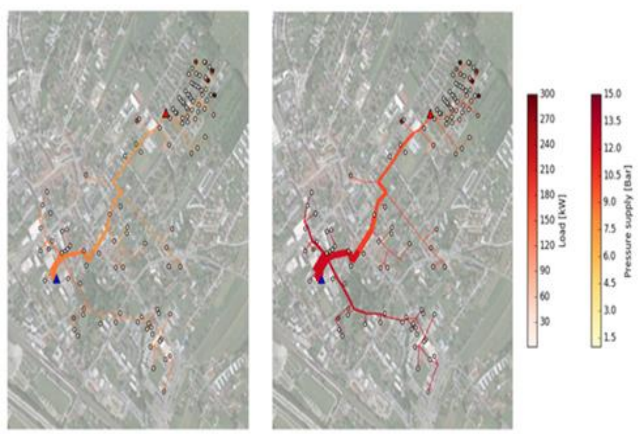

Figure 3: Network pressure distribution and consumer loads at (a) 17:00 afternoon lull and (b) 05:00 morning peaks on a typical spring day.

The edges here are colour coded to represent areas of highest and lowest pressure in the supply pipeline. The width of the edges are also scaled based on the mass flow rates. The plots show a clear difference in overall network pressure levels during a morning peak and afternoon lull 12 hours later. The regions of highest pressure and mass flows are located closest to the production sites as to be expected ranging from approximately 8-15bar from the lull to the peak times of the day. The lowest pressures can be observed at the periphery consumers as expected. An animation could be made by compiling the plots at each time step allowing one to see the propagation of temperature waves and other dynamic phenomena over time.

5.2 Upgraded Case results

A detailed simulation was ran over a four month period from late winter into spring (Jan 1st to April 30th). Spring time was chosen to observe a period with significant heating demand with growing solar thermal potential throughout the period. To observe the daily heat flows in and out of the storage as well as the heat production at the additional solar collector sites, a one week period of the results are presented in simulated plots in Figure 4. The top graph illustrates the total network load over a one week period with clear times of tank charging and discharging shaded. The tank was initialised in a fully discharged condition hence the peak of the first day is not able to be covered by the tank. The corresponding state of charge of the stratified tank can be overserved in the lower plot with the temperature distribution shown throughout.

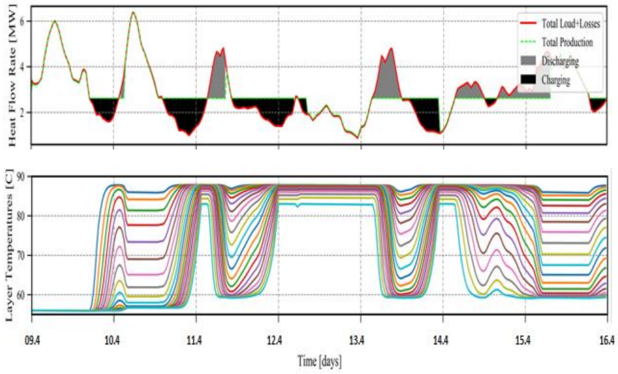

Figure 4: Top: Spring week simulation of total network production with indicated accumulator storage charge and discharge times. Bottom: Corresponding temperature distribution in tank

The heat output from the four solar thermal sites are seen for the corresponding week in Figure 5.

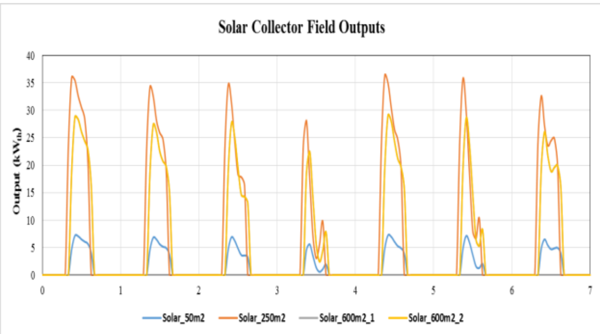

Figure 5: Thermal output from each solar system embedded in the network.

The blue curve represents the heat produced by the upgraded prosumer which is fed directly to its consumption needs over the simulation period.

A longer simulation over a four month period from the beginning of January to end of April was carried out to investigate the relative increase in biomass/solar heat in the overall energy mix with the addition of the storage and solar thermal collectors respectively. The bar chart in Figure 6 gives a breakdown of the energy mix over the given period for three different scenarios: the base case with assumers no storage tank, an intermediate case with the 750m^3 storage tank and the fully upgraded case with an additional 1500m^2 of solar thermal collectors incorporated alongside the storage tank.

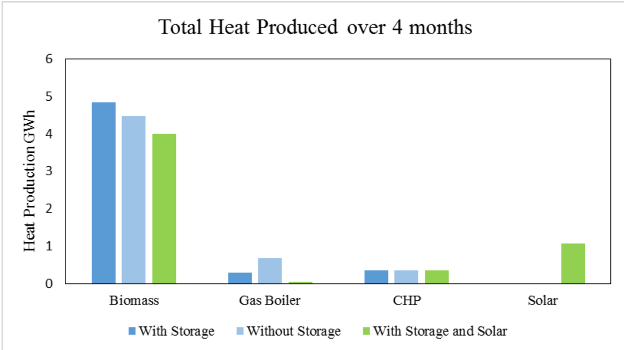

Figure 6: Energy Mix Jan 1st to May 1st – Scenario comparison

The dependency of the gas boiler is significantly reduced with the addition of the large storage tank from 671MWh down to 291MWh. With the addition of the solar collectors, its output is further reduced to just 48MWh over the given period. The heat output from the CHP is fixed and not affected by the implementation of storage or solar components. The corresponding percentage breakdown for the period for the three different scenarios is given in Figure 7.

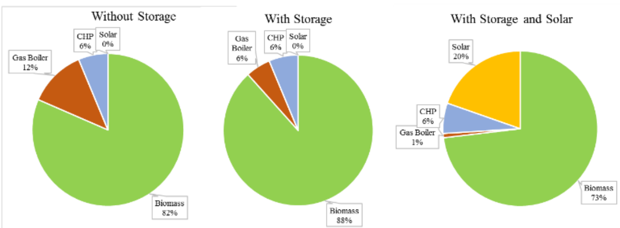

Figure 7: Energy Mix Percentage Breakdown Jan 1st to May 1st – Scenario comparison. (a) no storage or solar (b) with 750m^3 storage (c) with 750m^3 storage and 1500m^2 of solar collectors

The solar energy produced here was fed directly into the grid which is favourable over such a Winter/Spring period with a reasonably high heat demand. The 1,500m^2 of solar collector surface added here accounted for approximately 20% of the overall heat demand of the network over the given period. For a summer period simulation, further control strategies will need to be implemented to store as much excess solar heat as possible, which can be discharged at times of higher demand in autumn and Winter.

6. CONCLUSION

The work carried out in this paper is to give an overview of the capabilities of Modelica when simulating district heating networks with influx from renewable energy sources. In combination with Python packages such as NetworkX, both the pre and processing of data can be largely assisted, as it serves not only as a means to automate the modelling process but also to visualise results and track the changes in pressure and temperature distributions around the network. The demonstrated use case avails of some readily existing solar and storage components and by implementing control strategies, can be integrated into standard district heating network models. Their performance evaluated from an economical or environmental point of view to various levels of detail.

7. REFERENCES

Lund, H. et al. 2014: “4th Generation District Heating (4GDH) Integrating smart thermal grids into future sustainable energy systems”, Energy, 68, 1–11.

Schweiger G, et al. 2017: “The potential of power-to-heat in Swedish district heating systems”, Energy, http://dx.doi.org/10.1016/j.energy.2017.02.075“

J. Allegrini, et al. 2015: “A review of modelling approaches and tools for the simulation of district-scale energy systems" Renewable and Sustainable Energy Reviews, vol. 52, 1391-1404.

Fritzson, P. 2015: “Principles of Object-Oriented Modeling and Simulation with Modelica 3.3” 2nd edition. Wiley-IEEE Press, Piscataway, NJ.

M. Wetter and C. van Treeck, “BIM/GIS and Modelica Framework for building and community energy system design and
operation.” Presentation of IBPSA Project 1, 2016.

Schweiger, G. et al. 2017: “District heating and cooling systems – framework for Modelica-based simulation and dynamic optimization, Energy, https://doi.org/10.1016/j.energy.2017.05.115.

Larson H. 2015: ”District Heating Network Models for Production Planning”, Lund University, Department of Automatic Control.

Fuchs M., Streblow R., and Müller D., (2015).Visualising Simulation Results from Modelica Fluid Models Using Graph Drawing in Python. Proceedings of the 11thInternational Modelica Conference September 21-23, 2015, Versailles, France

SCFW - SOLAR YIELD PREDICTION TOOL FOR SOLAR DISTRICT HEATING SYSTEMS BASED ON SCENOCALC

Magdalena Berberich, Laure Deschaintre, Thomas Schmidt, Dirk Mangold
Solites – Steinbeis Research Institute for Solar and Sustainable Thermal Energy Systems
Meitnerstr. 8, 70563 Stuttgart, Germany
Phone: +49 (0)711 673 2000-55, Fax: +49 (0)711 673 2000-99, berberich@solites.de

Abstract – SCFW is an open-source calculation tool in MS Excel. The tool predicts the solar yield of solar thermal plants, which are integrated in district heating networks. It is based on international standards (Solar Keymark, ISO 9806) and comprises an entire solar thermal system including storage. The current version of the tool ‚ScenoCalc - Fernwärme' (SCFW 2.0) is available in German language.

1. INTRODUCTION

Large-scale solar thermal plants integrated in district heating systems are supplying renewable, zero-emission heat to residential and industrial areas. The technology can play an important role in the energy transition of the heating sector in Europe and beyond and the market is growing. However, one big challenge in developing solar district heating (SDH) systems remains in the yield prediction of solar thermal collectors. So far, there are different simulation tools for experts available, which are very detailed. A simple calculation tool, which is easy to use for everyone and gives a first impression of the expectable solar yield was missing.

Collector testing institutes use the Excel tool ScenoCalc (ESTIF, 2017) to calculate the annual collector output for Solar-Keymark certification (Solar Keymark, ISO 9806). Therefore it is limited to consider one single collector with constant average collector temperatures. In the project SCFW (Solites, 2017) an open-source calculation tool was developed in MS Excel, which is transparent in the calculation methods and based on ScenoCalc . SCFW enables the hourly calculation and comparison of different solar system designs with all components of a SDH system. The calculation result is the solar net gain at the point where it is fed into the district heating network. Another option is to calculate the solar gain of a single collector according to the solar Keymark certificate. Figure 1 shows the user interface of SCFW 2.0.

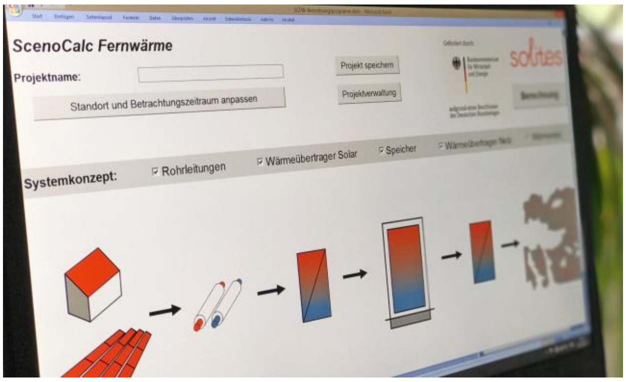

Figure 1: User interface of ScenoCalc Fernwärme SCFW 2.0

The calculation tool SCFW 2.0 was published in June 2017. It is free of charge and available online on www.scfw.de. The language of the tool is only German, however in case of growing interest it might be translated in English.

2. METHODS

As a first step for developing SCFW, the calculation and formulas of ScenoCalc were implemented in an MS Excel calculation sheet to get a transparent structure of calculation. To ensure the accuracy of this first version, the new tool was verified against ScenoCalc.

In a second step, the tool was developed further to calculate not just one collector but the solar net gain at the point where it is fed into the district heating network. The calculation follows strictly the formulas of ScenoCalc and ISO 9806 (DIN, 2014) on the one hand and considers relevant effects of the different solar system components on the other hand. To calculate these effects, the components collector field, pipes, heat exchanger in the solar circuit, buffer storage, heat exchanger in the net circuit and the load of the district heating network were integrated into the calculation model. The complete solar thermal system is shown in Figure 2. The broken grey line shows the system boundary for the solar system (left side of broken grey line). To separate the solar circuit and the net circuit hydraulically a heat exchanger is applied. Often a heat storage is integrated into the system to store the heat from the solar collectors before it is transported to the additional heater and then delivered at supply temperature to the district heating net. The district heating net itself is not considered in the calculation.

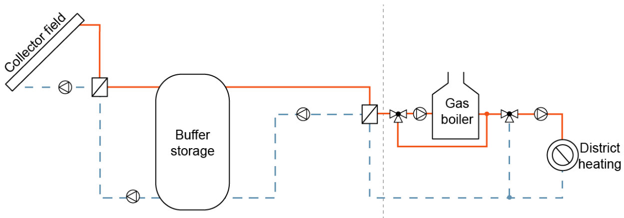

Figure 2: Schematic of a solar thermal plant for solar district heating

For each solar system component, the thermodynamic dependencies were analysed mathematically and transferred into formulas. For some cases a mathematical solution was found to solve the thermodynamical problems. However, if it was not possible to solve the single problem with a mathematical solution or this solution would have needed iterative calculation, an approximation was developed in an empirical approach. The use of iterations was avoided to keep the MS Excel calculations fast and reliable. The empirical solutions were developed by using simulation results of a Trnsys model, which was validated against measured data of real plants. The developed entire approximation formulas were validated against calculations with simple and constant system parameters, Trnsys simulations with broad changes of the most influencing parameters, and measurement data of real plants.

With the developed calculation methods, which are integrated in the published version SCFW 2.0, effects caused by the heat capacity of collectors, heat losses of pipes, fittings and optional storage, antifreeze protection and heat exchangers can be considered.

In addition, a high usability of the tool was developed by the following measures:

- In a graphical user interface in one sheet of the MS Excel workbook the system components can be chosen and its specific parameters can be set in separate user interfaces, which are opened by choosing the single component.
- A collector database containing the collector products for SDH systems available in the German market was integrated and can be expanded with further collector data.
- The calculation can be done for one year or shorter ranges in an hourly time step.
- Different profiles for the hourly supply and return temperatures and the load of the district heating network can be entered and saved.
- Climate data for Athens, Davos, Stockholm and Würzburg are included according to ScenoCalc. As it is a German tool, climate data for Frankfurt and Hamburg were added and data for other locations can be entered and saved. To consider not just one year, average climate data over 10 years from Meteotest is used (Meteotest, 2017).
- Whole calculation projects with all parameters can be saved in a project archive and loaded again.

The user interface is working with VBA macros (Visual Basic for Applications), which are separated from the calculation formulas, because the results needed to be calculated only based on formulas in MS Excel sheets to keep the calculation methods transparent.

In order to meet the market needs, the tool was discussed and tested in an early stage by companies producing and designing solarthermal systems for district heating. These companies are cooperating in the initiative IniSW, which was set up in 2015 and is chaired by Solites. In these discussions important new ideas were suggested and some of them are now implemented in the final version.

To prove the correctness of the calculations in the tool the hourly and yearly results were compared to Trnsys simulations. Some results are shown in Figure 3 with different supply and return temperatures for high temperature flat plate as well as vacuum tube collectors. For all other parameters the same values were used to compare the calculation methods. The results show just small differences between SCFW and Trnsys calculations.

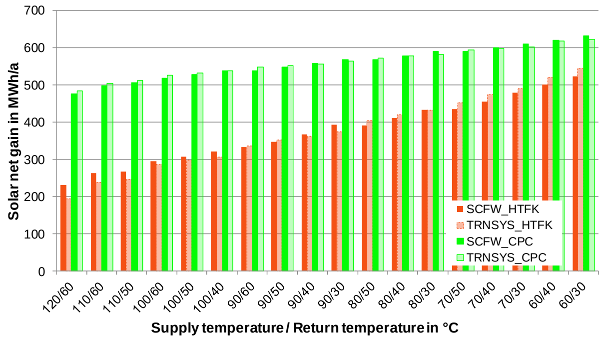

Figure 3: Comparison of yearly solar net gain calculated in SCFW and by Trnsys simulations – example for 1000 m² collector aperture area (HTFK: High temperature flat plate collector, CPC: Vacuum tube collector)

3. OPTIONS IN SCFW 2.0

With the tool SCFW solar thermal systems can be calculated, which are integrated in the heating central or directly in a district heating network.

The options of SCFW 2.0 are described in the following points:

- For the collector field the heat transfer fluid can be chosen between water and water-glycol. In case of water-glycol, a value for the energy loss by the reduced heat transfer can be set. In case of water, a parameter to consider the heat demand of the antifreeze protection can be set.
- Pipes in the collector field and for the connection to the buffer storage can be considered. The heat losses are calculated according to the given parameters and calculated in the energy balance. For the connecting pipes of the collector field to the district heating net it is possible to choose between pipes above ground, buried in the ground or with constant ambient temperature.
- The consideration of heat exchangers is possible between the collector field and the buffer storage and between the buffer storage and the district heating network by the implementation of a temperature

decrease. In case of heat exchangers, the increasing collector average temperature is more relevant than additional heat losses.

- A buffer storage can be calculated with a temperature filling level as a balance. This enables the calculation of charged and discharged heat, heat losses and surplus solar heat. In addition to that, an increase in the return temperature to the solar collectors can be calculated depending on the filling level to get realistical average collector temperatures.
- One important point is to consider the district heating network in which the solar thermal collectors are feeding. The district heating net is not calculated, but it represents the system boundary. The conditions at the point where the solar heat is fed into the district heating net are described by hourly data for thermal power in the district heating net and its supply and return temperatures. The hourly thermal power can be entered or chosen from pre-defined data, which can be scaled to the individual yearly heat demand. The supply and return temperature can be entered as well or calculated in a course of one year from two set points for summer and winter. The data can be saved to use it again.
- Two different operation modes are available: pre-heating or delivering the supply temperature. In the preheating mode the collectors can supply heat at a lower temperature level than needed in the district heating net. In case of the second operation mode, solar heat is produced only, if the irradiation is high enough to deliver the supply temperature.
- If the direct feed-in is chosen, it is assumed that the entire solar gain is used in the district heating net in each time step and the thermal power of the network is not considered.

In SCFW 2.0 the main parameters and monthly results are shown in a separate sheet and can be saved as a report in pdf format. Figure 4 shows the monthly results for irradiation on the collector (yellow), the heat demand (grey), the solar gain of the collector field (red), and the solar net gain at the point where it is fed into the district heating net (green).

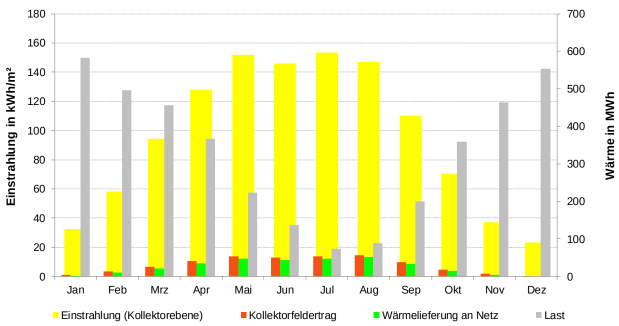

Figure 4: Diagram showing the calculation results in SCFW 2.0

4. CALCULATIONS WITH SCFW 2.0

In this chapter, some calculations done with SCFW 2.0 are described.

For a favorable performance of the solar thermal system, the overall system design is important. First of all the location of the solar thermal plant decides about the amount of solar irradiation the collectors receive. The solar thermal plant is able to heat its inlet temperature only if the irradiation is high enough. The following Figure 5 shows the differences between the global irradiation of two cities in Germany over ten years, whereas Würzburg is a location with very good solar irradiation conditions and Hamburg is a location with quite low solar irradiation. The solar irradiation in the years 2007 to 2016 fluctuates with +4 to -6 % of the average from the ten years for Würzburg (broken line). For Hamburg, the variation comprises the range of +7 to -5 % of the average level. There is a significant difference in the global solar irradiation of the two locations, which is very variable over the ten years.

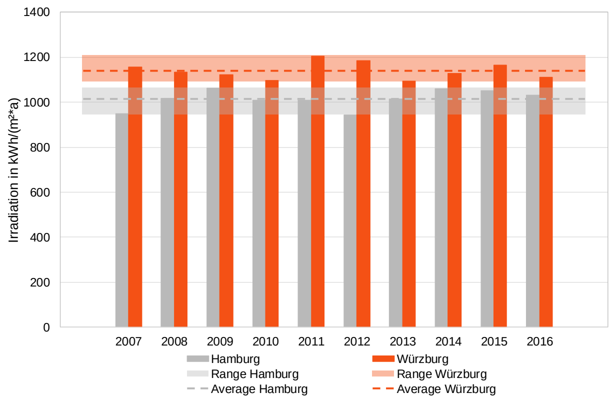

Figure 5: Yearly global solar irradiation in the years 2007 to 2016 for Würzburg and Hamburg (Deutscher Wetterdienst, 2017) on horizontal plane

Therefore, it is recommended to dimension a solar thermal plant using climate data of the location of the plant over a longer period, e.g. 10 years (like it is included in SCFW 2.0). By varying the solar irradiation in a sensitivity analysis within a system simulation program, its effect on the energy gain of the solar system can be analysed and valuated. If necessary, the solar thermal plant can be dimensioned with a safety factor to reach a needed solar heat gain even in years with poor irradiation.

In addition to that, the solar heat gain depends on the operation temperatures. The higher the average operation temperature of the collectors is, the lower the efficiency of the collectors gets because of higher heat losses of each collector. Therefore, the return temperature to the collector field and the needed supply temperature are decisive for the achievable solar heat gain.

This correlation is shown by calculations in SCFW 2.0 for high-temperature flat plate and vacuum tube collectors in the German market (Figure 6). The sample collector is a high-temperature flat plate collector with average specific values. The results are calculated with average climate data over 10 years (Meteotest, 2017) of the German city Frankfurt. The average net temperatures in the diagram are the yearly average for the arithmetic mean value of the supply and return temperatures of the regarded collector in each hour of the year.

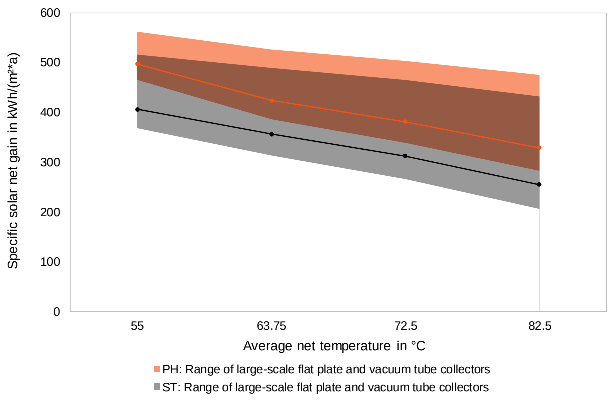

Figure 6: Usable solar heat of large-scale collectors in the German market with two different control strategies for the delivered temperature of the solar thermal plant: ST = heating up to the supply temperature, PH = preheating. The lines represent a sample collector (m²: brutto collector area)

In the preheating mode (PH, Figure 6), the solar thermal plant delivers heat at a lower temperature level than the supply temperature of the district heating net. Therefore, the solar thermal plant can produce heat even if the solar irradiation is low. The solar heat production in this mode mainly depends on the return temperature of the district heating net that should be heated by the solar thermal plant. This is visible by the strong reduction of the solar heat gain between the cases with 55 °C and 63.75 °C average temperature. The return temperature increases between these two cases from 40 to 50 °C in a yearly average.

A first idea of the performance of one single collector gives the Solar Keymark certificate (ESTIF, 2017). Each collector is tested and certified under standardized conditions with a constant average temperature in the collector. Neither the influence of the system integration nor the realistic supply and return temperatures are considered in the tests. In the certificate the performance indicators and yearly heat productions are declared for the climate data of four different locations in Europe.

As mentioned above, the solar irradiation influences the solar heat production of the collector field to a strong extend. This is shown in Figure 7 for the sample collector and with the application of the formerly mentioned climate data from Würzburg and Hamburg (see Figure 5).

The calculations of the solar heat production, whose results are shown in Figure 7, are based on a solar thermal system with a direct feed-in and without a heat storage. This system is operated to deliver always the supply temperature of the district heating net. The average net temperature is 63.75 °C, in summer the supply temperature amounts to 75 °C and the return temperature to 55 °C. The results show the direct dependency of the solar heat gain on the solar irradiation and the strong variation in single years from the average. The variation from the 10-years-average lies in a range of +10 to -15 % for Würzburg and +20 to -14 % for Hamburg.

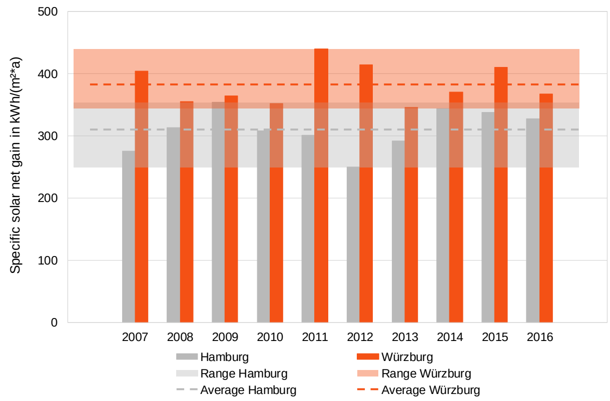

Figure 7: Calculated specific solar heat gain per m² brutto collector area of a sample collector with climatic data for the years 2007 to 2016 of the cities of Würzburg and Hamburg. The solar thermal plant is operated to always reach the supply temperature in a district heating network with 63.75 °C average temperature.

Such variations in the solar heat gain need to be considered in the dimensioning of a solar thermal plant. That is why the careful calculation of the solar heat gain with all available data and, in addition, based on realistic assumptions is essential for the feasibility of solar district heating systems. Compared to conventional heat producers, dynamic system behavior and the variations of the solar irradiation, the mass flow, and the temperatures of the district heating net need to be considered in detail.

If a solar thermal plant is dimensioned to deliver the entire heat demand of the district heating net during the summer time, in most cases a short-term heat storage is necessary to store the heat from day to night and for the case of some cloudy days. In Europe during summer, the heat demand of district heating systems usually is defined by tap water heating and the heat demand of industrial processes. The solar fraction of these solar thermal systems depends on the seasonal distribution of the yearly heat demand and is usually between 10 to 15 %. The higher the solar fraction, the more solar heat needs to be stored, not only for some days but for weeks. In case of high solar fractions in the range of more than 40 % of the yearly heat demand, a seasonal heat storage is necessary, because the solar heat gain from summer has to be used in winter. Due to the longer storage time of the solar heat, the heat losses increase and the specific net solar heat gain of the collectors decreases. **Fehler! Verweisquelle konnte nicht gefunden werden.** gives an example for the interrelations of the main parameters for such systems.

Therefore, it is assumed that the collector field comprises high temperature flat plate collectors of the sample type (see Figure 6), located in the city of Frankfurt in Germany. The collector field feeds in directly into a district heating net with a supply temperature of 78 °C in a yearly average and a yearly heat demand of 4 GWh/a. To increase the solar fraction of the yearly heat demand of the district heating net (see red line in **Fehler! Verweisquelle konnte nicht gefunden werden.**), the collector area has to be increased (see x-axis in **Fehler! Verweisquelle konnte nicht gefunden werden.**). The higher the solar fraction gets, the larger the heat storage volume has to be. The dashed grey line shows the specific storage volume in m³ water, related to the brutto collector area, which is necessary to reach the intended solar fraction. By mathematical variation, the specific storage volume was fitted to the respective collector area in a way that the storage volume is used completely and stagnation in the collector field is just avoided. For a solar collector area of 10,000 m² a solar fraction of 70 % of the yearly heat demand of the district heating net can be reached with a specific storage volume of 2.3 m³/(m² brutto collector area). In Figure 8, this specific storage volume is set to 100 % (see y-axis). The black broken line in Figure 8 gives the specific solar net gain of the entire solar thermal system (see Figure 2). The solar net gain is the usable solar thermal energy that is fed into the district heating net. Heat losses by the storage etc. are already subtracted. The maximum value of 313 kWh/(m² a), equals 100 %, is quite low and caused by the overall system layout that asks for a feed-in of the net solar heat gain always on the supply temperature of the district heating net of 78 °C in a yearly average. This specific net solar heat gain declines with the rising solar fraction due to rising heat losses of the necessary storage and rising average operation temperatures in the collector field.

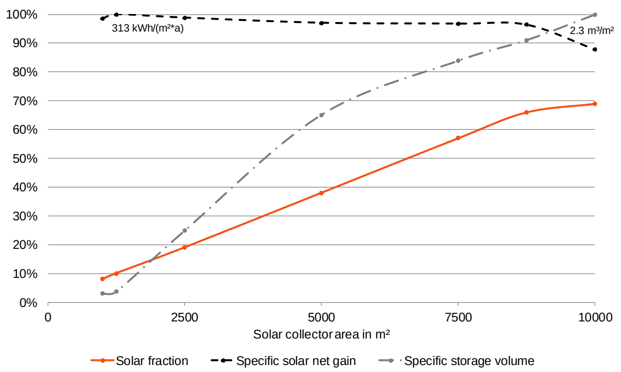

Figure 8: Correlation of solar collector area, specific heat storage volume, solar fraction of the yearly heat demand and solar heat gain for a solar thermal plant that feeds directly in a district heating net and always delivers the supply temperature of 78 °C in a yearly average (sample collector and weather data of the German city Frankfurt (see Figure 6))

For a real plant, possible next steps in the overall system design could be to change the system integration of the solar thermal system to a preheating mode (see Figure 6) or to integrate a heat pump into the solar system to unload the heat storage to lower temperatures. Both possibilities allow to reduce the operation temperatures of the solar collector field to reach higher specific solar net gains per year.

5. CONCLUSIONS

The examinations in chapter 4 show that SCFW 2.0 can be used for first assessments of SDH systems as well as for comparison of different system boundaries.

Since the publication of SCFW 2.0 in June 2017, there are about 330 downloads. Besides the calculation tool a handbook was published, which explains the use and the options of SCFW 2.0.

REFERENCES

Deutscher Wetterdienst (07.09.2017) ftp://ftp-cdc.dwd.de/pub/CDC/observations_germany/

DIN Deutsches Institut für Normung e.V. (2014) DIN EN ISO 9806:2014-06, Beuth Verlag GmbH, Berlin

ESTIF – European Solar Thermal Industry Federation (15.09.2017) http://www.estif.org/solarkeymarknew/index.php

Meteotest, Meteonorm: Einstrahlungsdaten für jeden Ort des Planeten (22.08.2017) http://meteonorm.com/de/

Solites (2017) ScenoCalc Fernwärme – Ertragsvorhersagetool für Solarthermie-Anlagen in Wärmenetzen, https://www.scfw.de/

The research project has been funded by the German Federal Ministry for Economic Affairs and Energy (BMWi, FKZ 0325554A and B) by reason of a decision of the German Parliament. The sole responsibility for the content of this publication lies with the authors. Neither the funding organization nor the authors are responsible for any use that may be made of the information contained therein.

MONITORING, SIMULATION AND REAL TIME CONTROL OF LARGE SOLAR COLLECTOR FIELDS - CASE OF LØGUMKLOSTER

Jan Erik Nielsen
PlanEnergi, A.C. Meyers Vænge 15, Copenhagen 2450 SV, Denmark
jen@planenergi.dk

Abstract – In Løgumkloster in the South-West of Denmark, solar collectors with two different types of absorbers are installed. The collector fields have been monitored and the measurements show that the multi-channel absorber performs almost 10 % better than the strip-type absorber. Simulations with a quasi-dynamic model are performed for a "real time control": The model is described.

1. INTRODUCTION

In Løgumkloster in the South-West of Denmark, solar collectors with two different types of absorbers are installed. The collectors are supplying to the same district heating network. The collectors are made by Savosolar - all together approx. 15 000 m².

The two different types are shown in fig. 1.

Strip type	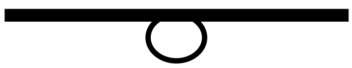
Multi-channel type	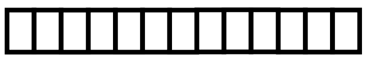

Figure 1. Different absorber types

It would be expected that the multi-channel absorber will perform better due better cooling of the radiated surface.

Apart from the different absorber the collectors are the same.

The collector fields have been monitored and the measurements have been used for check of performance.

Simulations with a quasi-dynamic model are performed for a "real time control": The model is described.

2. ANNUAL PERFORMANCE

The annual performance for the two collector fields is shown in table 1.

Absorber type	Annual output in kWh/m²	% of output of strip type
Strip type	410	100 %
Multi-channel type	447	109 %

Table 1. Annual output of collector fields

It is seen that the collector with the multi-channel absorber performs almost 10 % better than the collector with the strip type absorber. This is what could be expected due to higher absorber fin efficiency factor ***F***, and hence higher collector efficiency factor, ***F'***.

The better efficiency is paid by use of more material.

3. QUASI-DYNAMIC SIMULATION MODEL

A very simple quasi-dynamic model for simulating a collector field has been elaborated.

In the following differential equation, the change in the heat capacity of the solar collector loop is equal to "gathered" solar heat minus heat losses, minus the heat delivered to the district heating plant by means of the heat exchanger:

$$C \cdot dT_m/dt = \eta_0 \cdot G_{res} - U_L \cdot (T_m - T_a) - m \cdot c_p \cdot (T_o - T_i) \qquad (1)$$

where:

C	Heat capacity in solar collector loop per m^2 of collector [J/(K·m²)]
dT_m	Change in solar collector mean temperature over time step [K]
dt	Time step (e.g. 1 hour = 3600 s) [s]
G_{res}	Resulting radiation on collector surface [W/m²]
U_L	Solar collector heat loss coefficient (linearized) [W/(m²·K)]
T_m	Mean temperature in solar collector loop (mean over a time step) [°C]
m	Mass flow rate in collector loop (mean over time step) per m^2 collector [kg/(s·m^2)]
c_p	Specific heat capacity of solar collector fluid [J/(kg·K)]
T_o	Solar collector loop outlet temperature (mean over a time step) [°C]
T_i	Solar collector loop inlet temperature (mean over a time step) [°C]

Since the collector *fluid* represent most of the thermal capacity of the collector loop, only the liquid is used when calculating the thermal capacity, C:

$$C = V_{fluid}/1{,}000 \cdot \rho \cdot c_p \qquad (2)$$

where:

V_{fluid}	Fluid content in pipes and solar collector field per m2 solar collector [l/m²]
ρ	Density of solar collector fluid [kg/m3]

The linearized heat loss coefficient for the solar collector loop, UL is approximated by

$$U_L = a_1' + a_2 \cdot (T_{m,0} - T_a) \qquad (3)$$

where

a_1'	Solar collectors 1st order heat loss coefficient plus heat loss in pipes [W/(m²·K)]
a_2	Solar collectors 2nd order heat loss coefficient [W/(m²·K^2)]
$T_{m,0}$	Mean temperature in solar collector loop in the beginning of time step [°C]

In general, an index "comma null" or "comma one" is added to a parameter to describe a value at the beginning or at the end of a time step respectively. This means for example that $T_{m,0}$ is the parameter T_m in the beginning of a time step, while $T_{m,1}$ is the same parameter at the end of a time step. The mean temperature in the solar collector loop in the beginning of a time step ($T_{m,0}$) is equal to the mean temperature in the solar collector loop in the end of the previous time step i.e. $T_{m,1}$ from the previous time step.

The mass flow rate in kg/s per m² solar collector is calculated based on measured flow in m^3/h:

$$m = V/3600 \cdot \rho / A_{total} \qquad (4)$$

where

V	Volume flow rate in solar collector loop [m^3/h]

By defining two expressions for B_1 and B_2 respectively as:

$$B_1 = (U_L + 2 \cdot m \cdot c_p) \cdot dt/C \qquad (5)$$

$$B_2 = (\eta_0 \cdot G_{res} + U_L \cdot T_a + 2 \cdot m \cdot c_p \cdot T_i) \cdot dt/C \qquad (6)$$

Equation (1) can be rewritten to:

$$dT_m + T_m \cdot B_1 = B_2 \qquad (7)$$

Per definition, the change in T_m (i.e. dT_m) is equal to the difference between the value at the end of a time step and at the beginning of the time step, which as is stated in equation (8):

$$dT_m = T_{m,1} - T_{m,0} \qquad (8)$$

Correspondingly, Tm is defined as the average of values during the time step, which is calculated by:

$$T_m = (T_{m,1} + T_{m,0})/2 \qquad (9)$$

where:

$T_{m,0}$	is the mean collector loop temperature in the beginning of the present time step (which is known from the previous time step) and
$T_{m,1}$	is the mean collector loop temperature in the end of the present time step (which is saved and used as $T_{m,0}$ for the upcoming calculation of the next time step)

By inserting the expression for Tm from equation (9) into equation (7) and inserting the expression for dT_m from equation (8) into equation (7), an expression is created of which $T_{m,1}$ can be isolated:

$$T_{m,1} = [T_{m,0} \cdot (1 - B_1/2) + B_2] / [1 + B_1/2] \qquad (10)$$

T_m (mean of inlet and outlet temperature) can be expressed both by equation (9) and can be calculated as

$$T_m = (T_o + T_i)/2 \qquad (11)$$

By combining these two expressions, T_m can be eliminated, and the outlet temperature can be isolated:

$$T_o = T_{m,1} + T_{m,0} - T_i \quad (12)$$

This calculated outlet temperature is in the validation compared with the measured outlet temperature.

With a known T_o the energy yield Q can be calculated for the given values of flow and inlet temperature.

The measured energy yield is given by equation (13). (Since **m** is the mass flow rate in the solar collector loop per m^2 of solar collector, it is necessary to multiply with the total collector area, A_{total} to get the total energy yield.)

$$Q = \mathbf{m} \cdot A_{total} \cdot c_p \cdot (T_o - T_i) \cdot dt \quad (13)$$

The unit for Q is joule, but if a time step (dt) of 1 hour is used, i.e. dt = 3600 seconds, Q can be calculated in MWh by the expression

$$Q\ [\mathrm{MWh}] = \mathbf{m} \cdot A_{total} \cdot c_p \cdot (T_o - T_i)/10^6 \quad (14)$$

The calculated energy yield is validated by the measured yield.

4. REAL TIME CONTROL / SURVEILLANCE

This very simple quasi-dynamic model is used for simulating the collector field with the multi-channel absorber. Field measurements and simulation results using this simple model are compared – with very good agreement – see figures below.

Fig. 2 shows the measured and simulated in- and outlet temperatures. When the field is in operation the values fit quite well. At night the values differ quite a lot because the measured temperature is indoor near the heat exchanger, whereas the simulated temperature is the temperature inside the collector. Indication on temperatures of warnings / errors can be implemented for real time control - but although the overall picture looks good, large differences in temperatures occurs once a while – especially in the start phase (which is rather difficult to simulate precisely with this simple model).

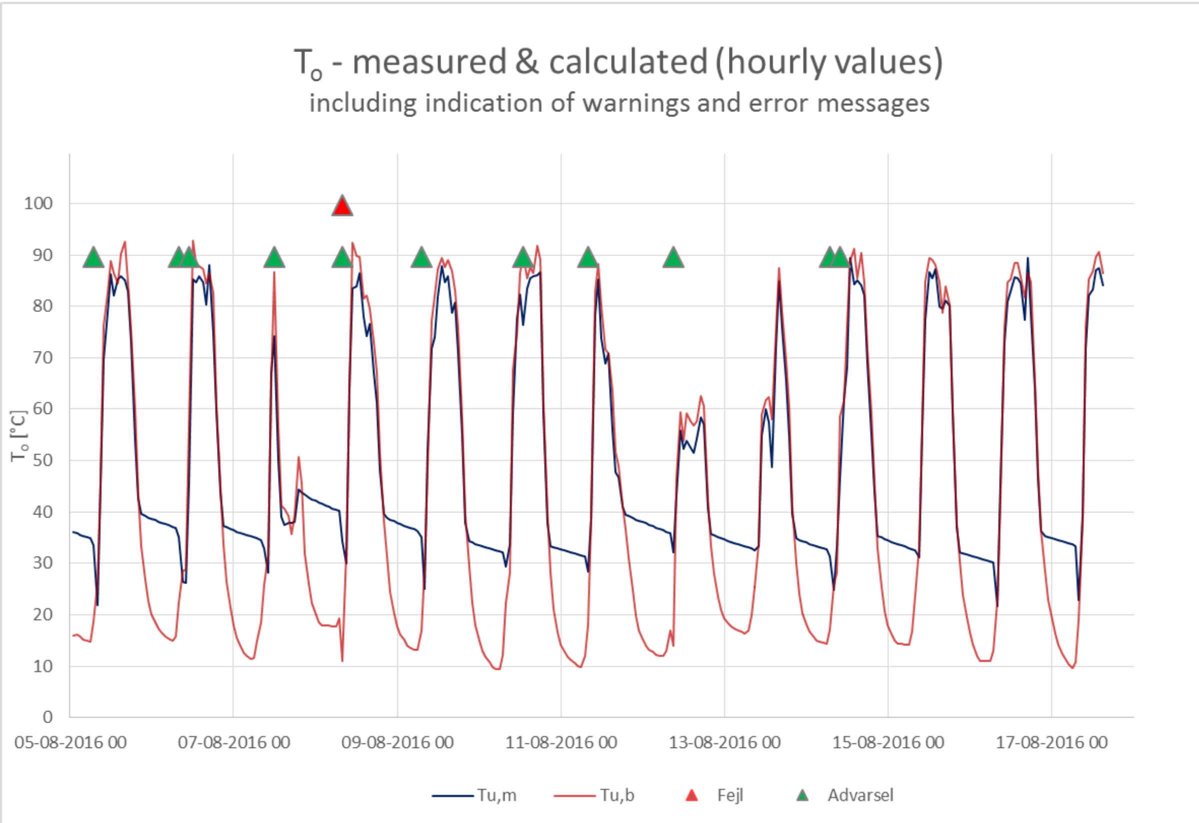

Figure 2. Example of comparison between measured and calculated outlet temperatures including indication of warnings and error messages. $\Delta T_{warning}$ = 10 K; ΔT_{error} = 20 K.

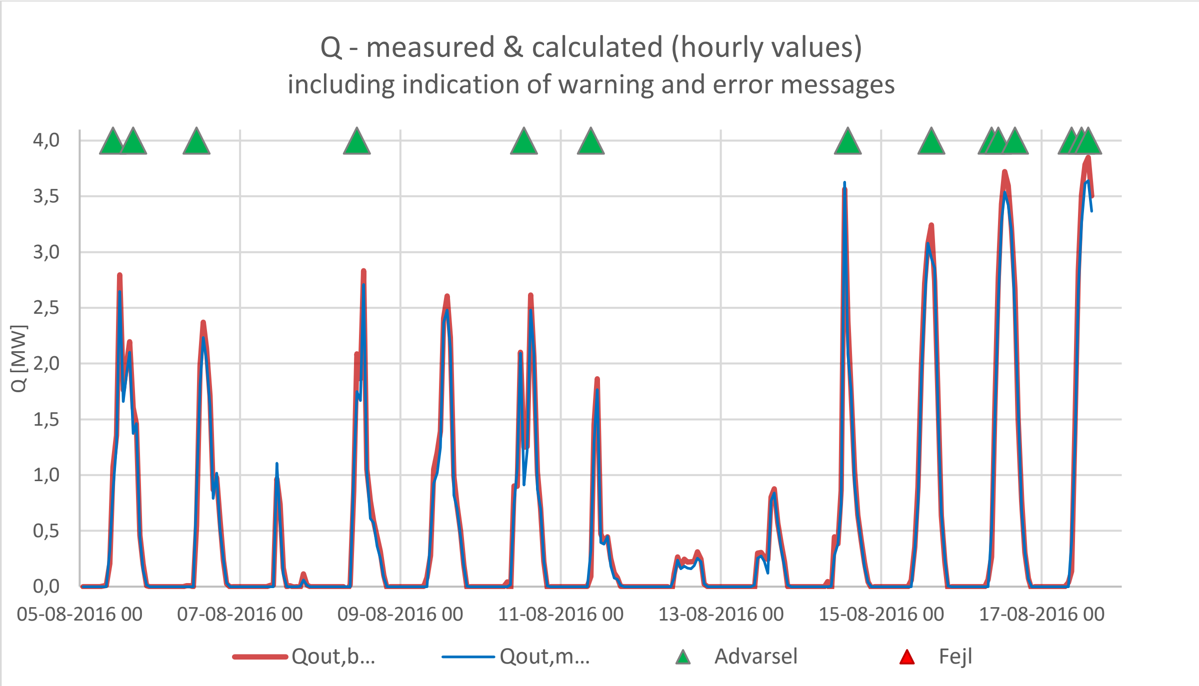

Figure 3. Example of comparison between measured and calculated energy yields including indication of warnings and error messages. $\Delta Q_{warning}$ = 5 % of Q_{nom}; ΔQ_{error} = 10 % of Q_{nom} (at Q_{nom} set to 4 MW).

The collector field in Løgumkloster is operating well in the chosen period in the example. Therefore, criteria should be chosen to avoid error messages and give very few warnings.

One option is to choose only to have the surveillance (and associated warnings and error messages) connected to the energy yield.

In the example shown in fig.3, a margin for warnings of 5 % is chosen to show some examples of warnings. This is however a small margin when taking model and measurement uncertainties into account. A margin for warnings of 10 % and an error margin of 15-20 % are deemed more realistic.

General recommendations for the Løgumkloster system:

- For hourly mean values of the solar energy yield the margin for warnings are set to 10 % of nominal yield.
- For hourly mean values of the solar energy yield the margin for errors are set to 20 % of nominal yield. (For outlet temperature, warning and error messages are deactivated.)

Measurements and system operation should be checked if error messages or several warnings are seen.

5. REFERENCES

[1] “Aluminium Solar Collectors for District Heating” February 2017 (revised November 2017), SAPA Precision Tubing, Løgumkloster Fjernvarme, Ramböll, PlanEnergi, DTU Byg

6. ACKNOWLEDGEMENT

The project is financed by the National Danish EUDP programme.

Long term measured and simulated performance of a combined solar district heating plant with flat plate collectors and parabolic trough collectors in series

Zhiyong Tian[1], Bengt Perers[1], Simon Furbo[1], Jianhua Fan[1], Andreas Zourellis[2]
1, Department of Civil Engineering, Technical University of Denmark, Nordvej Building 119, Kgs. Lyngby, 2800, Denmark, 0045-52781629, zhiytia@byg.dtu.dk

2, Aalborg CSP A/S, Aalborg, Denmark, azo@aalborgcsp.com

TOPIC: Advanced concepts and components- monitoring results

SUMMARY

Large scale solar heating plants develop fast in Europe, especially in Denmark. Most solar collectors used in previous solar heating plants are flat plate collectors. Flat plate collectors have relatively low efficiency at high temperature levels, such as 70 - 95 ℃, which is the supply temperature of district heating networks. Parabolic trough collectors keep a high efficiency at the high temperature level. To maximize the advantages of flat plate collectors and parabolic trough collectors, a novel combined solar heating plant with flat plate collectors and parabolic trough collectors in series has been constructed in Taars, Denmark. The flat plate collectors preheat the return water from the district heating networks to about 75℃, then the parabolic trough collectors heat the preheated water from the flat plate collector field to the required supply temperature of the district heating network. The thermal performance of the combined plant was measured from September, 2015. More than 2 years` thermal performance will be presented in this paper.
Key-words: Taars solar heating plant, parabolic trough collector, flat plate collector, thermal performance

1. Introduction

The number of large solar heating plants in Denmark has increased strongly during the last couples of years. Most solar collectors in the solar heating plants are flat plate collectors. The feasibility of parabolic trough collectors in solar heating plants has been investigated for Danish conditions [1]. A combined solar heating plant with a 5960 m^2 flat plate collector field and a 4032 m^2 parabolic trough collector field has been in operation in Taars since August 2015 [2], see Figs.1-2. The flat plate collectors preheat the return water from the district heating network to about 75℃, then the parabolic trough collectors heat the preheated water from the flat plate collector field to the required supply temperature of the district heating network.

Fig.1. Overview of the flat plate and parabolic trough collector fields in Taars solar heating plant [2].

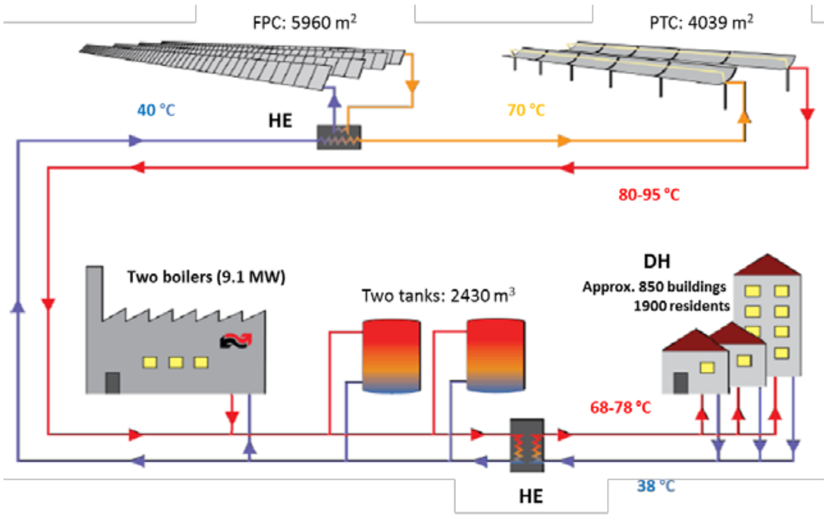

Fig.2. Schematic illustration of Taars solar heating plant.

2. Methods

The inlet temperature, outlet temperature, flow rate etc. of the parabolic trough collector field and the flat plate collector field have been measured. Daily and monthly thermal performances of the parabolic trough collector field and the flat plate collector fields are determined based on the measured data. A Trnsys model has been validated by the measurements [3].

3. Results and conclusions

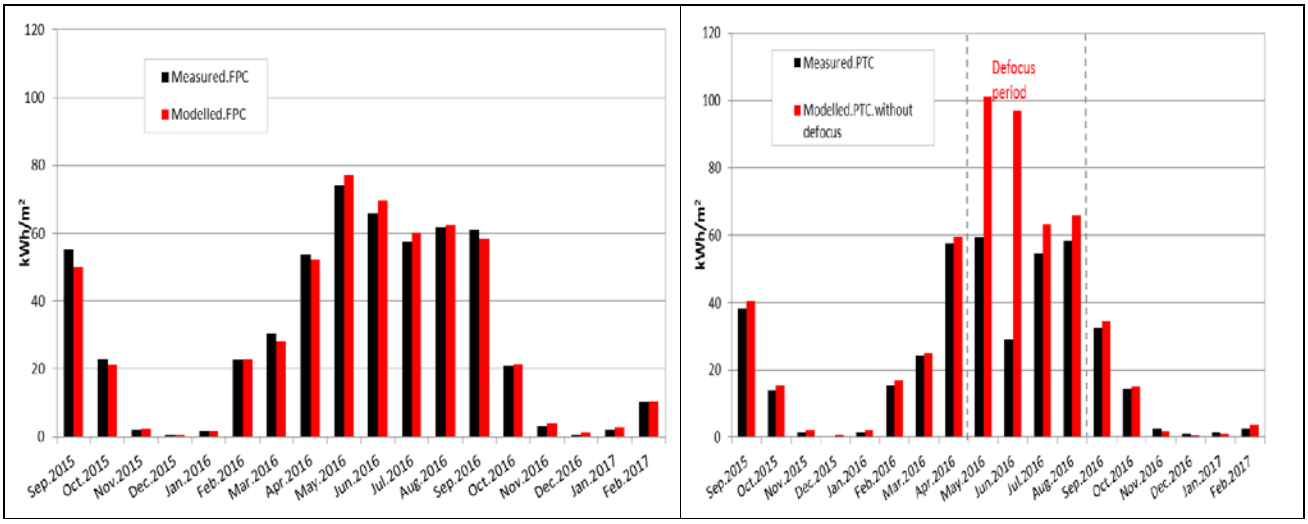

Fig.3. Thermal performances of flat plate collector field and parabolic trough collector field.

Fig.3. shows both measured and simulated performances of the flat plate collector field and parabolic trough collector field. Simulated and measured performances from September 2015 to February 2017 have a good agreement. More measurements and calculations of the thermal performances of both fields will be presented in the paper.

References

[1] B. Perers, S. Furbo, and J. Dragsted, “Thermal performance of concen- trating tracking solar collectors,” *DTU.Report*, vol. 292, no. August, 2013.

[2] Aalborg CSP A/S, “Aalborg CSP,” *http://www.aalborgcsp.com/*, 2017. [Online]. Available: July.2017.

[3] Z. Tian, B. Perers, S. Furbo, and J. Fan, “Analysis and validation of a quasi-dynamic model for a solar collector field with flat plate collectors and parabolic trough collectors in series for district heating,” *Energy*, Sep. 2017.

POTENTIALS FOR GROUND-MOUNTED SDH IN EUROPE

Daniel Trier, Christian Kok Skov and Simon Stendorf Sørensen
PlanEnergi, A.C. Meyers Vænge 15, DK-2450 Copenhagen SV, Denmark
+45 2517 0400, dt@planenergi.dk

Abstract – The trends of the Danish large-scale solar district heating (SDH) development have been investigated and it has been analysed if similar SDH systems could be deployed extensively in other countries. By combining a typical SDH setup with databases of DH networks across Europe, solar radiation etc. the potentials are investigated case by case. The outcomes indicate both availability of suitable land for the collector field and the feasibility of each potential system. The analysis only includes the potential for large ground-mounted solar collector fields outside of cities though roof-mounted (and similar) collector fields could also represent a feasible solution. Besides this, cities with waste incineration facilities and/or excess heat options are excluded as these may cause SDH to become infeasible. This means that the majority of existing DH demand and most big cities are omitted from the further analysis. Hence, the identified potentials only represent a first step in identifying widespread SDH possibilities. The results show that the availability of suitable land is in general not a limiting factor. In most of the investigated 22 countries many options for reasonably priced SDH have been identified, which encourages to exploit this potential. The analysis is carried out within the IEA SHC Task 52 "Solar Heat and Energy Economics in Urban Environments". A complete description of this work is included in the task reporting (Task52, 2018).

1. INTRODUCTION

The background behind the study described in this paper are two main questions:

- A strong solar district heating (SDH) development has been seen in Denmark during the past decade – what are the characteristics of the Danish SDH systems?
- Would it be possible to see a similar development in other countries?

To answer these questions, the Danish SDH systems have been evaluated to derive trends and highlight general (technical and non-technical) characteristics in this sector. A resulting list of typical SDH configurations and replicable boundary conditions of this well-established market is then applied consistently across 22 countries[1].

2. SUMMARY OF TRENDS IN DANISH SDH

Though all values have a significant spread, trends can be seen when analysing the list of more than 100 Danish DH plants having (at least one) solar heating system installed. A typical Danish SDH system could have the following characteristics:

- Solar collector gross area of 13,500 m^2 (This value has been increasing over the years, because new plants tend to be increasingly larger and existing SDH plants often choose to expand their solar heat capacity after some years.)
- Annual solar heat yield of around 400 kWh/m^2 (The yield depends on temperature levels of the district heating (DH) network, storage capacity, operation strategy (i.e. the combination with other units) and the yearly solar irradiation level.)
- Distance from collector field to DH network within 200 m.
- SDH installed in connection to a small town of up to around 5,000 inhabitants or 60,000 MWh of annual DH heat demand.
- Solar fraction typically around 20 %[2].
- DH plant mainly based on natural gas resulting typically in higher heat prices than DH plants using other heat sources.
- Ratio between storage volume and collector area around 0.2 m^3/m^2.
- No problems in finding suitable and available land near the town for the collector field.
- "Cost-of-service" (or "non-profit") principle means that consumer prices must reflect the true cost of heat production. This also means that for the DH utility long-term investments are not considered a problem, while their access to cheap financing[3] improves the economic feasibility.
- For the heat supply taxation on fossil fuels – together with penalties if continuous efficiency improvements[4] are not achieved – have increased the interest for alternative heat supply options by making the business-as-usual scenario more costly.

[1] The countries included in this analysis are Austria, Belgium, Bulgaria, Croatia, Czech Republic, Denmark, Estonia, Finland, France, Germany, Hungary, Italy, Latvia, Lithuania, the Netherlands, Poland, Romania, Slovakia, Slovenia, Spain, Sweden and the United Kingdom.

[2] In this paper solar fraction refers to the share of the heat demand at the DH plant which is covered by solar heat.

[3] This is offered by the Credit Institution for Local and Regional Authorities in Denmark (Kommunekredit, 2006).

[4] Some heat supply technologies are in the agreement (Danish Ministry et. al, 2016) considered equal to actual savings, e.g. solar thermal.

3. METHODOLOGY OF THE EUROPEAN SDH POTENTIAL ANALYSIS (SDHEP1)

3.1 Steps of the Analysis – Methodology Overview

As seen in figure 1 a stepwise approach is used to estimate the possibilities for solar heating systems like the ones found in the Danish DH sector.

The steps include a spatial analysis using GIS software in order to

- check city surroundings for suitable land by applying categories of land use typically suitable for solar collector fields
- check which networks to focus on (and which ones not) based on alternative heat supply options (see section 3.3)
- identify the heat demand of a wide range of DH networks incl. the urban area in which they are located
- apply data on solar radiation for every location to estimate the required area to produce a certain share of the heat demand

The GIS analysis is carried out in a collaboration with the Heat Roadmap Europe project work related to the mapping of renewable heat resources (Persson, 2017).

Cost estimations for the SDH systems are afterwards applied to estimate the cost of solar heat for each individual SDH system. By applying various maximum acceptable heat costs the potentials for feasible ground-mounted SDH systems can be quantified for the DH networks included in the analysis.

Since the list of DH networks included in the analysis is omitting a significant share of the total DH demand (which potentially could also introduce SDH), the analysis can be considered a first step in terms of quantifying and estimating feasibility of large scale SDH potentials in Europe. The overall analysis is therefore referred to as "Solar District Heating – European Potentials version 1" or in short "SDHEP1"

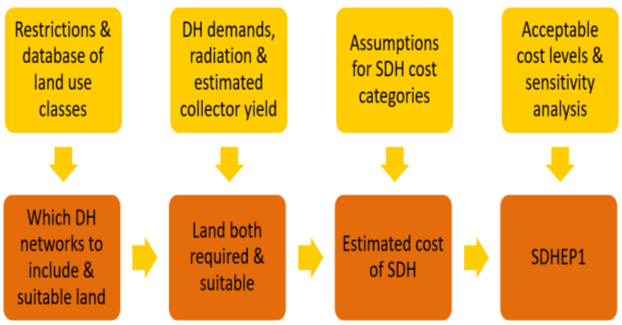

Figure 1. Stepwise approach of the SDH analysis of European potentials.

3.2 GIS Analysis of Land Availability

The Corine Land Cover data is used to define areas which could be suitable for ground-mounted SDH systems.

Table 1. Land use classes considered suitable for SDH systems in the SDHEP1 analysis.

CLC code	General land use class	Detailed land use class
12	Agricultural areas	Non-irrigated arable land
13	Agricultural areas	Permanently irrigated land
18	Agricultural areas	Pastures
21	Agricultural areas	Land principally occupied by agriculture
26	Forest and semi natural areas	Natural grasslands
27	Forest and semi natural areas	Moors and heathland
32	Forest and semi natural areas	Sparsely vegetated areas

Table 1 shows the land use classes considered suitable in the analysis. The outcome shows that most of the identified land suitable for SDH is in category (CLC code) 12 (approx. 2/3) followed by category 18 and 21 comprising almost all remaining areas.

3.3 Restricting the List of DH Networks

Note that the analysis does not represent the full potential for SDH in either Europe as a whole or in the individual countries. The objective has been to identify the most obvious candidate SDH cities, based on general qualifying conditions. This means that only the DH networks without opportunity to access waste incineration ("waste-to-energy" or WtE) or excess heat (e.g. from industrial processes) are included in this analysis. The reason for this limitation is that it does not seem logical to establish a SDH system in places where there is simultaneously a need to cool down a similar (or even larger) amount of excess heat. In these cases, it should be explored if it would make sense to utilise the excess heat already available.

To identify relevant cities for SDH the following criteria are applied:

- No excess heat source within 20 km
- No WtE facility within 20 km
- Suitable land for solar collectors available in the city vicinity (distances of 200 m and 1,000 m from the city boarder are investigated)

3.4 Defining Required Land Area and Collector Area

For each DH network the calculations aim at a solar heat production providing approximately a solar fraction of 20 % and 40 % respectively. In cases where there is not enough suitable land for this, the system is sized according to the land available.

To estimate the yield per square meter of solar collector, the solar radiation on horizontal (Joint Research Center, 2017) is used for every location together with a factor of

0.4 to convert solar radiation on horizontal to the yield from solar collector system at optimum orientation (IEA SHC, 2011). The land area to install one square meter of solar collector (surface) is assumed to be 3.5 m^2.

Heat losses in the transmission pipe between the collector field and the DH network as well as in the associated heat storage are included.

3.5 Cost Assumptions

Four investment categories are considered:

- Solar collector field including the collectors, piping heat exchanger, installation etc.
- Thermal energy storage
- Transmission line to the town
- Cost of land

It is assumed that all associated investments costs are covered within one of these categories. Figure 2, 3 and 4 show indications of the categories covering solar collector field, storage and land investment costs respectively.

For the transmission line the cost is estimated based on the size required to transport the thermal power. Cost assumptions are in the range of 600 €/m for a 10,000 m^2 solar collector field.

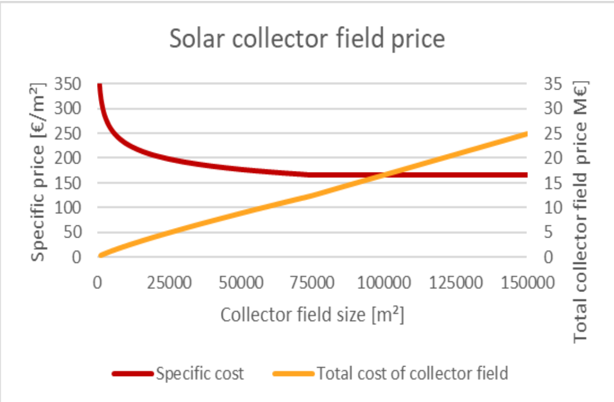

Figure 2. Cost of solar collector field investment depending on collector area.

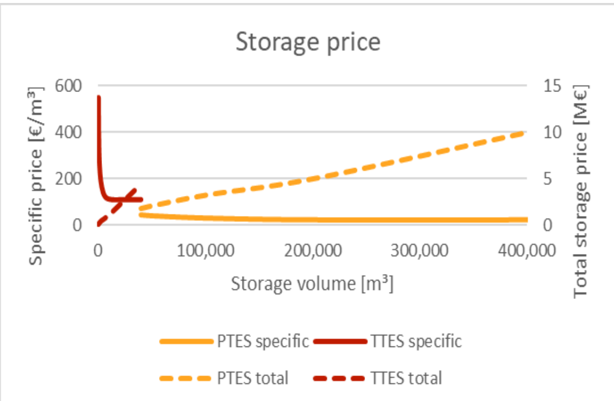

Figure 3. Cost of the thermal storage investment depending on storage volume.

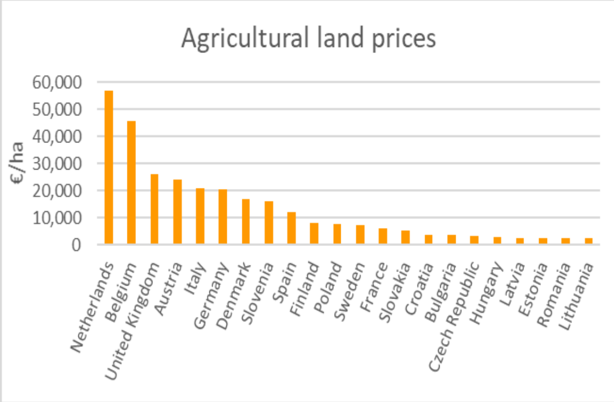

Figure 4. Assumed land investment costs by country.

The investment is assumed financed with an interest rate of 3 % p.a. over 25 years (except for the storages for which 20 years is assumed). No scrap value is assumed though the technical lifetimes of both collector field and transmission line in practice are expected to be longer than 25 years. Also, it will be possible to sell the land after decommissioning of the SDH system. Only including the investment of the land area can therefore be considered a conservative estimate. In that context, the assumed land costs could be considered a rent instead of a purchase. In practice significant deviations are seen even within countries. However, the land costs in this analysis does not cover a major share of the total SDH system cost even with increased cost levels in the sensitivity analysis.

4. RESULTS

4.1 Spatial Analysis of Land Availability

3,280 DH networks have been identified with an accumulated annual demand of 340 TWh. The number of analysed DH systems after excluding networks with/near WtE and/or excess heat is 2,480 i.e. 76 %. However, the corresponding known annual demand of these remaining DH networks is only 71 TWh (21 %). This indicates that the restriction typically excludes the largest DH networks.

The availability of suitable areas for 20 % or 40 % solar fraction in distances of 200 m and 1,000 m from the towns have been investigated. The results show that for only 3 % of the accumulated demand 200 m is not enough to locate suitable land. When aiming at a solar fraction of 40 %, this number is 5 %. Using 1,000 m as distance reduces these values to 1 %. In figure 5 it is illustrated how land availability in general does not seem to be a major issue.

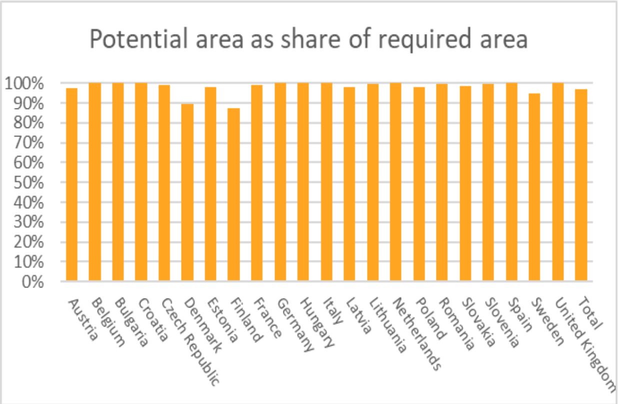

Figure 5. Ratio between the identified suitable land area within 200 m distance from the town and the required area when aiming at a solar fraction of 20 %.

4.2 Feasibility of SDH

In some cases, the estimated average cost of the solar heat becomes too high for the system to be realistically feasible when considering possible alternatives. Therefore, the results are shown for various cost limitations to indicate the accumulated identified potentials depending on which cost level is considered acceptable.

As seen in figure 6, when aiming at 20 % solar fraction (SF) 90 % of the identified SDH potentials (in terms of energy yield) is expected to be possible to realise at solar heat costs of maximum 45 €/MWh. Similarly, more than 70 % should be possible to realise below 35 €/MWh. In comparison, 40 % solar fraction is more expensive to realise. This is (among other things) influenced by the fact that the associated seasonal storage is only used for solar heat even though in practice the most feasible solutions are achieved when the storage also interacts with other DH plant units.

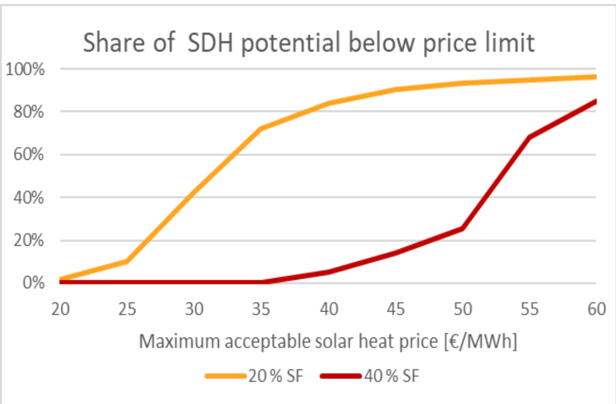

Figure 6. The share of the total identified solar heat production potential depending on solar heat price limit.

The total identified solar collector area potential depending on the maximum acceptable solar heat price is illustrated in figure 7.

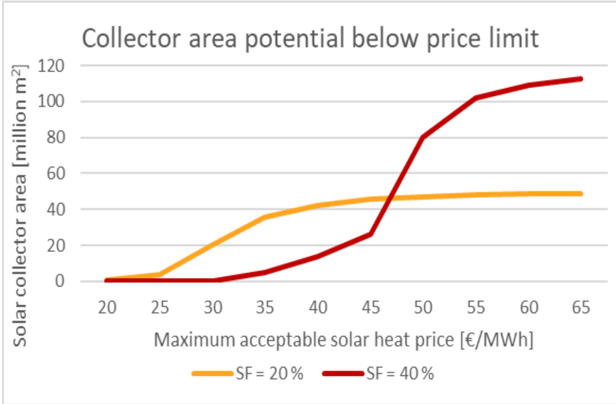

Figure 7. Identified solar collector potential in SDHEP1.

Similar to figure 6 the share of the identified potentials which should be possible to realise within certain price levels can be illustrated by country as shown in figure 8 below. This indicates several countries where low-cost ground-mounted SDH should be possible.

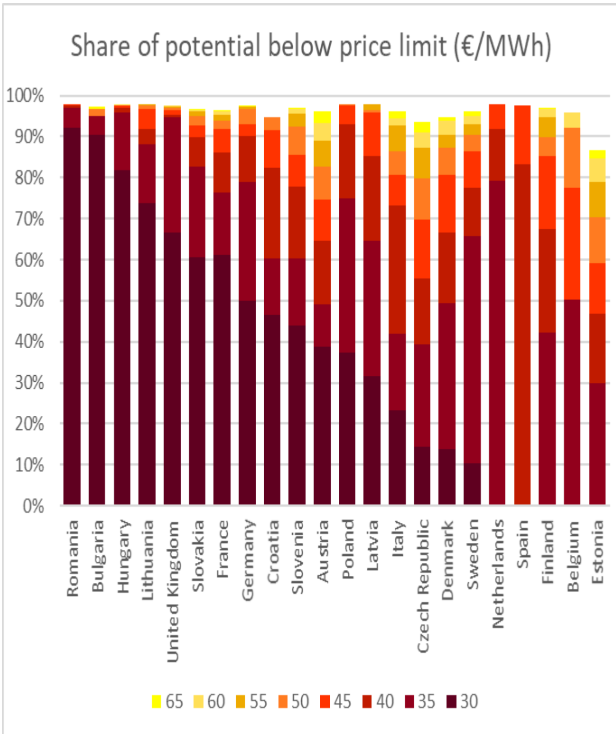

Figure 8. Share of the total identified solar heat potential below certain maximum allowed price limits when aiming at 20 % solar fraction.

Occupying agricultural land for non-food related purposes is not a discussion dealt with in detail within this analysis. However, it is worth considering that the alternative of growing biomass with the purpose of producing fuel will in general have a much lower energy yield per hectare than a solar heating system.

It should be noted that any legislative restrictions on the use of land for ground-mounted SDH systems could reduce these potentials.

5. CONCLUSIONS

The analysis reveals widespread possibilities for the deployment of large scale SDH by using agricultural land for the collector fields and supplying the heat by means of a transmission line to the nearby town. The results do not indicate that boundary conditions for Denmark should be favourable to an extent which makes it impossible to replicate the SDH development elsewhere.

The following key conclusions can be derived from the analysis:

- Disqualifying DH with WtE or excess heat available nearby means that the majority of existing DH demand and most big cities are omitted from the further analysis.
- The availability of suitable land is in general not a significant limiting factor when it comes to the potential for the investigated DH networks.
- Large scale systems are key to reach a low cost per m^2 of collector and thereby also low average costs of the solar heat produced.
- In most of the investigated countries many options for SDH at reasonable price levels have been identified, which encourages to exploit this potential.
- Increasing fossil fuel taxes can be an incentive for renewable energy (RE). With a carefully structured and stable political framework, incentives for RE can counterbalance the associated cost increase for utilities presently basing their supply on fossil fuels. By planning ahead all stakeholders can thereby maintain the same overall cost range while a green transition is facilitated.

ACKNOWLEDGEMENT

This paper is realised as part of the Heat Roadmap Europe project (HRE) which has received funding from the European Union's Horizon 2020 research and innovation programme under grant agreement no. 695989. The sole responsibility of this publication lies with the authors. It does not necessarily reflect the opinion of the funding authorities. Neither the authors nor the European Union is responsible for any use that may be made of the information contained herein.

The methodology and analysis were carried out in a collaboration between HRE and the IEA SHC Task 52 "Solar Heat and Energy Economics in Urban Environments".

The authors' participation in IEA SHC Task 52 is funded by the Energy Technology Development and Demonstration Program of the Danish Energy Agency under the grant number 64013-0533.

REFERENCES

(Task 52, 2018):
Reports are downloadable upon publication. See the IEA SHC Task 52 website task52.iea-shc.org.

(Kommunekredit, 2006):
Act on the Credit Institution for Local and Regional Authorities in Denmark (Lov om Kreditforeningen af kommuner og regioner i Danmark). ACT no. 383 of 3 May 2006.
www.kommunekredit.dk/wp-content/uploads/2017/09/act_on_kk.pdf

(Danish Ministry et. al, 2016):
Danish Ministry of Energy, Utilities and Climate, The Danish Energy Agency, the Danish District Heating Association, the Association of Danish CHP Plant, HMN GasNet, Danish Gas Distribution, NGF Nature Energy and the Danish Oil Industry Association. Agreement on the energy companies' energy savings effort. December 16th 2016. (Following up on an agreement from 2012). ens.dk/sites/ens.dk/files/Energibesparelser/energispareaftale_161216mbilag_6_eng.pdf

(Persson, 2017):
Urban Persson, Bernd Möller, Eva Wiechers. Heat Roadmap Europe – Methodologies and assumptions used in the mapping. August 2017.
heatroadmap.eu/resources/HRE4_D2.3.pdf

(Joint Research Center, 2017):
Joint Research Center, Institute for Energy and Transport (IET), European Commission. Ground-station based solar radiation data hor_rad_PVGIS_classic_year_latlon. Downloaded dataset (accessed 13-01-2017).

(IEA SHC, 2011):
IEA SHC Common Calculation Method: Solar Collector Energy Output, March 2011, iea-shc.org/common-calculation-method

ENERGY AND CLIMATE RELATED SPATIAL PLANNING IN THE PROVINCE OF STYRIA

Mag. Christine Schwaberger, Provincial Government of Styria, Department of Environment and Spatial Planning, Stempfergasse 7, 8010 Graz, Austria, Tel: +43 316 877 4197, christine.schwaberger@stmk.gv.at

Dipl. Ing. Dr. Lore Abart-Heriszt, University of Natural Resources and Life Sciences, Peter Jordan Straße 82 1190 Wien, Austria, Tel: +43 1 47654 85523, lore.abart@boku.ac.at

Spatial planning and urban planners play a key role in creating urban environments that support less energy-intense lifestyles and communities. The **SPECIAL project** has been set up to bridge the gap between climate/energy strategies and spatial/urban planning and to promote the integration of sustainable energy aspects into spatial planning strategies especially at a local level.

SPECIAL was a project from 2013 to 2016 funded by **Intelligent Energy Europe** and based on a partnership between eight Town Planning Associations (TPAs) and planning authorities across Europe. The Town and Country Planning Association (TCPA) was the lead partner; other partner planning associations were located in Sweden, Ireland, Hungary, Italy, Greece, Germany and Austria. The Department of Spatial Planning in the Provincial Government of Styria was one of the eight partners in the European project SPECIAL.

The **Department of Spatial Planning** is the institution responsible for the spatial planning at local level for the entire province of Styria (287 municipalities). It is mainly busy with the consultation of municipalities in terms of the development of their land use maps, zoning plans, master plans and development concepts, which have to be elaborated according to the Styrian Spatial Planning Law.

Furthermore, the department deals with the development of the planning law and its corresponding instruments. Another task of the department is the coordination of spatial and urban planning with other disciplines (e.g. climate protection, transport and housing). Finally, the department aims to stimulate the exchange of experiences and competences among the Austrian provinces (to integrate new methods and to learn from good practice examples).

During the SPECIAL project it became obvious that a **wide range of regulations** with regard to energy- and climate-related issues is already in place within the Styrian Spatial Planning Law. To this effect it is “just” the task of the planners at local level and of the Department of Spatial Planning to apply the planning instruments in a more “energy spatial planning” way than before.

Since the start of the project SPECIAL the Department of Spatial Planning has increasingly put emphasise on the **significance of integrated spatial and energy planning** in diverse Styrian development strategies.

Several steps have already been taken or are in preparation:

In September 2015 the Styrian Government decided the **“Climate Change Adaptation Strategy of Styria 2050”** which had been elaborated in the Energy Department in the Provincial Government of Styria. It includes aims and activities for the implementation of solutions for climate change adaption by means of spatial planning (safeguarding open land, protection against natural hazards, conservation of green and blue infrastructure, establishing integrated spatial and energy planning…). These measurements have to be partly implemented within the next 2-3 years.

From spring 2016 to spring 2017 a project concerning the implementation of integrated spatial and energy planning at local level was carried out by the Institute of Spatial Planning, Environmental Planning and Land Rearrangement of the BOKU (University of Natural Resources and Life Sciences, Vienna). Based on two case studies possible **contents of an “energy strategy”** as contribution to the spatial development concept of municipalities was assessed in this project.

In January 2018 the **“Climate and Energy Strategy of Styria 2030”** which had been elaborated in the Energy Department of the Provincial Government of Styria was decided by political will. It comprises integrated spatial and energy planning strategies focussing on the local level (strengthening of inner cities, development of tightly arranged settlement structures, climate friendly organisation of infrastructure and mobility, …).

In March 2018 a **guideline for municipalities** has been presented to public which gives recommendations for drafting an “energy strategy”. This guideline is based on the before mentioned project of the BOKU Vienna and illustrates to what extent the “energy strategy” supports the integration of energy-related issues in the spatial planning process.

Currently, the BOKU Vienna is preparing a **spatially and factually highly differentiated database** with information about “energy consumption and greenhouse gas emissions” for all 287 Styrian municipalities as a basis for the elaboration of “energy strategies” according to the guideline.

The database represents the energy- and climate-related status-quo at local level (“opening balance”). It delivers an extensive picture of the structural data considering all kinds of land use and mobility as well as of total energy consumption, heat density and greenhouse-gas emissions (in a 250m-grid). Moreover, it delivers potentials of renewable energy sources available at local level.

This database provides a sound foundation for drafting strategies to dispose future spatial development on priority areas of integrated spatial and energy planning. These areas encompass spatial structures characterised by energy consumption and greenhouse gas emissions at a low level.

Within the energy strategy considerations for pursuing spatially differentiated approaches with respect to heat supply and for concentrating future spatial development to **priority areas for district heating** (from renewable energy sources) are of crucial importance. In areas with conduction-bound heat-supply systems integrated spatial and energy planning is centred on the (further) development of multi-purpose settlement structures with moderate density. This meets the requirement to provide and develop the spatial frame for a sufficiently high number of heat recipients and hence for the mid- to long-term warranty for an economic operation of a district heating network.

In addition, the energy strategy focuses on directing the future settlement development on **priority areas for energy saving mobility**. Accounting for different quality grades of public transport (which also include information on the service level) and the intensity of land use (depending on the mix of different kinds of land use and the settlement density) more differentiated statements can be made in the energy strategy than in the conventional planning procedure. The options of integrated spatial and energy planning for promoting an energy-saving mobility refer to the design of compact settlement structures following the principle of short connections and to the adaptation of the settlement development to the structures of public transport.

Binding regulations towards **steering the spatial development on priority areas** of integrated spatial and energy planning need to be established in the spatial development concept on local level. In this context, statements should be made regarding the spatial and functional pattern of the municipality, development directions for building areas can be defined and priorities for the settlement development can be set. The principles, targets and regulations in the spatial development concept are to be implemented in the subordinated instruments (e.g. land use plans). In particular, this concerns the site of building areas, the mix of different kinds of land use, the settlement density as well as housing type and mode of infrastructure development.

The preparation of the database with the opening balances for all Styrian municipalities will be finished by the end of the year 2018. The database will be available at free access for municipalities via the GIS Styria.

From autumn 2018 to summer 2019 planners and municipalities will have the opportunity to join an **education and consulting service** to be advised in terms how to use the manifold information of the database for the elaboration of energy strategies with the help of the abovementioned guideline.

To this effect, Styria is well on the way to enable decision-makers in spatial planning at local level to **merge spatial planning policy with energy and climate related targets**. Henceforward, Styrian municipalities can contribute to the development of spatial preconditions for the energy transition and for the compliance with international commitments of climate protection.

HAMBURG INSTITUT
sustainable strategy consultants

5th International Solar District Heating Conference

in Graz/Austria, April 2018

Submission of abstract

Topic

2: SDH in urban context

- integration in larger urban DH systems
- large collector fields in urban environment

Intuition: Hamburg Institut
Speaker: Simona Weisleder / Christian Maaß

Title: MULTI-CODED AREAS FOR SDH

Solar District Heating is a simple, proven and cost-efficient option to integrate RES in DH if large areas are available and “plug and play” solutions can be realised. This approach has been very successful in Denmark.

Transferring this approach to other central European countries has so far only succeeded in a few cases. The experience of the last years shows that scarcity of areas is a major barrier to implement SDH, particularly in urbanized regions.

The development of SDH projects often fails due to a lack of available space. In densely populated urban areas like the Hamburg Metropolitan Region, space is needed for many other competing purposes like housing, traffic infrastructure, industry and commerce, nature conservation or - in the rural parts of the region - for agriculture.

To overcome these barriers, policy instruments are needed to facilitate the usage of urban areas for SDH – in the best case for simple, large and cost-efficient solutions. At the same time, it seems necessary to find instruments that enable SDH on areas with additional usages – in parallel and on the same ground with SDH. We have to re-think our perspective and our understanding of monovalent land use and we need to develop multi-coded areas. Those solutions might be at first glance more complicated, more experimental and maybe more expensive, but the transformation of the heating sector especially in the urban regions might only be successful in cooperation-models with other land usages.

Within the EU project, SDHp2m the Hamburg Institut is working on a best practice guide for the Metropolitan Region of Hamburg, which points out possibilities to develop SDH areas and double usages of urban areas with best practice examples. On this basis, recommendations for policy instruments to facilitate such solutions will be developed.

Examples of such multi-coded areas for SDH have been developed as concepts but have been so far rarely been implemented in practice. SDH land area development and double usage of areas for SDH and other purposes is so far hardly addressed in national or regional planning law or other policy instruments. Examples from many regions in the EU show that solutions for SDH land development and for parallel land use through SDH and other purposes can be found.

Categories for multi-coded areas for SDH include:

- large scale roof areas (existing and new build)
- large infrastructure installations (e.g. parking decks, sewage treatment plants)
- polluted or contaminated areas (e.g. former landfills or sludge hills)
- areas used for noise protection along traffic routes (e.g. motorway, railway)
- agricultural production (e.g. so called “Solar Neighbourhood Greenhouse”)
- nature preservation and water protection areas

Some experiences can be transferred from large photovoltaic installations, where multi-coding already is more common, e.g. on large parking decks, as noise protection and on greenhouses. But in several questions we need to investigate the special technical case of double-utilization with solar thermal installations, e.g. the hydraulic system of elongated installations along traffic routes or safety issues roofing parking decks with hot liquids in pipes. Furthermore, issues of cost efficiency have to be investigated, including a comparison to “plug and play” solutions. Or can we generate additional income with the double utilization? Are those solutions scalable or will they stay a niche product?

In the presentation, the above mentioned questions will be addressed and best practise examples for SDH projects from across the EU will be presented. The presentation will also point out policy instruments that foster SDH on multi coded land areas.

Creativity and open-minded discussions are important to gain solutions for multi-coded areas for SDH. It is not a question, that we need areas for energy production in the Regions, but how we can organize them in a sustainable and compatible way. The SDH conference should be used as a platform to lead this discussion among international experts.

Solar Neighbourhood Greenhouses developed by Hamburg Institut use urban open spaces twice: for solar thermal energy and urban gardening. They provide neighbourhoods with renewable energy trough SDH and healthy food, encourage community building and promote public acceptance.

INTEGRATED AND SUSTAINABLE ENERGY CONCEPTS FOR URBAN NEIGHBOURHOODS – A GENERIC APPROACH BASED ON AUSTRIAN EXPERIENCES

DI (FH) Gerhard Hofer, DI Christof Amann, Daniela Bachner, MSc
e7 Energie Markt Analyse GmbH, Walcherstraße 11, 1020 Vienna, Austria, Phone Number: +43 1 907 80 26-55, Fax Number: +43 1 907 80 26-10, e-mail adress: gerhard.hofer@e-sieben.at

Abstract – Larger Austrian cities are confronted with the necessity to develop new districts and to revitalise existing neighbourhoods. This process includes the development of new energy supply systems. Conventional in Vienna usually are gas grids for decentralised use on the one hand and district heating systems on the other hand. But both systems remain unsatisfactory: The simple gas supply is not in line with sustainability and greenhouse gas (GHG) emission reduction goals, whereas district heating (with combined heat and power (CHP) as one major source) is confronted with serious economic problems due to changes at the electricity markets and municipal utilities thus refuse to enlarge their district heating systems.

The paper describes the process for selecting alternative heat supply concept for a new urban settlement. The assessment of locally available renewable resources and infrastructures sets the basis for the identification of technically feasible options. After definition of specific heat supply ideas, concept design phase leads to dimensioning of elements of the heat supply concepts. Based on the technical description an environmental and economical assessment was carried out. The different technical and energy-economical energy concept options are assessed by means of a life-cycle cost analysis.

This generic approach was applied in the concept phase of the development of a new neighbourhood area in the City of Vienna called Donaufeld. In this feasibility study several technical options for heat supply were developed together with experts within the administration of the city and the municipal energy supplier.

Main outcome of the project are life-cycle costs for every heat supply concept. Alternative concepts with heat pumps and geothermal probes as main elements have similar life cycle costs than district heating. These concepts have a high share of locally produced renewable energy and can meet local 2000 Watt targets. However, higher investment costs have to be covered at the very beginning which is crucial for existing funding conditions for buildings.

1. BACKGROUND

Cities are facing the challenge of developing new districts and increasing the density of existing districts' due to constant urbanisation. In addition, the development of energy supply solutions for these city districts is part of this process. Conventional solutions are gas networks and decentralised use of gas boilers in buildings or district heat supply - but both systems are unsatisfactory with regard to new urban areas. The increasing need for sustainability and the targets of reducing the GHG emissions are not in line with simple gas supply. Owing to the changes in the electricity market, district heating (with cogeneration and gas as one of the main sources) is confronted with serious economic problems recently. Hence, urban energy suppliers avoid expanding the district heating plants. In addition, district heat supply reaches its limits of economic efficiency at lower energy density in the supply areas. Moreover, the question rises whether it makes a good economic sense to have two infrastructures for heating and energy at decreasing heat consumption.

The city of Vienna faces a particularly big challenge. There are 1.77 million people living in Vienna at the moment (as of 2013) [1]. Forecasts say that the city will have more than 2 million inhabitants by 2028 already. This means an average increase of more than 15,000 people per year [2]. Therefore, numerous new districts are built in the "green fields" to meet the housing demand.

The city sets great value on the sustainability of these development areas. In the course of the Smart City initiative [3], targets for living quality, conserving resources and innovation as well as the target values for CO_2 emissions and primary energy demand defined in accordance with the requirements of the Zurich 2000-watt society [4]. In order to achieve a sustainable and fair society, the city of Zurich has decided upon the 2000-watt model. According to this model, the known overall average primary energy usage of 2,000 Watt is sufficient for every human being, which equals a yearly energy demand of about 17,500 kWh electricity and heat per person. Thereby, about one fourth of this output (500 Watt primary energy) is available for housing purposes [5].

For the above reasons, the Municipal Department for Energy Planning (MA 20) of the city of Vienna commissioned a study to examine the technical energy supply solutions that are both environmental and economically viable for a concrete urban construction site while taking account of local renewable energy sources. The construction site is the city development area Donaufeld in the north of Vienna.

2. CITY DEVELOPMENT AREA DONAUFELD

The city development area Donaufeld has a size of about 60 hectares and is located in Floridsdorf, the 21th district of Vienna. According to the guiding principles [6], the target is to develop an energy strategy that leads to an environment and climate friendly district.

This area will be mostly used for residential buildings. There are plans to construct buildings on an area of 757,000 square metres gross floor area and 6,000 apartments. A very dense development is intended with buildings having 5-7 upper floors.

Figure 1: Overview and site plan of the city development area Donaufeld (Source: Guiding principles of Donaufeld, own additions)

The area will be realised in three construction phases. The first construction site is located southeast of the Donaufeld; the second construction site is located in the northeast. Both are situated east of the grass strip and will be set up in the coming years. The third construction site is located in the west of the green area and will probably only be built in the mid-2020s.

3. METHODS

3.1 Development process

It was the target of the project to develop possible energy supply solutions for the new district Donaufeld in consideration of local renewable energy resources, the examination of the technical feasibility as well as the environmental and economical evaluation. Moreover, it was aimed at involving essential stakeholders of the city of Vienna for new heat supply solutions. For this reason, a project advisory board was announced that includes municipal stakeholders. However, the municipal energy supplier is the main addressee of the study: the energy supplier’s next step should be the implementation of the newly developed heat supply solution in concrete development areas.

At the beginning of the project, the members of the project advisory board were asked to submit proposals on how to create a sustainable heat supply for Donaufeld. After that, agreement on a shortlist of possible heat supply options was reached. During the following meetings of the project advisory board, the current status and the interim results were presented and discussed in order to keep the participants informed and give them the possibility to actively contribute their experience and know-how. Thus, the heat supply options could be adjusted to the Viennese general conditions and can expect a higher acceptance.

3.2 Calculating and dimensioning methods

The development of heat supply solutions is built on determining the level and density of energy demand as well as analysing the local energy resources. On the basis of the values found, the performance values for space heating and hot water were calculated. The size and the operating mode of the plant were defined according to the heat supply solution.

On the one hand, the energy demand definition is based on determining the maximum permissible value of the heating demand and the expectable building compactness in the construction site; on the other hand, it relies on internal surveys and measurements of buildings that are similar in size and built with a construction standard of about 2010 conducted by the municipal energy supplier. In order to determine the hot water demand [7,8,9] and energy demand of households [10,11,12] further studies were taken into account.

The heat amount necessary to satisfy the demand for heating and hot water as well as the upstream losses up to the building’s technical centre is the relevant factor to determine the heat demand. The system boundary of the value is comparable to the Q*H of room heating as well as the Q*TW of hot water according to the Austrian Standard (ÖNORM) H 5056 [13]. The level for these indicators for room heating is 35 kWh/m²year and 28 kWh/m²year for hot water (referring to the conditioned gross floor area). These values are measured values and are based on a study of similar buildings by the municipal energy supplier. In comparison to the calculated heat demand of a passive house (about 10 kWh/m²year per gross floor area), these values seem to be relatively high. The differences to heat demand calculations according to the requirements for energy performance certificates are additional losses because of heat emission and distribution and higher indoor temperature than used in heat demand calculations. The assessment of the differences to energy consumption is calculated by using the monthly energy balance method for issuing the energy performance certificate in Austria [14]. The design values for the building envelope are as followed: U-value for wall = 0.12 W/m²K, U-value for windows (total) = 0.90 W/m²K, U-values for roof = 0.10 W/m²K. The ratio between surface and building volume = 0.35 1/m and indoor temperature was set to 22°C in contrast to 20°C based to the requirements of the energy performance certificate.

The construction site and the surrounding exploitations were examined to define the local renewable energy resources. A first limitation was done by the study “Options for designing the Viennese energy systems in the future” (Ger. „Optionen für die Gestaltung des Wiener Energiesystems der Zukunft“) [15] of the Vienna University of Technology (TU Wien). This study gives an overview of plausible options for renewable energy sources within the city of Vienna. With respect to the energy resources mentioned in the study, the local circumstances were examined regarding renewable energy resources as a second limitation. The use of ground-source heat pump and solar energy is regarded as promising.

This city development area consists almost entirely of residential buildings. There is no remarkable amount of waste heat within the construction site (e.g. due to cooling systems of commercial areas) that could be included in the concept. Unfortunately, big potential for waste heat lies outside of the construction site, e.g. in buildings such as the indoor sporting arena "Albert-Schulz-Halle" or the shopping mall "Donauzentrum". These objects were not taken into consideration, because their distance to the border of the construction site is bigger than 500 metres and other city development areas are planned that are closer to those objects.

4. RESULTS

4.1 List of energy supply solutions that have been examined in detail (shortlist)

The selection of energy supply options is divided into reference options, options with heat network (with/without district heating) and an option without heat network (see figure 2).

Reference options are those options that are normally used at the moment in Vienna. On the one hand, there is the option of district heating connected to the building (option 0); on the other hand, there is the option of a gas boiler in every building (option 4). According to the requirements of the Viennese building regulations, however, heat supply must not be provided by a gas boiler only. In order to reduce the CO2 emissions, solar thermal energy of one square meter collector surface per 100 square meters living area of the building has to be considered when using gas boilers as main heat generation system.

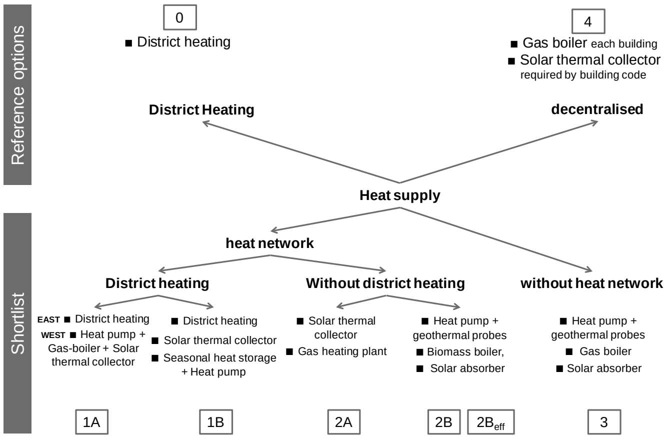

Figure 2: Shortlist of energy supply options

Options including a heat network and district heating are divided as follows:

- Option 1A: Construction phase 1 and 2 (east of the green area) will be supplied with district heating. The supply of construction phase 3 (west of the green area) will be ensured with a heat pump on the building site and a central gas boiler to cover peak loads as well as solar thermal energy on the roof of the building.
- Option 1B: This option tries to reach a maximum coverage with solar thermal energy. The solar heat will be saved in seasonal storages. One heat pump per seasonal storage as well as district heating is available to cover the additional heat demand. The seasonal storage should be a concrete container filled with water for thermal storage. There are two additional heat systems as heat pump is used for base load and district heating just for peak load.

Options including a heat network without district heating are divided as follows:

- Option 2A: Solar thermal energy is intended on about 30% of the roof surface. The remaining heat demand will be supplied with central gas heating plants per construction phase.
- Option 2B: Option 2B consists of a small micro heat networks for around 4 - 7 buildings. This covers an area without street crossings. Heat is

provided by heat pumps and geothermal probes. An exhaust air heat pump for buildings will be used for hot water. The electricity yield of the photovoltaic system on the roof will be directly utilised for the pump. Solar absorbers and heat pumps are used for regeneration of geothermal probes.

- Option 2Beff: Option 2Beff complies with option 2B, but has a reduced energy demand and thermal load by integrated ventilation systems with heat recovery.

Option 3 is planned without a heat network. Instead, one heat pump per construction site will be installed. The heating resources are geothermal probes. Solar absorbers and heat pumps are used for regeneration of geothermal probes in summer.

In the course of this study, the examination of a high number of technologies and supply systems was intended. Figure 3 provides an overview about the different possibilities to design the single options. It depicts the determinations for heat supply, heat networks, the temperature level of heat networks, ways of storage, hot water supply as well as the way of solar energy usage.

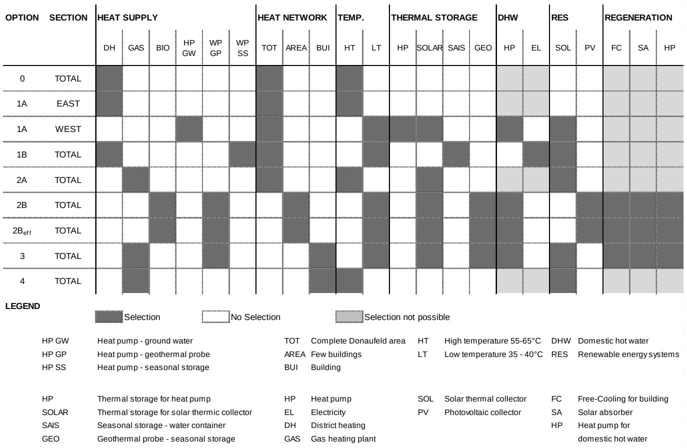

Figure 3: Overview about the different technologies of energy supply options

With regard to the option using geothermal probes, heat supply for the building as well as the regeneration of the geothermal probes have to be considered. According to the concepts of option 2B, 2Beff and 3, which include fields of geothermal probes, it is necessary to balance the heat exchange in geothermal probes equally. That means that the energy amount used for room heating and hot water in winter has to be reproduced in summer. Otherwise, there is the threat of the soil cooling down in the long-term (up to the freezing of probes) and a decrease in the efficiency of the energy supply solutions [16].

In order to regenerate the geothermal probes, free cooling of the apartments as well as the storage of heat from heat supply systems is intended. The following methods are examined to be used as heat supply systems: solar absorbers, reverse cycle heat exchangers (used as recovered heat), photovoltaic-thermal collectors (PVT), thermal solar plants and hot water heat pumps. The decisive factors are their possible application in summer and low production costs for the heat. For this project, solar absorbers and heat pumps are selected for thermal regeneration purposes.

4.2 Environmental evaluation of energy supply solutions

For environmental assessment, the indicators primary energy and CO_2 emissions are used. The energy consumption per supply option is calculated by means of an annual balance based on the calculation methods according to the Austrian Standard (ÖNORM) H 5056. This is a monthly energy balance taking into account energy losses for heat emission, distribution, storage and generation. The heat demand for room heating and hot water has already been defined (see chapter "Method"). Based on these values, the losses outside of the building due to heat distribution, heat storage as well as heat supply were calculated.

The results are annual balanced final energy parameters of every energy supply option. In order to identify the CO_2 emissions and primary energy parameters, the final energy was multiplied by the conversion factors in table 1:

Table 1: Conversion factors for primary energy and CO2 (source: OIB Richtlinie 6, edition 2015; Wien Energie)

Source of energy	Primary energy factor	Primary energy factor renewable	Unit	CO_2 emission parameter	Unit
Electrici-ty	1.91	0.59	-	276	g/kWh
Gas	1.17	0.00	-	236	g/kWh
District heating in Vienna	0.33	0.06	-	20	g/kWh
Biomass	1.08	1.02	-	4	g/kWh

The values for specific primary energy demand per square meter gross floor area of the options are between 21 and 75 kWh/m²year. The lowest primary energy demand (about 21 kWh/m²year) is caused by district heat supply (option 0). This value is enabled by a low primary energy factor of 0.33 for district heating in Vienna caused by the allocation between electricity and heat for CHP plants. By contrast, the values for gas heating are the highest (option 4 and 2A). The options with heat pumps (2B, 2Beff and 3) have a specific primary energy demand between 40 and 50 kWh/m²year. Primary energy factor for electricity is 1,91 and is based on a the mix of electricity production in Austria. This value is stated in the OIB G 6 which defines minimum energy performance requirements for buildings and primary energy factos for the Energy Performance Certificate. Efficient heat pumps lay good foundations for a low primary energy value, whereas peak load boilers increase this value. The options that use a mixture of district heating and heat pumps (option 1A and 1B) require around 30 kWh/m²year.

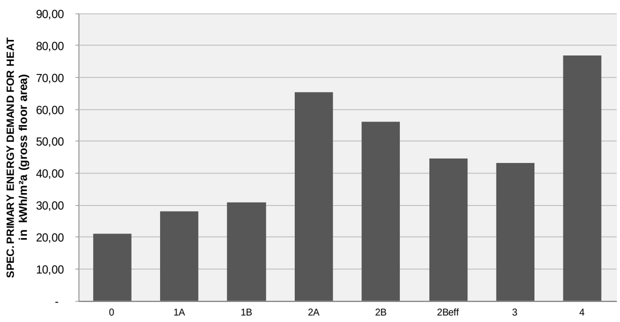

Figure 4: Area specific primary energy of the energy supply options

A similar picture can be seen when evaluating the CO_2 emissions (see Figure 5). In terms of this indicator, options with gas supply are responsible for the highest CO_2 emissions; whereas options with district heating cause only very low emissions. In comparison to primary energy, options with biomass boilers (option 2B and 2Beff) achieve better value due to a low CO_2 factor of 4 g/kWh.

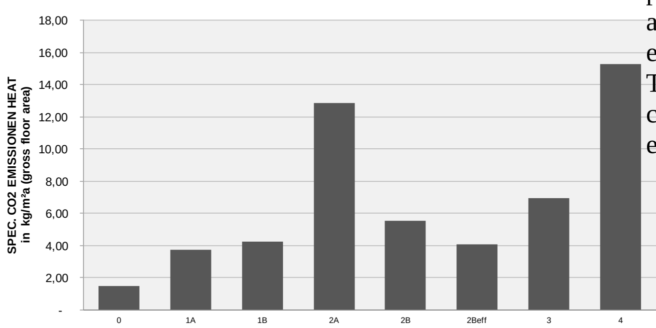

Figure 5: Area specific CO2 emissions of the energy supply options

In figure 6, the energy supply options were measured by the primary energy performance target of 500 W/person (based on the non-renewable primary energy factor). This value is related to the 2000 Watt model of Zurich. The value 500 W is the share for residential buildings. The figure shows that the options using mainly gas supply cannot keep the 2000 watt targets, as they already shortly fall below or even exceed the targets regarding the energy demand of room heating and hot water. The values for the use of electricity in apartments (248 Watt/person) have not been considered here. The options using district heating as well as those using heat pumps, are significantly below the value of 500 W/person and can meet the target also when taking the electricity use of the apartments into account.

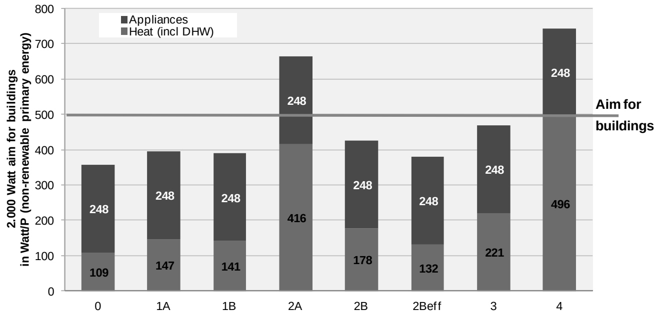

Figure 6: Orientation towards 500 Watt non-renewable primary energy performance per person for living

4.3 Economical evaluation of energy supply solutions

The economic evaluation is separated into investment costs for the construction of heat supply and life cycle costs over a period of 40 years.

The life-cycle costs contain investment costs, operational costs and the residual value of the energy supply systems. The operational costs include energy, maintenance, renewal at the end of its service life, management and a profit margin for energy supply companies. The nominal discount rate is 3%/a. The life-cycle costs shown in figure 7 present bandwidths of net present value taking into account following sensitivity analysis: with/without consideration of residual value, energy price increases of 2%/a and 4%/a. The assumptions for the cost calculation were chosen cautiously, so as not to imply too many expectations, for example by high energy price increases.

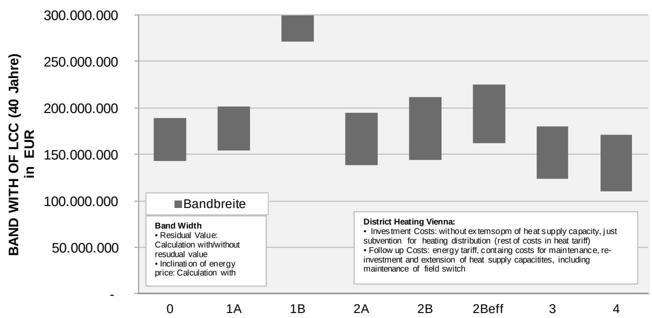

Figure 7: Bandwidths of life-cycle costs for heat supply options

The results in figure 7 show advantages for gas boiler solutions (variant 4). The heat pump solution without heating networks (variant 3) as well as with micro-heat network (variant 2B) come to similar cost levels as district heating (variant 0). Additional energy efficiency measures in variant 2Beff are not cost optimal. The variant with maximum amount of thermal solar collectors on buildings (1B) shows that this concept is not economically feasible for the framework conditions of this area.

Regarding investment costs in Figure 8, those variants with a low share of local, renewable energy sources have lower investment costs (variants 0 and 4). Variants with a high share of local renewables, in particularly those with large areas of thermal solar systems (variant 1B), have the highest investment costs. Combined solutions of heat pump and peak load boilers in variants 2B and 3 have slightly higher investment costs than district heating.

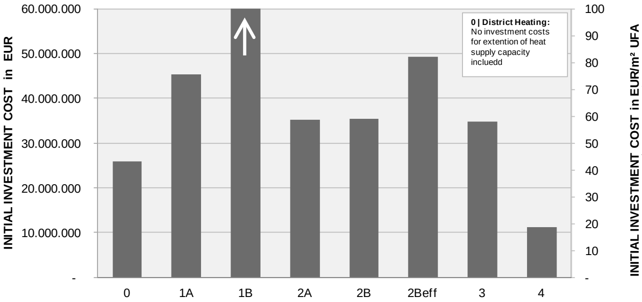

Figure 8: Initial investment costs for heat supply options

The paper must be submitted by e-mail to: **SDHConference@solar-district-heating.eu** not later than **March 9**, 2018.

5. CONCLUSIONS

5.1 Conclusions of environmental evaluation

In environmental terms, the decisive indicators are non-renewable primary energy demand and CO_2 emissions. The options with gas supply (option 2A and 4) have the highest values of primary energy and CO_2. The gas supply options do not meet the 2000 Watt targets of the city of Vienna and can thus be excluded from a future-oriented heat supply model.

The district heat supply (option 0) reaches the lowest values for both indicators. Hence, district heating plays a leading role at the environmental level. In order to maintain the good environmental evaluation, the low conversion factors for primary energy and CO_2 for district heating must be continuously achieved in the future.

For heat pumps with geothermal probes, the level of primary energy and CO_2 emission are higher than district heating. However, the 2000 watt targets can be fulfilled easily. For technical reasons, it is necessary to produce regeneration heat when using geothermal probes to have a seasonal balance between heat extraction and heat storage. This leads to an additional energy demand that is taken into account in the environmental evaluation. From the environmental point of view, heat pump concepts are a meaningful way of heat supply.

5.2 Conclusions of economical evaluation

The option with gas supply (option 4) has the lowest value for construction costs, followed by the district heating option (option 0). For district heating different system boundaries are applied: investment costs for district heating do not consider the costs for heat generation, because investments in new heat plans for district heating is included in the energy tariff.

Regarding the heat pump options (options 2B and 3) it is crucial whether the peak load is covered by heat pumps and geothermal probes or by boilers. Peak load boilers can significantly reduce the construction costs. At this point, it is important to consider the disadvantages in environmental evaluation of gas or biomass boilers (CO2 emission, fine dust). Moreover, the supply of regenerated heat in summer does burden the construction costs.

The gas option (option 4) is the most economic option concerning the life-cycle costs. High investment costs and lower operation costs of the option with heat pumps and geothermal probes lead to the same level of life-cycle costs in comparison with district heating.

5.3 General conclusions

Heat supply by means of heat pumps and geothermal probes has higher construction costs than district heating and gas supply. These additional costs have to be covered during the construction phase of the building. However, there are difficulties to cover additional costs as there are upper limits for construction costs in the residential housing funding program in Vienna. This upper limit is already hard to meet at the moment.

Higher initial investment costs of alternative heat concepts lead to the consideration of new business models regarding the abovementioned cases in order to enable the financing of initial investment. After all, options featuring heat pump solutions can also be used in smaller development areas and independent of district heating. Hence, it is possible to realise the presented plans without a “traditional” energy supplier.

From a technical point of view, the option with heat pumps is far more complex than a district heat supply solution. A heat supply concept with heat pumps considers several heat pumps, numerous geothermal probes that are distributed in the supply area, heating storages in the buildings and systems to regenerate the geothermal probes. The technologies for heat supply in the supply area are arranged in a decentralised way and demand higher management, maintenance and repair efforts.

At the same time, this means a higher degree of local added value. The financial resources for heat supply will be spent for the acquisition of energy sources (e.g. gas or oil) to a smaller share and be used to build and operate heat supply plants instead. In comparison to heat supply concepts such as district heating, the expenses for energy are significantly lower.

For now, heat supply in the City of Vienna is mainly covered by district heating and gas boilers in the buildings. In areas where district heating is economically feasible, it is still meaningful to use district heating. However, there are many areas without district heat supply. This can apply to existing buildings and city districts as well as newly build supply areas. For environmental reasons, the new construction of a heat supply system based on gas supply does not contribute to the reduction of CO2 emissions and the primary energy demand in a sustainable way. At this point, it is expedient to provide alternative solution concepts. The option of heat supply by means of heat pumps and geothermal probes offers a meaningful concept for urban heat supply.

Last but not least, an additional benefit of the heat pump solutions is the gain in comfort for the apartments: The first measure to generate regenerated heat in summer is free cooling of apartments. Thereby, the heat is extracted from the apartments and made available for the geothermal probes. In view of the hot summers in the last years, this solution offers a great benefit to the apartments. The “costless” temperature conditioning of apartments in summer provides a high level of comfort for the residents. This benefit should be considered in the overall evaluation of heat supply solutions.

6. ACKNOWLEDGEMENT

The project advisory board includes local institutions such as the wohnfonds_wien, the Municipal Department or Urban Renewal and Testing Agency for Residential Buildings (MA 25), the Energy Center of Vienna, the urban energy supplier Wien Energie as well as the client MA 20, responsible for urban planning. Wohnfonds_wien is the biggest property owner in Donaufeld and processes the urban developers’ competition. The MA25 establishes criteria for housing subsidy. The MA20 together with Energy Center of the TINA Vienna have the task to set the framework in the city in order to reduce the use of energy and the CO2 emissions.

This paper was supported by activities from the projects ecoregeneration (Development of a "Merit-Order" in order to assess regeneration heat for geothermal probes within urban residential neighbourhoods.) and INFINITE (INnovative FINancing models for sustaInable urban energy sysTEms). Both projects are funded by the Austrian Ministry for Transport, Innovation and Technology (BMVIT) in the framework of the City of Tomorrow programme.

7. REFERENCES

Wien wächst…, Bevölkerungsentwicklung in Wien und den 23 Gemeinde- und 250 Zählbezirken. Magistrat der Stadt Wien, MA 23 – Wirtschaft, Arbeit und Statistik, Statistik Journal Wien 1/2014. p. 20, Wien 2014. [1] [2]

Smart City Wien, Rahmenstrategie. Magistrat der Stadt Wien, MA 18 Stadtentwicklung und Stadtplanung, Wien 2014. [3]

Fachstelle 2000-Watt-Gesellschaft: Bilanzierungskonzept 2000-Watt-Gesellschaft. Zürich, 2014. [4]

Leichter Leben, Auf dem Weg zu einer nachhaltigen Energiezukunft — am Beispiel der 2000-Watt-Gesellschaft. Novatlantis, SIA, EnergieSchweiz. Bern, 2010. [5]

Magistrat der Stadt Wien, MA 21 – Stadtteilplanung und Flächennutzung: Leitbild Donaufeld (2010). [6]

Fanninger, G (2013): Präsentationsfolien „TOOL zur Vorprojektierung von thermischen Solaranlagen für Warmwasser & Raumheizung. AEE Intec, Gleisdorf 2013. [7]

Solar Guide (2002): Handbuch zur Planung von thermischen Solaranlagen für Mehrfamilienhäuser, Austria Solar Innovation Center, 2002. [8]

Recknagel, Sprenger, Schramek (2008): Taschenbuch für Heizung + Klimatechnik, 74. Auflage. Oldenbourg Industrieverlag 2008, Seite 1491. [9]

Nipkow, J. (2013): Der typische Haushalt-Stromverbrauch. Schweizerische Agentur für Energieeffizienz S.A.F.E., Dezember 2013. [10]

Schlomann et al. (2004): Energieverbrauch der privaten Haushalte und des Sektors Gewerbe, Handel, Dienstleistungen (GHD). Abschlussbericht an das Bundesministerium für Wirtschaft und Arbeit, 2004. [11]

Strasser, M. (2013): Strom- und Gastagebuch 2012. Strom- und Gaseinsatz sowie Energieeffizienz österreichischer Haushalte. Projektbericht. Statistik Austria, Direktion Raumwirtschaft, Energie, 2013. [12]

ÖNORM H 5050:2011-03-02: Gesamtenergieffizienz von Gebäuden, Heiztechnik-Energiebedarf. Österreichisches Normungsinstitut (2011). [13]

ÖNORM B 8110-6:2014-11-15:Wärmeschutz im Hochbau - Teil 6: Grundlagen und Nachweisverfahren - Heizwärmebedarf und Kühlbedarf - Nationale Festlegungen und nationale Ergänzungen zur ÖNORM EN ISO 13790. [14]

Haas, R. et al. (2013): Optionen für die Gestaltung des Wiener Energiesystems der Zukunft, Endbericht. Wiener Stadtwerke Holding AG, Wien 2013. [15]

Erdsondenpotenzial in der Stadt Zürich. Schlussbericht. Stadt Zürich, Amt für Hochbauten (2015). [16]

ENERGIEINSEL LANDSKRON

Christoph Aste
Ingenieurbüro für erneuerbare Energie, Hauptstrasse 244, 9201 Krumpendorf am Wörthersee, Österreich
phone: +43-664-3823812 / mail: office@asteenergy.at /www.asteenergy.com

In 2013 started the development for an ecological oriented large real estate in the district Landskron in the city of Villach. 215 flats in 11 house are under construction until Mai 2018 situated on an abundant industrial area. The heat supply area is between the water mouth of Moosbach and Seebach the runoff of Ossiacher See.

Embedded between these two rivers the project Landsitz will be a home for about 700 people. For those the heat supply will be maximum self-sufficient from local sustainable resources. The heat supply of this project relies on a small hydro power plant (electrical energy), a heat pump and a big solar thermal plant. To guarantee the residences 100% security of supply a cooperation with the district heating provider was made so they can back up when the other resources aren't available e.g. when no sun shines.

For the heat supply of 20.000 m² living and business space the Energieinsel Landskron GmbH built a 1000 m² solar plant on the roofs of Landsitz corresponding with a 68.000 liter buffer, which will produce nearly 27% of the local heating demand. If there is a heat surplus from the solar plant it's possible to deliver into the district heating system of Villach. This is one of the innovation from this project.

The other 60% of the heat will be from the project owned heat pump (using a fountain as source to raise low solar temperature up to 60°C) and from the Kelag Wärme GmbH connection. This three heat source supply via low temperature heating system (Flow 60 °C/ Return 30°C) the 11 new constructed multi-storey houses.

This concept enables a maximum self-sufficiency with 100 % security of supply and highest energy efficiency. Because of the low temperature heating system, it’s possible to use all resources at their best operating point and this gains maximum efficiency and this without

losing the high hygiene criteria. Another very important point was the cooperation with the investor because he enables an ecological construction, floor heating and fresh water modules which supports the overall heating concept.

2018 a small hydro power plant with a 80 kW capacity will be established nearby and the generated power supplies three e-charging stations, the electricity for the pumps of solar and low temperature distribution grid and for the heat pump. Another benefit will be an VW eGolf which will be available for inhabitants of Landsitz Landskron as a carsharing project.

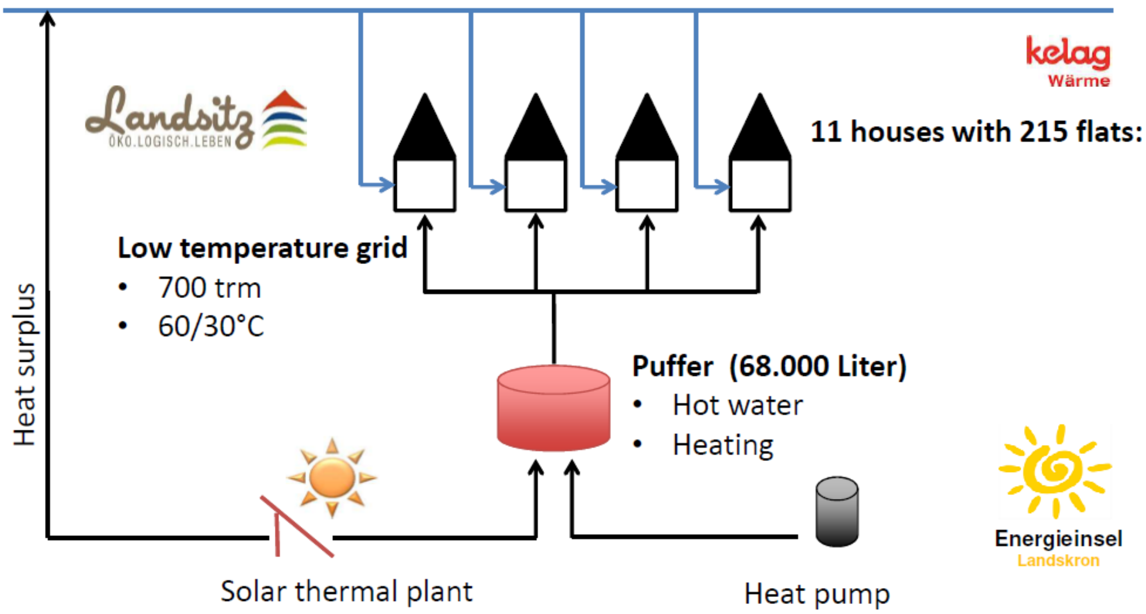

Fig.1 Heat Supply System Energieinsel Landskron

COMBINED SOLAR THERMAL GROUND SOURCE HEAT PUMP SYSTEM DELIVERS HEAT FOR A MICRO GRID HEATING NETWORK IN THE CITY OF ST. PÖLTEN 2018

Daniel Blasel and Sebastian Ager
BES BuildingEnergySolutions GmbH, Robert-Koch-Str. 50, 55129 Mainz, Germany,
Phone Number: +43 664 910 57 59, e-mail address: sag@bes-eu.com

Abstract – This paper describes the BES System and its practical implementation using the example of project Fuxsteiner and Heimberger, Schloßbergstraße St. Pölten.

1. INTRODUCTION

BES Building Energy Solutions GmbH, formerly Immosolar Group, was established in 1996. Since then the company has sought to develop, manufacture and sell energy systems for the sustainable provision of heating and cooling. The company's core values are centred on maximum energy efficiency and a responsibility for the sustainable, secure an affordable provision of energy based on renewables. With our partners, certified planners and architects, we design highly efficient energy systems. Over two decades we successfully implemented these systems with our system partners, i.e. experienced and certified contractors in industrial buildings, office buildings and in multi and single family homes. Building on the experience of the past decades, the next step was to further develop and implement the BES system into thermal micro-grid applications.

2. THE BES SYSTEM

The BES-System from BES Building Energy Solutions produces, distributes, stores and transfers energy in an efficiency way and offers a higher annual energy efficiency. The main components of each BES-System are the IS-heat pumps, the IS-solar collectors, the ground as a geothermal storage via ground collectors, the IS-Solar Central Processing Unit (SCPU4) and the IS-floor and wall radiant system. BES Systems for thermal micro-grid applications include additional gas boilers to provide the required temperatures for domestic hot water production.

3. THE PRACTICAL IMPLEMENTATION OF THE BES SYSTEM

A project that represents the further development of the BES system towards microgrid heating network integration is the project “Fuxsteiner und Heimberger / Schloßbergstraße” in the city of St.Pölten. The project has been successfully completed in 2017 with our partners and is currently under monitoring due to a scientific monitoring program performed by the research institute AEE INTEC from Gleisdorf. BES implemented in the scope of the project a microgrid heating network with the BES System for a new housing estate with several modern residential buildings with a total 36 housing units. The energy is provided by a 90kW heat pump, a gas fired boiler (85kW) and solar thermal system with a gross collector area of around 108m² mounted on the roof of the heating stations which is expected to provide 30% of the annual heating demand.

A simplified schema of the project is shown in Figure 1. Depending on the temperature level and needs, the solar thermal system can feed heat into two buffer storages for direct use (one for hot water preparation and one for space heating demand) or into the ground collector with the aim of seasonal storage. Due to the low feed temperature into the ground, normally unused low irradiation power can be used and additionally the solar collectors can operate in a favourable operating range and high solar yields of up to 540kWh/m²a_apertur can expected.

The heat pump uses the ground collector as a source for heat production and due the comparatively high source temperature between max. 25 °C and min. +5 °C a high efficiency of the heat pump during operation is ensured, which furthermore reduces external energy costs to a minimum. System annual performance figures (SJAZ) of 5 to 7 are expected.

Higher temperatures needed for hot water preparation are provided with a 85 kW gas-fired boiler which together with the solar thermal collector field feed into one central hot water buffer (4,000 liters). Lower temperature for the space heating demand are provided by the solar collector field as well as in combination with heat pump. Both feed into a 2,000 liters buffer storage from which the consumers are supplied via the microgrid heating network.

On the consumer side each housing unit has an underfloor heating system and a 120 litre hot water boiler. The hot water boilers are loaded twice a day in the time windows 03:00-05:00 and 12:00-14:00. Outside this time window, the microgrid heating network is operated exclusively at the low temperature level of the underfloor heating system to reduce heat losses to a minimum.

5. MONITORING RESULTS

Furthermore detailed technical data regarding the operational behaviour of the project “Fuxsteiner und Heimberger / Schloßbergstraße” in St.Pölten are presented using the latest results available by Samuel Knabl, AEE INTEC.

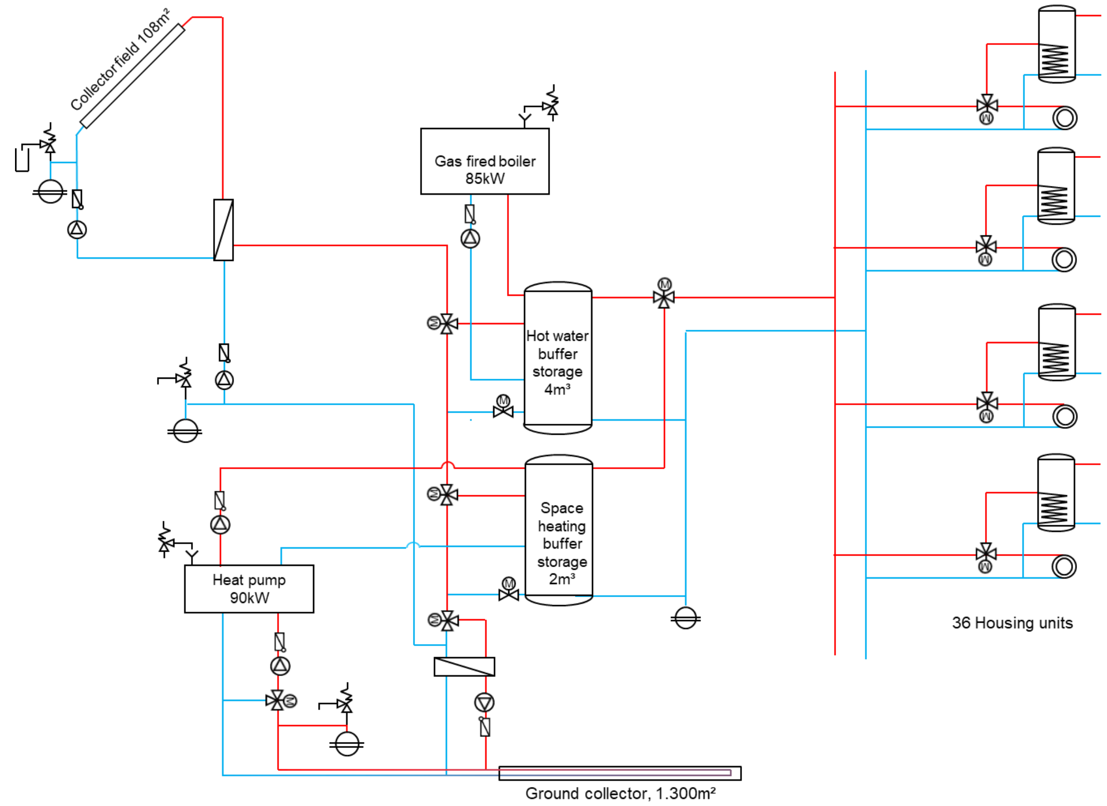

Figure 1: Scheme of the combined solar thermal ground source heat pump system for the microgrid heating network project "Fuxsteiner und Heimberger" in St.Pölten

Seasonal heat storage

Flemming Ulbjerg
Ramboll, Englandsgade 25
DK-5100 Odense C, Denmark

T +45 5161 1000
F +45 5161 1001
www.ramboll.com/energy

It has for many years been common knowledge, that large-scale Solar water heating due to economy of scale, is far more cost effective than small-scale solutions and even competitive against biomass and gas without taxes.
Today several commercial projects show, that solar water heating also is a driver for increasing the heat storage capacities in the district heating systems, not least underground heat storage pits, for storing solar heat up to a market share of around 60%.
These storages have available storage capacity half of the year and there is a potential for increasing the storage capacity at a low marginal cost in order to store other surplus heat sources from summer to winter.
Thereby the solar heating paves the way for integrating other surplus and cheap energy sources, e.g. surplus heat from combined heating and cooling. That is heat from surplus cheap electricity from wind via electric boilers, as well as efficient heat from electric heat pumps and fast regulating combined heat and power plants, which supplementing each other optimize the remaining heat production in accordance with the market prices for electric energy and for frequency regulation.

A community which has a developed district heating and cooling infrastructure including large scale solar heating, electric boilers, large heat pumps for combined heating and cooling, combined heat and power plants and not least large thermal storages, has the answer to one of the biggest challenges in the world, namely to integrate the fluctuating renewable energy. During a year it uses a lot of electricity for heating and cooling. At moderate electricity prices the consumption of electricity is close to the average. At low electricity prices the consumption is several times larger. At high electricity prices there is no consumption, or there may even be a net production of electricity to the grid based on CHP fueled by biomass or renewable gas.

Seen from the power system it seems that the city has the world record in demand response and that it must have a huge battery.

But we know the secret. There is no battery, only a smart integrated energy system.

We have in Denmark two remarkable cases to demonstrate the synergies between large scale solar water heating and this smart integrated energy system.

The town of Silkeborg has a 100 MW gas fuelled CC CHP plant, a 157,000 m2 large scale solar water heating plant covering 20% of the market and a heat pump. The heat pump increases the production of the solar heating plant by ~10% and it increases the total efficiency of the CHP plant from 86 to 102% (based on lower calorific value), which increases the operation hours of the CHP plant in the market by 100 %. The CHP plant which is important back-up for wind energy is supplemented by electric boiler and can be implemented with electric driven heat pumps.

The town of Toftlund has benefitted from previous demonstration projects and implemented in 2017 a 80.000 m3 heat storage pit combined with a 25.000 m2 solar heating plant and a heat pump.

STORAGE MANAGEMENT AND SYSTEM CONCEPT FOR A SOLAR DISTRICT HEATING SYSTEM

Nirendra Lal Shrestha, Thorsten Urbaneck, Thomas Oppelt, Bernd Platzer
Department of Mechanical Engineering, Professorship Technical Thermodynamics, Chemnitz University of Technology, 09107, Chemnitz, Germany
Tel: +49 371 531 32637, email: nirendra-lal.shrestha@mb.tu-chemnitz.de

Thomas Göschel, Ulf Uhlig, Holger Frey
inetz GmbH, Augustusburger Straße 1, 09111, Chemnitz, Germany
Tel: +49 371 489 4743, email: thomas.goeschel@inetz.de

Abstract – The paper presents the storage operation management and system concept of a large-scale solar district heating system. The integration of a short-term flat-bottom storage with stratification (non-pressurized) into the solar thermal system along with the conventional combined heat and power plant for supplying heat to the low-temperature network requires a special concept. The first monitoring results show that the system in general operates as expected. The operating strategy of the two-zone storage, capable of storing hot water of about 108 °C, is investigated for the summer and winter periods. There is a potential of improvement in the utilisation of the storage capacity. Furthermore, different operating modes of heat supply to the network are presented.

1. INTRODUCTION

The integration of solar heat in conventional district heating systems requires special concepts. The potential competition between solar and cogeneration heat has to be avoided (Urbaneck et al., 2015). Moreover, in recent years, the use of a short-term thermal energy storage (TES) in solar district heating systems (DHS) has been widely expanding and is an established technology. This paper is intended to describe a particular solution for the implementation of TES in a DHS together with a solar thermal plant and combined heat and power (CHP), which can be transferred to other urban quarters.

From 2011 to 2014, the Professorship Technical Thermodynamics at the Chemnitz University of Technology and the inetz company (heating network operator) have developed a highly efficient DHS with solar thermal plant and CHP for the urban quarter Brühl in Chemnitz (Germany) under the consideration of complex urban development conditions (Urbaneck et al., 2015). The system was built between 2015 and 2016. In summer 2016, the solar plant was put into operation.

2. DESCRIPTION OF THE SYSTEM

The Brühl solar district heating system (Figure 1) basically consists of two solar collector fields, a two-zone storage, a low-temperature network and a heat transfer substation (HTST) which connects the system to the primary district heating network via heat exchangers. The quarter covers an area of approx. 100,000 m^2 and includes mainly apartment buildings with more than 1300 residential units and the university library (Staedtebaufoerderung, 2017). The special feature of the Chemnitz solar DHS is that water is used as heat transfer fluid from the collector to the house without using heat exchangers. As a result, loss of temperature along the supply line decreases and the collector efficiency increases. In the collector, heat transfer is also improved due to the thermo-physical properties of water. From a practical point of view, venting is facilitated leading to a simple and efficient operation. A cost reduction can be achieved by eliminating large heat exchangers, by avoiding water-glycol mixtures, by eliminating pumps, valves on the secondary side, etc. However, the implementation of an active anti-freeze or safety technology is necessary. For the efficient utilization of the solar thermal energy, the supply network and the buildings have to meet certain requirements. A buried two-pipe network with a supply and return temperature of 70 °C and 40 °C, respectively, was built in the quarter. This low-temperature network connects the buildings' heat transfer substations to the supply center and distributes heat with constant/annually varying supply temperature. So far, the owners of 198 out of 259 buildings (76 %) have accepted the connection offer by the utility inetz. In 2017, the 5th construction phase of the low-temperature district heating network was completed. The installed load of the connected buildings amounts to 12.6 MW (as of 09/2017). In Figure 2, the system is shown schematically with the current expansion status of the network. The network length is about 3 km (without house connections).

2.1 Solar collector fields

The solar thermal system consists of two collector fields, south and north field (Figure 3). Table 1 shows the general characteristics of the collectors and the fields. The large-size flat plate collectors were mounted on the ground and are used for charging the storage and for supplying hot water directly to the network. The solar fields are operated with matched flow.

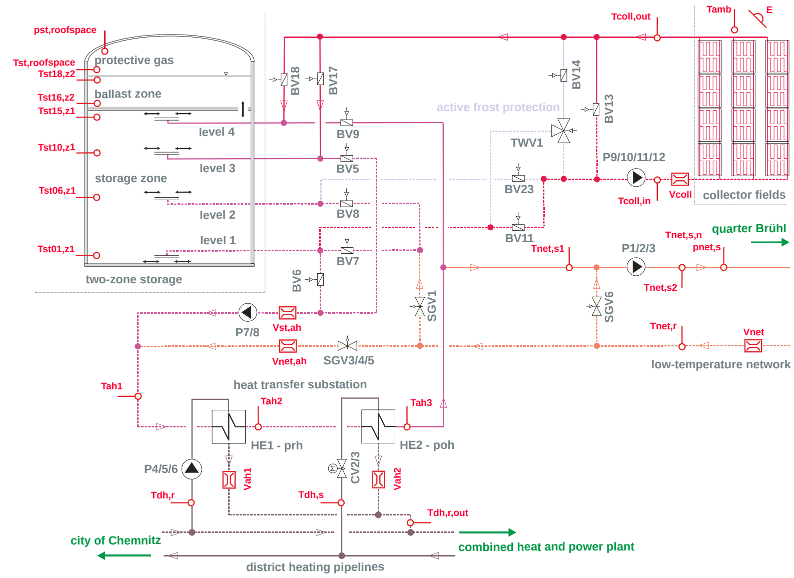

Figure 1: Structure of the heat transfer substation (supply center), solar collector fields and two-zone storage

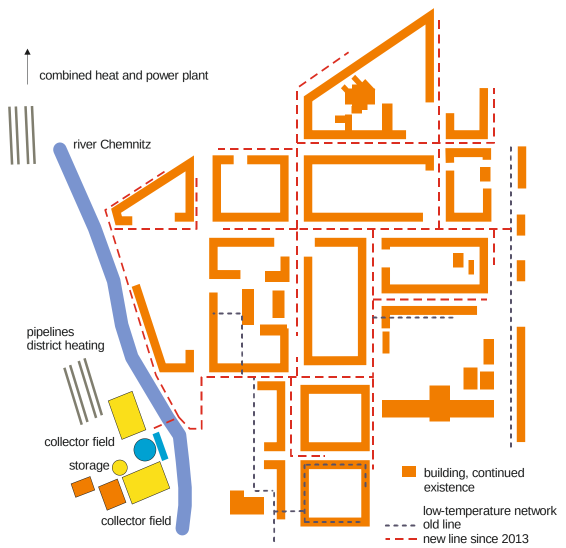

Figure 2: Schematic representation of the district heating system Brühl Chemnitz, low-temperature network

Table 1: Parameters of the collector fields

Collector type	Wagner WGK133AR, WGK80AR	
Collector inclination	35°	
Specific volume flow rate	15 l /(m^2·h)	
	South field	North field
Field azimuth	0° (south)	- 30° (south-east)
Aperture area	1007 m^2	1086 m^2
No. of WGK133AR	79	86
No. of WGK80AR	4	3
No of rows	10	17
Interconnection of the collectors	Parallel, according to Tichelmann	
Interconnection of the rows	Parallel, one-sided connection	

Figure 3: South solar collector field and two-zone storage (left) and north collector field (right) in the Brühl system, Chemnitz

2.2 Storage

As short-term storage, a welded flat bottom tank was installed above the ground close to the south field (Figure 4). It is constructed as two-zone storage according to a patent application by Thümmler (Thümmler, 2014) with a thermal useful volume of 1000 m^3 (storage zone) and a volume in the ballast zone of approx. 500 m^3. With this type of storage it is feasible to store hot water with a charging temperature of up to 108 °C. The high temperature is possible due to the hydrostatic load of the upper zone (ballast zone) which increases the pressure in the lower storage zone and thus influences the boiling temperature of the water to be stored. The increased temperature leads to a higher storage capacity. The two zones (Figure 5) are separated by a rigid and tightly sealed intermediate ceiling with insulation. For pressure balancing, both zones are interlinked by a pipe system. Likewise, the volume change which occurs during the heating or cooling of the storage and network water due to the change of density is absorbed by the ballast zone. In order to reliably avoid corrosion, nitrogen is injected which is obtained from compressed air by means of a nitrogen generator. Normally, the overpressure in the gas chamber is kept in the range between 3 and 70 mbar.

Figure 4: Mounting of the segment with intermediate floor

The total height of the storage is 20 m and the two zones are separated at a height of 13.4 m. The inner diameter of the storage is approx. 10 m and it is insulated with mineral wool being 0.50 m thick. The outer surface of the insulation is covered by aluminum trapezoidal profiles. Four radial diffusers with diameters of 1.4 m are arranged in different levels in order to charge and discharge the storage at different temperatures. The maximum charging and discharging flow rate of the storage is about 125 m^3/h (inetz, 2017). At the highest point in the storage volume, degasification of the district heating system takes place by means of the expansion device and safety valves.

2.3 Heat transfer substation

Since the solar energy yield can only cover the whole network demand on favorable summer days, auxiliary heat for charging the storage and direct supply to the low-temperature network is provided by the existing district heating system. For this purpose, a two-stage system was installed in the heat transfer substation. The first group of heat exchangers (pre-heating stage, HE1-prh in Figure 1) contains two parallel plate heat exchangers for transferring heat from the main district heating return line. Depending on the return temperature from the low-temperature network or the storage (Tah1 in Figure 1) and the current temperature of the main return line (Tdh,r), pre-heating can be conducted. Then the water with the temperature Tah2 flows to the post-heating stage (HE2-poh) where two parallel shell and tube heat exchangers supply heat from the main supply line in order to reach the desired supply temperature.

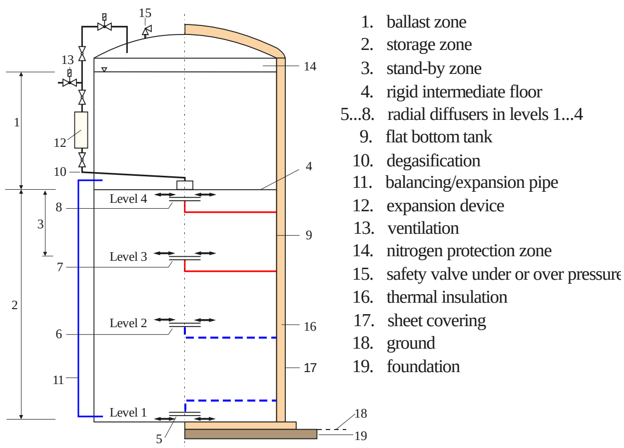

Figure 5: Schematic view of the two-zone storage (Thümmler, 2014)

Table 2: Technical parameter of the heat transfer substation (inetz, 2017)

plate heat exchangers (pre-heating)		**shell and tube heat exchangers (post-heating)**	
capacity	1.2+1.5 MW, activation of 2nd HE at $\dot{V}$ > 80 m^3/h, hysteresis 20 m^3/h	capacity	1.0+2.3 MW, activation of 2nd HE at $\dot{V}$ > 40 m^3/h or load of post-heating > 1 MW
primary design temperature	65/50 °C	primary design temperature	120/63 °C
secondary design temperature	45/57 °C	secondary design temperature	60/80 °C

2.4 Modes of system operation

The operating modes of the supply center can be classified into five groups according to the source of the heat supplying the low-temperature network (Table 3):

1. heat transfer substation (HTST) supplying the low-temperature network alone (OM A),
2. discharging capacity of the storage sufficient for network supply (full storage operation strategy) (OM B),
3. discharge from the storage and additional heating by HTST (OM C),
4. collector fields yield sufficient for network supply (OM D) and
5. collector fields yield and storage together supplying the low-temperature network (OM E).

It is assumed that the storage is never charged with solar heat and CHP heat (via HTST) simultaneously.

Table 3: Operating modes of the supply center for supplying the low-temperature network

Operating modes of the supply center	Heat source		
	HTST	Storage	Collector fields
OM A	Yes		
OM B		Yes	
OM C	Yes	Yes	
OM D			Yes
OM E		Yes	Yes

Table 4 shows the operating states of the storage which are possible in the Brühl system. These states are categorized according to the charging and discharging operation of the four diffusers.

One of the useful parameters which need to be observed during operation of the storage is the volumetric state of charge. It provides information on a useable volume which is above a certain limit temperature and set in relation to the total volume (Urbaneck, 2012). Furthermore, the energetic state of charge can also be calculated. The static energetic state of charge is related to the minimum and maximum design temperature of the storage. The limit temperature was set to 67 °C according to the 90 % criteria (system temperature 40/70 °C) and the maximum and minimum design temperature was set to 40 and 108 °C, respectively, to evaluate the state of charge of the storage.

3. MONITORING RESULTS

The Brühl DHS is equipped with an extended monitoring system allowing detailed performance analysis of components and determination of solar yield, supporting commissioning and optimization of the plant and protection of the system. Due to a problem in the data logger during the initial period of operation, the measurement data are only available from May 2017 onwards. As the active frost protection strategy has not yet been implemented in the solar system, the solar system has been turned off since the second week of December 2017. It will be activated again during April when the weather conditions are favourable.

Monthly heat quantities for the year 2017 (May-December) are shown in Figure 6. The specific collector gain delivered to the low-temperature district heating network was 305 kWh/m^2 (aperture) which was about 76 % of the predicted annual yield. In the design phase, a specific collector yield of about 402 kWh/(m^2·a) was simulated for the first stage of construction (Urbaneck et al., 2015). The solar fraction for the analysed period amounts to 8.2 % and for the whole year it is predicted to reach 5 %.

The relative duration of the operating modes of the supply center for supplying the low-temperature network during the analysed period is depicted in Figure 7. It can be seen that most of the time, heat for the low-temperature network is supplied by the auxiliary heating system alone (OM A). This mode covers ca. 74 % of the total operating duration of the supply center. Secondly, ca. 21 % of the supply center's operating duration was fulfilled by discharge from storage combined with heating by HTST (OM C). In the months of December and few weeks of November, the storage was not operated, leading to the relatively high share of mode OM A. Without solar heat and additional heat from the HTST, discharging capacity of the storage was used for about 2 % of the total operating duration of the system (OM B). Combined heat supply from collector fields and storage

Table 4: Operating states of the two-zone storage

Operating states	Feed into level				Extraction from level				Comments
	L1	L2	L3	L4	L1	L2	L3	L4	
OS0									no charging / discharging of the storage
OS1	x							x	discharging into the network, return flow to L1
OS2		x						x	discharging into the network, return flow to L2
OS3				x	x				charging with solar heat into L4
OS4			x		x				charging with solar heat into L3
OS5			x	x	x				charging with solar heat into L3 and L4
OS6	x		x		x			x	combination of OS1 and OS4
OS7		x	x		x			x	combination of OS2 and OS4
OS8				x	x				charging with primary district heating, return flow from L1
OS9				x			x		charging with primary district heating, return flow from L3

share about 3 % of the operating duration of the supply system (OM E). The collector fields did never supply the network alone (OM D).

For the two-zone storage, the relative duration of the operating states is shown in Figure 8. There is no charging and discharging of the storage taking place for about half of the system's operating duration (OS0). Relative duration for charging with solar heat into the storage is about 11 %, comprising feed-in of solar heat into the upper level 4 with 6 % (OS3) and into level 3 with 4 % (OS4) as well as into both levels at the same time with 1 % (OS5). Adding the combination of charging the solar heat into the storage and discharging heat into the network, simultaneously, relative duration is about 17 % (OS3 – OS7). 16 % of the relative duration of the system operation is used for discharging into the network without solar charging (OS1 + OS2). Discharging heat from level 4 into the network with solar heat being charged into level 3 at the same time took place during 6 % of the time (OS6 + OS7). During another 6 % of the duration, the storage was charged by the auxiliary heating system (OS8 + OS9). In the remaining duration of ca. 14 %, (other) tests and active anti-frost operation were performed.

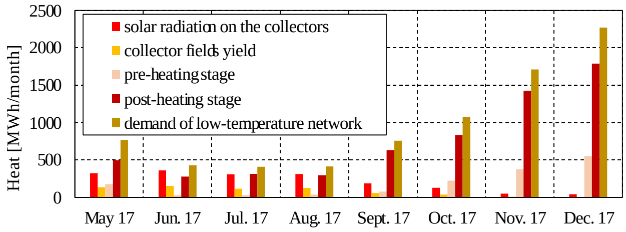

Figure 6: Monthly heat quantities for the year 2017 from May

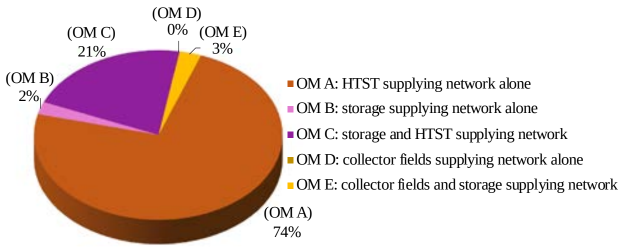

Figure 7: Relative duration of the operating modes of the supply center for supplying the low-temperature network for the year 2017 from May

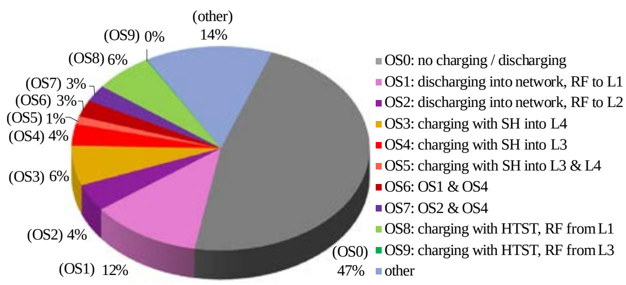

Figure 8: Relative duration of the operating states of the two-zone storage for the year 2017 from May

Based on the practical operation, relation between the system and storage as well as the storage behaviour are explained in the following section. Figure 9 to Figure 12 show an example of the storage operation in summer (week 25, 2017). The demand of the low-temperature network is almost constant and relatively low during summer operation (Figure 9). During the daytime, the storage is charged with heat from the collector fields and at the same time the collector fields deliver heat into the low-temperature network. Discharging of the storage and auxiliary heat from the primary district heating network together cover the low-temperature network's demand in the night and morning periods. In the early morning as the storage is completely discharged, the primary district heating network delivers heat to the low-temperature network. The supply temperatures from the auxiliary heating system and the collector fields and the return temperature from the low-temperature network influence the operation of the storage (Figure 10). At low network demand, the return temperature of the network increases (60…65 °C) and this causes the reduction of the vertical temperature difference in the storage (Figure 10, Figure 12). The charging temperature is almost constant and depends significantly upon the operation of the collector fields and the auxiliary heating system. The discharging temperature decreases slightly during the discharge process. This can be explained by the temperature distribution in the storage (Figure 12). Depending on the state of charge, the temperatures in the upper level of the storage zone fluctuate in the range of 65…80 °C (Figure 10). Generally, the network supply temperature which is dependent to the outside temperature is adjusted to a set point value by admixing.

The operation of the storage in winter is shown in Figure 13 and Figure 14. In contrast to summer operation, the demand of the low-temperature network is now higher. It can be seen that the auxiliary heating systems operates continuously and the collector fields yield is very low. The storage has not yet been applied for optimizing the heat supply from CHP via HTST.

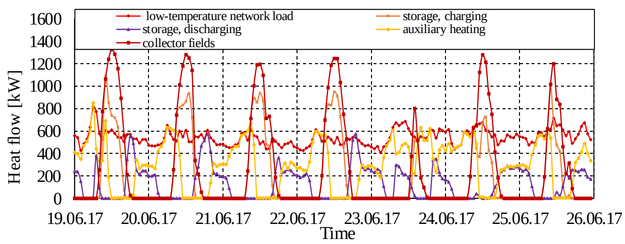

Figure 9: Low-temperature network load, charging and discharging of the storage, auxiliary heating demand and collector fields yield, summer operation, hourly measured values

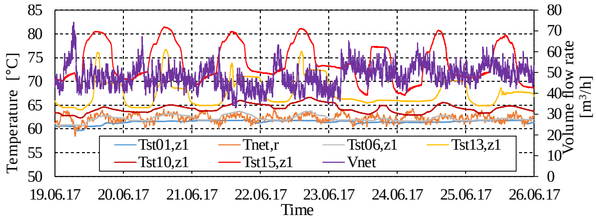

Figure 10: Temperatures, two-zone storage; return temperature and volume flow rate of low-temperature network, summer operation, 1-minute average values

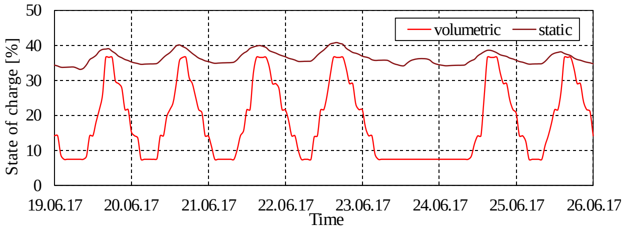

Figure 11: State of charge of the two-zone storage, summer operation, hourly values

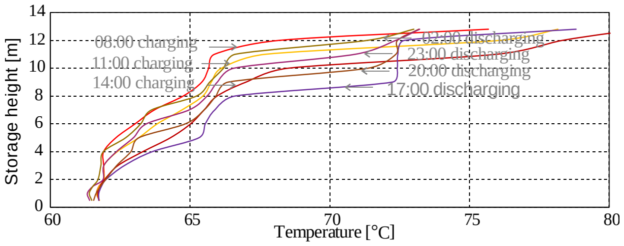

Figure 12: Vertical temperature distribution over the storage height, summer operation, 22.06.2017 08:00 – 23.06.2017 02:00, 3 hours measured values

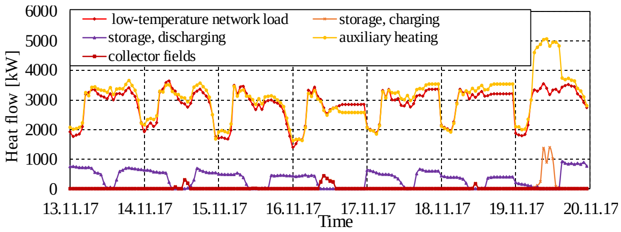

Figure 13: Low-temperature network load, charging and discharging of the storage, auxiliary heating demand and collector fields yield, winter operation, hourly measured values

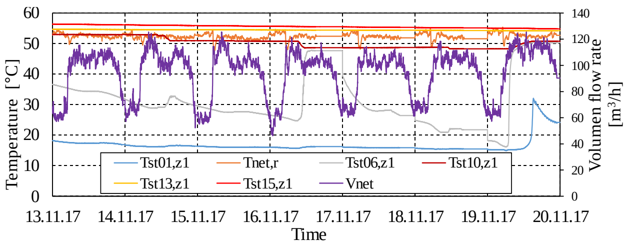

Figure 14: Temperatures, two-zone storage and return temperature and volume flow rate of low-temperature network, winter operation, 1-minute average values

4. CONCLUSIONS

In this paper, the operations management for the two-zone storage and system concept for a solar district heating system is presented. The initial monitoring results show that the system in general operates as expected. For an efficient operation of the system, there should be an optimum and balanced interaction between the heat sources (collector field, auxiliary heating system and storage) and the demand of the low-temperature network (peak or base load).

Relative duration of the different operation modes of the whole system (supply of low-temperature network) and the storage was analysed. There is a large number of possible modes due to four diffuser levels in the storage combined with two collector fields and the HTST as heat sources. During the analysed period, the storage has not yet been applied with advanced concepts. Thus, the HTST supplied the low-temperature network alone during 74 % of the time and no charging or discharging of the storage took place during 47 % of the time.

The boundary conditions of the system influence the storage operation. These are essentially the inlet temperatures (return temperature of the network and supply temperatures from the auxiliary heating system and the collector fields) and the modes of operation which are associated with different volume flow rates. The operating strategy of the storage is determined by the mode of operation of the system. Thus two typical operating modes of the storage (summer and winter operation) can be detected.

The monitoring results indicate that the operating strategy of the storage during the winter periods needs to be improved. Generally, during winter operation or the transitional period with higher heat demand, the storage can be used to optimize the heat generation. The storage can be charged when there is surplus of excess heat in the primary district heating network. Furthermore, during the winter operation of the storage with a longer operating period of the auxiliary system, cyclic charging and discharging can lead to the complete utilization of the storage capacity. At low demand of the network, however, one must pay attention to the influence of the return temperature from the network.

Further work will be conducted in modelling the two-zone storage, full utilization of the storage capacity, calculating the external loses of the storage, analysing the operation with thermal stratification and investigating the operating behaviour of the radial diffusors. Studying the control strategies of the system is also planned here (Urbaneck, 2017). There is still a significant potential of optimization in the operating strategy of the storage and the operating modes of the system. It is possible to transfer this concept to other urban quarters.

5. ACKNOWLEDGEMENTS

The project underlying this report is funded by the German Federal Ministry for Economic Affairs and Energy under the code 0325871 following a decision by the German parliament. Special thanks also go to the Project Management Jülich for supporting the project. The sole responsibility for the report's contents lies with the authors.

REFERENCES

Urbaneck, T., Oppelt, T., Platzer, B., Frey, H., Uhlig, U., Göschel, T., Zimmermann, D. and Rabe, D. (2015) Solar District Heating in East Germany – Transformation in a Cogeneration Dominated City. *Energy Procedia*, Vol. 70, pp. 587–594. - doi: 10.1016/j.egypro.2015.02.090.

Staedtebaufoerderung - Federal Institute for Research on Building, Urban Affairs and Spatial Development within the Federal Office for Building and Regional, http://www.staedtebaufoerderung.info/StBauF/DE/Programm/-AktiveStadtUndOrtsteilzentren/Praxis/Massnahmen/Chemnitz/Chemnitz_node.html. Internet-Plattform zum Städtebauförderprogramm Aktive Stadt- und Ortsteil zentren (in German), (21.02.2018).

Thümmler, E. (2014) DE102013111543 A1.

inetz GmbH. (2017) Funktionsbeschreibung MSR solar-unterstützte LowEx-WÜST Brühl (not published).

Urbaneck, T. (2012) *Kältespeicher – Grundlagen, Technik, Anwendung*. pp. 261-262. Oldenbourg, München

Urbaneck, T. www.solfw.de. Project website, (22.02. 2018).

NOMENCLATURE

ah	auxiliary heating	P	pump
amb	ambient	poh	post-heating
BV	butterfly valve	prh	pre-heating
coll	collector(-field)	Q	heat
CV	control valve	r	return
CW	calendar week	s	supply
dh	district heating	SGV	sliding gate valve
E	solar radiation (measurement)	SH	solar heat
HE	heat exchanger	st	storage
L	level	T	temperature (measurement)
OM	operating mode	TWV	Three-way valve
OS	operating state	V	volume flow rate (measurement)
net	network	z	zone
p	pressure (measurement)		

COMPARISON OF METHODS FOR STORAGE SIZING IN SOLAR DISTRICT HEATING NETWORKS

MSc. Olatz Terreros, MSc. Roman Geyer, MSc. Daniele Basciotti, Dr.-Ing. Ralf-Roman Schmidt

Austrian Institute of Technology GmbH, Energy Department, Giefinggasse 2, 1210 Vienna.

olatz.terreros@ait.ac.at, tel. +43 50550 6359

Introduction and aim

Thermal storage technologies are a key component in the transition towards 100% renewable energy systems. The implementation of storages in district heating networks leads to an increase of the integration of renewable and industrial waste energy sources, reduces peak loads and improves the system stability. Furthermore, thermal storages provide flexibility to the network, decoupling production and consumption over time, especially in combination with solar thermal plants.

The sizing of storages is usually based on engineering methods (e.g. design rules from manufacturers), however, additional methods exist, like mathematical methods (e.g. analyses of producers and consumers profiles) and simulation methods.

This contribution, which has been developed in the framework of the national project heat_portfolio, analyses relevant case studies of solar district heating networks and compares the current used engineering methods with a simulation method for storage sizing.

Method

Existing significant solar District heating plants in Austria, Germany and Demark have been analyzed for key figures, such as investments costs and design parameters.

Further on, a parametric study covering typical Austrian district heating networks has been performed, with the objective of generalizing the thermal storage design. Multiple rural and urban scenarios, characterised by different shares of solar thermal energy, are established in order to develop and test the different storage sizing methods.

For the simulation method, an operation optimisation model has been developed based on the mixed integer linear programming (MILP) method. It provides the cost optimal operation strategy for every scenario, evaluating the most suitable storage size, for both short-term and long-term storages. The model has been implemented in Matlab and executed through the intlinprog solver.

Results

As an example of the results from this study, figure 1 shows a comparison between the engineering and simulation methods as well as the storage size of existing plants.

The engineering methods determine the recommended storage volume for rural and urban scenarios based on the total nominal thermal capacity or the collector gross area installed in the network. The red dots represent the optimal storage volume determined by the simulation method, while the black, yellow and blue dots illustrate respectively the storage volume implemented in existing district heating networks in Austria.

For rural and urban baseline scenarios, where no or low integration of solar thermal technology is considered, the calculated storage volumes by the simulation methods fit the trendline set up by the engineering methods, and they approximate to the real storages already implemented in the existing networks. For rural methods, the results show that the storage volume calculated by the simulation methods is usually lower than those recommended by engineering methods.

This deviation could be explained due to the small difference in the investment costs of the storages, which allows the planner to select a larger storage in order to gain flexibility for future network extensions. Scenarios with high solar thermal integration are located in the upper area of the figure and some of them are in fact outside due to the large storage volumes required.

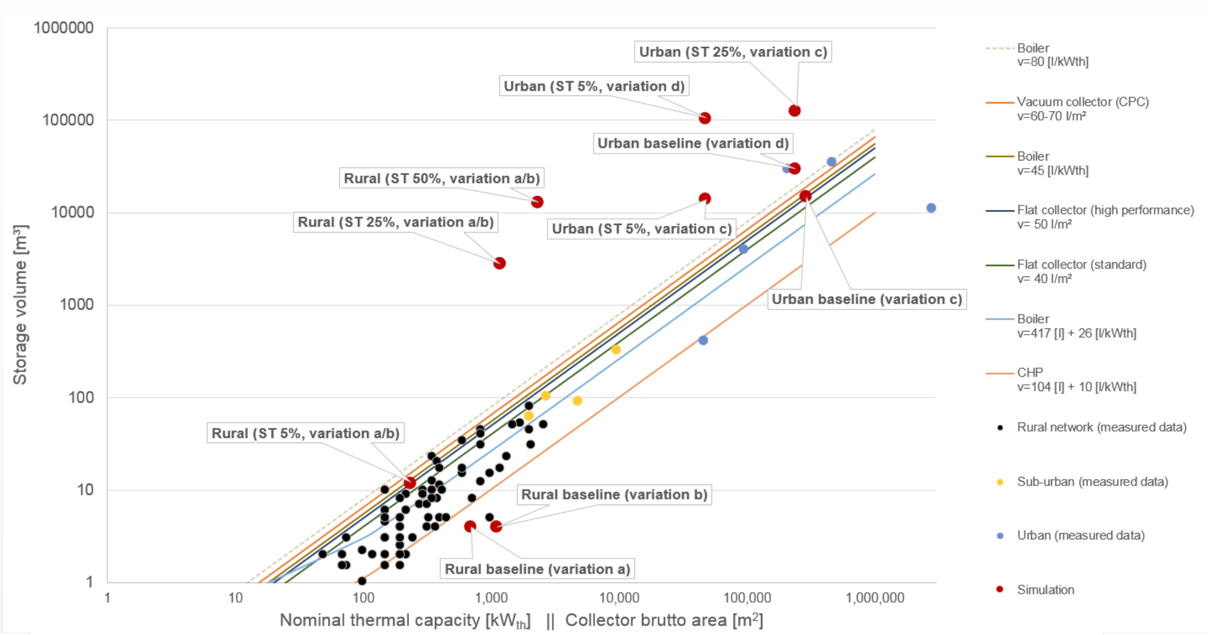

-Heat demand coverage with solar thermal plants: 5%, 25%, 50%.
-Rural scenarios: "variation a" contains a biomass boiler and an oil boiler; "variation b" contains a gas boiler.
-Urban scenarios: "variation c" contains a CHP and a gas boiler; "variation d" contains a gas boiler, a CHP and an incineration plant.

Figure 1: Comparison of engineering and simulation methods for storage sizing.

<u>Discussion and outlook</u>

It can be seen, that the investigated engineering methods are only limited suitable for storage sizing in scenarios with high integration of renewable technologies, while simulation methods are a good option due to the potential to analyze the network though a holistic approach, considering consumers, power plants and storages. Therefore, simulation methods are suitable for helping relevant stakeholders in decision making and pre-dimensioning storage sizes in solar DH-networks.

However, since simulation methods are very time consuming and require expert know-how, future work might include the investigation of mathematical methods, such as the rainflow counting algorithm, fourier transformation and the minimum load of the boiler algorithm.

OPERATIONAL ANALYSIS AND DETAILED MONITORING RESULTS OF SOLAR THERMAL HEAT PUMP COMBINATIONS INTEGRATED INTO AUSTRIAN DISTRICT HEATING NETWORKS

S. Knabl, W. Becke, C. Fink, R. Pertschy
AEE – Institute for Sustainable Technologies
Feldgasse 19, 8200 Gleisdorf, Austria
Tel.:+43 (0) 3112 - 5886 – 229
E-Mail: s.knabl@aee.at
Web: www.aee-intec.at

F. Helminger, B. Windholz
AIT – Austrian Institute of Technology
Giefinggasse 2, 1210 Vienna
Tel.:+43(0) 50550-6385
E-Mail: bernd.windholz@ait.ac.at
Web: www.ait.ac.at

Abstract – In 2009 the Austrian Klima- und Energiefonds started a funding programme for the development and further market penetration of large-scale solar thermal systems for industrial and commercial applications. Funding could be obtained for innovative system concepts between 100 and 10,000 m². In order to ensure high quality and functionality the most interesting projects in terms of innovation and replicability were chosen for a 12 months solar thermal system monitoring, analysis and optimization. Between September 2009 and September 2017 301 application forms were successfully handed in, summing up to a total collector area of around 150.000 m². Of these, 100 projects were equipped with additional sensors for monitoring in which 41 furthermore can be assigned to the solar district heating category. Of the 41 SDH-systems, a total of 6 systems were implemented as solar thermal heat pump combination projects. These systems are characterised by a wide variety of system designs with collector areas between 255 m² and 2,048 m² as well as heat pump capacities between 160 kW and 2,400 kW. Solar fractions between 3% and 29% reflect furthermore the broad spectrum of solar thermal heat pump combinations that have been realised in recent years in Austrian district heating networks. In this paper monitoring results covering both the characteristics of the solar circuit as well as the entire energy balance of selected SDH-heat pump combination including auxiliary energy flows, heat losses and parasitic energy consumption are presented.

1. INTRODUCTION

For six years the Austrian Climate and Energy Fund (KLIEN) has been sponsoring a subsidy program specifically for large-scale solar thermal plants for industrial applications, including scientific monitoring. In total, 301 projects were submitted covering around 150,000 m² of gross collector area. In order to gain knowledge essential for the further development of the solar thermal technology, the 100 most innovative and promising were selected for scientific monitoring which includes analysing monitoring data over one operational year.

2. THE FUNDING PROGRAMM

The programme managed by the Austrian Klima- und Energiefonds (KLIEN) is aimed at the implementation of solar thermal energy in the industrial and commercial sector according to four categories:

- Solar process heat applications
- Solar district heating (SDH)
- High solar fraction (> 20 %) in buildings for industry and services
- New system intelligence (hybrid systems such as PVT, new collector and storage developments, etc.) bridging the gap between R&D and market entry

Funding is provided for a maximum of 40% of the environmentally relevant additional costs (environmentally relevant investment costs minus the costs of a reference heating system based on oil) with an additional 5 % for projects implemented by SMEs. The total maximum funding rate therefore is 45 % of the environmentally relevant additional costs. The funding is intended for covering the entire material and labour costs related to the solar thermal circuit including storage for systems with a gross collector area of at least 100 m² and a maximum of 10,000 m² (respectively 50 m² to 200m² in category five “New system intelligence”). Caps are implemented specifically for each category in order to limit the maximum funding per plant. In summary 301 projects with a total gross collector area of around 150.000 m² has been submitted to the programme.

Image 1 provides an overview on the projects submitted for funding so far according to category and size.

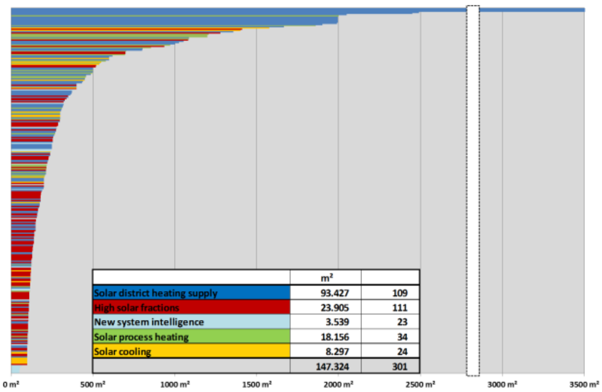

Image 1: Presentation of the total of submitted projects arranged by gross collector area and colour-coded according to the category of application.

From this image it becomes clear that around 20% of the plants have gross collector areas of larger than 500 m². The categories “solar district heating” and “high solar fraction (> 20 %) in buildings for industry and services” make up most of the projects (around 110 projects each).

3. SCIENTIFIC MONITORING PROGRAMME OF AUSTRIAN SDH PLANTS

In order to maximize the benefit and effectiveness of the previously described funding plan, the KLIEN assigned a scientific monitoring programme headed by AEE INTEC (in cooperation with AIT). The main tasks of this monitoring are:

- Technical consulting preparatory to submission to the funding programme
- Supervision for projects with highly innovative approaches in during the phase of detailed planning and in the course of the implementation of the plant
- Definition of the monitoring concept (input and output of the energy balance) for projects with a highly innovative approach
- Implementation of the metrological monitoring of the heating system for at least one year of operation for selected projects with a highly innovative approach
- Plant analysis and benchmarking
- Deduction of possibilities for technical improvements and identification of need for further research
- Consulting services to the funding agency (KLIEN) for adjustments and further development of the programme

Up to now 100 projects have been selected for the one year monitoring phase by a panel of experts and by end of February 2018 in which 41 out of the 100 projects can be assigned to the solar district heating category.

Of the 41 SDH-systems, a total of 6 projects were implemented as solar thermal heat pump combination systems (see table 1). The size and type of the monitored projects vary as well as the different heat distribution networks characteristics in which the systems are implemented. As shown in table 1 the monitored SDH-heat pump combination systems are integrated in small micrograms as well as in urban heating networks and also into typical biomass fired district heating grids.
The 6 projects are characterised by a wide variety of system designs with collector areas between 113 m² and 2,048 m² and heat pump capacities between 160 kW and 2,400 kW. In four of the six hybrid combination the solar collectors are used via the storage as the provider of the primary heat for the heat pump. Ground which is regenerated by solar energy (ground collectors as well as bore holes) is used as a heat pump source in two system designs.

4. DESCRIPTION OF REPRESENTATIVE AUSTRIAN SDH PILOT PLANTS

This chapter presents the experience gained from four SDH-heat pump systems constructed and monitored in the framework of the Austrian funding programme. Moreover the most important technical benchmark figures are shown separately for each plant.

4.1 Solar assisted low-temperature district heating grid Salzburg-Lehen (2.048 m² gross collector area)

In 2011 an entirely new residential area has been constructed in the district of „Lehen” in the city of Salzburg on the former operation site of Stadtwerke Salzburg, consisting of two- to eight-storey apartment buildings with a total of 300 housing units plus a students’ residence, a kindergarten, offices and shops (see image 3 for an impression of the area). The total housing and commercial area amounts to 38,000 m². The heat supply is provided by a newly constructed low-temperature heat network (65/35°C). Roughly one third of the energy is covered by solar thermal energy from 2,048 m² of gross collector area implemented in combination with an energy storage of 200 m³.
The collector area is composed of 13 fields which have been mounted on the flat roofs of the buildings and which feed into the central energy storage. Furthermore, a heat pump with a peak capacity of 160 kW has been installed and connected to the energy storage. This leads to lower temperatures in the lower part of the energy storage and therefore allows for higher solar energy yields and higher energy densities to be achieved at a given volume. The Salzburg community heating provides auxiliary energy whenever necessary and also feeds into the central energy storage. From here the heat is distributed to the different consumers via a two-pipe network (decentralized hydraulic units in the multi-storey buildings). This way not only the newly constructed objects but also some refurbished apartment buildings with a total of 160 housing units are supplied.

Table 1: SDH heat pump combination plants monitored by AEE INTEC in the framework of an Austrian funding programme

	Networks type in which systems are implemented	Collector area [m²]	Solar yield (direct/indirect) [$kWh/m^2a_{apert.}$]	Solar fraction (direct/ indirect) [%]	Heat pump power [kW]	Source for the heat pump	Auxiliary heatin
Salzburg Lehen	Urban heating network	2048	534* (221/313)	29* (12/17)	160	Puffer storage	District heati (1800kW
Salzburg Bergheim	Biomass district heating systems	215	252*	-	1100	Puffer storage	Biomass boiler + condensation Biogas-CHP (0,56 Gas boiler (5
SFL technologies,	Microgrid integration	255	459* (258/201)	8* (4,5/3,5)	360	Solar regenerated ground	2 Gas boiler (5 Oil boiler (14
Waldmühle Rodaun	Microgrid integration	1667	551**	20**	2400	Puffer storage	3 Gas Boi (2x1048 kW, 1x
NW Ebenthal	Biomass district heating systems	366	526**	2,9**	659	Puffer storage	Biomass boiler + condensation (Oil boiler (2.0
Fuxsteiner und Heimberger	Microgrid integration	113	504**	20**	90	Solar regenerated ground	Gas boile (80kW)

* As measured during the one year monitoring phase
** As simulated in the planning phase. Monitoring for these projects is ongoing.


Image 2: View on part of the 2,048 m² gross collector area distributed over 13 buildings. Picture source: AEE INTEC

The monitoring phase of one year for this project was completed in July 2014. The analysis showed very satisfying system performance and functionality. The specific solar yield for this plant was 534 kWh/m²$a_{aperture}$, covering more than 29 % of the thermal energy demand. The measured monthly SPFs of the heat pump range from 4.1 (August) to 5.1 (February) and a annual SPF of 4.7 was achieved.

4.4. Integration of 255 m² gross collector area in a low-temperature micro-network

In 2014, SFL technologies GmbH expanded their company premises in Stallhofen near Voitsberg. In order to cover the heat supply of the whole site, a micro-network assisted by solar thermal energy was implemented. The installed total collector area is divided into two collector fields with 127.5 m² each and totals 255 m² (see image 6). Four heat pumps with a total thermal output of 360 kW serve as the primary heating system. A gas boiler with 450 kW supports the heat pumps if needed. Two more existing boilers (gas boilers with 125 kW and an oil boiler with 140 kW) are used as emergency boilers.

The solar thermal system is used for helping to provide the energy for heating and hot water throughout the year as well as for regenerating the deep geothermal heat exchanger during summer. The geothermal field consists of 42 probes with a depth of 147 m each. Furthermore, three storage tanks with a combined volume of 15.5 m³ were installed for storing the solar heat.


Image 6: View on the 255 m² collector area installed on the roofs of the two production buildings. Picture source: H. Traussnigg GmbH.

The monitoring phase was completed in August 2016. The functionality of the plant was proved to be unproblematic. The solar yield for the monitoring phase was 459 kWh/(m²$a_{aperture}$) and a solar fraction of 8 % was reached. The average measured SPF of the heat pumps during the monitoring phase was 3,3.

4.2. Supply of a low-temperature network via 3 decentralised heat pump solar thermal combinations with a total collector area of 1,667 m²

On the site of a former cement factory on the outskirts of Vienna, a new housing estate with several modern residential buildings, local infrastructure and a total of 450 housing units was built in 2016.

The heating and hot water supply for the residential buildings is provided by a low-temperature network with a total of three heating stations. A total of four heat pumps (à 600 kW) were installed in the respective heating stations, each of which uses a buffer storage tank (total volume 50,000 litres) as source. The buffer storage tanks are loaded via the low-temperature network and a solar thermal system, consisting of three partial collector fields installed on a total of 5 roofs of the residential complex with a gross collector area of around 1,667 m². The failure safety of the micro network is guaranteed by three central gas boilers (2x1048 kW and 1x455 kW).

The monitoring phase started in June 2017 and in this point of time the functionality of the plant is unproblematic. At the time of submission, a solar yield of 551 kWh/ (m²$a_{aperture}$) was simulated with a solar share of 20 %. The operation of the solar plant has so far shown a good operating performance.


Image 3: View of the housing estate "Waldmühle Rodaun" (Bildquelle: www.immobilien-wirtschaft.at/)

4.3. 366 m² of gross collector area supports a multivalent heat supply system for the community district heating network Ebenthal

The energy plant in Ebenthal operates a district heating network with roughly 4 MW of connected load, supplying 100 buildings (commercial buildings, primary school, single-family houses, apartment buildings, swimming pool, etc.).

The energy is provided by a 2,000 kW biomass boiler, a solar thermal system with a gross collector area of 366 m², two flue gas condensation stages (409 kW and 530 KW) as well as heat pump with a thermal output of 650 kW. The heat pump is integrated into the second condensation stage in order to further increase the waste heat level. In addition, heat from the solar system can be used via an extra storage tank by the heat pump if required, thus further increasing the efficiency of the heat pump. This project is particularly interesting because of the operating behaviour of the solar system in a multivalent heat supply system.

The monitoring phase required by the funding programme started in July 2017. The solar yield simulated for the submission to the programme is

526 kWh/($m^2a_{aperture}$) and the solar fraction is aimed to be 2.9 %. The data measured up to now coincides with these values and therefore indicates that the target can be achieved.

Image 6: View on the 366m² of collectors on the roof of the heating building during the construction phase. Picture source: regionalwaerme.com

5 BENCHMARKS AND COMPARISON TO SIMULATION VALUES

The four projects described above are subject to the scientific monitoring programme. For this purpose all heat inputs as well as outputs are registered. The main benchmarks of the plants have been defined as: the specific solar yield, thermal energy supply and resulting here from the solar fraction (definition: solar input in relation to the sum of solar input and conventionally generated heat). The following image 7 shows these benchmarks for the four exemplary plants compared to the respective values predicted by simulation. Furthermore the measured yearly SPF of the installed heat pumps is given in the figure.

Two of the plants (Salzburg Lehen and SFL technologies) have already completed the monitoring phase while for two (Waldmühle Rodaun and NW Ebenthal) it is still ongoing (shaded bars in figure 7).

The specific solar yield of the project Salzburg Lehen was 534 kWh/m² $a_{aperture}$. 41% of the total solar yield resp. 221kWh/m² $a_{aperture}$ was used to directly fed into the grid. The remaining 313 kWh/m² $a_{aperture}$ was used as source energy for the heat pump. The total solar fraction of the project was 29%, with a direct share of 12% and an indirect share of 17%. The measured annual SPF of the system was 4.7.

For the SFL technologies project, a total solar yield of 459 kWh/$m^2a_{aperture}$ was measured. The share of direct solar yield is 258 kWh/m² $a_{aperture}$ and the remaining 201 kWh/m² were used for the regeneration of the geothermal probes. The SPF of the heat pump was 3,3 at the end of the one-year measurements.

The results and operating experience of the two remaining plants (Waldmühle Rodaun and NW Ebenthal), which are still in the monitoring phase, indicate that the simulated benchmarks can be achieved or even exceeded.

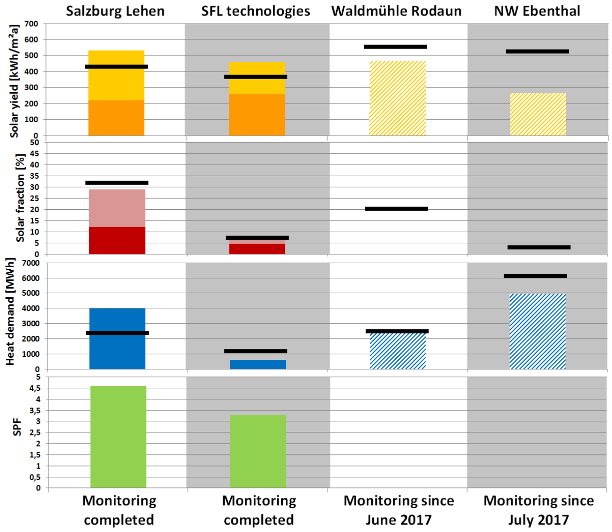

Image 7: Comparison of the measured specific solar yield (direct-orange, indirect - yellow), solar fraction (direct-red, indirect – light red)), heat demand (blue) and SPF of four solar thermal plants compared to the simulation values (black lines). The plants which have not yet completed the monitoring phase are marked by shaded bars (solar yield and het demand).

6 OUTLOOK

The Austrian funding programme for large-scale solar thermal plants has been well received on the market in the past years. The scientific monitoring for the plants has proved to be an essential part of the initiative and provides valuable feedback for the adaptation of the programme as well as for the further development of the technology.

7 REFERENCES

C. Fink, S. Knabl, W. Wagner, R. Stelzer, B. Windholz,: Endbericht – Wissenschaftliche Begleit-forschung „Solare Großanlagen 2011“ – Salzburg Lehen, http://www.solare-grossanlagen.at/files/pdf/2011_SalzburgLehenSbg.pdf (07.03.2018).

C. Fink, S. Knabl, Stelzer, B. Windholz, F. Helminger: 2. Zwischenbericht – Wissenschaftliche Begleitforschung „Solare Großanlagen 2013“ – SFL technologies, http://www.solare-srossanlagen.at/files/pdf/Begleitforschung_Zwischenbericht2_2013.compressed.pdf (07.03.2018).

C. Fink, S. Knabl, R. Stelzer, B. Windholz, F. Helminger: 2. Zwischenbericht – Wissenschaftliche Begleitforschung „Solare Großanlagen 2013“ – Waldmühle Rodaun, http://www.solare-grossanlagen.at/files/pdf/Begleitforschung_Zwischenbericht2_2013.compressed.pdf (07.03.2018).

C. Fink, S. Knabl, Stelzer, B. Windholz, F. Helminger: 1. Zwischenbericht – Wissenschaftliche Begleitforschung „Solare Großanlagen 2014“ – NW Ebenthal, http://www.solare-grossanlagen.at/files/pdf/Begleitforschung_Zwischenbericht_2014.pdf (07.03.2018)

SDH PLANT WITH 5000 M² FLAT-PLATE COLLECTORS FEEDING IN THE DISTRICT NETWORK OF MÜRZZUSCHLAG, ÖSTERREICH

Anja Raab[1*], *Robert Söll*

[1]S.O.L.I.D. Gesellschaft für Solarinstallation und Design mbH, Puchstrasse 85, Graz, 8020, Austria
+43 (0) 316-292840-54, p.reiter@solid.at

Starting in 2017, SOLID and the public utility of Mürzzuschlag developed a concept for a large-scale solar thermal plant on the basis of an ESCO model. Mürzzuschlag is a town with 8600 inhabitants, which covers its district heating (DH) demand using a biomass plant (50 %) and a gas cogeneration unit, which operates mainly in summer. The demand for DH has increased significantly in the Mürzzuschlag area in recent years. In the course of enlarging the DH, the project "Solarthermieanlage Mayerhofwiese" was launched. Primary goal of the project is to achieve a high solar fraction in summer and thus a large reduction in the use of natural gas.

Resulting from calculations by Stadtwerke Mürzzuschlag GmbH, a collector area of 5000 m² is needed for an economic operation. In this dimension the plant will yield 2,5 MW full load. Since the networks summer load is 700 kW (topload in winter 10 MW), a storage is needed to temporarily store surpluses in summer.

The yearly solar yield of 2.450 MWh is being transferred to the network via the 200 m³ storage tanks with network temperatures of 85°C/55°C in winter and 80°C/60°C in summer. Based on simulations a specific yield of 490 kWh/m²a is expected. That way the plant will cover 9 % of the town's annual heat demand. In summer months a solar coverage of up to 80 % will be reached. The average solar fraction in summer will be 57 %.

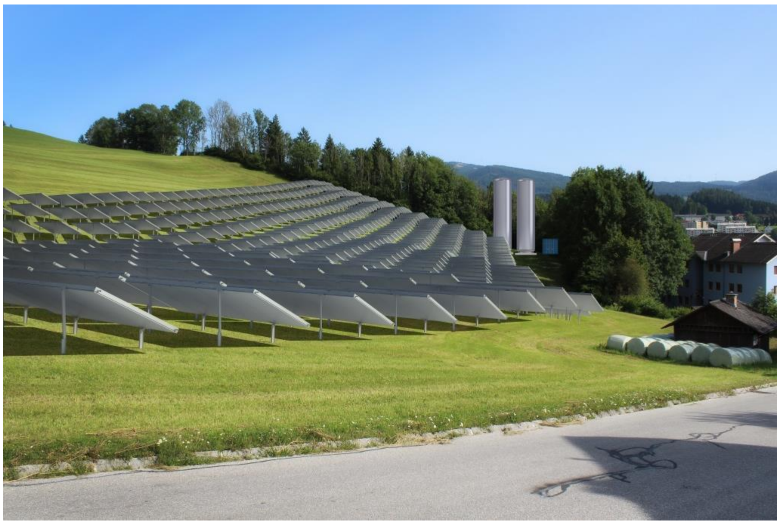

Fig. 1: Visualization of project "Solarthermieanlage Meyerhofwiese"

Detailed planning is in progress since September 2017. The collectors will be installed *ground mounted* on the northern outskirts of Mürzzuschlag. Except all required permissions still outstanding, the plant will be built during the next 5-8 months. SOLID shall be in charge of the design and construction process while solar.nahwaerme.at Energiecontracting GmbH shall finance and operate the plant.

Investments in solar district heating are being supported with about 40 % facilitation by the "Klima- und Energiefonds im Förderprogramm Solare Großanlagen".

The general conditions are convenient: space is available, high facilitations, high heat demand in summer. This project can thus be a flagship, to strikingly represent the technical and economical feasibility of such plants.

SMALL HEATING GRIDS FOR COMMUNITIES IN BALKAN COUNTRIES: THE COOLHEATING PROJECT

Dominik Rutz, Rainer Janssen
Unit Bioenergy & Bioeconomy, WIP Renewable Energies, Sylvensteinstr. 2, D - 81369 Munich, Germany
Tel. +49 89 720 12743, Fax +49 89 720 12791
E-Mail: dominik.rutz@wip-munich.de
Internet: www.wip-munich.de, www.coolheating.eu

Jakob Worm[2], Christian Doczekal[3], Richard Zweiler[3], Tomislav Puksec[4], Neven Duic[4], Borna Doracic[4], Rok Sunko[5], Blaž Sunko[5], Vladimir Gjogievski[6], Ljupco Dimov[6], Natasa Markovska[6], Vasil Bozikaliev[6], Nikola Rajkovic[7], Ilija Batas Bjelic[7], Anes Kazagic[8], Elma Redzic[8], Dino Tresnjo[8], Slobodan Jerotic[9], Bojana Mladenović[9], Emir Fejzovic[10], Amra Babić[10], Marin Petrovic[10], Mitja Kolbl[11]
[2]PlanEnergi, Denmark, [3]Güssing Energy Technologies GmbH, Austria, [4]University of Zagreb, Croatia, [5]Skupina fabrika d.o.o., Slovenia, [6]International Centre for Sustainable Development of Energy, Water and Environment Systems - Affiliate Skopje, Macedonia, [7]School of Electrical Engineering, Serbia, [8]Elektroprivreda, Bosnia and Herzegovina, [9]Municipality of of Sabac, Serbia, [10]Municipality of Visoko, Bosnia and Herzegovina, [11]Municipality of Ljutomer, Slovenia

Abstract – The CoolHeating project promotes the implementation of "small modular renewable heating and cooling grids" for communities in South-Eastern Europe. The objective of CoolHeating is to support the implementation of "small modular renewable heating and cooling grids" for communities in South-Eastern Europe. CoolHeating transfers knowledge from partners in countries where renewable district heating and cooling examples exist (Austria, Denmark, Germany) to countries where there are less examples in the sector (Croatia, Slovenia, Macedonia, Serbia, Bosnia-Herzegovina). Core activities, besides techno-economical assessments, include measures to stimulate the interest of communities and citizens to set-up renewable district heating systems as well as the capacity building about financing and business models. The outcome is the initiation of new small renewable district heating and cooling grids in 5 target communities up to the investment stage.

1. INTRODUCTION

The heating and cooling demand in Europe accounts for around half of the EU's final energy consumption. Renewable energy policies often mainly focus on the electricity market, whereas policies for renewable heating and cooling are usually much weaker. Therefore, it is important to support and promote renewable heating and cooling concepts.

Small modular district heating/cooling (DHC) grids have several benefits. They contribute to increase the local economy due to local value chains of local biomass supply. Local employment is enhanced as well as security of supply. The comfort for the connected household is higher as only the heat exchanger is needed in the basement of the buildings and no fuel purchase has to be organised. Small modular district heating/cooling grids can be fed by different heat sources, including from solar collectors, biomass systems, heat pumps and from surplus heat sources (e.g. heat from industrial processes or biogas plants that is not yet used).

Especially the combination of solar heating and biomass heating (*Figure 1*) is a very promising strategy for smaller rural communities due to its contribution to security of supply, price stability, local economic development, local employment, etc. On the one hand, solar heating requires no fuel and on the other hand biomass heating can store energy and release it during winter when there is less solar heat available. Thereby, heat storage (buffer tanks for short-term storage and seasonal tanks/basins for long-term storage) needs to be integrated. With increasing shares of fluctuating renewable electricity production (PV, wind), the Power-to-Heat conversion through heat pumps can furthermore help to balance the power grid. If the planning process is done in a sustainable way, small modular district heating/cooling grids have the advantage, that at the beginning only part of the system can be realised, and additional heat sources and consumers can be added later. This modularity requires well planning and appropriate dimensioning of the equipment (e.g. pipes). It reduces the initial demand for investment and can grow steadily. (Rutz et al. 2017b)

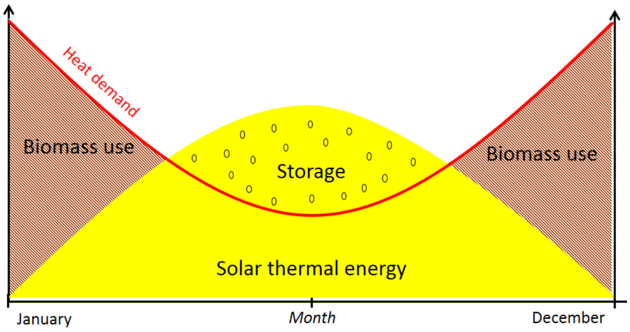

Figure 1 Synergies of the combination of solar thermal and biomass for DH (Rutz et al. 2017a)

2. THE COOLHEATING PROJECT

The objective of the CoolHeating project, funded by the EU's Horizon2020 programme, is to support the implementation of "small modular renewable heating and cooling grids" for communities in South-Eastern Europe (*Figure 2*). This is achieved through knowledge transfer and mutual activities of partners in countries where renewable district heating and cooling examples exist (Austria, Denmark, Germany) and in countries which have less development (Croatia, Slovenia, Macedonia, Serbia, Bosnia-Herzegovina). Core activities, besides techno-economical assessments, include measures to stimulate the interest of communities and citizens to set-up renewable district heating systems as well as the capacity building about financing and business models. The outcome is the initiation of new small renewable district heating and cooling grids in 5 target communities (*Figure 3*) up to the investment stage. These lighthouse projects will have a long-term impact on the development of "small modular renewable heating and cooling grids" at the national levels in the target countries.

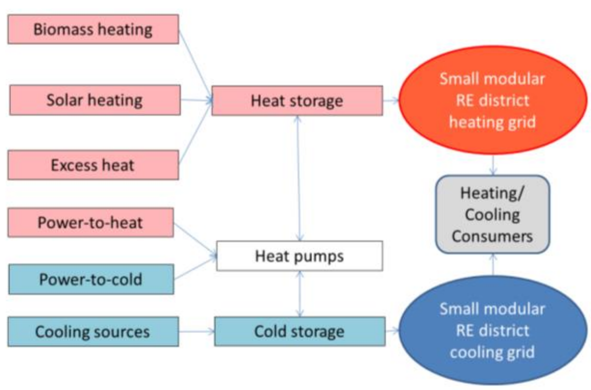

Figure 2: Concept of small modular renewable heating & cooling grids


Figure 3 Target countries of the CoolHeating project with best practice examples (dark blue) and target communities (light blue, red point) with less developed renewable distgrict heating sector

3. CONCEPTS FOR SMALL DISTRICT HEATING PROJECTS

Within the CoolHeating project, concepts for small modular renewable heating and cooling grids were elaborated by the project partner Güssing Energy Technologies GmbH, together with the project partners of the target countries, as well as with local stakeholders. In total, concepts for seven projects in the five target municipalities were developed, in order to supply them with 202 GWh/a heat and cold from renewable energies and just supported in selected cases by fossil peak load boilers. In order to develop the concepts, surveys about the heat demand were made and options were discussed with the local stakeholders. The following chapters briefly summarize the concepts (Doczekal et al. 2018a,b,c,d,e,f,g), which are available on the CoolHeating website (www.coolheating.eu).

3.1 Cven, Slovenia

The rural settlement of Cven in Slovenia has 226 households and a few larger buildings – the school, a culture hall and a shop. There is also a polyethylene foils factory.

All public buildings should be connected to the DH grid, as well as 90% of the households. The buildings should be supplied with heat for space heating and hot water in winter and for hot water in summer. The technical concept considers a small biomass CHP (combined heat and power) unit for the baseload, a biomass boiler and a natural gas peak load boiler. A buffer storage tank could decrease the peaks after night setback time in the morning, when most households start heating again. Biomass (e.g. wood chips) is available in this region.

About 2.24 GWh heat per year could be sold to the consumers, plus 943 MWh per year for wood drying. In total, 3.93 GWh/a are needed to feed the DH grid, including heat losses.

3.2 Karposh, Macedonia

The surroundings of the area Zajcev Rid in the Municipality of Karposh is located in the North-West of Skopje. There, it is planned to build a new efficient and highly sustainable residential neighbourhood. The heat supply of this new neighbourhood is an important issue due to the high air-pollution in Skopje and Karposh.

For the heat supply of the planned buildings, different options are discussed, such as connecting to the existing DH grid in the vicinity, choosing individual heating solutions, utilizing a natural gas distribution system or implementing a small DHC grid. The area is currently not covered by the major DH system of Skopje nor by a natural gas distribution system. The technical concept developed by the CoolHeating project proposes a small, modular, renewable DHC system for the neighbourhood.

The system for heat generation could contain a groundwater electric heat pump (about 15 MW_{th}), 5,000 m^2 flat plate solar collectors, a peak oil boiler (26 MW), and a seasonal thermal storage unit (55,000 m^3). The groundwater heat pump could be used to cover about 88.5% of the heat demand.

In total 47,835 MWh/a heat could be fed into the DH grid. Using the DH gird for cooling in summer could also be an option. The DHC grid could be fed with an electric chiller with about 15 MW_{th} to produce 9,000 MWh/a cooling.

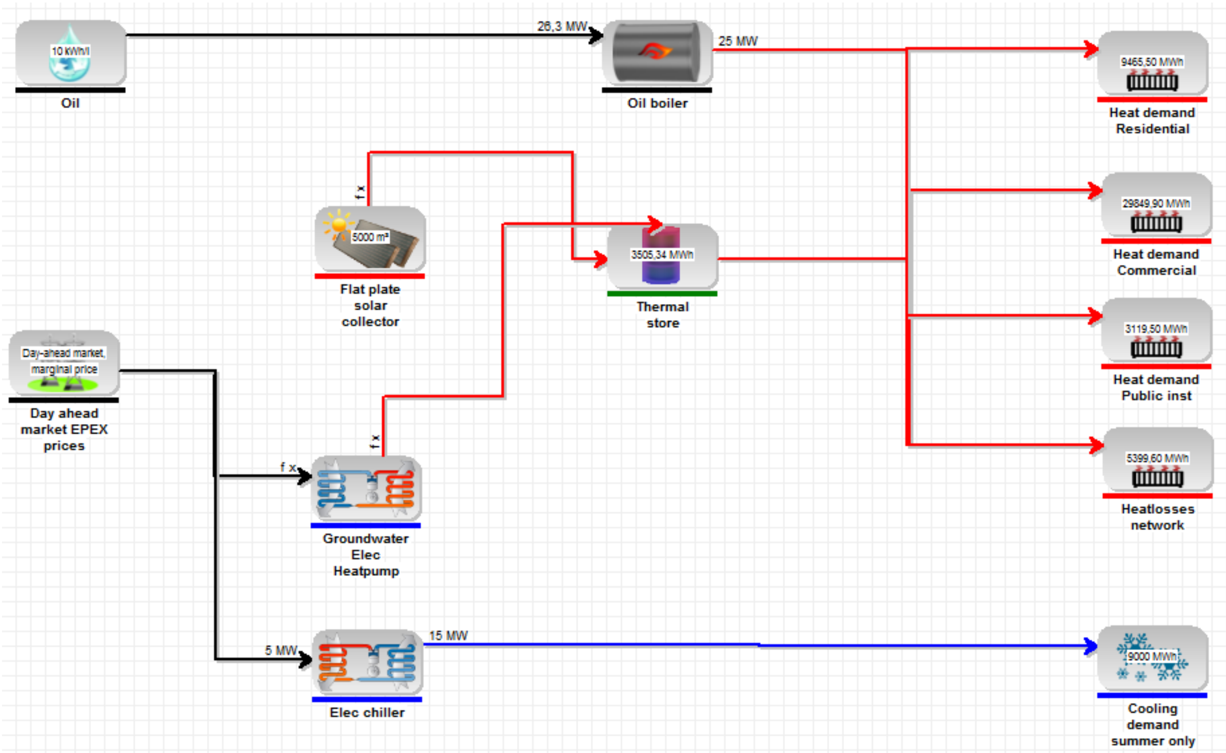

Figure 4: Scheme of heating and cooling production units and consumers in Karposh, calculated in energyPRO

3.3 Ljutomer, Slovenia

The CoolHeating target community in Slovenia is the city of Ljutomer, which has about 4,500 households. The Municipality of Ljutomer selected the industrial zone as one of two perspective locations for developing a DHC project. The industrial zone of Ljutomer is organised in three sectors.

The technical concept for the industrial zone in Ljutomer includes the industrial consumers as well as the heat production units. The total heat demand for the DH grid, including losses and steam supply is 23,715 MWh/a. The peak load is about 4,500 kW for the DH grid.

Two scenarios for the technical concepts were elaborated. For scenario 1 a biomass CHP, a biomass boiler, a natural gas peak load boiler, a buffer storage tank and a biomass steam boiler is considered. This scenario also covers the cooling needs from a dairy with an absorption chiller, operated with the DH grid. The grid density of the DH grid is very high with 3,524 kWh/m/a and about 15,001 kWh/m/a for the steam pipeline. About 48% of the DH grid needs are produced with the biomass CHP, 51% with the biomass boiler and a very low about of about 2% with the natural gas peak load boiler. The

DH grid heat losses in this scenario are about 6% (915 MWh/a).

In scenario 2 no biomass CHP units are included and no cooling for the dairy company is considered. This scenario shows an alternative if the integration of CHP units is not feasible. Because of higher heat production prices, the cooling might not be feasible in this scenario.

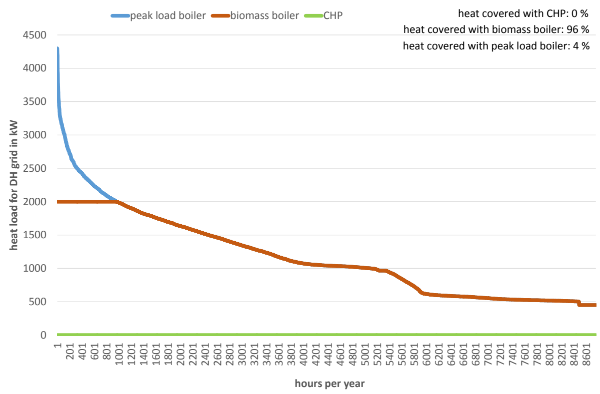

Figure 5: Annual load line of the heat production units of the heating plant at industrial zone in Ljutomer

3.4 Ozalj, Croatia

Currently, there is no district heating system in Ozalj so all the heat is supplied individually, at dwelling level. Regarding energy sources that are used for heating in households, biomass covers the largest share, followed by fuel oil. The reason for such a high share of biomass is the high amount of biomass available locally and no existing gas network in the city. Also, a fair number of citizens own a part of surrounding forests and therefore only encounter costs for transferring biomass to their home.

The main problem is that most of individual furnaces currently being used are old and therefore result in high environmental impact. Public buildings mainly use fuel oil (91%), while the rest is covered by electricity. Furthermore, electricity is used in the majority of households for the preparation of domestic hot water. The survey carried out in Ozalj showed that the building stock is rather old and inefficient, reflecting the current state of buildings in Croatia. Therefore, specific heat demands of households are relatively high.

The technical concept for Ozalj includes two different combinations of biomass boiler and flat plate solar collectors for baseload. The first combination uses solar collectors to cover a minor part of the heat demand, mainly during summer. The second one uses solar collectors in combination with a seasonal thermal storage. Every combination has an additional fuel oil peak load boiler for covering the peak load. During summer, domestic hot water is being provided by the system. The grid density is quite high, that would lead to a more economic operation of the system.

The overall heat demand which could be covered by a district heating system equals to 41,755 MWh/a in the central scenario and 66,413 MWh in the expanded scenario. These figures include the grid losses.

A biomass boiler could supply the DH grid with about 65.6% (Central Scenario 2) to 88.1% (Expended Scenario 1) of the annual heat demand and a fuel oil peak load boiler needs only 3.4% (Expended Scenario 2) to 5% (Central Scenario 1) of the annual heat demand.

The flat plate solar collectors could cover about 8.1% (Expended Scenario 1) to 30% (Central Scenario 2) with a size of 8,000 m² (Central Scenario 1) to 25,000 m² (Expended Scenario 2). Storage capacities of the seasonal storage were 30,000 m^3 for Central Scenario 2 and 40,000 m^3 for Expended Scenario 2.

The buffer storage tank with about 300 m³ could reduce the usage of the peak load boiler, mainly caused by the night setback of some consumers.

3.5 Letnjikovac, Serbia

The elementary school "Stojan Novaković" in Letnjikovac, a suburban settlement of Šabac, was built in 2004. For heating purposes of the building, a boiler room with 2 x 400 kW hot water oil boilers is installed. The heat supply is carried-out by pre-insulated pipelines to the school building and to an education center. The heat demand of these two buildings is: 280 kW and 20 kW.

The average fuel consumption (fuel oil) during the previous period was 24,000 l/year with 103 t/year CO_2 emissions and average fuel costs of 33,000 EUR/year including excise tax. There is no central system for sanitary hot water heating nor central systems for space cooling in both buildings. There is no heat consumption outside the heating season, so the installation of CHP plants at this moment is more investment intensive than heat only.

In the surrounding area there are blocks of single family buildings where individual stoves or central heating systems are used. In those furnaces logwood is burned, but sometimes coal is burned as well. Most of the buildings were built before 2012 when there were no strict regulations on the energy properties of buildings. For this reason, the heat consumption is extremely high.

The concept for Letnjikovac could include a biomass boiler with 150 kW and the existing fuel oil boilers for peak load for phase 1 (public buildings) and a 1.5 MW biomass boiler with a 3.5 MW fuel oil boiler for phase 2 (public buildings and about 248 households). Thermal storages with 6 m³ (phase 1) and 60 m³ (phase 2) helps to decrease peak load and to optimize the operation of the biomass boilers.

The DH grid could be 420 m at phase 1 and 7,656 m in phase 2. The grid density in phase 1 with 762 kWh/m/a is higher than in phase 2 with 462 kWh/m/a. The feasibility study could show if this DH grid is economic, due to the low grid density. In total 4,275 MWh/a heat are needed to feed the DH grid, including heat losses.

3.6 Šabac, Serbia

Šabac is one of 58 cities in Serbia where a district heating system exist. This system is managed by the Public Utility Company "Toplana-Šabac", whose founder is the city of Šabac. In the mid-1980s, two city heating plants - "Trkalište" and “Benska Bara” were built. All existing local boiler rooms have been reconstructed and converted into heating substations. Since the heating season 2016/17 for the heat production in the DH in Šabac, only natural gas is used.

The CoolHeating concept for the implementation of renewable energy in the DH grid Šabac could include three biomass boilers with 4.5 MW nominal capacity each. This could lead to about 61% coverage of the annual heat demand and supply the DH grid with 37,688 MWh/a renewable energy. The rest could be covered with the existing natural gas boilers (39% annual coverage). The new biomass plant should be connected to the main heating plant Trkalište with a new DH pipeline with DN 350, or at least DN 250 for 9 MW thermal load. The fuel for the biomass boilers could be wood chips or local agro-biomass. A buffer storage tank with 200 m³ at the new plant could improve the controlling of the biomass boilers and decrease peak load.

3.7 Visoko, Bosnia and Herzegovina

District heating systems were well developed in towns and cities before the war in Bosnia and Herzegovina. During the war, many systems fell into disrepair and after the war could not recover customers due to a fall in the purchasing power of the population. The maintenance and investment in the remaining functioning district heating systems has been low, leading to obsolete technologies, as well as low efficiency and large heat losses on the network. In last decade, traditional fossil-based DH system have been improved and some new ones built, the latest mainly based on biomass.

A DHC concept based on renewable energy sources would help to meet rising urban energy needs, to improve efficiency, to reduce emissions, and to improve the local air quality in the Municipality of Visoko. Air quality especially badly suffers during the heating season due to heavy use of coal for heating. Existing heating systems are mainly individual and currently dominated by coal as the cheapest energy source on the market. Therefore, they should be upgraded or new networks should be created, using solid biomass as well as solar and geothermal energy technologies. Depending on local conditions, renewable-based DHC would bring a range of benefits, including increased energy security, improved health and reduced climate impact.

The CoolHeating concept shows the possibility of using solar thermal heat, a heat pump from the river, in combination with a seasonal storage, as well as a natural gas peak load boiler. The system would supply around 150 private houses, 30 collective housing facilities and 6 public buildings. About 4,000 of Visoko Municipality's 40,000 citizens would be covered by this DH system.

A thermal seasonal storage with a capacity of 13,500 m³ would ensure the reliability and efficiency of the heat generation technologies. One of the main problems in the energy supply especially in the case of the renewable technologies is the temporary gap between the availability of the resource and the demand. The storage would allow filling this gap, therefore it is a key factor for improvement of the renewable rate in such energy mix. Base heat production would be achieved through solar collectors (15.8%) and heat pumps (78.5%), which would be connected to storage, while the rest and peak loads would cover the gas boiler.

The DH grid was calculated with 5,500 m. A direct supply system is suggested for individual households, with one heat exchanger for all private housing facilities and one heat exchanger per collective housing facilities. The predicted heat consumption for the connection rate of 80% private housing facilities and 100% connection rate for public buildings is 18,13 GWh including grid heat losses with about 5.9%. The temperature level of the DH grid will be designed with 80°C outgoing flow and 60°C return flow.

4. CONCLUSION

In conclusion, DH system on renewable energy sources would achieve a number of advantages in the target municipalities: reduction of emissions currently being reflected in considerable pollution, increasing reliability and efficiency, helping to manage the supply and demand of heat, reducing labour and maintenance costs associated with individual systems, variety of renewables used, etc.

This paper presented DHC concepts for seven projects in the five CoolHeating target municipalities, in order to supply them with 202 GWh/a heat and cold.

In the next step, economic calculations will be made for the developed scenarios and concepts in order to facilitate the selection of the best concept. Furthermore, individual business models will be developed. In the final step, a feasibility check will be made to present the potential project with most feasible technologies and business options to decision makers and investors until the end of 2018.

REFERENCES

Doczekal C., Gjorgievski V., Dimov L., Bozhikaliev V., Markovska N., (2018a) Heating/cooling demand and technical concept for district heating/cooling in Karposh. – Report elaborated in the CoolHeating project (Project-No. 691679); www.coolheating.eu

Doczekal C., Laurberg Jensen L., Worm J., Doračić B., Pukšec T., (2018b) Heating/cooling demand and technical concept for district heating/cooling in Ozalj. – Report elaborated in the CoolHeating project (Project-No. 691679); www.coolheating.eu

Doczekal C., Laurberg Jensen L., Worm J., Kazagić A., Merzić A., Redžić E., Trešnjo D., Petrović M., (2018c) Heating/cooling demand and technical concept for district heating/cooling in Visoko. – Report elaborated in the CoolHeating project (Project-No. 691679); www.coolheating.eu

Doczekal C., Rajaković N., Batas Bjelić I., Jerotić S., (2018d) Heating/cooling demand and technical concept for district heating/cooling in Šabac, Letnjikovac (Suburban Settlement of Šabac) – Report elaborated in the CoolHeating project (Project-No. 691679); www.coolheating.eu

Doczekal C., Rajaković N., Batas Bjelić I., Jerotić S., (2018e) Heating/cooling demand and technical concept for district heating/cooling in Šabac, Plan to implement biomass boilers for district heating in Šabac. – Report elaborated in the CoolHeating project (Project-No. 691679); www.coolheating.eu

Doczekal C., Sunko R., Kolbl M. (2018f) Heating/cooling demand and technical concept for district heating/cooling in Cven. – Report elaborated in the CoolHeating project (Project-No. 691679); www.coolheating.eu

Doczekal C., Sunko R., Kolbl M. (2018g) Heating/cooling demand and technical concept for district heating/cooling in Ljutomer. – Report elaborated in the CoolHeating project (Project-No. 691679); www.coolheating.eu

Rutz, D., Doczekal C., Zweiler R., Hofmeister M., Laurberg Jensen L. (2017a) Small Modular Renewable Heating and Cooling Grids - A Handbook. - ISBN 978-3-936338-40-9; WIP Renewable Energies, Munich, Germany, 110p.

Rutz, D., Mergner, R., Janssen, R., Soerensen, P.A., Jensen, L.L., Doczekal, C., Zweiler, R., Pukšec, T., Duić, N., Doracic, B., Sunko, R., Sunko, B., Markovska, N., Gjorgievski, V., Bozhikaliev, V., Rajkovic, N., Bjelic, I.B., Kazagic, A., Redzic, E., Smajevic, I., Jerotic, S., Mladenović, B., Fejzovic, E., Babić, A., Petrovic, M., Kolbl, M. (2017b) The Combination of Biomass with Solar Thermal Energy and other Renewables for Small Heating Grids: The Coolheating Project. - Proceedings of the 25th European Biomass Conference and Exhibition, Stockholm, Sweden; ISBN: 978-88-89407-17-2; DOI: 10.5071/25thEUBCE2017-5BV.2.6; pp. 1896 - 1898

FEASIBILITY STUDIES FOR SDH IN REGION VÄSTRA GÖTALAND

Jan-Olof Dalenbäck[1,2] and Gustaf Zettergren[3]

[1]CIT Energy Management AB, 412 88 Göteborg, Sweden
Phone: +46 31 772 1153;E-mail: jan-olof.dalenback@cit.chalmers.se

[2]Chalmers University of Technology, Building Services Engineering,
412 96 Göteborg, Sweden

[3]VGR Koncernstab, PO Box 1091, 405 23 Göteborg, Sweden,
Phone: +46 10 441 1600: E-mail: gustaf.zettergren@vregion.se

Abstract – Region Västra Götaland is associated to the EC project SDHp2m. which primarily has a focus on the implementation of solar district heating in three European regions: Styria (AT), Thuringia (DE) and Auvergne Rhone Alpes (FR). The aim here is to investigate the interest and the possibilities to complement existing block and district heating systems based on solid biofuels with a solar heating system within Region Västra Götaland. The paper summarises the second step of the project, comprising feasibility studies for a number of existing heating plants. The paper summarises the result for one plant in Region Västra Götaland, one plant in Region Gotland and one in Region Östergötland. The design heat loads in the studied plants vary from 3.5 to 10 MW. The proposed solar heating plants comprises 3 000 – 5 000 m^2 solar collector arrays combined with 300 – 500 m^3 of buffer storage. The resulting solar heat costs vary from 450 – 500 SEK/MWh, which is 30 – 50% higher than typical operational costs in this type of plants using wood chips. The experiences from the feasibility studies confirm that the implementation of solar heating plants rely on the possibilities to increase interest and knowledge, e.g. via demonstration plants, as there is a large potential to improve the efficiency of existing plants.

1. INTRODUCTION

Region Västra Götaland comprises 1.6 million inhabitants on 24 000 km^2, i.e. 66 inhabitants per km^2, which is equal to the average population density within Europe.

The region has 49 municipalities, the smallest with 5 000 inhabitants and the largest with 500 000 inhabitants (City of Gothenburg). All municipalities have one or more block and/or district heating plants using solid wood fuels. A couple of municipalities have one or more solar heating plants, e.g. Lerum and Orust.

Many heating plants using solid biofuels, especially wood chips, have often only one boiler that runs all year around, commonly without a buffer storage tank. This means in many cases that the boiler runs on very low power with low efficiency due to the low heat demand during the summer months.

A combination with a storage and solar collectors makes it possible to run the boiler with a higher efficiency (and less emissions) and thereby save more wood fuels than the amount replaced by the solar heat. However, the low price for wood fuels together with lack of awareness about solar collectors, etc. creates small incentives to invest in a solar system.

2. PROJECT DESCRIPTION

Region Västra Götaland is associated to the EC-project SDHp2m which primarily has a focus on the implementation of solar district heating in three European regions: Styria (AT), Thuringia (DE) and Auvergne Rhone Alpes (FR). The aim here is to investigate the interest and the possibilities to complement existing block and district heating systems based on solid biofuels with a solar heating system within Region Västra Götaland. The project will be carried out in three steps as described below.

First, a survey is initiated and evaluated. The survey will show the interest in the municipalities and potential plants that may be complemented with a solar system. A relevant number of plants will be selected for the next step.

Second, feasibility studies will be carried out for the plants identified in the first step. The most feasible plants (site and economics) will go on to a pre-design study and an application for co-financing, if and when required, before the third step.

Third, individual or common calls for tenders will be prepared and communicated to interested contractors, with the aim to realize at least one plant during 2017-2018 that can be used as a demonstration pant for other interested actors.

3. SURVEY

3.1 Gathering data

There is not one single source that provides information about heating plants with biofuel boilers in Sweden, so data were gathered based on two main sources.

First, a questionnaire was developed and distributed to all municipalities asking for basic information about their heating plants, especially those with biofuel (wood) boilers with a nominal power of 200 kW or more.

Second, information available on the homepages of members of the Swedish District Heating Association Region Västra Götaland, was gathered.

Third, the above was evaluated for duplicates and complemented with data from some other sources.

Fourth, the result of the survey was communicated by e-mail and presented at a seminar in order to be as complete as possible, at least regarding heating plants using biofuels (primarily wood).

3.2 Heating plants

Altogether >110 heating plants were found within the 49 municipalities in Region Västra Götaland (Figure 1). There are more heating plants, but the most important for the feasibility study are likely included.

***Figure 1.** Municipalities in Region Västra Götaland.*

The number of district heating systems is less than the number of heating plants as there may be several heating plants in one district heating system and the district heating systems in Ale and Partille are parts of the main district heating system in Göteborg.

There are also connections between Göteborg, Kungälv and Mölndal. Some of the municipalities have district heating from industries (e.g. Stenungsund, Vänersborg and Lilla Edet) and only two small municipalities lack district heating (Sotenäs and Öckerö).

The survey is presented in a Master thesis by Thrysøe Ekström (2016) and a conference paper by Dalenbäck et al (2016).

3.3 Wood fuel boilers

There are >40 identified wood chips boilers, out of which >25 are owned by the municipalities and the rest are owned by ESCO's.

There are >35 identified wood pellets boilers, out of which about 30 are owned by the municipalities and the rest are owned by ESCO's.

There are <10 identified wood briquettes boilers, all owned by the municipalities.

There are four plants with solar heating plants.

The sizes of the wood chips boilers vary from a few MW up to 130 MW (often for combined heat and power), the sizes of the wood briquettes boilers vary between 1 and 10 MW, while the sizes of the wood pellet boilers, with one exception (100 MW), vary from 100 kW up to a couple of MW.

3.4 Ownership

The fact that there are not only municipalities, but also ESCO's (e.g. Agrovärme) that operate heating plants was known, but maybe not that there are a couple of rather new operators. Besides the municipalities a couple of the ESCO's also seem to be interested in the project.

3.5 Available space

One of the prerequisites to complement an existing heating plant with solar heating is that there is some place where the collector array, and a storage tank, can be mounted. Therefore, the location of the heating plant has been identified in order to rank them from a feasibility point of view. The information required to evaluate the possibility to connect distributed collector arrays, i.e. available areas and buildings in connection to the district heating networks, was not gathered at this early stage.

4. FEASIBILITY STUDIES

4.1 Initial scanning

The survey and the connected info about SDH triggered the interest to have more information about the possibilities to complement existing plants with solar heating systems only in a few cases.

Thus, the initial scanning of potential plants has mainly been based on previous knowledge about existing plants and maps on internet together the interest shown on the first project seminar.

4.2 Feasibility studies

The aim is to get the first impression about the possibilities to complement small wood chips plants (from 4 up to about 30 MW) with a solar collector array. This approach is based on the fact that small wood chips plants have a large potential to improve the system efficiency (poor part load efficiency). It is further not likely to be able to build very large demonstration plants.

Wood briquettes boilers may also be interesting, while pellet boilers are less interesting as they usually have a higher efficiency at varying load conditions. Local conditions and the interest for solar heating expressed by the plant owners might however change that situation.

The feasibility studies were supposed to cover initial plant sizing, placing of collector arrays and a storage tank, as well as the possibilities to lower the return temperatures. The studies will also consider planned boiler replacements and extensions of the district heating networks, and result in initial cost estimates.

The existing plant in Ellös district heating network, design power 2-3 MW and a wood chips boiler with 2 MW design power, with 1 000 m^2 of solar collectors and 200 m^3 storage tank, will work as a reference for new plants.

4.3 Initial interest

The initial feasibility studies were supposed to be carried out for Herrljunga (6 MW), Vara (10 MW), Tibro (19 MW) and Töreboda (20 MW).

Further feasibility studies were supposed to be develop based on individual contacts with plants owners.

5. FEASIBILITY STUDIES

5.1 Introduction

The interest for feasibility studies in Region Västra Götaland has unfortunately been lower than expected, but luckily a couple plant owners in other regions have shown interest.

So far, three feasibility studies have been carried out: Vara (10 MW) in Region Västra Götaland, Borensberg (4.5 MW) in Region Östergötland and Hemse (4 MW) in Region Gotland. Two feasibilities are ongoing: Herrljunga (6 MW) and Tidaholm (15 MW).

The feasibility studies for Hemse (Dalenbäck, 2018a), Vara (Dalenbäck, 2018b) and Borensberg (Dalenbäck, 2017) are presented in the following.

5.2 Hemse

The heating plant is located on the island Gotland, with a lot of wind power plants and a rather high penetration of small solar heating and solar PV plants, i.e. a region with an above average knowledge and interest for renewable energy.

The present heat load varies between 500 kW in Summer and 3-4 MW in winter. The heating plant comprises an old wood chips boiler (7 MW) and old oil boilers for back-up (2 x 4 MW).

The feasibility study is part of a study to refurbish the heating plant with a new wood chips boiler, a possible solar heating plant and an electric boiler.

The present operation of the plant with a too large wood chips boiler results in high heat distribution temperature (forward 95 °C; return 50-60 °C) and high heat distribution heat losses, especially in the summer. Thus a new boiler is supposed to decrease the heat load as the heat distribution losses will decrease.

Figure 2. *Heating plant in Hemse.*

Figure 2 shows a bird eye view of the existing heating plant with nearby suitable land for placing a collector array in the east part of Hemse.

The proposed solar heating plant comprises 3 000 m^2 solar collectors (requiring about 10 000 m^2 land area) and a 300 m^3 buffer storage tank that is expected to gain about 1 200 MWh/a. The annual load is about 11 500 MWh/a, which means that solar heat is expected to cover about 10% of the total heat load.

The budget investment is estimated to 12 MSEK and with annuity 0.05 this results in a solar heat cost of 500 SEK/MWh.

5.2 Vara

The heating plant is located in the middle of Region Västra Götaland, surrounded by large farming fields with a couple of wind power plants.

Figure 3. *Heating plant in Vara.*

Figure 3 shows a bird eye view of the existing heating plant situated in an industrial area with nearby suitable land for placing a collector array in the south part of Vara.

The present heat load varies between 1 MW in summer and about 10 MW in winter. The heating plant comprises old wood chips boilers (5 + 6 MW) and old oil boilers for back-up (4 + 6 MW).

The intention with the feasibility study is to get a first understanding of the possibilities to complement, and improve the performance of the heating plant with a solar heating plant.

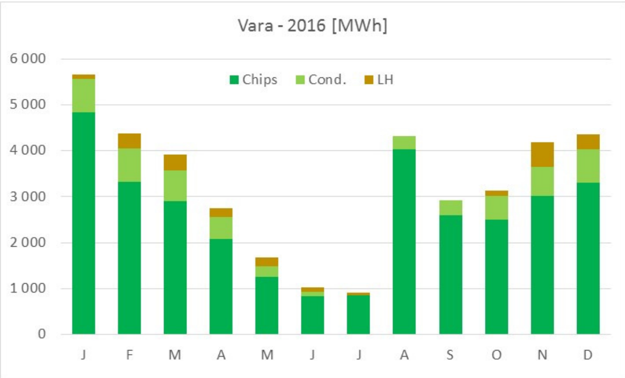

Figure 4. *Heating load in Vara. Chips = Wood chips; Cond. = Exhaust condenser; LH = Boiler for crop residues at Lagerhuset.*

Figure 4 shows the heat load in 2016. The high load in August (and September) is due to that the heating plant is also used to supply heat to a large crop dryer in operation in connection to the harvest period. The crop dryer is supplied with higher temperatures (>100 °C) than required for district heating via an extra heat distribution pipe. This together with other circumstances related to the heat distribution system may imply that a refurbishment of the heating plant may result in reduced heat loads.

The proposed solar heating plant comprises 5 000 m^2 solar collectors (requiring about 15 000 m^2 land area) and a 500 m^3 buffer storage tank that is expected to gain about 2 000 MWh/a. The annual load is about 35 000 MWh/a, which means that solar heat is expected to cover about 6% of the total heat load. Thus a larger plant size would be more feasible assuming that it is possible to find suitable land for solar collectors.

The budget investment is estimated to 18.5 MSEK and with annuity 0.05 this results in a solar heat cost of 450 SEK/MWh.

5.2 Borensberg

The heating plant is located in the northern part of Region Östergötland surrounded by forest. Borensberg has developed around the locks in Göta Kanal.

The present heat load varies between 300 kW in Summer and about 4.5 MW in winter. The heating plant comprises one wood chips boiler (3 MW) and one oil boiler (5 MW). The oil boiler fuel is HVO (bio diesel).

The intention with the feasibility study is to get a first understanding of the possibilities to stop the wood chips boiler for a long period in the summer with the help of a solar heating plant.

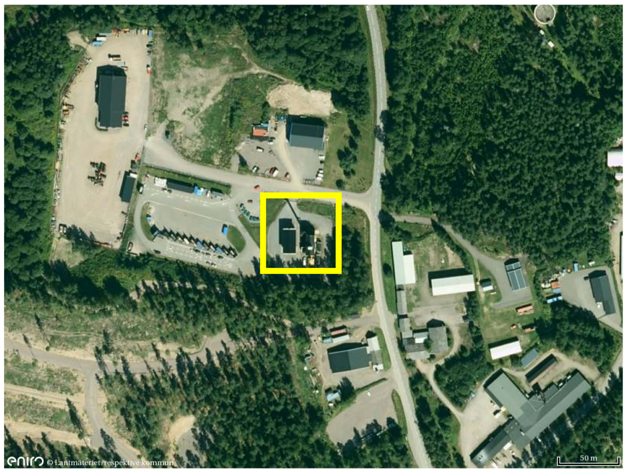

Figure 5. *Heating plant in Borensberg.*

Figure 5 shows a bird eye view of the existing heating plant situated in an industrial area surrounded by forest. Two land areas in the forest close to the heating plant and one open land area in another site close to the main heat distribution pipe may be possible for the placing of a collector array.

The proposed solar heating plant comprises 3 000 m^2 solar collectors (requiring about 10 000 m^2 land area) and a 300 m^3 buffer storage tank that is expected to gain about 1 200 MWh/a. The annual load is about 16 000 MWh/a, which means that solar heat is expected to cover about 8% of the total heat load. Thus a larger plant size would be more feasible assuming that it is possible to find suitable land for solar collectors.

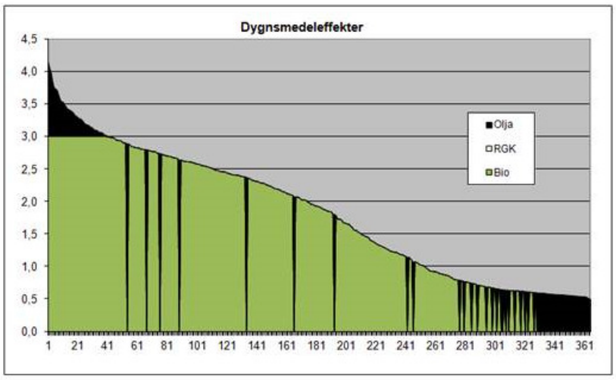

Figure 6. *Heating load in Borensberg presented as a power [MW] duration graph based on daily averages. Bio = Wood chips; Oil = HVO; RGK = Exhaust condenser (not used).*

The budget investment is estimated to 12 MSEK and with annuity 0.05 this results in a solar heat cost of 500 SEK/MWh.

Figure 6 shows the heat load in 2014. The district heating system is connected to a large number of small buildings whereas the utilization time (3 500 h) and the heat losses are rather high (about 250 kW).

The operational costs with wood chips is around 300 SEK/MWh, while the operational cost with HVO is around 1 100 SEK/MWh. Thus it is less feasible to replace wood chips than HVO from an economic point of view.

5.3 Comparisons

All studied plants have in common that they have rather high return temperatures in summer (50-60 °C). It is therefore recommended to evaluate the possibilities to lower them, influencing the solar yield as well as the buffer storage capacity.

Table 1. *Load characteristics.*

	MW	MWh/a	h/a
Hemse	3-4	11 500	3 300
Vara	10	35 000	3 500
Borensberg	4.5	16 000	3 500

Table 1 shows the load characteristics for the studied plants. All three plants are rather small. This is positive as the possibilities to get financial support are improved, but it is negative as it will be difficult to demonstrate competitive heat costs.

Hemse and Borensberg have about the same size, but there are large differences related to the present performance of the plants and possible placing of the solar collector arrays.

Hemse needs to be refurbished and is located close to suitable land areas, while Borensberg has rather new equipment and poor conditions to find suitable land areas for the solar collector array. Vara is 2-3 times larger, but has neither poor, nor very good conditions, for a solar heating plant.

Therefore, there are large possibilities that a solar system will be realised in Hemse, assuming it is possible to find favourable enough economic conditions.

5.4 Ownership

The studied heating plants have different ownerships, which may result in different decision procedures and different economic considerations.

Borensberg is owned and managed by the large municipal energy utility, Tekniska Verken in the City of Linköping. Hemse is owned and managed by Gotlands Energi (GEAB), which in turn is owned by Vattenfall (75%) and Region Gotland (25%). Vara is owned and managed by a small company owned by Vara Energi ek.för, which is a cooperative comprising citizens in Vara (similar to the Danish ownership of small DH systems).

5.5 Economic considerations

There are different ways to present the economic feasibility. Here the estimated solar heat cost (budget investment and average performance using annuity 0.05) is compared with the present operational cost (fuel plus O&M) during the summer.

The estimated solar costs are about 30 - 50% higher than the typical operational costs, but they relate only to 5 – 15% of the total load, i.e. they will only result in a small increase of the total operational costs, requiring a rather small financial support in order to keep the same district heating fee as without the solar system.

6. DISCUSSION

6.1 Survey

The existing information about heating plants had to be gathered from different sources which was rather time consuming.

The information about the heating plants that can be found on internet (municipalities, district heating association, district heating providers themselves, etc.) is very different. Some information contains everything from detailed data and pictures of heating plants to detailed descriptions of the heat distribution system connected to the plants, while there is lack of any information in some cases.

The same is valid for contact information. Some organisations present lists of employees with their responsibilities, while others only have information how district heating customers can send questions to a help desk.

In our case we were helped by the regional energy office – Hållbar Utveckling Väst - which had contact persons (energy advisors) in all municipalities. The knowledge about the local situation varied however among the contact persons and thereby the quality of data and contacts received.

6.2 Challenges

The main advantage is that district heating is established so the feasibility studies can focus on the potential possibilities to complement existing plants with a solar collector array and a storage tank (in case a storage tank is not already available).

The main challenge is that there are no strong incentives to complement existing plants with solar heating. The plants provide already renewable heat and the operation costs are low using wood fuels.

It is also a challenge to present a system design that the operation staff is convinced will improve the operation as well as the plant efficiency.

6.3 Experiences

The experience from the feasibility studies confirm the lack of incentives and knowledge among plant owners. Thus it confirms the necessity to create incentives and the need to be able to demonstrate up-to-date plants to prove performance and enable knowledge dissemination.

The experiences also show that the presently abundant resources and thereby low price of wood chips encourages plant operation with a lower than necessary performance. For example managed one of the plant owners to negotiate a new favorable wood chips delivery contract during the feasibility study.

In the long term, it is likely that bio energy resources will be more valuable in the future as it is one of the main renewables that can replace fossil resources in fuels and other products. Thus it should be increasingly important to nurse the use of bio energy. To use solar heat when available is thus a technology that should be encouraged. We are however far from this insight being realized.

The experiences also show that there are two main concerns or beliefs, the availability of space for solar collectors and the importance of short-term economics.

7. NEXT STEPS

7.1 Technology procurement

The aim now is to take one or two feasibility studies a step further and make pre-designs that can be used to apply for co-financing and to make call for tenders.

The finished and ongoing feasibility studies will be presented and discussed at a seminar with the plant owners and other stakeholders. The seminar will also be used to inform and encourage the Swedish Energy Agency to create a technology procurement project.

7.1 Evaluation and dissemination

The initial aim to realize at least one plant during 2017-2018 seems simply too optimistic.

The technology procurement should include funding for evaluation and dissemination in order to encourage the realization of larger plants that can show competitive economics.

REFERENCES

Reports:

Thrysøe Ekström, L. (2016). *Feasibility for solar district heating in Region Västra Götaland.* MSc thesis BOMX02-16-150. Chalmers University of Technology, Gothenburg.

Dalenbäck, J-O (2017). *Solvärme i Borensberg.* För-studie för Tekniska Verken, Linköping inom ramen för EU-projektet SDHp2m. CIT Energy Management AB, Gothenburg.

Dalenbäck, J-O (2018a). *Solvärme i Hemse.* Förstudie för GEAB inom ramen för EU-projektet SDHp2m. CIT Energy Management AB, Gothenburg.

Dalenbäck, J-O (2018b). *Solvärme i Vara.* Förstudie för Vara Energi Värme AB inom ramen för EU-projektet SDHp2m. CIT Energy Management AB, Gothenburg.

Conference proceeding:

Dalenbäck, J-O., L. Thrysøe Ekström and G. Zettergren (2016). Feasibility for SDH in Region Västra Götaland. *Proceedings 4th International Solar District Heating Conference*, Billund, Denmark.

FLAT PLATE AND VACUUM COLLECTORS SDH PLANTS: PERFORMANCE COMPARISON AFTER ONE YEAR OF OPERATION AND FUTURE EXPANSION OF THE SYSTEM USING NATIONAL INCENTIVES SCHEME

Luca Degiorgis[a, *], Michel Noussan[a], Matteo Jarre[a], Alberto Poggio[a], Giorgio Marcon[b]
[a] Politecnico of Torino, Department of Energy
C.so Duca degli Abruzzi 24, 10125, Torino, Italy.
Phone number: +39 011 0904529; +39 3493566826;
e-mail address: luca.degiorgis@gmail.com

[b] STUDIO INGEGNERIA ing. Marcon
C.so Marconi 34, 10125 Torino

TOPIC 4 Monitoring Results.

SUMMARY

A test site SDH solar plant has been built to provide heat to an existing district heating system in the Italian Alps, at 1600 m above sea level. The plant uses both flat plate and evacuated solar collectors and the two systems are equipped with a performance control system that allows to investigate the behavior of the two collectors' typologies separately. Due to the particularly mountainous environment, external temperatures and snow levels, coupled with high supply temperatures of the district heating network, can affect significantly the energy production of the solar plant. , where one of the biggest DH systems, that provides heat to the city of Torino, is located

After one year of operation it is possible to report a very good energy production and high availability of the plant. This allows to investigate a significant expansion of the plant, for maximizing the contribution of national incentives and reduce the heat cost production.

Keywords: solar plant, district heating, performance monitoring, flat plate collectors, vacuum collectors, economic analysis.

1. ABSTRACT FORMATTING

The SDH plant is located in an alpine village in the Susa Valley, 100 km North of Turin, at approximately 1600m above sea level. The DH plant has been turned into operation in 2005, providing heat to 54 substations for a total heated volume of 350,000 m^3, using a distribution network of insulated pipes 5km long.

In 2016 a solar pilot plant has been developed and turned into operation to provide heat to the existing DH system. The pilot plant is made of two small solar collector fields, one using parabolic evacuated tube collectors and the other one using large scale flat plate double glazed collectors.

The system is equipped with energy measurement probes and sensors, to determine operating conditions, efficiency and its behavior in relation with the operation of the district heating system. A meteorological station provides detailed weather information.

During the design of the plant several questions raised, especially linked to the mountain location: how a system like this will face the abundant snow that can accumulate on the roof and on the collectors? Will it be necessary to melt it? Is it necessary to provide extra heat or solar-based heat can be used for snow melting? A mechanical system will be necessary?

The performances of the flat plate collectors and the evacuated ones are also under investigation: which system will be better suited for the application? Which will be more performing? Will the two systems be reliable? Do they present specific weak points, especially because of snow and ice formation?

How about the economic point of view, are they comparable?

The two systems also differ for the heat transfer fluid: water for the ETC, a mixture of water and anti-freezing for FPC.

The control systems are dedicated, one for each system: variable mass flow and an on-off management, developed by the producer of the collectors for the ETC; variable mass flow and a commercial controller with quite simple ΔT control logic for the FPC.

The system has been in operation for one year and it is now possible to analyze a relevant amount of useful information: the main result is that the availability of the system has been extremely high, and the specific performances are at 700kWh/m^2 of collector surface.

The paper describes the monitoring system and the data analysis of a whole year of operation, in terms of delivered temperature, performance of the plants, efficiency of the systems, management of the flows, ratio between thermal energy production and electric energy use.

The availability of operation data and the ease to manage them with the special tools developed by the control system providers will be presented. Some alerts or alarm automatic detection and information are under development.

Due to good measured performances, an increase in the size of the solar plant is conceivable: a feasibility study is presented, based on real installation costs and on the current incentive schemes available in Italy.

MODELING AND SIMULATIONS OF SOLAR TWO-WAY SUBSTATION

Nicolas Lamaison[1,2], David Chèze[1,2] and Cédric Paulus[1,2]
CEA LITEN - 17 Rue des Martyrs, 38054 Grenoble (France)
INES - 50 Avenue du Lac Léman, 73375 Le Bourget du Lac (France)
+33 479792153, nicolas.lamaison@cea.fr

Abstract – Decentralized surplus feed-in of solar heat into a District Heating Network (DHN) is here addressed. The heat collected from solar panels located on rooftops of DHN connected buildings may either be used locally for domestic hot water and space heating or fed into the DHN. Two-way substations able to transfer heat from and into the network seem then to be required utilities. The present paper presents the specifications (60kW capacity, return-to-supply connection) and promising architectures of such two-way substation based on a previous analysis. A first-of-a-kind Modelica-based dynamic model of the substation together with the consumer and the solar field connected to it is then detailed. Two-day simulations considering real operating conditions of DHN were then performed. The results highlighted i) the good match between the periods of solar heat reinjection with the periods of low supply temperature and differential pressure and ii) the decisive benefit of the reinjection to increase the part of useful solar energy.

1. INTRODUCTION

In the "2way District Heating" course of action from the 4GDH concept (Lund et al., 2014), decentralized feed-in of solar heat from prosumers seems to be a promising solution to increase the share of renewable energy in District Heating Networks (DHN), especially in dense urban areas with limited ground surface. However, when scattered customers roofs are used to collect and inject heat locally in a network, new problematics arise. Local consumption or total feed-in of the collected solar energy, use of storage at the building level, and management of the local differential pressure and supply temperature are the most decisive ones.

Among the various reinjection principles, Return to Supply feed-in is considered since it seems to be the most flexible option from the DHN point of view (Beckenbauer et al., 2017; Lennermo and Lauenburg, 2016; Schäfer and Schmidt, 2016). However, R/S feed-in implies to overcome the local differential pressure between the return and supply lines, which usually exhibits significant variations due to rapid load fluctuations. Moreover, the feed-in temperature must be superior or equal to the local network supply line temperature. The latter constraints on the local differential pressure and the local supply temperature involve at the two-way substation level the use of at least a variable speed pump and a finely tuned control strategy.

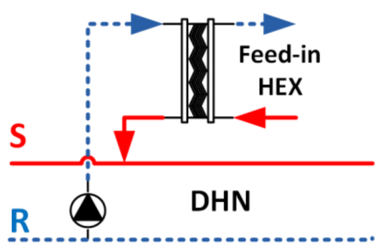

Figure 1: Schematic of Return to Supply (R/S) feed-in

At the network scale, various studies investigate decentralized reinjection and its effect on the thermo-hydraulic behavior of the network (Brange et al., 2016; Hassine and Eicker, 2014; Heymann et al., 2017). However, at the component scale i.e. the substation, only few studies from the open literature address the topic of the reinjection. From the simulation point of view, Paulus and Papillon (2014) compared nine different substation architectures, however connected in a Return to Return fashion, using TRNSYS and evaluated the influence of the return temperature, solar collectors area and type of solar collectors on thermal performances only. From the experimental point of view, Rosemann et al. (2017) addressed the challenging topic of innovative control algorithm at the substation level with Hardware-In-The-Loop testing. There conclusions were used to build various first-of-a-kind solar prosumers and decentralized feed-in substations (Rosemann et al., 2017a).

In the frame of the Horizon 2020 "THERMOSS" project, specifications, modelling and prototype testing of a two-way substation for a multi-family building is performed.

In the present paper, specifications and promising architectures are first presented in the basis of what was presented in Lamaison et al. (2017). Second, a first-of-a-king Modelica-based dynamic model of the most promising two-way substation together with the consumer and the solar field connected to it is then detailed. The control strategies and operating principles associated to this substation are then discussed. Third, results of a two-day simulation considering real DHN operating conditions in terms of differential pressure and temperatures (supply and return) is then detailed in terms of temperatures, flow rates and heat power. Finally, a sensitivity analysis on the DHN operating conditions is presented.

2. SPECIFICATIONS AND ARCHITECTURE

2.1 Specifications

During the first year of the THERMOSS project, specifications and architecture of a two-way substation were addressed. In order to give a precise frame to study, it was decided to specifically consider the decentralized reinjection of solar heat on a DHN. Extrapolation to other local heat sources is also envisioned and will use the current development as basis.

As stated in the Introduction, R/S feed-in is considered since it is the most promising option. As highlighted schematically in Figure 2, the solar collectors are assumed to be on the rooftop of a multi-family building, equipped with a unique two-way substation. Variants relying on individual two-way stations at the apartment level have been discarded from this study due to prohibitive cost and increased complexity. Indeed, solar two-way substations seem more appropriate for multi-family buildings rather than for individual apartments (Rosemann et al., 2017b) since it simplifies the hydraulic connections at the building level while reducing the costs. It also reduces the number of reinjection points in the DHN, aggregate heat inputs and thus simplifies the operation of the network.

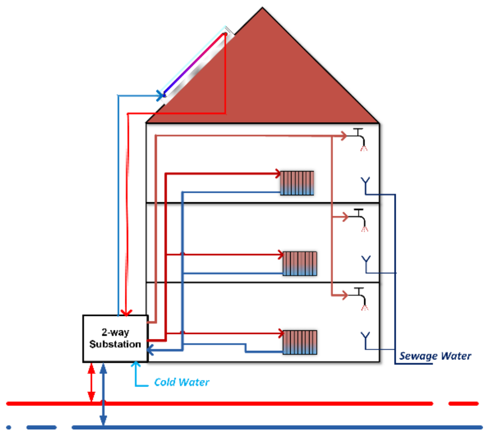

Figure 2: Schematic of a two-way substation in a multi-family building prosumer

Regarding the order of magnitudes involved for the present study, it is considered that the building consists in 6 apartments of 70m² organized in 3 floors of 2 apartments, leading to a building footprint of 7.5m of height, 10m of width and 14m of length. Firstly, assuming a rather poorly insulated envelope, the required Space Heating (SH) power is approximately 42kW (i.e. around 100W/m²). Secondly, using the daily draw-offs from COSTIC (2016), i.e. about 150 liters for an apartment of 3 people, and the “DHW-calc” calculator (Jordan and Vajen, 2005) to obtain a distributed daily profile, the maximum 10 minutes average is about 16kW/apartment. The latter leads to 60kW of Domestic Hot Water (DHW) power consumption for the entire building when accounting for a simultaneity coefficient of 0.62. Finally, accounting for the building geometry, it is calculated that the maximum solar collector area is about 80m² (which covers one side of the rooftop with a 30° of inclination angle). The building solar production would reach 56kW with an assumption of 700W/m² of production based on IEA SHC recommendations (IEA SHC, 2004).

2.2 Substation architectures chosen

The present work is a continuation of the study presented in (Lamaison et al., 2017) that discussed the possible architectures of such two-way substation based on a set of features and selected the most promising ones based on a set of criteria.

Features such as the location of the hydraulic separation between the network and the building, local consumption of the heat or total feed-in and control strategies were combined to build an exhaustive list of possible configurations. Promising setups were chosen from that list based on a multi-criteria analysis (cost, operation, ownership, etc.). These setups are presented in Figure 3, Figure 4 and Figure 5. The two first architectures exhibit complete reinjection of the solar heat on the network without direct local consumption of this heat while the last one promotes a local usage for DHW preheating while reinjecting the excess heat into the network.

On the three Figures, various control strategies are highlighted (S0, S1 and S2). The goal of these control strategies is to obtain a feed-in temperature level above the local supply temperature in the DHN, while also addressing the following constraints:

i) Minimize the temperature in the solar field to reach high efficiencies,
ii) Overcome the strongly varying local flow resistance, i.e. differential pressure drop,
iii) Adjust the feed-in flow rate so that the feed-in rate matches the strongly varying heat rate produced by the solar field.

S0 consists in a pump and a valve in series, S1 consists in a pump and a bypass valve, and S2 consists in a hydraulic separator and two pumps. It should be noted that for the present study, only Architecture 2 (C2U0) with control strategy S0 is considered.

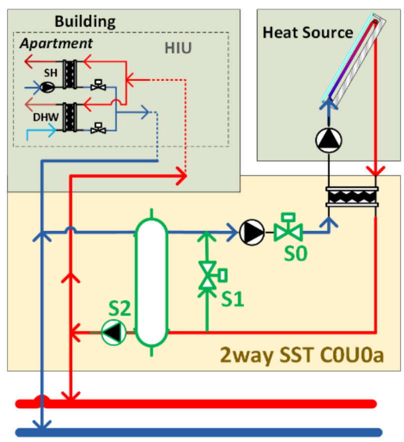

Figure 3: Schematic of Architecture 1 (C0U0)

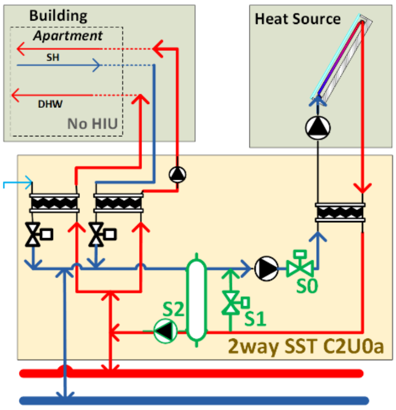

Figure 4: Schematic of Architecture 2 (C2U0)

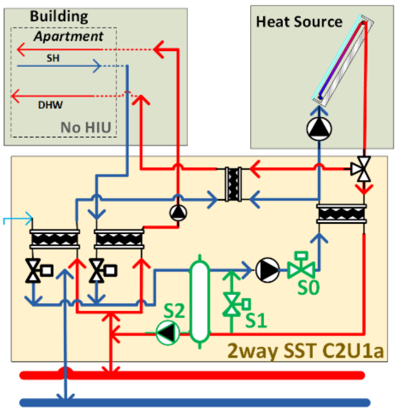

Figure 5: Schematic of Architecture 3 (C2U1)

3. MODELING

The present section introduces first the modelling framework. Second, it presents in sequence the models for the consumer (SH and DHW), the solar field and the substation. Third, the network boundary conditions used in the present study are highlighted. Finally, the control associated to the operation of the substation and the basic operating principles are discussed.

3.1 Modelling Framework

The modelling framework is based on the open source modelling language Modelica used in the commercial simulation environment Dymola. Modelica is an acausal (equation-base) and object-oriented programming language with a large and fast-growing community both for industrial and academic applications (Schweiger et al., 2017). Modelica has native multi-physical modelling capabilities (thermo-hydraulic), is structured in libraries enabling exchange of methods in the scientific community and allows for implementing new components. Moreover, the Annex 60 project from the IEA (Wetter, et al., 2015) promotes the development of computational tools for building and community energy systems based on Modelica and FMI standards, motivating the choice of this modelling framework.

As mentioned in the introduction, the Modelica "Standard" Library for its common connectors and fluid ports, the "Buildings" library (Wetter et al., 2014) for its general building models and the "DistrictHeating" library (Giraud et al., 2015) for its DHN piping and solar collectors models will be used.

3.2 Consumer

The consumer is modelled in terms of space heating consumption using the 'Buildings' library (Wetter et al., 2014) from Modelica and in terms of domestic hot water consumption using the 'DHW-calc' draw-offs profile (Jordan and Vajen, 2005).

Space heating is modelled with i) a heating system and ii) a mono-zone building. Concerning the heating system, it is composed of a thermostatic valve and a radiator modelled using the "RadiatorEN442_2" model from the library "Buildings" (Wetter et al., 2014). In this model, the transferred heat is computed using a discretization along the water flow path, and heat is exchanged between each compartment and a uniform room air and radiation temperature. Concerning the mono-zone building, it is modelled using the "mixed air" model (Wetter et al., 2011) from the same library. It considers a perfectly mixed air in the room and takes into account heat exchange through convection, conduction, infrared radiation and solar radiation. Internal heat gains due to occupation (latent heat), lighting (radiation) and home appliances (convection) are included in the model. Constant single-flow ventilation is considered with a flow-rate of about 0.4 room volume per hour. For the present study, the dimension of the building considered were listed in Section 2.1. The total glazed area for the building represents 1/6 of the building living area, shared as follows, 50% on the South wall, 15% on the West wall and 35% on the East wall. The envelope of the building (layers composition and infiltration) is set to follow the RT2000 French thermal regulations.

Concerning the equivalent radiator, it is assumed to have a nominal inlet temperature, a nominal difference and a nominal power of respectively 70°C, 15K and 42kW. For the obtained nominal mass flow rate of 0.7kg/s, a nominal pressure drop of 1bar is assumed (together with a quadratic pressure drop law). The set point for the building ambient temperature is set at 20°C.

The model requires as inputs the outside temperature and the set point for the radiator inlet temperature. In the present study, the analysis of the operation of the two-way substation is studied for 2 days. Thus, Figure 6 gives this 2 days outside temperature profile calculated using the weather station of Chambéry-Aix les Bains in the software Meteonorm (2017). The 2 days considered are the 11 and 12th of March. The associated set point for the thermostatic valve is also given in Figure 6. The latter follows a heating curve, i.e. 60°C as radiator inlet set point temperature for -10°C as outside temperature and 25°C for 15°C).

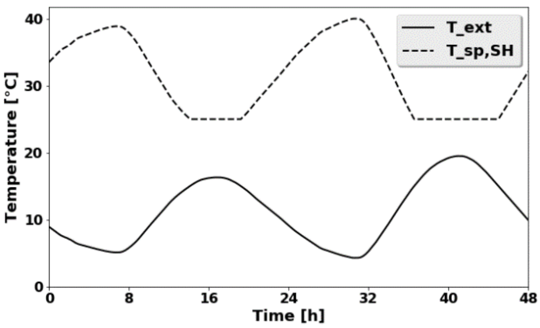

Figure 6: Two days outside temperature and associated radiator inlet temperature set point profiles

The water draw-off system is considered without sanitary loop. As explained initially, the daily profile of draw-offs are obtained from the software DHW-calc (Jordan and Vajen, 2005) from Task 26 of IEA which distributes DHW draw-offs throughout the year or the day with statistical means, according to a probability function. The mean daily DHW consumption was set to 900litres, i.e. 150l/apartment. The latter was obtained from a report of COSTIC (2016) based on the type of apartment and the number of people living in it. Figure 7 shows the 2 days profile considered (6 minutes time-step). The cold water temperature is considered constant equal to 10°C.

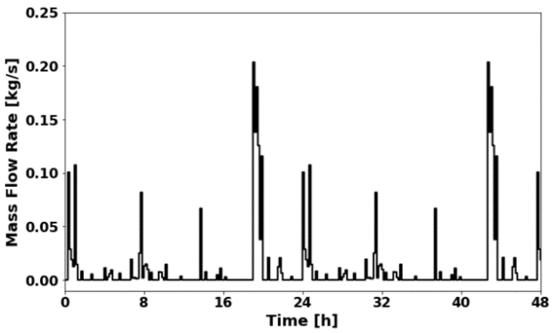

Figure 7: Two days DHW draw-offs profile at 10 minutes time step (obtained from DHW-calc software)

3.3 Solar Field

The solar field on the rooftop is modelled using a component developed inside the 'DistrictHeating' library specifically for the present study. It is a thermo-hydraulic model that considers collectors arranged in rows, each row being discretized in a number of element superior or equal to the number of collectors in the row. The energy balance of each discretized element follows is shown in Eq.(1) which comes from the norm NF EN ISO 9806 (2017).

In that equation, the thermal capacity C accounts for the fluid and material capacities, T_m is the mean temperature of the fluid through the field, T_a is the ambient temperature, A_{field} refers to the total collector field area, η_0 is the collector optical efficiency and a_1 and a_2 are respectively the linear and quadratic heat loss coefficients. The three latter coefficients are obtained using the Solar Keymark test results report ("Solar Keymark Database," 2018).

Finally, in Eq.(1), G_T is calculated using Eq.(2) in which I_b and I_d are the direct and diffuse solar irradiations, obtained from weather data and K_b and K_d are the incidence angle modifiers for the direct and diffuse irradiations, obtained from the Solar Keymark test results report ("Solar Keymark Database," 2018). More specifically, K_b depends on the incidence angle θ and is obtained using input table from manufacturer.

$$C\frac{dT_m}{dt} = A_{field}(\eta_0 G_T - a_1(T_m - T_a) - a_2(T_m - T_a)^2) + \dot{m}_{sol}cp(T_{in} - T_{out}) \tag{1}$$

$$G_T = I_b K_b + I_d K_d \tag{2}$$

The direct irradiation I_b and incidence angle θ must be calculated on the tilted plan of the collectors while to obtain the diffuse irradiation I_d on the tilted surface, the model of Perez et al. (1990) is used. For both irradiation calculations, the horizontal solar irradiation obtained from the weather station of Chambéry-Aix les Bains in the software Meteonorm (2017) is used. Figure 8 presents the resulting total solar irradiation for the 2 days considered.

Hydro-dynamically speaking, the mass flow is considered perfectly distributed in the different rows for the present study. Thus, the solar field pressure drop is calculated with a quadratic law using the total solar loop flow rate $\dot{m}_{sol}$, the single collector nominal pressure drop $\Delta P_{nom,c}$ and flow rate $\dot{m}_{nom,c}$, and the number of rows N_{rows} and collectors per row $N_{coll\_per\_row}$, as shown by Eq. (3).

$$\Delta P_{solar,field} = N_{coll\_per\_row}\Delta P_{nom,c}\left(\frac{\dot{m}_{sol}}{N_{rows}\dot{m}_{nom,c}}\right)^2 \tag{3}$$

Finally, there are two pipes on the solar field (return and supply lines) modelled using finite volumes with heat losses (see Eq. (4) with 'z' being the abscissa along the pipe and UA_{loss} the overall heat transfer coefficient). For the heat losses, the piping are considered to be in contact with the ambient air. The pressure drop in this piping also follows a quadratic law (see Eq. (5)).

$$C\frac{dT}{dt} = \dot{m}cp\frac{dT}{dz} - UA_{loss}(T - T_{ext}) \tag{4}$$

$$\Delta P_{pipe} = \Delta P_{nom,pipe}\left(\frac{\dot{m}}{\dot{m}_{nom,pipe}}\right)^2 \tag{5}$$

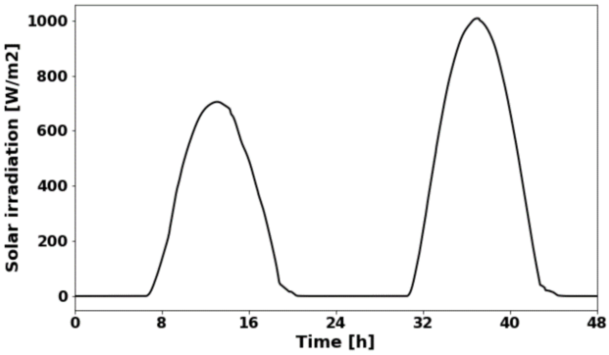

Figure 8: Total (diffuse + direct) solar irradiation on the tilted plan (30°) of the solar collectors for 2 days considered

In the present study, two rows of two double-glazing solar thermal panels ("SavoSolar SF500-15DG - Solar Keymark," 2016) with a gross unit area of 15.96m² (2.6m x 6.2m) leads to a gross area of about 64m² (5.2m x 12.4m) that fits in the estimated space in Section 2.1. The solar collector coefficients and unit capacity are respectively 0.793, 2.52 W/m²/K, 0.004W/m²/K and 12 KJ/K/m². Both the supply and return lines of the solar field are considered to be 20m long with an internal diameter of 32mm and insulated with 3cm of PUR Foam.

3.4 Substation

As shown in Figure 9, the C2U0 two-way substation is modelled with 3 Heat Exchangers, 2 valves and 2 pumps. Concerning the heat exchangers (HEX_{sol}, HEX_{DHW} and HEX_{SH}), they are discretized with finite volume method on both sides. A constant overall heat transfer UA is assumed, sized for the nominal operating conditions listed in Table 1 below.

Table 1: Heat Exchanger sizing

HEX	Thot,in [°C]	Thot,out [°C]	Tcold,in [°C]	Tcold,out [°C]	Q [kW]
Solar	90	60	50	80	60
DHW	80	45	10	45	60
SH	80	50	40	70	42

The service lines between the network and the substation are modelled using the finite volume model of long pipes form the 'DistrictHeating' library (Giraud et al., 2015). The flow in these lines can switch direction. They are sized for 60kW for a temperature difference of 30°C. The latter means a flow rate of 0.47kg/s, which leads to a DN32 for a nominal pressure drop of 100Pa/m (usual sizing value for DHN). The nominal velocity is thus calculated to be about 0.6m/s below the advised limit of 2m/s. A quadratic model (similar to Eq. (5)) is then used to obtain the pressure drop during the simulations. A length of 50m is chosen for these service lines with an insulation of 3cm of PUR Foam.

For the consumer two-way valves (V_{SH} and V_{DHW}), a linear characteristic is considered assuming that the nominal flow rate of 0.47kg/s should be ensured for a differential pressure drop of 1bar. For the SH pump (P_{SH}), it is assumed to operate at a constant differential pressure drop of 1bar in accordance with the equivalent radiator characteristics as described in Section3.2.

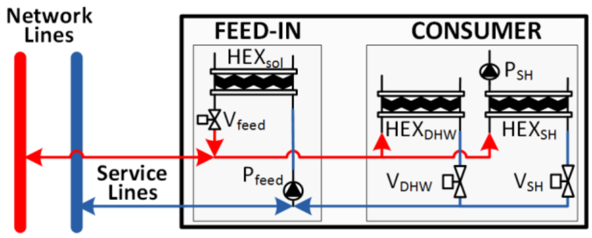

Figure 9: Two-Way Substation model (Similar to Figure 4 with S0 strategy only)

Finally, the feed-in pump (P_{feed}) is considered to be subjected to the network pressure drop and its flow rate is controlled as explained later in Section 3.6. For the calculation of the feed-in pump consumption, an isentropic efficiency of 80% is accounted for.

3.5 Network boundary conditions

The network side inputs are the local differential pressure and supply/return temperatures. In the present model, these two variables can either be set to constants to study specific operational conditions or set to follow real DHN variations. For the latter, data were collected by Veolia Giroa in the frame of the THERMOSS project at the DHN of San Sebastian, Spain. Figure 10 below presents these data for the two consecutive days of interest (2nd and 3rd of March 2017) with a time step of 15 minutes. These data are here only used as typical DHN data and are not correlated to the other boundary conditions such as the outside temperature for example.

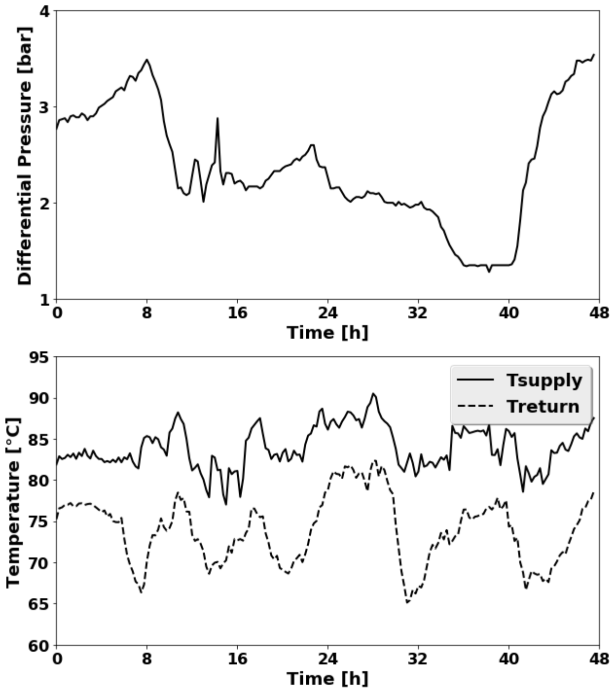

Figure 10: Differential Pressure and Supply/Return Temperatures used as DHN inputs for the simulations

3.6 Control and Operating Principles

The control strategy of the two-way substation concerns first the valves on the consumer side, second the solar field pump speed and third, the feed-in pump speed:

- Consumers: The DHW valve (V_{DHW}) opening is controlled using a pure proportional controller so that the secondary hot temperature on the consumer side is equal to 45°C. Similarly, a pure proportional controller is used for the opening of the SH valve (V_{SH}) so that the secondary hot temperature is equal to the set point defined in Figure 6.
- Solar field: The solar field pump starts when the irradiation in the plane of the solar field is above 100W/m² and its flow rate is controlled by a PI controller so that the outlet temperature of the solar field is constant (set at the DHN supply temperature plus a margin of 10°C). The flow rate on the field is bounded between 10 and 50 kg/hr/m² of solar panels.
- Feed-In: The feed in pump (P_{feed}) starts when the solar field outlet temperature is above the supply temperature of the DHN plus a margin of 5°C. The speed of the feed-in pump is controlled so that the outlet temperature of the feed-in heat exchanger is above the supply temperature of the DHN plus a margin of 5°C.

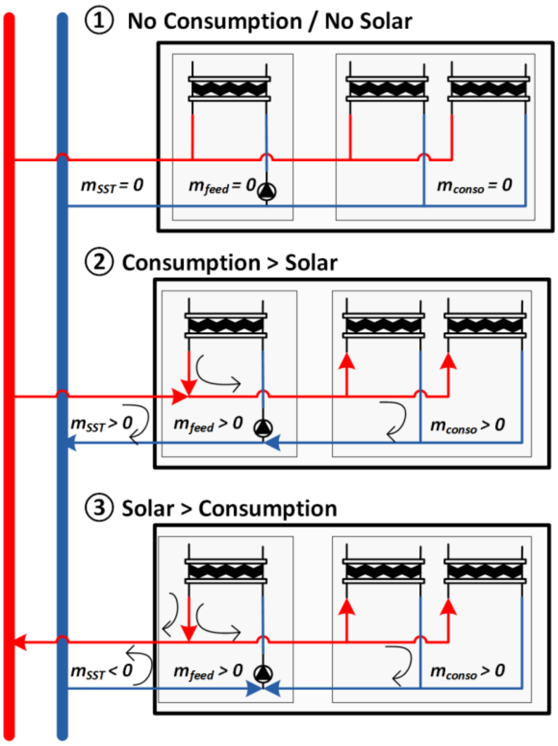

Figure 11: Operating principles of the C2U0 Substation

The operating principles of the substation are presented in Figure 11. At a given instant of time, there are three cases possible:

i) In case 1, there is no heat consumption or solar production and thus there is no flow through the service lines;

ii) In case 2, the heat consumption for domestic hot water and space heating is larger than the solar production. The solar energy is used for the consumer needs in addition to the heat coming from the network. The flow in the service lines is thus from the supply to the return line;

iii) In case 3, the heat consumption is lower than the solar production. The solar energy is used to entirely satisfy the consumer needs and the surplus heat is reinjected to the network. The flow in the service lines is thus from the return to the supply line.

4. SIMULATION RESULTS

4.1 Two days operation analysis

Figure 12 presents first the results in terms of mass flow rate in the solar field, from the network, from the feed-in pump and to the consumer (DHW+SH). The 3 operating cases described in the previous Section are specifically highlighted. The peaks in the consumer flow rates are due to the DHW draw-offs. The oscillations observed for the feed-in are due to the PI controller that requires a better identification, or even a gain schedule-like identification due to the strongly varying operating conditions. The conclusion of this graph is that reinjecting the solar heat on the network when no local storage facilities are available is of prime interest since the solar production periods do not match the local consumption periods.

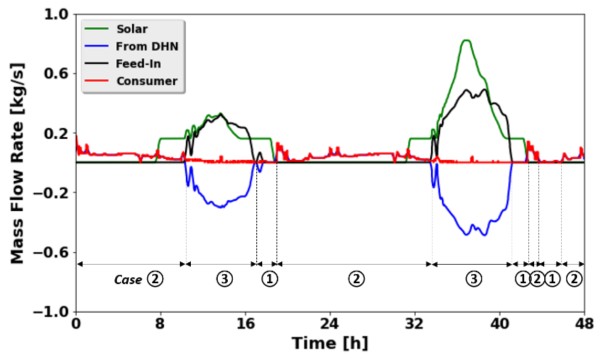

Figure 12: Mass flow rates in the two-way substation and in the solar field for the 2-days simulation period

Figure 13 presents the results of the 2days simulation in terms of temperature. The periods of consumption and reinjection are noticeable on the temperature chart, i.e. when the temperature at the entrance of the service line is the same as the DHN supply temperature, the substation consumes heat, when it is above, it reinjects heat. It is here interesting to note that solar energy production periods are coincident with the periods where the heating demand is the lowest (due to high outside temperature and passive gains) for which in general the supply temperature from the network is also the lowest. The latter is favourable for the reinjection. A similar analysis can be performed for the network differential pressure.

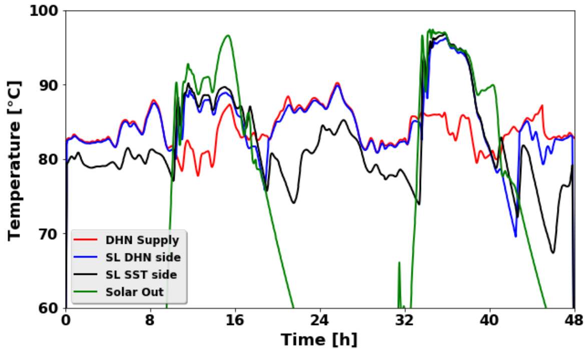

Figure 13: Temperatures in the supply line of the DHN, the supply service line (SL) and the solar field for the 2-days simulation period

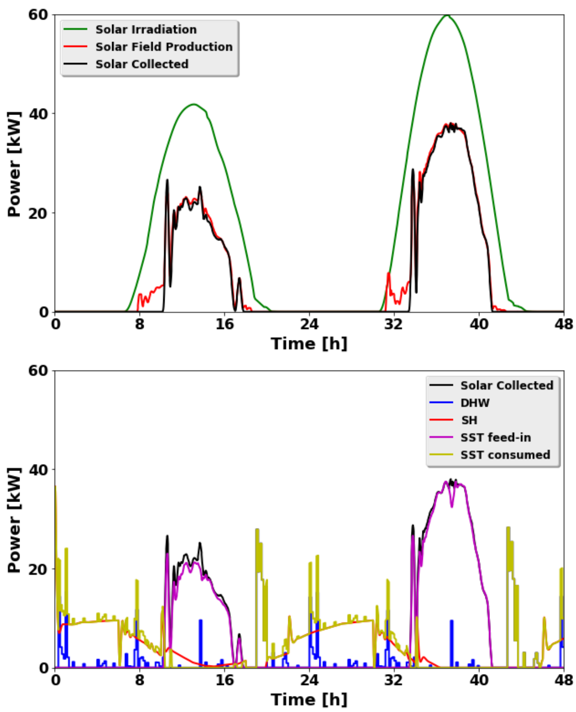

Figure 14: Heat power in the substation for the 2-days simulation period

Figure 14 presents the results of the 2days simulation in terms of heat power. On the top chart, the difference between the solar irradiation (Q_{sol}) and the solar field production (Q_{field}) is due to the solar collectors' efficiency. The difference between the solar field production (Q_{field}) and the collected energy (Q_{coll}) is due to the losses in the solar field piping mostly during the start-up phase (warming up of the volume of water that cooled down at night). On the bottom chart, all the heat power related to streams from or to the two-way substation are shown. It is worth noticing that the part of self-consumption is rather small (SH and DHW curves below the Solar Collected curve). A schematic explanation of all the heat power from Figure 14 is given in Figure 15.

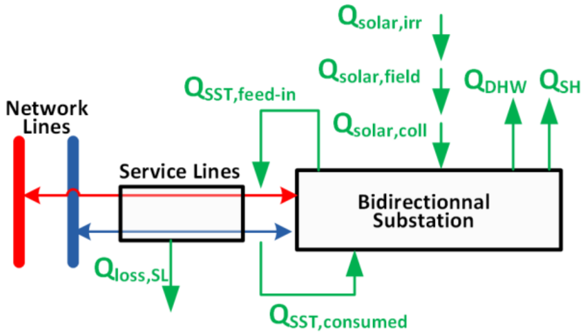

Figure 15: Schematic of the power streams used in Figure 14

4.2 Influence of DHN differential pressure, supply temperature and return temperature

Using the previous simulation as a base case scenario, 3 additional simulations for which respectively the DHN differential pressure was increased by 1bar, the DHN supply temperature was increased by 10°C and the DHN return temperature was reduced by 10°C were performed. Table 2 summarizes the results in terms of energy, using the same nomenclature as Figure 15. The feed-in pump consumption is also calculated. In general, the increase of the differential pressure has only an impact on the feed-in pump consumption while an increase of either the supply or the return temperature will reduce the solar plant production (lower field efficiency and larger heat losses).

Table 3 presents 5 ratios of interest using the energies presented in Table 2. As shown before, both the efficiencies of the solar field ($E_{solar,field}/E_{solar,irr}$) and the plant ($E_{solar,coll}/E_{solar,irr}$) are reduced with an increase of either DHN lines temperature. Additionally, the ratio of the self-consumed solar energy ($E_{solar,coll}$- $E_{loss,SL}$) to the total energy consumed (E_{SH}+E_{DHW}) referred as $\eta_{self\_vs\_cons}$ and to the collected solar energy referred as $\eta_{self\_vs\_solar}$ are rather small when considering that the solar energy produced is larger than the consumed energy. The reinjection is thus primordial in such situation since it transforms the collected solar energy into useful energy (for other DHN users). Finally, the pump ($E_{feed,pump}$) to collected solar energy ($E_{solar,coll}$) referred as $\eta_{pump\_vs\_solar}$ increases with a higher differential pressure and decreases with higher supply and lower return temperature.

Table 2: Sensitivity on DHN operating conditions (unit: kWh)

Case	Base	ΔP+1bar	T_s+10°C	T_r-10°C
$E_{solar,irr}$	760.19	760.19	760.19	760.19
$E_{solar,field}$	361.13	361.09	342.63	372.78
$E_{solar,coll}$	332.74	332.71	310.58	345.04
E_{SH}	194.28	194.42	194.34	194.28
E_{DHW}	74.16	74.78	74.41	74.15
$E_{SST,consumed}$	250.09	250.85	252.16	250.73
$E_{SST,feed-in}$	315.84	316.22	295.14	328.53
$E_{loss,SL}$	89.70	89.81	92.58	85.04
$E_{feed,pump}$	1.05	1.59	0.63	0.73

Table 3: Energy Ratios (unit: %)

Case	Base	ΔP+1bar	T_s+10°C	T_r-10°C
$\eta_{solar,field}$	47.5	47.5	45.1	49.0
$\eta_{solar,plant}$	43.8	43.8	40.9	45.4
$\eta_{self\_vs\_cons}$	6.3	6.1	5.7	6.2
$\eta_{self\_vs\_solar}$	5.1	5.0	5.0	4.8
$\eta_{pump\_vs\_solar}$	0.32	0.48	0.20	0.21

5. CONCLUSIONS

The present paper presented the modelling of a specific architecture of two-way substation together with the solar field and the consumer connected to it. Real DHN operating conditions were used as boundary conditions to dynamically simulate two days of operation. The latter showed that the developed framework was appropriate to perform detailed thermo-hydraulic simulations of such solar two-way substations.

Further steps will include the generalization of these results on seasonal and yearly basis, the simulations of the other promising architectures and the evaluation of the influence of a storage.

ACKOWLEDGEMENTS

This project has received funding from the European Union's Horizon 2020 research and innovation program under grant agreement No 723562. The authors also wish to thank Bosch Thermotechnik GmbH and Giroa-Veolia for their valuable inputs.

REFERENCES

Beckenbauer, D., Ehrenwirth, M., Klärner, M., Zörner, W., Cheng, V., 2017. Validation of a District Heating System Model and Simulation-Based Investigation of Bidirectional Heat Transport by Decentralized Solar Thermal Plants. Presented at the SWC/SHC 2017, Abu Dhabi, UAE.

Brange, L., Englund, J., Lauenburg, P., 2016. Prosumers in district heating networks – A Swedish case study. Appl. Energy 164, 492–500. https://doi.org/10.1016/j.apenergy.2015.12.020

COSTIC, 2016. besoin-eau-chaude-sanitaire-habitat-individuel-et-collectif.pdf (Guide Technique : Les besoins d'eau chaude sanitaire en habitat individuel et collectif).

Giraud, L., Baviere, R., Vallée, M., Paulus, C., 2015. Presentation, Validation and Application of the DistrictHeating Modelica Library. pp. 79–88. https://doi.org/10.3384/ecp1511879

Hassine, I.B., Eicker, U., 2014. Control Aspects of Decentralized Solar Thermal Integration into District Heating Networks. Energy Procedia, Proceedings of the 2nd International Conference on Solar Heating and Cooling for Buildings and Industry (SHC 2013) 48, 1055–1064. https://doi.org/10.1016/j.egypro.2014.02.120

Heymann, M., Rühling, K., Felsmann, C., 2017. Integration of Solar Thermal Systems into District Heating – DH System Simulation. Energy Procedia, 15th International Symposium on District Heating and Cooling, DHC15-2016, 4-7 September 2016, Seoul, South Korea 116, 394–402. https://doi.org/10.1016/j.egypro.2017.05.086

IEA SHC, 2004. Recommendation: Converting solar thermal collector area into installed capacity (m2 to kWth).

Jordan, U., Vajen, K., 2005. DHWcalc: Program to generate domestic hot water profiles with statistical means for user defined conditions, in: ISES Solar World Congress. pp. 1–6.

Lamaison, N., Baviere, R., Cheze, D., Paulus, C., 2017. A multi-criteria analysis of bidirectional solar district heating substation architecture. Presented at the SWC/SHC 2017, Abu Dhabi, UAE.

Lennermo, G., Lauenburg, P., 2016. Distributed heat generation in a district heating system. Presented at the International Conference on Solar-Heating and Cooling, Gleisdorf, Austria.

Lund, H., Werner, S., Wiltshire, R., Svendsen, S., Thorsen, J.E., Hvelplund, F., Mathiesen, B.V., 2014. 4th Generation District Heating (4GDH). Energy 68, 1–11. https://doi.org/10.1016/j.energy.2014.02.089

Meteonorm, 2017. Meteonorm: Irradiation data for every place on Earth [WWW Document]. URL http://www.meteonorm.com/en/ (accessed 7.10.17).

NF EN ISO 9806, 2017.

Paulus, C., Papillon, P., 2014. Substations for Decentralized Solar District Heating: Design, Performance and Energy Cost. Energy Procedia 48, 1076–1085. https://doi.org/10.1016/j.egypro.2014.02.122

Perez, R., Ineichen, P., Seals, R., Michalsky, J., Stewart, R., 1990. Modeling daylight availability and irradiance components from direct and global irradiance. Sol. Energy 44, 271–289. https://doi.org/10.1016/0038-092X(90)90055-H

Rosemann, T., Heymann, M., Rühling, K., Hafner, B., 2017a. DH Networks - Concept, Construction and Measurements Results of a Decentralized Feed-In Substation. Presented at the SWC/SHC 2017, Abu Dhabi, UAE.

Rosemann, T., Löser, J., Rühling, K., 2017b. A New DH Control Algorithm for a Combined Supply and Feed-In Substation and Testing Through Hardware-In-The-Loop. Energy Procedia, 15th International Symposium on District Heating and Cooling, DHC15-2016, 4-7 September 2016, Seoul, South Korea 116, 416–425. https://doi.org/10.1016/j.egypro.2017.05.089

SavoSolar SF500-15DG - Solar Keymark, 2016.

Schäfer, K., Schmidt, T., 2016. Technical challenges for solar thermal plants with decentralized feed-in into district heating networks and deduced plant concept for the experimental feed-in station in the SWD.SOL project. Presented at the 4th International Solar District Heating Conference, Billund, p. 8.

Schweiger, G., Larsson, P.-O., Magnusson, F., Lauenburg, P., Velut, S., 2017. District heating and cooling systems – Framework for Modelica-based simulation and dynamic optimization. Energy. https://doi.org/10.1016/j.energy.2017.05.115

Solar Keymark Database [WWW Document], 2018. URL http://www.solarkeymark.dk/CollectorCertificates (accessed 3.22.18).

Wetter, M., Fuchs, M., Grozman, P., Helsen, L., Jorissen, F., Lauster, M., Dirk, M., Nytsch-geusen, C., Picard, D., Sahlin, P., Thorade, M., 2015. IEA EBC Annex 60 Modelica library an international collaboration to develop a free open-source model library for buildings and community energy systems. Presented at the BS2015, pp. 395–402.

Wetter, M., Zuo, W., Nouidui, T.S., 2011. Modeling of heat transfer in rooms in the Modelica" Buildings" library. Lawrence Berkeley National Lab.(LBNL), Berkeley, CA (United States).

Wetter, M., Zuo, W., Nouidui, T.S., Pang, X., 2014. Modelica Buildings Library. J. Build. Perform. Simul. 7, 253–270.

CONCEPT, CONSTRUCTION AND MEASUREMENT RESULTS OF A DECENTRALIZED FEED-IN SUBSTATION

Martin Heymann, Toni Rosemann, Karin Rühling
Institute of Power Engineering, Professorship of Building Energy Systems and Heat Supply,
Technische Universität Dresden, Dresden, 01062, Germany, +49-351 / 463-34709,
martin.heymann@tu-dresden.de

Bernd Hafner
Viessmann Werke GmbH & Co. KG,
+49-6452-701583; drhf@viessmann.com

Abstract – This paper presents the concept and measurement results of a solar thermal pilot plant for decentralized feed-in into a 2nd generation district heating network. Ambitious conditions for both target temperature level and pressure difference are fulfilled by a return to supply line feed-in (RL/SL) design. The use of water as solar liquid requires an active frost protection using the district heating network. The measurement results include two frost protection seasons and one feed-in season.

1. INTRODUCTION

Decentralized feed-in of solar thermal gains can contribute to the decarbonisation and flexibilisation of modern district heating networks (e.g. Heymann, et. al., 2017). The development of standards concerning network feed-in substations and their control concepts are the research goals of the ongoing project “Kostenreduktions-potential beim Ausbau der Solarisierung von Fernwärme-netzen durch Standardisierung”[1]. These standards are derived from practical experiences by designing, commissioning and operating pilot plants – including the solar thermal system and the substation itself – as well as simulation studies.

This paper presents the design and control concept of a pilot plant which is in regular operation at the Centre for Energy Technology (CET) in Dresden since November 2016 (see Figure 1). The network feed-in substation is connected to a 2nd generation network (according to IEA DHC Annex X classification) and was developed in cooperation with the local network operator as part of a feasibility study for larger collector fields. The pilot plant is designed for the RL/SL feed-in into the district heating network - the most common and variable way of decentralized network integration.

Detailed measurement results consider two of three main operation modes of the network feed-in substation:

- *Feed-in* of solar energy,
- *Stagnation* (see Rosemann, et.al. 2017b) and
- Active *Frost Protection* of the water-based solar circuit.

[1]Founded by Federal Ministry for Economic Affairs and Energy FKZ 0325553A.

2. CONCEPT OF THE DISTRICT HEATING NETWORK FEED-IN SUBSTATION

The pilot plant is connected to the primary district heating network of the city with a nominal pressure stage of PN25 and a nominal target feed-in temperature of 110 °C. Therefore solar vacuum tube collectors working according to the heat pipe principle are used in the collector field (CF). The collector field, consisting of six subfields C1..C6 connected in series, has a total gross area of 84 m² (total aperture area 48 m²) and an inclination of about 31° facing south. The design heat flow rate is 30 kW based on a total incline irradiance $G_{t,i}$= 1000 W/m² and collector field temperatures of 115/70 °C.

The circulation pump in the solar circuit Pu_{STS} is a speed-controlled pump group where only one pump is used in main operation at a time and where the other pump is hold as a spare component. The redundancy will be important to guarantee the functionality of frost protection for big collector fields. The compressor-based pressure maintenance is connected to the system in the supply line of the collector field with an integrated stagnation cooler. This cooler is built as a finned tube radiator which limits the maximum steam spread in case of stagnation, reduces the design volume of the common additional auxiliary vessel and thereby the design volume of the pressure maintenance expansion vessel.

The speed-controlled feed-in pump $Pu_{DH,F}$ is necessary to overcome the pressure difference Δp_{DH} in the DH network and generates the feed-in volume flow. The proper selection of this component is essential to assure the feed-in of the solar yields into the network. This is often complicated due to the lack of information about Δp_{DH}, $T_{SL,DH}$ and $T_{RL,DH}$ at the feed-in point for the course of the year and the future development of these values. The bypass valve Va1 will be opened before feed-in to

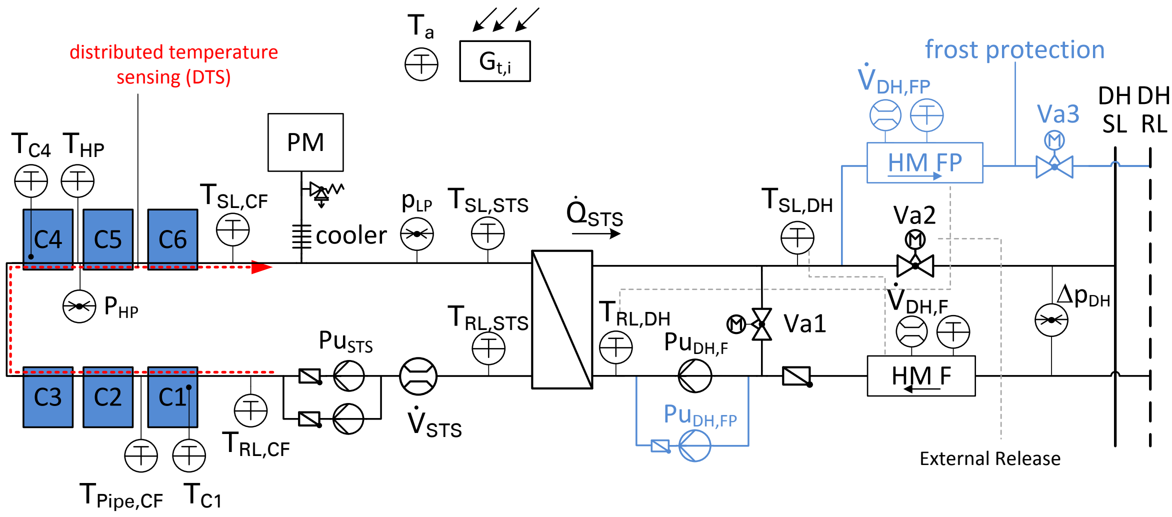

Figure 1: Schematic of the feed-in substation (Ta – ambient temperature, C – collector, CF – collector field, DH – district heating, HM – heat meter, F – feed-in, FP – frost protection, HP – highest point, LP – lowest point, PM – pressure maintenance, Pu – pump, Va – valve, STS – solar thermal system)

heat up the medium in the district heating side of the substation to prevent cold plugs in the network, but will be closed during feed-in. The valve Va2 is used to realize an external unblocking. If necessary the network operators can withdraw the release signal and prevent/stop the feed-in by closing the valve and power off the pumps. The valves Va2 and Va3 are used to switch the flow direction between RL/SL in the state *Feed-in* (Va2 open, Va3 closed) and RL/RL for heating the STS in the state *Frost Protection* (Va2 closed, Va3 open). A separate frost protection pump $Pu_{DH,FP}$ is used because of different design parameter for the RL/RL frost protection heating (low discharge head) and due to redundancy.

A minimum sensor equipment is necessary for the plant operation. It consists of five temperature sensors ($T_{SL,CF}$ $T_{SL,STS}$ $T_{RL,CF}$ and $T_{SL,DH}$, T_a), the radiation sensor $G_{t,i}$ as well as two heat meters. The heat meter HM F measures the heat fed into the network. The volume flow signal $\dot{V}_{DH,F}$ of the feed-in heat meter is used for a control loop by an analogue module. There is a second heat meter HM FP, which measures the heat required for frost protection. These two separate heat meters are necessary as long as no bidirectional heat meter is available on the market that is certified for billing.

The monitoring package consists of additional temperature sensors, three pressure sensors (p_{HP}, p_{LP}, Δp_{DH}), a flow meter $\dot{V}_{STS}$, as well as a distributed temperature sensing system (DTS see Herwig, Rühling, 2014). The DTS uses an optical sensor cable, which is attached to the collector pipe of the system in order to measure the temperature distribution with a high spatial and time resolution. This is helpful for detailed analysis of the states *Frost Protection* and *Stagnation*.

3. STATE FEED-IN

3.1 Controller

In order to operate the network feed-in substation in the *Feed-in* state a set of three controllers is used (see Table 1). The controller C1 is used for the matched-flow control of the collector field output temperature $T_{SL,CF}$ by adapting the pump speed of Pu_{STS}. This controller compensates changes mainly in the radiation $G_{t,i}$ and the return line temperature $T_{RL,STS}$. The objective is to keep the heat exchanger input temperature $T_{SL,STS}$ higher than the setpoint of the feed-in temperature $T_{SL,DH}$ – to guarantee heat transfer – and to keep the average temperature of the solar thermal system low to minimize losses.

The two general main tasks of controlling the feed-in pump $Pu_{DH,F}$ are:

Table 1: Closed-loop PI-controllers for state Feed-in

Name	*Control variable*	*Setpoint*	*Output*
C1	$T_{SL,CF}$	115..120°C	speed Pu_{STS}
C21	$T_{SL,DH}$	110°C	setpoint C22
C22	$\dot{V}_{DH,F}$	results from control signal of	speed $Pu_{DH,F}$

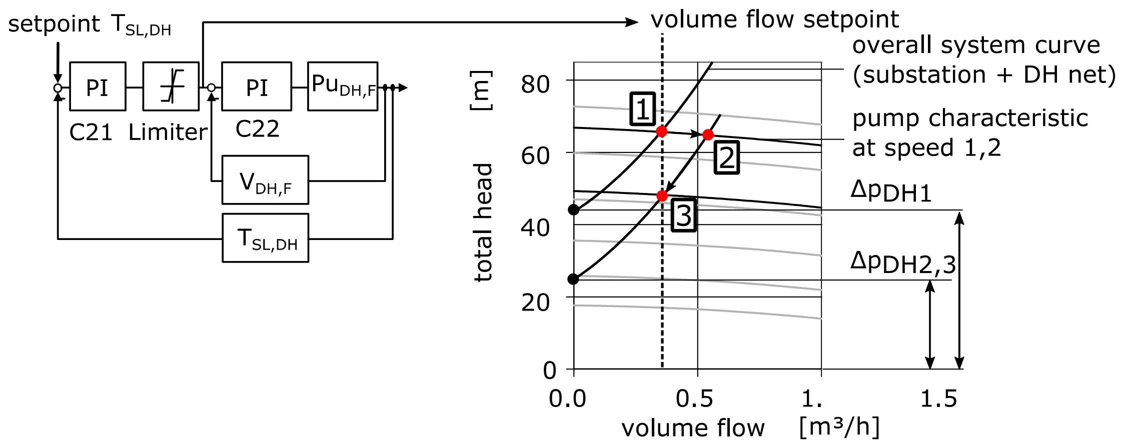

Figure 2: Left: Cascade controller for the feed-in temperature $T_{SL,DH}$,
Right: Characteristic curves of the feed-in pump $Pu_{DH,F}$ and the operation points 1..3 during the control action of C22 reacting on a step of ΔpDH
(1 – Starting point, 2 – after step of Δp_{DH} without reaction of C22, 3 – final stage after correction of the pump speed)

- to guarantee a stable volume flow $\dot{V}_{DH}$ despite the strongly changing pressure difference of the network Δp_{DH} but corresponding to the current solar yields and
- to operate with minimal power consumption.

A cascaded controller is used (see Figure 2 left) to achieve both tasks. The temperature controller C21 finds a solution for Equation (1) by adjusting the volume flow setpoint $\dot{V}_{SP}$ of the controller C22 and thereby the volume flow $\dot{V}_{DH}$. The inner controller compensates any change of the pressure difference of the network $\Delta p_{DH.}$ This is energetic efficient, because the pump speed is changed to manipulate $\dot{V}_{DH}$ directly instead of using a throttling or bypass valve. The volume flow signal of the heat meter HM F can be used directly e.g. through an additional analogue module, depending on the kind of heat meter and the achievable update interval. The tested substation works well when controllers are updated every four seconds.

$$T_{SP} = T_{SL,DH} = \frac{\dot{V}_{SP} \cdot \varrho \cdot c_p}{\dot{Q}_{STS}} + T_{RL,DH} \qquad (1)$$

with T_{SP} .. setpoint for $T_{SL,DH}$, $\dot{V}_{SP}$ .. setpoint for $\dot{V}_{DH}$

The compensation of the variable pressure difference Δp_{DH} by using the volume flow controller C22 (see Figure 2 right) is realized in three steps:

1. The setpoint volume flow is reached at the actual pressure difference $\Delta p_{DH,1}$ (steady state)
2. The volume flow $\dot{V}_{DH}$ differs from the setpoint as a result of the disturbing pressure difference $\Delta p_{DH,23}$. The feed-in temperature $T_{SL,DH}$ will differ from its setpoint as well. (instationary)
3. The controller C22 compensates the pressure difference variation and the feed-in temperature will not be affected. (stationary)

The volume flow signal $\dot{V}_{DH}$ of the HM F can also be used to find the right pump speed to overcome the pressure difference Δp_{DH} when the feed-in starts (Rosemann, et. al., 2017a). The integration of this signal into the plant control as described above is recommended because of the low additional costs for reading out this signal and the high advantages for solving the common technical pressure difference Δp_{DH} problems in district heating networks (Lennermo and Lauenburg, 2015).

3.2 State Machine

For the correct operation of a district heating network feed-in substation, the controller and actuators of the plant have to be de-/activated and set to corresponding values at the right moment. This task is solved with a state machine (see Figure 3). A state is a set of actor and controller settings which structures the operation of the plant into sequential steps. The entry point of the state machine is "Start". There is always only one active state. The active state checks the criteria pointing to the connected states and starts a transition if the logical expression of all criteria is true. Global states are special states that always check their entry criteria because of their high priority, which is used e.g. for safety technology. States can consist of sub-states. This is used to cluster states to visualize their coherence (e.g. to heat up the solar thermal system is always a part of the feed-in).

A criterion is based on measurements of physical values and durations. A duration can be based on a physical criterion (additional time criterion, "How long is a physical condition met") or on the active time of a state (τ_{State}, "How long is a state active"). The parameters of the criteria depend on the concrete plant and its constraints.

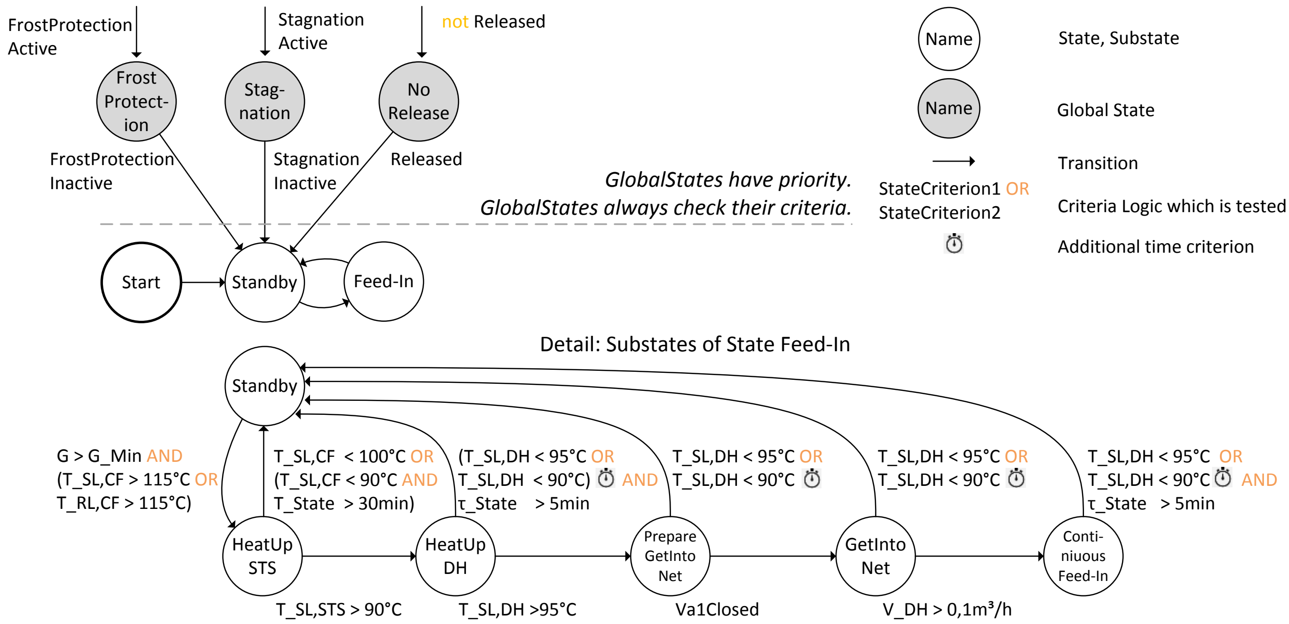

Figure 3: State diagram of the net feed-in substation with detailed sub-states of the state Feed-in
Released – External release signal is true and feed-in allowed
G_Min – minimal radiation threshold calculated on basis of the collector curve
The criteria for Stagnation and Frost protection are discussed in the corresponding section.

3.3 Measurement results

The exemplary measurement results of the state *Feed-in* (see Figure 4) start at 8:00 of 22th of June and end at 18:00 with an average radiation of 530 W m^{-2} and an average ambient temperature of 31 °C.

The plant is operated according to the state machine described above with the substates from Table 2. In the morning, the system starts in *Standby* until $T_{CF,SL}$ or $T_{CF,RL}$ exceeds 115 °C. The collector field return line temperature $T_{RL,CF}$ is remarkable higher than the collector field supply line temperature mainly due to shading of C6. From 9:20 to 10:00 the active state falls back to *Standby*. The fallback is triggered by the low solar thermal supply line temperature $T_{SL,CF}$ < 90 °C criterion. This undesired behavior sometimes happens due to mentioned collector temperature variation during the heat up and is a specialty of the collector field design of the pilot plant. After reaching the state *HeatUpSTS* again the hot medium is transported to the heat exchanger and the district heating side gets heated up. During the *Continuous Feed-in* from 11:20 to 17:10 three different disturbances occur, which are well compensated. $T_{SL,DH}$ very accurately reaches its dynamic setpoint:

Table 2: Description of the substates for the state Feed-in and controller activity (○ – inactive, ● - active)

State	Description	C1	C21	C22
Standby	Default State with no activity of the plant (night, cloudy day, winter day)	○	○	○
HeatUpSTS	When high temperatures are detected in the collector field, Pu_{STS} is activated and the hot fluid is moved into the network feed-in substation.	●	○	○
HeatUpDH	When the hot plug reaches the heat exchanger, the district heating side of the network feed-in substation is heated up by opening the bypass valve Va1 and starting the feed-in pump $Pu_{DH,F}$.	●	○	○
PrepareGetIntoNet	The bypass valve Va1 is closed.	●	○	○
GetIntoNet	The pump speed $Pu_{DH,F}$ rises until a volume flow $\dot{V}_{DH}$ is detected.	●	○	●
ContinuousFeed-In	Hot water heated by the collector field is fed into the district heating network	●	●	●

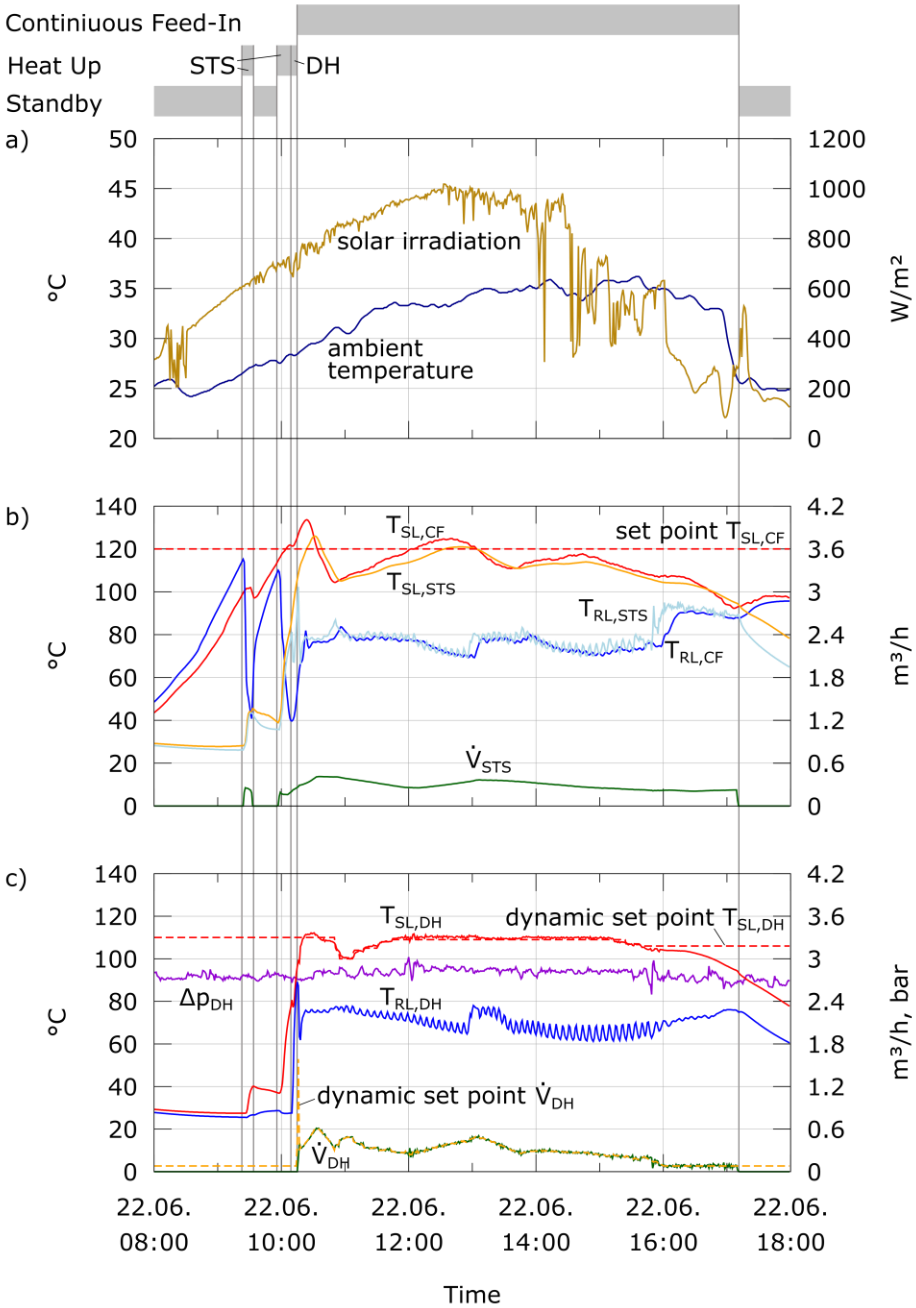

Figure 4: Measurement data for state Feed-in,
a) ambient, b) solar system, c) district heating side

- 12:00, 15:50 – Peaks in the pressure difference Δp_{DH} are compensated by the pump speed adaption of the controller C22.
- 13:30 - The rising of the return line temperature $T_{RL,DH}$ by 10 K is compensated with a higher volume flow $\dot{V}_{DH}$ by the controller C21.
- 14:30 – The radiation starts to drop caused by clouds. The solar volume flow $\dot{V}_{STS}$ is reduced by the controller C1. The high thermal capacity of the collector and the medium as well reduces the sensitivity to radiation disturbances.

The continuous volatility of the district heating return line temperature $T_{RL,DH}$ is caused by the periodic opening and closing of the control valve of a district heating substation located in the long stub pipe to the district heating network.

In the evening the feed-in temperature $T_{SL,DH}$ falls below 95 °C and the feed-in is stopped by falling back to *Standby*. During the day 82 kWh solar thermal energy where fed into the district heating network mainly at the desired feed-in temperature of 110 °C. The current amount of heat fed into the network from January to September 2017 – without final optimization of the state machine and controller – is 8.556 kWh.

Table 3: Tested criteria for the de-/activation of the state Frost protection (○ – on, ● - off, | - “or”, & - “and”)

Name	Frost protection	Criteria	Pump activity	
			Pu_{STS}	$Pu_{DH,FP}$
5 °C, 13min	Enter	$(T_{SL,CF} \mid T_{RL,CF} \mid T_{Pipe,CF} \mid T_{HP}) < 5$ °C	●	●
	Exit	$(T_{SL,CF}$ & $T_{RL,CF}$ & $T_{Pipe,CF}$ & $T_{HP}) > 10$ °C AND RUNTIME $Pu_{STS} > 13$ min	○	○
5 °C, 13min, CS	Enter	$(T_{SL,CF} \mid T_{RL,CF} \mid T_{Pipe,CF} \mid T_{HP} \mid T_{C1} \mid T_{C4}) < 5$ °C	●	●
	Exit	$(T_{SL,CF}$ & $T_{RL,CF}$ & $T_{Pipe,CF}$ & T_{HP} & T_{C1} & $T_{C4}) > 10$ °C AND RUNTIME $Pu_{STS} > 13$ min	○	○

4. STATE ACTIVE FROST PROTECTION

Controller and State Machine

The frost protection has to prevent all parts of the installation from cooling down to a temperature near the melting point of the solar liquid. To achieve this, a lower limit for the medium temperature in the solar system of 5 °C is defined. If any of the temperature criteria goes below this threshold, the state *Frost Protection* is activated. This state is defined as a global and is checked in every iteration.

If activated, heating water from the district heating return line flows through the district heating side of the station and back to the return line via the frost protection branch with the heat meter. The separate pump $Pu_{DH,FP}$ (see Figure 1), which is installed in parallel to the feed-in pump $Pu_{DH,F}$, is used for this issue. The frost protection stops and returns to the *Standby* state, when all observed sensors exceed the upper threshold value of 10 °C and a minimum runtime is reached.

The tested variants concerning the details of the state *Frost Protection* made during winter season 2016/2017 and 2017/18 are shown in Table 3. First tests were done with the activation of the pumps when any of the collector field temperatures falls below the lower limit. These temperatures are reported by sensors installed in the piping of the supply and return line ($T_{SL,CF}$ $T_{RL,CF}$) and sensors in the connection pipes of the collector field (T_{HP}, $T_{Pipe,CF}$). The pumps are stopped if all measured temperatures go above the upper threshold. It has been shown, that a minimum runtime of 13 min is necessary to assure at least one turn of the fluid through the solar thermal system. Furthermore detailed evaluations using the DTS showed that under some conditions the collectors cool down faster than the piping of the collector field (see

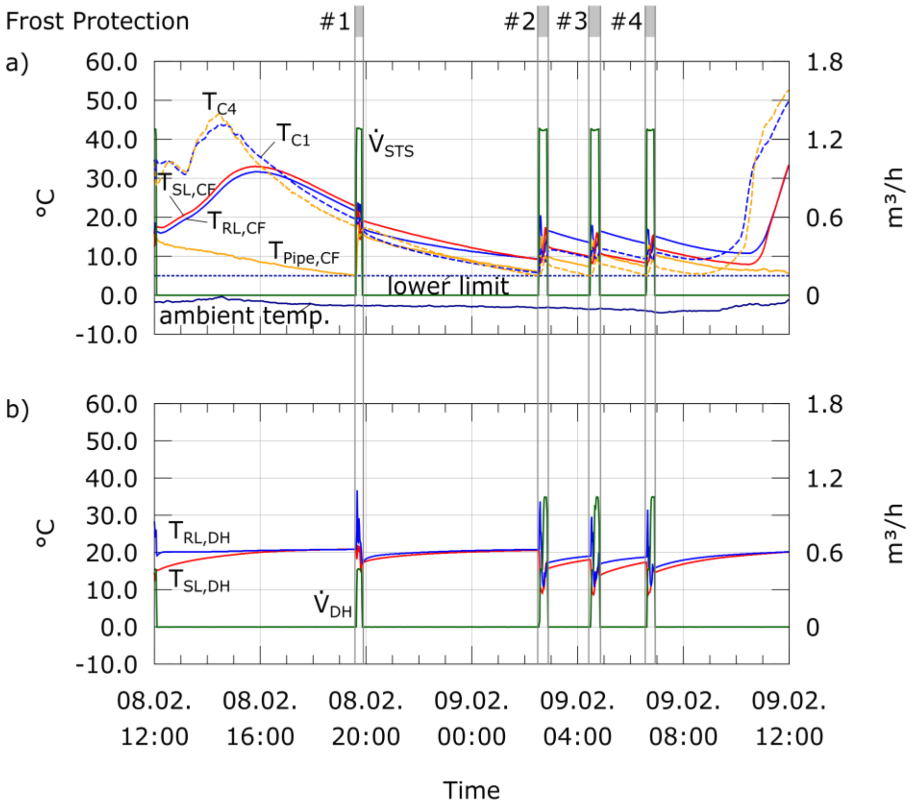

Figure 5: Measurement data for state Frost Protection, a) solar system, b) district heating side

Rosemann, et. al., 2017b). Therefore two collector sensors CS (T_{C1}, T_{C4}) had been included in the scanning routine to detect low medium temperature within the collectors.

4.2 Measurement results

In Figure 5 the measurement data for the operation of the frost protection using the latest level of development are shown (5°C, 13min, CS). The measurement period starts at midday of the 8th of February and ends at midday the day after. The average ambient temperature was -2.7 °C, at minimum -4.7 °C and the sky was clouded. The upper chart illustrates temperature profiles gained from the sensors of the solar thermal system and the collector field. The lower chart contains the temperature values on the district heating side.

The temperatures in the collector field increase in the afternoon due to solar gains and are dropping constantly afterwards. The solar gains only effect the sensors located directly next to the collectors. The temperature in the 25 m long connection pipe between C1 and C2 $T_{Pipe,CF}$ is not raised. At 19:50 $T_{Pipe,CF}$ triggers the first frost protection period (#1). All other frost protection periods (#2 to #4) are triggered by the collector sensor T_{C4}.

The solar pump operates at its maximum speed ($\dot{V}_{STS}$) when the state *Frost Protection* is active. The volume flow on the district heating side $\dot{V}_{DH}$ is controlled in order to reach a supply line temperature of 20 °C in the solar circuit. The temperatures on the district heating side $T_{RL,DH}$ and $T_{SL,DH}$ are very low, almost at room temperature.

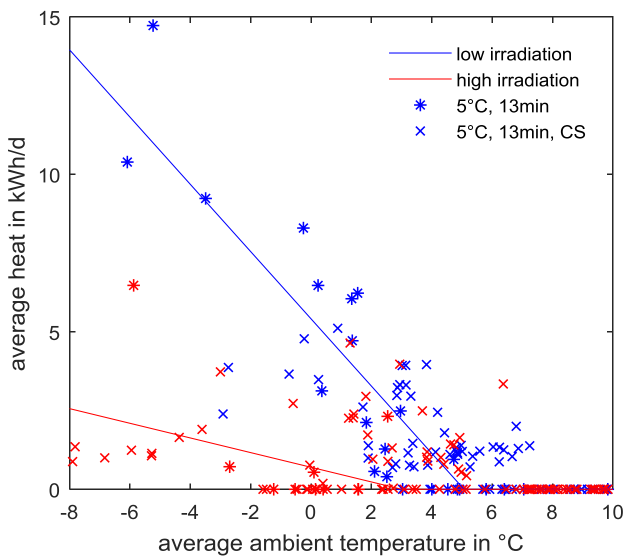

Figure 6: Statistical evaluation of the frost protection season in winter 2016/17 and 2017/18, daily average, low irradiation < 1,2 kWh/(m² d) in collector plane ≤ high irradiation

The solar thermal plant is connected to the district heating network via a long stub pipe. In the presented time period the connected consumers have no heat demand and the return line cools down. The frost protection can be guaranteed anyway, because it's little heat demand and the big transfer surface of the heat exchanger. Overall a heat demand for the frost protection of 4 kWh was measured at that day.

Figure 6 shows the daily heat demand for the frost protection over the daily ambient temperature for two winter seasons. Days with a relatively high irradiation (> 1,2 kWh/m² in collector plane) are colored red, others blue. As expected the heat demand for frost protection increases with decreasing ambient temperatures. This demand is clearly reduced at days with high solar gains. The frost protection starts at daily average ambient temperatures of about 3 to 5 °C. The heat demand can go up to 14 kWh per day at very cold and cloudy days with daily average ambient temperatures under -5 °C.

The heat demand added up to 380 kWh for the whole winter season, which is about 2 – 3% of the annual heat output fed into the district heating system. This is in the range of known plants with active frost protection.

5. CONCLUSIONS/PROSPECTS

The planning of the pilot plant, the realization and the operating experience of one and a half year have already provided valuable information which can be used for standardization of decentralized feed-in substations. There is a need for clarification with the district heating companies regarding the control accuracy of the feed-in temperatures. A high control accuracy of the feed-in temperature always is reached at the expense of a higher variation of the feed-in volume flow and vice versa. For solar thermal systems, a higher temperature tolerance especially in the morning during heat up or during phases of clouds would ease the general operation. Especially for district heating systems with a crucial solar fraction a high variation of the feed-in volume flow can cause hydraulic problems and interference.

The use of water as solar liquid is feasible with an active frost protection in the winter season. It is necessary to take the different cooling behavior of the collectors and the piping into consideration. A well designed separate stagnation cooler combined with a small additional auxiliary vessel can safely limit the steam spread and protect the membrane of the expansion vessel. This combination can reduce the design volume of the expansion vessel thus reduce investment costs.

Solar thermal gain prognoses will be possible after the validation of a simulation model for the decentralized solar thermal feed-in substations. It is intended to make simulations studies regarding the generalization of the current control concept (state machine). The commissioning of a combined supply and feed-in substation connected to a low temperature district heating network in Berlin Adlershof[2] is in progress. This will extent the monitoring portfolio of the research project.

REFERENCES

Lennermo, G., Lauenburg, P., 2015. Variation in Differential Pressure at a District Heating Prosumer Substation, 3nd International Solar District Heating Conference, Toulouse

Herwig, A., Rühling, K., 2014. Fiber-Optic Distributed Temperature Sensing Of Large Hot Water Storage Tanks. 15th International Symposium on District Heating and Cooling, Stockholm

Heymann, M., Rühling, K., Felsmann, C., 2017. Integration of Solar Thermal Systems into District Heating – DH System Simulation, Energy Procedia, 116, Seoul doi:https://doi.org/10.1016/j.egypro.2017.05.086

Rosa, A. D., Li, H., Svendsen, S., Werner, S., Persson, U., Rühling, K., Felsmann, C., Crane, M., Burzynski, R. and Bevilacqua, C. 2014. Annex X Final Report: Toward 4th Generation District Heating, Tech. rep., IEA DHC|CHP

Rosemann, T., Löser, J., Rühling, K., 2017a. A New DH Control Algorithm for a Combined Supply and Feed-In Substation and Testing Through Hardware-In-The-Loop, Energy Procedia, 116, 416-425. doi:https://doi.org/10.1016/j.egypro.2017.05.089

Rosemann, T., Heymann, M., Rühling, K., Hafner, B., 2017b. DH Networks - Concept, Construction and Measurement Results of a Decentralized Feed-In Substation, International Conference on Solar Heating and Cooling for Buildings and Industry

APPENDIX: UNITS AND SYMBOLS

Table 4: Symbols

Quantity	Symbol	Unit
Area	A	m^2
Global irradiance or solar flux density	G	$W\ m^{-2}$
System mass	m	kg
Mass flow rate	$\dot{m}$	$kg\ s^{-1}$
Pressure (absolute)	p	bar
Pressure difference	Δp	bar
Heat	Q	kWh
Heat flow rate	$\dot{Q}$	kW
Temperature	T	°C
Efficiency	η	
Time	τ	s

Table 5: Abbreviations and subscripts

Quantity	Symbol
Ambient	a
Collector	Col
Collector field	CF
Collector sensor	CS
District heating	DH
Feed-in	F
Frost protection	FP
Heat meter	HM
Highest point in system	HP
Lowest point in system	LP
Network feed-in Substation	NFS
Pressure maintenance	PM
Pump	Pu
Return line	RL
Valve	Va
Solar thermal system	STS
Supply line	SL

[2] Founded by Federal Ministry for Economic Affairs and Energy FKZ 03ET1155B.

Solar thermal prosumer in Lodi District Heating network

Marco Calderoni, Alice Dénarié
Department of Energy, Politecnico di Milano, via Lambruschini, 4, Milano, 20156, Italy,
+39 02 2399 3931, marco.calderoni@polimi.it
Andrea Barcellesi
Linea Reti e Impianti srl, viale Trento e Trieste 38, Cremona, 26100, Italy
+39 0372 4181, a.barcellesi@linea-ri.it

Abstract – District Heating is acknowledged as an infrastructure which can exploit local heat sources by collecting heat where it is available and transporting it where it is needed. This opens doors to the birth of heat prosumers, a well-known concept in the power sector. The case of Lodi, a 45.000 inhabitants' city 30 km from Milano, offers an exemplary case study in this regard.
After connecting a sport centre to the local district heating network, Linea Reti Impianti [1], the district heating network operator of Lodi, proposed the integration in the network of the solar thermal plant installed on the roof of the pool building, collecting all available solar heat. This connection has a twofold benefit: from the point of view of Linea Reti Impianti, an additional heat source is available – small in quantitative terms, but valuable in qualitative terms, solar heat being 100% renewable; from the perspective of the solar plant, a relatively high demand is constantly available, thus improving efficiency and avoiding stagnation in the collectors. The present article shows the results of technical investigations on the hydraulic connection and on the adopted control strategy, leading to the proposal for an improved control logic.

1. INTRODUCTION

Lodi district heating (DH) network, operated by Linea Reti e Impianti (LRI), serves almost 200 buildings, corresponding to approximately 2,5 Mm^3 of heated volume. The 25 km piping transports some 60 GWh per year, mixing several energy sources: natural gas, CHP, biomass and, since 2017, also solar thermal energy. The solar heat is produced by a 192 m^2 solar thermal system, owned by Sporting Lodi [2], a public-private company operating the local sport centre, which includes a large swimming pool.

Before the sport centre was connected to the DH network, the pool has undergone major changes. Due to these changes, the solar plants has come out to be oversized with respect to the new building configuration in recent years. Therefore, efficiency of the solar thermal plant has been very low. The decision by LRI to connect the solar plant to the DH network, thus benefitting from excess heat to feed in the network, resulted in a better exploitation of the solar thermal plant; nevertheless monitoring data showed a relatively low energy yield.

This article describes the analysis carried out by Politecnico di Milano, in cooperation with LRI, aimed at improving solar energy yield.

2. INTEGRATION OF THE SOLAR THERMAL PLANT IN THE DH NETWORK

2.1 General information

Hydraulic integration is shown in Figure 1. The DH substation is connected to the secondary loop (intermediate loop) of the solar thermal plant. No storage is present in the solar loop, so the connection between solar plant and DH network is direct [3] . The two heat exchangers (HX1 and HX2), on the left side of the picture, connect the demand (pool heating above, domestic hot water below) to DH. On the DH side of these two HXs, two flow meters and two electro-mechanic valves are installed (M_{pool} and M_{DHW}): according to the amount of energy required on the demand side, valves open or close, thus varying the amount of DH water entering HX1 and HX2.

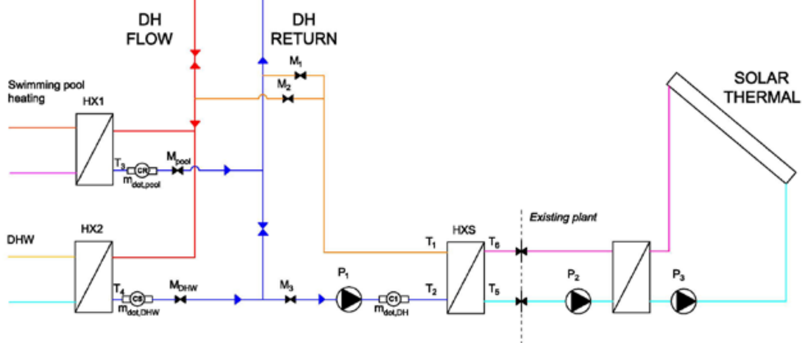

Figure 1 Integration of ST plant in the DH network

Main characteristics of the solar plant are listed in **Table 1**.

Component	Size	Unit	Comments
Solar collectors	9,6	m^2	Aperture area Model Big Sol 10,5
Solar aperture area	192	m^2	20 collectors
Solar gross area	210	m^2	20 collectors
Collectors slope	40	°	
Collectors azimuth	9	°	
Storage	No storage	-	
Pipe length	140 + 140 (supply + return)	m	Due to the construction of a new pool, connection required long piping
Primary loop flow-rate	17	$l/(m^2\ h)$	Low-flow mode

Table 1 Main characteristics of the solar plant

2.2 Control strategy

Control strategy is based on parameters listed in **Table 2**.

Measured parameter	Short name
Flow rate pool heating on DH side of HX1	$m_{dot,pool}$
Flow rate DHW heating on DH side of HX2	$m_{dot,DHW}$
Inlet temperature pool heating on DH side of HX1	$T_{s,pool}$
Outlet temperature pool heating on DH side of HX1	$T_{r,pool}$
Inlet temperature DHW heating on DH side of HX2	$T_{s,DHW}$
Outlet temperature DHW heating on DH side of HX2	$T_{r,DHW}$
Flow rate DH side of HXS	$m_{dot,DH}$
Inlet temperature on DH side of HXS	T2
Outlet temperature on DH side of HXS	T1
Inlet temperature on intermediate loop side of HXS	T6
Outlet temperature on intermediate loop side of HXS	T5

Table 2: Main characteristics of the solar plant

Control strategy A (50°C < T6 < 75°C)

Flow meters measure the flow rates in HX1 and HX2 and enable the control system to consequently set pump P1 velocity (given that solar heat is available, that is when T6 > 50°C) so as to meet the sum of the two flow rates. P1 pushes DH water inside the HXS, where it is heated according to the amount of available solar heat. If T1 is lower than 75°C, water flows finally into the DH return pipe.

In case solar irradiation is too low (T6 < 50°C), P1 does not start and DH water flows directly into the DH return pipe, bypassing HXS.

In brief, if 50°C < T6 < 75°C:

$m_{dot,p1} = m_{dot,pool} + m_{dot,DHW}$

M2 close, M1 open

Control strategy B (T6 > 75°C)

P1 runs at nominal velocity, that is 8 m^3/h. If the flow rate generated by P1 is lower than the sum of the demand (HX1 and HX2), all solar heat is self-consumed and the amount of energy needed to match the demand is collected from the DH supply pipe. Contrariwise, if P1 flow rate is higher than the demand, additional water is collected from the DH return pipe, heated in HXS and conveyed to the DH supply pipe.

In brief, if T6 > 75°C:

$m_{dot,DH} = 8\ m^3/h$

M2 open, M1 close

3. SYSTEM OPERATION DURING THE FIRST YEAR

LRI has been monitoring some parameters related to the heat demand and to the solar plant since its installation in March, 2017.

Figure 2 Solar collectors in the installation phase

Due to a first commissioning period, monitoring data can be considered useful for validating the simulation model starting from 15.05.2017.

Elaboration of monitoring data enabled to quantify the amount of energy delivered from the solar heat exchanger to the DH network (as explained above, part of such energy is directly used for swimming pool heating and DHW heating, while the other part flows in the DH supply pipe).

With regard to meteorological data, solar irradiation on horizontal and ambient temperature measured in 2017 have been obtained from Lombardy region's environmental protection agency (ARPA) [4].

During the period 15/05/2017-15/06/2017, when good quality monitoring data was available, the solar system delivered to the DH network 13.600 kWh, corresponding to an overall efficiency of 33%. Figure 3 shows five days monitoring.

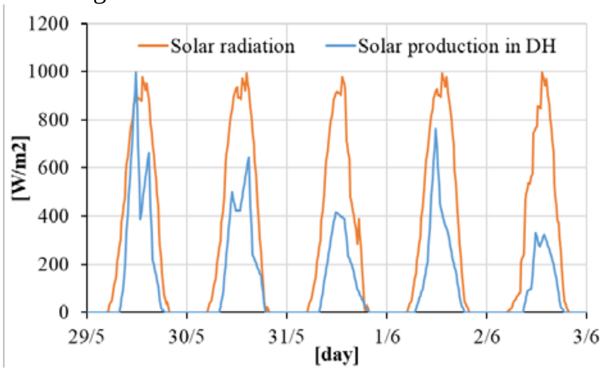

Figure 3 Solar radiation and energy integration in DH

Efficiency is lowered by the significant losses along the long connection pipes, which cause almost 10% losses. Looking at monitoring data in detail, it is quite evident that T5, that is the outlet temperature from HXS in the intermediate loop between solar plant and DH network, is relatively high, even if the solar plant is operated in low-flow regime, as.Figure 4 shows. This is a consequence of the control strategy, which in case "B", when the user flows are quite low, it collects relatively hot water from the DH return pipe, mixes it with return water from HX1 and HX2 and sends it to the HXS.

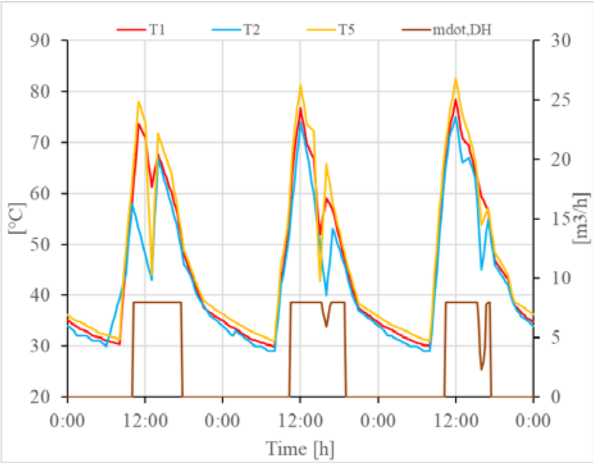

Figure 4 Monitoring data of heat exchanger HXS

LRI actually chose such control strategy aiming at maximising the flow rate in HXS when the demand is low, thus cooling the solar loop as much as possible, in order to avoid stagnation. Due to the fact that DH return water is high, though, the result turns out to be sub-optimal, leading to return high temperatures in the intermediate loop and, consequently to low collectors' efficiency.

The fact that T5 is high is likely to be the main reason for relatively low plant efficiency. In order to verify this assumption a simulation model in TRNSYS [5] has been set-up and validated in order to try an optimised control strategy and evaluate its impact on plant's efficiency.

4. VALIDATION OF THE SIMULATION MODEL AND IMPROVEMENT VIA OPTIMISED CONTROL STRATEGY

For validating the TRNSYS simulation model the same monitoring interval (15/06/2017 to 15/07/2017) was used. LRI stated that during this time frame control strategy B was in place and the simulation model has been set accordingly. Thanks to monitoring data and some components data sheet, the unknown parameters characterising simulation have been regressively estimated such as thermal conductivity of insulated pipes, dead bands in solar control system and aging of the collectors. Simulation's inputs and outputs are listed here:

Input data

$m_{dot,pool}$, $m_{dot,DHW}$, $m_{dot,DHW}$

T2, T3, T4

Solar radiation and ambient temperature

Output data - validation

HXS energy delivery

T1, T5

P1 control strategy

Simulation results showed a solar energy delivery to the DH network of 12.700 kWh, resulting in an error of 7%. Such accuracy was considered satisfactory for the scope of the study, but required some further investigation to make sure not only the overall energy delivery, but also temperature profiles are actually matching. For this purpose, the monitored values of flow temperature exiting the HXS, T_1, has been compared with the simulated one. Results for 3 days are shown in Figure 5.

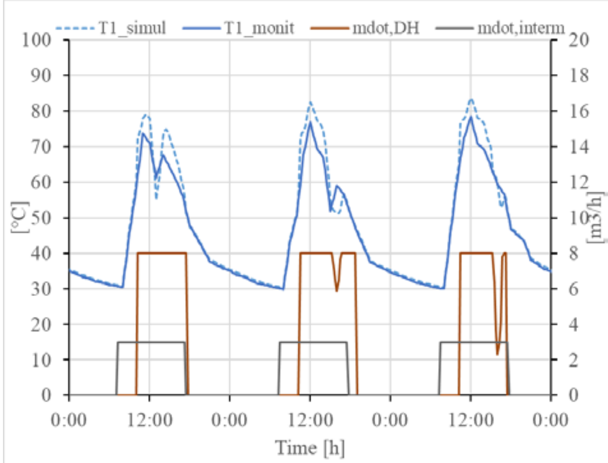

Figure 5 Monitoring data vs simulation results of DH supply temperature

There is a good match between monitored and simulated values. It can be also observed that switch-on and switch-off of solar pump P2 and DH pump P1 match in the simulation model (grey and brown curves): P2 start is followed with some delay by P1 start, as the intermediate solar loop needs to be heated up before it can supply heat to the DH network.

The good match between temperatures confirmed that the simulation model is providing reliable results and can therefore be used to simulate the effect of changes in the control strategy.

After validating the simulation model, an improved control strategy was applied in order to verify the room for improvement with a zero-cost measure. Such improvement of control strategy “B” consists of reducing the flow rate m_{dot_DH}, matching it to the flow-rate in the demand-side HXs HX1 and HX2, as happens in strategy “A”. In this way no hot water from the DH return pipe is mixed to the flow exiting HX1 and HX2, resulting in lower input temperature in HXS and, consequently, in higher collectors’ efficiency.

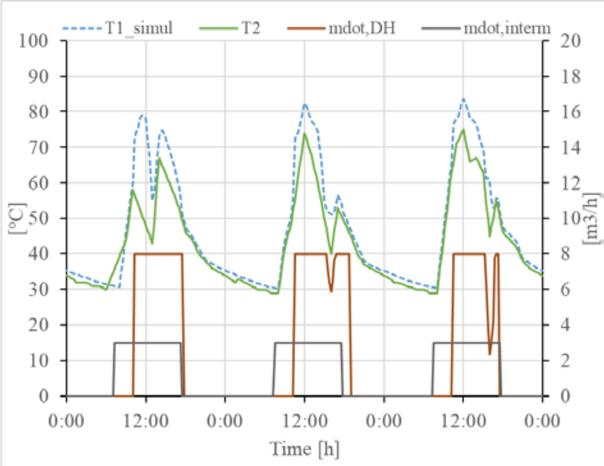

Figure 6 Simulation results with original control strategy ”B”

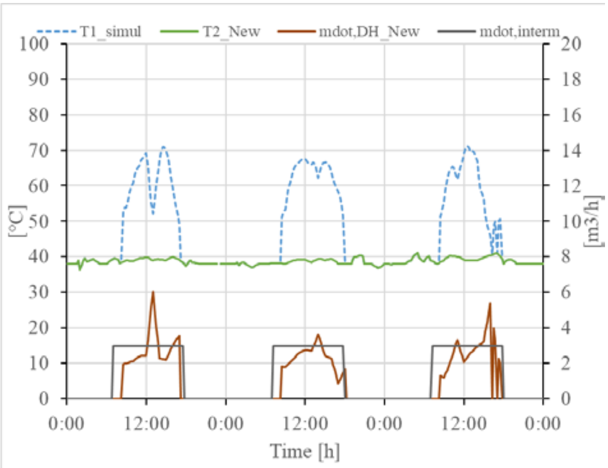

Figure 7 Simulation results with improved control strategy ”B_New”

Figure 6 and Figure 7 shows the results of simulation with original control strategy and with the new one.

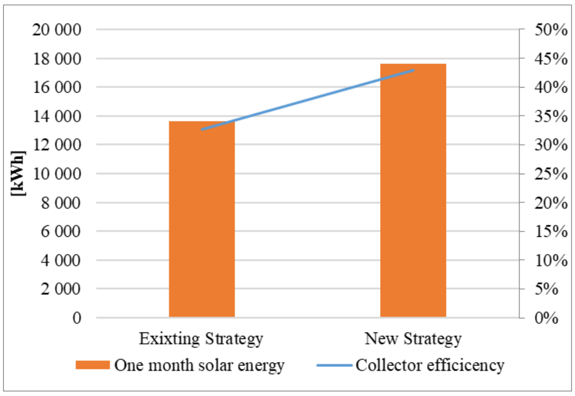

Figure 8 Simulation results in temrs of energy production and average collector efficiency

Simulations show that such control strategy improvement leads to higher collector efficiency (43% against 33%) and to an increased solar yield of about 30% (considering the accuracy mentioned above).

It’s worth noticing that this new control strategy allows for an efficiency improvement but also for a reduction of temperature in T1. Still the level of temperature is higher than the one required as supply temperature in the users’ heat exchangers; thus a general increase of the self-consumption can be noticed.

5. CONCLUSIONS

Feed-in of solar thermal heat in existing DH networks is affected by technical and economic problems, especially in case of small residential systems: from the technical point of view, temperature is a big issue, solar thermal collectors not being able to provide required DH temperatures along significant time laps; from the economic perspective, the fact that solar thermal is a relatively cheap technology makes any additional investment, such as additional piping and control to connect the solar plant to a DH network, little appealing, as it worsens economic performance, which is per se usually not strongly attractive. These barriers can be partly overcome in case of larger solar thermal systems (e.g. in the range of some hundreds of m^2), which can easier reach higher temperatures and may have better economics per se due to scaling effect. Unfortunately, such large solar thermal systems are rare in Italy (as they are in many European countries).

The case of Lodi made the feed-in of solar heat in the DH possible because boundary conditions were favourable: a large solar plant already installed on a swimming pool and operating in sub-optimal way due to oversizing, and a DH network already supplying heat to the pool.

Despite favourable boundary conditions, this case study shows that many technical issues must be considered when coupling solar thermal with DH. In particular, hydraulic integration and control strategy are crucial due to limited temperature available at the solar plant and may prevent solar collectors from working efficiently, if conceived wrongly.

Simulations performed in the present study investigated monitoring data and control strategy, identified the reason for sub-optimal performance of the solar thermal system and suggested a zero-cost improvement in the control logics, leading to some 30% of increase in the solar yield.

REFERENCES

[1] Linea Reti Impianti: District Heating Utility of Lodi, http://www.linea-ri.it/

[2] Faustina Sporting: Sport centre in Lodi, http://www.faustinasportingclub.it/

[3] Schäfer, K., Mangold, D. Decentralized Feed-In of Solar Heat into District Heating Networks Results of a Simulation Case Study in the Joint Research Project DEZENTRAL, Proceedings o SDH conference 2015, Toulouse

[4] ARPA Lombardia: Regional Environmental Protection Agency, www.arpalombardia.it

[5] TRNSYS: Transient System Simulation Tool, http://www.trnsys.com/

IN-SITU TESTING AND MODELING OF LARGE COLLECTOR ARRAYS

D. Tschopp, Ph. Ohnewein, Ch. Rohringer, R. Hausner
AEE – Institute for Sustainable Technologies (AEE INTEC)
Feldgasse 19, A-8200 Gleisdorf
phone: +43-(0)3112-5886-252; email: d.tschopp@aee.at

Summary

For most district heating applications, large-scale solar thermal plants are a technically and economically viable option to feed solar thermal energy into the heating net. We present the results of the project MeQuSo: Within the project, a new in-situ test procedure for large collector arrays is developed. The test aims at providing a thorough method for evaluating the thermal power output of large collector arrays under "real-life", transient conditions.

In the conference contribution the major challenges, a framework how to address them and collector array models suitable for in-situ testing will be presented in connection with the evaluation of measurement data of the SDH plant “Fernheizwerk” in Graz (Austria).

Keywords: in-situ testing, collector array, in-situ measurement, large solar thermal plants

1. Large-scale solar thermal plants for SDH applications

Currently there are more than 5,000 medium and large-scale district heating (DH) networks in operation in Europe, supplying 10% of the total heat demand, but until now, there is only a small share of around 150 DH networks that integrate solar thermal energy as a heat source [1], [2].

Key factors to increase the market penetration of large-scale solar thermal plants are the reduction of investment risks and the realization of cost saving potentials during the plant operation by means of performance guarantees, efficient monitoring and ongoing optimization. These measures rely on an accurate and reliable characterization of the collector array performance. In the presented research project MeQuSo, an in-situ test procedure is developed with the objective of evaluating the thermal power output of large collector arrays under transient conditions.

2. Research focus

The cornerstones and characteristics of the in-situ test procedure are:

- Consideration of ‘real operation conditions’, i.e. dealing with soiling, shading, etc.
- Provision of a standardized and traceable framework for data acquisition, data selection and parameter estimation
- Modeling of the collector array focuses on the most important influencing factors on the thermal performance, but restrains from a detailed representation to facilitate the application of the procedure
- Applicability of the procedure to common plant configurations and measurement setups
- Characterization of the collector array performance with a set of characteristic parameters

The in-situ test procedure will have some similarities with the ISO 9806 standard for single collector tests [3], but it differs from ISO 9806 in two important aspects:

1) The new test procedure focuses on large collector arrays instead of single collectors.
2) The new test procedure moves from the laboratory to ‘real-world’ conditions.

A cornerstone to develop the in-situ test procedure is the availability of high-precision measurement data. In the research project, the large-scale solar thermal plant “Fernheizwerk” in Graz (Austria) was equipped with high-precision measurement equipment. Measurements are done for six individual collector arrays with large-scale flat plate collectors of five different producers. This allows a direct side-by-side comparison of the arrays.

3. Results

Based on the evaluation of measurement data of this plant and literature studies, the major challenges that an in-situ test procedure needs to address were identified, a methodological approach how to meet these challenges was developed as well as collector array models suitable for in-situ testing (see table 1).

challenge	issues	solution
dynamics	• dwelling time of the fluid is not neglectable (often in the range of 2…3 minutes) • transient behaviour (varying volume flows, irradiance, etc.) needs to be accounted for	plug-flow model with fluid and solid part capacity terms
irradiance distribution	• external and internal shading, irradiance varies across the array, sensor readings are not representative	models of the irradiance distribution of the plant
narrow data range	• measurement data lie in a narrow range • strong correlation of irradiance and flow temperature	statistical analysis and design of experiments (DoE)

TABLE 1: MAJOR CHALLENGES FOR IN-SITU TEST PROCEDURES

In fig. 1a, some issues regarding the dynamics are exemplified by showing the delayed reaction of the flow temperature to input changes and the superimposition of various effects, when the return temperature and the volume flow rate vary. Fig. 1b depicts a screenshot of a 3D-model of the plant "Fernheizwerk". The differential equation used for the plug-flow model is shown in equation (1).

In the conference contribution, the major challenges, a framework how to address them and collector array models suitable for in-situ test procedures will be presented in connection with the evaluation of measurement data of the solar district heating plant "Fernheizwerk".

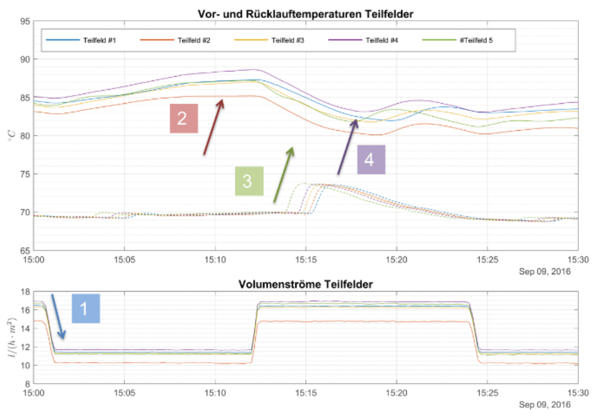

FIG. 1A (LEFT): COLLECTOR ARRAY DYNAMICS; FIG. 1B (RIGHT): 3D-MODEL OF THE PLANT "FERNHEIZWERK"

$$\frac{\partial T_f(z,t)}{\partial t} = -\frac{V(t)}{A_f} \cdot \frac{V_{col}}{A_{col}} \cdot \rho_f \cdot c_f \cdot \frac{A_{col}}{(mc)} \cdot \frac{\partial T_f(z,t)}{\partial z} + \frac{A_{col}}{(mc)} \cdot \alpha(t) \cdot R(t) - \frac{A_{col}}{(mc)} \cdot \gamma \cdot (T_f(z,t) - T_a(t)) \qquad \text{EQ. (1)}$$

4. References

[1] Dalenbäck, J.-O.; Werner, S. (2012): *Solar District Heating - Boundary Conditions and Market Obstacles*, CIT Energy Management AB, Gothenburg

[2] AEBIOM (2012): *EU Handbook District Heating Markets*, AEBIOM, Brussels

[3] ISO 9806:2013 *Solar energy – Solar thermal collectors – Test methods*. International Standards Organization, Geneva

Author Index